STEM CELLS AND AGING

EDITED BY: Cesar V. Borlongan and Gary K. Steinberg
PUBLISHED IN: Frontiers in Aging Neuroscience

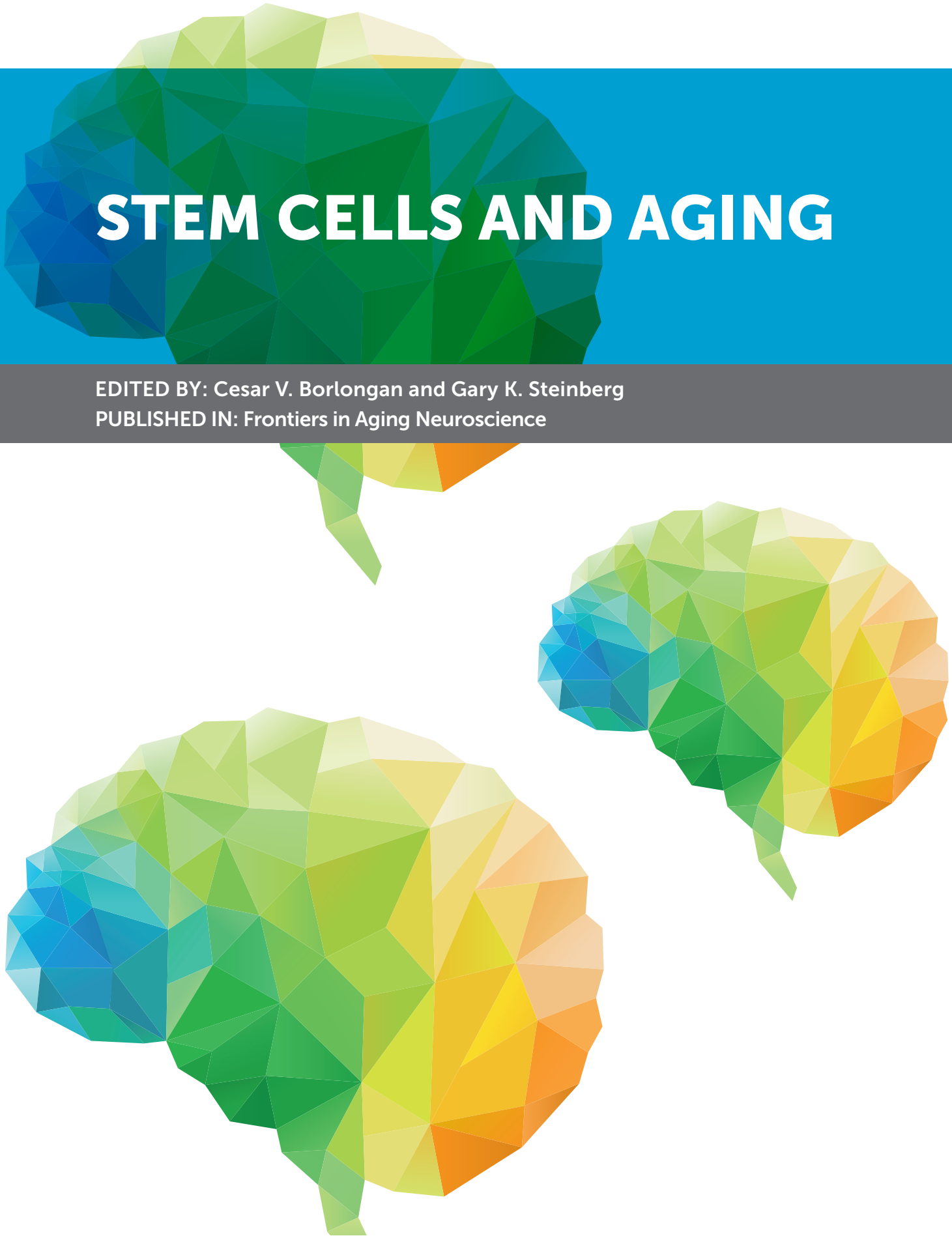

frontiers Research Topics

ISSN 1664-8714
ISBN 978-2-88971-034-8
DOI 10.3389/978-2-88971-034-8

About Frontiers

Frontiers is more than just an open-access publisher of scholarly articles: it is a pioneering approach to the world of academia, radically improving the way scholarly research is managed. The grand vision of Frontiers is a world where all people have an equal opportunity to seek, share and generate knowledge. Frontiers provides immediate and permanent online open access to all its publications, but this alone is not enough to realize our grand goals.

Frontiers Journal Series

The Frontiers Journal Series is a multi-tier and interdisciplinary set of open-access, online journals, promising a paradigm shift from the current review, selection and dissemination processes in academic publishing. All Frontiers journals are driven by researchers for researchers; therefore, they constitute a service to the scholarly community. At the same time, the Frontiers Journal Series operates on a revolutionary invention, the tiered publishing system, initially addressing specific communities of scholars, and gradually climbing up to broader public understanding, thus serving the interests of the lay society, too.

Dedication to Quality

Each Frontiers article is a landmark of the highest quality, thanks to genuinely collaborative interactions between authors and review editors, who include some of the world's best academicians. Research must be certified by peers before entering a stream of knowledge that may eventually reach the public - and shape society; therefore, Frontiers only applies the most rigorous and unbiased reviews.
Frontiers revolutionizes research publishing by freely delivering the most outstanding research, evaluated with no bias from both the academic and social point of view. By applying the most advanced information technologies, Frontiers is catapulting scholarly publishing into a new generation.

What are Frontiers Research Topics?

Frontiers Research Topics are very popular trademarks of the Frontiers Journals Series: they are collections of at least ten articles, all centered on a particular subject. With their unique mix of varied contributions from Original Research to Review Articles, Frontiers Research Topics unify the most influential researchers, the latest key findings and historical advances in a hot research area! Find out more on how to host your own Frontiers Research Topic or contribute to one as an author by contacting the Frontiers Editorial Office: frontiersin.org/about/contact

STEM CELLS AND AGING

Topic Editors:
Cesar V. Borlongan, University of South Florida, United States
Gary K. Steinberg, Stanford University, United States

Dr. Borlongan and Dr. Steinberg serve as consultants to stem cell-based companies, hold patents and patent applications, and have funded grants related to stem cell biologics and applications.

Citation: Borlongan, C. V., Steinberg, G. K., eds. (2021). Stem Cells and Aging Lausanne: Frontiers Media SA. doi: 10.3389/978-2-88971-034-8

Table of Contents

04 ***Editorial: Stem Cells and Aging***
Cesar V. Borlongan and Gary K. Steinberg

06 ***Long-Term Continuous Cervical Spinal Cord Stimulation Exerts Neuroprotective Effects in Experimental Parkinson's Disease***
Ken Kuwahara, Tatsuya Sasaki, Takao Yasuhara, Masahiro Kameda, Yosuke Okazaki, Kakeru Hosomoto, Ittetsu Kin, Mihoko Okazaki, Satoru Yabuno, Satoshi Kawauchi, Yousuke Tomita, Michiari Umakoshi, Kyohei Kin, Jun Morimoto, Jea-Young Lee, Naoki Tajiri, Cesar V. Borlongan and Isao Date

18 ***Estradiol Replacement at the Critical Period Protects Hippocampal Neural Stem Cells to Improve Cognition in APP/PS1 Mice***
Yaoyao Qin, Dong An, Weixing Xu, Xiuting Qi, Xiaoli Wang, Ling Chen, Lei Chen and Sha Sha

32 ***Stem Cells of the Aging Brain***
Alexandra M. Nicaise, Cory M. Willis, Stephen J. Crocker and Stefano Pluchino

55 ***HUCBC Treatment Improves Cognitive Outcome in Rats With Vascular Dementia***
Poornima Venkat, Lauren Culmone, Michael Chopp, Julie Landschoot-Ward, Fengjie Wang, Alex Zacharek and Jieli Chen

69 ***LncRNAs Stand as Potent Biomarkers and Therapeutic Targets for Stroke***
Junfen Fan, Madeline Saft, Nadia Sadanandan, Bella Gonzales-Portillo, You Jeong Park, Paul R. Sanberg, Cesario V. Borlongan and Yumin Luo

85 ***Effect of Bone Marrow Stromal Cells in Parkinson's Disease Rodent Model: A Meta-Analysis***
Jianyang Liu, Jialin He, Yan Huang and Zhiping Hu

95 ***Revisiting Stem Cell-Based Clinical Trials for Ischemic Stroke***
Joy Q. He, Eric S. Sussman and Gary K. Steinberg

107 ***Age-Dependent Activation and Neuronal Differentiation of Lgr5+ Basal Cells in Injured Olfactory Epithelium*** **via** ***Notch Signaling Pathway***
Xuewen Li, Meimei Tong, Li Wang, Yumei Qin, Hongmeng Yu and Yiqun Yu

120 ***Conversion of Reactive Astrocytes to Induced Neurons Enhances Neuronal Repair and Functional Recovery After Ischemic Stroke***
Michael Qize Jiang, Shan Ping Yu, Zheng Zachory Wei, Weiwei Zhong, Wenyuan Cao, Xiaohuan Gu, Anika Wu, Myles Randolph McCrary, Ken Berglund and Ling Wei

frontiers in Aging Neuroscience

EDITORIAL
published: 17 May 2021
doi: 10.3389/fnagi.2021.690613

Editorial: Stem Cells and Aging

Cesar V. Borlongan[1]* *and Gary K. Steinberg*[2]*

[1] Department of Neurosurgery and Brain Repair, University of South Florida, Tampa, FL, United States, [2] Department of Neurosurgery, Stanford University, Stanford, CA, United States

Keywords: stem cells, aging, transplantation, brain, regeneration

Editorial on the Research Topic

Stem Cells and Aging

Stem cells have emerged as a key scientific tool and potent therapeutic agent for both understanding the mechanism of aging, as well as treating diseases that arise as cells lose their resilience in later years of life. Science continues to advance our comprehension and capacity to harness the innumerable possibilities that stem cells hold for ameliorating disease burden and improving the quality of life. Collaborative efforts across the globe have helped elucidate the role of stem cells in reversing the consequences of age-related neurologic disorders, including stroke, Parkinson's disease (PD), and Alzheimer's disease (AD). This special issue is a testimony to the enthralling breakthroughs over the past year in stem cell therapy for aging-related disorders.

PD manifests as neurodegenerative destruction of dopaminergic neurons in the substantia nigra pars compacta due to pathological accumulation of misfolded alpha-synuclein inclusions. This aberrant protein aggregation precipitates disabling motor deficits and poor quality of life in millions of patients globally. Dr. Zhiping Hu of Central South University, an innovative mind in the field of ischemic stroke research, has also led critical efforts to advance our understanding of PD in the laboratory and the literature. In the present issue, Liu et al. clarify the importance of bone marrow stromal cells in PD models by investigating the pooled effects observed in 27 major animal studies to date.

Spinal cord stimulation (SCS) is a promising focus of PD research that leverages implantable electrodes to deliver controlled electrical signals to the spine. This represents an alternative therapeutic approach to traditional pharmacological options that mirrors concepts inherent to deep brain stimulation, another treatment that demonstrates success in certain PD patients. Dr. Isao Date of Nagoya City University is a world-renowned researcher who has contributed crucial data to the PD field. Here, Kuwahara et al. present novel findings that continuous SCS effects positive behavioral and histological changes in PD. The principles outlined in this study contain tremendous translational value that underscores the potential utility of SCS in the clinical setting.

Human umbilical cord blood cells (HUCBCs) signify a potent source of stem cells that have demonstrated advantageous outcomes across a diverse array of conditions. Dr. Jieli Chen is an esteemed stroke expert from the Henry Ford Hospital who has leveraged HUCBC stem cells in her research to contribute compelling evidence for the neuroprotective efficacy of these cells against devastating conditions such as stroke. In the accompanying article, Venkat et al. set the stage for the use of HUCBCs in vascular dementia. They provide compelling evidence of white matter remodeling with cognitive functional improvements that establish HUCBCs as a potentially robust therapeutic tool.

Dr. Stefano Pluchino of the University of Cambridge has led pioneering studies on developing experimental molecular stem cell-based medicines designed to transform our understanding of the mechanisms of intercellular neuro-immune signaling into therapeutics for multiple sclerosis (MS) and other inflammation-plagued disorders, such as stroke and traumatic brain injury. Here, Nicaise et al. discuss the regenerative capabilities of the resident stem cells in the aging brain. They investigate factors that influence neural stem cell aging and provide both *in vivo* and *in vitro* models to illustrate their findings.

Edited and reviewed by:
Thomas Wisniewski,
New York University, United States

***Correspondence:**
Cesar V. Borlongan
cborlong@health.usf.edu
Gary K. Steinberg
cerebral@stanford.edu

Received: *03 April 2021*
Accepted: *12 April 2021*
Published: *17 May 2021*

Citation:
Borlongan CV and Steinberg GK (2021) Editorial: Stem Cells and Aging. Front. Aging Neurosci. 13:690613. doi: 10.3389/fnagi.2021.690613

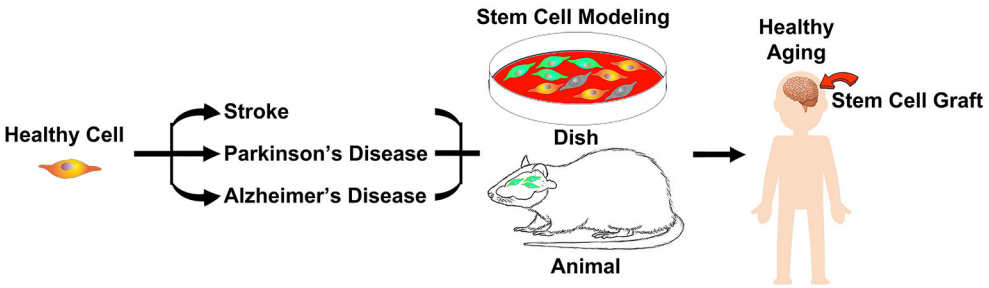

FIGURE 1 | During aging and disease states, such as stroke, Parkinson's disease and Alzheimer's disease, brain cells become vulnerable to injury, which can be captured in a pertri dish or animal models. Stem cell therapy stands as a robust approach in harnessing healthy aging.

Limited data have supported a critical time period for menopausal women with AD to undergo estrogen replacement therapy (ERT). Dr. Sha Sha is a senior lecturer at Nanjing Medical University with many years of experience in the field. Here, Qin et al. elucidate the effective window of estradiol treatment utilizing an AD mouse model. They examine β-amyloid accumulation, telomerase activity, hippocampal neurogenesis, hippocampal dependent behavior and neural stem cell (NSC) proliferation to discover an effective window for treatment.

The utilization of stem cells has provided a potent therapeutic for the treatment of central nervous system disorders. He et al. boasts years of experience as a cerebrovascular neurosurgeon and scientist focused on translating key scientific findings to the clinic. Here, Dr. Steinberg of Stanford University and colleagues discuss past and current clinical trials utilizing stem cell-based therapy as a treatment for ischemic stroke. Specifically, they discuss the recurring use of hematopoietic, mesenchymal, and neural cell lineages and the reasoning behind this.

Stroke is a debilitating illness with limited therapeutic options. Dr. Yumin Luo is a leader in the field of cerebrovascular disease from Capital Medical University, who specializes particularly in stroke. Here, Fan et al. explored the role of long non-coding RNAs (lncRNAs) in the pathology of ischemic stroke and intracerebral hemorrhage. The authors explicate the diagnostic and therapeutic capacity of lncRNAs in stroke and the potential for stem cells to further bolster lncRNA function.

Aging-induced deterioration of olfactory sensory neurons in the olfactory epithelium (OE) can be alleviated by promoting OE regeneration through certain chemical factors. Dr. Yiqun Yu has led remarkable studies investigating the molecular mechanisms of the olfactory bulb. Li et al. at Fudan University found that levels of G-protein coupled receptor 5 (Lgr5)-positive cells were reduced substantially in the injured OE of aged mice, and Notch signaling promoted OE regeneration.

The neuronal transcription factor NeuroD1 has been shown to promote the differentiation of neurons (iNeurons) from astrocytes following a stroke, suggesting a potential regenerative therapy. Dr. Ling Wei from Emory University has led innovative studies investigating neuroprotective agents in stroke. Here, Jiang et al. found that NeuroD1 administration *via* lentivirus culminated in the transformation of the infected astrocytes into iNeurons in mice, which rehabilitated impaired neuronal circuitry induced by stroke.

These milestone studies in basic science, translational medicine, and clinical research demonstrate the therapeutic potential of stem cells in aging-related neurological disorders (**Figure 1**). The present pandemic highlights age as a primary factor driving mortality and morbidity. Age serves as a significant determinant of health not just for COVID-19, but for most of the diseases that we endeavor to treat. Our scientific efforts to understand the mechanisms of cell death and survival in the brain toward therapeutically harnessing healthy aging will benefit from the rigorous investigations into the clinical applications of stem cells.

AUTHOR CONTRIBUTIONS

All authors conceptualized and wrote the manuscript.

FUNDING

CB was funded by National Institutes of Health (NIH) R01NS090962, NIH R01NS102395, and NIH R21NS109575. GS was funded by NIH R01NS058784, NIH R01NS093057, and NIH R01NS064136, California Institute for Regenerative Medicine (CIRM) CLIN1-09433, and was supported in part by funding from Bernard and Ronni Lacroute, the William Randolph Hearst Foundation, Marc Paskin, and Penny Bradley.

ACKNOWLEDGMENTS

The authors thank the excellent technical assistance of Jeffrey Farooq, Zhen-Jie Wang, Blaise Cozene, Nadia Sadanandan, and Jea-Young Lee for drafting this Editorial and creating the summary figure.

Conflict of Interest: CB and GS serve as consultants to stem cell-based companies, hold patents and patent applications, and have funded grants related to stem cell biologics and applications.

frontiers in Aging Neuroscience

ORIGINAL RESEARCH
published: 16 June 2020
doi: 10.3389/fnagi.2020.00164

Long-Term Continuous Cervical Spinal Cord Stimulation Exerts Neuroprotective Effects in Experimental Parkinson's Disease

Ken Kuwahara[1], Tatsuya Sasaki[1], Takao Yasuhara[1], Masahiro Kameda[1], Yosuke Okazaki[1], Kakeru Hosomoto[1], Ittetsu Kin[1], Mihoko Okazaki[1], Satoru Yabuno[1], Satoshi Kawauchi[1], Yousuke Tomita[1], Michiari Umakoshi[1], Kyohei Kin[1], Jun Morimoto[1], Jea-Young Lee[2], Naoki Tajiri[3], Cesar V. Borlongan[2] and Isao Date[1]*

[1] Department of Neurological Surgery, Graduate School of Medicine, Dentistry and Pharmaceutical Sciences, Okayama University, Okayama, Japan, [2] Department of Neurosurgery and Brain Repair, Morsani College of Medicine, University of South Florida, Tampa, FL, United States, [3] Department of Neurophysiology and Brain Science, Graduate School of Medical Sciences, Nagoya City University, Nagoya, Japan

OPEN ACCESS

Edited by:
Xinglong Wang,
Case Western Reserve University,
United States

Reviewed by:
Timothy J. Collier,
Michigan State University,
United States
Kaneyasu Nishimura,
Kyoto Pharmaceutical University,
Japan
Heather Boger,
Medical University of South Carolina,
United States

***Correspondence:**
Tatsuya Sasaki
tatu_tatu_sasa@yahoo.co.jp

Received: 28 March 2020
Accepted: 12 May 2020
Published: 16 June 2020

Citation:
Kuwahara K, Sasaki T, Yasuhara T, Kameda M, Okazaki Y, Hosomoto K, Kin I, Okazaki M, Yabuno S, Kawauchi S, Tomita Y, Umakoshi M, Kin K, Morimoto J, Lee J-Y, Tajiri N, Borlongan CV and Date I (2020) Long-Term Continuous Cervical Spinal Cord Stimulation Exerts Neuroprotective Effects in Experimental Parkinson's Disease. Front. Aging Neurosci. 12:164. doi: 10.3389/fnagi.2020.00164

Background: Spinal cord stimulation (SCS) exerts neuroprotective effects in animal models of Parkinson's disease (PD). Conventional stimulation techniques entail limited stimulation time and restricted movement of animals, warranting the need for optimizing the SCS regimen to address the progressive nature of the disease and to improve its clinical translation to PD patients.

Objective: Recognizing the limitations of conventional stimulation, we now investigated the effects of continuous SCS in freely moving parkinsonian rats.

Methods: We developed a small device that could deliver continuous SCS. At the start of the experiment, thirty female Sprague-Dawley rats received the dopamine (DA)-depleting neurotoxin, 6-hydroxydopamine, into the right striatum. The SCS device was fixed below the shoulder area of the back of the animal, and a line from this device was passed under the skin to an electrode that was then implanted epidurally over the dorsal column. The rats were divided into three groups: control, 8-h stimulation, and 24-h stimulation, and behaviorally tested then euthanized for immunohistochemical analysis.

Results: The 8- and 24-h stimulation groups displayed significant behavioral improvement compared to the control group. Both SCS-stimulated groups exhibited significantly preserved tyrosine hydroxylase (TH)-positive fibers and neurons in the striatum and substantia nigra pars compacta (SNc), respectively, compared to the control group. Notably, the 24-h stimulation group showed significantly pronounced preservation of the striatal TH-positive fibers compared to the 8-h stimulation group. Moreover, the 24-h group demonstrated significantly reduced number of microglia in the

striatum and SNc and increased laminin-positive area of the cerebral cortex compared to the control group.

Conclusions: This study demonstrated the behavioral and histological benefits of continuous SCS in a time-dependent manner in freely moving PD animals, possibly mediated by anti-inflammatory and angiogenic mechanisms.

Keywords: electrical stimulation, neuroinflammation, neuromodulation, neuroprotection, 6-hydroxydopamine

INTRODUCTION

Parkinson's disease manifests as a progressive neurodegenerative disease resulting from the loss of dopaminergic neurons in the nigrostriatal system. Cardinal symptoms of PD include bradykinesia, rigidity, resting tremor, and postural instability. Levodopa treatment stands as the first-line therapy for PD. However, long-term medication often results in adverse events, including motor fluctuation and dyskinesia.

Deep brain stimulation (DBS) improves motor symptoms in advanced PD patients. In animal models of PD, DBS may increase BDNF (Spieles-Engemann et al., 2010) and may prevent DA neuron loss in the SNc (Maesawa et al., 2004; Spieles-Engemann et al., 2011). However, DBS entails an invasive surgical procedure that damages brain tissue and involves a permanent system implant. The estimated risk of intracranial hemorrhage in DBS ranges from 0.8 to 2.8% (Obeso et al., 2001; Herzog et al., 2003; Sansur et al., 2007; Weaver et al., 2009; Fenoy and SimpsonJr., 2014). Moreover, the efficacy of DBS appears effective only in cases with motor fluctuation responsive to levodopa therapy, thus, limited PD patients are eligible for DBS.

Spinal cord stimulation in the management of intractable neuropathic pain demonstrates a solid track record of effectiveness and safety. Although neurological injuries account for the most serious complication in SCS procedure, they are rare with an incidence rate of only 0.6% (Levy et al., 2011). In animal models of PD, SCS alleviates motor deficits (Fuentes et al., 2009; Santana et al., 2014; Shinko et al., 2014; Yadav et al., 2014) and protects nigrostriatal dopaminergic neurons (Fuentes et al., 2009; Shinko et al., 2014). In advanced PD patients with lumbago and leg pain, SCS improves motor function such as posture, postural stability, and gait ability (Agari and Date, 2012).

Electrical stimulation shows efficacy in PD animal models. However, technical problems plague the SCS animal model, including the short duration of the stimulation (no more than 1 h per day) and the highly restricted movement of animals (i.e., due to anesthesia) (Maesawa et al., 2004; Boulet et al., 2006; Spieles-Engemann et al., 2010, 2011; Shinko et al., 2014; Yadav et al., 2014; Huotarinen et al., 2018). The advent of small mobile stimulators enables continuous DBS in freely moving parkinsonian rats (Badstübner et al., 2012; Badstuebner et al., 2017). Cognizant of SCS in PD animal models not closely replicating the clinical application, customizing the small mobile stimulators used in DBS for SCS may overcome these preclinical limitations. To date, continuous SCS in freely moving PD animals remains unexplored. In the present study, we developed a small mobile device for continuous SCS in freely moving parkinsonian rats.

Abbreviations: BDNF, brain-derived neurotrophic factor; DA, dopamine; DBS, deep brain stimulation; Iba1, ionized calcium-binding adaptor molecule 1; PD, Parkinson's disease; SCS, spinal cord stimulation; SNc, substantia nigra pars compacta; TH, tyrosine hydroxylase; VEGF, vascular endothelial growth factor; 6-OHDA, 6-hydroxydopamine.

MATERIALS AND METHODS

Animals and Animal Care

All animal procedures in this study followed specifically the approved guidelines by the Institutional Animal Care and Use Committee of Okayama University Graduate School of Medicine (Protocol# OKU-2018807). Adult female Sprague-Dawley rats (Shimizu Laboratory Supplies Co., Ltd., Japan) weighing 200–250 g at the beginning of the study served as subjects for all experiments. Animal housing consisted of individual cages in a temperature and humidity-controlled room and maintained on a semidiurnal light-dark cycle.

Small Mobile Device for Continuous Electrical Stimulation

We developed an electrical stimulation device called SAS-200 (Unique Medical Co., Ltd., Japan) that offered convenient adjustment of stimulation conditions via Bluetooth and allowed free movement of rats owing to its small size. The SAS-200SCS, which was attached to the back of the rats and connected to the SCS electrode, delivered the stimulation. This stimulation required no anesthesia, thereby allowing rats to freely move around, making continuous stimulation possible. Additionally, the stimulation conditions could be easily adjusted wirelessly.

The SAS-200 measured 20 mm × 40 mm × 20 mm, with a net weight of 26 g (including the battery) (**Figure 1A**). It consisted of a control panel, a rechargeable lithium-ion battery, and an aluminum case. An aluminum case covered the unit and fixed by screws on two sides. The SAS-200 generated biphasic square pulses with stimulation conditions programmed in the control panel, and as many as 1,650 patterns of stimulation could be adjusted accordingly. Based on pilot stimulation optimization studies, we selected 10 stimulation parameters for stimulation intensity (0.25, 0.4, 0.5, 0.6, 0.7, 0.8, 1.0, 1.2, 1.5, and 2.0 mA), 11 for frequency (1, 2, 5, 10, 20, 30, 50, 100, 150, 200, and 300 Hz), three for pulse width (100, 250, and 500 μs), and five for stimulation cycle [(A) continuous stimulation, (B) 8 h on 16 h off, (C) 12 h on 12 h off, (D) 30 s on 5 min off, and (E) 15 trains every 12 s]. A standard Windows PC with a specific application controlled these stimulation conditions, such

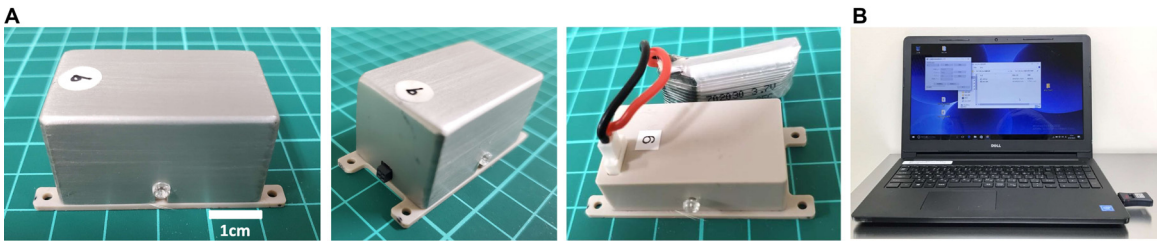

FIGURE 1 | Wireless controllable electrical stimulation system (SAS-200). **(A)** The stimulation device measures 20 mm × 40 mm × 20 mm, with a net weight of 26 g (including the battery). The control panel is covered by an aluminum case and fixed by screws on two sides. **(B)** Stimulation conditions can be changed using a Windows PC and transmitted through Bluetooth.

as beginning, duration, and particular conditions (**Figure 1B**). An LED light, which was placed below the transparent screw on the right side, served as the stimulation and battery indicator; when Bluetooth initiated the stimulation, the light turned on, and the light flickered when the battery dropped below 20%. We used a rechargeable battery with an AC adaptor. In our experiments, we fixed and encased in a protective jacket the SAS-200 to the back of the animals through threads at four fixing holes. A battery change involved simply removing the screws and replacing the depleted battery with a fully charged battery.

Experimental Design

Rats were randomly divided into three groups: the control, 8-h stimulation, and 24-h stimulation groups (30 rats total, $n = 10$ in each group) (see study time course in **Figure 2**). On day 0, all rats received 6-OHDA, which was injected into the right striatum. Subsequently, all rats underwent C2 laminectomy and implanted with an electrode in their epidural space, with the external mobile stimulator subsequently attached to their back. After recovery from anesthesia, stimulation commenced in the 8- and 24-h stimulation groups (see detailed stimulation protocol below). On days 7 and 14, all rats received behavioral tests, and thereafter euthanized for immunohistochemical investigations and morphological analyses.

Surgical Procedure

6-OHDA Lesioning

All rats received anesthesia with 0.3 mg/kg of medetomidine, 4.0 mg/kg of midazolam, and 5.0 mg/kg of butorphanol by intraperitoneal injection and placed in a stereotaxic instrument (Narishige, Japan). The animals underwent a midline head skin incision on and a small hole drilled in their skull. Twenty μg of 6-OHDA (4 μl of 5 mg/ml dissolved in saline containing 0.2 mg/ml of ascorbic acid; Sigma, United States) was injected into the right striatum (1.0 mm anterior and 3 mm lateral to the bregma and 5.0 mm ventral to the surface of the brain with the tooth-bar set at −1.0 mm) with a 28G Hamilton syringe that delivered an injection rate of the drug at 1 μl/min. Syringe withdrawal commenced after a 5-min absorption time following injection.

Implantation of Stimulation Electrode

Following 6-OHDA injection, animals received a midline skin incision that extended to the back, and carefully dissecting the spinal muscles to expose and to eventually perform a C2 laminectomy. We implanted a silver bipolar ball electrode, with a diameter of 2 mm, epidurally on the dorsal surface of the spinal cord and fixed to the muscle using a 5-0 silk thread (**Figures 3A,B**). We then placed a ground electrode in the skull of the rat, with the lead tunneled subcutaneously to the back of rats. Finally, the rats received the stimulation device that was fixed on their back using 1-0 silk threads at four fixing holes and encased in a protective jacket (**Figure 3C**).

Electrical Stimulation

After recovery from anesthesia, the stimulation device commenced by wireless command from Windows PC via Bluetooth in the 8- and 24-h stimulation groups. In the 8-h stimulation group, the stimulator automatically delivered biphasic square pulses for 8 h then switched off for 16 h. Stimulation continued for 14 consecutive days, and with battery changed every 3 days. Stimulation consisted of 50 Hz pulses in 100 μs. Intensities corresponded to the 80% of motor threshold (**Supplementary Video S1**). The parameter was determined based on the results of our previous studies demonstrating neuroprotective effects for PD model rats (Shinko et al., 2014).

Behavioral Tests

Cylinder Test

To assess the degree of forepaw asymmetry, we performed the cylinder test on days 7 and 14. This test involved placing individual animals in a transparent cylinder (diameter: 20 cm, height: 30 cm) for 3 min and recording the number of forepaw contacts on the cylinder wall (Schallert et al., 2000; Shinko et al., 2014). The score of the cylinder test reflected a contralateral bias: ([number of contacts with contralateral limb] − [number of contacts with ipsilateral limb]/[number of total contacts] × 100) (Roof et al., 2001; Shinko et al., 2014; Sasaki et al., 2016). This contralateral bias indicated successful 6-OHDA-induced unilateral depletion of nigrostriatal dopaminergic neurons and fibers.

Methamphetamine-Induced Rotation Test

Rats received an intraperitoneal injection of methamphetamine (3.0 mg/kg; Dainippon Sumitomo Pharma, Japan) on days 7 and 14. We assessed for 90 min with a video camera the full 360° turns in the direction ipsilateral to the lesion. Such drug-induced

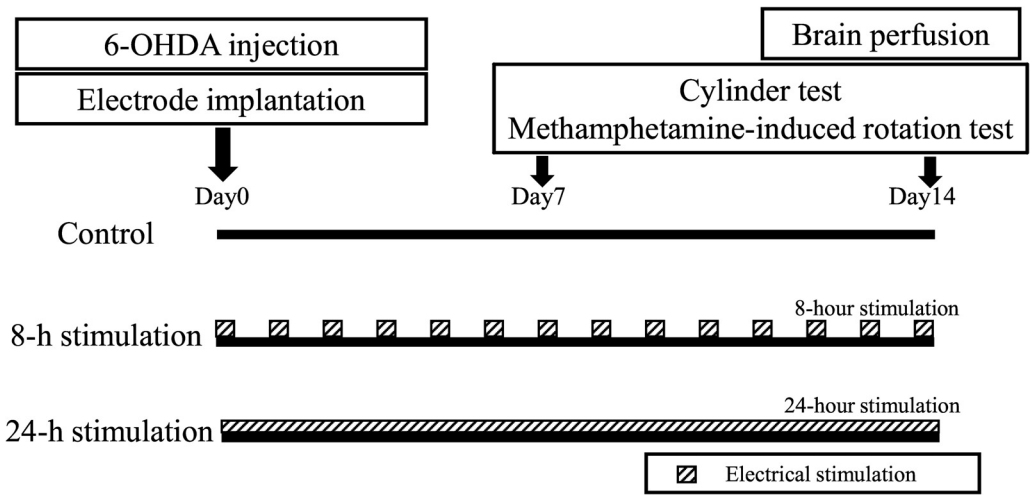

FIGURE 2 | Time course of this study.

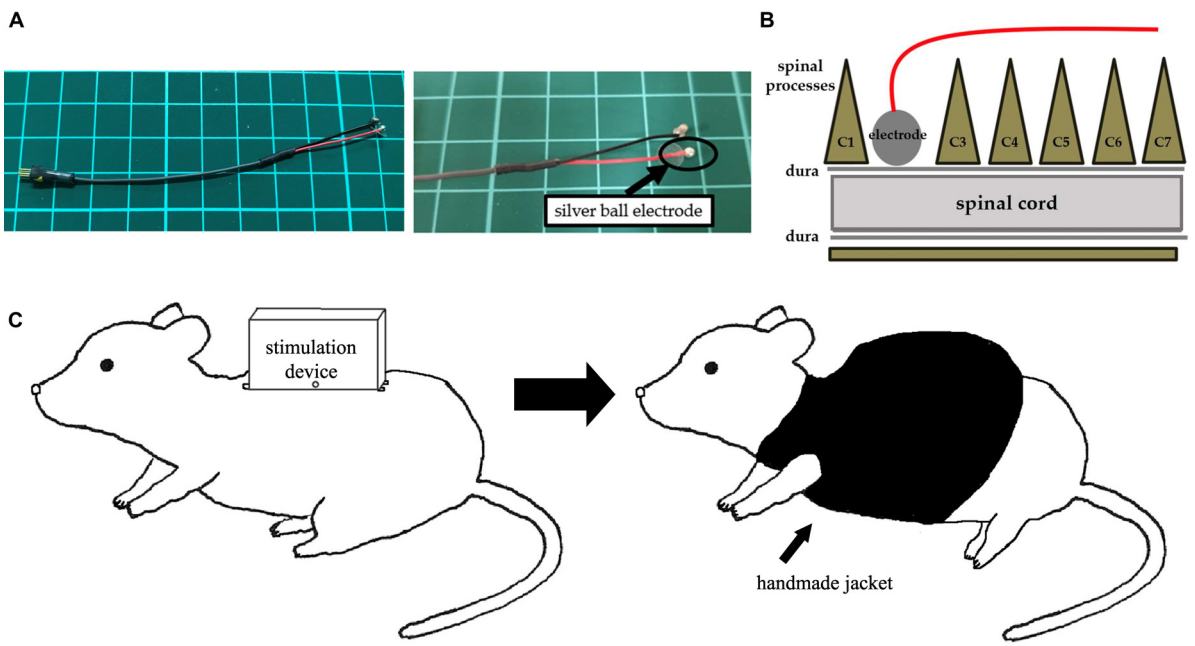

FIGURE 3 | An electrode and images of surgery. **(A)** A silver ball SCS electrode used in this study (diameter: 2 mm). **(B)** An image showing electrode implantation. A silver ball electrode was placed on the dorsal surface of the spinal cord and fixed by a silk thread. **(C)** An image showing a rat with a stimulation device. After fixation of the stimulation device on the back, a handmade jacket was put on the rat.

ipsilateral rotations also indicated successful 6-OHDA-induced unilateral nigrostriatal dopaminergic depletion.

Immunohistochemical Investigations

Processing for immunohistochemistry started after completion of behavioral tests on day 14. Animals underwent euthanasia with an overdose of pentobarbital (100 mg/kg). The rats then received transcardial perfusion with 150 ml of cold phosphate-buffered saline (PBS) and 150 ml of 4% paraformaldehyde (PFA) in PBS. We then harvested the brains carefully, post fixed in 4% PFA in PBS overnight at 4°C, and subsequently stored in 30% sucrose in PBS until completely submerged. Thereafter, we sectioned the brains coronally at a thickness of 40 μm.

For assessing nigrostriatal dopaminergic pathways, we used TH staining. We initially exposed free-floating sections to a blocking solution using 3% hydrogen peroxide in 70% methanol for 7 min. After three washes in PBS, we incubated the sections overnight at 4°C, with rabbit anti-TH antibody (1:500; Chemicon, Temecula, CA, United States) with 10% normal horse serum. We then washed the sections three times for 5 min in PBS

and incubated them for 1 h in biotinylated donkey anti-rabbit IgG (1:500; Jackson ImmunoResearch Lab, West Grove, PA, United States), followed by 30 min in avidin-biotin-peroxidase complex (Vector Laboratories, Burlingame, CA, United States). We next treated the sections with 3, 4-diaminobenzidine (DAB; Vector) and hydrogen peroxide, then mounted on albumin-coated slides, and embedded them with cover glass.

Next, we performed Iba-1 and laminin staining to evaluate activated microglial cells and blood vessels, respectively. We initially washed 40-μm-thick sections three times in PBS and incubating them in 10% normal horse serum and primary antibodies: rabbit anti-Iba1 antibody (1:250; Wako Pure Chemical Industries, Osaka, Japan) and rabbit anti-laminin antibody (1:500; AB11575, Abcam plc, Cambridge, United Kingdom) overnight at 4°C. Thereafter, we washed the sections three times in PBS, incubated them for 1 h in FITC-conjugated affinity-purified donkey anti-rabbit IgG (H + L) in a dark chamber, then washed them three more times in PBS and finally mounted and embedded them with cover glass as above.

Morphological Analyses

We assessed the density of TH-positive fibers in the striatum with a computerized analysis system as described previously (Shinko et al., 2014). Investigators blinded to the treatment conditions randomly selected three sections at 0.5, 1.0, and 1.5 mm anterior to the bregma for quantitative analysis. The two areas adjacent to the needle tract of the lesion side and the symmetrical areas in the contralateral side served as the brain region of interest. We then converted the brain photographs into binary images using an appropriate threshold (Image J; National Institutes of Health, Bethesda, MD, United States), and calculated the percentages of the lesion to the intact side in each section, with the averages subsequently used for statistical analyses. We counted all the number of TH-positive dopaminergic neurons in three sections at 4.8, 5.3, and 5.8 mm posterior to the bregma in the SNc, but not in the ventral tegmental area. We then calculated the percentage of the lesioned side to the intact side, then using the averages for the statistical analyses. We also counted the number of Iba-1 positive cells with nuclei in the lesion side of the striatum and SNc using randomly selected fixed areas (500 μm × 500 μm square) from two different sections (0.5 and 1.0 mm anterior to the bregma), then used the averages used for statistical analyses. Additionally, we measured the area of laminin-positive structures as percentages relative to the area of the randomly captured images (500 μm × 500 μm square) from two different sections of the cortex (4 mm lateral to the midline and 0.5 and 1.0 mm anterior to the bregma) then also used the averages for statistical analyses.

Statistical Analyses

We used the software package SPSS 20.0 (SPSS, Chicago, IL, United States) to perform one-way analysis of variance (ANOVA) with subsequent Tukey's tests, with significance set at $p < 0.05$. Data showed here represented means ± standard deviation (SD).

RESULTS

Body Weight

Body weight decreased at day 7 and nearly recovered at day 14 in all groups (**Figure 4**). Body weights did not significantly differ on days 0, 7, and 14 between the control, 8-, and 24-h stimulation groups (body weight on days 0, 7, and 14: control group: 229.2 ± 13.7, 216.0 ± 13.8, and 229.5 ± 14.0 g; 8-h stimulation group: 228.8 ± 11.3, 214.5 ± 7.76, and 230.6 ± 8.01 g; and 24-h stimulation group: 230.9 ± 13.8, 214.4 ± 10.8, and 228.9 ± 14.9 g, respectively).

Behavioral Tests

Cylinder Test

The 24-h stimulation group performed significantly better in the cylinder test than the control group on days 7 and 14.

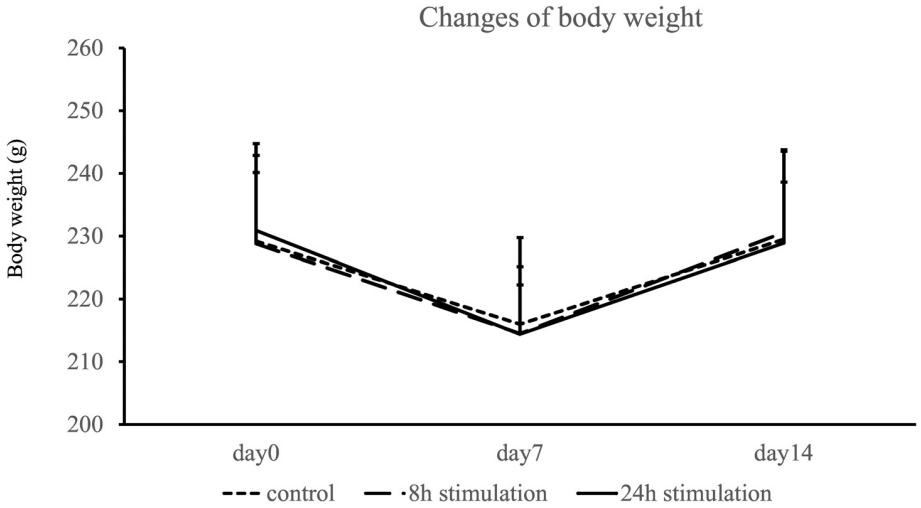

FIGURE 4 | Changes in body weight.

In the 8-h stimulation group, the treated animals displayed significant improvement in the contralateral bias on day 14 compared to the control group (contralateral bias: control group: 25.0 ± 10.1 and 47.6 ± 28.4%; 8-h stimulation group: 22.7 ± 14.7 and 23.3 ± 12.3%; 24-h stimulation group: 11.6 ± 9.56 and 9.80 ± 6.39% at 1 and 2 weeks, respectively; **Figure 5A**). For comparison, the contralateral bias before 6-OHDA lesion was 1.3 ± 0.8%.

Methamphetamine-Induced Rotation Test

The number of methamphetamine-induced rotations on days 7 and 14 in the 8- and 24-h stimulation groups statistically decreased compared to that of the control group (control group: 1292 ± 239 and 1518 ± 172 turns/90 min; 8-h stimulation group: 893 ± 217 and 1,020 ± 146 turns/90 min; 24-h stimulation group: 670 ± 244 and 820 ± 289 turns/90 min at 1 and 2 weeks, respectively; **Figure 5B**). The 8- and 24-h stimulation groups did not significantly differ in their rotational behaviors. For comparison, the rotational number before 6-OHDA lesion was 18 ± 10 turns/90 min.

Immunohistochemical Investigations

TH (Tyrosine Hydroxylase) Staining

The stimulation groups exhibited significant preservation of TH-positive fibers in the striatum and TH-positive neurons in the SNc compared to the control group (control group: 21.9 ± 7.16%; 8-h stimulation group: 45.3 ± 12.6%; 24-h stimulation group: 57.2 ± 9.11% relative to the intact side of TH-positive fibers in the striatum, **Figure 6**; control group: 25.9 ± 4.99%; 8-h stimulation group: 49.2 ± 9.24%; 24-h stimulation group: 57.9 ± 10.6% relative to the intact side of TH-positive neurons in the SNc, **Figure 7**). The 24-h stimulation group displayed significant preservation of TH-positive fibers in the striatum. Additionally, the 24-h stimulation group demonstrated more preserved TH-positive neurons in the SNc than the 8-h stimulation group.

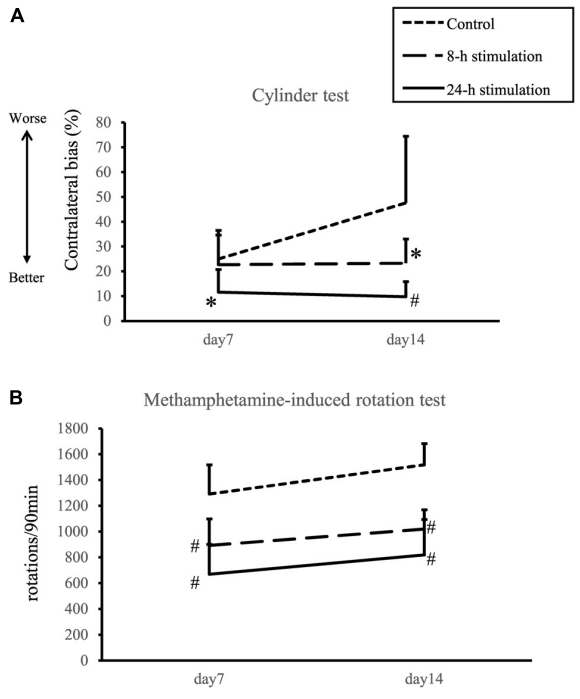

FIGURE 5 | Spinal cord stimulation and behavioral outcomes. **(A)** Contralateral bias in the cylinder test. In the 24-h stimulation group, improvement of contralateral bias was observed from days 7 to 14. In the 8-h stimulation group, improvement was observed on day 14 ($^{\#}p < 0.01$, $^{*}p < 0.05$). **(B)** Methamphetamine-induced rotations per 90 min. The number of methamphetamine-induced rotations significantly decreased in the 8- and 24-h stimulation groups compared to the control group ($^{\#}p < 0.01$).

Iba1 Staining

The number of Iba1-positive cells in the striatum and the SNc of rats in the 24-h stimulation group decreased significantly compared to the control group. In the 8-h stimulation group, the number of Iba1-positive cells tended to decrease in the striatum, and was significantly decreased in the SNc (control group: 37.9 ± 7.55; 8-h stimulation group: 31 ± 8.73; 24-h stimulation group: 23.5 ± 6.13 cells/field of view in the striatum; control group: 40.6 ± 6.26; 8-h stimulation group 32.4 ± 6.30; 24-h stimulation group 25.1 ± 5.62 cells/field of view in the SNc; **Figure 8**).

Laminin Staining

The laminin-positive area in the lesioned cortex significantly increased in the 8- and 24-h stimulation groups compared to the control group of the intact and lesion side (control group intact side: 4.59 ± 1.89%; control group lesion side: 6.23 ± 2.63%; 8-h stimulation group intact side: 7.90 ± 2.82%; 8-h stimulation group lesion side: 8.04 ± 3.19%; 24-h stimulation group intact side: 9.12 ± 2.58%; 24-h stimulation group lesion side: 10.8 ± 3.90%; **Figure 9**). Laminin-positive area in the striatum and the SNc were also explored, but there were no differences among all the groups (data not shown).

DISCUSSION

The present study demonstrated that a small mobile device efficiently delivered continuous SCS and exerted neuroprotective effects behaviorally and immunohistochemically on PD rats in a time-dependent manner. While both SCS-treated groups generally improved their performance in both contralateral bias and methamphetamine rotations, and displayed an increase in laminin-labeled cerebral blood vessels, The 24-h stimulation group conferred better therapeutic effects than the 8-h stimulation group, in that the longer continuous SCS regimen significantly reduced microglial cells both in the lesioned striatum and SNc compared to rats in the control group (**Supplementary Figure S1**).

Small Mobile Device for Continuous SCS

Until now, conventional SCS machines allow limited control of stimulation parameter and highly restrict the movements of animals. Current SCS machines consist of a large electrical stimulator and an electrode implanted in the animals with wire connections (Maesawa et al., 2004; Spieles-Engemann et al., 2010,

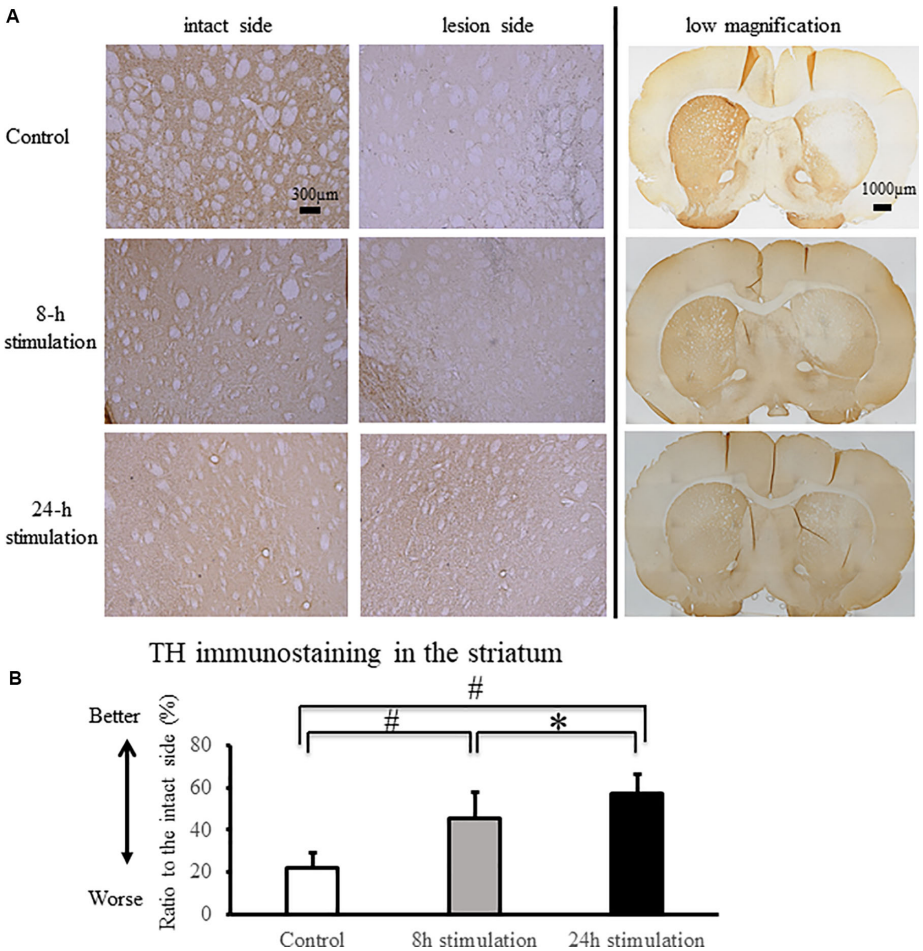

FIGURE 6 | Spinal cord stimulation and TH staining in the striatum. **(A)** TH-positive fibers were preserved in the striatum of the 8- and 24-h stimulation groups (10×). In the right column, the low magnified images are shown (2×). **(B)** The ratio of TH-positive fibers in the lesioned striatum to the intact side was significantly preserved in the stimulation groups compared to that in the control group ($^{\#}p < 0.01$). TH-positive fibers in the striatum of rats in the 24-h stimulation group were significantly preserved compared to those in the 8-h stimulation group ($^{*}p < 0.05$).

2011; Santana et al., 2014; Sato et al., 2014; Shinko et al., 2014; Brys et al., 2017). Long-term adhesion of the wire to the skin results in erosion or infection of the animals. Moreover, the routine use of general anesthesia when delivering fSCS (Shinko et al., 2014) restricts free movement of the animals. Additionally, the invasive nature of current SCS procedure likely alters experimental outcomes. Because of the large size of stimulator, hard-wired connections between stimulator and electrodes, use of anesthesia, and invasive procedure, the duration and timing of electrical stimulation remain limited with conventional SCS.

A small mobile electrical stimulator may circumvent the technical limitations of current SCS machines. Indeed, such mobile device shows efficacy as a DBS apparatus for PD animals (Badstübner et al., 2012; Badstuebner et al., 2017). In this study, we developed a small mobile device for continuous SCS. This system achieved minimal invasiveness, free movement with a wireless system, easily accessible adjustment of stimulation conditions, and robust and stable stimulation for at least 2 weeks in PD animals. Notably, Bluetooth signaling efficiently controlled stimulation parameters. The present study thus extended the utility of small mobile device originally employed in DBS to SCS, the latter being less invasive with the electrode epidurally implanted as opposed to the former that targets the deep regions of the brain (e.g., thalamus, subthalamic nucleus, and globus pallidus). We envision that a closed-loop stimulation device harboring a stimulation/receiving function will allow SCS to respond in real time and in a graded manner based on the individual's disease state. Such mobile SCS device will likely become available in the near future in view of technological developments in downsizing and wireless communication.

Prolonged SCS Improves Therapeutic Outcomes in PD Animals

Although neuroprotective effects of SCS have been documented in PD animals, the optimal electrical stimulation conditions remain unclear. Effective electrical stimulation parameters in PD rats vary in pulse width (400–1,000 μs), frequency (300–333 Hz), stimulation duration (30 min at 2 times/week for

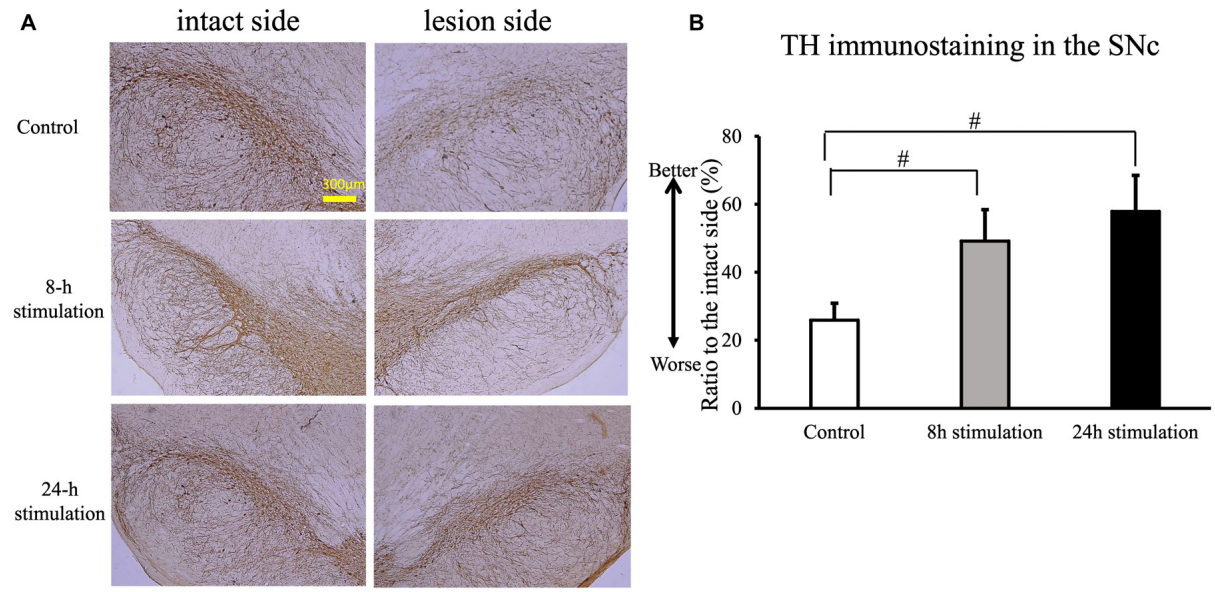

FIGURE 7 | Spinal cord stimulation and TH staining in the SNc. **(A)** TH-positive neurons in the SNc were preserved in the stimulation groups (10×). **(B)** TH-positive neurons in the SNc in the 8- and 24-h stimulation groups were significantly preserved compared to those in the control group ($^{\#}p < 0.01$).

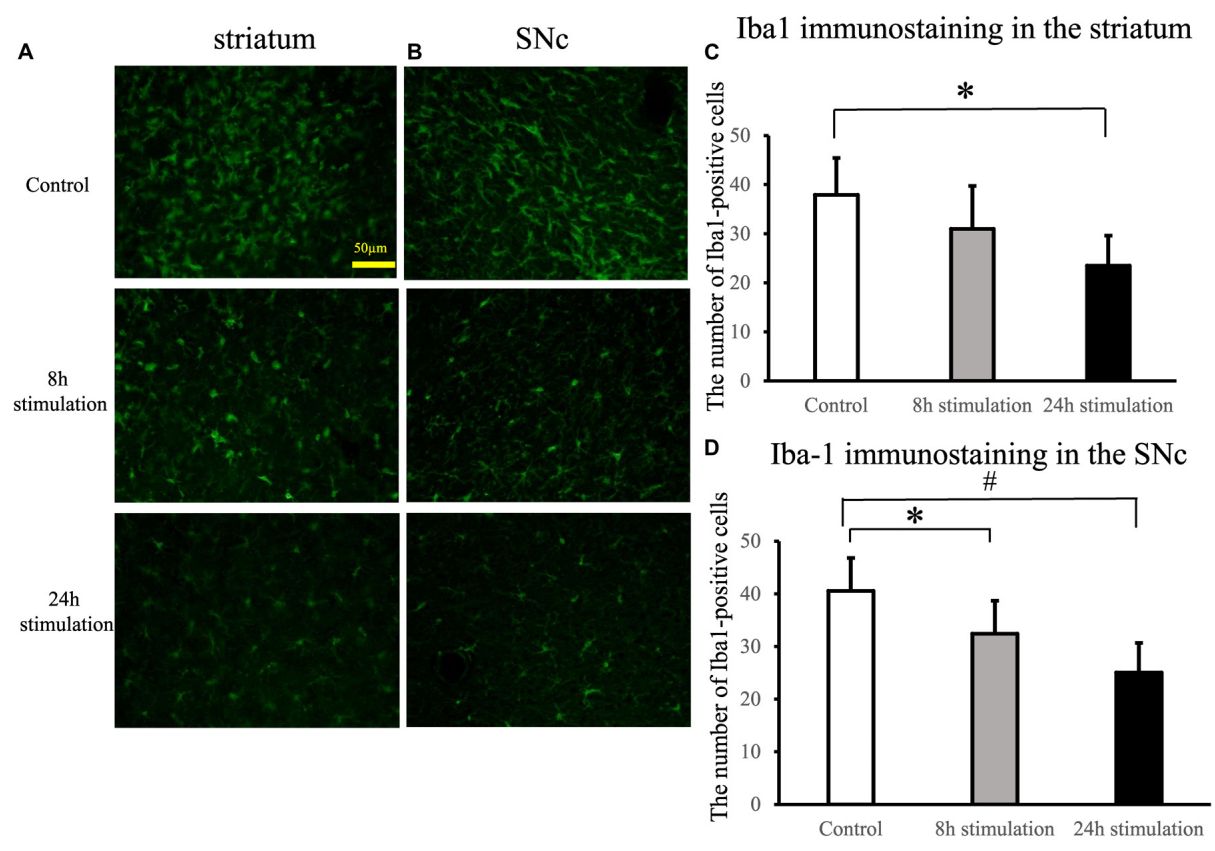

FIGURE 8 | Spinal cord stimulation and Iba1 staining in the striatum and SNc. **(A,B)** Iba1 staining in the striatum **(A)** and the SNc **(B)** of the lesion side (40×). **(C,D)** The number of Iba1-positive cells in the lesioned striatum **(C)** significantly decreased in the 24-h stimulation group compared to the control group ($^{*}p < 0.05$). Similarly, the number of Iba1-positive cells in the lesioned SNc **(D)** significantly decreased in the 24-h stimulation group compared to the control group ($^{\#}p < 0.01$, $^{*}p < 0.05$).

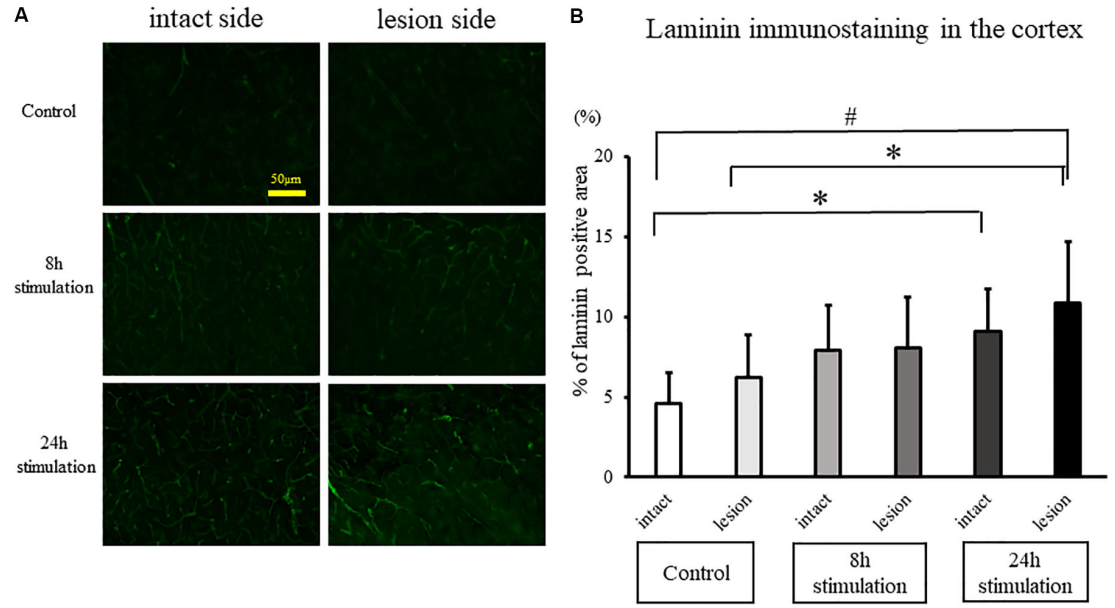

FIGURE 9 | Spinal cord stimulation and laminin staining in the cerebral cortex. **(A)** Laminin-positive areas in the cerebral cortex of rats in the stimulation groups were augmented compared to those in the control group (40×). **(B)** Laminin-positive cells in the cerebral cortex in the 24-h stimulation group were augmented compared to those in the control group ($^{\#}p < 0.01$, $^{*}p < 0.05$).

4.5 weeks – 30 min at once a week for 5 weeks) (Yadav et al., 2014; Brys et al., 2017). Previously we showed that the optimal conditions of "short burst" of SCS were as follows: pulse width, 100 μs; frequency, 2, 50, and 100 Hz; stimulation duration, 1 h for 16 consecutive days (Shinko et al., 2014). In the present study, we now tested the "continuous" SCS approach. Here, we confirmed that 50 Hz was the optimal frequency. To simulate the clinical settings and to reveal the time-dependency of SCS, we set stimulation duration at 8 and 24 h. Whereas behavioral amelioration, preservation of nigral TH-positive neurons, and level of angiogenesis did not differ between the 8- and 24-h stimulation groups, the longer SCS preserved more striatal TH-positive fibers and exerted better anti-inflammatory effects than the shorter SCS treatment. The dampened microglial cell activation produced by longer SCS treatment suggests that a progressive detrimental neuroinflammation may accompany PD requiring prolonged anti-inflammatory treatment to effectively sequester such cell death pathway.

Anti-inflammatory Effects of SCS

Parkinson's disease neurodegeneration manifests in part as a chronic neuroinflammation characterized by activated microglial cells in the striatum and SNc (Hirsch et al., 2012). Electrical stimulation may modulate neuroinflammation in that-DBS treatment in normal SD rats reduces the number of activated microglia around the electrode (Vedam-Mai et al., 2016). In tandem, SCS treatment also confers such anti-inflammation in an animal model of spinal cord ischemic reperfusion injury by reducing microglial activation through downregulation of the ERK1/2 pathway (Dong et al., 2018), a signaling pathway supported by pain studies (Morioka et al., 2013; Jiang et al., 2016; Liu et al., 2016; Huang et al., 2019; Zhong et al., 2019). In our study, SCS after intrastriatal 6-OHDA administration in the 24-h stimulation group decreased the number of microglia cells likely by exerting anti-inflammatory effects through the signaling pathways originating from the dorsal column-medial lemniscus then propagating to the SNc and striatum. Probing this anti-inflammatory signaling mechanism warrant electrophysiological experiments.

Enhanced Angiogenesis by SCS

Low-frequency cervical SCS increases cerebral blood flow (Isono et al., 1995; Zhong et al., 2004; Yang et al., 2008), which persists up to at least 15 min after discontinuation of SCS (Isono et al., 1995). However, there has been no report about the relationship between the vasculostructural changes of cerebral blood vessels and SCS. In the present study, SCS increased the laminin-positive areas in the cerebral cortex of the lesion side compared to the control group. These results resemble the observation that intrastriatal transplantation of encapsulated VEGF-secreting cells in PD rats enhances angiogenesis (Yasuhara et al., 2004). Moreover, these findings parallel the upregulation of VEGF in the lesioned striatum of PD rats that received intermittent SCS (1 h/day for 7 consecutive days) (Shinko et al., 2014). That SCS modulates specific vasculature-associated growth factors suggests a crosstalk between electrical stimulation and growth factor secretion (Bagetta et al., 2011; Escamilla-Sevilla et al., 2011; Seifried et al., 2013; Maioli et al., 2015; Muñoz et al., 2016), which may mediate the observed increase in laminin-positive vascular area in the cerebral cortex of SCS-treated PD rats.

Clinical Application of SCS for PD in the Future

Neuroinflammation in PD pathogenesis may involve multi-pronged neurodegenerative processes, such as inflammation and downregulation of neurotrophic factors (Yasuhara et al., 2004; Shinko et al., 2014; Chen et al., 2018; Kim et al., 2018; Troncoso-Escudero et al., 2018). This neurodegeneration plagued with aberrant inflammation and dampened neurotrophic factor levels manifests as a key secondary cell death pathway in other neurological disorders, such as stroke, traumatic brain injury, Huntington's disease, and peripheral nerve injury (Borlongan et al., 2000; Xia et al., 2004; Emerich et al., 2006; Shojo et al., 2010; Rodrigues et al., 2012), which equally poses as a potent therapeutic target. Probing the potential of SCS to abrogate these cell death pathways may provide novel insights into the mechanism of electrical stimulation and further optimize its therapeutic outcomes.

Deep brain stimulation stands as an effective treatment for motor symptoms in advanced PD patients. SCS offers a less invasive approach compared to DBS in that the procedure spares the brain from surgical manipulations. Such minimally invasive SCS may be equally effective as DBS in reducing the hallmark PD motor deficits. Indeed, SCS alleviates motor deficits in PD marmosets (Santana et al., 2014). However, a case report shows that SCS fails to relieve akinesia or restore locomotion in two PD patients (Thevathasan et al., 2010). Optimization of SCS, including the use of continuous stimulation produced by a small mobile stimulator, may improve the clinical benefits of this minimally invasive electrical stimulation.

Study Limitations

In this study, we used PD model of rats induced by 6-OHDA. The main advantages of this model include the ease of creating the lesion that produces loss of dopaminergic fibers in the striatum and of dopaminergic neurons in the substantia nigra. One of the disadvantages of this model is that it does not resemble the natural pathology of PD, which is slow progression of the degeneration of nigrostriatal dopaminergic neurons with degradation of α-synuclein. Therapeutic potentials of the SCS should be explored with other PD models of neurodegeneration and α-synucleinopathy reminiscent of the clinical scenario.

The aim of this study was to explore the neuroprotective effects of the SCS with duration of treatment as a factor. Here, treatment was started immediately after 6-OHDA lesion induction, which may not be applicable in the clinical setting since PD symptoms do no manifest when at least 80% of the dopaminergic neurons have already been depleted. Testing SCS in a late-stage PD model is warranted. Another limitation is that elucidating the therapeutic mechanism of SCS will require additional studies. In our study, the neuroprotective effects with angiogenic potentials were shown, but whether the neuroprotective effects of SCS during the pre-symptomatic phase is sustained during the symptomatic stage warrants further examination. In the future, behavioral changes over time after discontinuation of the SCS may reveal long-lasting effects of SCS, as well as its mechanism of actions, on PD symptoms.

CONCLUSION

We demonstrated that a small mobile stimulator afforded continuous SCS and exerted neuroprotective effects in PD rats in a time-dependent manner. SCS attenuated behavioral and histological deficits associated with 6-OHDA-induced PD symptoms, possibly by mitigating microglial activation while enhancing angiogenesis. The newly developed device for continuous SCS serves as a useful tool for basic research in our understanding of interplay across electrical stimulation, neurodegeneration, and neural repair, but also advances its utility as a therapeutic modality for PD.

DATA AVAILABILITY STATEMENT

The raw data supporting the conclusions of this article will be made available by the authors, without undue reservation, to any qualified researcher.

ETHICS STATEMENT

The animal study was reviewed and approved by Institutional Animal Care and Use Committee of Okayama University Graduate School of Medicine (Protocol# OKU-2018807).

AUTHOR CONTRIBUTIONS

KeK and TS contributed conception and design of the study. KeK, TY, YO, KH, IK, MO, SY, SK, YT, and MU performed the experiments. KeK and JM collected the data. KyK and NT performed the statistical analysis. KeK wrote the first draft of the manuscript. KyK, TS, TY, and J-YL wrote sections of the manuscript. CB performed the critical editing. ID supervised the study. All authors contributed to manuscript revision, read and approved the submitted version.

FUNDING

This research was supported by scientific research grants from the Ministry of Health, Labor, and Welfare of Japan (09156274 and 24592129). All data collection, analysis, writing, and submission decisions were made by the authors of this manuscript, not by funding sources.

SUPPLEMENTARY MATERIAL

The Supplementary Material for this article can be found online at: https://www.frontiersin.org/articles/10.3389/fnagi.2020.00164/full#supplementary-material

FIGURE S1 | The graphic abstract showing therapeutic effects of SCS against 6-OHDA-induced PD model of rats through angiogenesis and anti-inflammation.

VIDEO S1 | The video showing twitching rats with SCS. The intensities corresponded to the 80% of motor threshold were used for each rat.

REFERENCES

Agari, T., and Date, I. (2012). Spinal cord stimulation for the treatment of abnormal posture and gait disorder in patients with Parkinson's disease. *Neurol. Med. Chirurg.* 52, 470–474. doi: 10.2176/nmc.52.470

Badstübner, K., Kröger, T., Mix, E., Gimsa, U., Benecke, R., and Gimsa, J. (2012). "Electrical impedance properties of deep brain stimulation electrodes during long-term in-vivo stimulation in the Parkinson model of the rat," in *Biomedical Engineering Systems and Technologies, BIOSTEC*, Vol. 357, eds J. Gabriel, J. Schier, S. Van Huffel, E. Conchon, C. Correia, A. Fred, et al. (Berlin: Springer), 287–297. doi: 10.1007/978-3-642-38256-7_19

Badstuebner, K., Gimsa, U., Weber, I., Tuchscherer, A., and Gimsa, J. (2017). Deep brain stimulation of hemiparkinsonian rats with unipolar and bipolar electrodes for up to 6 weeks: behavioral testing of freely moving animals. *Parkinsons Dis.* 2017:5693589. doi: 10.1155/2017/5693589

Bagetta, V., Picconi, B., Marinucci, S., Sgobio, C., Pendolino, V., Ghiglieri, V., et al. (2011). Dopamine-dependent long-term depression is expressed in striatal spiny neurons of both direct and indirect pathways: implications for Parkinson's disease. *J. Neurosci.* 31, 12513–12522. doi: 10.1523/JNEUROSCI.2236-11.2011

Borlongan, C. V., Su, T. P., and Wang, Y. (2000). Treatment with delta opioid peptide enhances in vitro and in vivo survival of rat dopaminergic neurons. *Neuroreport* 11, 923–926. doi: 10.1097/00001756-200004070-00005

Boulet, S., Lacombe, E., Carcenac, C., Feuerstein, C., Sgambato-Faure, V., Poupard, A., et al. (2006). Subthalamic stimulation-induced forelimb dyskinesias are linked to an increase in glutamate levels in the substantia nigra pars reticulata. *J. Neurosci.* 26, 10768–10776. doi: 10.1523/JNEUROSCI.3065-06.2006

Brys, I., Bobela, W., Schneider, B. L., Aebischer, P., and Fuentes, R. (2017). Spinal cord stimulation improves forelimb use in an alpha-synuclein animal model of Parkinson's disease. *Int. J. Neurosci.* 127, 28–36. doi: 10.3109/00207454.2016.1138296

Chen, X., Hu, Y., Cao, Z., Liu, Q., and Cheng, Y. (2018). Cerebrospinal fluid inflammatory cytokine aberrations in Alzheimer's disease, Parkinson's disease and amyotrophic lateral sclerosis: a systematic review and meta-analysis. *Front. Immunol.* 19:2122. doi: 10.3389/fimmu.2018.02122

Dong, X., Li, H., Lu, J., Jing, H., Cheng, Y., Jin, M., et al. (2018). Spinal cord stimulation postconditioning reduces microglial activation through down-regulation of ERK1/2 pathway phosphorylation during spinal cord ischemic reperfusion in rabbits. *NeuroReport* 29, 1180–1187. doi: 10.1097/WNR.0000000000001093

Emerich, D. F., Thanos, C. G., Goddard, M., Skinner, S. J., Geany, M. S., Bell, W. J., et al. (2006). Extensive neuroprotection by choroid plexus transplants in excitotoxin lesioned monkeys. *Neurobiol. Dis.* 23, 471–480. doi: 10.1016/j.nbd.2006.04.014

Escamilla-Sevilla, F., Pérez-Navarro, M. J., Muñoz-Pasadas, M., Sáez-Zea, C., Jouma-Katati, M., Piédrola-Maroto, G., et al. (2011). Change of the melanocortin system caused by bilateral subthalamic nucleus stimulation in Parkinson's disease. *Acta Neurol. Scand.* 124, 275–281. doi: 10.1111/j.1600-0404.2010.01469.x

Fenoy, A. J., and Simpson, R. K. Jr. (2014). Risks of common complications in deep brain stimulation surgery: management and avoidance. *J. Neurosurg.* 120, 132–139. doi: 10.3171/2013.10.JNS131225

Fuentes, R., Petersson, P., Siesser, W. B., Caron, M. G., and Nicolelis, M. A. (2009). Spinal cord stimulation restores locomotion in animal models of Parkinson's disease. *Science* 323, 1578–1582. doi: 10.1126/science.1164901

Herzog, J., Volkmann, J., Krack, P., Kopper, F., Potter, M., Lorenz, D., et al. (2003). Two-year follow-up of subthalamic deep brain stimulation in Parkinson's disease. *Mov. Disord.* 18, 1332–1337. doi: 10.1002/mds.10518

Hirsch, E. C., Vyas, S., and Hunot, S. (2012). Neuroinflammation in Parkinson's disease. *Park. Relat. Disord.* 18, S210–S212. doi: 10.1016/S1353-8020(11)70065-7

Huang, H., Wang, M., and Hong, Y. (2019). Intrathecal administration of adrenomedullin induces mechanical allodynia and neurochemical changes in spinal cord and DRG. *Neurosci. Lett.* 18, 196–201. doi: 10.1016/j.neulet.2018.10.037

Huotarinen, A., Penttinen, A. M., Back, S., Voutilainen, M. H., Julku, U., Piepponen, T. P., et al. (2018). Combination of CDNF and deep brain stimulation decreases neurological deficits in late-stage model Parkinson's disease. *Neuroscience* 374, 250–263. doi: 10.1016/j.neuroscience.2018.01.052

Isono, M., Kaga, A., Fujiki, M., Mori, T., and Hori, S. (1995). Effect of spinal cord stimulation on cerebral blood flow in cats. *Stereotact. Funct. Neurosurg.* 64, 40–46. doi: 10.1159/000098732

Jiang, B. C., Cao, D. L., Zhang, X., Zhang, Z. J., He, L. N., Li, C. H., et al. (2016). CXCL13 drives spinal astrocyte activation and neuropathic pain via CXCR5. *J. Clin. Invest.* 126, 745–761. doi: 10.1172/JCI81950

Kim, H. W., Lee, H. S., Kang, J. M., Bae, S. H., Kim, C., Lee, S. H., et al. (2018). Dual effects of human placenta-derived neural cells on neuroprotection and the inhibition of neuroinflammation in a rodent model of Parkinson's disease. *Cell Transplant.* 27, 814–830. doi: 10.1177/0963689718766324

Levy, R., Henderson, J., Slavin, K., Simpson, B. A., Barolat, G., Shipley, J., et al. (2011). Incidence and avoidance of neurologic complications with paddle type spinal cord stimulation leads. *Neuromodulation* 14, 412–422; discussion 422. doi: 10.1111/j.1525-1403.2011.00395.x

Liu, C. C., Gao, Y. J., Luo, H., Berta, T., Xu, Z. Z., Ji, R. R., et al. (2016). Interferon alpha inhibits spinal cord synaptic and nociceptive transmission via neuronal-glial interactions. *Sci. Rep.* 27:34356. doi: 10.1038/srep34356

Maesawa, S., Kaneoka, Y., Kajita, Y., Usui, N., Misawa, N., Nakayama, A., et al. (2004). Long-term stimulation of the subthalamic nucleus in hemiparkinsonian rats: neuroprotection of dopaminergic neurons. *J. Neurosurg.* 100, 679–687. doi: 10.3171/jns.2004.100.4.0679

Maioli, M., Rinaldi, S., Migheli, R., Pigliaru, G., Rocchitta, G., Santaniello, S., et al. (2015). Neurological morphofunctional differentiation induced by REAC technology in PC12. A neuro protective model for Parkinson's disease. *Sci. Rep.* 15:10439. doi: 10.1038/srep10439

Morioka, N., Tokuhara, M., Harano, S., Nakamura, Y., Hisaoka-Nakashima, K., and Nakata, Y. (2013). The activation of P2Y6 receptor in cultured spinal microglia induces the production of CCL2 through the MAP kinases-NF-κB pathway. *Neuropharmacology* 75, 116–125. doi: 10.1016/j.neuropharm.2013.07.017

Muñoz, M. D., Antolín-Vallespín, M., Tapia-González, S., and Sánchez-Capelo, A. (2016). Smad3 deficiency inhibits dentate gyrus LTP by enhancing GABAA neurotransmission. *J. Neurochem.* 137, 190–199. doi: 10.1111/jnc.13558

Obeso, J. A., Olanow, C. W., Rodriguez-Oroz, M. C., Krack, P., Kumar, R., and Lang, A. E. (2001). Deep-brain stimulation of the subthalamic nucleus or the pars interna of the globus pallidus in Parkinson's disease. *N. Engl. J. Med.* 345, 956–963. doi: 10.1056/NEJMoa000827

Rodrigues, M. C., Rodrigues, A. A. Jr., Glover, L. E., Voltarelli, J., and Borlongan, C. V. (2012). Peripheral nerve repair with cultured schwann cells: getting closer to the clinics. *ScientificWorldJournal* 2012:413091. doi: 10.1100/2012/413091

Roof, R. L., Schielke, G. P., Ren, X., and Hall, E. D. (2001). A comparison of long-term functional outcome after 2 middle cerebral artery occlusion models in rats. *Stroke* 32, 2648–2657. doi: 10.1161/hs1101.097397

Sansur, C. A., Frysinger, R. C., Pouratian, N., Fu, K. M., Bittl, M., Oskouian, R. J., et al. (2007). Incidence of symptomatic hemorrhage after stereotactic electrode placement. *J. Neurosurg.* 107, 998–1003. doi: 10.3171/JNS-07/11/0998

Santana, M. B., Halje, P., Simplicio, H., Richter, U., Freire, M. A. M., Petersson, P., et al. (2014). Spinal cord stimulation alleviates motor deficits in a primate model of Parkinson disease. *Neuron* 84, 716–722. doi: 10.1016/j.neuron.2014.08.061

Sasaki, T., Liu, K., Agari, T., Yasuhara, T., Morimoto, J., Okazaki, M., et al. (2016). Anti-high mobility group box 1 antibody exerts neuroprotection in a rat model of Parkinson's disease. *Exp. Neurol.* 275(Pt 1), 220–231. doi: 10.1016/j.expneurol.2015.11.003

Sato, K. L., Johanek, L. M., Sanada, L. S., and Sluka, K. A. (2014). Spinal cord stimulation reduces mechanical hyperalgesia and glial cell activation in animals with neuropathic pain. *Anesth. Analg.* 118, 464–472. doi: 10.1213/ANE.0000000000000047

Schallert, T., Fleming, S. M., Leasure, J. L., Tillerson, J. L., and Bland, S. T. (2000). CNS plasticity and assessment of forelimb sensorimotor outcome in unilateral rat models of stroke, cortical ablation, parkinsonism and spinal cord injury. *Neuropharmacology* 39, 777–787. doi: 10.1016/s0028-3908(00)00005-8

Seifried, C., Boehncke, S., Heinzmann, J., Baudrexel, S., Weise, L., Gasser, T., et al. (2013). Diurnal variation of hypothalamic function and chronic subthalamic nucleus stimulation in Parkinson's disease. *Neuroendocrinology* 97, 283–290. doi: 10.1159/000343808

Shinko, A., Agari, T., Kameda, M., Yasuhara, T., Kondo, A., Tayra, J. T., et al. (2014). Spinal cord stimulation exerts neuroprotective effects against experimental Parkinson's disease. *PLoS One* 9:e101468. doi: 10.1371/journal.pone.0101468

Shojo, H., Kaneko, Y., Mabuchi, T., Kibayashi, K., Adachi, N., and Borlongan, C. V. (2010). Genetic and histologic evidence implicates role of inflammation in traumatic brain injury-induced apoptosis in the rat cerebral cortex following moderate fluid percussion injury. *Neuroscience* 171, 1273–1282. doi: 10.1016/j.neuroscience.2010.10.018

Spieles-Engemann, A. L., Behbehani, M. M., Collier, T. J., Wohlgenant, S. L., Steece-Collier, K., Paumier, K., et al. (2010). Stimulation of the rat subthalamic nucleus is neuroprotective following significant nigral dopamine neuron loss. *Neurobiol. Dis.* 39, 105–115. doi: 10.1016/j.nbd.2010.03.009

Spieles-Engemann, A. L., Steece-Collier, K., Behbehani, M. M. J., Collier, T., Wohlgenant, S. L., Kemp, C. J., et al. (2011). Subthalamic nucleus stimulation increases brain-derived neurotrophic factor in the nigrostriatal system and primary motor cortex. *J. Parkinsons Dis.* 1, 123–136. doi: 10.3233/JPD-2011-11008

Thevathasan, W. M. P., Mazzone, P., Jha, A., Djamshidian, A., Dileone, M., Di Lazzaro, V., et al. (2010). Spinal cord stimulation failed to relieve akinesia or restore locomotion in Parkinson disease. *Neurolgy* 74, 1325–1327. doi: 10.1212/WNL.0b013e3181d9ed58

Troncoso-Escudero, P., Parra, A., Nassif, M., and Vidal, R. L. (2018). Outside in: unraveling the role of neuroinflammation in the progression of Parkinson's disease. *Front. Neurol.* 15:860. doi: 10.3389/fneur.2018.00860

Vedam-Mai, V., Baradaran-Shoraka, M., Reynolds, B. A., and Okun, M. S. (2016). Tissue response to deep brain stimulation and microlesion: a comparative study. *Neuromodulation* 19, 451–458. doi: 10.1111/ner.12406

Weaver, F. M., Follett, K., Stern, M., Hur, K., Harris, C., Marks, W. J., et al. (2009). Bilateral deep brain stimulation vs best medical therapy for patients with advanced Parkinson disease: a randomized controlled trial. *JAMA* 301, 63–73. doi: 10.1001/jama.2008.929

Xia, C. F., Yin, H., Borlongan, C. V., Chao, J., and Chao, L. (2004). Adrenomedullin gene delivery protects against cerebral ischemic injury by promoting astrocyte migration and survival. *Hum. Gene Ther.* 15, 1243–1254. doi: 10.1089/hum.2004.15.1243

Yadav, A. P., Fuentes, R., Zhang, H., Vinholo, T., Wang, C. H., Freire, M. A., et al. (2014). Chronic spinal cord electrical stimulation protects against 6-hydroxydopamine lesions. *Sci. Rep.* 4:3839. doi: 10.1038/srep03839

Yang, X., Farber, J. P., Wu, M., Foreman, R. D., and Qin, C. (2008). Roles of dorsal column pathway and TRPV1 in augmentation of cerebral blood flow by upper cervical spinal cord stimulation in rats. *Neuroscience* 152, 950–958. doi: 10.1016/j.neuroscience.2008.01.009

Yasuhara, T., Shingo, T., Kobayashi, K., Takeuchi, A., Yano, A., Muraoka, K., et al. (2004). Neuroprotective effects of vascular endothelial growth factor (VEGF) upon dopaminergic neurons in a rat model of Parkinson's disease. *Eur. J. Neurosci.* 19, 1494–1504. doi: 10.1111/j.1460-9568.2004.03254.x

Zhong, J., Huang, D. L., and Sagher, O. (2004). Parameters influencing augmentation of cerebral blood flow by cervical spinal cord stimulation. *Acta Neurochir.* 146, 1227–1234. doi: 10.1007/s00701-004-0364-7

Zhong, Y., Chen, J., Chen, J., Chen, Y., Li, L., and Xie, Y. (2019). Crosstalk between Cdk5/p35 and ERK1/2 signalling mediates spinal astrocyte activity via the PPARγ pathway in a rat model of chronic constriction injury. *J. Neurochem.* 151, 166–184. doi: 10.1111/jnc.14827

Conflict of Interest: The authors declare that the research was conducted in the absence of any commercial or financial relationships that could be construed as a potential conflict of interest.

frontiers in Aging Neuroscience

ORIGINAL RESEARCH
published: 04 August 2020
doi: 10.3389/fnagi.2020.00240

Estradiol Replacement at the Critical Period Protects Hippocampal Neural Stem Cells to Improve Cognition in APP/PS1 Mice

Yaoyao Qin[1], Dong An[1], Weixing Xu[1], Xiuting Qi[1], Xiaoli Wang[1], Ling Chen[1,2], Lei Chen[1] and Sha Sha[1,2]**

[1]*Department of Physiology, Nanjing Medical University, Nanjing, China,* [2]*State Key Lab of Reproductive Medicine, Nanjing Medical University, Nanjing, China*

It has been suggested that there is a critical window for estrogen replacement therapy (ERT) in postmenopausal women with Alzheimer's disease (AD); however, supporting evidence is lacking. To address this issue, we investigated the effective period for estradiol (E2) treatment using a mouse model of AD. Four-month-old female APPswe/PSEN1dE9 (APP/PS1) mice were ovariectomized (OVX) and treated with E2 for 2 months starting at the age of 4 months (early period), 6 months (mid-period), or 8 months (late period). We then evaluated hippocampal neurogenesis, β-amyloid (Aβ) accumulation, telomerase activity, and hippocampal-dependent behavior. Compared to age-matched wild type mice, APP/PS1 mice with intact ovaries showed increased proliferation of hippocampal neural stem cells (NSCs) at 8 months of age and decreased proliferation of NSCs at 10 months of age; meanwhile, Aβ accumulation progressively increased with age, paralleling the reduced survival of immature neurons. OVX-induced depletion of E2 in APP/PS1 mice resulted in elevated Aβ levels accompanied by elevated p75 neurotrophin receptor ($p75^{NTR}$) expression and increased NSC proliferation at 6 months of age, which subsequently declined; accelerated reduction of immature neurons starting from 6 months of age, and reduced telomerase activity and worsened memory performance at 10 months of age. Treatment with E2 in the early period post-OVX, rather than in the mid or late period, abrogated these effects, and $p75^{NTR}$ inhibition reduced the overproliferation of NSCs in 6-month-old OVX-APP/PS1 mice. Thus, E2 deficiency in young APP/PS1 mice exacerbates cognitive deficits and depletes the hippocampal NSC pool in later life; this can be alleviated by E2 treatment in the early period following OVX, which prevents Aβ/$p75^{NTR}$-induced NSC overproliferation and preserves telomerase activity.

Keywords: Alzheimer's disease (AD), β-amyloid (Aβ), estradiol (E2), hippocampus, neurogenesis

OPEN ACCESS

Edited by:
Cesar V. Borlongan, University of South Florida, United States

Reviewed by:
Tiantian Zhang, Ocean University of China, China
David J. Koss, Newcastle University, United Kingdom

****Correspondence:***
Sha Sha
shashass@njmu.edu.cn
Lei Chen
chenl@njmu.edu.cn

Received: *22 May 2020*
Accepted: *10 July 2020*
Published: *04 August 2020*

Citation:
Qin Y, An D, Xu W, Qi X, Wang X, Chen L, Chen L and Sha S (2020) Estradiol Replacement at the Critical Period Protects Hippocampal Neural Stem Cells to Improve Cognition in APP/PS1 Mice. Front. Aging Neurosci. 12:240. doi: 10.3389/fnagi.2020.00240

INTRODUCTION

The risk for Alzheimer's disease (AD) is associated with age-related loss of ovarian hormones in women (Marongiu, 2019). Prospective and case-control studies have demonstrated that estrogen replacement therapy (ERT) can effectively reduce cognitive deficits in some but not all postmenopausal women (Espeland et al., 2004; Vedder et al., 2014). Growing evidence suggests that the effectiveness of ERT depends on its application during a critical period and a specific treatment duration (Espeland et al., 2004; Zandi et al., 2002). Experiments in aged nonhuman primates and rodents have revealed that 17β-estradiol (E2) treatment following ovariectomy can improve cognitive function (Baxter et al., 2018; Pollard et al., 2018) and alleviate cognitive decline in aged animals with long-term E2 deficiency (Luine, 2014). This critical treatment window may be related to changes in brain responsiveness to E2.

The generation and progression of β-amyloid (Aβ) accumulation in the brain is a pathologic hallmark of AD (Benilova et al., 2012). Many experiments have demonstrated the ability of Aβ to cause synaptic dysfunction and mature neuron death (He et al., 2019; Xu et al., 2012). Neurogenesis in the adult hippocampus involves the proliferation of NSCs and their terminal differentiation into neurons, which is important for preserving cognitive function (Ager et al., 2015). Improving hippocampal neurogenesis can ameliorate cognition in mouse models of AD (Xu et al., 2012), which exhibit a pathologic Aβ plaque burden accompanied by decreased hippocampal neurogenesis and impaired hippocampal-dependent spatial memory (Moon et al., 2014). A previous study has reported that Aβ impairs the proliferation of NSCs in the adult subventricular zone *via* $p75^{NTR}$ (Sotthibundhu et al., 2009). Also, both *in vitro* and *in vivo* experiments have proven that the aggregated form of Aβ can inhibit telomerase activity (Wang et al., 2015), which has been proposed to preserve stem cell function by the promotion of resting stem cell proliferation and maintaining in telomere length (Boccardi and Paolisso, 2014). Postmenopausal women who received long-term estrogen therapy had longer telomeres than those who did not receive this therapy (Lee et al., 2005). There is increasing evidence that E2 can alter hippocampal structure and function (Frick et al., 2015), with long-term administration of E2 at physiologic doses reducing Aβ accumulation in 3xTg-AD mice (Carroll et al., 2007).

To explore the effective time window of E2 treatment for alleviating AD-associated cognitive impairment and the hippocampal mechanisms, we used female transgenic mice carrying mutant human *APPswe* and *PS1dE9* genes (APP/PS1 mice), in which the production of Aβ appears at approximately 4–5 months of age and dramatically accelerates during 6–8 months of age (Garcia-Alloza et al., 2006). In this study, 4-month-old female APP/PS1 mice were ovariectomized (OVX) to induce an acute decline in E2(surgical menopause), and then we evaluated the effects of E2 administered at different time points postsurgery on hippocampal neurogenesis, Aβ accumulation, and the causal link between the neuroprotective effect of E2 and its hippocampal-dependent memory performance.

MATERIALS AND METHODS

Animals

APP/PS1 transgenic mice (Stock No. 34829) with a C57BL/6J × C3H hybrid background (Stock No. 004462) were obtained from Jackson Laboratory (Bar Harbor, ME, USA). APP/PS1 mice were maintained by crossing the hemizygotes with noncarrier siblings [later referred to as wild-type (WT) mice], and genotyped by polymerase chain reaction (PCR) analysis of genomic DNA from tail biopsies according to the instructions and our previous publication (Xu et al., 2012). Female hemizygous APP/PS1 mice aged 4–10 months and their WT littermates were used in this study. The present study was approved by the Institutional Animal Care and Ethical Committee of Nanjing Medical University (No. 2014-153), and conducted in accordance with the guidelines of the Institute for Laboratory Animal Research of the Nanjing Medical University. Mice were housed in plastic cages at 23 ± 2°C and 55% relative humidity with a 12:12 h light/dark cycle. Water and food were given *ad libitum*. Body weight was measured weekly.

Ovariectomy and Drug Administration

Ovariectomy

All surgeries were performed under ketamine (100 mg/kg)/xylazine (10 mg/kg; i.p.) anesthesia using aseptic conditions following institutional guidelines. Female mice in diestrus were bilaterally ovariectomized (OVX) at the age of 4 months (**Figure 1**). The dorsal surface was shaved and the vascular supply was ligated, then ovaries dissected out through bilateral incisions. Sham-operated (sham-op) control mice were subjected to surgery and ovaries were manipulated but left intact.

E2 Treatment

A pellet containing 0.18 mg of E2 (Innovative Research of America, Sarasota, FL, USA) was subcutaneously implanted

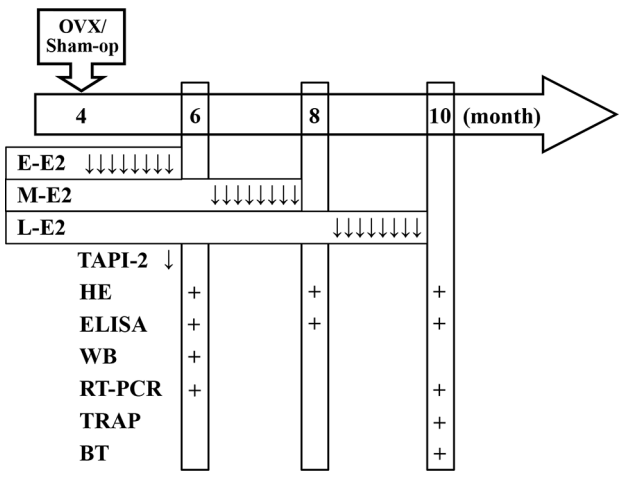

FIGURE 1 | Time chart of the experimental procedure. Horizontal arrow indicates the mouse age (month). ↓, E2/TAPI-2 administration; +, time point of experiment examination; E-E2, early period; M-E2, mid period; L-E2, late period; HE, histological examination; WB, western blotting; BT, behavioral tests.

at the following three time points: immediately after OVX, 2 months after OVX (6-month-old), or 4 months after OVX (8-month-old). The pellet continuously releases E2 for 60 days, resulting in serum levels of estrogen in the physiological range (Carroll et al., 2007). At the end of each period of E2 treatment, specimens were collected or behavioral tests were carried out (see time chart of the experimental procedure in **Figure 1**).

TAPI-2 Treatment

The $p75^{NTR}$ metalloprotease inhibitor TAPI-2 (Sigma–Aldrich, St. Louis, MO, USA) was intracerebroventricular injected by the osmotic pump infusion 4 days before 5-bromo-2′-deoxyuridine (BrdU) injection (**Figure 1**). The mouse was placed in the stereotaxic instrument (Stoelting, Wood Dale, IL, USA), and a 7-day Alzet osmotic minipump (mean flow rate, 0.25 μl/h) containing TAPI-2 (50 mmol/l; Katakowski et al., 2007) or sterile saline was placed subcutaneously in the back. A brain infusion cannula connected to the pump that was positioned at right lateral ventricle (0.3 mm posterior, 1.0 mm lateral, and 2.3 mm ventral to Bregma).

Histological Examination and Quantitative Evaluation

The mice were injected (i.p.) with BrdU (50 mg/kg; Sigma–Aldrich) twice daily at 6 h intervals for three consecutive days as previously described (Taniuchi et al., 2007). At 24 h after the last BrdU injection, the mice were anesthetized and perfused transcardially with cold phosphate-buffered saline (PBS) followed by 4% paraformaldehyde (PFA). Brains were post-fixed overnight in 4% PFA at 4°C and coronal section (40 μm) were cut using a vibrating microtome (Microslicer DTK 1500, Dousaka EM Company, Kyoto, Japan).

BrdU, Ki67 and Doublecortin (DCX) Immunostaining

Every 5th free-floating section (200 μm apart) was treated with 2 M HCl for 30 min and then with 3% hydrogen peroxide for 10 min at room temperature. The sections were incubated with PBS containing 0.3% Triton X-100 and 3% normal goat serum for 45 min, followed by overnight incubation at 4°C with mouse monoclonal anti-BrdU antibody (1:1,000; Millipore, Billerica, MA, USA) or mouse monoclonal anti-DCX antibody (1:500; Santa Cruz, CA, USA). After several PBS rinses, the sections were incubated in biotin-labeled goat anti-mouse IgG antibody (1:500; Santa Cruz) under agitation. Immunoreactivities were visualized based on avidin-biotin horseradish peroxidase complex (ABC Elite; Vector Laboratories, Inc., Burlingame, CA, USA) using 3,3′-diaminobenzidine (DAB; Vector Laboratories). For Ki67 immunostaining, the sections were incubated with rabbit monoclonal anti-Ki67 antibody (1:500; Abcam, Cambridge, UK) followed by Cy3-conjugated goat anti-rabbit IgG antibody (1:200, Jackson ImmunoResearch Laboratories, PA, USA).

Quantitative Evaluation of Immuno-Positive Cells

Immuno-positive BrdU ($BrdU^+$) and DCX (DCX^+) cells were assessed using a conventional light microscope (Olympus DP70, Japan) with a 40× objective. Images of Ki67-immunolabeled sections were observed using a fluorescence microscope (Olympus DP70, ×100). The total number of $BrdU^+$ cells or $Ki67^+$ cells was calculated from 12 sections and multiplied by 5 to obtain a total number for each mouse. The number of DCX^+ cells in the subgranular zone (SGZ) was counted and divided by the length of SGZ to obtain the density of DCX^+ cells (per micrometer; Sha et al., 2016).

Aβ Immunochemistry and Plaque Counting

The blocked sections were incubated in rabbit polyclonal anti-Aβ (1:300; Invitrogen, Carlsbad, CA, USA). Immuno-reactivities were visualized by the ABC method. Aβ-labeled plaques in the hippocampus with a diameter of more than twice the size of a neuronal cell body (the mean diameter is approximately 15 μm; Gilman et al., 2017; Weisenburger and Vaziri, 2018) were counted, and the number was multiplied by 5 to obtain the total number of plaques in the hippocampus (Carroll et al., 2007).

Enzyme-Linked Immunosorbent Assay (ELISA)

Sandwich Aβ ELISAs were performed as previously described (Heikkinen et al., 2004). Briefly, hippocampal samples were dissected from the mice under deep isoflurane anesthesia and homogenized in 8× cold guanidine buffer (50 mM Tris-HCl, pH 8.0, 5 M guanidine-HCl). The samples and Aβ-peptides used as standards were diluted with reaction buffer containing protease inhibitors and AEBSF (Roche, Mannheim, Germany) to prevent degradation of Aβ and centrifuged at 16,000× *g* for 20 min at 4°C. The quantity of total protein in the supernatants was quantified by bicinchoninic acid (BCA) protein assay kit (Pierce Biotechnology Inc., Rockford, IL, USA). The total levels of hippocampal Aβ were quantified using human $Aβ_{42}$ and $Aβ_{40}$ELISA kits (Invitrogen #KHB3441 and #KHB3481, respectively) following the manufacturer's instructions. Absorbance at 450 nm was measured with an automated microplate reader (ELx800 BioTek Inc., Winooski, VT, USA). $Aβ_{42}$ and $Aβ_{40}$ concentrations in the samples were standardized to total protein levels and are expressed in nanograms per milligram of total protein.

Western Blotting Analysis

The brains were rapidly removed and the coronal brain slices (1 mm) were cut in ice-cold PBS. The dentate gyrus (DG) of the hippocampus was micro-dissected from the sections on dry ice and homogenized. The protein (50 μg) was separated by SDS-PAGE and transferred to membranes. The antibodies used were rabbit polyclonal anti-$p75^{NTR}$ (1:200; Santa Cruz) and mouse monoclonal anti-β-actin (1:2,000; Millipore). Horseradish peroxidase-conjugated secondary antibodies were applied and the immunoreactive signals visualized with enhanced chemiluminescence detection system (Millipore). Protein band intensity was quantified using the image analysis software package (ImageJ; NIH Image, Bethesda, MD, USA) and is expressed as the ratio relative to β-actin level.

Reverse Transcription-Polymerase Chain Reaction (RT-PCR)

Total RNA from DG regions was extracted using TRIzol reagent kit (Invitrogen). cDNA synthesis was performed using

the Prime Script RT reagent kit (TaKaRa; Japan), according to manufacturer's instructions. Briefly, 500 ng of RNA was used as a template to prepare cDNA. A 1 μl 20-fold diluted cDNA (each sample in triplicate) was then used for each run. The primer sets used for *p75*^{NTR}, *GAPDH*, *TERT*, and β-*actin* were designed according to the previous publications (AlMatrouk et al., 2018; Zhang et al., 2019). PCR conditions for *TERT* and β-*actin* were 30 cycles of denaturation at 94°C for 45 s, annealing at 65°C for 45 s, and extension at 72°C for 45 s. PCR product of *TERT* was resolved by 1.5% agarose gel electrophoresis and visualized by ethidium bromide staining. The band intensities were determined using the image analysis software package (ImageJ), and β-*actin* gene expression was detected as the internal control. The other PCR products were assessed using an ABI Prism 7300 Sequence Detection System (Applied Biosystems, Foster City, CA, USA) in the presence of a fluorescent dye (SYBR Green I; TaKaRa). The relative expression of genes was determined using the $2^{-\Delta\Delta Ct}$ method, with normalization to *GAPDH* expression. The values were averaged from four sets of independent experiments and are expressed as a percentage relative to WT mice.

Telomeric Repeat Amplification Protocol (TRAP) Assay

The telomerase activity was measured from fresh hippocampal DG regions using the TRAP$_{EZE}$® XL Telomerase Detection Kit (#S7707; Millipore), following the manufacturer's instruction and previously described (An et al., 2017) with some modifications. All samples were analyzed in triplicate. Briefly, samples were resuspended in CHAPS lysis buffer and incubated on ice for 30 min. Each reaction contained 10 μl 5× TRAP$_{EZE}$RT Reaction mix, 0.4 μl (2 U) Taq polymerase, 37.6 μl nuclease-free H_2O, and 2 μl sample extract (500 ng/μl). The TSR8 control template was used to generate a standard curve. After a 30 min incubation at 30°C, the samples were amplified over 38 cycles at 94°C for 30 s 59°C for 30 s and 72°C for 1 min. The amplified telomerase products were quantified using a fluorescence plate reader (MQX200 BioTek Inc.). Telomerase activity was calculated from the ratio of telomerase products to an internal standard for each lysate (ΔFL/ΔR).

Behavioral Tests

Y-Maze Test

Working memory performance was assessed by recording spontaneous alternation behavior (SAB) in a single-session Y-maze as described before (Zhang et al., 2019). The custom-made maze had wooden arms separated by 120° angle. Each arm was 30 cm long, 10 cm wide, and restricted by 20 cm high walls. The mice were placed at the center of the Y-maze and were allowed to freely explore for 8 min. The series of arm entries was recorded visually. An arm entry was considered to be complete when the mouse placed all four paws into a given arm. The percentage alternation was calculated as the ratio of actual alternations (the number of triads containing successive entries into the three arms) to the maximum possible alternations (the total number of arms entered minus 2).

Morris Water Maze (MWM) Test

Two days after Y-maze test, spatial learning and memory ability were evaluated with the MWM test (Zhang et al., 2019). A circular water tank made of white polypropylene (diameter = 120 cm; height = 45 cm) was prepared. The pool was filled to a depth of 33 cm with water (24 ± 1°C) made opaque by adding a small amount of non-toxic white paint. Swimming paths were analyzed using a computer system with a video camera (AXIS-90 Target/2; Neuroscience Inc., Tokyo, Japan). During the visible-platform training (2 days), a cylindrical dark-colored platform (7 cm in diameter) was placed 0.5 cm above the water surface with the position of the midpoint of one of the four quadrants. The mouse was randomly released from four different quadrants, respectively, and allowed to swim for 90 s. During the hidden-platform training (5 days), the platform was submerged 1 cm below the water surface opposite to the position in the visible-platform training. Four trials were conducted per day with a 30-min intertrial interval. Average swimming speed (m/s) and latency (s) to reach the platform were scored on all trials. On day 8 of training, a probe trial was carried out by removing the platform. The mouse was released from the opposite quadrant in which the platform was located in the hidden-platform training and allowed to swim for 90 s, and the percentage of time spent in the target quadrant was used to evaluate memory retention.

Data Analysis/Statistics

All of the outcome analyses were carried out by the independent investigators blinded to the treatment conditions and mouse types. Data were retrieved and processed with the software Micro cal Origin 9.1 (Origin Lab Corp., Northampton, MA, USA). Group data were expressed as mean ± standard error (SE), and statistical analyses were performed using SPSS software, version 18.0 (SPSS Inc., Chicago, IL, USA). Experimental results were compared among treatment groups by analysis of variance (ANOVA) or Student's *t*-test, followed by Bonferroni's *post hoc* analysis for significant effects. $P < 0.05$ was considered statistically significant.

RESULTS

Age-Related Changes in Hippocampal Neurogenesis in APP/PS1 Mice and WT Mice

Our previous study reported that the proliferation of NSCs in the DG of male 8-month-old (8 m)-APP/PS1 mice is increased compared with that in age-matched male WT mice (Xu et al., 2012). In the present study, we used exogenous (BrdU) and endogenous (Ki67) markers of mitosis to examine the proliferation of NSCs and the microtubule-associated protein DCX to detect newly generated healthy neurons in female APP/PS1 mice and WT mice at the ages of 6 months, 8 months and 10 months (6m, 8m and 10m). Interestingly, we observed that the numbers of BrdU$^+$ cells ($t_{(14)} = -0.688$, $P = 0.503$;

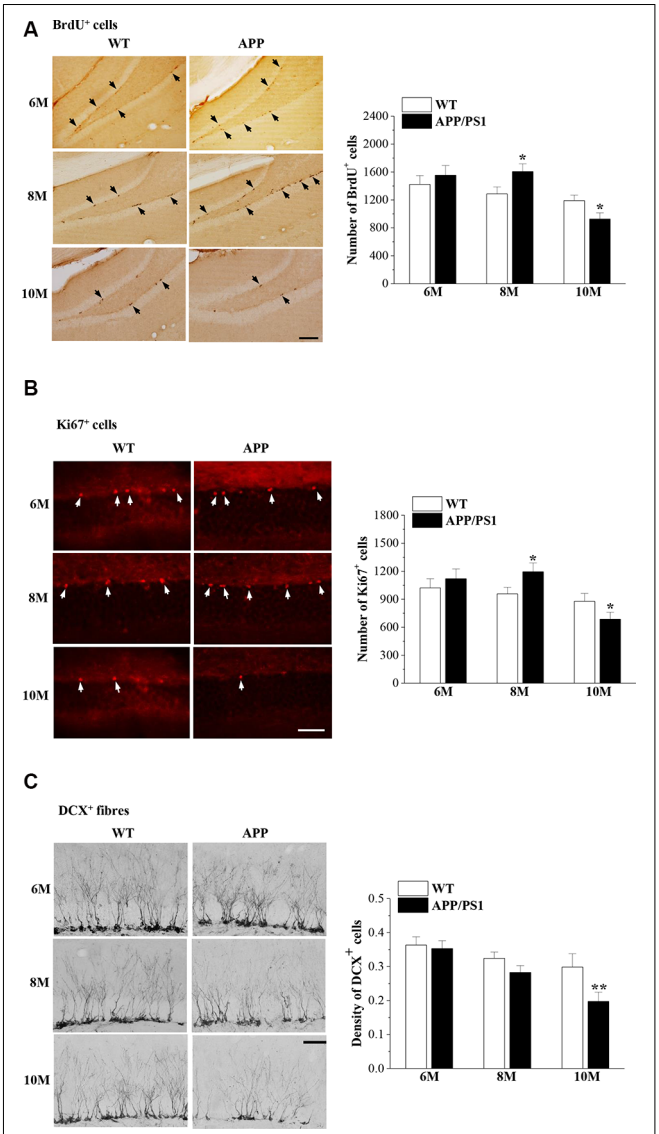

FIGURE 2 | Abnormal neurogenesis in the dentate gyrus (DG) of APP/PS1 mice. **(A)** Representative images of 5-bromo-2′-deoxyuridine (BrdU) immunostaining in 6-month-old, 8-month-old, and 10-month-old APP/PS1 mice and age-matched wild-type (WT) mice (upper panels). $BrdU^+$ cells are indicated by black arrows. Scale bar = 50 μm. The bar graphs show the mean number of $BrdU^+$ cells in APP/PS1 mice and WT mice. $^*P < 0.05$ vs. age-matched WT mice (Student's *t*-test). **(B)** Ki67 immunostaining in 6-month-old, 8-month-old, and 10-month-old APP/PS1 mice and age-matched WT mice (upper panels). $Ki67^+$ cells are indicated by white arrows. Scale bar = 50 μm. The bar graphs show the mean number of $Ki67^+$ cells in APP/PS1 mice and WT mice. $^*P < 0.05$ vs. age-matched WT mice (Student's *t*-test). **(C)** Representative pictures of doublecortin (DCX) immunostaining in 6-month-old, 8-month-old, and 10-month-old APP/PS1 mice and age-matched WT mice (upper panels). Scale bar = 50 μm. The bars indicate the mean density of DCX^+ cells in APP/PS1 mice and WT mice. $^{**}P < 0.01$ vs. 10-month-old WT mice (Student's *t*-test).

Figure 2A) and $Ki67^+$ cells ($t_{(14)} = -0.685$, $P = 0.504$; **Figure 2B**) in the SGZ of 6m-APP/PS1 mice were not significantly different from those of 6m-WT mice. Notably, the numbers of $BrdU^+$ cells ($t_{(14)} = -2.787$, $P = 0.015$) and $Ki67^+$ cells ($t_{(14)} = -2.290$, $P = 0.038$) in 8m-APP/PS1 mice were markedly higher than those in 8m-WT mice. In contrast, an obvious decline in the number of $BrdU^+$ cells ($t_{(14)} = 2.738$, $P = 0.016$) or $Ki67^+$ cells ($t_{(14)} = 2.578$, $P = 0.022$) was observed in 10m-APP/PS1 mice compared to 10m-WT mice. In addition, the density of DCX^+ cells in 10m-APP/PS1 mice ($t_{(14)} = 6.303$, $P < 0.001$; **Figure 2C**), but not 6m-APP/PS1 mice ($t_{(14)} = 0.309$, $P = 0.762$) or 8m-APP/PS1 mice ($t_{(14)} = 1.521$, $P = 0.151$), was lower than that in age-matched WT mice. Thus, hippocampal NSC proliferation initially increases and then decreases while the survival of immature neurons decreases with age in APP/PS1 mice.

Effects of E2 on Hippocampal Neurogenesis in APP/PS1 Mice and WT Mice

To test the effects of E2 on the age-related changes in NSC proliferation and neuron production in APP/PS1 mice, 4m-APP/PS1 mice and 4m-WT mice were bilaterally OVX and treated with E2 for 2 months at three different stages (early period: E-E2; mid period: M-E2; and late period: L-E2; **Figure 1**). Compared to sham-op 6m-APP/PS1 mice, OVX-6m-APP/PS1 mice showed an increase in the number of $BrdU^+$ cells ($P = 0.028$, $n = 8$; **Figure 3A**), which was abrogated by the administration of E-E2 ($P = 0.005$, $n = 8$). However, OVX-8m-APP/PS1 mice ($P = 0.040$, $n = 8$) or OVX-10m-APP/PS1 mice ($P = 0.023$, $n = 8$) showed a significant decrease in the number of $BrdU^+$ cells compared to the age-matched sham-op APP/PS1 mice. The number of $BrdU^+$ cells was comparable between M-E2 treated OVX-8m-APP/PS1 mice and vehicle-treated OVX-8m-APP/PS1 mice ($P = 0.292$, $n = 8$). E-E2 treated OVX-10m-APP/PS1 mice exhibited more $BrdU^+$ cells ($P = 0.017$, $n = 8$) than their vehicle-treated counterparts, but the M-E2 ($P = 0.452$, $n = 8$) and L-E2 ($P = 0.588$, $n = 8$) treatment groups had no change. The number of $BrdU^+$ cells did not differ between OVX-WT mice and sham-op WT mice ($F_{(1,42)} = 0.057$, $P = 0.813$; **Figure 3B**), or between E2- and vehicle-treated OVX-WT mice ($F_{(3,56)} = 0.399$, $P = 0.754$) at these three ages.

OVX-6m-APP/PS1 mice ($P = 0.044$, $n = 8$; **Figure 3C**), OVX-8m-APP/PS1 mice ($P = 0.018$, $n = 8$) and OVX-10m-APP/PS1 mice ($P = 0.007$, $n = 8$) showed obvious loss of DCX^+ cells when compared to the age-matched sham-op APP/PS1 mice. However, the density of DCX^+ cells was unchanged in OVX-6m-WT mice ($P = 0.654$, $n = 8$; **Figure 3D**) and OVX-8m-WT mice ($P = 0.701$, $n = 8$), but was reduced in OVX-10m-WT mice ($P = 0.023$, $n = 8$) compared to age-matched sham-op WT littermates. The administration of E-E2 reversed the decrease in DCX^+ cell density in OVX-6m-APP/PS1 mice ($P = 0.032$, $n = 8$), but E-E2 administration was ineffective in OVX-6m-WT mice ($P = 0.401$, $n = 8$). Furthermore, the administration of M-E2 did not alter the DCX^+ cell density in OVX-8m-APP/PS1 mice ($P = 0.161$, $n = 8$) or OVX-8m-WT mice ($P = 0.364$, $n = 8$); and the decreases in DCX^+ cell density in OVX-10m-APP/PS1 mice ($F_{(3,28)} = 0.213$, $P = 0.887$)

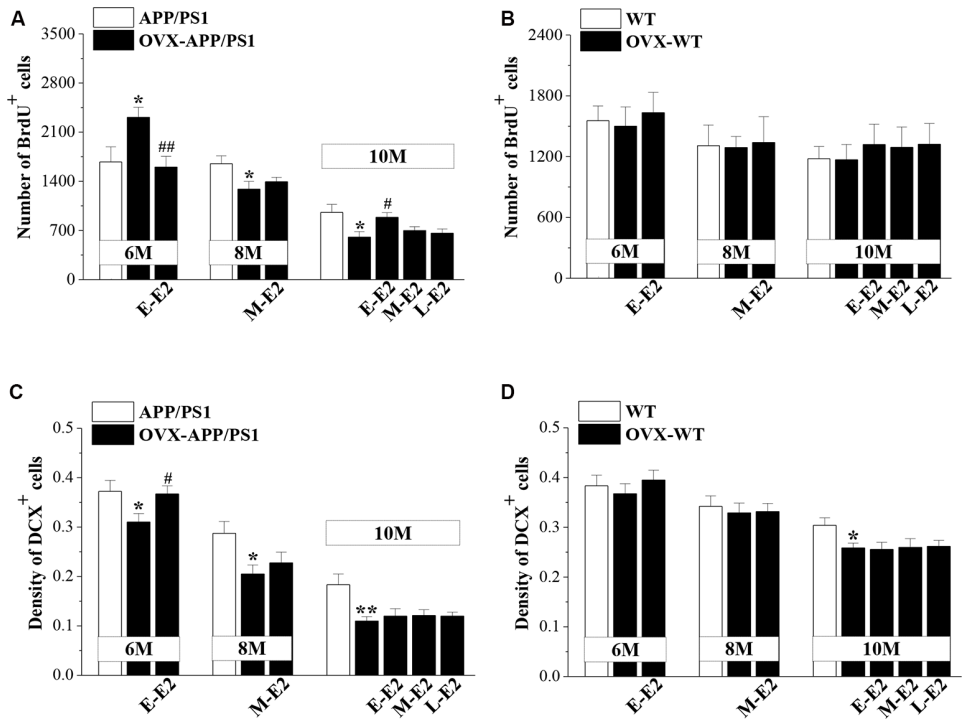

FIGURE 3 | Influence of E2 on the proliferation of neural stem cells (NSCs) and the survival of immature neurons in the DG of APP/PS1 mice. **(A,B)** Bar graphs showing the numbers of $BrdU^+$ cells in APP/PS1 mice or WT mice that were sham-operated (sham-op; open bars) or OVX (black bars). $^*P < 0.05$ vs. age-matched sham-op APP/PS1 mice; $^{\#}P < 0.05$ and $^{\#\#}P < 0.01$ vs. age-matched OVX-APP/PS1 mice (two-way ANOVA). **(C,D)** The mean density of DCX^+ cells in APP/PS1 mice or WT mice. $^*P < 0.05$ and $^{**}P < 0.01$ vs. age-matched sham-op mic; $^{\#}P < 0.05$ vs. 6-month-old OVX-APP/PS1 mice (two-way ANOVA).

and OVX-10m-WT mice ($F_{(3,28)}$ = 0.478, P = 0.700) were insensitive to the administration of E2. These results indicate that E2 treatment in the early period post-OVX prevents excessive proliferation of NSCs and preserves immature neurons at the initiation of pathogenesis in APP/PS1 mice, which may have a certain protective effect on the proliferative capacity of NSCs at the advanced stages of the disease.

Effects of E2 on Aβ Secretion and Deposition in APP/PS1 Mice

To explore the mechanisms underlying E2-induced protection of neurogenesis in APP/PS1 mice, we evaluated the secretion and deposition of Aβ. OVX-6m-APP/PS1 mice showed elevated levels of $A\beta_{42}$ (P = 0.025, n = 8; **Figure 4A**) and $A\beta_{40}$ (P = 0.034, n = 8; **Figure 4B**) compared to sham-op 6m-APP/PS1 mice, which were reduced by the administration of E-E2 ($A\beta_{42}$: P = 0.027, n = 8; $A\beta_{40}$: P = 0.042, n = 8). However, OVX did not affect $A\beta_{42}$ or $A\beta_{40}$level in the hippocampus of 8m-APP/PS1 mice ($A\beta_{42}$: P = 0.818, n = 8; $A\beta_{40}$: P = 0.597, n = 8) or 10m-APP/PS1 mice ($A\beta_{42}$: P = 0.365, n = 8; $A\beta_{40}$: P = 0.604, n = 8). Furthermore, the administration of E2 in OVX-8m-APP/PS1 mice ($A\beta_{42}$: P = 0.572, n = 8; $A\beta_{40}$: P = 0.757, n = 8) or OVX-10m-APP/PS1 mice ($A\beta_{42}$: $F_{(3,28)}$ = 0.734, P = 0.540; $A\beta_{40}$: $F_{(3,28)}$ = 0.088, P = 0.966) had no effect on the level of $A\beta_{42}$ or $A\beta_{40}$. The number of Aβ plaques—another index of Aβ pathology—did not differ between OVX-APP/PS1 mice and the age-matched sham-op mice ($F_{(1,42)}$ = 0.797, P = 0.377; **Figure 4C**) or between E2-treated OVX-APP/PS1 mice and the vehicle-treated groups at these three ages ($F_{(3,56)}$ = 1.518, P = 0.220). The results indicate that E2 is beneficial for the hippocampi at the initiation stage of Aβ formation rather than at the more advanced stage of Aβ deposition.

Involvement of $p75^{NTR}$ in the Effects of E2-Induced Protection of Neurogenesis in APP/PS1 Mice

Activated $p75^{NTR}$ ligands were shown to be involved in the neurogenic effect of Aβ (Sotthibundhu et al., 2009). To test the role of $p75^{NTR}$ in the preservation of neurogenesis by E2 in APP/PS1 mice, we examined $p75^{NTR}$ expression in 6-month-old mice that were OVX or sham-op at 4 months old and treated with E2 or vehicle for 2 months (**Figure 1**). Compared to 6m-WT mice, levels of $p75^{NTR}$ protein (P = 0.082, n = 8; **Figure 5A**) and mRNA (P = 0.056, n = 8; **Figure 5B**) in 6m-APP/PS1 mice had a slight but insignificant increase. OVX-6m-APP/PS1 mice showed markedly higher levels of $p75^{NTR}$ protein ($P < 0.001$, n = 8) and mRNA ($P < 0.001$, n = 8) than sham-op 6m-APP/PS1 mice. The application of E2 abolished the increases in $p75^{NTR}$ expression in OVX-6m-APP/PS1 mice ($P < 0.001$, n = 8 for both protein and mRNA). We further used TAPI-2 to prevent the activation of $p75^{NTR}$ and examined Aβ-impaired neurogenesis. Compared to vehicle-treated OVX-

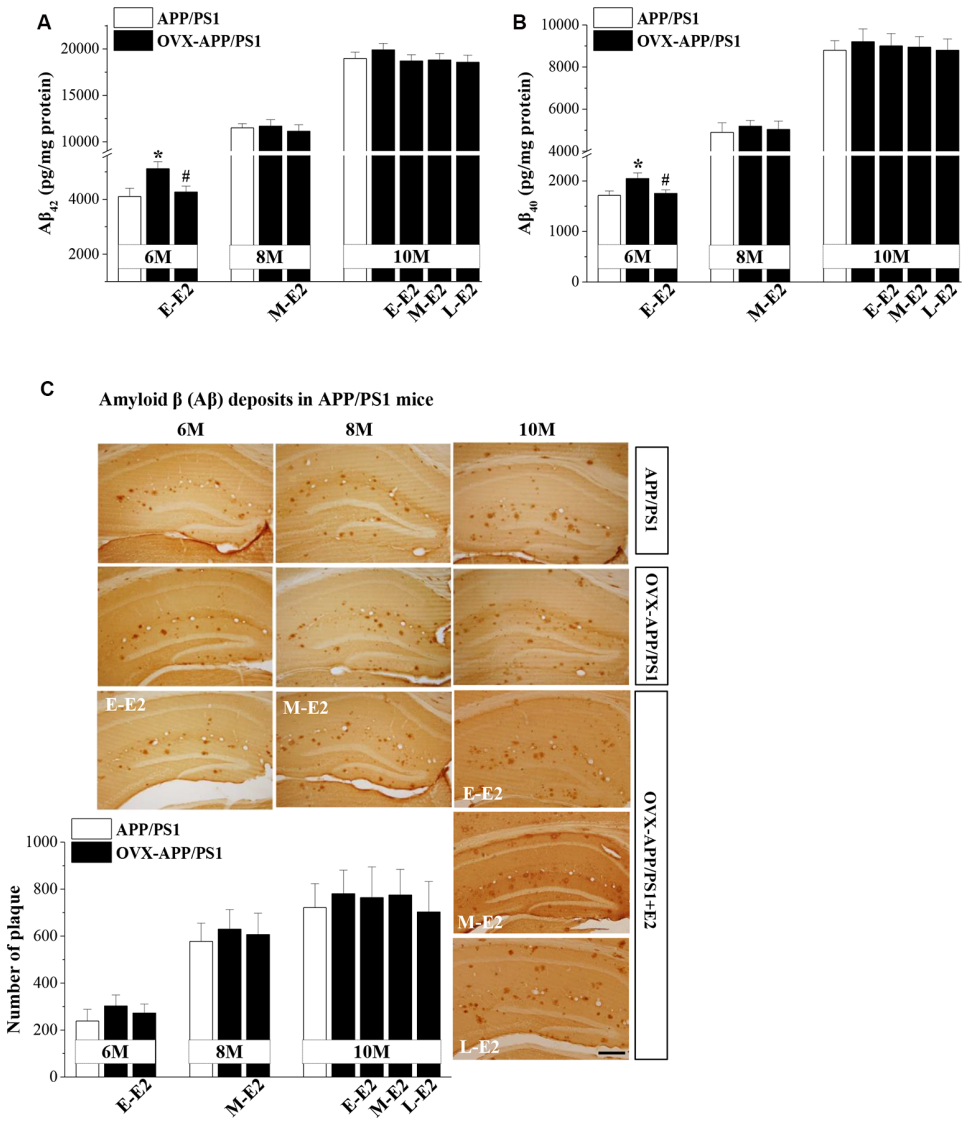

FIGURE 4 | Age-related increase in Aβ accumulation and the influence of E2 on Aβ formation in the hippocampus of APP/PS1 mice. **(A,B)** Bar graphs showing the level of total $A\beta_{1-42}$ or $A\beta_{1-40}$in APP/PS1 mice that were sham-op (open bars) or OVX (black bars). $^{*}P < 0.05$ vs. 6-month-old sham-op APP/PS1 mice; $^{\#}P < 0.05$ vs. 6-month-old OVX-APP/PS1 mice (two-way ANOVA). **(C)** Representative images showing Aβ immunostaining in 6-month-old, 8-month-old, and 10-month-old APP/PS1 mice that were sham-op or OVX with vehicle or E2 treatment in the early period (E-E2), mid period (M-E2), or late period (L-E2). The data show the mean counts of Aβ deposits in the hippocampus of APP/PS1 mice. Scale bar = 200 μm.

6m-APP/PS1 mice, the number of $BrdU^{+}$ cells was significantly reduced in TAPI-2-treated OVX-6m-APP/PS1 mice ($P = 0.014$, $n = 8$; **Figure 5C**); however, the density of DCX^{+} cells was unchanged ($P = 0.636$, $n = 8$; **Figure 5D**). Thus, E2 deficiency results in elevated expression of $p75^{NTR}$ and consequently, increased proliferation of hippocampal NSCs in APP/PS1 mice, but has no effect on the reduction of immature neurons.

Effects of E2 on Telomerase Regulation in Aged APP/PS1 Mice

Telomerase, a reverse transcriptase, is required for embryonic and adult neurogenesis (Lobanova et al., 2017). To investigate whether telomerase is implicated in the E2 mediated protection of NSCs in APP/PS1 mice, we analyzed the levels of TERT and telomerase activity in 10-month-old APP/PS1 mice. Compared to 10m-WT mice, 10m-APP/PS1 mice displayed significantly lower *TERT* mRNA level ($P < 0.001$, $n = 8$; **Figure 6A**) and telomerase activity ($P < 0.001$, $n = 8$; **Figure 6B**). However, *TERT* level ($P < 0.001$, $n = 8$) and telomerase activity ($P < 0.001$, $n = 8$) were markedly lower in OVX-10m-APP/PS1 mice than in sham-op 10m-APP/PS1 mice, but were increased by the administration of E-E2 (mRNA: $P = 0.011$, $n = 8$; activity: $P = 0.037$, $n = 8$; the administration of E2 is shown in **Figure 1**). However, compared to sham-op 10m-APP/PS1 mice, the *TERT* level ($P = 0.016$, $n = 8$) and telomerase activity ($P = 0.032$, $n = 8$) in OVX-10m-APP/PS1 mice that received E-E2 treatment were not

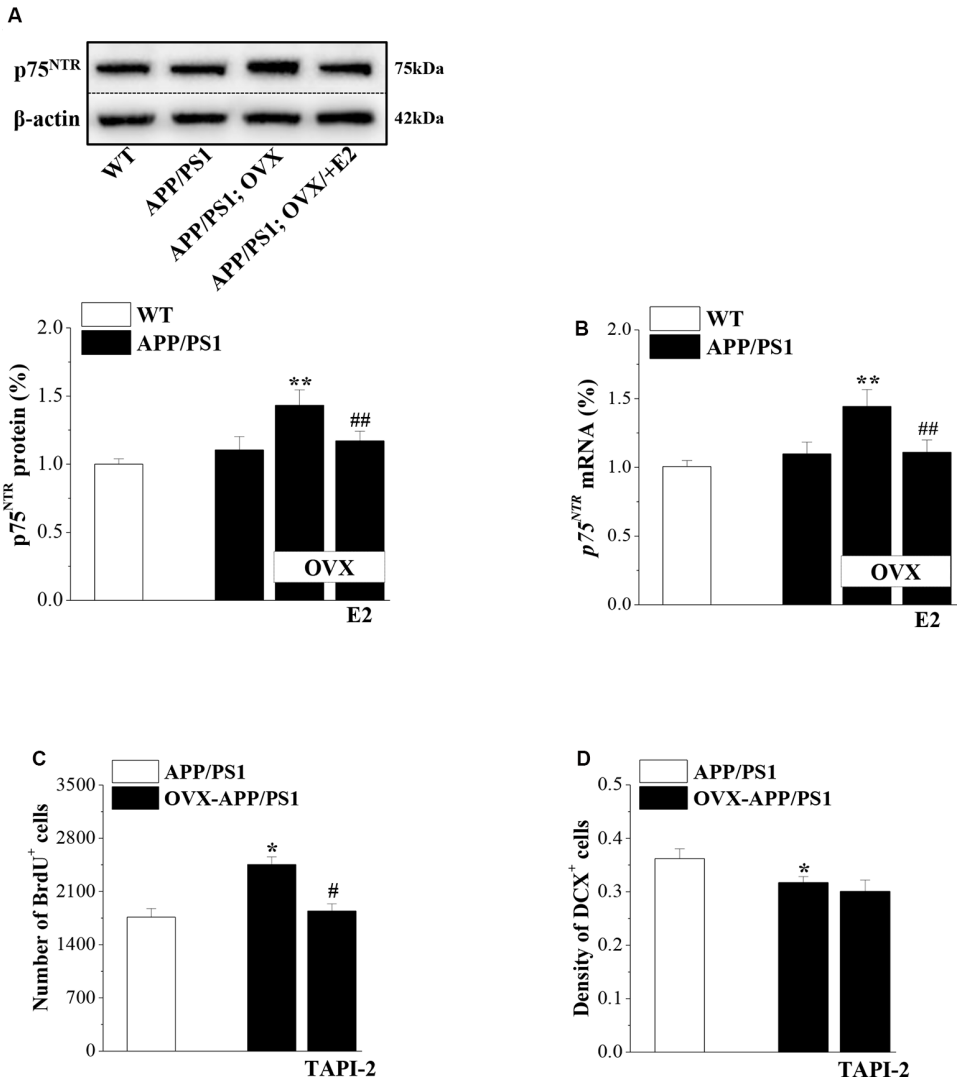

FIGURE 5 | p75^{NTR} participates in E2-induced protection of NSC proliferation in APP/PS1 mice. **(A,B)** Influence of E2 on the level of p75^{NTR} in 6-month-old APP/PS1 mice. The upper panels represent representative blots of p75^{NTR}. Bar graphs show the level of p75^{NTR} protein or *p75^{NTR}* mRNA in APP/PS1 mice or OVX-APP/PS1 mice treated with vehicle or E2 for 2 months. $^{**}P < 0.01$ vs. sham-op APP/PS1 mice; $^{\#\#}P < 0.01$ vs. OVX-APP/PS1 mice (two-way ANOVA). **(C,D)** Influence of the p75^{NTR} inhibitor TAPI-2 on the excessive proliferation of NSCs and survival of immature neurons in the DG of 6-month-old APP/PS1 mice. The bar graphs show the number of BrdU$^+$ cells and the density of DCX$^+$ cells in APP/PS1 mice or OVX-APP/PS1 mice treated with vehicle or TAPI-2 for 7 days. $^{*}P < 0.05$ vs. sham-op APP/PS1 mice; $^{\#}P < 0.05$ vs. OVX-APP/PS1 mice (two-way ANOVA).

completely restored. The administration of M-E2 or L-E2 had no effect on *TERT* expression (all $P > 0.05$, $n = 8$) or telomerase activity (all $P > 0.05$, $n = 8$) in OVX-10m-APP/PS1 mice. These results indicate that telomerase activity declines in the Aβ-impaired hippocampus, which is exacerbated by E2 deficiency; however, this is reversed by early period E2 treatment.

Effects of E2-Induced Protection of Neurogenesis on Cognitive Deficits in Aged APP/PS1 Mice

Adult hippocampal neurogenesis has been implicated in the cognitive deficits that are a signature abnormality of AD (Gonçalves et al., 2016). Thus, it is critically important to assess whether E2-mediated protection of neurogenesis in APP/PS1 mice is linked to improvements in cognitive function. Hippocampal-dependent learning and memories were evaluated by the Y-maze and MWM at the age of 10 months (**Figure 1**). The SAB rate in the Y-maze, which is regarded as a measure of short-term working memory, was remarkably reduced in 10m-APP/PS1 mice compared with that in 10m-WT mice ($P < 0.001$, $n = 10$; **Figure 7A**). Moreover, OVX-10m-APP/PS1 mice showed a distinctly decreased rate compared to sham-op 10m-APP/PS1 mice ($P < 0.001$, $n = 10$). Central to our analysis was the observation that E-E2 administration partly restored the alternation rate ($P = 0.003$, $n = 10$) but did not

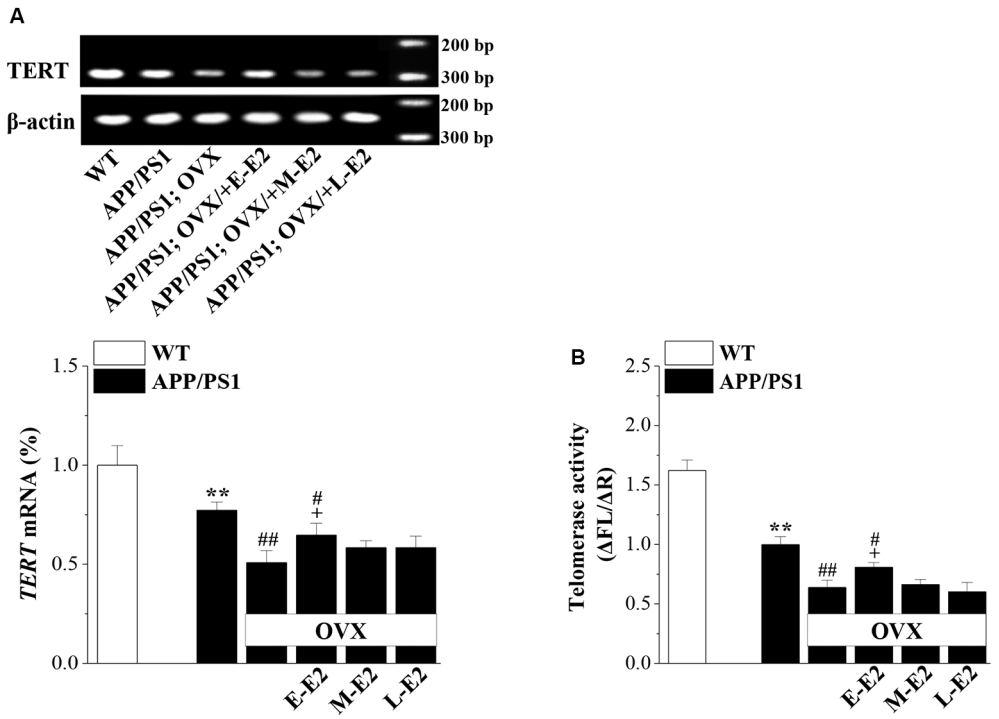

FIGURE 6 | The administration of E2 in the early period post-OVX rescues the impaired telomerase activity in the DG in aged APP/PS1 mice. **(A)** Representative RT-polymerase chain reaction (PCR) analysis showing mRNA levels of *TERT* in 10-month-old APP/PS1 mice that were sham-op or OVX with vehicle or E2 treatment in the early period (E-E2), mid period (M-E2), or late period (L-E2). The bar graphs show the mRNA percentage level of *TERT*. $^{**}P < 0.01$ vs. WT mice; $^{\#}P < 0.05$ and $^{\#\#}P < 0.01$ vs. sham-op APP/PS1 mice; $^{+}P < 0.05$ vs. OVX-APP/PS1 mice (two-way ANOVA). **(B)** Bar graphs showing the quantification of telomerase activity by telomeric repeat amplification protocol (TRAP; ΔFL/ΔR). $^{**}P < 0.01$ vs. WT mice; $^{\#}P < 0.05$ and $^{\#\#}P < 0.01$ vs. sham-op APP/PS1 mice; $^{+}P < 0.05$ vs. OVX-APP/PS1 mice (two-way ANOVA).

completely reverse the impairment in working memory in OVX-10m-APP/PS1 mice relative to sham-op 10m-APP/PS1 mice ($P = 0.026$, $n = 10$). Additionally, the administration of M-E2 and L-E2 had no effect on the SAB rate in OVX-10m-APP/PS1 mice (all $P > 0.05$, $n = 10$). The rate in 10m-WT mice was unaffected by E2 deprivation and E2 treatment (data not shown). To exclude the possibility that the changes in SAB performance were caused by differences in motility, we quantified the number of arms entered by mice in the Y-maze. As shown in **Figure 7B**, there was no significant effect of genotype ($F_{(1,54)} = 0.582$, $P = 0.449$), ovariectomy ($F_{(1,54)} = 0.005$, $P = 0.944$) or E2 treatment ($F_{(3,54)} = 1.191$, $P = 0.322$) on the number of arm entries.

In the MWM, the visible-platform on days 1–2 was used to examine search behavior or visual acuity, and the hidden-platform on days 3–7 was used to evaluate hippocampal-dependent spatial cognitive function. During acquisition, mice showed no difference in the latency to reach the visible-platform based on genotype ($F_{(1,108)} = 0.356$, $P = 0.552$; **Figure 7C**), OVX ($F_{(1,108)} = 0.000$, $P = 0.996$), or E2 treatment ($F_{(3,108)} = 0.371$, $P = 0.774$). On days 4–7 of training, the latency to reach the hidden platform in 10m-APP/PS1 mice was significantly increased compared to that in the 10m-WT mice (all $P < 0.05$, $n = 10$), but there was no difference in swim speed between these two groups (all $P > 0.05$, $n = 10$). Furthermore, compared to sham-op 10m-APP/PS1 mice, OVX-10m-APP/PS1 mice required a longer time to find the hidden platform on days 5–7 (all $P < 0.05$, $n = 10$) with no change in swimming speed (all $P > 0.05$, $n = 10$). Interestingly, the increased latency on days 5–7 of training in OVX-10m-APP/PS1 mice was reversed by the administration of E-E2 (day 5: $P = 0.015$, $n = 10$; day 6: $P = 0.016$, $n = 10$; day 7: $P = 0.012$, $n = 10$), but not by the administration of M-E2 or L-E2 (all $P > 0.05$, $n = 10$). However, the administration of E-E2 alone in OVX-10m-APP/PS1 mice did not completely recover the prolonged latency compared to sham-op 10m-APP/PS1 mice (day 5: $P = 0.048$; day 6: $P = 0.011$; day 7: $P = 0.013$). No significant difference was found in the swimming speed between E2- and vehicle-treated OVX-10m-APP/PS1 mice (all $P > 0.05$).

A probe trial was carried out 24 h after the last day of training, and the percentage of time spent in the target quadrant was measured to evaluate the strength of the memory trace. As shown in **Figure 7D**, 10m-APP/PS1 mice spent less time in the target quadrant than 10m-WT mice ($P < 0.001$). OVX-10m-APP/PS1 mice showed much shorter swimming time in the target quadrant than sham-op 10m-APP/PS1 mice ($P < 0.001$). In addition, the swimming time in the target quadrant was longer for E-E2–treated OVX-10m-APP/PS1 mice than for vehicle-treated OVX-10m-APP/PS1 mice ($P = 0.021$), but shorter than for sham-op 10m-APP/PS1 mice ($P = 0.023$). The performance in the target quadrant by OVX-10m-APP/PS1 mice was unaltered

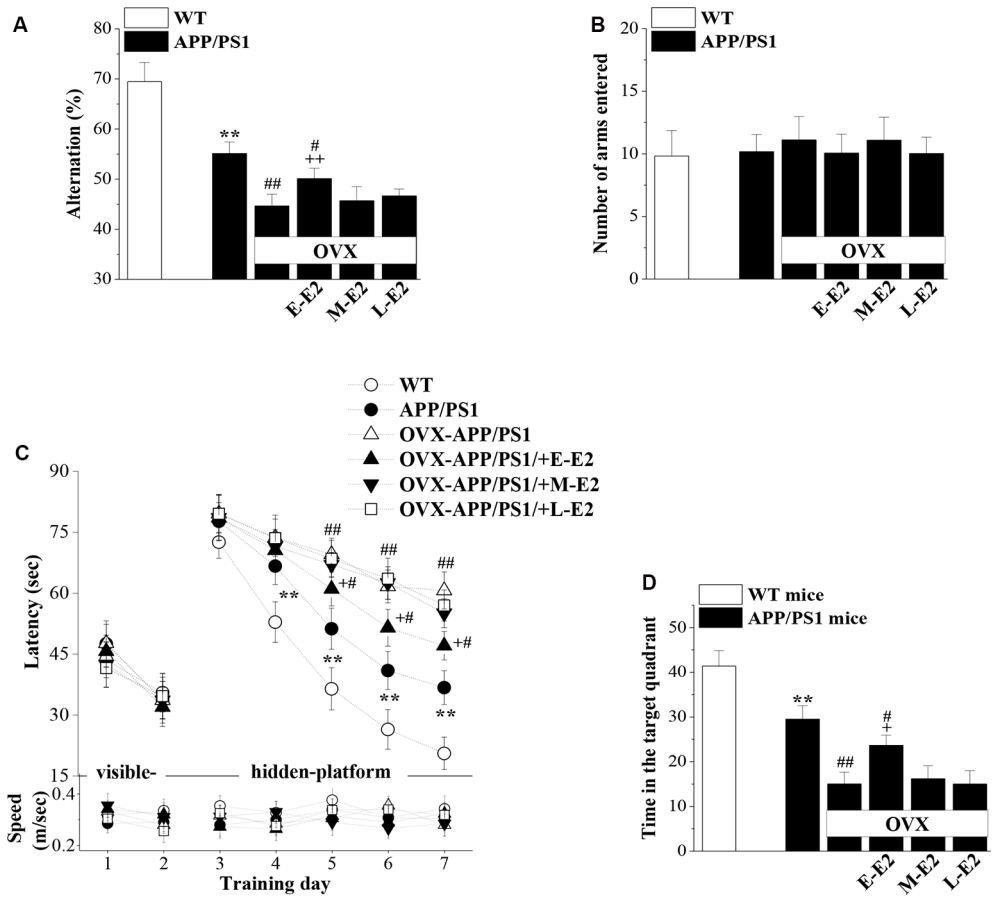

FIGURE 7 | The administration of E2 in the early period post-OVX alleviates the cognitive deficits in aged APP/PS1 mice. **(A,B)** Influence of E2 treatment in the early period (E-E2), mid period (M-E2), or late period (L-E2) on working memory as assessed by the Y-maze test in 10-month-old APP/PS1 mice. The bar graphs show the spontaneous alternation ratio (%) and the total number of arm entries in the Y-maze test of APP/PS1 mice. $^{**}P < 0.01$ vs. WT mice; $^{\#}P < 0.05$ and $^{\#\#}P < 0.01$ vs. sham-op APP/PS1 mice; $^{++}P < 0.01$ vs. OVX-APP/PS1 mice (two-way ANOVA). **(C)** Spatial learning and memory were assessed by the Morris water maze (MWM). Each point represents the mean latency (sec) to reach the platforms (upper panel) and the swimming speeds (m/s; bottom panel). $^{**}P < 0.01$ vs. WT mice; $^{\#}P < 0.05$ and $^{\#\#}P < 0.01$ vs. sham-op APP/PS1 mice; $^{+}P < 0.05$ vs. OVX-APP/PS1 mice (repeated measure ANOVA). **(D)** Probe trial test. The bars represent the percentages of swimming time spent in the platform quadrant. $^{**}P < 0.01$ vs. WT mice; $^{\#}P < 0.05$ and $^{\#\#}P < 0.01$ vs. sham-op APP/PS1 mice; $^{+}P < 0.05$ vs. OVX-APP/PS1 mice (two-way ANOVA).

by the administration of M-E2 or L-E2 ($P > 0.05$ in each group). Taken together, these results imply that E2 alleviates cognitive deficits in aged APP/PS1 mice, but only when administered during the early period post-OVX.

DISCUSSION

Consistent with the evidence supporting the existence of a critical period for the benefit of ERT on cognitive function in postmenopausal women with AD (Vedder et al., 2014), here, we showed in AD model mice that E2 treatment in the early, but not in the late period post-OVX, prevented cognitive decline. This involved inhibition the excessive proliferation of hippocampal NSCs by suppression of Aβ-induced overexpression of $p75^{NTR}$ in young APP/PS1 mice, and preservation of telomerase activity and proliferation capability of NSCs in aged APP/PS1 mice. The positive effects on cognition were evidenced by better scores in the Y-maze and MWM tests.

APP/PS1 mouse models develop AD pathology at young age, enabling the study of exogenous E2 efficiency on cognitive performance under varying conditions of ovarian function. Whilst OVX can be used to study the consequences of menopause in women, the procedure induces a rapid gonadal hormone decline in contrast to the progressive decline associated with natural menopause in women. Nevertheless, a recent review has suggested that OVX results in a "blank ovarian hormone state," which is an ideal model to evaluate the effects of ovarian hormone deprivation and the outcomes of subsequent exogenous hormone treatments on the brain (Koebele and Bimonte-Nelson, 2016). Indeed, epidemiological data regarding women who underwent OVX before the onset of natural menopause indicate a long-term increased risk of AD (Rocca et al., 2010) and furthermore ERT efficacy is similar in both natural menopause and oophorectomy in women, depending on the timing of treatment initiation (Mosconi et al., 2004; Maki et al., 2019). Given that female mice continue to experience hormonal cycles

with age (Hung et al., 2003), the use of OVX can be considered an effective model to mimic human/primate menopause in mice.

The results presented here are in line with previous studies demonstrating that the proliferation of hippocampal NSCs is increased at the Aβ plaque initiation stage while subsequently decreased at the Aβ plaque progressive stage in the same mouse model as ours (Taniuchi et al., 2007; Xu et al., 2012), indicating a similar "bell-shaped" proliferation curve. However, the survival of immature neurons declined faster with age in APP/PS1 mice, showing a steeper curve than that in WT mice. The turning point seems to be at the age of occurrence of massive Aβ deposits. Meanwhile, in agreement with earlier findings, our results showed progressive exacerbation of Aβ pathology in APP/PS1 mice from the age of 6–10 months (Garcia-Alloza et al., 2006). Our previous report demonstrated that Aβ impairs the survival of immature neurons by downregulating the PI3K-Akt-mTOR signaling pathway (Li et al., 2010). The sensitivity of the adult brain to Aβ was found to be reduced after 10 months of age in mice, indicating an age-dependent decrease in the neurogenic effect of Aβ (Sotthibundhu et al., 2009). Therefore, the bell-shaped curve may be attributed to the gradual desensitization of the nervous system to Aβ and depletion of the NSC pool; the decline in NSC proliferation could contribute to the progressive reduction in new neuron production in aged APP/PS1 mice. However, another AD mouse model, APP/PS1 mice on a C57BL/6J background exhibit seizure activity at the age of 3–4 months, and show different hippocampal neurogenesis from our model (Unger et al., 2016). These heterogeneities of phenotypes may be attributable to genetic background and inter-animal variability. Additionally, although APP/PS1 transgenic mouse models have been commonly used in AD research, the pathogenesis in these models has distinctions from sporadic AD patients such as lacking of widespread neurodegeneration and none developed neurofibrillary tangles (NFTs; Drummond and Wisniewski, 2017). Further study is needed to determine the critical period of E2 on an ideal model contains both plaques and NFTs.

Our results showed that estrogen deficiency caused an increase in NSC proliferation at the Aβ initiation stage and a decrease at the Aβ progressive stage, showing a leftward shift of the proliferation curve. The survival of immature neurons showed a sharper decline in APP/PS1 mice than in WT mice. E2 treatment in the early period post-OVX prevented the over-proliferation of NSCs and increased the immature neuron. The relationship between E2 and hippocampal neurogenesis has been controversial. Exogenous E2 administration enhances hippocampal cell proliferation by activating estrogen receptor, whereas long-term E2 deficiency has no effect on cell proliferation in the DG in female rats or mice (Tanapat et al., 2005; Galea et al., 2006; Lagace et al., 2007). Importantly, E2 treatment at the early period post-OVX decreased the levels of Aβ. According to previous studies, E2 treatment for 3 months reduces the enhanced Aβ accumulation in OVX-3xTg-AD mice (Carroll et al., 2007). E2 treatment can increase Aβ clearance *via* regulation of β-secretase (BACE1) activity and expression in APP23 mice (Li et al., 2013). A 2-month administration of docosahexaenoic acid-enriched phospholipids inhibits the generation and accumulation of Aβ by suppressing BACE1 expression in senescence-accelerated prone eight mice (Wang et al., 2019). These evidences may explain the effect of E2 on Aβ accumulation. Investigations into the relationship between Aβ and hippocampal neurogenesis have proven that exogenous and endogenous Aβ promote the proliferation of NSCs in the subventricular zone *via* $p75^{NTR}$ (Sotthibundhu et al., 2009; Zheng J. Y. et al., 2017), and Aβ inhibits the endocytosis of $p75^{NTR}$ in cholinergic basal forebrain neurons (Ovsepian et al., 2014). $p75^{NTR}$ is shown to stimulate the proliferation of cultured neurospheres by interacting with several cell-cycle regulatory proteins (Provenzano et al., 2011). Our findings showed that the levels of Aβ and $p75^{NTR}$ were elevated by OVX, both prevented by E2 treatment in the early period post-OVX; blocking $p75^{NTR}$ activation reduced NSC proliferation without affecting the survival of immature neurons. Thus, the increased survival of immature neurons by early-period E2 treatment might be related to the reduction in Aβ levels. One study has demonstrated that the deletion of the $p75^{NTR}$ gene suppresses Aβ production in APP/PS1 mice (Wang et al., 2011). Lower $p75^{NTR}$ mRNA and protein levels have been observed following chronic E2 treatment (Hasan et al., 2005). Thus, there are multiple levels of interaction between E2, Aβ, and $p75^{NTR}$. Combined with these observations, our results indicate that early period E2 treatment blocked the hyperproliferation of NSCs by inhibiting Aβ-induced $p75^{NTR}$ expression, and alleviated the depletion of the NSC pool in aged APP/PS1 mice, thereby abolishing the leftward overproliferation curve. In accordance with the E2-induced preservation of NSC proliferation in aged OVX-APP/PS1 mice, we found that telomerase activity was reduced in aged APP/PS1 mice, which was exacerbated by OVX and rescued by early-period E2 treatment post-OVX. These observations imply that changes in telomerase activity are accompanied by altered NSC number in the DG. Telomerase is expressed at high levels in NSCs and neural progenitor cells in the adult brain (Liu et al., 2018), and Aβ aggregates are shown to inhibit telomerase activity in senescent human cells (Wang et al., 2015). This implies that the decrease in telomerase activity in aged APP/PS1 mice may be related to the Aβ accumulation. However, we observed that there were no significant differences in Aβ levels between aged APP/PS1 mice, OVX-APP/PS1 mice and E2 treated OVX-APP/PS1 mice, raising the possibility that the NSC pool provides a supply of telomerase. Additionally, pharmacologic induction of TERT is found to increase the expression of nerve growth factor and brain-derived neurotrophic factor (BDNF) while protecting neurons from oxidative stress and the cytotoxic effects of Aβ (Baruch-Eliyahu et al., 2019), implying an interaction between the NSC pool and telomerase.

Interestingly, E2 had beneficial effects on neurogenesis and Aβ levels in APP/PS1 mice only when administered during the early period post-OVX. Our findings in this regard can be explained by previous studies showing that the neuroprotective actions of E2 are dependent on time since OVX. The administration of E2 within 3 months, but not delayed

10 months post-OVX, has efficacy in rats (Walf et al., 2009). It has been proposed that the responsiveness of the brain to hormones declines after an extended period of hormone depletion (Hamilton et al., 2011). E2 deficiency or administration after the progressive stage did not affect Aβ levels or the plaque numbers in APP/PS1 mice. Although some studies suggest that estrogen deprivation for 3 months could enhance the deposition of Aβ in APPswe transgenic mice that underwent OVX at 4 weeks old (Levin-Allerhand and Smith, 2002), estrogen treatment after a similar interval following OVX has no effect on Aβ levels in mice that underwent OVX at an older age (Heikkinen et al., 2004). This is in general agreement with earlier work demonstrating that long-term E2 deficiency increased Aβ production at the initiation stage of amyloid pathology but has no effect on Aβ aggregation and plaque formation (Heikkinen et al., 2004; Levin-Allerhand et al., 2002). E2 had no effect on hippocampal neurogenesis in WT mice, although 10-month-old OVX-WT mice showed fewer immature neurons, which is supported by reports that E2 does not affect neurogenesis in normal mice (Lagace et al., 2007).

In addition to E2-mediated effects on hippocampal NSC proliferation, we also observed that E2 treatment in the early period post-OVX partially alleviated cognitive deficits in aged APP/PS1 mice. Adult neurogenesis depends on the function and stable numbers of NSCs. Continuous neurogenesis in the DG is essential for maintaining normal hippocampal-dependent cognitive behavior. The hippocampal mechanism of context encoding is considered to depend on a subset of immature adult-born neurons in the DG (Adlaf et al., 2017). NSC transplantation restores spatial learning ability in 18-month-old 3xTg-AD mice by elevating hippocampal BDNF level (Blurton-Jones et al., 2009), and stimulating NSC proliferation in 7-month-old 3xTg-AD mice by activating the PI3K-AKT-GSK3β-Wnt pathway results in increased cognitive function (Zheng R. et al., 2017). The relationship between NSC and synaptic resistance to Aβ toxicity has been confirmed by *in vivo* and *in vitro* experiments: a larger pool of NSC is associated with reduced Aβ binding to the synapse, while transgenic ablation of endogenous NSC increases synaptic Aβ binding (Micci et al., 2019). Factors secreted during the proliferation of hippocampal NSCs create a favorable microenvironment for the proper functioning of the nervous system (Lee et al., 2007). Moreover, E2 treatment in young OVX mice can lead to a long-lasting enhancement of classical estrogen response element-dependent gene activation in the hippocampus, the effects of which can persist even after cessation of E2 treatment (Pollard et al., 2018).

A recent multimodality brain imaging study has shown that declines in circulating estrogens are a major risk factor for female-specific brain AD abnormalities, and suggests that the therapeutic window of ERT for AD preventive interventions in women might be early in menopause (Rahman et al., 2020). The present study provides evidence that the early period following OVX is the critical window for E2 treatment to alleviate cognitive deficits in aged APP/PS1 mice. E2 likely acts by preventing depletion of the hippocampal NSC pool and preserving basal neurogenesis. Our findings reveal the mechanisms underlying the cognitive efficacy of E2 treatment, especially as related to a critical window after hormone declines, and provide experimental evidence that can guide clinical decision-making for the initiation of ERT in postmenopausal women, particularly those with or at risk of developing AD.

DATA AVAILABILITY STATEMENT

The raw data supporting the conclusions of this article will be made available by the authors, without undue reservation.

ETHICS STATEMENT

The animal study was reviewed and approved by Institutional Animal Care and Ethical Committee of Nanjing Medical University.

AUTHOR CONTRIBUTIONS

SS conceived and designed the experiments. YQ and DA performed the experiments. WX and XQ analyzed the data. XW contributed reagents and materials. LiC, LeC, and SS drafted the manuscript. All authors contributed to the article and approved the submitted version.

FUNDING

This work was supported by the National Natural Science Foundation of China (31600835; 81971274).

REFERENCES

Adlaf, E. W., Vaden, R. J., Niver, A. J., Manuel, A. F., Onyilo, V. C., Araujo, M. T., et al. (2017). Adult-born neurons modify excitatory synaptic transmission to existing neurons. *Elife* 6:e19886. doi: 10.7554/elife.19886

Ager, R. R., Davis, J. L., Agazaryan, A., Benavente, F., Poon, W. W., LaFerla, F. M., et al. (2015). Human neural stem cells improve cognition and promote synaptic growth in two complementary transgenic models of Alzheimer's disease and neuronal loss. *Hippocampus* 25, 813–826. doi: 10.1002/hipo.22405

AlMatrouk, A., Lemons, K., Ogura, T., Luo, W., Wilson, C., and Lin, W. (2018). Chemical exposure-induced changes in the expression of neurotrophins and their receptors in the main olfactory system of mice lacking TRPM5-expressing microvillous cells. *Int. J. Mol. Sci.* 19:2939. doi: 10.3390/ijms19102939

An, K., Liu, H. P., Zhong, X. L., Deng, D. Y. B., Zhang, J. J., and Liu, Z. H. (2017). hTERT-immortalized bone mesenchymal stromal cells expressing rat galanin *via* a single tetracycline-inducible lentivirus system. *Stem Cells Int.* 2017:6082684. doi: 10.1155/2017/6082684

Baruch-Eliyahu, N., Rud, V., Braiman, A., and Priel, E. (2019). Telomerase increasing compound protects hippocampal neurons from amyloid β toxicity by enhancing the expression of neurotrophins and plasticity related genes. *Sci. Rep.* 9:18118. doi: 10.1038/s41598-019-54741-7

Baxter, M. G., Santistevan, A. C., Bliss-Moreau, E., and Morrison, J. H. (2018). Timing of cyclic estradiol treatment differentially affects cognition in aged female rhesus monkeys. *Behav. Neurosci.* 132, 213–223. doi: 10.1037/bne0000259

Benilova, I., Karran, E., and De Strooper, B. (2012). The toxic Aβ oligomer and Alzheimer's disease: an emperor in need of clothes. *Nat. Neurosci.* 15, 349–357. doi: 10.1038/nn.3028

Blurton-Jones, M., Kitazawa, M., Martinez-Coria, H., Castello, N. A., Muller, F. J., Loring, J. F., et al. (2009). Neural stem cells improve cognition *via* BDNF in

a transgenic model of Alzheimer disease. *Proc. Natl. Acad. Sci. U S A* 106, 13594–13599. doi: 10.1073/pnas.0901402106

Boccardi, V., and Paolisso, G. (2014). Telomerase activation: a potential key modulator for human healthspan and longevity. *Ageing Res. Rev.* 15, 1–5. doi: 10.1016/j.arr.2013.12.006

Carroll, J. C., Rosario, E. R., Chang, L., Stanczyk, F. Z., Oddo, S., LaFerla, F. M., et al. (2007). Progesterone and estrogen regulate Alzheimer-like neuropathology in female 3xTg-AD mice. *J. Neurosci.* 27, 13357–13365. doi: 10.1523/jneurosci.2718-07.2007

Drummond, E., and Wisniewski, T. (2017). Alzheimer's disease: experimental models and reality. *Acta Neuropathol.* 133, 155–175. doi: 10.1007/s00401-016-1662-x

Espeland, M. A., Rapp, S. R., Shumaker, S. A., Brunner, R., Manson, J. E., Sherwin, B. B., et al. (2004). Conjugated equine estrogens and global cognitive function in postmenopausal women: women's health initiative memory study. *JAMA* 291, 2959–2968. doi: 10.1001/jama.291.24.2959

Frick, K. M., Kim, J., Tuscher, J. J., and Fortress, A. M. (2015). Sex steroid hormones matter for learning and memory: estrogenic regulation of hippocampal function in male and female rodents. *Learn. Mem.* 22, 472–493. doi: 10.1101/lm.037267.114

Galea, L. A., Spritzer, M. D., Barker, J. M., and Pawluski, J. L. (2006). Gonadal hormone modulation of hippocampal neurogenesis in the adult. *Hippocampus* 16, 225–232. doi: 10.1002/hipo.20154

Garcia-Alloza, M., Robbins, E. M., Zhang-Nunes, S. X., Purcell, S. M., Betensky, R. A., Raju, S., et al. (2006). Characterization of amyloid deposition in the APPswe/PS1dE9 mouse model of Alzheimer disease. *Neurobiol. Dis.* 24, 516–524. doi: 10.1016/j.nbd.2006.08.017

Gilman, J. P., Medalla, M., and Luebke, J. I. (2017). Area-specific features of pyramidal neurons-a comparative study in mouse and rhesus monkey. *Cereb. Cortex* 27, 2078–2094. doi: 10.1093/cercor/bhw062

Gonçalves, J. T., Schafer, S. T., and Gage, F. H. (2016). Adult neurogenesis in the hippocampus: from stem cells to behavior. *Cell* 167, 897–914. doi: 10.1016/j.cell.2016.10.021

Hamilton, R. T., Rettberg, J. R., Mao, Z., To, J., Zhao, L., Appt, S. E., et al. (2011). Hippocampal responsiveness to 17β-estradiol and equol after long-term ovariectomy: implication for a therapeutic window of opportunity. *Brain Res.* 1379, 11–22. doi: 10.1016/j.brainres.2011.01.029

Hasan, W., Smith, H. J., Ting, A. Y., and Smith, P. G. (2005). Estrogen alters trkA and p75 neurotrophin receptor expression within sympathetic neurons. *J. Neurobiol.* 65, 192–204. doi: 10.1002/neu.20183

He, Y., Wei, M., Wu, Y., Qin, H., Li, W., Ma, X., et al. (2019). Amyloid β oligomers suppress excitatory transmitter release *via* presynaptic depletion of phosphatidylinositol-4,5-bisphosphate. *Nat. Commun.* 10:1193. doi: 10.1038/s41467-019-09114-z

Heikkinen, T., Kalesnykas, G., Rissanen, A., Tapiola, T., Iivonen, S., Wang, J., et al. (2004). Estrogen treatment improves spatial learning in APP + PS1 mice but does not affect β amyloid accumulation and plaque formation. *Exp. Neurol.* 187, 105–117. doi: 10.1016/j.expneurol.2004.01.015

Hung, A. J., Stanbury, M. G., Shanabrough, M., Horvath, T. L., Garcia-Segura, L. M., and Naftolin, F. (2003). Estrogen, synaptic plasticity and hypothalamic reproductive aging. *Exp. Gerontol.* 38, 53–59. doi: 10.1016/s0531-5565(02)00183-3

Katakowski, M., Chen, J., Zhang, Z. G., Santra, M., Wang, Y., and Chopp, M. (2007). Stroke-induced subventricular zone proliferation is promoted by tumor necrosis factor-α-converting enzyme protease activity. *J. Cereb. Blood Flow Metab.* 27, 669–678. doi: 10.1038/sj.jcbfm.9600390

Koebele, S. V., and Bimonte-Nelson, H. A. (2016). Modeling menopause: the utility of rodents in translational behavioral endocrinology research. *Maturitas* 87, 5–17. doi: 10.1016/j.maturitas.2016.01.015

Lagace, D. C., Fischer, S. J., and Eisch, A. J. (2007). Gender and endogenous levels of estradiol do not influence adult hippocampal neurogenesis in mice. *Hippocampus* 17, 175–180. doi: 10.1002/hipo.20265

Lee, D. C., Im, J. A., Kim, J. H., Lee, H. R., and Shim, J. Y. (2005). Effect of long-term hormone therapy on telomere length in postmenopausal women. *Yonsei Med. J.* 46, 471–479. doi: 10.3349/ymj.2005.46.4.471

Lee, J. P., Jeyakumar, M., Gonzalez, R., Takahashi, H., Lee, P. J., Baek, R. C., et al. (2007). Stem cells act through multiple mechanisms to benefit mice with neurodegenerative metabolic disease. *Nat. Med.* 13, 439–447. doi: 10.1038/nm1548

Levin-Allerhand, J. A., Lominska, C. E., Wang, J., and Smith, J. D. (2002). 17α-estradiol and 17β-estradiol treatments are effective in lowering cerebral amyloid-β levels in AβPPSWE transgenic mice. *J. Alzheimers Dis.* 4, 449–457. doi: 10.3233/jad-2002-4601

Levin-Allerhand, J. A., and Smith, J. D. (2002). Ovariectomy of young mutant amyloid precursor protein transgenic mice leads to increased mortality. *J. Mol. Neurosci.* 19, 163–166. doi: 10.1007/s12031-002-0027-1

Li, R., He, P., Cui, J., Staufenbiel, M., Harada, N., and Shen, Y. (2013). Brain endogenous estrogen levels determine responses to estrogen replacement therapy *via* regulation of BACE1 and NEP in female Alzheimer's transgenic mice. *Mol. Neurobiol.* 47, 857–867. doi: 10.1007/s12035-012-8377-3

Li, L., Xu, B., Zhu, Y., Chen, L., Sokabe, M., and Chen, L. (2010). DHEA prevents Aβ25–35-impaired survival of newborn neurons in the dentate gyrus through a modulation of PI3K-Akt-mTOR signaling. *Neuropharmacology* 59, 323–333. doi: 10.1016/j.neuropharm.2010.02.009

Liu, M. Y., Nemes, A., and Zhou, Q. G. (2018). The emerging roles for telomerase in the central nervous system. *Front. Mol. Neurosci.* 11:160. doi: 10.3389/fnmol.2018.00160

Lobanova, A., She, R., Pieraut, S., Clapp, C., Maximov, A., and Denchi, E. L. (2017). Different requirements of functional telomeres in neural stem cells and terminally differentiated neurons. *Genes Dev.* 31, 639–647. doi: 10.1101/gad.295402.116

Luine, V. N. (2014). Estradiol and cognitive function: past, present and future. *Horm. Behav.* 66, 602–618. doi: 10.1016/j.yhbeh.2014.08.011

Maki, P. M., Girard, L. M., and Manson, J. E. (2019). Menopausal hormone therapy and cognition. *BMJ* 364:l877. doi: 10.1136/bmj.l877

Marongiu, R. (2019). Accelerated ovarian failure as a unique model to study peri-menopause influence on Alzheimer's disease. *Front. Aging Neurosci.* 11:242. doi: 10.3389/fnagi.2019.00242

Micci, M. A., Krishnan, B., Bishop, E., Zhang, W. R., Guptarak, J., Grant, A., et al. (2019). Hippocampal stem cells promotes synaptic resistance to the dysfunctional impact of amyloid β oligomers via secreted exosomes. *Mol. Neurodegener.* 14:25. doi: 10.1186/s13024-019-0322-8

Moon, M., Cha, M. Y., and Mook-Jung, I. (2014). Impaired hippocampal neurogenesis and its enhancement with ghrelin in 5XFAD mice. *J. Alzheimers Dis.* 41, 233–241. doi: 10.3233/jad-132417

Mosconi, L., Pupi, A., De Cristofaro, M. T., Fayyaz, M., Sorbi, S., and Herholz, K. (2004). Functional interactions of the entorhinal cortex: an 18F-FDG PET study on normal aging and Alzheimer's disease. *J. Nucl. Med.* 45, 382–392.

Ovsepian, S. V., Antyborzec, I., O'Leary, V. B., Zaborszky, L., Herms, J., and Oliver Dolly, J. (2014). Neurotrophin receptor p75 mediates the uptake of the amyloid β (Aβ) peptide, guiding it to lysosomes for degradation in basal forebrain cholinergic neurons. *Brain Struct. Funct.* 219, 1527–1541. doi: 10.1007/s00429-013-0583-x

Pollard, K. J., Wartman, H. D., and Daniel, J. M. (2018). Previous estradiol treatment in ovariectomized mice provides lasting enhancement of memory and brain estrogen receptor activity. *Horm. Behav.* 102, 76–84. doi: 10.1016/j.yhbeh.2018.05.002

Provenzano, M. J., Minner, S. A., Zander, K., Clark, J. J., Kane, C. J., Green, S. H., et al. (2011). p75(NTR) expression and nuclear localization of p75(NTR) intracellular domain in spiral ganglion Schwann cells following deafness correlate with cell proliferation. *Mol. Cell. Neurosci.* 47, 306–315. doi: 10.1016/j.mcn.2011.05.010

Rahman, A., Schelbaum, E., Hoffman, K., Diaz, I., Hristov, H., Andrews, R., et al. (2020). Sex-driven modifiers of Alzheimer risk: a multimodality brain imaging study. *Neurology* doi: 10.1212/wnl.0000000000009781 [Epub ahead of print]

Rocca, W. A., Grossardt, B. R., and Shuster, L. T. (2010). Oophorectomy, menopause, estrogen, and cognitive aging: the timing hypothesis. *Neurodegener. Dis.* 7, 163–166. doi: 10.1159/000289229

Sha, S., Xu, J., Lu, Z. H., Hong, J., Qu, W. J., Zhou, J. W., et al. (2016). Lack of JWA enhances neurogenesis and long-term potentiation in hippocampal dentate gyrus leading to spatial cognitive potentiation. *Mol. Neurobiol.* 53, 355–368. doi: 10.1007/s12035-014-9010-4

Sotthibundhu, A., Li, Q. X., Thangnipon, W., and Coulson, E. J. (2009). Aβ(1–42) stimulates adult SVZ neurogenesis through the p75 neurotrophin receptor. *Neurobiol. Aging* 30, 1975–1985. doi: 10.1016/j.neurobiolaging.2008.02.004

Tanapat, P., Hastings, N. B., and Gould, E. (2005). Ovarian steroids influence cell proliferation in the dentate gyrus of the adult female rat in a dose- and

time-dependent manner. *J. Comp. Neurol.* 481, 252–265. doi: 10.1002/cne.20385

Taniuchi, N., Niidome, T., Goto, Y., Akaike, A., Kihara, T., and Sugimoto, H. (2007). Decreased proliferation of hippocampal progenitor cells in APPswe/PS1dE9 transgenic mice. *Neuroreport* 18, 1801–1805. doi: 10.1097/wnr.0b013e3282f1c9e9

Unger, M. S., Marschallinger, J., Kaindl, J., Hofling, C., Rossner, S., Heneka, M. T., et al. (2016). Early changes in hippocampal neurogenesis in transgenic mouse models for Alzheimer's disease. *Mol. Neurobiol.* 53, 5796–5806. doi: 10.1007/s12035-016-0018-9

Vedder, L. C., Bredemann, T. M., and McMahon, L. L. (2014). Estradiol replacement extends the window of opportunity for hippocampal function. *Neurobiol. Aging* 35, 2183–2192. doi: 10.1016/j.neurobiolaging.2014.04.004

Walf, A. A., Paris, J. J., and Frye, C. A. (2009). Chronic estradiol replacement to aged female rats reduces anxiety-like and depression-like behavior and enhances cognitive performance. *Psychoneuroendocrinology* 34, 909–916. doi: 10.1016/j.psyneuen.2009.01.004

Wang, C. C., Guo, Y., Zhou, M. M., Xue, C. H., Chang, Y. G., Zhang, T. T., et al. (2019). Comparative studies of DHA-enriched phosphatidylcholine and recombination of DHA-ethyl ester with egg phosphatidylcholine on ameliorating memory and cognitive deficiency in SAMP8 mice. *Food Funct.* 10, 938–950. doi: 10.1039/c8fo01822g

Wang, Y. J., Wang, X., Lu, J. J., Li, Q. X., Gao, C. Y., Liu, X. H., et al. (2011). p75NTR regulates Aβ deposition by increasing Aβ production but inhibiting Aβ aggregation with its extracellular domain. *J. Neurosci.* 31, 2292–2304. doi: 10.1523/JNEUROSCI.2733-10.2011

Wang, J., Zhao, C., Zhao, A., Li, M., Ren, J., and Qu, X. (2015). New insights in amyloid β interactions with human telomerase. *J. Am. Chem. Soc.* 137, 1213–1219. doi: 10.1021/ja511030s

Weisenburger, S., and Vaziri, A. (2018). A guide to emerging technologies for large-scale and whole-brain optical imaging of neuronal activity. *Annu. Rev. Neurosci.* 41, 431–452. doi: 10.1146/annurev-neuro-072116-031458

Xu, B., Yang, R., Chang, F., Chen, L., Xie, G., Sokabe, M., et al. (2012). Neurosteroid PREGS protects neurite growth and survival of newborn neurons in the hippocampal dentate gyrus of APPswe/PS1dE9 mice. *Curr. Alzheimer Res.* 9, 361–372. doi: 10.2174/156720512800107591

Zandi, P. P., Carlson, M. C., Plassman, B. L., Welsh-Bohmer, K. A., Mayer, L. S., Steffens, D. C., et al. (2002). Hormone replacement therapy and incidence of Alzheimer disease in older women: the Cache County Study. *JAMA* 288, 2123–2129. doi: 10.1001/jama.288.17.2123

Zhang, T., Chen, P., Li, W., Sha, S., Wang, Y., Yuan, Z., et al. (2019). Cognitive deficits in mice lacking Nsun5, a cytosine-5 RNA methyltransferase, with impairment of oligodendrocyte precursor cells. *Glia* 67, 688–702. doi: 10.1002/glia.23565

Zheng, J. Y., Liang, K. S., Wang, X. J., Zhou, X. Y., Sun, J., and Zhou, S. N. (2017). Chronic estradiol administration during the early stage of Alzheimer's disease pathology rescues adult hippocampal neurogenesis and ameliorates cognitive deficits in $A\beta_{1-42}$ mice. *Mol. Neurobiol.* 54, 7656–7669. doi: 10.1007/s12035-016-0181-z

Zheng, R., Zhang, Z. H., Chen, C., Chen, Y., Jia, S. Z., Liu, Q., et al. (2017). Selenomethionine promoted hippocampal neurogenesis via the PI3K-Akt-GSK3β-Wnt pathway in a mouse model of Alzheimer's disease. *Biochem. Biophys. Res. Commun.* 485, 6–15. doi: 10.1016/j.bbrc.2017.01.069

Conflict of Interest: The authors declare that the research was conducted in the absence of any commercial or financial relationships that could be construed as a potential conflict of interest.

frontiers in Aging Neuroscience

REVIEW
published: 06 August 2020
doi: 10.3389/fnagi.2020.00247

Stem Cells of the Aging Brain

Alexandra M. Nicaise[1]*, *Cory M. Willis*[1], *Stephen J. Crocker*[2] and *Stefano Pluchino*[1]*

[1]Department of Clinical Neurosciences and NIHR Biomedical Research Centre, University of Cambridge, Cambridge, United Kingdom, [2]Department of Neuroscience, University of Connecticut School of Medicine, Farmington, CT, United States

The adult central nervous system (CNS) contains resident stem cells within specific niches that maintain a self-renewal and proliferative capacity to generate new neurons, astrocytes, and oligodendrocytes throughout adulthood. Physiological aging is associated with a progressive loss of function and a decline in the self-renewal and regenerative capacities of CNS stem cells. Also, the biggest risk factor for neurodegenerative diseases is age, and current *in vivo* and *in vitro* models of neurodegenerative diseases rarely consider this. Therefore, combining both aging research and appropriate interrogation of animal disease models towards the understanding of the disease and age-related stem cell failure is imperative to the discovery of new therapies. This review article will highlight the main intrinsic and extrinsic regulators of neural stem cell (NSC) aging and discuss how these factors impact normal homeostatic functions within the adult brain. We will consider established *in vivo* animal and *in vitro* human disease model systems, and then discuss the current and future trajectories of novel senotherapeutics that target aging NSCs to ameliorate brain disease.

Keywords: neural stem cells, aging, senescence, cell metabolism, mitochondria, disease modeling, senotherapeutics

OPEN ACCESS

Edited by:
Cesar V. Borlongan, University of South Florida, United States

Reviewed by:
Claudio Grassi, Catholic University of the Sacred Heart, Italy
Laura Trujillo-Estrada, University of Malaga, Spain

***Correspondence:**
Alexandra M. Nicaise
an574@cam.ac.uk
Stefano Pluchino
spp24@cam.ac.uk

Received: *18 May 2020*
Accepted: *20 July 2020*
Published: *06 August 2020*

Citation:
Nicaise AM, Willis CM, Crocker SJ and Pluchino S (2020) Stem Cells of the Aging Brain. Front. Aging Neurosci. 12:247. doi: 10.3389/fnagi.2020.00247

INTRODUCTION

Aging is defined as the time-related decline of physiological functions that are necessary for survival eventually leading to the cessation of life (Harman, 2001; López-Otín et al., 2013). The general characteristics of aging, such as cognitive decline, cardiovascular defects, and metabolic changes affect all individuals at varying rates. While some endure aging in a healthy manner, defined as *healthy* aging, others age *unhealthily*, developing age-related disorders such as cardiovascular disease, cancer, Alzheimer's disease (AD), and diabetes (Chang et al., 2019; Cole et al., 2019). Genetic and environmental factors, such as smoking, exercise, and diet, impart significant alterations to normal physiology that define the rate an organism ages (Harman, 2001). This implies that though two people are the same chronological age their biological brain age may be significantly different (Franke and Gaser, 2019).

Measures have been developed and refined over the preceding decade to assay human brain age *in vivo*, including MRI to both measure gray matter volume and alterations in neural activity. The results from these studies, with due consideration to all caveats and limitations, have demonstrated that a "brain age" can be computed, establishing a novel idea of a "brain age gap." The "brain age gap" is defined as the gap between a person's chronological age and their biological brain age based on a pre-determined set of MRI criteria. This computational approach establishes how *healthy* or *unhealthy* an individual's brain age is and this data can then be extrapolated to then anticipate risk in the development of age-associated brain diseases and can be extended to anticipate the risk of developing age-associated brain diseases (Cole and Franke, 2017). For example, dementia/AD

and multiple sclerosis (MS) exhibit the strongest discordance between actual chronological age and predicted age using an unbiased machine MRI learning tool (Kaufmann et al., 2019). Typically, the effects of advancing chronological age, including cognitive decline, become significantly apparent between the ages of 60–75 years as evidenced by the significant loss of total tissue volume, which coincides with the peak onset of age-associated neurodegenerative diseases (Scahill et al., 2003; Chad et al., 2018; Franceschi et al., 2018). These diseases can also occur earlier in life in subjects with higher genetic and environmental risk factors, which suggests an accelerated aging phenotype may play a role. Similar deficits in cognitive function correlated with changes in brain volume are observed in aged humans and rodents (20–24 months old), making them a valuable model (Hamezah et al., 2017). Furthermore, most of these morphological changes are correlated with increased synaptic dysfunction, which leads to the gain-of-function of behavioral deficits observed in aging, such as cognitive decline, learning, memory, and sensory deficits (Petralia et al., 2014). Both human and rodent work has suggested a correlation between a decrease in the number of synaptic connections and an increase age-related cognitive decline (Dickson et al., 1995; Peters et al., 2008). The predominant hallmark used to compute biological age in humans is brain volume, which is associated with a decrease in synaptic connections, suggesting a lack of renewal, replacement, and regeneration on a cellular level.

Neural stem cells (NSCs) persist throughout mammalian life, residing within the subgranular zone (SGZ) of the hippocampus and the subventricular zone (SVZ) of the lateral ventricles, where they maintain the capacity for self-renewal and maturation into new neurons and glia. NSCs are mitotic cells characterized by symmetric divisions (self-renewal) during early development. They gradually shift to asymmetrical division to generate differentiated cells and maintain a multipotent reservoir (Gage, 2000; Alvarez-Buylla and Lim, 2004; Zhao et al., 2008; Gage and Temple, 2013; Obernier and Alvarez-Buylla, 2019). Although the proliferation and differentiation of NSCs are predominantly restricted to the embryonic period in rodents, the capacity to produce new neurons has been shown to persist into adulthood, however, whether this is an evolutionarily conserved process in humans remains controversial (Sorrells et al., 2018; Moreno-Jiménez et al., 2019). Evidence for neurogenesis in healthy adult humans is provided by the presence of NSCs and immature neurons both expressing cell division markers (Moreno-Jiménez et al., 2019; Tobin et al., 2019). Also, neurogenesis has been reported using radioactive carbon-based cell dating and BrdU incorporation studies (Eriksson et al., 1998; Spalding et al., 2013). These dynamics in humans have been observed to change with disease, such as AD, where immature neurons are found greatly reduced, and MS, where NSCs are found increased in the SVZ (Nait-Oumesmar et al., 2007; Moreno-Jiménez et al., 2019).

In adult mice, NSCs residing within the specialized niches are known to play important roles in maintaining cognitive functions, such as learning and memory formation, and contributing to repair and regeneration of injured tissue, which includes their neurogenic capability (Imayoshi et al., 2008; Lugert et al., 2010). These new neurons contribute to learned behavior such as odor reward association and discrimination (Grelat et al., 2018; Li et al., 2018). Advancing age-related biological changes are associated with a significant decline in neurogenesis, concomitant with dynamic alterations to the niche microenvironment that disrupt normal homeostatic functions (Kuhn et al., 1996).

Several tissues and cell-based biological biomarkers have been identified that reflect age-related processes, such as senescent cell burden, genomic instability, on-going chronic inflammation, and telomere attrition (**Figure 1**; López-Otín et al., 2013). The accumulated burden of aging defects contributes to overall brain degeneration, drastically impacting the regenerative potential of the NSC niches. Also, ongoing disease burden has been shown to accelerate biological brain aging in AD/dementia, PD, amyotrophic lateral sclerosis (ALS), MS, and Huntington's disease (HD), all neurodegenerative diseases with demonstrated dysfunction in NSC compartments (Horgusluoglu et al., 2017; Hou et al., 2019).

In this review article, we will highlight how intrinsic, as well as extrinsic regulators of age and disease, impart drastic changes to the endogenous NSC niche, how this is modeled *in vitro* and *in vivo*, and new therapies on the horizon targeted at aging NSCs to ameliorate brain disease.

BRAIN STEM CELL NICHES IN AGING AND DISEASE

Mammalian NSCs within niches adopt various states including quiescence, activation, and differentiation, however, the proportions of cells in those states change dramatically with increasing biological age (Obernier and Alvarez-Buylla, 2019). A large body of evidence has revealed that aging negatively impacts these niches, ultimately impacting regenerative functions. One major component being cellular senescence, which is a process in which cells experience a decrease in their proliferative capacity and undergo profound alterations which inherently changes their normal functions, impacting surrounding cells, and eventually leading to age-associated organ dysfunction (Baker and Petersen, 2018). Senescent cells accumulate with age and impact regeneration and homeostatic functions within stem cell niches, and experimental evidence in mice has linked the elimination of these cells to an increase in lifespan and a delay in age-associated disorders (Baker et al., 2011; Yousefzadeh et al., 2020). They disturb the microenvironment by secreting a wide-range of factors, including pro-inflammatory proteins, chemokines, and interleukins (ILs) which have a profound effect on other cells around them, termed the senescence-associated secretory phenotype (SASP; Coppé et al., 2010; Angelova and Brown, 2019; Cohen and Torres, 2019). Senescent cells have been identified in the aging brain of both humans and rodents, particularly in the context of neurodegenerative disease (Baker and Petersen, 2018). Senescence is initiated by a myriad of aging-related factors, both intrinsic and extrinsic, which will be reviewed in this section.

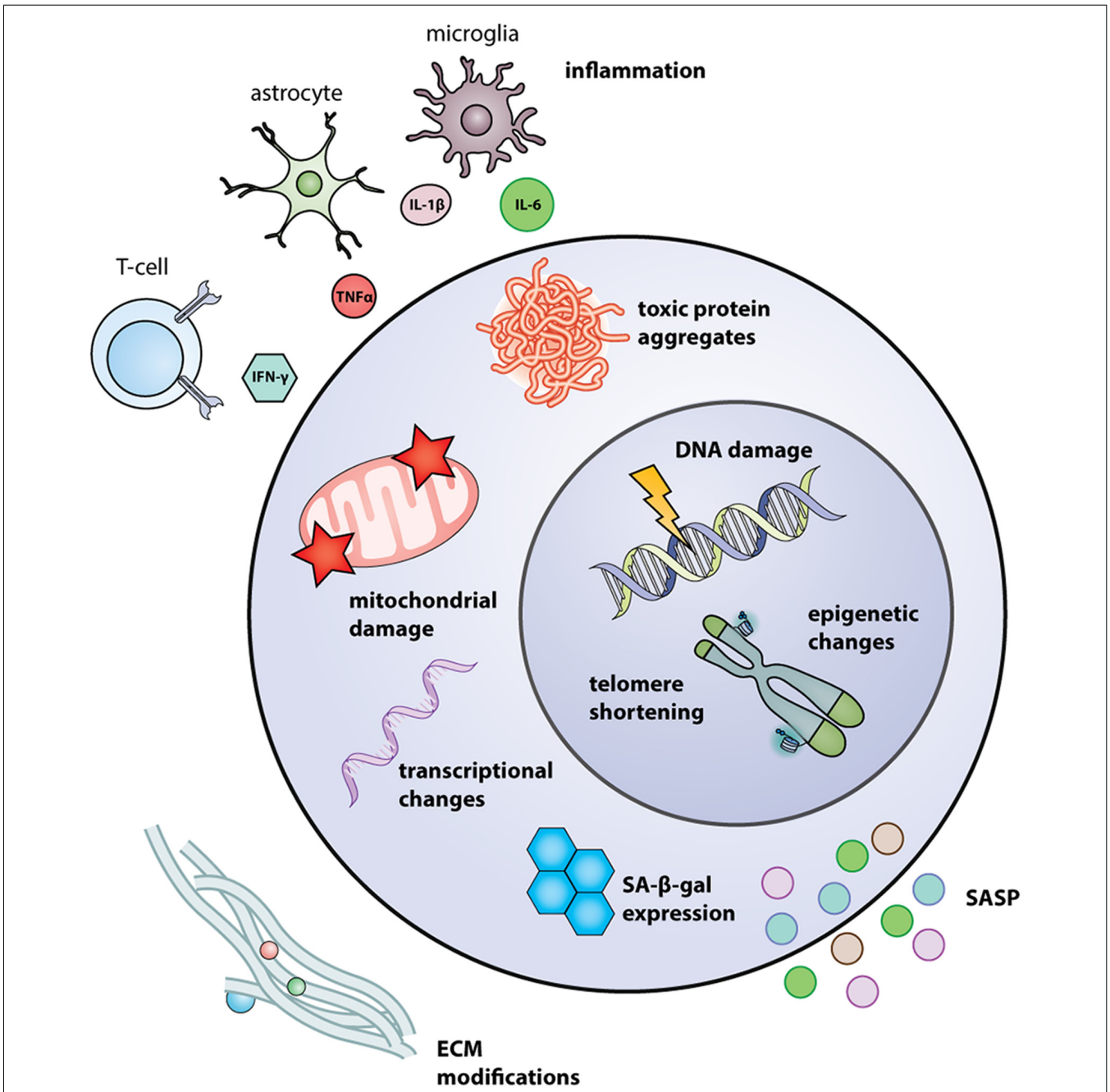

FIGURE 1 | Intrinsic and extrinsic regulators of NSC aging. Intrinsic regulators include transcriptional changes, such as upregulation of $p16^{Ink4a}$ and p53; mitochondrial damage, resulting from mtDNA mutations and excessive ROS; toxic protein aggregates, due to a dysregulation in proteostasis; SA-β-gal expression, induced by senescence; telomere shortening and DNA damage caused by replication-associated stress and dysfunctional repair amongst other factors; and changes in epigenetic patterns. Extrinsic regulators include SASP, secreted by nearby senescent cells, and secreted by senescent NSCs themselves; modifications in ECM, such as increases in HA composition; and inflammatory molecules secreted by activated astrocytes, microglia, and T-cells. Abbreviations: ECM, extracellular matrix; HA, hyaluronic acid; mtDNA, mitochondrial DNA; NSC, neural stem cells; ROS, reactive oxygen species; SASP, senescence-associated secretory phenotype.

DNA Damage and Repair

Several studies have demonstrated that chronological aging results in the increased accumulation of DNA damage in tissues and cells (Kenyon, 2010; Sperka et al., 2012). For example, replication-associated DNA damage leads to mutations and increases genomic instability with advancing age (Adams et al., 2015). In line with this observation, NSCs isolated from the SVZ of 20-month old-aged mice displayed significant genetic aberrations compared to NSCs isolated from 2-month old mice, which is attributed to the increased accumulation of

mutations over replicative cycles (Bailey et al., 2004). NSCs avoid replication stress by entering an inactive stage called quiescence, highlighted by a low basal metabolic rate and limited self-renewal. Following disease or tissue damage, reactive oxygen species (ROS) production stimulates adult NSCs to re-enter the cell cycle to replenish damaged and dying cells. Coincidentally, this results in replication-induced stress and an increased frequency of DNA mutations (Wang Y. Z. et al., 2011). This highlights the importance of maintaining a proper balance between quiescence and activation within NSC niches to minimize replicative stress and maximize DNA integrity during chronological and biological aging.

Genomic instability with advancing age is thought to be the result of increased accumulation of DNA damage in tandem with a diminished DNA damage response. It has been reported that NSCs fail to proliferate and undergo appropriate differentiation in the absence of functional DNA repair mechanisms (**Figure 2**; Marin Navarro et al., 2020). Under normal non-aged conditions cells still face genotoxic insults from endogenous by-products such as ROS, inflammatory mediators, and lipid peroxidation while maintaining DNA damage response and repair processes (Mani et al., 2020). This includes the five major repair pathways, base excision repair (BER), nucleotide excision repair (NER), mismatch repair (MMR), homologous recombination (HR), and non-homologous end joining (NHEJ), which all involve a complex interplay of genes and their ensuing proteins. These pathways attempt to repair the lesioned area, however, breakdowns in signaling activate apoptotic mechanisms to inhibit the propagation of the lesioned DNA (Petr et al., 2020). The efficiency in these processes declines with age for reasons that remain unclear leading to a build-up of DNA damage. Evidence points to transcriptional repression of DNA repair genes in aging cells as well as age-related decreases in repair enzymes and activities accounting for the increased DNA damage with age (Szczesny et al., 2003; Imam et al., 2006; Collin et al., 2018). Additionally, DNA damage response elements such as NER, BER, MMR, and NHEJ are important in the maintenance of the NSC niche with defective elements associated with age-related neurodegenerative diseases such as ALS, AD, and PD (Liu and Martin, 2006; Sepe et al., 2016; Shanbhag et al., 2019).

Retrotransposable elements (RTEs) are DNA elements that have been copied and pasted from one location to another and can also give rise to genomic instability through mutations and double-strand breaks which in turn impacts gene regulation (Terry and Devine, 2019). Further, increased activity of RTEs has been observed in the aged human brain and results in genome instability in NSCs (Bollati et al., 2009; Maxwell et al., 2011). One example being long interspersed nuclear element-1 (LINE-1), which is normally repressed by *Sox2*, a gene required for the maintenance of NSCs with diminished expression in the hippocampal SGZ with advancing age (Muotri et al., 2005; Carrasco-Garcia et al., 2019). Decreased expression of *Sox2* within the hippocampal SGZ in aged mice is inversely correlated with the increased expression of the cyclin-dependent kinase inhibitor $p16^{Ink4a}$, an established biomarker of senescent cells (Carrasco-Garcia et al., 2019). Specifically, LINE-1 becomes transcriptionally derepressed in $p16^{Ink4a}$ expressing cells, which triggers a type-I interferon (IFN-1) response and initiates the secretion of pro-inflammatory cytokines, proteases, and immune modulators inhibiting NSC proliferation and leading to age-associated chronic inflammation (Coppé et al., 2010; Kulkarni et al., 2017; De Cecco et al., 2019).

Genomic instability can also result from telomere shortening, one of the major mechanisms proposed to induce organismal aging (López-Otín et al., 2013). Telomeres are specialized structures that cap the ends of chromosomes protecting from gene erosion and fusion with neighboring chromosomes (Sahin and Depinho, 2010). In humans, the average telomere length declines in advancing age due to truncation occurring following a lifetime of cell division, with the endogenous enzyme telomerase maintaining telomere length to protect against genomic instability and intrinsic DNA damage (Arai et al., 2015). Importantly, adult NSCs within the rodent SVZ are known to have high telomerase activity to meet the proliferative and self-renewal needs of the cell (Caporaso et al., 2003), however telomerase in isolation cannot maintain telomere length within NSC niches. In fact, the deleterious effects of shortened telomeres in NSCs are mediated, in part, by p53, a tumor suppressor protein and potential biomarker of aging and senescence with increased expression in aged tissues (Rodier et al., 2007). Mutant mice overexpressing p53 have a reduction in NSC proliferation, highlighting a role for p53 in the aging NSC niche (Medrano et al., 2009). When considered together, this work underscores the importance of genomic stability in the maintenance and proper functioning of adult NSCs (**Figure 2**).

Intrinsic Regulators

The frequency of intrinsic regulators of DNA damage increases with advancing age, negatively influencing the expression of regulatory genes important for homeostasis (**Figure 2**; Espada and Ermolaeva, 2016). For example, members of the forkhead box transcription factor family O (FoxO) are indispensable in maintaining NSC proliferation and self-renewal throughout adulthood by regulating a program of genes that controls quiescence, differentiation, and oxygen metabolism (Paik et al., 2009; Renault et al., 2009). Constitutive knock-out of *Foxo3* in mice reduces the total NSC pool and leads to decreased self-renewal and impaired ability to generate different neural lineages (Renault et al., 2009). Supporting this notion, diminished regulatory gene expression either indirectly or directly underlies NSC dysfunction in advancing age. A follow-up study identified an alternative function of *Foxo3* in directly regulating autophagy genes in NSCs with its loss leading to the accumulation of protein aggregates and resultant homeostatic dysfunction (Audesse et al., 2019). This is of particular importance as protein aggregation is a key histological hallmark in many age-related neurodegenerative diseases, such as the accumulation of amyloid-β (Aβ) and tau tangles in AD and alpha-synuclein deposits in PD. *Foxo3* remains an attractive target for further functional studies and therapeutic targeting as genome-wide association studies have identified a single-nucleotide polymorphism (SNP) within the *FOXO3* gene that

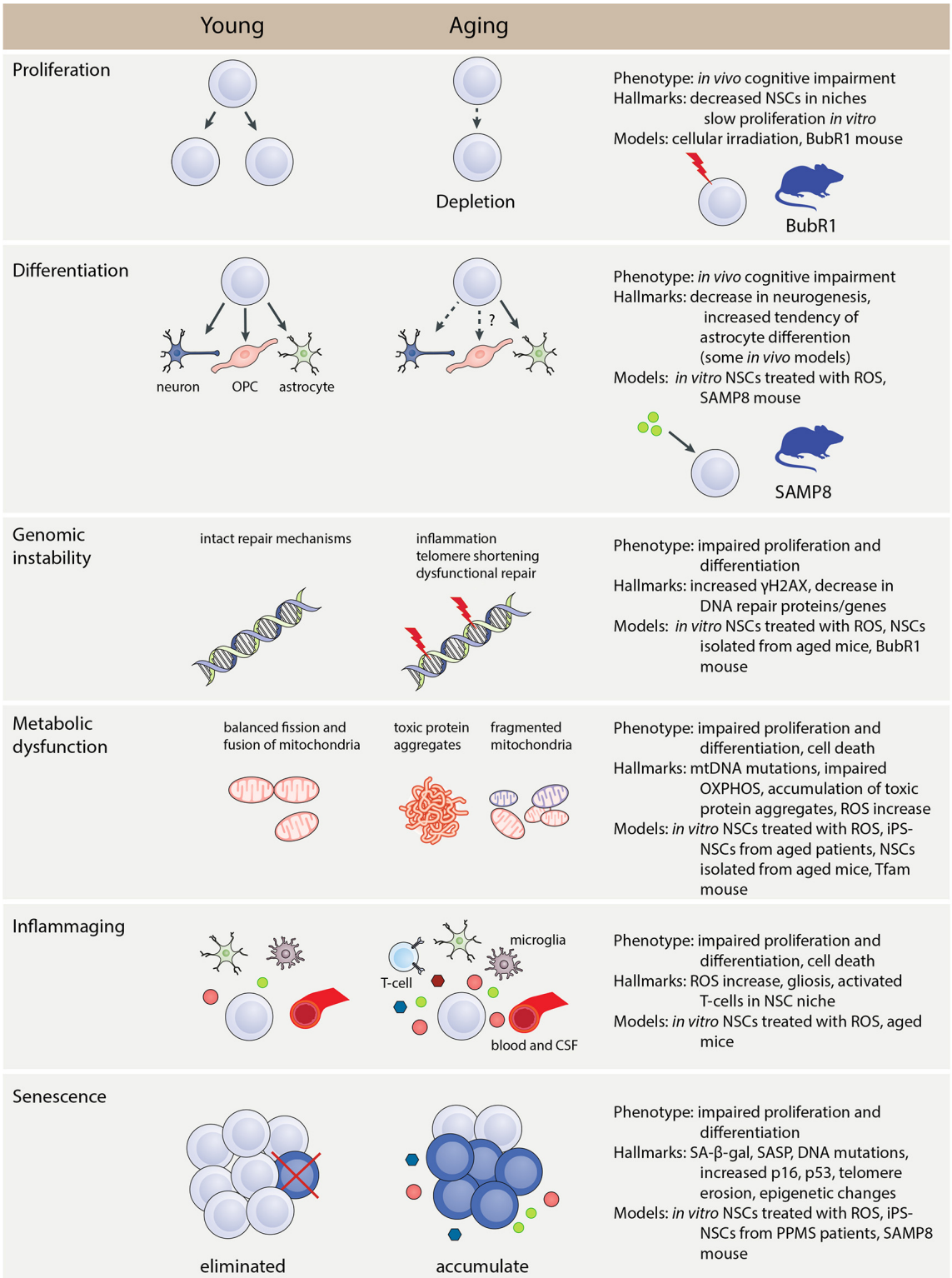

FIGURE 2 | Hallmarks and phenotype of NSC aging. The main phenotypes, hallmarks, and models that can be used to investigate aspects of NSC aging. Genomic instability, metabolic dysfunction, inflammaging, and senescence are all aspects that affect the normal proliferation and differentiation function of NSCs. These causes of aging have specific hallmarks that can be identified using *in vivo* and *in vitro* methods. Abbreviations: CSF, cerebrospinal fluid; iPSC, induced pluripotent stem cell; mtDNA, mitochondrial DNA; NSC, neural stem cell; OPC, oligodendrocyte progenitor cell; OXPHOS, oxidative phosphorylation; PPMS, primary progressive multiple sclerosis; ROS, reactive oxygen species; SA-β-gal, senescence-associated β-galactosidase; SASP, senescence-associated secretory phenotype.

is associated with extreme longevity in humans (Willcox et al., 2008; Flachsbart et al., 2009).

Intrinsic DNA damage also occurs in mitochondrial (mt)DNA. A higher incidence of mtDNA mutations is known to be associated with physiological brain aging and in age-related neurodegenerative diseases such as AD and PD (Zapico and Ubelaker, 2013; Cha et al., 2015). Somatic mtDNA mutations accumulate in all tissues with age in a stochastic manner (Chinnery et al., 2002; Bratic and Larsson, 2013). It is still unclear why somatic mutations in mtDNA increase with age, but most evidence points to increased pro-inflammatory insults (Larsson, 2010). An alternative hypothesis implicates replication errors that occur during embryogenesis which undergo expansion in adult life and accumulate (Larsson, 2010). Therefore, further studies investigating the cause of mtDNA mutations in aging are warranted.

Once an arbitrary threshold is surpassed, where the levels of accumulated mtDNA mutations surpass normal/healthy mtDNA, energy metabolism is impaired (**Figure 2**; Wallace, 2010). This is significant in tissues with high energy demands such as the NSC niches of the developing and injured adult brain (Cavallucci et al., 2016). mtDNA integrity is maintained *via* repair machinery such as 8-oxoguanine DNA glycosylase (OGG1), a DNA repair protein that restores damaged mtDNA. This repair machinery is important in maintaining NSC multipotency as evidenced in NSCs from *Ogg1* knockout-mice which spontaneously accumulate mtDNA damage, shifting their differentiation pattern towards an astrocytic lineage vs. neuronal (Wang W. et al., 2011). Further, two separate reports have identified a decrease in human *OGG1* activity in the AD brain (Mao et al., 2007; Jacob et al., 2013). mtDNA is also susceptible to damage due to a lack of histone protection and proximity to ROS generated by mitochondria (Alexeyev et al., 2013). An overabundance of ROS in NSC niches impairs adult neurogenesis (Rola et al., 2007). The accumulation of mtDNA mutations over time results in respiration deficiency and the further, excessive production of ROS (Murphy, 2009). Mitochondrial ROS act as regulators to facilitate gene expression changes that impact NSC fate decisions (Maryanovich and Gross, 2013). Ablating the mitochondrial transcription factor A (*Tfam*) in mice produces histological and pathological hallmarks of aging in the hippocampus of mice, including impaired proliferation and neurogenesis in NSCs (Beckervordersandforth et al., 2017a). Interestingly, reductions in the TFAM gene and protein expression are observed in advancing age and age-associated neurodegenerative diseases such as PD, AD, and HD (Kang et al., 2018). Overall, these studies point to the natural accumulation of mtDNA mutations in normal aging, which may be accelerated in neurodegenerative disorders, leading to widespread NSC dysfunction.

Epigenetics

Epigenetic modifications naturally occur and accumulate with age resulting in long-lasting functional changes to cells and tissues (**Figure 1**). These modifications are attributed to cell-intrinsic and extrinsic factors inherited through subsequent cell divisions (Feil and Fraga, 2012; Podobinska et al., 2017). An example of this is histone acetylation and deacetylation, which is regulated by histone acetyltransferase (HAT) and deacetylase (HDAC) enzymes, respectively. Acetylation of histones relaxes the chromatin structure increasing accessibility to the gene for transcription. In aged mice, an imbalance in the acetylation and deacetylation of genes in the hippocampus is correlated with memory impairment (Peleg et al., 2010). Epigenetic modifications also occur through DNA methylation, a crucial process regulating and controlling gene expression by various DNA methyltransferases (DNMTs). Changes in the DNA methylation status are observed in the brain of human post-mortem subjects with advanced age (Numata et al., 2012). Interestingly, the biological aging of tissue correlates with patterns in DNA methylation termed the "epigenetic clock" (Horvath et al., 2012). Tet methylcytosine dioxygenase 2 (TET2), a regulator of DNA methylation, is reduced in human aging and somatic mutations are associated with an elevated risk of developing age-related disorders such as stroke (Burgess, 2015). Similarly, Tet2 expression is reduced in NSCs from aged rodents with complete ablation inhibiting normal neurogenesis (Gontier et al., 2018). Many different epigenetic factors are known to alter adult NSC renewal and differentiation capacity, such as mixed-lineage leukemia 1 (Mll1), a chromatin remodeling factor identified in mice, yet their role in age and age-associated diseases remain to be elucidated (Lim et al., 2009).

Nucleoporins (Nups) are a family of proteins that form channels within the nuclear envelope, thus regulating the flow of macromolecules, and have emerged as epigenetic regulators of NSC differentiation (Raices and D'Angelo, 2017). Differentiation of NSCs is accompanied by changes in nuclear reorganization which result in gene expression changes mediated by Nup expression (Capelson et al., 2010). Furthermore, Nups physically interact with the genome to control transcriptional programs. In NSCs, NUP153 is essential for maintaining stemness *via* its complex with the transcription factor *Sox2*. In turn, the silencing of *Nup53* results in neuronal differentiation, associated with a loss of *Sox2* expression (Toda et al., 2017). NUP153 has also been implicated in age-related diseases, such as AD (Sakuma and D'Angelo, 2017; Leone et al., 2019). In NSCs isolated from the 3xTg-AD mouse model, *Nup153* expression was significantly reduced, inhibiting proliferation, migration, and neuronal differentiation. Instead, *Nup153* overexpression in AD NSCs rescued defective proliferation and migration and enhanced neuronal differentiation. Thus, *Nup153* acts as an epigenetic hub for a variety of co-regulators (Leone et al., 2019). Different outcomes in NSC differentiation associated with *Nup153* expression may also be context dependent and in turn change the epigenetic behavior of *Nup153*. A further understanding in how Nups alter NSC behavior in aging and disease is warranted.

Cell Metabolism

The metabolism of stem cells plays a vital role in maintaining cellular homeostasis through the regulation of various processes, such as the generation of energy and proteins along with the breakdown and elimination of waste. Changes in the balance of these functions alter NSC behavior, especially the

propensity to proliferate and differentiate (**Figure 2**). Many of these basic homeostatic functions, such as mitochondrial maintenance, proteostasis, and nutrient sensing, are altered with age and considered hallmarks of aging (López-Otín et al., 2013). Rapamycin, a drug that targets the mammalian target of rapamycin (mTOR) pathway, which is critical to cellular metabolism, has been identified to prolong rodent lifespan, further elucidating the importance of cellular metabolism in aging (Harrison et al., 2009). Probing the mechanisms by which aging alters the variety of metabolic aspects is important in the discovery of new avenues for therapeutic targeting.

Considerable activity into understanding the biological processes that modify NSC metabolism in advancing age have demonstrated the importance of proteostasis, or protein homeostasis, in maintaining cellular health. During advancing age, breakpoints in proteostasis result in the accumulation of misfolded proteins and associated cellular damage and dysfunction (**Figure 1**; Koga et al., 2011). Several neurodegenerative diseases are identified by the accumulation of misfolded and damaged proteins, such as Aβ in AD, alpha-synuclein deposits in PD, and Lewy bodies in dementia, which are known to negatively affect NSC niches (Basaiawmoit and Rattan, 2010). NSCs from aged mice have been shown to accumulate protein aggregates in defective lysosomes, limiting normal digestion and removal in quiescent NSCs of aged rodents. Lysosomal dysfunction, and in turn accumulation of insoluble protein aggregates, prevented quiescent NSCs from aged animals to return to an activated, proliferative state. Enhancing lysosomal function through transcription factor EB (TFEB) activity, a master regulator of lysosomes restores NSC activation ability (Leeman et al., 2018). A functional outcome of damaged protein accumulation in NSCs with advancing age is a weakening of the diffusion barrier which maintains the distribution of cellular components during replication or differentiation. This prevents asymmetric segregation of damaged proteins and further propagates the accumulation of misfolded proteins in daughter cells (Moore et al., 2015). Also, accumulation of protein fragments in neurodegenerative diseases such as AD, PD, and HD alters normal NSC function and can promote a senescent phenotype (Conforti et al., 2013; He et al., 2013; Zasso et al., 2018).

Changes in NSC metabolism help balance self-renewal and differentiation, which includes mechanisms involved in energy generation (Rafalski and Brunet, 2011; Ochocki and Simon, 2013). A major emphasis has been placed on contextualizing mitochondrial dysfunction and NSC aging and whether it supports the *mitochondrial theory of aging*, which proposes that chronic mitochondrial dysfunction underlies the great majority of age-related deficits (López-Otín et al., 2013). This theory is not without merit, as the capacity of antioxidants to scavenge ROS in the brain is impaired with age, allowing the extra- and intracellular accumulation of ROS and subsequent oxidative stress and damage (Siqueira et al., 2005). Quiescent NSCs are intrinsically glycolytic unless activated for proliferation wherein a metabolic switch to mitochondrial respiration *via* oxidative phosphorylation (OXPHOS) occurs to meet the new energy demands of the cell (Coller, 2019). However, aging impairs mitochondrial respiration through a variety of factors that damages the machinery necessary for controlled activation of NSC proliferation and differentiation, directly impacting adult neurogenesis (**Figure 2**; Llorens-Bobadilla et al., 2015; Stoll et al., 2015). For example, conditional deletion of the energy-producing mitochondrial enzyme complex alpha-ketoglutarate-dehydrogenase reduces the proliferative potential of NSCs residing in the SGZ of the hippocampus (Calingasan et al., 2008). Alterations in other mitochondrial properties, such as fusion and fission, impair NSC proliferation in the SGZ of the adult rodent hippocampus leading to deficits in spatial learning (Khacho et al., 2016). Additionally, stem cells upon division apportion aged mitochondria, leaving a daughter cell with an accumulation of aged, fragmented mitochondria causing a deficit in stemness properties (Katajisto et al., 2015). Therefore, normal mitochondrial function is critical in maintaining healthy NSC niches, allowing NSCs to react appropriately to the changing energy needs of the brain.

Nutrient sensing by NSCs within niches is inherently linked to the regulation of their activation state. Recently, mechanisms through which calorie restriction promotes longevity in NSCs have been uncovered (Van Cauwenberghe et al., 2016). Calorie restriction prevents age-related declines in neurogenesis, which likely occurs *via* a decrease in pro-inflammatory signaling in the niche (Apple et al., 2019). The effects of calorie restriction are partly mediated through the insulin/insulin-like growth factor (IGF)-1 signaling (IIS) pathway which responds to changes in glucose and is found to regulate NSC function (Rafalski and Brunet, 2011; Vitale et al., 2019). Inhibition of IGF-1 signaling in rodent NSCs inhibits age-related declines and promotes self-renewal of the NSC niche (Chaker et al., 2015). Intriguingly, signaling through the IIS pathway results in the downstream activation of mTOR, a pathway with major implications in aging (Verburgh, 2015). The mTOR pathway acts as a nexus in amino acid concentration signaling and is a critical regulator of cellular metabolism and growth. mTOR signaling is important in regulating the quiescent vs. an active proliferative state of adult NSCs (Nieto-González et al., 2019). For example, inhibition of mTOR complex 1 (mTORC1) induces a reversible quiescent phenotype, which is corroborated by *in vivo* findings that diminished mTOR activity in the aged NSC niche can be reversed by pharmacological intervention leading to increased proliferation and neurogenesis (Paliouras et al., 2012; Romine et al., 2015). However, future studies must proceed with caution when artificially increasing and decreasing mTOR activity. The mTOR pathway is hyperactivated in both pre-clinical rodent models of AD and in AD patients with associated NSC dysfunction, suggesting that finely-tuned mTOR activity is needed to maintain niche homeostasis (Perluigi et al., 2015). In this regard, recent evidence has identified reductions in mTOR activity *via* rapamycin supplementation concomitant with the amelioration of age-dependent spatial memory deficits and increased lifespan in mice (Majumder et al., 2012). Whether rapamycin treatment has an indirect or direct role in modulating the aged NSC niche has yet to be tested.

Physical exercise has a positive effect on cognitive functions in older adults, also reflected in rodent research (Colcombe et al.,

2006). It has been suggested that aerobic exercise boots aspects of brain metabolism, including upregulation in the hippocampus of enzymes involved in glutamate turnover and glucose catabolism (Ding et al., 2006; Matura et al., 2017). This results in enhanced proliferation of NSCs and increases in the number of immature neurons in middle-aged mice (Wu et al., 2008). Voluntary running in aged mice increases secretion of growth hormone stimulating proliferation and neurogenesis in the hippocampal niche of aged mice (Yang et al., 2015). Moreover, increases in BDNF and IGF-1 significantly increase after voluntary running, improving neurogenic potential (Adlard et al., 2005). This data suggests that exercise aids in the proliferation of NSC niches, and the eventual production of immature neurons through overall changes in metabolic components.

Oxygen Sensing

Oxygen sensing is a potent regulator of the aged NSC niche. Hypoxia-inducible factors (HIFs) are transcription factors that regulate the cellular response to changes in oxygen levels, of which HIF1α plays a prominent role in NSCs. Conditional deletion of HIF1α in NSCs of adult mice resulted in a loss of NSC proliferation within the SVZ, highlighting its importance in maintaining the adult NSC niche (Li et al., 2014). Further, chronic mild hypoxia results in dual yet opposing NSC functions. Chronic mild hypoxia increases NSC proliferation in the presence of mitogens such as EGF and bFGF, whereas chronic mild hypoxia promotes differentiation into neurons in the absence of these mitogens (Xie and Lowry, 2018). Hypoxia is known to play a role in multiple neurodegenerative diseases, including AD, PD, ALS, and HD, where it promotes inflammation and neuronal damage. However, the extent of the alterations to the NSC niche is unknown (Jha et al., 2018). Impaired oxygen sensing is reported in aged rodent brains suggesting a potential mechanism leading to neurogenic decline with age (Yeo, 2019).

Extracellular Matrix

It is well-established that the ECM is an important component of the NSC niche serving as an inert scaffold to anchor cells and dynamically regulate cell fate (**Figure 1**; Gattazzo et al., 2014). NSC adherence to ECM molecules such as laminin (Ln), fibronectin (Fn), and hyaluronan (HA) is facilitated *via* integrin receptors, which initiate cellular responses stimulating proliferation or differentiation. Concerning advancing age, Su et al. (2017) demonstrated that increased HA deposition within the dentate gyrus (DG) directly contributes to age-related reductions in NSC proliferation and differentiation by overactivation of the CD44 receptor. Further, increased HA deposition is observed in aged human brain tissue and in demyelinated MS plaques, the latter impeding remyelination (Back et al., 2005; van Horssen et al., 2007; Lepelletier et al., 2017). Stem cell behavior is also dependent on tissue stiffness, which is determined by ECM composition and organization. ECM-derived mechanical signals act through Rho GTPases to activate cellular pathways to alter NSC lineage commitment. When NSCs are cultured on stiff matrices neurogenesis is suppressed whereas blocking Rho GTPase in NSCs rescues differentiation on stiff matrices (Keung et al., 2011). Follow-up studies identified that soft hydrogels direct cultured adult NSCs to differentiate into neurons, whereas harder gels were biased towards glial cell differentiation (Saha et al., 2008). Counterintuitively, despite overall brain stiffness increasing with age in both rodents and humans (Elkin et al., 2010; Takamura et al., 2020), decreased stiffness in neurodegenerative diseases is linked to a loss of adult neurogenesis (Klein et al., 2014). These differences could be due to regional heterogeneity in brain stiffness, which is observed in post-mortem tissue of AD and PD patients, highlighting the complexity of ECM regulation and deposition in the aging and diseased brain (Berg, 2011; Murphy et al., 2016). Moreover, the presence of glial scar tissue and brain tumors can drastically change the mechanical properties of the affected brain region in near an NSC niche and, in turn, the behavior. Thus, the ECM plays a major role in modulating the activity of the NSC niche in both aging and disease, although the extent to which it drives total brain aging, and perhaps neurodegeneration, remain outstanding lines of research.

Extrinsic Regulators, Immunity, and Inflammation

Key drivers in the development of an aged phenotype in adult NSCs involve extrinsic large-scale systemic changes reflected in circulating fluids, including blood, cerebrospinal fluid (CSF), and lymph which can affect the NSC niche (**Figure 1**). The blood, CSF, and lymph display increases in pro-inflammatory mediators with both age and neurodegenerative disease exacerbating ongoing brain-wide inflammation and NSC niche dysfunction (Pluvinage and Wyss-Coray, 2020). Recent work has uncovered alterations in the human plasma proteome with age, which become exacerbated with AD (Lehallier et al., 2019). Further study in what these proteomic changes biologically confer is warranted.

Due to the SVZ being uniquely situated above the lateral ventricles, exposure to blood and CSF factors routinely occurs. Systemic factors have been identified in aged mice that promote age-induced dysfunction, such as C-C motif chemokine 11 (CCL11), a chemokine increased in the blood of aged mice which directly correlates with a decrease in neurogenesis. Systemic exposure of young mice to recombinant CCL11 impaired hippocampal neurogenesis, which is rescued with a CCL11 blocking antibody. Interestingly, CCL11 is increased in aged human plasma and CSF (Villeda et al., 2011). β2-microtubulin (B2M) is another circulating pro-aging factor identified in old mice as well as humans. It negatively regulates regenerative functions in the hippocampus, including NSC proliferation and neurogenesis (Smith et al., 2015).

On the other hand, aged mice with cognitive deficits show improvement after parabiosis with young mice, highlighting how circulating systemic factors can directly influence brain homeostasis (Villeda et al., 2011, 2014). For example, several circulating factors have been identified in young mice which provide rejuvenation to aged NSC niches, one being growth differentiation factor 11 (GDF11), a bone morphogenetic protein. This protein was found to be present in higher concentrations in young mouse serum compared to aged mouse

serum. Also, after heterochronic parabiosis of aged mice to young mice, GDF11 was found increased in the aged mice. Administration of a recombinant version of GDF11 to aged mice reproduces similar beneficial effects, such as increased NSC proliferation and differentiation, as observed in the parabiosis studies (Katsimpardi et al., 2014). Further work delving into an earlier developmental stage found that umbilical cord plasma from humans contains proteins that improve cognitive function in aged mice, namely tissue inhibitor of metalloproteinases 2 (TIMP2). TIMP2 is enriched in human cord plasma, young mouse plasma, and in young mouse hippocampi, and declines with age. Immunodepletion of TIMP2 from cord plasma before intravenous administration into aged mice blocked the beneficial cognitive effects emphasizing the importance of systemic factors in brain aging (Castellano et al., 2017).

The blood-brain barrier (BBB) is comprised of a microvasculature unit of brain endothelial cells (BECs), which are exposed to circulating factors on their luminal side and brain cells on their abluminal side. BECs in aged mice express an inflammatory transcriptional profile, including upregulation of vascular cell adhesion molecule 1 (VCAM1). Soluble VCAM1 is increased in the plasma of both aged humans and mice. Plasma collected from aged mice and infused into young mice induced a significant increase in VCAM1 expression in the BEC population, which caused microglial activation and decreased the amount of proliferating NSCs. Genetic deletion of *Vcam1* in BECs during adulthood reduced microglial activation and increased NSC proliferation (Yousef et al., 2019). Given that aged BECs display a pro-inflammatory profile, exposure to circulating pro-inflammatory factors may further amplify this phenotype through induction of VCAM1 expression as well as induce intrinsic cellular changes associated with aging.

Aging and neurodegenerative diseases are associated with impaired integrity of the BBB, which creates a more permissive environment for the entry of peripheral immune cells into the brain parenchyma (Erdö et al., 2017). Infiltrating T cells secreting high levels of IFN-γ have been identified in aged NSC niches. Here, increased IFN-γ led to impaired NSC proliferation and maintenance of a quiescent phenotype, impeding differentiation. Markedly, histological analysis of post-mortem human brain tissue from elderly individuals identified a similar pro-inflammatory T cell infiltrate in the SVZ (Dulken et al., 2019). The aberrant infiltration of T cells into the SVZ in aged mice is supported by previous work demonstrating that under chronic inflammatory conditions, such as in the rodent model of MS, experimental autoimmune encephalomyelitis (EAE), an autoreactive T-cell-mediated disease model, T cell activation is associated with a dysfunction in the proliferation and migration of NSCs due to persistent inflammation (Pluchino et al., 2008; Rasmussen et al., 2011).

The term *inflammaging* is used to describe major changes in aging associated with the accumulation of soluble inflammatory factors, tissue damage burden, and activation of immune cells (López-Otín et al., 2013). Overall, the above work supports the concept that pro-inflammatory molecules from circulating fluids as well as infiltrating cells affect the NSC niche (**Figure 1**). Progenitor cells in the brain also have the capability of secreting pro-inflammatory factors. One example being senescent stem cells in progressive MS brains secreting high mobility group box 1 (HMGB1), a known SASP factor and inflammatory molecule, which inhibits the differentiation of oligodendrocyte progenitor cells (OPCs) *in vitro* (Davalos et al., 2013; Nicaise et al., 2019). HMGB1 has previously been found to be elevated in the hippocampus and CSF of aged rats where it promotes microglial inflammation by stimulating toll-like receptors (TLR)-2 and -4 (Fonken et al., 2016). Inflammatory factors can also be secreted by brain cells within the niche microenvironment. A recent article highlighted the impact of age-associated changes within the niche, including the activation of microglia, the resident brain macrophage population (Solano Fonseca et al., 2016). Increased clusters of activated microglia and peripheral infiltrating monocytes expressing increased levels of tumor necrosis factor-α (TNF-α), interleukin-1 β (IL-1β), and IL-6 were identified in the aged SVZ while increased levels of TGF-β1 were found to be released from SVZ endothelial cells (Pineda et al., 2013). *In vitro* modeling demonstrated that resting, non-activated microglia promote NSC proliferation and differentiation into neuronal lineages, whereas activated pro-inflammatory microglia suppressed differentiation (Solano Fonseca et al., 2016). The pro-inflammatory cytokine IL-1β, which is released by activated microglia and astrocytes, increases VCAM1 expression in NSCs repressing them in a quiescent state, inhibiting neurogenesis, and diminishing expansion of the NSC pool through self-renewal (Kokovay et al., 2012). Microglia are not the only contributors to *inflammaging*. Astrocytes become reactive with advancing age wherein they secrete pro-inflammatory molecules (e.g., IFNs) directly impacting local cell networks (Clarke et al., 2018). Corroborating data from animals lacking global expression of IFN receptors demonstrate an absence of age-related declines in NSC activation; rather, NSCs readily activate from quiescence as observed in young animals (Kalamakis et al., 2019). Unsurprisingly, an increased response to IFN is detected in the aged human brain which is thought to negatively affect brain functions (Baruch et al., 2014). Overall, these data suggest that chronic inflammation in the brain, whether a result of age, on-going neurodegenerative disease activity, or a combination of both, maintains NSCs in a quiescent state, repressing their capacity to proliferate and differentiate (**Figure 2**).

These findings demonstrate that both systemic and local factors are altered with age and disease, as well as widespread accumulation of senescent cells, leading to profound impacts on NSCs and niche microenvironment. However, it remains to be understood how alterations in the absolute amounts of these factors in advancing age and age-related neurodegenerative diseases lead to enhanced or diminished endogenous NSC function.

Importantly, intrinsic and extrinsic changes associated with aging do not occur in isolation, rather they interact synergistically. For example, changes in diet are reflected in fluctuations of physiologic factors in the CSF, such as IGF-1 and insulin, which in turn contributes to intrinsic epigenetic regulation of NSCs (Mihaylova et al., 2014; Mir et al., 2017).

Further, cell-intrinsic aging, which is reflected in senescent NSCs, alters the extrinsic microenvironment *via* the activity of the SASP.

SASP then leads to an amplification of local cellular dysfunction as SASP factors spread to and impair the normal functioning of local cells which in turn leads to further cell-intrinsic changes and beginning the cycle anew (Coppé et al., 2010).

Therefore, NSC aging cannot be attributed to a single factor, rather it involves a complex interplay of both intrinsic, including DNA damage, and extrinsic factors, such as secretion of inflammatory factors, which all contribute to dysfunction alterations in the stem cell niche.

MODELING BRAIN AGING *IN VIVO*

Studying brain aging *in vivo* is a challenging endeavor given that the regulation of age is heterogenous amongst different tissues and species (Zahn et al., 2007), however, research has primarily focused on evolutionarily conserved mechanisms that control aging to better facilitate data extrapolation to humans. Numerous mouse models of aging have been established and extensively reviewed (Yeoman et al., 2012; Heng et al., 2017; Folgueras et al., 2018). Nevertheless, the field is still in its infancy, and major gaps in our knowledge exist regarding how the aging process impacts the central nervous system (CNS), specifically NSC function and maintenance. Here, we are going to briefly cover findings from mouse models of accelerated aging in which an NSC phenotype has been described.

Mouse models recapitulating aspects of genomic instability associated with aging have been established and extensively used to study this biological process in non-CNS tissue as reviewed elsewhere (Specks et al., 2015; Folgueras et al., 2018). Many mouse models of aging have been generated based on genetic correlates of progeroid human syndromes. Progeroid syndromes are a group of genetic disorders that make individuals biologically older than they are, typically due to a monogenic mutation in DNA repair mechanisms or lamin (Gordon et al., 2014). However, there are some mouse models based on progeroid syndromes that do not exhibit an NSC dysfunction, one example being a mouse model Hutchinson-Gilford progeria syndrome (HGPS). HGPS is caused due to a mutation in the lamin A gene, resulting in the build-up of the truncated form of lamin A, called progerin. Despite lamin A being ubiquitously expressed by various cell types, induced mutation of *LMNA* in the brain of mice did not affect behavior or neurogenesis assays of hippocampal cells, suggesting a protective mechanism (Baek et al., 2015). However, there are other relevant mouse models of aging that possess an NSC phenotype which will be further discussed.

Benzimidazole-Related 1 (BubR1) Mutants

BubR1 is a spindle assembly checkpoint kinase, encoded by *Bub1b*, that is critical for the accurate separation of duplicated chromosomes during cell division and maintaining genomic stability (Wassmann and Benezra, 2001; Cleveland et al., 2003). Reduced BubR1 expression induces aneuploidy, which affects genomic stability (Baker et al., 2004). Further, deficiencies in DNA repair pathways cause progeria syndromes in humans which display CNS pathologies (Gordon et al., 2014). Natural aging significantly reduces BubR1 expression within the DG of the hippocampus in an age-dependent manner, with the largest reductions observed at 24 months of age. Interestingly, it only takes 2 months for BubR1 insufficient mice ($BubR1^{H/H}$) to reach a similar expression level to that of wild-type mice at 24 months of age. NSC proliferation and maturation were significantly reduced in $BubR1^{H/H}$ mice impairing hippocampal neurogenesis despite having no impact on neuronal survival (**Figure 2**; Yang et al., 2017). An independent study identified a similar impairment in NSC proliferation following lentiviral knockdown of *BubR1* in wild-type adult mice, confirming the strength of the $BubR1^{H/H}$ mouse model in recapitulating aspects of NSC aging. Further, a follow-up study using the $BubR1^{H/H}$ mice found that inhibition of the endogenous Wnt antagonist, secreted frizzled-related protein 3 (sFRP3), rescued NSC proliferation in the hippocampal DG in these mice (Cho et al., 2019).

These data highlight how mouse models of genomic stability can be employed to not only rapidly and faithfully recapitulate specific hallmarks of aging *in vivo* but allow for a mechanistic understanding of the aged NSC phenotype.

Telomerase Mutants

Telomerase-deficient mice have served as a model system to study the adverse cellular and organismal consequences of wide-spread endogenous DNA damage signaling activation *in vivo*. In these mice, telomere loss and uncapping provoke progressive tissue atrophy, stem-cell depletion, and impaired tissue injury responses (Sahin and Depinho, 2010). Telomere attrition in NSCs is of particular interest as loss of proliferative potential and stem cell exhaustion with age is thought to be correlated with the age-related cognitive decline observed in mice and humans (Ferrón et al., 2009). Currently, there are two established telomere attrition mouse models with an associated NSC phenotype.

In one mouse model, mice carrying a homozygous germline deletion for the telomerase RNA component gene ($Terc^{-/-}$) showed a complete loss of *Terc* expression and telomerase activity (Blasco et al., 1997). Inducing telomere shortening in these mice requires successive generations (>3 generations) of mating to establish phenotypic changes (Blasco et al., 1997). Third generation $Terc^{-/-}$ mice show reduced neurogenesis in the SVZ of the DG and loss of neurons in the hippocampus and frontal cortex, suggestive of an impairment in the proliferation and maturation capacity of NSCs (Ferrón et al., 2004; Rolyan et al., 2011; Khan et al., 2015).

In the other mouse model, deficiency in telomerase reverse transcriptase ($Tert^{-/-}$), a catalytic subunit of the telomerase complex, induces aging phenotypes similar to that observed in $Terc^{-/-}$ mice, such as impaired spatial memory, dendritic development, and neurogenesis (Strong et al., 2011; Zhou et al., 2017).

Interestingly, in a tamoxifen-inducible $Tert^{-/-}$ mouse model (TERT-ER) somatic telomerase reactivation reversed these observed deficits through the restoration of proliferating $Sox2^{+}$

NSCs and new-born neurons, consistent with the integral role of SVZ NSCs in the generation and maintenance of mature neurons in adulthood (Jaskelioff et al., 2011).

Thus, these transgenic mice provide excellent models for the study of the deficits in proliferation observed in NSCs of aged animals.

Mitochondrial DNA Mutants

It is well accepted that mitochondria play a central role in the maintenance of NSCs in development and throughout adulthood, with oxidative phosphorylation an essential regulator of NSC proliferation and differentiation (Cabello-Rivera et al., 2019; Khacho et al., 2019). Consequently, age-associated alterations in mitochondrial function are thought to have a profound effect on the ability of NSCs to self-renew (Khacho et al., 2019). Mutations in the mitochondrial genome increase with age (Vermulst et al., 2007) and are associated with an increase in the production of mitochondrial ROS, which are potent signaling molecules that can impair stem cell self-renewal capacity (Hämäläinen et al., 2015).

Mouse models of advanced aging accumulate mtDNA mutations (PolgA and Tfam), associated with reductions in quiescent NSCs and a loss of self-renewal in the adult SVZ (Ahlqvist et al., 2012; Beckervordersandforth et al., 2017b). Further, NSC-specific ablation of nicotinamide phosphoribosyltransferase (Nampt), a rate-limiting enzyme that salvages the essential metabolic cofactor nicotinamide adenine dinucleotide (NAD^+) and the main source of NSC NAD^+ required for cell-cycle progression, reduced the NSC pool and their proliferation in adult mice (Stein and Imai, 2014). Importantly, these phenotypes can be rescued *via* supplementation of N-acetyl-L-cysteine and nicotinamide mononucleotide in the PolgA and Nampt mouse models, respectively (Ahlqvist et al., 2012; Stein and Imai, 2014).

Therefore, mouse models of accelerated aging as a result of mitochondrial dysfunction can serve not only a basic research role but also in the development of therapies aimed at reversing these aging phenotypes.

SAMP8 Mice

A non-transgenic mouse model of accelerated aging exists. SAMP8 mice are a specific strain of inbred mice that exhibit a senescence-accelerated phenotype, which could be used to study how intrinsic homeostatic mechanisms of NSCs change with age. This short-lived strain progressively develops learning and memory deficits, along with a multisystemic aging phenotype (Takeda, 2009). The mice develop increased oxidative stress and astrogliosis in the brain, along with an accelerated loss of the NSC pool associated with a rise in astrocyte differentiation (**Figure 2**; Soriano-Cantón et al., 2015).

Consideration must be taken when interpreting results from these mice as extensive astro- and microgliosis is observed in parallel with the deficits in NSCs (Soriano-Cantón et al., 2015). No current studies have investigated the potential impact activated astrocytes and microglia in the (accelerated) aging hippocampus have on resident NSCs. Therefore, these mouse models provide a valuable tool to not only study cell-specific effects of aging but also in untangling the cell-cell interactions of NSCs and resident (or peripheral) cells in the context of aging.

MODELING BRAIN AGING IN A DISH WITH STEM CELL TECHNOLOGIES

To model human brain diseases in a dish, many laboratories rely on induced pluripotent stem cells (iPSCs) rather than somatic aged brain cells, which are rare and difficult to obtain. Additionally, human post-mortem samples reflect cell states at the end stage of the disease, hindering the study of disease pathogenesis. To generate iPSCs, primary human cells, such as fibroblasts or blood cells, are reprogrammed to an embryonic-like state, similar to embryonic stem cells (ESCs), through the expression of Yamanaka transcription factors. iPSCs are then given cues to direct differentiation towards the mature cell of interest to model disease. Typically, iPSCs are used to model diseases with genetic origins, such as ALS (*SOD1* mutation), familial PD (mutations in *Parkin* and *PINK1*), and HD (*HTT* mutation), yet many sporadic forms of these and other diseases occur with increasing age, such as sporadic PD, ALS, and progressive MS (PMS; Niccoli and Partridge, 2012; Reeve et al., 2014). iPSCs generated with specific mutations and deletions reflective of the disease state are an invaluable tool for understanding how familial genetic alterations change cell phenotype. However, the consideration of aging signatures is rarely considered.

Mimicking age-related defects in cells has proven difficult as reprogramming acts as a *developmental reset*, removing some of the known aging markers that were evident in the somatic cell of origin (Studer et al., 2015). These markers include epigenetic patterns, DNA damage, mitochondrial dysfunction, telomere length, and senescence, which are diminished or absent either during iPSC induction and/or further differentiation into the cell of interest (López-Otín et al., 2013).

The following reprogramming into iPSCs, several age-associated markers (including genetic and proteomic signatures) were reset, and cells retained a youthful phenotype (Miller et al., 2013). Despite this evidence, it is still unclear to what extent markers of the cell of origin are retained as it has also been shown that reprogrammed iPSCs can exhibit differentiation biases when further differentiated into a cell type of interest. This is of particular importance not only for cells in disease models but identifying what constitutes an aging signature vs. a disease-related signature. For example, NSCs differentiated from iPSCs reprogrammed from primary progressive MS (PPMS) patient fibroblasts and primary blood mononuclear cells exhibit a senescence phenotype compared to age-matched healthy patients (Nicaise et al., 2019). PPMS NSCs secrete SASP factors *in vitro* and inhibit remyelination in an *in vivo* model of PPMS, which was attributed to a dysfunctional phenotype arising from intrinsic defects in NSC function (Nicaise et al., 2017). Whether the NSCs retained an epigenetic or genetic signature unique to PPMS disease during iPSC reprogramming is unknown (Nicaise et al., 2019). This may also indicate that labile disease-associated markers which are lost with reprogramming are not necessary to recapitulate salient features of the disease or aging

in the reprogrammed cells, therein pointing to the unmodified processes as playing a more important role in the preservation of "age" or disease underlying the utility of these cellular models. In support of these findings, a higher frequency of age-related mtDNA mutations is identifiable in iPSCs reprogrammed from fibroblasts of aged individuals compared to reprogrammed fibroblasts from young individuals. This work demonstrates that cellular reprogramming does not completely remove epigenetic markers nor the propensity of aged cells to accumulate mutations (Kang et al., 2016). Nor does iPSC reprogramming abrogate the potential for the study of idiopathic forms of the disease, as iPSC-derived astrocytes from non-genetic forms of ALS recapitulate the disease-related phenotypes of genetically confirmed ALS iPSC-astrocytes (Haidet-Phillips et al., 2011). Overall, these studies raise further questions regarding the conservation of age-related changes under disease conditions or whether disease conditions exacerbate the expression of markers of cellular aging (**Table 1**).

There is no universally agreed upon and established metric for determining cellular age, however, DNA methylation patterns are observed to correlate with chronological age, termed "epigenetic age." One model which uses DNA methylation patterns is named Horvath's model and is based on 353 CpG methylation sites in cells and tissues that allow for the quantifiable measurement of cellular biological age as well as an estimation of age acceleration (i.e., contrasting DNA methylation age with chronological age; Horvath et al., 2012). The specific methylation sites correlate to 0 years of age in ESCs, are reflected in somatic cells as the age of the donor but become largely erased upon iPSC reprogramming (Horvath et al., 2012; Horvath, 2013; Sheng et al., 2018).

Instead, direct induction of somatic cells to induced NSCs (iNSCs), retains 5–30% of the original aged methylation pattern according to the Horvath model, making them an ideal candidate to study aging both in the context of health and disease (Sheng et al., 2018). Direct induction of cells bypasses the pluripotency step, wherein somatic cells are forced to express the Yamanaka factors transiently then cued to become NSCs using growth factors *in vitro* (Thier et al., 2012). Recent work profiled markers of aging in young and aged blood cells, as well as iPS-NSCs and iNSCs from the same patients, and somatic fetal NSCs. Blood cells from aged patients match the estimated age based on Horvath's model and possess shortened telomeres and an aged transcriptome, which was absent in the iPS-NSCs. Rather, iNSCs retain specific methylation patterns observed in the blood cells and shortened telomere length, while iPS-NSCs closely match the somatic fetal-derived NSCs (Sheng et al., 2018; **Table 1**). Whether these DNA methylation patterns are reflective of aging within cells or causative transcriptomic changes inducing cellular dysfunction is unknown.

The forced expression of neurogenic transcription factors in fibroblasts results in the generation of directly induced neurons (iNs), which are further differentiated *in vitro* to obtain a more mature neuronal subtype (Vierbuchen et al., 2010).

Induced motor neurons (iMNs) from primary fibroblasts or iPS-NSCs retain many of the aging hallmarks of the old donors, including increased DNA damage foci (γH2AX), SA-β-galactosidase activity, and loss of heterochromatin and nuclear organization (Tang et al., 2017). Aging signatures in iMNs derived from iPS-NSCs were largely erased. Further work using both iPSC-derived neurons and iNs from aged patients identified that decreased Ran-binding protein 17 (RanBP17) in aged iNs is responsible for the age-dependent loss of nucleocytoplasmic organization, which is reset in iPSCs (Mertens et al., 2015). Also, mitochondrial dysfunction present in the somatic cell is exacerbated in aged iNs, supporting the theory of metabolic dysfunction driving brain aging (Hoffman et al., 2017; Kim et al., 2018; **Table 1**).

The culmination of this work highlights the power of direct induction in disease modeling to further our understanding of the processes underlying age-related deficits in cells (Liu et al., 2016; Nekrasov et al., 2016). Unfortunately, caveats remain with this technology, such as the glaring fact that neurons are post-mitotic, restricting their use in large-scale applications, such as drug screens, due to the lack of a proliferative intermediate cell. However, their value lies with the insight into understanding neuronal aging in the context of health and disease. In the future it will be important to explore how disease-associated and aging phenotypes can be retained in iNSCs, and if direct induction into other brain cell types, such as astrocytes and oligodendrocytes, will uncover unknown roles of these cells in aging and disease.

Despite iPSCs losing some markers of aging during the reprogramming process, they are a valuable tool that can generate, theoretically, endless amounts of specialized cells for researchers to investigate. Some genetic mutations have been found to accelerate aging, including point mutations within the lamin A (*LMNA*) gene, which was identified in HGPS. Modification of the *LMNA* transcript results in a truncated form of lamin A called progerin. Progerin acts to shorten telomeres, inflict DNA damage, and encourage cellular senescence. Interestingly, iPSCs from patients with HGPS do not show an accumulation of progerin and lack the cellular alterations associated with accelerated aging, however, this phenotype is reinstated following iPSC differentiation into smooth muscle cells (Liu et al., 2011). This system was applied to iPSC-derived neurons from PD patients to determine the effect of aging on this disease. The researchers transfected progerin into iPSC-derived dopaminergic (DA) neurons from both healthy and genetic PD subjects and discovered disease-specific phenotypes. Progerin transfected PD cells developed an aging phenotype displayed by the progressive loss of tyrosine hydroxylase (TH) expression, enlarged mitochondria, and Lewy-body-precursor inclusions compared to healthy cells transfected with progerin, despite these cells still displaying accelerated aging signatures such as DNA damage foci (Miller et al., 2013). This work indicates that forced progerin expression can induce age-associated marker expression, but it is unknown if this method faithfully recapitulates cellular phenotypes observed in advancing age and disease.

Hydroxyurea (HU), used for the treatment of leukemia, disrupts cellular proliferation, and has been found to induce senescence in human cells (Park et al., 2000). Treatment of rodent NSCs *in vitro* with (HU) robustly induces cellular senescence identified by increased p53 and $p16^{Ink4a}$ expression,

TABLE 1 | List of studies using human stem cells to study cellular brain aging and disease.

Cell type	Donor ages (years)	Disease	Phenotypes and markers	Reference
iPSCs	24–72	None	Increased frequency of mitochondrial DNA mutations with age.	Kang et al. (2016)
iPS-NSCs	45–66	PPMS	Displayed senescence markers, secreted pro-inflammatory factors inhibiting OPC differentiation.	Nicaise et al. (2019)
hES-NSCs treated with hydroxyurea	Embryonic	None	Exhibited cellular senescence, impaired mitochondrial metabolism.	Daniele et al. (2016)
iNSCs	30–60	None	Cells retained 5–30% of donor cells epigenetic aging markers.	Sheng et al. (2018)
iPS-neurons with progerin overexpression	11–96	PD and HGPS	Dendrite degeneration, loss of TH, increased DNA damage and mitochondrial ROS.	Miller et al. (2013)
iPS-neurons treated with telomerase inhibitor	N/A	PD	Increased DNA damage, reduction in dendrites, increased mitochondrial ROS.	Vera et al. (2016)
iNs	0–89	None	Transcriptomic aging, loss of nucleocytoplasmic organization.	Mertens et al. (2015)
iNs	6–71	HD	HD gene expression increased DNA damage and ROS production, protein aggregates.	Victor et al. (2018)
iNs	0–89	none	Mitochondrial dysfunction—impaired energy production, lower mitochondrial membrane potential.	Kim et al. (2018)
iNs	37–71	ALS	Soma shrinkage, hypoactivity.	Liu et al. (2016)

Abbreviations: ALS, amyotrophic lateral sclerosis; HD, Huntington's disease; hES, human embryonic; HGPS, Hutchinson-Gilford progeria syndrome; iNs, induced neurons; iNSCs, induced neural stem cells; iPS, induced pluripotent stem; NSC, neural stem cell; OPC, oligodendrocyte progenitor cell; PD, Parkinson's disease; PPMS, primary progressive multiple sclerosis; ROS, reactive oxygen species; TH, tyrosine hydroxylase.

SA-β-galactosidase staining, and downregulation of DNA repair proteins, which has also been replicated in human NSCs *in vitro* (Daniele et al., 2016). This model led to the formation of aging hallmarks through DNA damage, similar to ROS-induced damage in the brain, yet it is unknown if it faithfully recapitulates every aspect of aging, including telomere shortening and Horvath DNA methylation patterns (Dong et al., 2014; **Table 1**). HU treatment of NSCs derived from disease models, either directly induced or from iPSCs, has yet to be investigated but may yield interesting results.

Ionizing irradiation, which causes severe DNA damage and inhibits the proliferation of NSCs, is used to study senescence *in vitro*, however, it is unknown how well this faithfully recapitulates cellular hallmarks of aging (Schneider, 2014).

The aforementioned studies, which are summarized in **Table 1**, describe models that recapitulate some, but not all, of the key characteristics of cellular aging. However, each model comes with its own set of limitations. Thus far, iNs retain the largest number of aging markers identified within the parent cell, including maintenance of DNA methylation age, transcription of aging-associated factors, and mitochondrial dysfunction. Unfortunately, iNs do not capture the entire gestalt of the aging brain, nor do they have a proliferative intermediate to derive other cell types, but they are ideal for studying neurons in the context of diseases of aging. Their use in modeling aging and age-related disease is reviewed in depth elsewhere (Mertens et al., 2018). iNSCs may prove more useful for further interrogation of aging in disease as iNSCs are known to retain 5–30% of age-related DNA methylation markers from the cell of origin and have the capability to differentiate into astrocytes, oligodendrocytes, and microglia when prompted. iPS-NSCs from patients with PPMS have shown a senescent phenotype, however, iNSCs have yet to be used to model any age-associated disease. Forced expression of verified aging-associated proteins and treatment with inducers of senescence are viable alternatives in creating cellular aging hallmarks. Therefore, induced cellular aging may serve as a method to study how certain proteins or extrinsic factors affect pathways related to cellular aging in specific cell types, but their faithfulness in capturing the natural aging and disease process is debated. Since aging is a multifactorial process, applying a multipronged approach (i.e., disease based iNSCs or iPS-NSCs treated with cellular stressors) will help further elucidate new pathways and enhance our understanding of aging and disease. As such, these models may be especially useful in the sporadic forms of diseases, such as MS, PD, AD, and ALS, where no obvious genetic causes exist, or affect more than one cell type in the brain and involve aging.

NOVEL THERAPEUTICS FOR BRAIN AGING

With the emerging picture of experimental and pathological data pointing to disease-associated aging among progenitor cell populations, how might this be targeted for therapeutic benefit? Certainly, approaches such as caloric restriction and lifestyle can influence the risk of disease, but for some conditions, a patient's ability or compliance for these approaches would also represent a challenge. Hence, pharmacological approaches to affect the aged cells within tissues are being actively explored as viable strategies to limit disease progression and/or stimulate endogenous regeneration and recovery (**Table 2**).

Drug screens using NSCs are not as common as disease-specific cell types such as oligodendrocytes for MS or neurons in diseases such as AD and PD. However, when considering

TABLE 2 | List of novel therapeutics for brain aging.

Class	Definition	Drugs/Agents available	Mechanism of action	Citations using therapeutics on CNS cells
Senomorphics	Compounds that actively alter the physiology of senescent cells.	Metformin, rapamycin	Metformin—acts on Akt to inhibit mTOR Rapamycin—inhibits mTOR	Neumann et al. (2019) and Nicaise et al. (2019)
Senolytics	Compounds that actively kill senescent cells.	A combination of dasatinib (D) and quercetin (Q), fisetin	D—an inhibitor of tyrosine kinases. Q—inhibits PI3K Fisetin—inhibits mTOR	Currais et al. (2018) and Zhang et al. (2019)
NSC Transplantation	NSCs grafted into CNS.	Allogenic mouse NSCs, NSCs with neurotrophic supplementation.	Cell replacement strategy, secrete beneficial factors.	Park et al. (2013) and Zhang et al. (2017)

Abbreviations: CNS, central nervous system; mTOR, mammalian target of rapamycin.

the potentially influential role of senescent NSCs in the context of impaired regeneration or functionality, the paucity of high throughput or high content screens using rodent NSCs, or disease-specific NSCs, represents a potential opportunity for therapeutic interventions for a range of neurological conditions. Conceptually, the effect of NSCs as a source of disease-related impairment would mean that drug screens using NSCs would not only impart effects for neurogenesis but potentially also a means to address microgliosis, astrogliosis, and promote myelin regeneration (Kim and Jin, 2012). In terms of the latter, targeting cellular senescence in NSCs could represent a means by which to affect cognitive decline which is linked to reduced myelination with advancing age (Wang F. et al., 2020). Similarly, the diminished neuroendocrine function of the hypothalamus is associated with the cognitive decline with advancing age and a consequence of loss of hypothalamic NSC functions (Zhang et al., 2013). This loss of function is a result of the NSC senescence of hypothalamic NSCs (Xiao et al., 2020).

Using primary neurospheres of murine hypothalamic NSCs, the long non-coding RNA Gm31629 was found to be reduced with aging and function as a biomarker of cellular senescence through a stabilized interaction with Y-box1 (YB-1) protein (Xiao et al., 2020). Based on this, nuclear magnetic resonance (NMR) was applied to understand how Gm31629 conferred stability to YB-1 to then perform a molecular docking and virtual screen of a library of natural small molecule compounds that identified theaflavin 3-gallate (TF2A; Xiao et al., 2020). This compound, a theaflavin found in black tea, was found to reverse senescence-like changes in senescent cells, and administration to 12-month-old mice reduced the rate of age-related decline (Xiao et al., 2020). These findings prompt several conclusions: (i) NSCs are an important site of cellular senescence; (ii) NSCs can exert widespread functions in aged animals throughout the body; and (iii) NSCs can be effectively used to screen and identify anti-senescence agents. From these data, future screens employing human disease-specific NSCs would be warranted to address the role of cellular senescence in this population plays in contributing to neuropathology and disease progression.

Further screens of existing chemical libraries have yielded nomenclature to describe two categories of senotherapeutic agents, termed "senomorphics" and "senolytics" (**Table 2**).

Senomorphics

Senomorphic agents are compounds that actively alter the physiology of aged cells, thereby mitigating their influence on the cellular environments in which they reside (**Table 2**; Tchkonia et al., 2013). Specifically, these compounds disrupt or block the production and release of pro-inflammatory factors that comprise the SASP (Farr and Khosla, 2019). Senomorphics thereby block the paracrine effects of senescent cells on other cells, limiting the impact of the SASP on impaired tissue function and/or regenerative potential. Examples of senomorphic agents which have been explored in the context of aging in demyelinating disease include metformin and rapamycin. Of particular relevance to our discussion on NSCs is the recent report demonstrating the utility of metformin to enhance the myelinating capacity of OPCs in the aged CNS (Neumann et al., 2019). Rapamycin is a naturally occurring macrolide product first isolated in 1931 from a bacterium found in the soil on Easter Island (Rapa Nui) in the south Pacific Ocean (Vézina et al., 1975). The anti-inflammatory actions of rapamycin are mediated by the kinase mTORC1 (Brown et al., 1994). Similarly, metformin acts *via* Akt (PKB) to inhibit mTOR signaling (Dowling et al., 2007). Interestingly, a CRISPR-Cas9 knockout gene screen of senescent cells identified *MTOR* as a critical checkpoint required for the SASP (Liu et al., 2019), in part, *via* attenuated nuclear factor kappa-light-chain-enhancer of activated B cells (NFkB) signaling and suppressed IL-1RA levels (Laberge et al., 2015; Liu et al., 2019). Consistent with these findings, we had recently determined that NSCs derived from MS patient iPSC lines exhibit a cellular senescence phenotype and upregulated mTOR expression. Treatment of these patient NSCs with rapamycin was similarly found to both reduce mTOR expression and the senescent phenotype in this cellular model (Nicaise et al., 2019).

Senolytics

Senolytic agents represent the second class of agents to therapeutically address the impact of cellular aging in intractable or incurable diseases. The compound term senolytic refers to the mechanism of action of this class which is to selectively kill cells that are senescent to reduce the impact of these cells on tissues (**Table 2**). This novel class of agents was named by Zhu et al. (2015). Using irradiated fat cells, they validated

six anti-apoptotic targets by siRNA, which included B-cell lymphoma-extra large (BCL-XL) and ephrin type-B receptor 1 (EPHB1), that were found to promote senescent cell death but did not affect the viability or proliferation of non-senescent cells. From this, a limited biased screen of select compounds identified the combination of dasatinib (D), an SRC-family protein-tyrosine kinase inhibitor approved for the treatment of leukemia, and quercetin (Q), a dietary flavonoid with estrogen mimetic activity and pleotropic kinase inhibitor (Russo et al., 2014), were found to be most effective in clearing/killing senescent cells (Zhu et al., 2015). Other agents in the senolytic class, such as fisetin (Zhu et al., 2017), which mimics the effects of dietary restriction, are also in development for their potential to target senescent cells in disease models including CNS conditions (Currais et al., 2014, 2018). Characterization of the impact of these agents on the CNS requires more extensive study, as it is unknown to what extent killing senescent cells would alter the brain microenvironment. A potentially important caveat to the application of these agents to CNS disease is that in many instances the molecular basis for understanding cellular senescence is from irradiated (10 Gy) non-neural primary cells such as fibroblasts or fat cells. Although these studies and screens provide an important molecular template for identifying cellular senescence in other tissues, including CNS, the precise translation of changes evoked by irradiation to disease conditions within the CNS may be incomplete and likely there exist important differences requiring further characterization and study.

Experimental evidence from transgenic animal models has shown the potential utility of senolysis as an effective strategy to target senescent cells in the CNS *in vivo*. Currently, experimental models of AD are being tested as prototypic neurological diseases of aging (Mendelsohn and Larrick, 2018). For example, Baker et al. (2011) developed a transgenic mouse in which senescent $p16^{Ink4a+}$ cells are killed by the initiation of apoptosis through chemically included expression of ATTAC, a caspase inducer sequence. They recently reported that astrocytes and microglia develop an aged, $p16^{Ink4a+}$ (senescent) phenotype in a presenilin mouse model of AD-related tauopathy ($MAPT^{P301S}$PS19; Yoshiyama et al., 2007). Then, using the INK-ATTAC transgenic mice, they demonstrated that selective elimination of these $p16^{Ink4a+}$ cells improves the phenotype and amyloid load in a $MAPT^{P301S}$PS19 mouse model of tau-dependent AD-like disease (Bussian et al., 2018). Importantly, this study used electron microscopy to show that neurons do not develop a senescent-like phenotype. This was indicative that cells with proliferative potential may be key players in neurological illnesses associated with aging (Bussian et al., 2018), whereby microglia play an important role in shaping neuropathology. Consistent with this transgenic study, the identification of senescent-like changes in p21+ and $p16^{Ink4a+}$ OPCs is associated with amyloid plaques in human AD autopsy neurospecimens and in an APP/PS1 mouse model of AD (Zhang et al., 2019). They also demonstrated that the use of the senolytic combination D + Q effectively eliminates the abundance of senescent cells, which was coincident with a dramatic improvement of cognitive performance and lowered amyloid load in treated APP/PS1 mice (Zhang et al., 2019). Similarly, the senolytic fisetin has been reported to ameliorate cognitive deficits in APPswe/PS1dE9 AD mice (Currais et al., 2014). Hence, accumulating evidence supports a role for cellular senescence associated with cognition and neuroinflammation in AD. The impact of these agents on cognitive decline in aged individuals without associated neurological diagnosis or other neurodegenerative diseases will require further study.

Cell Transplantation

NSCs have shown promising effects as exogenous stem cell therapeutics in the treatment of many mouse models of neurodegenerative diseases, such as PD, AD, MS, and ALS (Martino and Pluchino, 2006; Pluchino et al., 2009; Willis et al., 2020). Major strides have been made in harnessing their restorative, regenerative, and protective potential in the hopes of treating these devasting diseases. NSC transplants not only act as a cell replacement strategy but also secrete factors that can promote endogenous regeneration (**Table 2**). However, if their usefulness becomes diminished in an aged milieu is unknown.

An important caveat in cell transplantation is the idea of host-to-graft transfer of disease, which has been observed in PD patients. Foetal-derived NSCs transplanted into patients were found to last up to 16 years but eventually developed alpha-synuclein-positive Lewy bodies (Li et al., 2008). This work stresses the importance of the extracellular milieu and how it can affect even NSCs of fetal origin. As described in the above section, there is a myriad of extrinsic aging factors that would affect the transplanted graft. For example, the increase in pro-inflammatory factors, as well as the build-up of dysregulated proteins may outweigh the benefit of the transplanted cells and affect the overall success, possibly even turning transplanted cells senescent. Early work points to the success of fetal NSC transplants into aged rats, resulting in cognitive improvements. However, cells transplanted into aged and damaged environments demonstrate lower graft survival (Winkler, 2001; Zaman and Shetty, 2002). Interestingly, combining neurotrophic supplementation of brain-derived neurotrophic factor (BDNF) and neurotrophin-3 (NT-3), along with a caspase inhibitor, allows the graft to survive. Genetically engineered NSCs, which are resilient to inflammation (expressing dominant-negative nuclear factor of kappa light polypeptide gene enhancer in B-cells inhibitor, alpha [IκBα]), display an improvement in survival after transplantation into aged mice (Zhang et al., 2017). Not only can cells be engineered to be more resistant to hostile conditions, but they can also be genetically altered to secrete increased growth factors and even enzymes, such as choline acetyltransferase (ChAT), which is found to improve cognitive function in aging animals (Park et al., 2013). These examples suggest the idea of a multifaceted approach where young NSCs can be harnessed to secrete pro-rejuvenating and neurotrophic factors, such as TIMP-2, to help promote endogenous niche activation and eventually brain regeneration in aging and disease (Castellano et al., 2017). This method could potentially be used in conjunction with a senomorphic approach to have the most effect. However, as noted above, to what extent young NSCs or genetically

modified NSCs remain healthy and unperturbed by the aged environment is unknown. Over time the chronically inflamed brain may confer age-related changes onto the transplanted cells rendering them as dysfunctional as the endogenous niche. Stem cell therapy for neurodegenerative disease and aging may hold the promise of regeneration, nevertheless, many hurdles remain.

CONCLUSION

Research on brain stem cell aging within the past decade has surged and we have made significant advances in understanding what happens to this cell population in aging and disease using a variety of *in vitro* and *in vivo* model systems. Intrinsic and extrinsic factors play a large role in the decline of the NSC niche over time, which can be exacerbated by the disease. These include DNA damage, changes in metabolism and nutrient sensing, as well as the chronic pro-inflammatory environment both within the niche and in systemic fluids, which can all act to maintain cells in either a quiescent or senescent state, inhibiting their proper function when needed. These putative markers of NSC aging may also lead to the identification of biomarkers predictive for the onset and/or progression of cognitive defects associated with advancing age and neurodegenerative diseases. For example, the blood-borne SASP proteins IL-15 and chemokine (C-C motif) ligand 3 (CCL3) are correlated with chronological age and cognitive decline (Lehallier et al., 2019; Schafer et al., 2020). However, the cellular sources of these SASP factors are currently unknown.

Therefore, using patient-derived NSCs generated from fibroblasts and profiled for senescence markers may identify the proportion of circulating proteins contributed by NSCs. Further study is needed to determine if the NSC senescence burden *in vitro* correlates with the development and progression of cognitive defects *in vivo*.

There is no single mechanism to aging, and multiple processes likely contribute to declining. Therefore, using models in which we can parse these details is important to understanding the fundamentals of this process. Interrogating how aging may differ from diseases associated with aging, both transcriptionally and proteomically, would allow us to better understand the discrepancy between those who do and do not develop the disease, but also identify what facets of aging portend disease. This includes *in vivo* models of aging using genetically altered mice in which certain genes are mutated affecting various age-associated pathways (i.e., mitochondrial dynamics), allowing researchers to study in detail how changes alter cellular and organismal aging. *In vitro* models using novel stem cell technologies also hold potential for studying NSC aging in humans as they retain aging and disease markers. Defining the mechanisms that trigger modifications in this cell population with age and in disease will allow for a more directed approach to developing preventative or curative treatments.

AUTHOR CONTRIBUTIONS

AN designed review outline, wrote manuscript, and designed figures. CW and SC contributed sections of manuscript. CW, SC, and SP critically reviewed manuscript.

FUNDING

This work was funded by the National Multiple Sclerosis Society (RG-1802-30211 to SC), the Italian Multiple Sclerosis Association (AISM, grant 2010/R/31 and grant 2014/PMS/4 to SP), the Italian Ministry of Health (GR08-7 to SP), the European Research Council (ERC) under the ERC-2010-StG grant agreement n° 260511-SEM_SEM, the Medical Research Council, the Engineering and Physical Sciences Research Council, the Biotechnology and Biological Sciences Research Council UK Regenerative Medicine Platform Hub "Acellular Approaches for Therapeutic Delivery" (MR/K026682/1 to SP), the Evelyn Trust (RG 69865 to SP), and the Bascule Charitable Trust (RG 75149 to SP).

ACKNOWLEDGMENTS

We wish to acknowledge the contribution of past and present members of the Pluchino laboratory, who have contributed to (or inspired) this review article. We are grateful to Jayden Smith, Luca Peruzzotti-Jametti, and Giovanni Pluchino for critical insights into this manuscript.

REFERENCES

Adams, P. D., Jasper, H., and Rudolph, K. L. (2015). Aging-induced stem cell mutations as drivers for disease and cancer. *Cell Stem Cell* 16, 601–612. doi: 10.1016/j.stem.2015.05.002

Adlard, P. A., Perreau, V. M., and Cotman, C. W. (2005). The exercise-induced expression of BDNF within the hippocampus varies across life-span. *Neurobiol. Aging* 26, 511–520. doi: 10.1016/j.neurobiolaging.2004.05.006

Ahlqvist, K. J., Hamalainen, R. H., Yatsuga, S., Uutela, M., Terzioglu, M., Gotz, A., et al. (2012). Somatic progenitor cell vulnerability to mitochondrial DNA mutagenesis underlies progeroid phenotypes in Polg mutator mice. *Cell Metab.* 15, 100–109. doi: 10.1016/j.cmet.2011.11.012

Alexeyev, M., Shokolenko, I., Wilson, G., and Ledoux, S. (2013). The maintenance of mitochondrial DNA integrity—critical analysis and update. *Cold Spring Harb. Perspect. Biol.* 5:a012641. doi: 10.1101/cshperspect.a012641

Alvarez-Buylla, A., and Lim, D. A. (2004). For the long run: maintaining germinal niches in the adult brain. *Neuron* 41, 683–686. doi: 10.1016/s0896-6273(04)00111-4

Angelova, D. M., and Brown, D. R. (2019). Microglia and the aging brain: are senescent microglia the key to neurodegeneration? *J. Neurochem.* 151, 676–688. doi: 10.1111/jnc.14860

Apple, D. M., Mahesula, S., Fonseca, R. S., Zhu, C., and Kokovay, E. (2019). Calorie restriction protects neural stem cells from age-related deficits in the subventricular zone. *Aging* 11, 115–126. doi: 10.18632/aging.101731

Arai, Y., Martin-Ruiz, C. M., Takayama, M., Abe, Y., Takebayashi, T., Koyasu, S., et al. (2015). Inflammation, but not telomere length, predicts successful ageing at extreme old age: a longitudinal study of semi-supercentenarians. *EBioMedicine* 2, 1549–1558. doi: 10.1016/j.ebiom.2015.07.029

Audesse, A. J., Dhakal, S., Hassell, L. A., Gardell, Z., Nemtsova, Y., and Webb, A. E. (2019). FOXO3 directly regulates an autophagy network to functionally regulate proteostasis in adult neural stem cells. *PLoS Genet.* 15:e1008097. doi: 10.1371/journal.pgen.1008097

Back, S. A., Tuohy, T. M., Chen, H., Wallingford, N., Craig, A., Struve, J., et al. (2005). Hyaluronan accumulates in demyelinated lesions and inhibits oligodendrocyte progenitor maturation. *Nat. Med.* 11, 966–972. doi: 10.1038/nm1279

Baek, J. H., Schmidt, E., Viceconte, N., Strandgren, C., Pernold, K., Richard, T. J., et al. (2015). Expression of progerin in aging mouse brains reveals structural nuclear abnormalities without detectible significant alterations in gene expression, hippocampal stem cells or behavior. *Hum. Mol. Genet.* 24, 1305–1321. doi: 10.1093/hmg/ddu541

Bailey, K. J., Maslov, A. Y., and Pruitt, S. C. (2004). Accumulation of mutations and somatic selection in aging neural stem/progenitor cells. *Aging Cell* 3, 391–397. doi: 10.1111/j.1474-9728.2004.00128.x

Baker, D. J., and Petersen, R. C. (2018). Cellular senescence in brain aging and neurodegenerative diseases: evidence and perspectives. *J. Clin. Invest.* 128, 1208–1216. doi: 10.1172/jci95145

Baker, D. J., Jeganathan, K. B., Cameron, J. D., Thompson, M., Juneja, S., Kopecka, A., et al. (2004). BubR1 insufficiency causes early onset of aging-associated phenotypes and infertility in mice. *Nat. Genet.* 36, 744–749. doi: 10.1038/ng1382

Baker, D. J., Wijshake, T., Tchkonia, T., Lebrasseur, N. K., Childs, B. G., Van De Sluis, B., et al. (2011). Clearance of $p16^{Ink4a}$-positive senescent cells delays ageing-associated disorders. *Nature* 479, 232–236. doi: 10.1038/nature10600

Baruch, K., Deczkowska, A., David, E., Castellano, J. M., Miller, O., Kertser, A., et al. (2014). Aging. Aging-induced type I interferon response at the choroid plexus negatively affects brain function. *Science* 346, 89–93. doi: 10.1126/science.1252945

Basaiawmoit, R. V., and Rattan, S. I. (2010). Cellular stress and protein misfolding during aging. *Methods Mol. Biol.* 648, 107–117. doi: 10.1007/978-1-60761-756-3_7

Beckervordersandforth, R., Ebert, B., Schäffner, I., Moss, J., Fiebig, C., Shin, J., et al. (2017a). Role of mitochondrial metabolism in the control of early lineage progression and aging phenotypes in adult hippocampal neurogenesis. *Neuron* 93:1518. doi: 10.1016/j.neuron.2017.03.008

Beckervordersandforth, R., Ebert, B., Schäffner, I., Moss, J., Fiebig, C., Shin, J., et al. (2017b). Role of mitochondrial metabolism in the control of early lineage progression and aging phenotypes in adult hippocampal neurogenesis. *Neuron* 93, 560.6–573.6. doi: 10.1016/j.neuron.2016.12.017

Berg, D. (2011). Hyperechogenicity of the substantia nigra: pitfalls in assessment and specificity for Parkinson's disease. *J. Neural Transm.* 118, 453–461. doi: 10.1007/s00702-010-0469-5

Blasco, M. A., Lee, H. W., Hande, M. P., Samper, E., Lansdorp, P. M., Depinho, R. A., et al. (1997). Telomere shortening and tumor formation by mouse cells lacking telomerase RNA. *Cell* 91, 25–34. doi: 10.1016/s0092-8674(01)80006-4

Bollati, V., Schwartz, J., Wright, R., Litonjua, A., Tarantini, L., Suh, H., et al. (2009). Decline in genomic DNA methylation through aging in a cohort of elderly subjects. *Mech. Ageing Dev.* 130, 234–239. doi: 10.1016/j.mad.2008.12.003

Bratic, A., and Larsson, N.-G. (2013). The role of mitochondria in aging. *J. Clin. Invest.* 123, 951–957. doi: 10.1172/JCI64125

Brown, E. J., Albers, M. W., Shin, T. B., Ichikawa, K., Keith, C. T., Lane, W. S., et al. (1994). A mammalian protein targeted by G1-arresting rapamycin-receptor complex. *Nature* 369, 756–758. doi: 10.1038/369756a0

Burgess, D. J. (2015). Human genetics: somatic mutations linked to future disease risk. *Nat. Rev. Genet.* 16:69. doi: 10.1038/nrg3889

Bussian, T. J., Aziz, A., Meyer, C. F., Swenson, B. L., Van Deursen, J. M., and Baker, D. J. (2018). Clearance of senescent glial cells prevents tau-dependent pathology and cognitive decline. *Nature* 562, 578–582. doi: 10.1038/s41586-018-0543-y

Cabello-Rivera, D., Sarmiento-Soto, H., López-Barneo, J., and Muñoz-Cabello, A. M. (2019). Mitochondrial complex I function is essential for neural stem/progenitor cells proliferation and differentiation. *Front. Neurosci.* 13:664. doi: 10.3389/fnins.2019.00664

Calingasan, N. Y., Ho, D. J., Wille, E. J., Campagna, M. V., Ruan, J., Dumont, M., et al. (2008). Influence of mitochondrial enzyme deficiency on adult neurogenesis in mouse models of neurodegenerative diseases. *Neuroscience* 153, 986–996. doi: 10.1016/j.neuroscience.2008.02.071

Capelson, M., Liang, Y., Schulte, R., Mair, W., Wagner, U., and Hetzer, M. W. (2010). Chromatin-bound nuclear pore components regulate gene expression in higher eukaryotes. *Cell* 140, 372–383. doi: 10.1016/j.cell.2009.12.054

Caporaso, G. L., Lim, D. A., Alvarez-Buylla, A., and Chao, M. V. (2003). Telomerase activity in the subventricular zone of adult mice. *Mol. Cell. Neurosci.* 23, 693–702. doi: 10.1016/s1044-7431(03)00103-9

Carrasco-Garcia, E., Moreno-Cugnon, L., Garcia, I., Borras, C., Revuelta, M., Izeta, A., et al. (2019). SOX2 expression diminishes with ageing in several tissues in mice and humans. *Mech. Ageing Dev.* 177, 30–36. doi: 10.1016/j.mad.2018.03.008

Castellano, J. M., Mosher, K. I., Abbey, R. J., Mcbride, A. A., James, M. L., Berdnik, D., et al. (2017). Human umbilical cord plasma proteins revitalize hippocampal function in aged mice. *Nature* 544, 488–492. doi: 10.1038/nature22067

Cavallucci, V., Fidaleo, M., and Pani, G. (2016). Neural stem cells and nutrients: poised between quiescence and exhaustion. *Trends Endocrinol. Metab.* 27, 756–769. doi: 10.1016/j.tem.2016.06.007

Cha, M. Y., Kim, D. K., and Mook-Jung, I. (2015). The role of mitochondrial DNA mutation on neurodegenerative diseases. *Exp. Mol. Med.* 47:e150. doi: 10.1038/emm.2014.122

Chad, J. A., Pasternak, O., Salat, D. H., and Chen, J. J. (2018). Re-examining age-related differences in white matter microstructure with free-water corrected diffusion tensor imaging. *Neurobiol. Aging* 71, 161–170. doi: 10.1016/j.neurobiolaging.2018.07.018

Chaker, Z., Aid, S., Berry, H., and Holzenberger, M. (2015). Suppression of IGF-I signals in neural stem cells enhances neurogenesis and olfactory function during aging. *Aging Cell* 14, 847–856. doi: 10.1111/acel.12365

Chang, A. Y., Skirbekk, V. F., Tyrovolas, S., Kassebaum, N. J., and Dieleman, J. L. (2019). Measuring population ageing: an analysis of the Global Burden of Disease Study 2017. *Lancet Public Health* 4, e159–e167. doi: 10.1016/s2468-2667(19)30019-2

Chinnery, P. F., Samuels, D. C., Elson, J., and Turnbull, D. M. (2002). Accumulation of mitochondrial DNA mutations in ageing, cancer and mitochondrial disease: is there a common mechanism? *Lancet* 360, 1323–1325. doi: 10.1016/s0140-6736(02)11310-9

Cho, C. H., Yoo, K. H., Oliveros, A., Paulson, S., Hussaini, S. M. Q., Van Deursen, J. M., et al. (2019). sFRP3 inhibition improves age-related cellular changes in BubR1 progeroid mice. *Aging Cell* 18:e12899. doi: 10.1111/acel.12899

Clarke, L. E., Liddelow, S. A., Chakraborty, C., Munch, A. E., Heiman, M., and Barres, B. A. (2018). Normal aging induces A1-like astrocyte reactivity. *Proc. Natl. Acad. Sci. U S A* 115, E1896–E1905. doi: 10.1073/pnas.1800165115

Cleveland, D. W., Mao, Y., and Sullivan, K. F. (2003). Centromeres and kinetochores: from epigenetics to mitotic checkpoint signaling. *Cell* 112, 407–421. doi: 10.1016/s0092-8674(03)00115-6

Cohen, J., and Torres, C. (2019). Astrocyte senescence: evidence and significance. *Aging Cell* 18:e12937. doi: 10.1111/acel.12937

Colcombe, S. J., Erickson, K. I., Scalf, P. E., Kim, J. S., Prakash, R., McAuley, E., et al. (2006). Aerobic exercise training increases brain volume in aging humans. *J. Gerontol. A Biol. Sci. Med. Sci.* 61, 1166–1170. doi: 10.1093/gerona/61.11.1166

Cole, J. H., and Franke, K. (2017). Predicting age using neuroimaging: innovative brain ageing biomarkers. *Trends Neurosci.* 40, 681–690. doi: 10.1016/j.tins.2017.10.001

Cole, J. H., Marioni, R. E., Harris, S. E., and Deary, I. J. (2019). Brain age and other bodily 'ages': implications for neuropsychiatry. *Mol. Psychiatry* 24, 266–281. doi: 10.1038/s41380-018-0098-1

Coller, H. A. (2019). The paradox of metabolism in quiescent stem cells. *FEBS Lett.* 593, 2817–2839. doi: 10.1002/1873-3468.13608

Collin, G., Huna, A., Warnier, M., Flaman, J. M., and Bernard, D. (2018). Transcriptional repression of DNA repair genes is a hallmark and a cause of cellular senescence. *Cell Death Dis.* 9:259. doi: 10.1038/s41419-018-0300-z

Conforti, P., Camnasio, S., Mutti, C., Valenza, M., Thompson, M., Fossale, E., et al. (2013). Lack of huntingtin promotes neural stem cells differentiation into glial cells while neurons expressing huntingtin with expanded polyglutamine tracts undergo cell death. *Neurobiol. Dis.* 50, 160–170. doi: 10.1016/j.nbd.2012.10.015

Coppé, J. P., Desprez, P. Y., Krtolica, A., and Campisi, J. (2010). The senescence-associated secretory phenotype: the dark side of tumor suppression. *Annu. Rev. Pathol.* 5, 99–118. doi: 10.1146/annurev-pathol-121808-102144

Currais, A., Farrokhi, C., Dargusch, R., Armando, A., Quehenberger, O., Schubert, D., et al. (2018). Fisetin reduces the impact of aging on behavior and physiology in the rapidly aging SAMP8 mouse. *J. Gerontol. A Biol. Sci. Med. Sci.* 73, 299–307. doi: 10.1093/gerona/glx104

Currais, A., Prior, M., Dargusch, R., Armando, A., Ehren, J., Schubert, D., et al. (2014). Modulation of p25 and inflammatory pathways by fisetin maintains cognitive function in Alzheimer's disease transgenic mice. *Aging Cell* 13, 379–390. doi: 10.1111/acel.12185

Daniele, S., Da Pozzo, E., Iofrida, C., and Martini, C. (2016). Human neural stem cell aging is counteracted by α-glycerylphosphorylethanolamine. *ACS Chem. Neurosci.* 7, 952–963. doi: 10.1021/acschemneuro.6b00078

Davalos, A. R., Kawahara, M., Malhotra, G. K., Schaum, N., Huang, J., Ved, U., et al. (2013). p53-dependent release of Alarmin HMGB1 is a central mediator of senescent phenotypes. *J. Cell Biol.* 201, 613–629. doi: 10.1083/jcb.201206006

De Cecco, M., Ito, T., Petrashen, A. P., Elias, A. E., Skvir, N. J., Criscione, S. W., et al. (2019). L1 drives IFN in senescent cells and promotes age-associated inflammation. *Nature* 566, 73–78. doi: 10.1038/s41586-018-0784-9

Dickson, D. W., Crystal, H. A., Bevona, C., Honer, W., Vincent, I., and Davies, P. (1995). Correlations of synaptic and pathological markers with cognition of the elderly. *Neurobiol. Aging* 16, 285–298; discussion 298–304. doi: 10.1016/0197-4580(95)00013-5

Ding, Q., Vaynman, S., Souda, P., Whitelegge, J. P., and Gomez-Pinilla, F. (2006). Exercise affects energy metabolism and neural plasticity-related proteins in the hippocampus as revealed by proteomic analysis. *Eur. J. Neurosci.* 24, 1265–1276. doi: 10.1111/j.1460-9568.2006.05026.x

Dong, C. M., Wang, X. L., Wang, G. M., Zhang, W. J., Zhu, L., Gao, S., et al. (2014). A stress-induced cellular aging model with postnatal neural stem cells. *Cell Death Dis.* 5:e1116. doi: 10.1038/cddis.2014.82

Dowling, R. J., Zakikhani, M., Fantus, I. G., Pollak, M., and Sonenberg, N. (2007). Metformin inhibits mammalian target of rapamycin-dependent translation initiation in breast cancer cells. *Cancer Res.* 67, 10804–10812. doi: 10.1158/0008-5472.can-07-2310

Dulken, B. W., Buckley, M. T., Navarro Negredo, P., Saligrama, N., Cayrol, R., Leeman, D. S., et al. (2019). Single-cell analysis reveals T cell infiltration in old neurogenic niches. *Nature* 571, 205–210. doi: 10.1038/s41586-019-1362-5

Elkin, B. S., Ilankovan, A., and Morrison, B. III. (2010). Age-dependent regional mechanical properties of the rat hippocampus and cortex. *J. Biomech. Eng.* 132:011010. doi: 10.1115/1.4000164

Erdö, F., Denes, L., and De Lange, E. (2017). Age-associated physiological and pathological changes at the blood-brain barrier: a review. *J. Cereb. Blood Flow Metab.* 37, 4–24. doi: 10.1177/0271678X16679420

Eriksson, P. S., Perfilieva, E., Bjork-Eriksson, T., Alborn, A. M., Nordborg, C., Peterson, D. A., et al. (1998). Neurogenesis in the adult human hippocampus. *Nat. Med.* 4, 1313–1317. doi: 10.1038/3305

Espada, L., and Ermolaeva, M. A. (2016). DNA damage as a critical factor of stem cell aging and organ homeostasis. *Curr. Stem Cell Rep.* 2, 290–298. doi: 10.1007/s40778-016-0052-6

Farr, J. N., and Khosla, S. (2019). Cellular senescence in bone. *Bone* 121, 121–133. doi: 10.1016/j.bone.2019.01.015

Feil, R., and Fraga, M. F. (2012). Epigenetics and the environment: emerging patterns and implications. *Nat. Rev. Genet.* 13, 97–109. doi: 10.1038/nrg3142

Ferrón, S. R., Marques-Torrejón, M. A., Mira, H., Flores, I., Taylor, K., Blasco, M. A., et al. (2009). Telomere shortening in neural stem cells disrupts neuronal differentiation and neuritogenesis. *J. Neurosci.* 29, 14394–14407. doi: 10.1523/JNEUROSCI.3836-09.2009

Ferrón, S., Mira, H., Franco, S., Cano-Jaimez, M., Bellmunt, E., Ramirez, C., et al. (2004). Telomere shortening and chromosomal instability abrogates proliferation of adult but not embryonic neural stem cells. *Development* 131, 4059–4070. doi: 10.1242/dev.01215

Flachsbart, F., Caliebe, A., Kleindorp, R., Blanche, H., Von Eller-Eberstein, H., Nikolaus, S., et al. (2009). Association of FOXO3A variation with human longevity confirmed in German centenarians. *Proc. Natl. Acad. Sci. U S A* 106, 2700–2705. doi: 10.1073/pnas.0809594106

Folgueras, A. R., Freitas-Rodríguez, S., Velasco, G., and López-Otín, C. (2018). Mouse models to disentangle the hallmarks of human aging. *Circ Res.* 123, 905–924. doi: 10.1161/circresaha.118.312204

Fonken, L. K., Frank, M. G., Kitt, M. M., D'angelo, H. M., Norden, D. M., Weber, M. D., et al. (2016). The alarmin HMGB1 mediates age-induced neuroinflammatory priming. *J. Neurosci.* 36, 7946–7956. doi: 10.1523/JNEUROSCI.1161-16.2016

Franceschi, C., Garagnani, P., Morsiani, C., Conte, M., Santoro, A., Grignolio, A., et al. (2018). The continuum of aging and age-related diseases: common mechanisms but different rates. *Front. Med.* 5:61. doi: 10.3389/fmed.2018.00061

Franke, K., and Gaser, C. (2019). Ten years of *BrainAGE* as a neuroimaging biomarker of brain aging: what insights have we gained? *Front. Neurol.* 10:789. doi: 10.3389/fneur.2019.00789

Gage, F. H. (2000). Mammalian neural stem cells. *Science* 287, 1433–1438. doi: 10.1126/science.287.5457.1433

Gage, F. H., and Temple, S. (2013). Neural stem cells: generating and regenerating the brain. *Neuron* 80, 588–601. doi: 10.1016/j.neuron.2013.10.037

Gattazzo, F., Urciuolo, A., and Bonaldo, P. (2014). Extracellular matrix: a dynamic microenvironment for stem cell niche. *Biochim. Biophys. Acta* 1840, 2506–2519. doi: 10.1016/j.bbagen.2014.01.010

Gontier, G., Iyer, M., Shea, J. M., Bieri, G., Wheatley, E. G., Ramalho-Santos, M., et al. (2018). Tet2 rescues age-related regenerative decline and enhances cognitive function in the adult mouse brain. *Cell Rep.* 22, 1974–1981. doi: 10.1016/j.celrep.2018.02.001

Gordon, L. B., Rothman, F. G., López-Otín, C., and Misteli, T. (2014). Progeria: a paradigm for translational medicine. *Cell* 156, 400–407. doi: 10.1016/j.cell.2013.12.028

Grelat, A., Benoit, L., Wagner, S., Moigneu, C., Lledo, P. M., and Alonso, M. (2018). Adult-born neurons boost odor-reward association. *Proc. Natl. Acad. Sci. U S A* 115, 2514–2519. doi: 10.1073/pnas.1716400115

Haidet-Phillips, A. M., Hester, M. E., Miranda, C. J., Meyer, K., Braun, L., Frakes, A., et al. (2011). Astrocytes from familial and sporadic ALS patients are toxic to motor neurons. *Nat. Biotechnol.* 29, 824–828. doi: 10.1038/nbt.1957

Hämäläinen, R. H., Ahlqvist, K. J., Ellonen, P., Lepistö, M., Logan, A., Otonkoski, T., et al. (2015). mtDNA mutagenesis disrupts pluripotent stem cell function by altering redox signaling. *Cell Rep.* 11, 1614–1624. doi: 10.1016/j.celrep.2015.05.009

Hamezah, H. S., Durani, L. W., Ibrahim, N. F., Yanagisawa, D., Kato, T., Shiino, A., et al. (2017). Volumetric changes in the aging rat brain and its impact on cognitive and locomotor functions. *Exp. Gerontol.* 99, 69–79. doi: 10.1016/j.exger.2017.09.008

Harman, D. (2001). Aging: overview. *Ann. N Y Acad. Sci.* 928, 1–21. doi: 10.1111/j.1749-6632.2001.tb05631.x

Harrison, D. E., Strong, R., Sharp, Z. D., Nelson, J. F., Astle, C. M., Flurkey, K., et al. (2009). Rapamycin fed late in life extends lifespan in genetically heterogeneous mice. *Nature* 460, 392–395. doi: 10.1038/nature08221

He, N., Jin, W. L., Lok, K. H., Wang, Y., Yin, M., and Wang, Z. J. (2013). Amyloid-β(1–42) oligomer accelerates senescence in adult hippocampal neural stem/progenitor cells *via* formylpeptide receptor 2. *Cell Death Dis.* 4:e924. doi: 10.1038/cddis.2013.437

Heng, Y., Eggen, B. J. L., Boddeke, E. W. G. M., and Kooistra, S. M. (2017). Mouse models of central nervous system ageing. *Drug Discov. Today Dis. Models* 25–26, 21–34. doi: 10.1016/j.ddmod.2018.10.002

Hoffman, J. D., Parikh, I., Green, S. J., Chlipala, G., Mohney, R. P., Keaton, M., et al. (2017). Age drives distortion of brain metabolic, vascular, and cognitive functions and the gut microbiome. *Front. Aging Neurosci.* 9:298. doi: 10.3389/fnagi.2017.00298

Horgusluoglu, E., Nudelman, K., Nho, K., and Saykin, A. J. (2017). Adult neurogenesis and neurodegenerative diseases: a systems biology perspective. *Am. J. Med. Genet. B Neuropsychiatr. Genet.* 174, 93–112. doi: 10.1002/ajmg.b.32429

Horvath, S. (2013). DNA methylation age of human tissues and cell types. *Genome Biol.* 14:R115. doi: 10.1186/gb-2013-14-10-r115

Horvath, S., Zhang, Y., Langfelder, P., Kahn, R. S., Boks, M. P., Van Eijk, K., et al. (2012). Aging effects on DNA methylation modules in human brain and blood tissue. *Genome Biol.* 13:R97. doi: 10.1186/gb-2012-13-10-r97

Hou, Y., Dan, X., Babbar, M., Wei, Y., Hasselbalch, S. G., Croteau, D. L., et al. (2019). Ageing as a risk factor for neurodegenerative disease. *Nat. Rev. Neurol.* 15, 565–581. doi: 10.1038/s41582-019-0244-7

Imam, S. Z., Karahalil, B., Hogue, B. A., Souza-Pinto, N. C., and Bohr, V. A. (2006). Mitochondrial and nuclear DNA-repair capacity of various brain regions in mouse is altered in an age-dependent manner. *Neurobiol. Aging* 27, 1129–1136. doi: 10.1016/j.neurobiolaging.2005.06.002

Imayoshi, I., Sakamoto, M., Ohtsuka, T., Takao, K., Miyakawa, T., Yamaguchi, M., et al. (2008). Roles of continuous neurogenesis in the structural and functional integrity of the adult forebrain. *Nat. Neurosci.* 11, 1153–1161. doi: 10.1038/nn.2185

Jacob, K. D., Noren Hooten, N., Tadokoro, T., Lohani, A., Barnes, J., and Evans, M. K. (2013). Alzheimer's disease-associated polymorphisms in human OGG1 alter catalytic activity and sensitize cells to DNA damage. *Free Radic Biol. Med.* 63, 115–125. doi: 10.1016/j.freeradbiomed.2013.05.010

Jaskelioff, M., Muller, F. L., Paik, J. H., Thomas, E., Jiang, S., Adams, A. C., et al. (2011). Telomerase reactivation reverses tissue degeneration in aged telomerase-deficient mice. *Nature* 469, 102–106. doi: 10.1038/nature09603

Jha, N. K., Jha, S. K., Sharma, R., Kumar, D., Ambasta, R. K., and Kumar, P. (2018). Hypoxia-induced signaling activation in neurodegenerative diseases: targets for new therapeutic strategies. *J. Alzheimers Dis.* 62, 15–38. doi: 10.3233/jad-170589

Kalamakis, G., Brune, D., Ravichandran, S., Bolz, J., Fan, W., Ziebell, F., et al. (2019). Quiescence modulates stem cell maintenance and regenerative capacity in the aging brain. *Cell* 176, 1407.e14–1419.e14. doi: 10.1016/j.cell.2019.01.040

Kang, I., Chu, C. T., and Kaufman, B. A. (2018). The mitochondrial transcription factor TFAM in neurodegeneration: emerging evidence and mechanisms. *FEBS Lett.* 592, 793–811. doi: 10.1002/1873-3468.12989

Kang, E., Wang, X., Tippner-Hedges, R., Ma, H., Folmes, C. D., Gutierrez, N. M., et al. (2016). Age-related accumulation of somatic mitochondrial DNA mutations in adult-derived human iPSCs. *Cell Stem Cell* 18, 625–636. doi: 10.1016/j.stem.2016.02.005

Katajisto, P., Döhla, J., Chaffer, C. L., Pentinmikko, N., Marjanovic, N., Iqbal, S., et al. (2015). Stem cells. Asymmetric apportioning of aged mitochondria between daughter cells is required for stemness. *Science* 348, 340–343. doi: 10.1126/science.1260384

Katsimpardi, L., Litterman, N. K., Schein, P. A., Miller, C. M., Loffredo, F. S., Wojtkiewicz, G. R., et al. (2014). Vascular and neurogenic rejuvenation of the aging mouse brain by young systemic factors. *Science* 344, 630–634. doi: 10.1126/science.1251141

Kaufmann, T., Van Der Meer, D., Doan, N. T., Schwarz, E., Lund, M. J., Agartz, I., et al. (2019). Common brain disorders are associated with heritable patterns of apparent aging of the brain. *Nat. Neurosci.* 22, 1617–1623. doi: 10.1038/s41593-019-0471-7

Kenyon, C. J. (2010). The genetics of ageing. *Nature* 464, 504–512. doi: 10.1038/nature08980

Keung, A. J., De Juan-Pardo, E. M., Schaffer, D. V., and Kumar, S. (2011). Rho GTPases mediate the mechanosensitive lineage commitment of neural stem cells. *Stem Cells* 29, 1886–1897. doi: 10.1002/stem.746

Khacho, M., Clark, A., Svoboda, D. S., Azzi, J., Maclaurin, J. G., Meghaizel, C., et al. (2016). Mitochondrial dynamics impacts stem cell identity and fate decisions by regulating a nuclear transcriptional program. *Cell Stem Cell* 19, 232–247. doi: 10.1016/j.stem.2016.04.015

Khacho, M., Harris, R., and Slack, R. S. (2019). Mitochondria as central regulators of neural stem cell fate and cognitive function. *Nat. Rev. Neurosci.* 20, 34–48. doi: 10.1038/s41583-018-0091-3

Khan, A. M., Babcock, A. A., Saeed, H., Myhre, C. L., Kassem, M., and Finsen, B. (2015). Telomere dysfunction reduces microglial numbers without fully inducing an aging phenotype. *Neurobiol. Aging* 36, 2164–2175. doi: 10.1016/j.neurobiolaging.2015.03.008

Kim, H. J., and Jin, C. Y. (2012). Stem cells in drug screening for neurodegenerative disease. *Korean J. Physiol. Pharmacol.* 16, 1–9. doi: 10.4196/kjpp.2012.16.1.1

Kim, Y., Zheng, X., Ansari, Z., Bunnell, M. C., Herdy, J. R., Traxler, L., et al. (2018). Mitochondrial aging defects emerge in directly reprogrammed human neurons due to their metabolic profile. *Cell Rep.* 23, 2550–2558. doi: 10.1016/j.celrep.2018.04.105

Klein, C., Hain, E. G., Braun, J., Riek, K., Mueller, S., Steiner, B., et al. (2014). Enhanced adult neurogenesis increases brain stiffness: *in vivo* magnetic resonance elastography in a mouse model of dopamine depletion. *PLoS One* 9:e92582. doi: 10.1371/journal.pone.0092582

Koga, H., Kaushik, S., and Cuervo, A. M. (2011). Protein homeostasis and aging: the importance of exquisite quality control. *Ageing Res. Rev.* 10, 205–215. doi: 10.1016/j.arr.2010.02.001

Kokovay, E., Wang, Y., Kusek, G., Wurster, R., Lederman, P., Lowry, N., et al. (2012). VCAM1 is essential to maintain the structure of the SVZ niche and acts as an environmental sensor to regulate SVZ lineage progression. *Cell Stem Cell* 11, 220–230. doi: 10.1016/j.stem.2012.06.016

Kuhn, H. G., Dickinson-Anson, H., and Gage, F. H. (1996). Neurogenesis in the dentate gyrus of the adult rat: age-related decrease of neuronal progenitor proliferation. *J. Neurosci.* 16, 2027–2033. doi: 10.1523/JNEUROSCI.16-06-02027.1996

Kulkarni, A., Scully, T. J., and O'donnell, L. A. (2017). The antiviral cytokine interferon-γ restricts neural stem/progenitor cell proliferation through activation of STAT1 and modulation of retinoblastoma protein phosphorylation. *J. Neurosci. Res.* 95, 1582–1601. doi: 10.1002/jnr.23987

Laberge, R. M., Sun, Y., Orjalo, A. V., Patil, C. K., Freund, A., Zhou, L., et al. (2015). MTOR regulates the pro-tumorigenic senescence-associated secretory phenotype by promoting IL1A translation. *Nat. Cell Biol.* 17, 1049–1061. doi: 10.1038/ncb3195

Larsson, N. G. (2010). Somatic mitochondrial DNA mutations in mammalian aging. *Annu. Rev. Biochem.* 79, 683–706. doi: 10.1146/annurev-biochem-060408-093701

Leeman, D. S., Hebestreit, K., Ruetz, T., Webb, A. E., Mckay, A., Pollina, E. A., et al. (2018). Lysosome activation clears aggregates and enhances quiescent neural stem cell activation during aging. *Science* 359, 1277–1283. doi: 10.1126/science.aag3048

Lehallier, B., Gate, D., Schaum, N., Nanasi, T., Lee, S. E., Yousef, H., et al. (2019). Undulating changes in human plasma proteome profiles across the lifespan. *Nat. Med.* 25, 1843–1850. doi: 10.1038/s41591-019-0673-2

Leone, L., Colussi, C., Gironi, K., Longo, V., Fusco, S., Li Puma, D. D., et al. (2019). Altered Nup153 expression impairs the function of cultured hippocampal neural stem cells isolated from a mouse model of Alzheimer's disease. *Mol. Neurobiol.* 56, 5934–5949. doi: 10.1007/s12035-018-1466-1

Lepelletier, F. X., Mann, D. M., Robinson, A. C., Pinteaux, E., and Boutin, H. (2017). Early changes in extracellular matrix in Alzheimer's disease. *Neuropathol. Appl. Neurobiol.* 43, 167–182. doi: 10.1111/nan.12295

Li, L., Candelario, K. M., Thomas, K., Wang, R., Wright, K., Messier, A., et al. (2014). Hypoxia inducible factor-1α (HIF-1α) is required for neural stem cell maintenance and vascular stability in the adult mouse SVZ. *J. Neurosci.* 34, 16713–16719. doi: 10.1523/JNEUROSCI.4590-13.2014

Li, W. L., Chu, M. W., Wu, A., Suzuki, Y., Imayoshi, I., and Komiyama, T. (2018). Adult-born neurons facilitate olfactory bulb pattern separation during task engagement. *Elife* 7:e33006. doi: 10.7554/eLife.33006

Li, J. Y., Englund, E., Holton, J. L., Soulet, D., Hagell, P., Lees, A. J., et al. (2008). Lewy bodies in grafted neurons in subjects with Parkinson's disease suggest host-to-graft disease propagation. *Nat. Med.* 14, 501–503. doi: 10.1038/nm1746

Lim, D. A., Huang, Y. C., Swigut, T., Mirick, A. L., Garcia-Verdugo, J. M., Wysocka, J., et al. (2009). Chromatin remodelling factor Mll1 is essential for neurogenesis from postnatal neural stem cells. *Nature* 458, 529–533. doi: 10.1038/nature07726

Liu, G. H., Barkho, B. Z., Ruiz, S., Diep, D., Qu, J., Yang, S. L., et al. (2011). Recapitulation of premature ageing with iPSCs from Hutchinson-Gilford progeria syndrome. *Nature* 472, 221–225. doi: 10.1038/nature09879

Liu, Z., and Martin, L. J. (2006). The adult neural stem and progenitor cell niche is altered in amyotrophic lateral sclerosis mouse brain. *J. Comp. Neurol.* 497, 468–488. doi: 10.1002/cne.21012

Liu, X., Wei, L., Dong, Q., Liu, L., Zhang, M. Q., Xie, Z., et al. (2019). A large-scale CRISPR screen and identification of essential genes in cellular senescence bypass. *Aging* 11, 4011–4031. doi: 10.18632/aging.102034

Liu, M. L., Zang, T., and Zhang, C. L. (2016). Direct lineage reprogramming reveals disease-specific phenotypes of motor neurons from human ALS patients. *Cell Rep.* 14, 115–128. doi: 10.1016/j.celrep.2015.12.018

Llorens-Bobadilla, E., Zhao, S., Baser, A., Saiz-Castro, G., Zwadlo, K., and Martin-Villalba, A. (2015). Single-cell transcriptomics reveals a population of dormant neural stem cells that become activated upon brain injury. *Cell Stem Cell* 17, 329–340. doi: 10.1016/j.stem.2015.07.002

López-Otín, C., Blasco, M. A., Partridge, L., Serrano, M., and Kroemer, G. (2013). The hallmarks of aging. *Cell* 153, 1194–1217. doi: 10.1016/j.cell.2013.05.039

Lugert, S., Basak, O., Knuckles, P., Haussler, U., Fabel, K., Gotz, M., et al. (2010). Quiescent and active hippocampal neural stem cells with distinct morphologies respond selectively to physiological and pathological stimuli and aging. *Cell Stem Cell* 6, 445–456. doi: 10.1016/j.stem.2010.03.017

Majumder, S., Caccamo, A., Medina, D. X., Benavides, A. D., Javors, M. A., Kraig, E., et al. (2012). Lifelong rapamycin administration ameliorates age-dependent cognitive deficits by reducing IL-1β and enhancing NMDA signaling. *Aging Cell* 11, 326–335. doi: 10.1111/j.1474-9726.2011.00791.x

Mani, C., Reddy, P. H., and Palle, K. (2020). DNA repair fidelity in stem cell maintenance, health and disease. *Biochim. Biophys. Acta Mol. Basis Dis.* 1866:165444. doi: 10.1016/j.bbadis.2019.03.017

Mao, G., Pan, X., Zhu, B. B., Zhang, Y., Yuan, F., Huang, J., et al. (2007). Identification and characterization of OGG1 mutations in patients with Alzheimer's disease. *Nucleic Acids Res.* 35, 2759–2766. doi: 10.1093/nar/gkm189

Marin Navarro, A., Pronk, R. J., Van Der Geest, A. T., Oliynyk, G., Nordgren, A., Arsenian-Henriksson, M., et al. (2020). p53 controls genomic stability and temporal differentiation of human neural stem cells and affects neural organization in human brain organoids. *Cell Death Dis.* 11:52. doi: 10.1038/s41419-019-2208-7

Martino, G., and Pluchino, S. (2006). The therapeutic potential of neural stem cells. *Nat. Rev. Neurosci.* 7, 395–406. doi: 10.1038/nrn1908

Maryanovich, M., and Gross, A. (2013). A ROS rheostat for cell fate regulation. *Trends Cell Biol.* 23, 129–134. doi: 10.1016/j.tcb.2012.09.007

Matura, S., Fleckenstein, J., Deichmann, R., Engeroff, T., Füzéki, E., Hattingen, E., et al. (2017). Effects of aerobic exercise on brain metabolism and grey matter volume in older adults: results of the randomised controlled SMART trial. *Transl. Psychiatry* 7:e1172. doi: 10.1038/tp.2017.135

Maxwell, P. H., Burhans, W. C., and Curcio, M. J. (2011). Retrotransposition is associated with genome instability during chronological aging. *Proc. Natl. Acad. Sci. U S A* 108, 20376–20381. doi: 10.1073/pnas.1100271108

Medrano, S., Burns-Cusato, M., Atienza, M. B., Rahimi, D., and Scrable, H. (2009). Regenerative capacity of neural precursors in the adult mammalian brain is under the control of p53. *Neurobiol. Aging* 30, 483–497. doi: 10.1016/j.neurobiolaging.2007.07.016

Mendelsohn, A. R., and Larrick, J. W. (2018). Cellular senescence as the key intermediate in tau-mediated neurodegeneration. *Rejuvenation Res.* 21, 572–579. doi: 10.1089/rej.2018.2155

Mertens, J., Paquola, A. C. M., Ku, M., Hatch, E., Bohnke, L., Ladjevardi, S., et al. (2015). Directly reprogrammed human neurons retain aging-associated transcriptomic signatures and reveal age-related nucleocytoplasmic defects. *Cell Stem Cell* 17, 705–718. doi: 10.1016/j.stem.2015.09.001

Mertens, J., Reid, D., Lau, S., Kim, Y., and Gage, F. H. (2018). Aging in a dish: ipsc-derived and directly induced neurons for studying brain aging and age-related neurodegenerative diseases. *Annu. Rev. Genet.* 52, 271–293. doi: 10.1146/annurev-genet-120417-031534

Mihaylova, M. M., Sabatini, D. M., and Yilmaz, O. H. (2014). Dietary and metabolic control of stem cell function in physiology and cancer. *Cell Stem Cell* 14, 292–305. doi: 10.1016/j.stem.2014.02.008

Miller, J. D., Ganat, Y. M., Kishinevsky, S., Bowman, R. L., Liu, B., Tu, E. Y., et al. (2013). Human iPSC-based modeling of late-onset disease *via* progerin-induced aging. *Cell Stem Cell* 13, 691–705. doi: 10.1016/j.stem.2013.11.006

Mir, S., Cai, W., Carlson, S. W., Saatman, K. E., and Andres, D. A. (2017). IGF-1 mediated neurogenesis involves a novel RIT1/Akt/Sox2 cascade. *Sci. Rep.* 7:3283. doi: 10.1038/s41598-017-03641-9

Moore, D. L., Pilz, G. A., Arauzo-Bravo, M. J., Barral, Y., and Jessberger, S. (2015). A mechanism for the segregation of age in mammalian neural stem cells. *Science* 349, 1334–1338. doi: 10.1126/science.aac9868

Moreno-Jiménez, E. P., Flor-García, M., Terreros-Roncal, J., Rábano, A., Cafini, F., Pallas-Bazarra, N., et al. (2019). Adult hippocampal neurogenesis is abundant in neurologically healthy subjects and drops sharply in patients with Alzheimer's disease. *Nat. Med.* 25, 554–560. doi: 10.1038/s41591-019-0375-9

Muotri, A. R., Chu, V. T., Marchetto, M. C., Deng, W., Moran, J. V., and Gage, F. H. (2005). Somatic mosaicism in neuronal precursor cells mediated by L1 retrotransposition. *Nature* 435, 903–910. doi: 10.1038/nature03663

Murphy, M. P. (2009). How mitochondria produce reactive oxygen species. *Biochem. J.* 417, 1–13. doi: 10.1042/bj20081386

Murphy, M. C., Jones, D. T., Jack, C. R. Jr., Glaser, K. J., Senjem, M. L., Manduca, A., et al. (2016). Regional brain stiffness changes across the Alzheimer's disease spectrum. *Neuroimage Clin.* 10, 283–290. doi: 10.1016/j.nicl.2015.12.007

Nait-Oumesmar, B., Picard-Riera, N., Kerninon, C., Decker, L., Seilhean, D., Hoglinger, G. U., et al. (2007). Activation of the subventricular zone in multiple sclerosis: evidence for early glial progenitors. *Proc. Natl. Acad. Sci. U S A* 104, 4694–4699. doi: 10.1073/pnas.0606835104

Nekrasov, E. D., Vigont, V. A., Klyushnikov, S. A., Lebedeva, O. S., Vassina, E. M., Bogomazova, A. N., et al. (2016). Manifestation of Huntington's disease pathology in human induced pluripotent stem cell-derived neurons. *Mol. Neurodegener.* 11:27. doi: 10.1186/s13024-016-0092-5

Neumann, B., Baror, R., Zhao, C., Segel, M., Dietmann, S., Rawji, K. S., et al. (2019). Metformin restores CNS remyelination capacity by rejuvenating aged stem cells. *Cell Stem Cell* 25, 473.e8–485.e8. doi: 10.1016/j.stem.2019.08.015

Nicaise, A. M., Banda, E., Guzzo, R. M., Russomanno, K., Castro-Borrero, W., Willis, C. M., et al. (2017). iPS-derived neural progenitor cells from PPMS patients reveal defect in myelin injury response. *Exp. Neurol.* 288, 114–121. doi: 10.1016/j.expneurol.2016.11.012

Nicaise, A. M., Wagstaff, L. J., Willis, C. M., Paisie, C., Chandok, H., Robson, P., et al. (2019). Cellular senescence in progenitor cells contributes to diminished remyelination potential in progressive multiple sclerosis. *Proc. Natl. Acad. Sci. U S A* 116, 9030–9039. doi: 10.1073/pnas.1818348116

Niccoli, T., and Partridge, L. (2012). Ageing as a risk factor for disease. *Curr. Biol.* 22, R741–752. doi: 10.1016/j.cub.2012.07.024

Nieto-González, J. L., Gómez-Sánchez, L., Mavillard, F., Linares-Clemente, P., Rivero, M. C., Valenzuela-Villatoro, M., et al. (2019). Loss of postnatal quiescence of neural stem cells through mTOR activation upon genetic removal of cysteine string protein-α. *Proc. Natl. Acad. Sci. U S A* 116, 8000–8009. doi: 10.1073/pnas.1817183116

Numata, S., Ye, T., Hyde, T. M., Guitart-Navarro, X., Tao, R., Wininger, M., et al. (2012). DNA methylation signatures in development and aging of the human prefrontal cortex. *Am. J. Hum. Genet.* 90, 260–272. doi: 10.1016/j.ajhg.2011.12.020

Obernier, K., and Alvarez-Buylla, A. (2019). Neural stem cells: origin, heterogeneity and regulation in the adult mammalian brain. *Development* 146:dev156059. doi: 10.1242/dev.156059

Ochocki, J. D., and Simon, M. C. (2013). Nutrient-sensing pathways and metabolic regulation in stem cells. *J. Cell Biol.* 203, 23–33. doi: 10.1083/jcb.201303110

Paik, J. H., Ding, Z., Narurkar, R., Ramkissoon, S., Muller, F., Kamoun, W. S., et al. (2009). FoxOs cooperatively regulate diverse pathways governing neural stem cell homeostasis. *Cell Stem Cell* 5, 540–553. doi: 10.1016/j.stem.2009.09.013

Paliouras, G. N., Hamilton, L. K., Aumont, A., Joppe, S. E., Barnabe-Heider, F., and Fernandes, K. J. (2012). Mammalian target of rapamycin signaling is a key regulator of the transit-amplifying progenitor pool in the adult and aging forebrain. *J. Neurosci.* 32, 15012–15026. doi: 10.1523/JNEUROSCI.2248-12.2012

Park, J. I., Jeong, J. S., Han, J. Y., Kim, D. I., Gao, Y. H., Park, S. C., et al. (2000). Hydroxyurea induces a senescence-like change of K562 human erythroleukemia cell. *J. Cancer Res. Clin. Oncol.* 126, 455–460. doi: 10.1007/s004320050013

Park, D., Yang, Y. H., Bae, D. K., Lee, S. H., Yang, G., Kyung, J., et al. (2013). Improvement of cognitive function and physical activity of aging mice by human neural stem cells over-expressing choline acetyltransferase. *Neurobiol. Aging* 34, 2639–2646. doi: 10.1016/j.neurobiolaging.2013.04.026

Peleg, S., Sananbenesi, F., Zovoilis, A., Burkhardt, S., Bahari-Javan, S., Agis-Balboa, R. C., et al. (2010). Altered histone acetylation is associated with age-dependent memory impairment in mice. *Science* 328, 753–756. doi: 10.1126/science.1186088

Perluigi, M., Di Domenico, F., and Butterfield, D. A. (2015). mTOR signaling in aging and neurodegeneration: at the crossroad between metabolism dysfunction and impairment of autophagy. *Neurobiol. Dis.* 84, 39–49. doi: 10.1016/j.nbd.2015.03.014

Peters, A., Sethares, C., and Luebke, J. I. (2008). Synapses are lost during aging in the primate prefrontal cortex. *Neuroscience* 152, 970–981. doi: 10.1016/j.neuroscience.2007.07.014

Petr, M. A., Tulika, T., Carmona-Marin, L. M., and Scheibye-Knudsen, M. (2020). Protecting the aging genome. *Trends Cell Biol.* 30, 117–132. doi: 10.1016/j.tcb.2019.12.001

Petralia, R. S., Mattson, M. P., and Yao, P. J. (2014). Communication breakdown: the impact of ageing on synapse structure. *Ageing Res. Rev.* 14, 31–42. doi: 10.1016/j.arr.2014.01.003

Pineda, J. R., Daynac, M., Chicheportiche, A., Cebrian-Silla, A., Sii Felice, K., Garcia-Verdugo, J. M., et al. (2013). Vascular-derived TGF-β increases in the stem cell niche and perturbs neurogenesis during aging and following irradiation in the adult mouse brain. *EMBO Mol. Med.* 5, 548–562. doi: 10.1002/emmm.201202197

Pluchino, S., Muzio, L., Imitola, J., Deleidi, M., Alfaro-Cervello, C., Salani, G., et al. (2008). Persistent inflammation alters the function of the endogenous brain stem cell compartment. *Brain* 131, 2564–2578. doi: 10.1093/brain/awn198

Pluchino, S., Zanotti, L., Brini, E., Ferrari, S., and Martino, G. (2009). Regeneration and repair in multiple sclerosis: the role of cell transplantation. *Neurosci. Lett.* 456, 101–106. doi: 10.1016/j.neulet.2008.03.097

Pluvinage, J. V., and Wyss-Coray, T. (2020). Systemic factors as mediators of brain homeostasis, ageing and neurodegeneration. *Nat. Rev. Neurosci.* 21, 93–102. doi: 10.1038/s41583-019-0255-9

Podobinska, M., Szablowska-Gadomska, I., Augustyniak, J., Sandvig, I., Sandvig, A., and Buzanska, L. (2017). Epigenetic modulation of stem cells in neurodevelopment: the role of methylation and acetylation. *Front. Cell. Neurosci.* 11:23. doi: 10.3389/fncel.2017.00023

Rafalski, V. A., and Brunet, A. (2011). Energy metabolism in adult neural stem cell fate. *Prog. Neurobiol.* 93, 182–203. doi: 10.1016/j.pneurobio.2010.10.007

Raices, M., and D'Angelo, M. A. (2017). Nuclear pore complexes and regulation of gene expression. *Curr. Opin. Cell Biol.* 46, 26–32. doi: 10.1016/j.ceb.2016.12.006

Rasmussen, S., Imitola, J., Ayuso-Sacido, A., Wang, Y., Starossom, S. C., Kivisakk, P., et al. (2011). Reversible neural stem cell niche dysfunction in a model of multiple sclerosis. *Ann. Neurol.* 69, 878–891. doi: 10.1002/ana.22299

Reeve, A., Simcox, E., and Turnbull, D. (2014). Ageing and Parkinson's disease: why is advancing age the biggest risk factor? *Ageing Res. Rev.* 14, 19–30. doi: 10.1016/j.arr.2014.01.004

Renault, V. M., Rafalski, V. A., Morgan, A. A., Salih, D. A., Brett, J. O., Webb, A. E., et al. (2009). FoxO3 regulates neural stem cell homeostasis. *Cell Stem Cell* 5, 527–539. doi: 10.1016/j.stem.2009.09.014

Rodier, F., Campisi, J., and Bhaumik, D. (2007). Two faces of p53: aging and tumor suppression. *Nucleic Acids Res.* 35, 7475–7484. doi: 10.1093/nar/gkm744

Rola, R., Zou, Y., Huang, T. T., Fishman, K., Baure, J., Rosi, S., et al. (2007). Lack of extracellular superoxide dismutase (EC-SOD) in the microenvironment impacts radiation-induced changes in neurogenesis. *Free Radic. Biol. Med.* 42, 1133–1145; discussion 1131–1132. doi: 10.1016/j.freeradbiomed.2007.01.020

Rolyan, H., Scheffold, A., Heinrich, A., Begus-Nahrmann, Y., Langkopf, B. H., Hölter, S. M., et al. (2011). Telomere shortening reduces Alzheimer's disease amyloid pathology in mice. *Brain* 134, 2044–2056. doi: 10.1093/brain/awr133

Romine, J., Gao, X., Xu, X. M., So, K. F., and Chen, J. (2015). The proliferation of amplifying neural progenitor cells is impaired in the aging brain and restored by the mTOR pathway activation. *Neurobiol. Aging* 36, 1716–1726. doi: 10.1016/j.neurobiolaging.2015.01.003

Russo, G. L., Russo, M., Spagnuolo, C., Tedesco, I., Bilotto, S., Iannitti, R., et al. (2014). Quercetin: a pleiotropic kinase inhibitor against cancer. *Cancer Treat. Res.* 159, 185–205. doi: 10.1007/978-3-642-38007-5_11

Saha, K., Keung, A. J., Irwin, E. F., Li, Y., Little, L., Schaffer, D. V., et al. (2008). Substrate modulus directs neural stem cell behavior. *Biophys. J.* 95, 4426–4438. doi: 10.1529/biophysj.108.132217

Sahin, E., and Depinho, R. A. (2010). Linking functional decline of telomeres, mitochondria and stem cells during ageing. *Nature* 464, 520–528. doi: 10.1038/nature08982

Sakuma, S., and D'Angelo, M. A. (2017). The roles of the nuclear pore complex in cellular dysfunction, aging and disease. *Semin Cell Dev. Biol.* 68, 72–84. doi: 10.1016/j.semcdb.2017.05.006

Scahill, R. I., Frost, C., Jenkins, R., Whitwell, J. L., Rossor, M. N., and Fox, N. C. (2003). A longitudinal study of brain volume changes in normal aging using serial registered magnetic resonance imaging. *Arch. Neurol.* 60, 989–994. doi: 10.1001/archneur.60.7.989

Schafer, M. J., Zhang, X., Kumar, A., Atkinson, E. J., Zhu, Y., Jachim, S., et al. (2020). The senescence-associated secretome as an indicator of age and medical risk. *JCI Insight* 5:133668. doi: 10.1172/jci.insight.133668

Schneider, L. (2014). Survival of neural stem cells undergoing DNA damage-induced astrocytic differentiation in self-renewal-promoting conditions *in vitro*. *PLoS One* 9:e87228. doi: 10.1371/journal.pone.0087228

Sepe, S., Milanese, C., Gabriels, S., Derks, K. W., Payan-Gomez, C., Van, I. W. F., et al. (2016). Inefficient DNA repair is an aging-related modifier of Parkinson's disease. *Cell Rep.* 15, 1866–1875. doi: 10.1016/j.celrep.2016.04.071

Shanbhag, N. M., Evans, M. D., Mao, W., Nana, A. L., Seeley, W. W., Adame, A., et al. (2019). Early neuronal accumulation of DNA double strand breaks in Alzheimer's disease. *Acta Neuropathol. Commun.* 7:77. doi: 10.1186/s40478-019-0723-5

Sheng, C., Jungverdorben, J., Wiethoff, H., Lin, Q., Flitsch, L. J., Eckert, D., et al. (2018). A stably self-renewing adult blood-derived induced neural stem cell exhibiting patternability and epigenetic rejuvenation. *Nat. Commun.* 9:4047. doi: 10.1038/s41467-018-06398-5

Siqueira, I. R., Fochesatto, C., De Andrade, A., Santos, M., Hagen, M., Bello-Klein, A., et al. (2005). Total antioxidant capacity is impaired in different structures from aged rat brain. *Int. J. Dev. Neurosci.* 23, 663–671. doi: 10.1016/j.ijdevneu.2005.03.001

Smith, L. K., He, Y., Park, J. S., Bieri, G., Snethlage, C. E., Lin, K., et al. (2015). β2-microglobulin is a systemic pro-aging factor that impairs cognitive function and neurogenesis. *Nat. Med.* 21, 932–937. doi: 10.1038/nm.3898

Solano Fonseca, R., Mahesula, S., Apple, D. M., Raghunathan, R., Dugan, A., Cardona, A., et al. (2016). Neurogenic niche microglia undergo positional remodeling and progressive activation contributing to age-associated reductions in neurogenesis. *Stem Cells Dev.* 25, 542–555. doi: 10.1089/scd.2015.0319

Soriano-Cantón, R., Perez-Villalba, A., Morante-Redolat, J. M., Marqués-Torrejón, M. A., Pallás, M., Pérez-Sánchez, F., et al. (2015). Regulation of the p19(Arf)/p53 pathway by histone acetylation underlies neural stem cell behavior in senescence-prone SAMP8 mice. *Aging Cell* 14, 453–462. doi: 10.1111/acel.12328

Sorrells, S. F., Paredes, M. F., Cebrian-Silla, A., Sandoval, K., Qi, D., Kelley, K. W., et al. (2018). Human hippocampal neurogenesis drops sharply in children to undetectable levels in adults. *Nature* 555, 377–381. doi: 10.1038/nature25975

Spalding, K. L., Bergmann, O., Alkass, K., Bernard, S., Salehpour, M., Huttner, H. B., et al. (2013). Dynamics of hippocampal neurogenesis in adult humans. *Cell* 153, 1219–1227. doi: 10.1016/j.cell.2013.05.002

Specks, J., Nieto-Soler, M., Lopez-Contreras, A. J., and Fernandez-Capetillo, O. (2015). Modeling the study of DNA damage responses in mice. *Methods Mol. Biol.* 1267, 413–437. doi: 10.1007/978-1-4939-2297-0_21

Sperka, T., Wang, J., and Rudolph, K. L. (2012). DNA damage checkpoints in stem cells, ageing and cancer. *Nat. Rev. Mol. Cell Biol.* 13, 579–590. doi: 10.1038/nrm3420

Stein, L. R., and Imai, S. (2014). Specific ablation of Nampt in adult neural stem cells recapitulates their functional defects during aging. *EMBO J.* 33, 1321–1340. doi: 10.1002/embj.201386917

Stoll, E. A., Makin, R., Sweet, I. R., Trevelyan, A. J., Miwa, S., Horner, P. J., et al. (2015). Neural stem cells in the adult subventricular zone oxidize fatty acids to produce energy and support neurogenic activity. *Stem Cells* 33, 2306–2319. doi: 10.1002/stem.2042

Strong, M. A., Vidal-Cardenas, S. L., Karim, B., Yu, H., Guo, N., and Greider, C. W. (2011). Phenotypes in mTERT+/− and mTERT−/− mice are due to short telomeres, not telomere-independent functions of telomerase reverse transcriptase. *Mol. Cell. Biol.* 31, 2369–2379. doi: 10.1128/mcb.05312-11

Studer, L., Vera, E., and Cornacchia, D. (2015). Programming and reprogramming cellular age in the era of induced pluripotency. *Cell Stem Cell* 16, 591–600. doi: 10.1016/j.stem.2015.05.004

Su, W., Foster, S. C., Xing, R., Feistel, K., Olsen, R. H., Acevedo, S. F., et al. (2017). CD44 transmembrane receptor and hyaluronan regulate adult hippocampal neural stem cell quiescence and differentiation. *J. Biol. Chem.* 292, 4434–4445. doi: 10.1074/jbc.m116.774109

Szczesny, B., Hazra, T. K., Papaconstantinou, J., Mitra, S., and Boldogh, I. (2003). Age-dependent deficiency in import of mitochondrial DNA glycosylases

required for repair of oxidatively damaged bases. *Proc. Natl. Acad. Sci. U S A* 100, 10670–10675. doi: 10.1073/pnas.1932854100

Takamura, T., Motosugi, U., Sasaki, Y., Kakegawa, T., Sato, K., Glaser, K. J., et al. (2020). Influence of age on global and regional brain stiffness in young and middle-aged adults. *J. Magn. Reson. Imaging* 51, 727–733. doi: 10.1002/jmri.26881

Takeda, T. (2009). Senescence-accelerated mouse (SAM) with special references to neurodegeneration models, SAMP8 and SAMP10 mice. *Neurochem. Res.* 34, 639–659. doi: 10.1007/s11064-009-9922-y

Tang, Y., Liu, M. L., Zang, T., and Zhang, C. L. (2017). Direct reprogramming rather than iPSC-based reprogramming maintains aging hallmarks in human motor neurons. *Front. Mol. Neurosci.* 10:359. doi: 10.3389/fnmol.2017.00359

Tchkonia, T., Zhu, Y., Van Deursen, J., Campisi, J., and Kirkland, J. L. (2013). Cellular senescence and the senescent secretory phenotype: therapeutic opportunities. *J. Clin. Invest.* 123, 966–972. doi: 10.1172/jci64098

Terry, D. M., and Devine, S. E. (2019). Aberrantly high levels of somatic LINE-1 expression and retrotransposition in human neurological disorders. *Front. Genet.* 10:1244. doi: 10.3389/fgene.2019.01244

Thier, M., Worsdorfer, P., Lakes, Y. B., Gorris, R., Herms, S., Opitz, T., et al. (2012). Direct conversion of fibroblasts into stably expandable neural stem cells. *Cell Stem Cell* 10, 473–479. doi: 10.1016/j.stem.2012.03.003

Tobin, M. K., Musaraca, K., Disouky, A., Shetti, A., Bheri, A., Honer, W. G., et al. (2019). Human hippocampal neurogenesis persists in aged adults and Alzheimer's disease patients. *Cell Stem Cell* 24, 974.e3–982.e3. doi: 10.1016/j.stem.2019.05.003

Toda, T., Hsu, J. Y., Linker, S. B., Hu, L., Schafer, S. T., Mertens, J., et al. (2017). Nup153 interacts with Sox2 to enable bimodal gene regulation and maintenance of neural progenitor cells. *Cell Stem Cell* 21, 618.e7–634.e7. doi: 10.1016/j.stem.2017.08.012

Van Cauwenberghe, C., Vandendriessche, C., Libert, C., and Vandenbroucke, R. E. (2016). Caloric restriction: beneficial effects on brain aging and Alzheimer's disease. *Mamm. Genome* 27, 300–319. doi: 10.1007/s00335-016-9647-6

van Horssen, J., Dijkstra, C. D., and De Vries, H. E. (2007). The extracellular matrix in multiple sclerosis pathology. *J. Neurochem.* 103, 1293–1301. doi: 10.1111/j.1471-4159.2007.04897.x

Vera, E., Bosco, N., and Studer, L. (2016). Generating late-onset human ipsc-based disease models by inducing neuronal age-related phenotypes through telomerase manipulation. *Cell Rep.* 17, 1184–1192. doi: 10.1016/j.celrep.2016.09.062

Verburgh, K. (2015). Nutrigerontology: why we need a new scientific discipline to develop diets and guidelines to reduce the risk of aging-related diseases. *Aging Cell* 14, 17–24. doi: 10.1111/acel.12284

Vermulst, M., Bielas, J. H., Kujoth, G. C., Ladiges, W. C., Rabinovitch, P. S., Prolla, T. A., et al. (2007). Mitochondrial point mutations do not limit the natural lifespan of mice. *Nat. Genet.* 39, 540–543. doi: 10.1038/ng1988

Vézina, C., Kudelski, A., and Sehgal, S. N. (1975). Rapamycin (AY-22,989), a new antifungal antibiotic. I. Taxonomy of the producing streptomycete and isolation of the active principle. *J. Antibiot.* 28, 721–726. doi: 10.7164/antibiotics.28.721

Victor, M. B., Richner, M., Olsen, H. E., Lee, S. W., Monteys, A. M., Ma, C., et al. (2018). Striatal neurons directly converted from Huntington's disease patient fibroblasts recapitulate age-associated disease phenotypes. *Nat. Neurosci.* 21, 341–352. doi: 10.1038/s41593-018-0075-7

Vierbuchen, T., Ostermeier, A., Pang, Z. P., Kokubu, Y., Sudhof, T. C., and Wernig, M. (2010). Direct conversion of fibroblasts to functional neurons by defined factors. *Nature* 463, 1035–1041. doi: 10.1038/nature08797

Villeda, S. A., Luo, J., Mosher, K. I., Zou, B., Britschgi, M., Bieri, G., et al. (2011). The ageing systemic milieu negatively regulates neurogenesis and cognitive function. *Nature* 477, 90–94. doi: 10.1038/nature10357

Villeda, S. A., Plambeck, K. E., Middeldorp, J., Castellano, J. M., Mosher, K. I., Luo, J., et al. (2014). Young blood reverses age-related impairments in cognitive function and synaptic plasticity in mice. *Nat. Med.* 20, 659–663. doi: 10.1038/nm.3569

Vitale, G., Pellegrino, G., Vollery, M., and Hofland, L. J. (2019). ROLE of IGF-1 system in the modulation of longevity: controversies and new insights from a centenarians' perspective. *Front. Endocrinol.* 10:27. doi: 10.3389/fendo.2019.00027

Wallace, D. C. (2010). Mitochondrial DNA mutations in disease and aging. *Environ. Mol. Mutagen.* 51, 440–450. doi: 10.1002/em.20586

Wang, W., Esbensen, Y., Kunke, D., Suganthan, R., Rachek, L., Bjoras, M., et al. (2011). Mitochondrial DNA damage level determines neural stem cell differentiation fate. *J. Neurosci.* 31, 9746–9751. doi: 10.1523/jneurosci.0852-11.2011

Wang, Y. Z., Plane, J. M., Jiang, P., Zhou, C. J., and Deng, W. (2011). Concise review: quiescent and active states of endogenous adult neural stem cells: identification and characterization. *Stem Cells* 29, 907–912. doi: 10.1002/stem.644

Wang, F., Ren, S. Y., Chen, J. F., Liu, K., Li, R. X., Li, Z. F., et al. (2020). Myelin degeneration and diminished myelin renewal contribute to age-related deficits in memory. *Nat. Neurosci.* 23, 481–486. doi: 10.1038/s41593-020-0588-8

Wassmann, K., and Benezra, R. (2001). Mitotic checkpoints: from yeast to cancer. *Curr. Opin. Genet. Dev.* 11, 83–90. doi: 10.1016/s0959-437x(00)00161-1

Willcox, B. J., Donlon, T. A., He, Q., Chen, R., Grove, J. S., Yano, K., et al. (2008). FOXO3A genotype is strongly associated with human longevity. *Proc. Natl. Acad. Sci. U S A* 105, 13987–13992. doi: 10.1073/pnas.0801030105

Willis, C. M., Nicaise, A. M., Peruzzotti-Jametti, L., and Pluchino, S. (2020). The neural stem cell secretome and its role in brain repair. *Brain Res.* 1729:146615. doi: 10.1016/j.brainres.2019.146615

Winkler, J. (2001). Human neural stem cells improve cognitive function of aged brain. *Neuroreport* 12:A33. doi: 10.1097/00001756-200105080-00002

Wu, C. W., Chang, Y. T., Yu, L., Chen, H. I., Jen, C. J., Wu, S. Y., et al. (2008). Exercise enhances the proliferation of neural stem cells and neurite growth and survival of neuronal progenitor cells in dentate gyrus of middle-aged mice. *J. Appl. Physiol.* 105, 1585–1594. doi: 10.1152/japplphysiol.90775.2008

Xiao, Y. Z., Yang, M., Xiao, Y., Guo, Q., Huang, Y., Li, C. J., et al. (2020). Reducing hypothalamic stem cell senescence protects against aging-associated physiological decline. *Cell Metab.* 31, 534.e5–548.e5. doi: 10.1016/j.cmet.2020.01.002

Xie, Y., and Lowry, W. E. (2018). Manipulation of neural progenitor fate through the oxygen sensing pathway. *Methods* 133, 44–53. doi: 10.1016/j.ymeth.2017.08.018

Yang, Z., Jun, H., Choi, C. I., Yoo, K. H., Cho, C. H., Hussaini, S. M. Q., et al. (2017). Age-related decline in BubR1 impairs adult hippocampal neurogenesis. *Aging Cell* 16, 598–601. doi: 10.1111/acel.12594

Yang, T. T., Lo, C. P., Tsai, P. S., Wu, S. Y., Wang, T. F., Chen, Y. W., et al. (2015). Aging and exercise affect hippocampal neurogenesis *via* different mechanisms. *PLoS One* 10:e0132152. doi: 10.1371/journal.pone.0132152

Yeo, E. J. (2019). Hypoxia and aging. *Exp. Mol. Med.* 51, 1–15. doi: 10.1038/s12276-019-0233-3

Yeoman, M., Scutt, G., and Faragher, R. (2012). Insights into CNS ageing from animal models of senescence. *Nat. Rev. Neurosci.* 13, 435–445. doi: 10.1038/nrn3230

Yoshiyama, Y., Higuchi, M., Zhang, B., Huang, S. M., Iwata, N., Saido, T. C., et al. (2007). Synapse loss and microglial activation precede tangles in a P301S tauopathy mouse model. *Neuron* 53, 337–351. doi: 10.1016/j.neuron.2007.01.010

Yousef, H., Czupalla, C. J., Lee, D., Chen, M. B., Burke, A. N., Zera, K. A., et al. (2019). Aged blood impairs hippocampal neural precursor activity and activates microglia *via* brain endothelial cell VCAM1. *Nat. Med.* 25, 988–1000. doi: 10.1038/s41591-019-0440-4

Yousefzadeh, M. J., Zhao, J., Bukata, C., Wade, E. A., Mcgowan, S. J., Angelini, L. A., et al. (2020). Tissue specificity of senescent cell accumulation during physiologic and accelerated aging of mice. *Aging Cell* 19:e13094. doi: 10.1111/acel.13094

Zahn, J. M., Poosala, S., Owen, A. B., Ingram, D. K., Lustig, A., Carter, A., et al. (2007). AGEMAP: a gene expression database for aging in mice. *PLoS Genet.* 3:e201. doi: 10.1371/journal.pgen.0030201

Zaman, V., and Shetty, A. K. (2002). Combined neurotrophic supplementation and caspase inhibition enhances survival of fetal hippocampal CA3 cell grafts in lesioned CA3 region of the aging hippocampus. *Neuroscience* 109, 537–553. doi: 10.1016/s0306-4522(01)00478-x

Zapico, S. C., and Ubelaker, D. H. (2013). mtDNA mutations and their role in aging, diseases and forensic sciences. *Aging Dis.* 4, 364–380. doi: 10.14336/ad.2013.0400364

Zasso, J., Ahmed, M., Cutarelli, A., and Conti, L. (2018). Inducible α-synuclein expression affects human neural stem cells' behavior. *Stem Cells Dev.* 27, 985–994. doi: 10.1089/scd.2018.0011

Zhang, P., Kishimoto, Y., Grammatikakis, I., Gottimukkala, K., Cutler, R. G., Zhang, S., et al. (2019). Senolytic therapy alleviates Aβ-associated oligodendrocyte progenitor cell senescence and cognitive deficits in an Alzheimer's disease model. *Nat. Neurosci.* 22, 719–728. doi: 10.1038/s41593-019-0372-9

Zhang, Y., Kim, M. S., Jia, B., Yan, J., Zuniga-Hertz, J. P., Han, C., et al. (2017). Hypothalamic stem cells control ageing speed partly through exosomal miRNAs. *Nature* 548, 52–57. doi: 10.1038/nature23282

Zhang, G., Li, J., Purkayastha, S., Tang, Y., Zhang, H., Yin, Y., et al. (2013). Hypothalamic programming of systemic ageing involving IKK-β, NF-κB and GnRH. *Nature* 497, 211–216. doi: 10.1038/nature12143

Zhao, C., Deng, W., and Gage, F. H. (2008). Mechanisms and functional implications of adult neurogenesis. *Cell* 132, 645–660. doi: 10.1016/j.cell.2008.01.033

Zhou, Q. G., Liu, M. Y., Lee, H. W., Ishikawa, F., Devkota, S., Shen, X. R., et al. (2017). Hippocampal TERT regulates spatial memory formation through modulation of neural development. *Stem Cell Reports* 9, 543–556. doi: 10.1016/j.stemcr.2017.06.014

Zhu, Y., Doornebal, E. J., Pirtskhalava, T., Giorgadze, N., Wentworth, M., Fuhrmann-Stroissnigg, H., et al. (2017). New agents that target senescent cells: the flavone, fisetin and the BCL-XL inhibitors, A1331852 and A1155463. *Aging* 9, 955–963. doi: 10.18632/aging.101202

Zhu, Y., Tchkonia, T., Pirtskhalava, T., Gower, A. C., Ding, H., Giorgadze, N., et al. (2015). The Achilles' heel of senescent cells: from transcriptome to senolytic drugs. *Aging Cell* 14, 644–658. doi: 10.1111/acel.12344

Conflict of Interest: SP is co-founder and CSO at CITC Limited and iSTEM Therapeutics, and co-founder and Non-executive Director at Asitia Therapeutics. AN is an advisor for iSTEM Therapeutics.

The remaining authors declare that the research was conducted in the absence of any commercial or financial relationships that could be construed as a potential conflict of interest.

frontiers in Aging Neuroscience

ORIGINAL RESEARCH
published: 18 August 2020
doi: 10.3389/fnagi.2020.00258

HUCBC Treatment Improves Cognitive Outcome in Rats With Vascular Dementia

Poornima Venkat[1], Lauren Culmone[1], Michael Chopp[1,2] Julie Landschoot-Ward[1], Fengjie Wang[1], Alex Zacharek[1] and Jieli Chen[1]**

[1]Department of Neurology, Henry Ford Hospital, Detroit, MI, United States, [2]Department of Physics, Oakland University, Rochester, MI, United States

Background and purpose: Vascular dementia (VaD) is the second common cause of dementia after Alzheimer's disease in older people. Yet, there are no FDA approved drugs specifically for VaD. In this study, we have investigated the therapeutic effects of human umbilical cord blood cells (HUCBC) treatment on the cognitive outcome, white matter (WM) integrity, and glymphatic system function in rats subject to a multiple microinfarction (MMI) model of VaD.

Methods: Male, retired breeder rats were subjected to the MMI model (800 ± 100 cholesterol crystals/300 μl injected into the internal carotid artery), and 3 days later were treated with phosphate-buffered saline (PBS) or HUCBC (5×10^6, i.v.). Sham rats were included as naïve control. Following a battery of cognitive tests, rats were sacrificed at 28 days after MMI and brains extracted for immunohistochemical evaluation and Western blot analysis. To evaluate the glymphatic function, fluorescent tracers (Texas Red dextran, MW: 3 kD and FITC-dextran, MW: 500 kD) was injected into the cisterna magna over 30 min at 14 days after MMI. Rats (3–4/group/time point) were sacrificed at 30 min, 3 h, and 6 h, and the tracer movement analyzed using laser scanning confocal microscopy.

Results: Compared to control MMI rats, HUCBC treated MMI rats exhibit significantly improved short-term memory and long-term memory exhibited by increased discrimination index in novel object recognition task with retention delay of 4 h and improved novel odor recognition task with retention delay of 24 h, respectively. HUCBC treatment also improves spatial learning and memory as measured using the Morris water maze test compared to control MMI rats. HUCBC treatment significantly increases axon and myelin density increases oligodendrocyte and oligodendrocyte progenitor cell number and increases Synaptophysin expression in the brain compared to control MMI rats. HUCBC treatment of MMI in rats significantly improves glymphatic function by reversing MMI induced delay in the penetration of cerebrospinal fluid (CSF) into the brain parenchyma *via* glymphatic pathways and reversing delayed clearance from the brain. HUCBC treatment significantly increases miR-126 expression in serum, aquaporin-4 (AQP4) expression around cerebral vessels, and decreases transforming growth factor-β (TGF-β) protein expression in the brain which may contribute to HUCBC induced improved glymphatic function.

OPEN ACCESS

Edited by:
Cesar V. Borlongan, University of South Florida, United States

Reviewed by:
Murali Vijayan, Texas Tech University Health Sciences Center, United States
Gary K. Steinberg, Stanford University, United States

***Correspondence:**
Poornima Venkat
pvenkat3@hfhs.org
Jieli Chen
jchen4@hfhs.org

Received: *23 April 2020*
Accepted: *27 July 2020*
Published: *18 August 2020*

Citation:
Venkat P, Culmone L, Chopp M, Landschoot-Ward J, Wang F, Zacharek A and Chen J (2020) HUCBC Treatment Improves Cognitive Outcome in Rats With Vascular Dementia. Front. Aging Neurosci. 12:258. doi: 10.3389/fnagi.2020.00258

Conclusions: HUCBC treatment of an MMI rat model of VaD promotes WM remodeling and improves glymphatic function which together may aid in the improvement of cognitive function and memory. Thus, HUCBC treatment warrants further investigation as a potential therapy for VaD.

Keywords: cognition, human umbilical cord blood cells, multiple microinfarcts, vascular dementia, white matter remodeling

INTRODUCTION

Vascular dementia (VaD) is a significant cause of cognitive impairment and accounts for nearly 15–20% of dementia incidence in the United States (Plassman et al., 2007; Wolters and Ikram, 2019). VaD is a complex neurodegenerative disease that is characterized by changes in behavior and a progressive decline in cognitive function including the impairment of executive functions such as thinking, planning, problem-solving, working memory, reasoning, judgment, and the execution of tasks. VaD is frequently present in patients after a stroke or a series of mini-strokes and may result from multiple pathologies. Decreased cerebral blood flow to deep white matter (WM) results in silent, multifocal, micro-infarcts in the brain that in turn cause blood-brain barrier disruption, glymphatic dysfunction, increased inflammation, neuronal loss and cognitive impairment in animals (Rapp et al., 2008b; Wang et al., 2012; Venkat et al., 2017). Improved control of vascular risk factors and treatment of the vascular disease may contribute to a decline in dementia incidence in high-income countries (Satizabal et al., 2016; Wolters and Ikram, 2019). There is a need for approved pharmacological and biological interventions that can directly target and improve underlying VaD pathology.

In the current study, we investigate whether human umbilical cord blood cells (HUCBCs) treatment of VaD improves cognition and memory in rats subjected to a multiple microinfarction (MMI) model of VaD. The MMI model in rodents decreases CBF and induces multiple diffuse cerebral microinfarcts, induces blood-brain abarrier dysfunction, WM injury, impairment of glymphatic waste clearance pathway, widespread reactive gliosis, demyelination, hippocampal neuronal damage and cognitive impairment (Rapp et al., 2008b; Wang et al., 2012, 2017; Venkat et al., 2017; Yu et al., 2019). The glymphatic system is a functional waste clearance system that facilitates the removal of interstitial metabolic wastes and neurotoxins from the brain parenchyma (Plog and Nedergaard, 2018; Zhang et al., 2019). This glial-dependent waste clearance mechanism involves cerebrospinal fluid (CSF) penetration into the brain along with periarterial spaces facilitated by perivascular astrocytic aquaporin-4 (AQP4), and interstitial fluid and solute drainage along perivenous channels (Plog and Nedergaard, 2018). AQP4 is an integral membrane pore protein that plays crucial roles in glymphatic waste clearance by facilitating CSF-interstitial fluid exchange and fluid movement throughout the brain (Badaut et al., 2011). Previous studies have reported that loss of AQP4 in AQP4 knockout mice is associated with delayed and suppressed CSF tracer influx compared to wild type mice (Iliff et al., 2012; Mestre et al., 2018). Also, loss of AQP4 exacerbates glymphatic dysfunction, increases amyloid-β (Aβ) accumulation and increases cognitive deficits in Alzheimer's disease (AD) mice (Xu et al., 2015). Transforming growth factor (TGF-β) is a multifunctional cytokine which can contribute to glymphatic dysfunction by causing vascular changes including the hardening of cerebral vessels (Howe et al., 2019). The hardening of vessels in the brain can lead to a reduction in CSF flow and this can hinder overall waste clearance from the brain parenchyma (Howe et al., 2019). In aging, AD, stroke, diabetes and an MMI model of VaD, impaired glymphatic functioning results in the accumulation of metabolic waste and neurotoxins in the brain which can impair brain homeostasis, injure brain cells and lead to cognitive impairment (Iliff et al., 2012; Gaberel et al., 2014; Kress et al., 2014; Jiang et al., 2017; Wang et al., 2017). Thus, the glymphatic system represents an important target for therapeutic intervention in neurological diseases.

The therapeutic effects of HUCBC transplantation have been previously investigated in several disease models, including stroke (Chen et al., 2001b; Yan et al., 2014, 2015), traumatic brain injury (Lu et al., 2002), and AD (Darlington et al., 2013; Ehrhart et al., 2016). In AD mice, repeated low dose HUCBC administration improves cognitive outcome, decreases glial activation, and Aβ pathology in the brain compared to control mice (Darlington et al., 2013). Also, HUCBC transplantation is safe and well-tolerated in human patients with AD in the Phase 1 clinical trial (Kim et al., 2015). In our previous study, we reported that mice subjected to MMI have significantly decreased miR-126 expression, and mice with endothelial miR-126 knockdown exhibit significant cognitive impairment, WM injury, and glymphatic dysfunction (Yu et al., 2019). MiRs, and particularly miR-126, are emerging as key players in the pathogenesis of vascular damage (Zampetaki et al., 2010). MiR-126, a secreted factor, is one of the most abundant miRs present in endothelial cells and plays integral roles in regulating endothelial cell function, angiogenesis, vascular integrity, and anti-inflammation (Fish et al., 2008; Hu et al., 2015). HUCBC treatment is known to increase miR-126 expression after stroke and contribute to improvement in neurological function in diabetic mice (Chen et al., 2016). Therefore, in this study, we test the therapeutic effects of HUCBC treatment on cognition and memory in rats subjected to an MMI model of VaD and investigate whether HUCBC treatment increases miR-126, improves WM remodeling and glymphatic waste clearance in the brain of retired breeder rats.

MATERIALS AND METHODS

All experimental procedures were carried out following the National Institutes of Health (NIH) Guide for the Care and Use of Laboratory Animals and were approved by the Institutional Animal Care and Use Committee (IACUC) of the Henry Ford Health System. This manuscript is prepared following ARRIVE guidelines (Kilkenny et al., 2010).

Experimental Groups and Timelines

Male, retired breeder (9–12 months old) Wistar rats (Charles River Laboratories, Wilmington, MA, USA) were randomized to one of three groups (n = 6/group): (1) sham control; (2) MMI control; and (3) MMI+HUCBC. Rats in the MMI+HUCBC group received 5×10^6 HUCBCs administered *via* tail vein injection at 3 days after MMI. HUCBCs were obtained from Saneron CCEL Therapeutics, Inc., Tampa, FL, USA, a cord blood cell bank. Cryopreserved HUCBCs were rapidly thawed at 37°C and resuspended into 10 ml of 1× phosphate-buffered saline (PBS; VWR) to wash and centrifuged at 100 rpm to pellet. The cell pellet was resuspended in 1× PBS and cell viability and cell quantification were performed using the trypan blue dye exclusion method; cells were diluted in 1× PBS to give the numbers required for the injections. HUCBCs were not labeled before injection. Cognitive tests were performed 21–28 days following MMI surgery, with no overlap in testing. At 28 days after MMI, rats were sacrificed, and brains extracted for immunohistochemical analysis and Western blot analysis. There was no mortality after MMI or treatment in either group. **Figure 1A** presents a schematic timeline of experiments.

Randomization and Blinding

Rats were randomly assigned to MMI or MMI+HUCBC treated groups on day 3 after MMI. Investigators performing cognitive tests, immunohistochemical staining, and analysis were blinded to treated groups. ANY-Maze (Stoelting Co.) was used to acquire and analyze cognitive function data.

MMI Model

Rats were subjected to MMI surgery following previously described methods (Rapp et al., 2008a,b; Wang et al., 2012; Venkat et al., 2017, 2019; Yu et al., 2019). Freshly prepared cholesterol crystals of size 70–100 μm were obtained by serial filtration through 100 μm and 70 μm cell strainers and counted on a hemocytometer. Spontaneous respiration of isoflurane mixed in 2:1 N_2O:O_2 mixture was used as an anesthetic and regulated with a modified FLUOTEC 3 Vaporizer (Fraser Harlake). For the entire procedure, rats were placed on a heating pad and body temperature maintained at 37°C. A PE-50 tube was tapered by heating over a flame, connected to a 1 ml syringe filled with cholesterol crystals/saline, and then inserted into the lumen of the internal carotid artery (ICA) through an incision made on the external carotid artery (ECA). A microsurgical clamp was applied to the common carotid artery (CCA) and the cholesterol crystals (800 ± 100 crystals/300 μl saline) were slowly injected into the ICA over a minute. After cholesterol crystal injection, the tube was withdrawn, ECA was permanently ligated with a 4–0 suture, microsurgical clamps removed such that the CCA and ICA remained patent. Rats regained consciousness in their home cages and received routine post-surgical care. Sham control rats underwent a similar surgical procedure and were injected with saline alone.

Cognitive Testing

(a) Using the novel object recognition (NOR) test, short-term memory was assessed by examining animals' biases to explore novel objects in their environment. The testing followed previously described methods (Stuart et al., 2013). Briefly, rats were allowed to freely explore two identical objects placed equidistant from the walls of a large box during a 5-min trial phase. Following a retention delay of 4 h, one of the trial objects was randomly replaced with a novel object during the test phase. The trial and test objects were made from hard plastic building blocks and were of comparable sizes but different shapes. Between each trial, the objects and the bin were wiped with water. Exploration times were recorded using ANY-Maze by defining trial and novel objects, exploration zones, and head orientation such that sniffing, biting, licking, pawing, touching with the snout or probing with whiskers <1 cm of the object was included as exploration while sitting on or climbing the object was not included. Discrimination index was defined as the ratio of novel exploration time to total exploration time and a higher discrimination index indicates better short term memory.

(b) The odor test has been described in detail previously (Spinetta et al., 2008) and was used to evaluate long-term memory based on the animal's preference for novel scents. One week before the test, 2.5 cm wooden beads[1] were placed in the home cages of two sets of donor rats to build up rat-specific odors, which were later used as novel odors N1 and N2. The test spans 3 days and includes a habituation phase, a trial phase, and a test phase. The habituation phase lasted 24-h during which rats were removed from social housing and placed in a single housing. Each cage had four beads placed in them for familiarization and to serve as a familiar odor (F). On day 2, before the trial phase, all 4 F beads were removed from the cages. The trial phase consisted of 3 1-min trials during which 3 F beads and 1 novel odor bead (N1) were placed in the center of the cage. In each trial, the N1 bead was placed in a new position to minimize spatial cues. An inter-trial interval of 1 min, during which the cage had no beads was used to minimize olfactory adaptation. The test phase occurred after a 24-h retention delay. During the 1-min test phase, four beads (N1, N2, and 2 F beads) were placed in the center of the cage. A four-choice procedure was used for assessing relative odor preference as this has been shown to greatly increase sensitivity and reliability when compared to a two-choice procedure (Spinetta et al., 2008). Time spent exploring (sniffing, licking, biting) each bead was recorded. Discrimination index defined as the ratio between time spent exploring N2 to the total exploration time was used to evaluate long-term memory.

(c) The Morris water maze (MWM) test (Darwish et al., 2012) evaluates hippocampus based spatial and visual learning

[1] https://www.craftparts.com/

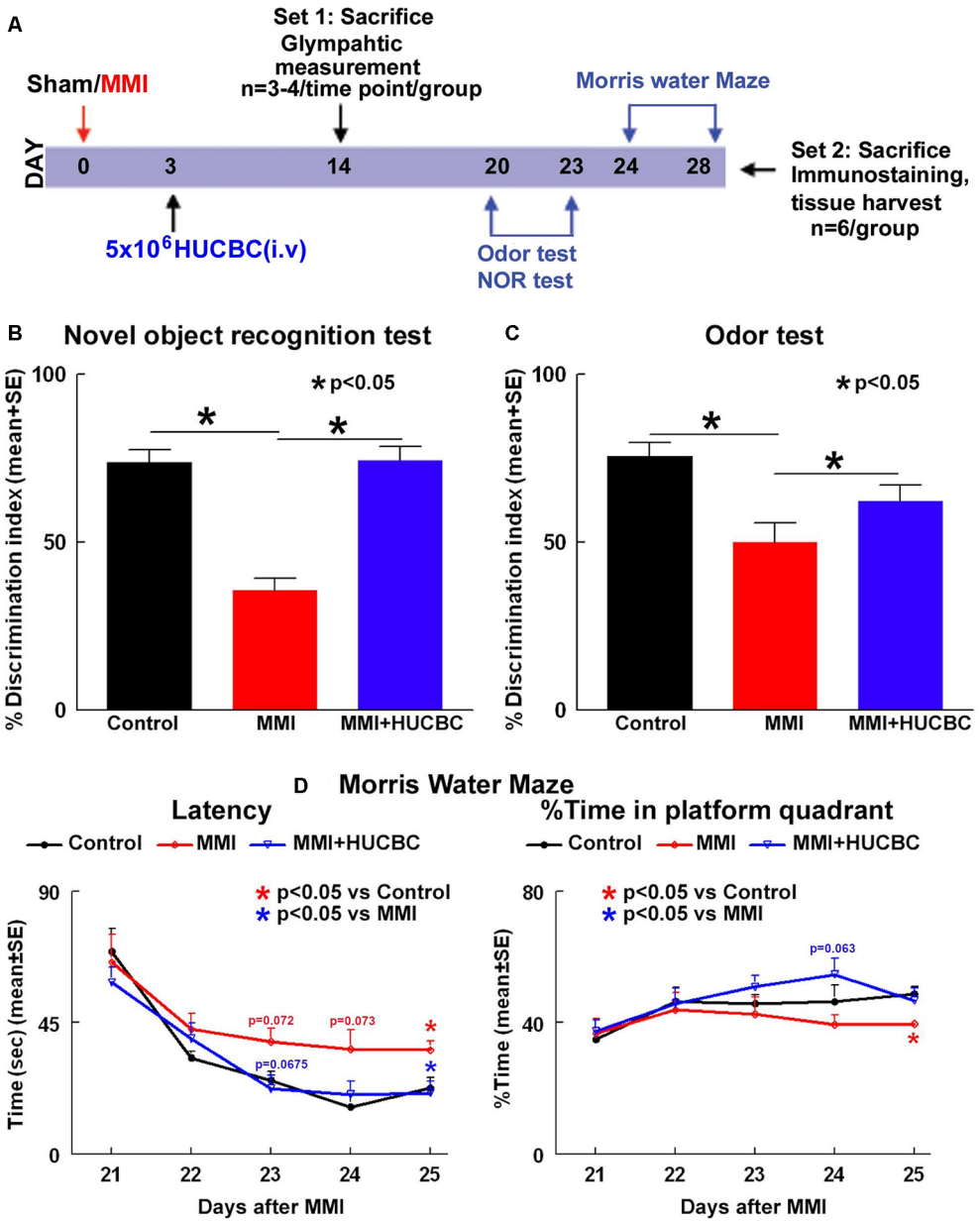

FIGURE 1 | Human umbilical cord blood cells (HUCBC) treatment improves cognitive outcome at 1 month in rats subject to multiple microinfarction (MMI). **(A)** Schematic timeline of the study. Rats were randomized to Sham, MMI, or MMI+HUCBC treatment groups. The MMI+HUCBC group received 5 × 10^6 HUCBCs administered *via* tail vein injection at 3 days after MMI. Cognitive tests were performed 21–28 days following MMI surgery. HUCBC treatment in retired breeder rats subjected to MMI significantly attenuates VaD-induced **(B)** short-term memory loss (NOR test), **(C)** long-term memory deficits (odor test), and **(D)** spatial learning and memory deficits (MWM test) compared to control MMI rats, *n* = 6/group.

and memory. The MWM test spans 5 days and consists of four 90-second trials per day. A dark-colored tank was halfway filled with water and virtually subdivided into four equal quadrants [northeast (NE), northwest, southeast, and southwest]. A clear, transparent platform was submerged in the NE quadrant and for every four trials, the platform was randomly moved within the NE quadrant. Rats were introduced into the pool facing the wall from one of four pre-designated starting points and allowed to swim freely for 90 s or until it reached the platform. Data collection including time spent in the target quadrant (NE) and escape latency i.e., time to reach the hidden platform was performed using ANY-Maze software and data were averaged over four trials for each day to yield a single value for each rat/day.

Glymphatic Measurement

An additional set of sham, MMI, and MMI+HUCBC rats (*n* = 3–4 rats/time point) were employed to evaluate glymphatic

function. Tracers including Texas Red conjugated dextran (MW: 3 kDa, Invitrogen) and FITC conjugated dextran (MW: 500 kDa, Invitrogen) were diluted to 1% in artificial CSF. At 2 weeks after MMI, 100 μl of 1% fluorescent tracers at a 1:1 ratio were slowly injected over 30 min using a syringe pump into the cisterna magna, as previously described (Yang et al., 2013; Venkat et al., 2017). Rats were sacrificed at 30 min, 3 h, and 6 h from the beginning of infusion and transcardially perfused with saline and 4% paraformaldehyde. Vibratome sections of brain coronal sections (80 μm thick) were cut and Laser scanning confocal microscopy was used to evaluate tracer intensity in brain sections.

Histological and Immunohistochemical Assessment

Rats were deeply anesthetized by intraperitoneal injection of ketamine (87 mg/Kg) and Xylazine (13 mg/Kg) which was followed by transcardial perfusion with 0.9% saline using a Simon Varistaltic Pump. For each rat, a section of the brain (frontal cortex) tissue was snapped frozen in liquid nitrogen and stored at −80°C for western blot analysis. The rest of the brain was immersion fixed in 4% paraformaldehyde for 48 h after which the brains were embedded in paraffin and seven equally spaced coronal blocks (∼2 mm) cut using a rat brain matrix, as previously described (Defazio et al., 2014). A series of adjacent 6 μm thick C sections were cut and employed for various staining. Brain coronal tissue sections were prepared and an antibody against AQP4 (Millipore, 1:1,000) was employed to assess water channel dysfunction. Antibodies against APC (oligodendrocyte marker, Genway, 1:20), NG2 (oligodendrocyte progenitor cell marker, MilliporeSigma, 1:400), Synaptophysin (synaptic protein, Abcam, 1:400) were also used. Bielschowsky silver was used to stain axons and Luxol fast blue was used to stain myelin. An antibody against amyloid-β 1–42 (amyloid-β 1–42, Abcam, 1:100) was used to assess amyloid-β levels. Similar procedures without the addition of primary antibodies were used as controls.

Quantification Analysis

As WM/axonal damage was observed in both hemispheres, eight fields of view consisting of corpus callosum (CC), cortex, striatum, and hippocampus were digitized for each brain section under a 20× or 40× objective (Olympus) using a color video camera interfaced with MCID image analysis system (Imaging Research). Positive cell numbers were counted for each field of view or the positively stained area was quantified using a built-in densitometry function in the MCID image analysis system with a density threshold set above unstained. For each animal, data were averaged to yield either percentage positive area or number of positive cells/mm^2.

MiR-126 Measurement

Samples were lysed and total RNA was extracted using Qiazol reagents and miRNeasy Mini kit (Qiagen), respectively. According to the manufacturer's protocols, miRNAs were reverse transcribed with the miRNA Reverse Transcription kit (Thermo Fisher Scientific) and PCR amplification was performed with the TaqMan miRNA assay kit (hsa-miR-126-3p, Thermo Fisher Scientific, catalog #4427975, which is specific for mature miRNA sequences) with U6 snRNA as an internal control (Chen et al., 2016). For the qPCR reactions, we used 2 μl of isolated RNA per cDNA reaction and then used 3 μl of cDNA for each PCR reaction.

Western Blot

Protein was extracted from samples using Trizol (Invitrogen). The BCA kit (Thermo Scientific) was used to measure protein concentration and 40 μg of protein/lane loaded in a 10% SDS PAGE precast gel (Invitrogen). The gel was placed in a tank where 120 volts of electrical current was run for approximately one and a half hours. The gel was subsequently transferred to a nitrocellulose membrane using the iBlot transfer system (Invitrogen). This membrane was blocked in 2% I-Block (Applied Biosystems) in 1× TBS-T for 1 h, and then either β-actin (Abcam, 1:10,000), TGF-β (R&D Sytems, 1:1,000), Amyloid-β 1–40 (MyBioresource, 1:500) or Amyloid-β 1–42 (Abcam, 1:1,000) was used. For Synaptophysin and PSD-95, 30 μg of protein/lane was loaded, and either GAPDH (Abcam, 1:5,000), PSD-95 (Cell signaling, 1:750) or Synaptophysin (Chemicon, 1:2,000) were used. Secondary antibodies (anti-mouse, Jackson ImmunoResearch) were added at 1:1,000 dilution in 2% I-Block in 1× TBS-T at room temperature. The membranes were washed with 1× TBS-T, and then Luminol Reagent (Santa Cruz) was added. The membranes were then developed using a FluorChem E Imager system (ProteinSimple). Grayscale images were analyzed using ImageJ and normalized to β-actin or GAPDH.

Statistical Analysis

Repeated measure analysis of variance (ANOVA) was used to test group differences in the water maze test. *Post hoc* analysis was performed, and p-values were adjusted following Tukey multiple comparison testing. Unpaired 2-tailed Student *t*-test was used for comparison of two groups with the use of GraphPad Prism 8. $P < 0.05$ was considered statistically significant.

RESULTS

HUCBC Treatment Improves Cognition and Memory in Rats Subjected to MMI

To test whether treatment of MMI with HUCBCs improves cognition and memory in rats, a battery of cognitive tests was performed 21–28 days after MMI. Data in **Figures 1B–D** show that rats subjected to MMI and treated with HUCBCs exhibit significantly higher discrimination index in NOR task indicating improved short-term memory, higher discrimination index in odor test indicating improved long-term memory, and decreased latency in MWM test indicating improved spatial learning and memory compared to MMI control rats.

HUCBC Treatment Promotes Glymphatic Clearance in Rats Subjected to MMI

Glymphatic dysfunction has been implicated to induce WM damage and cognitive decline in rats subject to MMI, stroke,

and other neurological diseases (Yan et al., 2015). Thus, we tested if HUCBC treatment improves glymphatic function in an additional set of sham, MMI, and MMI+HUCBC rats. At 14 days after MMI, fluorescent tracers (3 kDa Texas Red conjugated dextran and 500 kDa FITC conjugated dextran) were injected into the cisterna magna. To analyze tracer movement, rats (n = 3–4/time point/group) were sacrificed at 30 min, 3 h, and 6 h after tracer infusion and perfusion fixed. Tracer fluorescence intensities were quantified in whole-brain coronal sections using laser scanning confocal microscopy. Data in **Figures 2A,B** indicate that compared to the sham group, rats subjected to MMI exhibit a significant delay in tracer influx indicated by low tracer intensities at 30 mins and persisting tracer accumulation with poor clearance from brain parenchyma indicated by high fluorescent intensities at 6 h after tracer infusion. HUCBC treatment significantly improves glymphatic function and reverses MMI induced delay in CSF penetration into the brain parenchyma and clearance from the brain *via* perivascular pathways.

We have previously found that mice subjected to MMI have significantly decreased miR-126 expression which contributes to cognitive impairment, WM injury, and glymphatic dysfunction (Yu et al., 2019). Therefore, we measured serum miR-126 expression and found that HUCBC treatment significantly increases serum miR-126 expression compared to the control MMI rats (**Figure 3A**). AQP4 expression around cerebral blood vessels is closely related to the proper functioning of the glymphatic system and mice lacking AQP-4 exhibit delayed CSF influx *via* the glymphatic pathways and approximately a 70% reduction in interstitial solute clearance (Iliff et al., 2012; Venkat et al., 2017). Therefore, we evaluated AQP4 expression around cerebral blood vessels and found that HUCBC treatment of MMI significantly increases AQP4 expression compared to control MMI rats which may contribute to improved glymphatic function (**Figure 3C**). In addition to water channel dysfunction, vascular changes such as hardening of cerebral vessels caused by increased TGF-β may also contribute to the impaired glymphatic function. We found that HUCBC treatment of MMI significantly decreases brain TGF-β expression compared to control MMI rats which may contribute to improved glymphatic function (**Figure 3B**).

HUCBC Treatment Decreases WM Injury in Rats Subjected to MMI

WM injury is characteristic of VaD and is associated with cognitive decline in patients as well as in experimental animal models of dementia (Filley and Fields, 2016). MMI rats treated with HUCBCs exhibit significantly increased axon density (**Figures 4A,B**, Bielschowsky Silver) and myelin density (**Figures 4C,D**, Luxol Fast Blue) in WM tracts in the corpus callosum and WM bundles in the striatum, as well as significantly increased number of oligodendrocyte progenitor cell (**Figures 5A,B**, NG2) and oligodendrocytes (**Figures 5C,D**, APC) in the cortex and striatum when compared to control MMI rats.

HUCBC Treatment Increases Synaptophysin Expression in Rats Subjected to MMI

To assess whether HUCBC treatment improves synaptic protein expression in the brain of rats subjected to MMI, we measured the expression of Synaptophysin, the major integral membrane glycoprotein present in neuronal synaptic vesicles (Clare et al., 2010). HUCBC treatment of MMI in rats significantly increases Synaptophysin protein expression in the cortex and striatum compared to control MMI rats (**Figures 6A,B**). However, we could not detect significant differences in Synaptophysin or PSD-95 protein expression in cortical brain tissue using Western blot between Control and MMI or MMI and MMI+HUCBC groups (**Figure 6C**).

MMI or HUCBC Treatment Does Not Alter Amyloid-β in Rat Brain

HUCBC treatment has previously been shown to reduce cerebral and vascular β-amyloid plaques and $A\beta_{1-40,42}$ peptides in the brain tissue of transgenic AD mice (Nikolic et al., 2008). Therefore, we performed immunostaining to assess amyloid-β levels in Control, MMI, and MMI+HUCBC groups. However, we did not find significant positive staining for amyloid-β in control, MMI, or MMI+HUCBC group (**Figures 7A,B**). We also tested Aβ expression in the brain of sham, MMI, and MMI+HUCBC rats using Western blot. We did not find a significant increase in $A\beta_{1-40}$ or $A\beta_{1-42}$ levels in the brain of MMI animals compared to control animals and HUCBC treatment did not affect Aβ levels (**Figure 7C**).

DISCUSSION

In the current study, we show that HUCBC treatment of VaD in rats improves cognition and memory which may be mediated in concert by enhanced glymphatic clearance, increased miR-126 expression, WM remodeling, and increased synaptic protein expression. Cell therapy continues to be of growing interest as a promising disease-modifying treatment for multiple neurological conditions such as stroke and dementia (Darlington et al., 2015; Yan et al., 2015). HUCBC transplantation has been tested extensively as a treatment for AD (Nikolic et al., 2008; Kim et al., 2015) and stroke (Vendrame et al., 2004; Yan et al., 2014, 2015). There is currently a lack of studies that test the therapeutic benefits of HUCBCs for the treatment of VaD which holds high clinical significance. In this study, we provide evidence for the first time that HUCBC treatment improves cognitive function outcome in MMI-induced VaD model and demonstrates that HUCBC treatment improves glymphatic waste clearance in VaD which may contribute to its therapeutic effects.

HUCBC treatment improves cognitive outcomes in animal models of stroke, traumatic brain injury, and AD (Chen et al., 2001b; Lu et al., 2002; Darlington et al., 2013; Yan et al., 2014, 2015; Ehrhart et al., 2016). In elderly dementia patients, transplantation of HUCBC significantly improves early cognitive functions and daily living activity (He et al.,

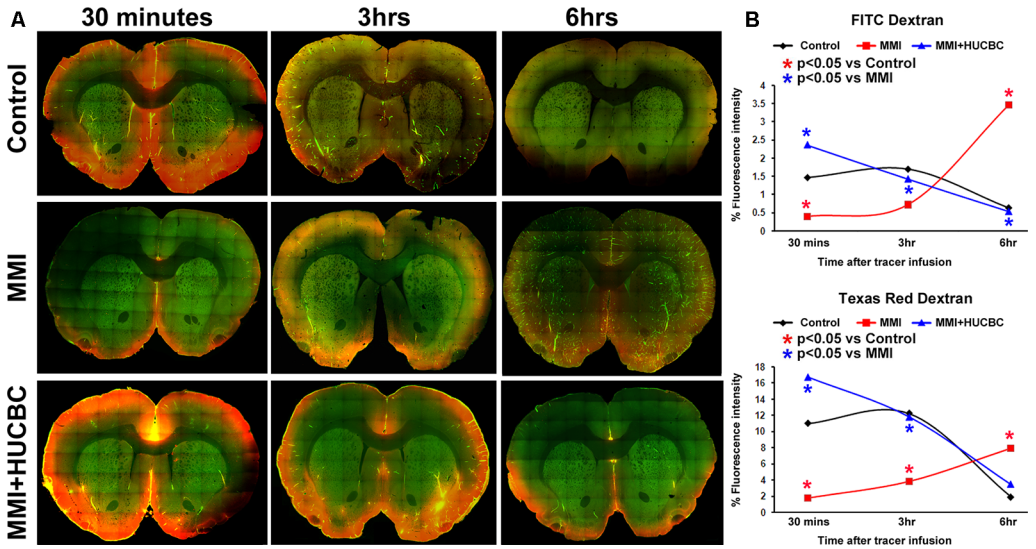

FIGURE 2 | HUCBC treatment improves glymphatic function at 14 days after MMI. In an additional set of sham, MMI, and MMI+HUCBC rats, at 14 days after MMI, 100 μl of 1% fluorescent tracers at a 1:1 ratio (3 kDa Texas Red conjugated dextran and 500 kDa FITC conjugated dextran) was slowly injected into the cisterna magna over 30 min. To analyze tracer movement, rats (*n* = 3–4/time point/group) were sacrificed at 30 min, 3 h, and 6 h after tracer infusion and perfusion fixed. **(A)** Representative images at 30 mins, 3 h, and 6 h after tracer infusion in Sham, MMI, and MMI+HUCBC treated groups. Whole-brain coronal sections (80 μm thick) were imaged under a 10× objective with tiling/image stitching using a laser scanning confocal microscope. **(B)** Tracer fluorescence intensities were quantified using the MCID image analysis system. Compared to the sham group, rats subjected to MMI exhibit a significant delay in tracer influx indicated by low tracer intensities at 30 mins and persisting accumulation with poor clearance from brain parenchyma indicated by high fluorescent intensities at 6 h after tracer infusion. HUCBC treatment significantly improves glymphatic function and reverses MMI induced delay in cerebrospinal fluid (CSF) penetration into the brain parenchyma and clearance from the brain *via* perivascular pathways.

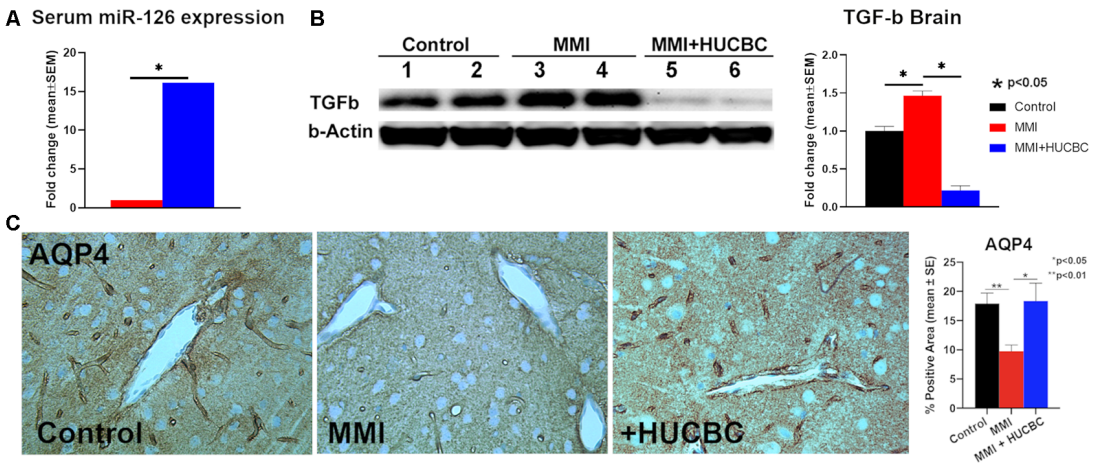

FIGURE 3 | HUCBC treatment increases serum miR-126, increases AQP-4 around cerebral blood vessels and decreases brain TGF-β at 1 month in rats subject to MMI. **(A)** HUCBC treatment significantly increases serum miR-126 expression compared to the control MMI rats, *n* = 6/group. **(B)** Western blot assay showing that HUCBC treatment significantly decreases brain TGF-β protein expression compared to control MMI rats evaluated using Western blot analysis. **(C)** HUCBC treatment significantly increases AQP4 expression around cerebral blood vessels compared to the control MMI rats, *n* = 6/group.

2017). In prior work, using a transient middle cerebral artery occlusion for stroke in rats, we and others have demonstrated that intravenously administered HUCBCs enter the brain and preferentially migrate to injured brain tissue (Chen et al., 2001b; Vendrame et al., 2004; Xiao et al., 2005). In rodent models of AD, intravenously injected HUCBCs were detected in the brain at both 7 and 30 days after transplantation (Ehrhart et al., 2016). A small percentage of HUCBCs were also distributed in the tissue of peripheral organs such as bone marrow, spleen, liver, and kidney, while they were not detected in the circulation at 24 h after injection (Chen et al., 2001b; Ehrhart et al., 2016). Even when HUCBCs

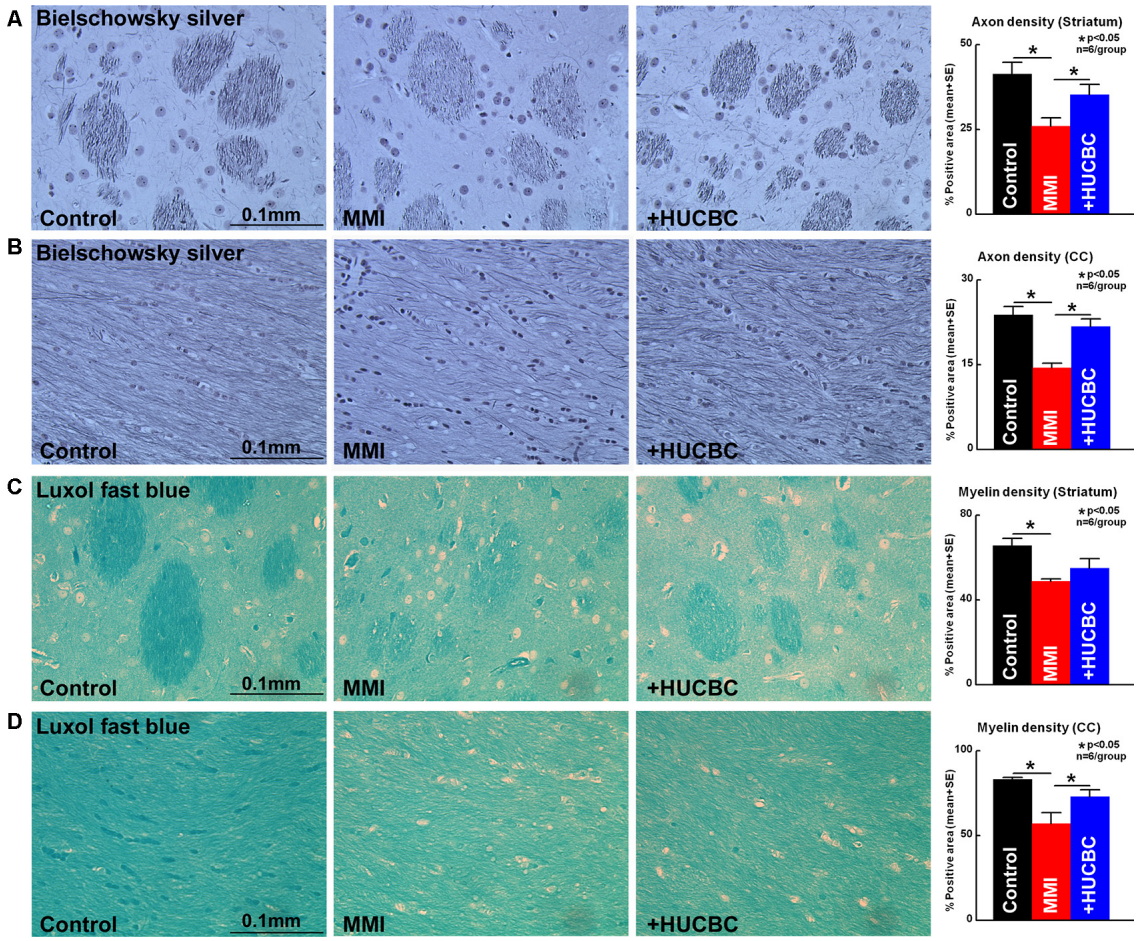

FIGURE 4 | HUCBC treatment improves axon and myelin density in rats subject to MMI. Treatment of MMI with HUCBCs improves white matter (WM) remodeling indicated by significantly increased **(A,B)** axon density and **(C,D)** myelin density in the WM tracts of the corpus callosum and WM bundles of the striatum compared to control MMI rats, *n* = 6/group.

were not detected in the brain following low dose HUCBC intravenous treatment, neuroprotective effects and improvement in neurological function were still observed in the low-dose HUCBC treatment group compared to controls indicating that homing of HUCBC to the brain is not mandatory and HUCBC derived paracrine effects and trophic and growth factors mediate recovery (Borlongan et al., 2004; Xiao et al., 2005). Thus, systemic administration of HUCBCs provides an optimal and viable therapeutic strategy to treat neurodegenerative diseases. VaD is characterized by a decline in cognitive function. Among other symptoms, patients with VaD exhibit memory impairment, disorientation, confusion, anxiety, depression, and attention deficits. Also, patients experience a loss of executive function such as planning, reasoning, organizing thoughts and behavior, and analyzing problems (Venkat et al., 2015). As cognitive impairment is recognized as a key feature in patients with VaD, improvement in memory and cognition is a primary measure for treatment efficacy. In the present study, we employed a battery of cognitive tests to account for the multiple dimensions of impairment seen in patients with VaD. Our data indicate that HUCBC treatment significantly improves short-term memory, long-term memory, and spatial learning and memory as displayed through improved performance in the NOR test, odor test, and MWM respectively when compared to control MMI rats. While HUCBC improves motor function after stroke (Chen et al., 2001b, 2016; Yan et al., 2014, 2015), the MMI model does not induce significant motor deficits in rats (Venkat et al., 2017). In our prior study, we subjected rats of various ages (3–4 months old: young, 6–8 months old: retired breeder and 16–18 months old: aged) to MMI model and performed modified neurological severity score (mNSS) evaluation which tests for motor, sensory, balance and reflex actions and the absence of a tested reflex or abnormal response receives one point (Chen et al., 2001a; Yan et al., 2014). Thus, on a scoring scale of 0–18, a score <6 indicates mild neurological deficits with possibly small to no lesion, a score of 6–12 indicates the presence of substantial neurological deficits with ischemic infarct and score >13 indicates the presence of a very large lesion and predicts poor survival. We found that MMI induces significant motor impairment only in aged

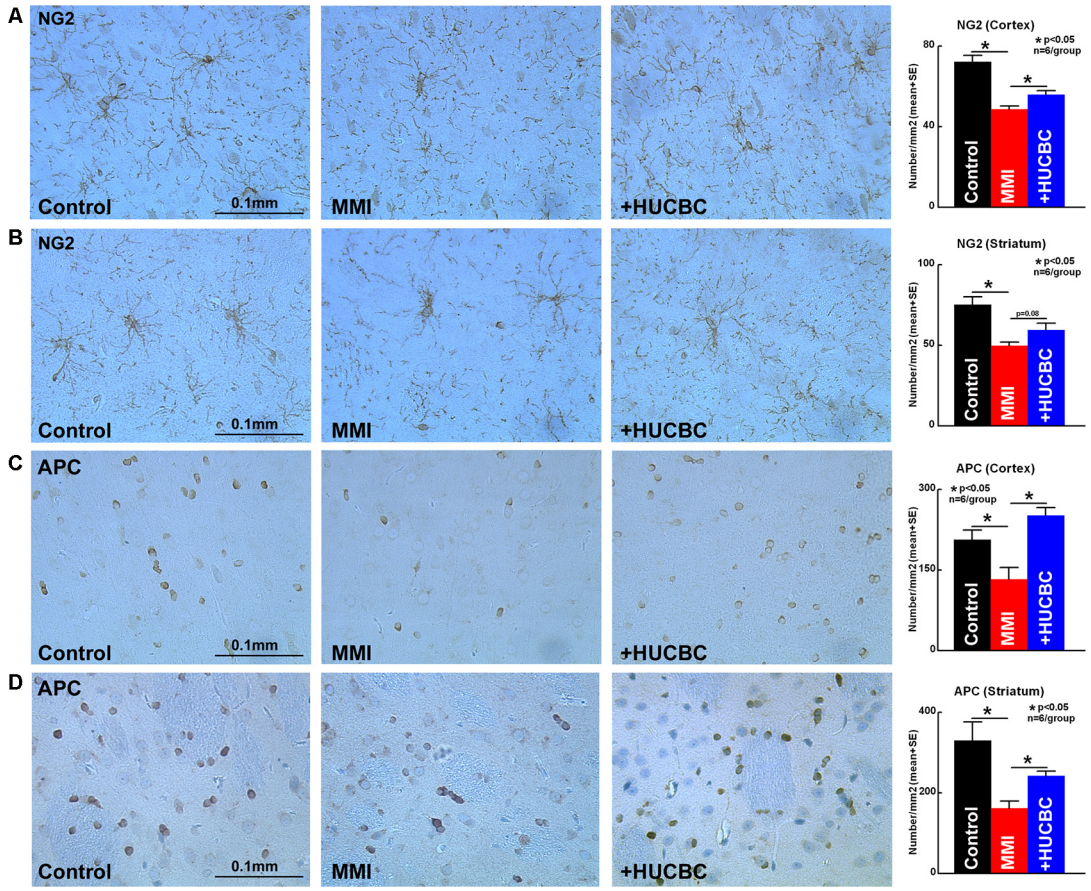

FIGURE 5 | HUCBC treatment improves oligodendrogenesis in rats subject to MMI. Treatment of MMI with HUCBCs improves oligodendrogenesis indicated by a significantly higher number of **(A,B)** OPC and **(C,D)** oligodendrocytes in the cortex and striatum compared to control MMI rats, *n* = 6/group.

rats (16–18 months), while in retired breeder rats there are very slight neurological deficits (average mNSS score of 2.5) on day 1 and low mNSS scores at 21–28 days indicate that motor deficits are unlikely to affect the cognitive outcome (Venkat et al., 2017).

The glymphatic system comprises a brain-wide waste clearance pathway that enables the drainage of CSF and interstitial fluid thereby facilitating the clearance of metabolic waste from the brain parenchyma (Zhang et al., 2019). Dysfunction within this system has been implicated in a variety of conditions including AD, diabetes mellitus, and VaD (Jessen et al., 2015; Venkat et al., 2017). Microinfarcts have been shown to impair the global influx of CSF along the glymphatic pathway and microlesions trap interstitial solutes within the brain parenchyma (Wang et al., 2017). This trapping of solutes and overall impairment of glymphatic function can lead to the aggregation of proteins and inflammation within the brain which can cause neurodegeneration and thus dementia (Wang et al., 2017). AQP4 is mainly present in cells lining the ventricles and in astrocytic end-feet near capillaries. AQP4 is essential in transporting and regulating water movement between cellular, vascular, and ventricular compartments as well as facilitating movement of CSF into the brain, CSF-interstitial fluid exchange, and interstitial solute clearance (Badaut et al., 2011). A widespread loss of AQP4 polarization and overall dysfunction in waste clearance has been found in the aging brain and this reduction in glymphatic clearance has been proposed to contribute to the cognitive decline seen among the elderly (Kress et al., 2014). In our previous study, we have demonstrated that MMI causes a reduction in AQP4 expression around cerebral vessels and induces glymphatic dysfunction with delayed penetration and clearance of CSF *via* paravascular pathways (Venkat et al., 2017; Yu et al., 2019). This glymphatic dysfunction was significantly correlated with reduced cognitive outcome. Our data in the present study indicate that treatment with HUCBCs significantly increases AQP4 expression and improves glymphatic system function at 14 days after MMI. As previously discussed, our data indicate that brain TGF-β expression is increased in MMI rats and subsequently decreased after treatment with HUCBC. TGF-β levels have also been shown to increase in models of stroke and have been implicated in stroke-induced glymphatic dysfunction (Howe et al., 2019). Specifically, increased levels of brain TGF-

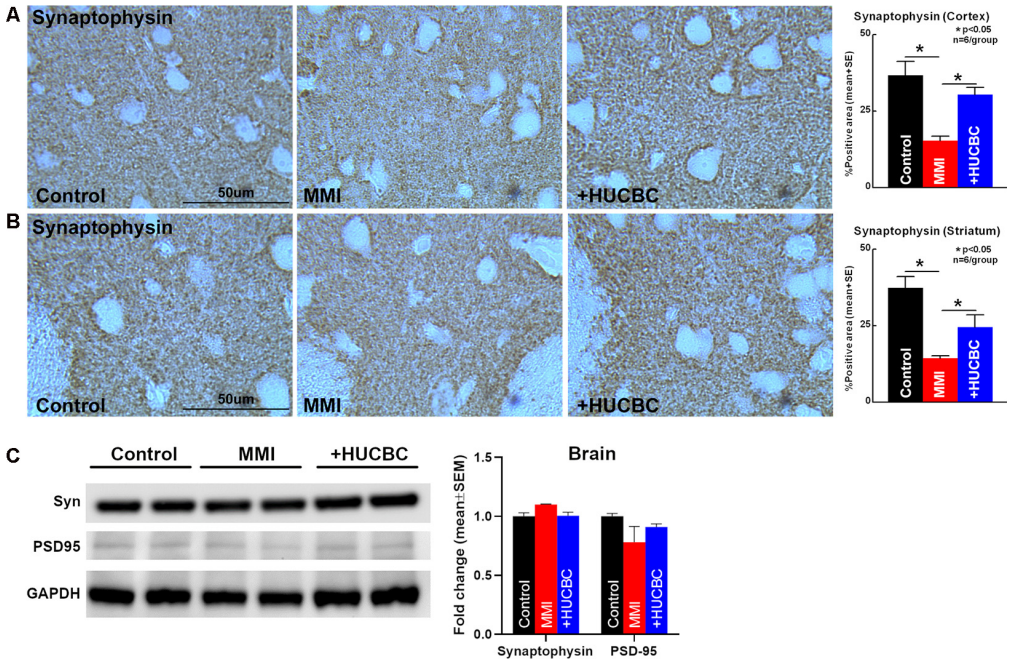

FIGURE 6 | HUCBC treatment improves synaptic vesicle protein in rats subject to MMI. **(A,B)** HUCBC treatment in rats subject to MMI significantly increases the expression of Synaptophysin, a major synaptic vesicle protein, in the cortex as well as striatum compared to control MMI rats, *n* = 6/group. **(C)** Western blot showing Synaptophysin and PSD-95 expression in the brain of sham, MMI, and MMI+HUCBC rats. MMI does not alter cortical brain levels of Synaptophysin or PSD-95 compared to control rats. HUCBC treatment does not alter cortical brain levels of Synaptophysin or PSD-95 compared to MMI rats, *n* = 6/group.

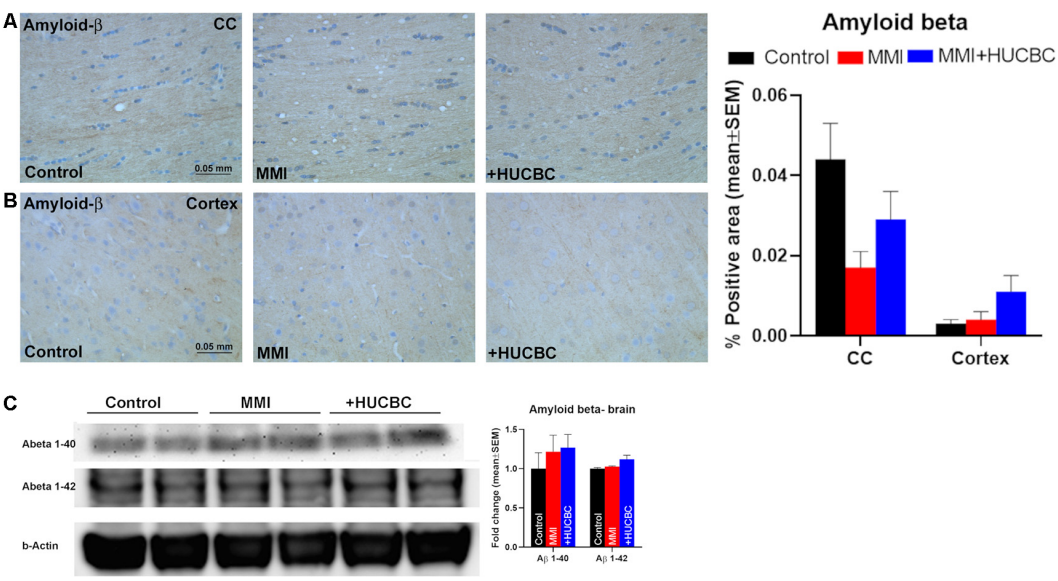

FIGURE 7 | MMI or HUCBC treatment does not alter Amyloid-β in rats subject to MMI. **(A,B)** MMI does not significantly increase Aβ expression in the corpus callosum or cortex compared to control rats. HUCBC treatment does not alter Aβ expression in the corpus callosum or cortex compared to MMI rats, *n* = 6/group. **(C)** Western blot showing Aβ expression in the brain of sham, MMI, and MMI+HUCBC rats. MMI does not increase brain $A\beta_{1-40}$ or $A\beta_{1-42}$ levels compared to control rats and HUCBC treatment does not affect Aβ levels compared to MMI rats, *n* = 6/group.

β expression are associated with an increase in fibronectin within the basement membrane which is an essential regulator of CSF distribution and waste clearance from the brain parenchyma (Engelhardt and Sorokin, 2009; Thomsen et al., 2017; Howe et al., 2018, 2019). Fibrosis of the basement membrane leads to the hardening of vessels and reduces

the overall flow of CSF, thus impairing glymphatic waste clearance (Howe et al., 2019). Therefore, an increase in TGF-β may contribute to the glymphatic dysfunction in VaD patients and a reduction in TGF-β levels contributes to the enhancement of glymphatic clearance observed with HUCBC treatment.

WM damage is a common pathology in VaD patients which arises from demyelination and axonal loss due to hypoxia-related damage to OLs (Ihara et al., 2010). WM damage progresses due to the failure of remyelination caused by impaired survival, proliferation, migration, recruitment, and differentiation of OPCs (Maki et al., 2013). Myelin is essential for the coordination and rapid conduction of impulses between cortical regions which are essential for learning and memory (Fields, 2008). As WM facilitates connectivity within the brain which is crucial for the vast array of human cognitive capacities, damage to WM is regarded as a cause of cognitive impairment (Filley and Fields, 2016). A reduction in frontal WM is associated with worse outcomes in working memory tasks (Ehrler et al., 2019) and working and episodic memory dysfunctions also increase with increasing severity of WM lesions (Zeng et al., 2019). HUCBCs have previously been shown to improve OL survival under hypoxia conditions and promote OPC to OL maturation *in vitro* (Hall et al., 2009; Rowe et al., 2010, 2012). In addition, HUCBCs protect striatal WM tracts in animal models of ischemia (Rowe et al., 2010, 2012). Our data show that treatment with HUCBCs significantly increases axon and myelin density in WM tracts in the corpus callosum and WM bundles in the striatum and increases OL and OPC number in the cortex and striatum when compared to untreated MMI rats. Therefore, the promotion of myelination and increase in axon density may be a major contributor to HUCBC induced improvement in cognitive function. Synaptophysin is the most abundant protein present in synaptic vesicles and is an essential factor in synaptic plasticity and memory storage (Clare et al., 2010). It has previously been reported that enhanced synaptic plasticity measured through an increase in synaptophysin expression mediates treatment benefits after stroke (Chen et al., 2010). Using immunohistochemical analysis and imaging under high magnification, we found that HUCBC treatment in MMI rats significantly increases synaptophysin expression compared to control MMI rats. However, we could not detect significant differences in Synaptophysin or PSD-95 protein expression in cortical brain tissue using Western blot between Control and MMI or MMI and MMI+HUCBC groups. The difference between Western blot data and imaging data may be attributed to imaging in specific brain regions compared to using cortical brain tissue for Western blot. Also, the MMI model does not induce wide spread brain damage while synaptophysin is expressed extensively brain wide. Further studies are warranted to test whether HUCBC treatment improves synaptic plasticity in VaD.

In this study, we have primarily examined whether HUCBC treatment improves cognitive outcome and improves VaD pathology but have not tested the underlying molecular mechanisms. MicroRNAs are small, non-coding RNA sequences that are known to regulate many genes, pathways, and biological networks within cells (Kress et al., 2014). MiR-126 is specifically expressed by endothelial cells and primary human endothelial cell lines from veins, arteries, skin, and brain were found to express miR-126 while vascular smooth muscle cells or leukocyte cell lines did not express miR-126 (Harris et al., 2008). Previous studies have analyzed miR-126 level in various murine tissue and found that miR-126 is enriched in tissues with a high vascular component such as heart and lung and expressed at lower levels in the brain, liver, and kidney (Landgraf et al., 2007; Harris et al., 2008; Wang et al., 2008). MiR-126 is significantly decreased in the serum and brain of various animal models of VaD, stroke, and diabetic stroke as well as in cellular models of ischemia/reperfusion (Venkat et al., 2019; Yu et al., 2019; Pan et al., 2020). In a model of transient ischemia, miR-126 was found to be significantly decreased in key brain regions such as the hippocampus and cerebral cortex compared to controls, with the lowest expression in these regions occurring at 24 h after stroke (Xiao et al., 2020). In humans with ischemic stroke, circulating miR-126 is significantly decreased compared to healthy subjects starting at 24 h and lasting until 24 weeks after stroke onset (Long et al., 2013). Serum miR-126 is also decreased in mild, moderate, and severe AD patients compared to healthy controls (Guo et al., 2017). Whether miR-126 expression is altered in human VaD brain is yet to be investigated. The increasing miR-126 expression has been shown to decrease infarct volume, WM and vascular damage, inflammation, and BBB leakage which translates to better cognitive outcomes in dementia and stroke (Venkat et al., 2019; Yu et al., 2019; Pan et al., 2020). Previously, we have found that mice subjected to MMI have significantly decreased miR-126 expression which may play a key role in mediating cognitive impairment after MMI (Yu et al., 2019). Also, mice with endothelial miR-126 knockdown exhibited significant cognitive dysfunction, reduced CBF, WM rarefaction including decreased myelin and axon density, increased inflammation and glial activation, and significant glymphatic dysfunction (Yu et al., 2019). We have previously demonstrated that HUCBC treatment increases miR-126 expression and improves functional outcome, promotes WM remodeling, and reduces inflammation after stroke in diabetic mice (Chen et al., 2016). Therefore, we measured serum miR-26 expression and found that the HUCBC treatment of MMI rats significantly increases serum miR-126 expression compared to the control MMI rats. Thus, it is likely that in MMI as well, HUCBC treatment-induced therapeutic effects are regulated at least in part by increasing miR-126 expression and future studies are warranted.

LIMITATION

In humans, as well as rodents, cognitive outcome deteriorates with increasing age (Goldman et al., 1992; Park et al., 2007). It is important to consider age as a factor and employ aged animals in studies investigating mechanisms and therapeutics for VaD. The MMI model effectively induces cognitive deficits

in middle-aged rats but not in young adult rats (Rapp et al., 2008b). However, our previous study found that aged rats (16–18 months) exhibit age-induced cognitive deficits, and MMI in aged rats induces significant neurological deficits that can potentially interfere with cognitive test outcomes (Venkat et al., 2017, 2019). Although aged-MMI rats have significant cognitive deficits compared to aged control, aged-MMI induced additional cognitive deficits were not detected using the water maze test compared to aged-control rats (Venkat et al., 2019). In addition to having worse outcomes after stroke than men fluctuations in endogenous estrogens levels can also affect the female brain (Bushnell et al., 2006; Lobo, 2007). Sex should also be considered as a factor that may regulate the association between depressive symptoms and WM lesions (Kirton et al., 2014). In this study, we have only tested the HUCBC effect in male middle-aged rats and future studies are warranted to test efficacy in female middle-aged rats. In the current study, we demonstrate using immunohistochemical analysis that HUCBC treatment of MMI significantly increases axon and myelin density in the WM of the corpus callosum and striatum and increases OPC and oligodendrocyte numbers in the cortex and striatum. However, we did not study the ultrastructure of myelin using Electron microscopy, and further studies are warranted. We have previously demonstrated the therapeutic potential of HUCBC in the treatment of stroke with co-morbid diabetes (Yan et al., 2014, 2015). Also, treatment with HUCBC-derived mesenchymal stem cells prevents inflammation, apoptosis, and remodeling in lung and heart tissue in a model of pulmonary hypertension (Kim et al., 2016). Since hypertension and diabetes are pertinent risk factors for VaD and patients often have co-morbidities, HUCBCs likely have therapeutic potential to treat this population, and future studies are warranted.

CONCLUSIONS

HUCBC treatment of an MMI rat model of VaD promotes WM remodeling, increases serum miR-126 expression, and improves glymphatic function which in concert may contribute to the recovery in the cognitive outcome. Thus, HUCBC treatment warrants further investigation as a potential therapy for VaD.

DATA AVAILABILITY STATEMENT

All datasets presented in this study are included in the article.

ETHICS STATEMENT

The animal study was reviewed and approved by Institutional Animal Care and Use Committee of Henry Ford Health System.

AUTHOR CONTRIBUTIONS

PV performed experiments, analyzed data, and wrote the manuscript. LC performed experiments and wrote the manuscript. AZ, FW, and JL-W performed experiments. MC and JC were involved in experimental design, made critical revisions, and gave final approval of the manuscript.

ACKNOWLEDGMENTS

We wish to thank Qinge Lu and Sutapa Santra for their technical assistance. HUCBC was obtained from Saneron CCEL Therapeutics, Inc., and we wish to thank Nicole Kuzmin-Nichols, Ph.D. (President and COO at Saneron CCEL Therapeutics, Inc.), Cyndy Davis Sanberg, Ph.D. (Sr. VP of R&D, Saneron CCEL Therapeutics, Inc.) for providing HUCBC.

REFERENCES

Badaut, J., Ashwal, S., and Obenaus, A. (2011). Aquaporins in cerebrovascular disease: a target for treatment of brain edema? *Cerebrovasc. Dis.* 31, 521–531. doi: 10.1159/000324328

Borlongan, C. V., Hadman, M., Sanberg, C. D., and Sanberg, P. R. (2004). Central nervous system entry of peripherally injected umbilical cord blood cells is not required for neuroprotection in stroke. *Stroke* 35, 2385–2389. doi: 10.1161/01.STR.0000141680.49960.d7

Bushnell, C. D., Hurn, P., Colton, C., Miller, V. M., del Zoppo, G., Elkind, M. S., et al. (2006). Advancing the study of stroke in women: summary and recommendations for future research from an NINDS-sponsored multidisciplinary working group. *Stroke* 37, 2387–2399. doi: 10.1161/01.STR.0000236053.37695.15

Chen, J., Li, Y., Wang, L., Zhang, Z., Lu, D., Lu, M., et al. (2001a). Therapeutic benefit of intravenous administration of bone marrow stromal cells after cerebral ischemia in rats. *Stroke* 32, 1005–1011. doi: 10.1161/01.str.32.4.1005

Chen, J., Sanberg, P. R., Li, Y., Wang, L., Lu, M., Willing, A. E., et al. (2001b). Intravenous administration of human umbilical cord blood reduces behavioral deficits after stroke in rats. *Stroke* 32, 2682–2688. doi: 10.1161/hs1101.098367

Chen, J., Ning, R., Zacharek, A., Cui, C., Cui, X., Yan, T., et al. (2016). MiR-126 contributes to human umbilical cord blood cell-induced neurorestorative effects after stroke in type-2 diabetic mice. *Stem Cells* 34, 102–113. doi: 10.1002/stem.2193

Chen, J., Zacharek, A., Cui, X., Shehadah, A., Jiang, H., Roberts, C., et al. (2010). Treatment of stroke with a synthetic liver X receptor agonist, TO901317, promotes synaptic plasticity and axonal regeneration in mice. *J. Cereb. Blood Flow Metab.* 30, 102–109. doi: 10.1038/jcbfm.2009.187

Clare, R., King, V. G., Wirenfeldt, M., and Vinters, H. V. (2010). Synapse loss in dementias. *J. Neurosci. Res.* 88, 2083–2090. doi: 10.1002/jnr.22392

Darlington, D., Deng, J., Giunta, B., Hou, H., Sanberg, C. D., Kuzmin-Nichols, N., et al. (2013). Multiple low-dose infusions of human umbilical cord blood cells improve cognitive impairments and reduce amyloid-β-associated neuropathology in Alzheimer mice. *Stem Cells Dev.* 22, 412–421. doi: 10.1089/scd.2012.0345

Darlington, D., Li, S., Hou, H., Habib, A., Tian, J., Gao, Y., et al. (2015). Human umbilical cord blood-derived monocytes improve cognitive deficits and reduce amyloid-β pathology in PSAPP mice. *Cell Transplant.* 24, 2237–2250. doi: 10.3727/096368915x688894

Darwish, H., Mahmood, A., Schallert, T., Chopp, M., and Therrien, B. (2012). Mild traumatic brain injury (MTBI) leads to spatial learning deficits. *Brain Inj.* 26, 151–165. doi: 10.3109/02699052.2011.635362

Defazio, R., Criado, A., Zantedeschi, V., and Scanziani, E. (2014). Neuroanatomy-based matrix-guided trimming protocol for the rat brain. *Toxicol. Pathol.* 43, 249–256. doi: 10.1177/0192623314538345

Ehrhart, J., Darlington, D., Kuzmin-Nichols, N., Sanberg, C. D., Sawmiller, D. R., Sanberg, P. R., et al. (2016). Biodistribution of infused human umbilical cord blood cells in Alzheimer's disease-like murine model. *Cell Transplant.* 25, 195–199. doi: 10.3727/096368915x689604

Ehrler, M., Latal, B., Kretschmar, O., von Rhein, M., and O'Gorman Tuura, R. (2019). Altered frontal white matter microstructure is associated with working memory impairments in adolescents with congenital heart disease: a diffusion

tensor imaging study. *Neuroimage Clin.* 25:102123. doi: 10.1016/j.nicl.2019.102123

Engelhardt, B., and Sorokin, L. (2009). The blood-brain and the blood-cerebrospinal fluid barriers: function and dysfunction. *Semin. Immunopathol.* 31, 497–511. doi: 10.1007/s00281-009-0177-0

Fields, R. D. (2008). White matter in learning, cognition and psychiatric disorders. *Trends Neurosci.* 31, 361–370. doi: 10.1016/j.tins.2008.04.001

Filley, C. M., and Fields, R. D. (2016). White matter and cognition: making the connection. *J. Neurophysiol.* 116, 2093–2104. doi: 10.1152/jn.00221.2016

Fish, J. E., Santoro, M. M., Morton, S. U., Yu, S., Yeh, R. F., Wythe, J. D., et al. (2008). miR-126 regulates angiogenic signaling and vascular integrity. *Dev. Cell* 15, 272–284. doi: 10.1016/j.devcel.2008.07.008

Gaberel, T., Gakuba, C., Goulay, R., Martinez De Lizarrondo, S., Hanouz, J. L., Emery, E., et al. (2014). Impaired glymphatic perfusion after strokes revealed by contrast-enhanced MRI: a new target for fibrinolysis? *Stroke* 45, 3092–3096. doi: 10.1161/STROKEAHA.114.006617

Goldman, H., Berman, R. F., Gershon, S., Murphy, S., Morehead, M., and Altman, H. J. (1992). Cerebrovascular permeability and cognition in the aging rat. *Neurobiol. Aging* 13, 57–62. doi: 10.1016/0197-4580(92)90009-m

Guo, R., Fan, G., Zhang, J., Wu, C., Du, Y., Ye, H., et al. (2017). A 9-microRNA signature in serum serves as a noninvasive biomarker in early diagnosis of Alzheimer's disease. *J. Alzheimers Dis.* 60, 1365–1377. doi: 10.3233/JAD-170343

Hall, A. A., Guyer, A. G., Leonardo, C. C., Ajmo, C. T. Jr., Collier, L. A., Willing, A. E., et al. (2009). Human umbilical cord blood cells directly suppress ischemic oligodendrocyte cell death. *J. Neurosci. Res.* 87, 333–341. doi: 10.1002/jnr.21857

Harris, T. A., Yamakuchi, M., Ferlito, M., Mendell, J. T., and Lowenstein, C. J. (2008). MicroRNA-126 regulates endothelial expression of vascular cell adhesion molecule 1. *Proc. Natl. Acad. Sci. U S A* 105, 1516–1521. doi: 10.1073/pnas.0707493105

He, Y., Jin, X., Wang, J., Meng, M., Hou, Z., Tian, W., et al. (2017). Umbilical cord-derived mesenchymal stem cell transplantation for treating elderly vascular dementia. *Cell Tissue Bank.* 18, 53–59. doi: 10.1007/s10561-017-9609-6

Howe, M. D., Atadja, L. A., Furr, J. W., Maniskas, M. E., Zhu, L., McCullough, L. D., et al. (2018). Fibronectin induces the perivascular deposition of cerebrospinal fluid-derived amyloid-β in aging and after stroke. *Neurobiol. Aging* 72, 1–13. doi: 10.1016/j.neurobiolaging.2018.07.019

Howe, M. D., Furr, J. W., Munshi, Y., Roy-O'Reilly, M. A., Maniskas, M. E., Koellhoffer, E. C., et al. (2019). Transforming growth factor-β promotes basement membrane fibrosis, alters perivascular cerebrospinal fluid distribution and worsens neurological recovery in the aged brain after stroke. *Geroscience* 41, 543–559. doi: 10.1007/s11357-019-00118-7

Hu, J., Zeng, L., Huang, J., Wang, G., and Lu, H. (2015). miR-126 promotes angiogenesis and attenuates inflammation after contusion spinal cord injury in rats. *Brain Res.* 1608, 191–202. doi: 10.1016/j.brainres.2015.02.036

Ihara, M., Polvikoski, T. M., Hall, R., Slade, J. Y., Perry, R. H., Oakley, A. E., et al. (2010). Quantification of myelin loss in frontal lobe white matter in vascular dementia, Alzheimer's disease and dementia with Lewy bodies. *Acta Neuropathol.* 119, 579–589. doi: 10.1007/s00401-009-0635-8

Iliff, J. J., Wang, M., Liao, Y., Plogg, B. A., Peng, W., Gundersen, G. A., et al. (2012). A paravascular pathway facilitates CSF flow through the brain parenchyma and the clearance of interstitial solutes, including amyloid beta. *Sci. Trans. Med.* 4, 147ra11. doi: 10.1126/scitranslmed.3003748

Jessen, N. A., Munk, A. S., Lundgaard, I., and Nedergaard, M. (2015). The glymphatic system: a beginner's guide. *Neurochem. Res.* 40, 2583–2599. doi: 10.1007/s11064-015-1581-6

Jiang, Q., Zhang, L., Ding, G., Davoodi-Bojd, E., Li, Q., Li, L., et al. (2017). Impairment of the glymphatic system after diabetes. *J. Cereb. Blood Flow Metab.* 37, 1326–1337. doi: 10.1177/0271678x16654702

Kilkenny, C., Browne, W., Cuthill, I. C., Emerson, M., and Altman, D. G. (2010). Animal research: reporting *in vivo* experiments: the ARRIVE guidelines. *Br. J. Pharmacol.* 160, 1577–1579. doi: 10.1111/j.1476-5381.2010.00872.x

Kim, K. C., Lee, J. C., Lee, H., Cho, M. S., Choi, S. J., and Hong, Y. M. (2016). Changes in Caspase-3, B cell Leukemia/Lymphoma-2, Interleukin-6, tumor necrosis factor-alpha and vascular endothelial growth factor gene expression after human umbilical cord blood derived mesenchymal stem cells transfusion in pulmonary hypertension rat models. *Korean Circ. J.* 46, 79–92. doi: 10.4070/kcj.2016.46.1.79

Kim, H. J., Seo, S. W., Chang, J. W., Lee, J. I., Kim, C. H., Chin, J., et al. (2015). Stereotactic brain injection of human umbilical cord blood mesenchymal stem cells in patients with Alzheimer's disease dementia: a phase 1 clinical trial. *Alzheimers Dement.* 1, 95–102. doi: 10.1016/j.trci.2015.06.007

Kirton, J. W., Resnick, S. M., Davatzikos, C., Kraut, M. A., and Dotson, V. M. (2014). Depressive symptoms, symptom dimensions and white matter lesion volume in older adults: a longitudinal study. *Am. J. Geriatr. Psychiatry* 22, 1469–1477. doi: 10.1016/j.jagp.2013.10.005

Kress, B. T., Iliff, J. J., Xia, M., Wang, M., Wei, H. S., Zeppenfeld, D., et al. (2014). Impairment of paravascular clearance pathways in the aging brain. *Ann Neurol.* 76, 845–861. doi: 10.1002/ana.24271

Landgraf, P., Rusu, M., Sheridan, R., Sewer, A., Iovino, N., Aravin, A., et al. (2007). A mammalian microRNA expression atlas based on small RNA library sequencing. *Cell* 129, 1401–1414. doi: 10.1016/j.cell.2007.04.040

Lobo, R. A. (2007). Menopause and stroke and the effects of hormonal therapy. *Climacteric* 10, 27–31. doi: 10.1080/13697130701550903

Long, G., Wang, F., Li, H., Yin, Z., Sandip, C., Lou, Y., et al. (2013). Circulating miR-30a, miR-126 and let-7b as biomarker for ischemic stroke in humans. *BMC Neurol.* 13:178. doi: 10.1186/1471-2377-13-178

Lu, D., Sanberg, P. R., Mahmood, A., Li, Y., Wang, L., Sanchez-Ramos, J., et al. (2002). Intravenous administration of human umbilical cord blood reduces neurological deficit in the rat after traumatic brain injury. *Cell Transplant.* 11, 275–281. doi: 10.3727/096020198389924

Maki, T., Liang, A. C., Miyamoto, N., Lo, E. H., and Arai, K. (2013). Mechanisms of oligodendrocyte regeneration from ventricular-subventricular zone-derived progenitor cells in white matter diseases. *Front. Cell. Neurosci.* 7:275. doi: 10.3389/fncel.2013.00275

Mestre, H., Hablitz, L. M., Xavier, A. L., Feng, W., Zou, W., Pu, T., et al. (2018). Aquaporin-4-dependent glymphatic solute transport in the rodent brain. *eLife* 7:e40070. doi: 10.7554/elife.40070.021

Nikolic, W. V., Hou, H., Town, T., Zhu, Y., Giunta, B., Sanberg, C. D., et al. (2008). Peripherally administered human umbilical cord blood cells reduce parenchymal and vascular beta-amyloid deposits in Alzheimer mice. *Stem Cells Dev.* 17, 423–439. doi: 10.1089/scd.2008.0018

Pan, J., Qu, M., Li, Y., Wang, L., Zhang, L., Wang, Y., et al. (2020). MicroRNA-126–3p/-5p overexpression attenuates blood-brain barrier disruption in a mouse model of middle cerebral artery occlusion. *Stroke* 51, 619–627. doi: 10.1161/strokeaha.119.027531

Park, L., Anrather, J., Girouard, H., Zhou, P., and Iadecola, C. (2007). Nox2-derived reactive oxygen species mediate neurovascular dysregulation in the aging mouse brain. *J. Cereb. Blood Flow Metab.* 27, 1908–1918. doi: 10.1038/sj.jcbfm.9600491

Plassman, B. L., Langa, K. M., Fisher, G. G., Heeringa, S. G., Weir, D. R., Ofstedal, M. B., et al. (2007). Prevalence of dementia in the United States: the aging, demographics and memory study. *Neuroepidemiology* 29, 125–132. doi: 10.1159/000109998

Plog, B. A., and Nedergaard, M. (2018). The glymphatic system in central nervous system health and disease: past, present and future. *Annu. Rev. Pathol.* 13, 379–394. doi: 10.1146/annurev-pathol-051217-111018

Rapp, J. H., Hollenbeck, K., and Pan, X. M. (2008a). An experimental model of lacunar infarction: embolization of microthrombi. *J. Vasc. Surg.* 48, 196–200. doi: 10.1016/j.jvs.2008.01.038

Rapp, J. H., Pan, X. M., Neumann, M., Hong, M., Hollenbeck, K., and Liu, J. (2008b). Microemboli composed of cholesterol crystals disrupt the blood-brain barrier and reduce cognition. *Stroke* 39, 2354–2361. doi: 10.1161/STROKEAHA.107.496737

Rowe, D. D., Leonardo, C. C., Hall, A. A., Shahaduzzaman, M. D., Collier, L. A., Willing, A. E., et al. (2010). Cord blood administration induces oligodendrocyte survival through alterations in gene expression. *Brain Res.* 1366, 172–188. doi: 10.1016/j.brainres.2010.09.078

Rowe, D. D., Leonardo, C. C., Recio, J. A., Collier, L. A., Willing, A. E., and Pennypacker, K. R. (2012). Human umbilical cord blood cells protect oligodendrocytes from brain ischemia through Akt signal transduction. *J. Biol. Chem.* 287, 4177–4187. doi: 10.1074/jbc.M111.296434

Satizabal, C. L., Beiser, A. S., Chouraki, V., Chêne, G., Dufouil, C., and Seshadri, S. (2016). Incidence of dementia over three decades in the

framingham heart study. *N. Engl. J. Med.* 374, 523–532. doi: 10.1056/NEJMoa1504327

Spinetta, M. J., Woodlee, M. T., Feinberg, L. M., Stroud, C., Schallert, K., Cormack, L. K., et al. (2008). Alcohol-induced retrograde memory impairment in rats: prevention by caffeine. *Psychopharmacology* 201, 361–371. doi: 10.1007/s00213-008-1294-5

Stuart, S. A., Robertson, J. D., Marrion, N. V., and Robinson, E. S. (2013). Chronic pravastatin but not atorvastatin treatment impairs cognitive function in two rodent models of learning and memory. *PLoS One* 8:e75467. doi: 10.1371/journal.pone.0075467

Thomsen, M. S., Routhe, L. J., and Moos, T. (2017). The vascular basement membrane in the healthy and pathological brain. *J. Cereb. Blood Flow Metab.* 37, 3300–3317. doi: 10.1177/0271678x17722436

Vendrame, M., Cassady, J., Newcomb, J., Butler, T., Pennypacker, K. R., Zigova, T., et al. (2004). Infusion of human umbilical cord blood cells in a rat model of stroke dose-dependently rescues behavioral deficits and reduces infarct volume. *Stroke* 35, 2390–2395. doi: 10.1161/01.STR.0000141681.06735.9b

Venkat, P., Chopp, M., and Chen, J. (2015). Models and mechanisms of vascular dementia. *Exp. Neurol.* 272, 97–108. doi: 10.1016/j.expneurol.2015.05.006

Venkat, P., Chopp, M., Zacharek, A., Cui, C., Landschoot-Ward, J., Qian, Y., et al. (2019). Sildenafil treatment of vascular dementia in aged rats. *Neurochem. Int.* 127, 103–112. doi: 10.1016/j.neuint.2018.12.015

Venkat, P., Chopp, M., Zacharek, A., Cui, C., Zhang, L., Li, Q., et al. (2017). White matter damage and glymphatic dysfunction in a model of vascular dementia in rats with no prior vascular pathologies. *Neurobiol. Aging* 50, 96–106. doi: 10.1016/j.neurobiolaging.2016.11.002

Venkat, P., Cui, C., Chopp, M., Zacharek, A., Wang, F., Landschoot-Ward, J., et al. (2019). MiR-126 mediates brain endothelial cell exosome treatment-induced neurorestorative effects after stroke in type 2 diabetes mellitus mice. *Stroke* 50, 2865–2874. doi: 10.1161/STROKEAHA.119.025371

Wang, S., Aurora, A. B., Johnson, B. A., Qi, X., McAnally, J., Hill, J. A., et al. (2008). The endothelial-specific MicroRNA miR-126 governs vascular integrity and angiogenesis. *Dev. Cell* 15, 261–271. doi: 10.1016/j.devcel.2008.07.002

Wang, M., Ding, F., Deng, S., Guo, X., Wang, W., Iliff, J. J., et al. (2017). Focal solute trapping and global glymphatic pathway impairment in a murine model of multiple microinfarcts. *J. Neurosci.* 37, 2870–2877. doi: 10.1523/JNEUROSCI.2112-16.2017

Wang, M., Iliff, J. J., Liao, Y., Chen, M. J., Shinseki, M. S., Venkataraman, A., et al. (2012). Cognitive deficits and delayed neuronal loss in a mouse model of multiple microinfarcts. *J. Neurosci.* 32, 17948–17960. doi: 10.1523/JNEUROSCI.1860-12.2012

Wolters, F. J., and Ikram, M. A. (2019). Epidemiology of vascular dementia. *Arterioscler. Thromb. Vasc. Biol.* 39, 1542–1549. doi: 10.1161/ATVBAHA.119.311908

Xiao, J., Nan, Z., Motooka, Y., and Low, W. C. (2005). Transplantation of a novel cell line population of umbilical cord blood stem cells ameliorates neurological deficits associated with ischemic brain injury. *Stem Cells Dev.* 14, 722–733. doi: 10.1089/scd.2005.14.722

Xiao, Z. H., Wang, L., Gan, P., He, J., Yan, B. C., and Ding, L. D. (2020). Dynamic changes in mir-126 expression in the hippocampus and penumbra following experimental transient global and focal cerebral ischemia-reperfusion. *Neurochem. Res.* 45, 1107–1119. doi: 10.1007/s11064-020-02986-4

Xu, Z., Xiao, N., Chen, Y., Huang, H., Marshall, C., Gao, J., et al. (2015). Deletion of aquaporin-4 in APP/PS1 mice exacerbates brain Aβ accumulation and memory deficits. *Mol. Neurodegener.* 10:58. doi: 10.1186/s13024-015-0056-1

Yan, T., Venkat, P., Chopp, M., Zacharek, A., Ning, R., Cui, Y., et al. (2015). Neurorestorative therapy of stroke in type 2 diabetes mellitus rats treated with human umbilical cord blood cells. *Stroke* 46, 2599–2606. doi: 10.1161/STROKEAHA.115.009870

Yan, T., Venkat, P., Ye, X., Chopp, M., Zacharek, A., Ning, R., et al. (2014). HUCBCs increase angiopoietin 1 and induce neurorestorative effects after stroke in T1DM rats. *CNS Neurosci. Ther.* 20, 935–944. doi: 10.1111/cns.12307

Yang, L., Kress, B. T., Weber, H. J., Thiyagarajan, M., Wang, B., Deane, R., et al. (2013). Evaluating glymphatic pathway function utilizing clinically relevant intrathecal infusion of CSF tracer. *J. Transl. Med.* 11:107. doi: 10.1186/1479-5876-11-107

Yu, P., Venkat, P., Chopp, M., Zacharek, A., Shen, Y., Ning, R., et al. (2019). Role of microRNA-126 in vascular cognitive impairment in mice. *J. Cereb. Blood Flow Metab.* 39, 2497–2511. doi: 10.1177/0271678X18800593

Zampetaki, A., Kiechl, S., Drozdov, I., Willeit, P., Mayr, U., Prokopi, M., et al. (2010). Plasma microRNA profiling reveals loss of endothelial miR-126 and other microRNAs in type 2 diabetes. *Circ. Res.* 107, 810–817. doi: 10.1161/CIRCRESAHA.110.226357

Zeng, W., Chen, Y., Zhu, Z., Gao, S., Xia, J., Chen, X., et al. (2019). Severity of white matter hyperintensities: lesion patterns, cognition and microstructural changes. *J. Cereb. Blood Flow Metab.* 271678x19893600. doi: 10.1177/0271678x19893600

Zhang, L., Chopp, M., Jiang, Q., and Zhang, Z. (2019). Role of the glymphatic system in ageing and diabetes mellitus impaired cognitive function. *Stroke Vasc. Neurol.* 4, 90–92. doi: 10.1136/svn-2018-000203

Conflict of Interest: The authors declare that the research was conducted in the absence of any commercial or financial relationships that could be construed as a potential conflict of interest.

frontiers in Aging Neuroscience

REVIEW
published: 19 October 2020
doi: 10.3389/fnagi.2020.594571

LncRNAs Stand as Potent Biomarkers and Therapeutic Targets for Stroke

Junfen Fan[1,2], Madeline Saft[3], Nadia Sadanandan[3], Bella Gonzales-Portillo[3], You Jeong Park[3], Paul R. Sanberg[3], Cesario V. Borlongan[3] and Yumin Luo[1,2,4]**

[1]Institute of Cerebrovascular Disease Research and Department of Neurology, Xuanwu Hospital of Capital Medical University, Beijing, China, [2]Beijing Geriatric Medical Research Center and Beijing Key Laboratory of Translational Medicine for Cerebrovascular Diseases, Beijing, China, [3]Department of Neurosurgery and Brain Repair, University of South Florida Morsani College of Medicine, Tampa, FL, United States, [4]Beijing Institute for Brain Disorders, Capital Medical University, Beijing, China

Stroke is a major public health problem worldwide with a high burden of neurological disability and mortality. Long noncoding RNAs (lncRNAs) have attracted much attention in the past decades because of their newly discovered roles in pathophysiological processes in many diseases. The abundance of lncRNAs in the nervous system indicates that they may be part of a complex regulatory network governing physiology and pathology of the brain. In particular, lncRNAs have been shown to play pivotal roles in the pathogenesis of stroke. In this article, we provide a review of the multifaceted functions of lncRNAs in the pathogenesis of ischemic stroke and intracerebral hemorrhage, highlighting their promising use as stroke diagnostic biomarkers and therapeutics. To this end, we discuss the potential of stem cells in aiding lncRNA applications in stroke.

Keywords: ischemic stroke, hemorrhagic stroke, long non-coding RNAs, biomarkers, therapeutics

OPEN ACCESS

Edited by:
Ashok K. Shetty, Texas A&M University College of Medicine, United States

Reviewed by:
Hua Su, University of California, San Francisco, United States
Ken Arai, Massachusetts General Hospital and Harvard Medical School, United States

****Correspondence:***
Cesario V. Borlongan
cborlong@usf.edu
Yumin Luo
yumin111@ccmu.edu.cn

Received: *13 August 2020*
Accepted: *18 September 2020*
Published: *19 October 2020*

Citation:
Fan J, Saft M, Sadanandan N, Gonzales-Portillo B, Park YJ, Sanberg PR, Borlongan CV and Luo Y (2020) LncRNAs Stand as Potent Biomarkers and Therapeutic Targets for Stroke. Front. Aging Neurosci. 12:594571. doi: 10.3389/fnagi.2020.594571

INTRODUCTION

Ischemic stroke is primarily characterized by insufficient blood flow to the brain, whereas hemorrhagic stroke leads to bleeding in the brain, with both types of stroke accompanied by a multitude of biological processes including oxygen deprivation, inflammatory response, oxidative stress, neurotoxicity of excitatory amino acids, apoptosis and edema formation, eventually culminating to severe neurovascular damage (Sahota and Savitz, 2011; Ahad et al., 2020; Virani et al., 2020). Intravascular thrombolysis and mechanical thrombectomy have significantly improved the prognosis of patients with acute ischemic stroke (AIS; Hacke et al., 1995; Berkhemer et al., 2015). However, only a small proportion of patients can receive these two treatments in clinical scenarios due to the narrow therapeutic time window and a considerable incidence of intracranial hemorrhagic conversion (Fonarow et al., 2011; Powers et al., 2018).

Abbreviations: AIS, acute ischemic stroke; BBB, blood-brain barrier; BMECs, brain microvascular endothelial cells; CAD, coronary artery disease; ceRNAs, competing endogenous RNAs; CNS, central nervous system; CMP, chromatin-modifying protein; coREST, corepressors of the RE-1 silencing transcription; C2dat1, CAMK2D-associated transcript 1; ERS, endoplasmic reticulum stress; I/R, ischemia/reperfusion; LAA, large-artery atherosclerosis; lncRNA, long noncoding RNA; MCAO, middle cerebral artery occlusion; MMPs, matrix metalloproteinases; MoDMs, monocyte-derived macrophages; mRNAs, messenger RNAs; ncRNAs, noncoding RNAs; NO, nitric oxide; OGD/R, oxygen and glucose deprivation/reoxygenation; NKILA, NF-kB interacting lncRNA; oxLDL, oxidized low-density lipoprotein; PBMCs, peripheral blood mononuclear cells; SAH, subarachnoid hemorrhage; SNPs, single nucleotide polymorphisms; VEGF, vascular endothelial growth factor.

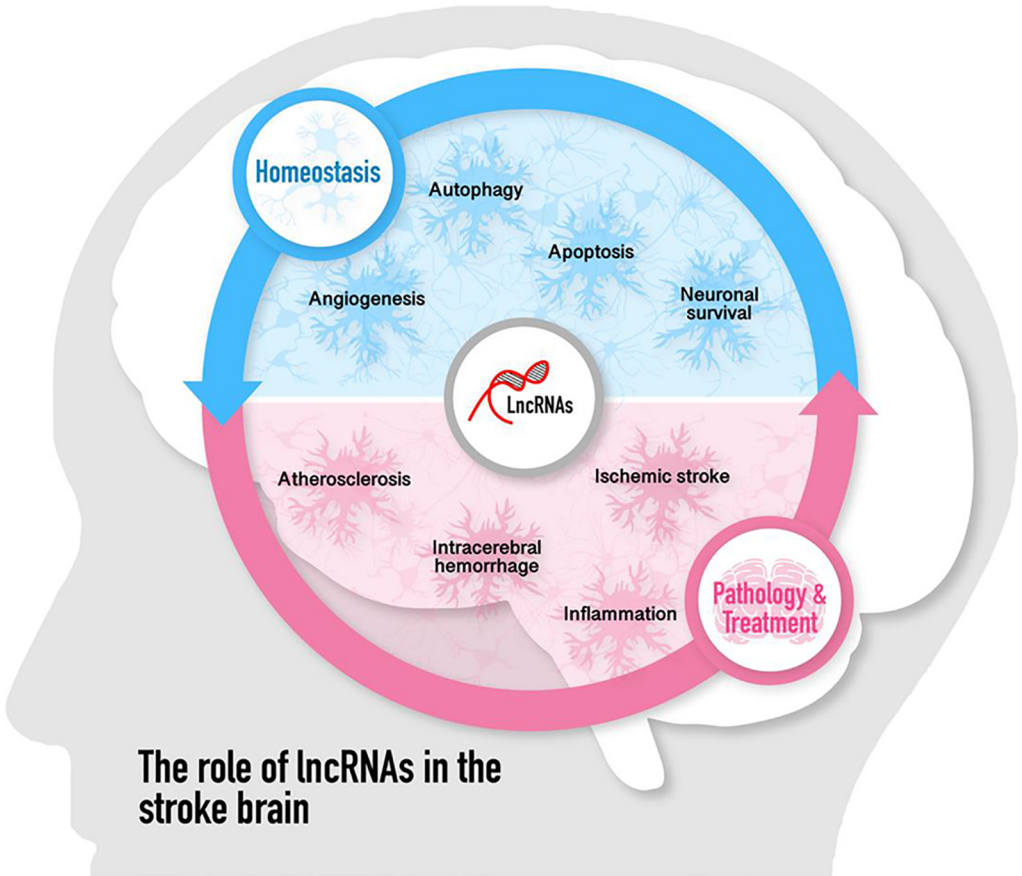

GRAPHICAL ABSTRACT

Little is known about the pathogenesis and treatment options of intracerebral hemorrhage. Surgical evacuation is the main therapeutic option for intracerebral hemorrhage (Gross et al., 2019). Although great efforts have been made in investigating the complex mechanism of stroke-induced neuronal death, there is still a lack of effective treatment for neurological deficits caused by stroke. Therefore, the discovery of new targets and biomarkers is of great significance for ischemic stroke and intracerebral hemorrhage therapy.

According to the Human Genome Project study, only a minor portion of the mammalian genome encodes the protein-coding transcriptome, whereas the vast majority (approximately 80%) is transcribed into non-coding RNAs (ncRNAs; Djebali et al., 2012). Long noncoding RNAs (lncRNAs) are transcripts longer than 200 nucleotides without or with the ability to encode proteins, but occupy a large part of the transcriptional output (Anderson et al., 2015; Matsumoto et al., 2017; Kopp and Mendell, 2018). LncRNAs were primarily considered as the "noise" of genomic transcription and had no biological functions (Ponting et al., 2009). Mounting evidence illustrates that lncRNAs are essential regulators of various biological processes including cell differentiation, proliferation, and apoptosis, as well as diseases such as cancer, metabolic disorders, cardiovascular diseases, and neurological disorders (Kurian et al., 2015; Bhan et al., 2017; Andersen and Lim, 2018; Yang Q. et al., 2018). LncRNAs also participate in brain development, neuron function, and progression of neurodegenerative diseases (Wan et al., 2017). Recently, lncRNAs have been highlighted to be involved in the pathological process of stroke.

A microarray profiling study firstly showed that lncRNA expression changes in the cerebral cortex at multiple time-points of reperfusion following transient middle cerebral artery occlusion (MCAO) in the adult rat (Dharap et al., 2012). Thereafter, altered lncRNA expression profiles have been investigated in rodent focal cerebral ischemia models, ischemic stroke patients as well as *in vitro* cultured cells following oxygen and glucose deprivation/reoxygenation (OGD/R; Zhao et al., 2015; Zhang et al., 2016; Guo et al., 2018). Kim et al. (2019) investigated the expression pattern of lncRNA from two different intracerebral hemorrhage rat models. The aberrant expression of lncRNAs uncovered in stroke has led researchers to explore the potential roles and mechanisms of specific lncRNA in brain physiology and pathology. We and other groups are among the first to elaborate on the functional significance of individual lncRNA in ischemic stroke. A recent study showed that the expression of lncRNA MEG3 was

significantly upregulated following ischemia *in vitro* and *in vivo*, and it mediates ischemic neuronal death by targeting the miR-21/PDCD4 signaling pathway (Yan et al., 2017). LncRNA MALAT1 exerted neuroprotective effects in the post-stroke cerebral microvasculature, resulting in reduced cerebral vascular and parenchymal damage (Zhang X. et al., 2017). Our group reported that compared with healthy controls, circulating lncRNA H19 levels were upregulated in patients with stroke. Knockdown of lncRNA H19 could decrease infarct volume, brain edema, and neuroinflammation by driving HDAC1-dependent M1 microglial polarization (Wang et al., 2017a). Moreover, lncRNA H19 induces cerebral ischemia-reperfusion injury *via* activation of autophagy through the DUSP5-ERK1/2 axis (Wang et al., 2017b). Taken together, these findings indicate that lncRNAs play multiple roles in the post-stroke brain and provide evidence for their importance in stroke pathophysiology.

To date, an increasing number of lncRNAs have been identified to be involved in the molecular processes of ischemic stroke and intracerebral hemorrhage cascade. Here, we provide a systematic and comprehensive summary of the existing knowledge of lncRNAs and stroke in hopes to further elucidate this new research area.

MECHANISMS OF LncRNAs FUNCTIONS

Historically, many of the non-protein-coding parts of the human genome have been considered as junk DNA. However, the development of high-throughput technologies including next-generation sequencing over the past decades allows the in-depth study of noncoding genomes with unprecedented resolution and scale. LncRNAs are defined as transcripts of greater than 200 nucleotides. Most of them cannot be translated into proteins while a few of them encode small peptides (Huang et al., 2017; Kopp and Mendell, 2018). The number of lncRNAs identified is much lower than that of coding protein genes (mRNAs), however, they have higher tissue and organ specificity. Based on the relative position on the chromosome, lncRNAs can be classified into sense lncRNAs, antisense lncRNAs, intronic lncRNAs, intergenic lncRNAs, divergent lncRNAs, promoter upstream lncRNAs, promoter-associated lncRNAs, and transcription start site-associated lncRNAs (St Laurent et al., 2015). LncRNAs are localized in the nucleus or the cytoplasm where they may regulate gene expression at transcriptional or posttranscriptional levels, respectively. Cytoplasmic lncRNAs can stabilize ribonucleoprotein complexes, regulate mRNA stability, or act as competing endogenous RNAs (ceRNAs) for the binding of miRNAs. By contrast, lncRNAs localized to the nucleus regulate gene expression in various modes such as sequestering transcription factors/protein complex away from chromatin (decoy), bringing together distinct proteins to form ribonucleoprotein complexes (scaffold), transcription in response to stimulation or signaling pathway (signal), or acting as a guide by recruiting chromatin-modifying enzymes to target genes (guide) and inducing chromosomal looping to increase the association between enhancer and promoter region (enhancer; Bär et al., 2016). Additionally, lncRNAs can interfere with DNA and form RNA-DNA triplex (Kuo et al., 2019). Because of these diverse and pervasive mechanisms, lncRNAs offer a unique perspective to understand gene regulatory networks. There has been a great deal of research on lncRNAs in different diseases such as cancer, cardiovascular diseases, immune system diseases, and the function of lncRNAs in stroke now is emerging (Taft et al., 2010).

Interestingly, a single lncRNA can modulate multiple targets while one target might be regulated by different lncRNAs, resulting in crosstalk signaling pathways in the network regulated by specific lncRNAs. Therefore, clarifying the molecular mechanism of these crosstalk signaling pathways in the progression of ischemic stroke may reveal key cell death and survival signaling pathways in the brain.

LncRNA EXPRESSION IN ISCHEMIC STROKE

LncRNAs are highly expressed in mammalian brain tissues (Mercer et al., 2008). LncRNA expression was first profiled in the cerebral cortex of adult rats at multiple time-points of reperfusion following transient MCAO. Three hundred and fifty-nine lncRNAs were identified to be significantly upregulated and 84 were downregulated at 3 to 12 h of reperfusion following MCAO compared to sham (Dharap et al., 2012). In the following study, they identified that stroke-induced lncRNAs combined with the chromatin-modifying protein (CMP) Sin3A and corepressors of the RE-1 silencing transcription factor (coREST) to regulate the epigenetic transcriptome post-ischemia (Dharap et al., 2013). Liu et al. (2018) demonstrated that a total of 255 lncRNAs (217 upregulated and 38 downregulated) and 894 mRNAs (870 upregulated and 24 downregulated) were significantly differentially expressed in the ischemic brain compared with sham controls. Also, they found that the alteration of lncRNAs expression was closely related to changes in mRNA expression involved in neuroinflammation, cell cycle, cell differentiation, and apoptosis (Liu et al., 2018). Another study used unbiased high-throughput RNA-seq to evaluate the genome-wide expression of lncRNAs in the mouse cortex following focal ischemia. A total of 259 lncRNA isoforms at 6 h, 378 isoforms at 12 h, and 217 isoforms at 24 h of reperfusion were differentially expressed vs. sham controls. Of these, 213, 322, and 171 isoforms at 6, 12, and 24 h of reperfusion, respectively, were novel lncRNAs (Bhattarai et al., 2017). More recently, the group of Frank R Sharp investigated the differential lncRNA expression signatures in peripheral blood samples of male and female humans after stroke. They observed that 299 lncRNAs were differentially expressed between stroke and control males, whereas 97 lncRNAs were altered between stroke and control females. Moreover, some of these differentially expressed lncRNAs mapped closely to previously identified putative stroke-risk genes, suggesting the potential value of lncRNAs as blood biomarkers of ischemic stroke (Dykstra-Aiello et al., 2016). Zhang et al. (2016) initially analyzed differential lncRNA expression in primary brain microvascular endothelial cells (BMECs) after OGD and found that the expression levels of 362 lncRNAs changed significantly. Moreover, they also discovered various conserved

transcription factor binding sites in the promoter region of these OGD-responsive endothelial lncRNAs (Zhang et al., 2016). Besides, Deng et al. (2018) identified the expression profile of lncRNAs in peripheral blood mononuclear cells (PBMCs) after AIS and confirmed that linc-DHFRL1-4, SNHG15, and linc-FAM98A-3 were dramatically elevated in ischemic stroke patients compared with healthy controls and transient ischemic attack patients.

The aforementioned studies provide ample evidence that the brain responds to stroke-associated stimuli by significantly altering lncRNAs transcriptomic profiles. This early and robust stroke-induced lncRNA aberration suggests potential functional roles and the predictive values of lncRNAs as new biomarkers for ischemic stroke. A better understanding of the molecular mechanisms after cerebral ischemia will provide an opportunity to explore potential strategies for early diagnosis and therapy of stroke.

ROLES OF LncRNAs IN THE PATHOGENESIS OF ISCHEMIC STROKE

Cumulative studies have indicated that lncRNAs play pivotal roles in regulating the pathological process of ischemic stroke by affecting atherosclerosis, which is a risk factor for stroke, and post-stroke pathophysiology such as inflammation, neuronal injury, and survival (including autophagy and cell apoptosis), angiogenesis as well as neurogenesis. The role of lncRNAs in the pathogenesis of ischemic stroke is discussed in the following paragraphs and summarized in **Figure 1**.

LncRNAs in Atherosclerosis

Atherosclerosis is a complex, chronic polygenic disease and the major cause of stroke and heart disease. Endothelial cell proliferation and migration play important roles in the initiation and pathological development of atherosclerosis. Recently, the expression level of lncRNA HOTTIP was found to be upregulated in coronary artery disease (CAD) tissues than in normal arterial tissues. Ectopic expression of HOTTIP promoted endothelial cell proliferation and migration *via* activation of the Wnt/β-catenin pathway (Liao et al., 2018). Located on human chromosome 11, LncRNA H19 is one of the first identified lncRNAs. It has been reported to be upregulated in atherosclerotic patients and regarded as a potential target in the prevention of atherosclerosis and a new biomarker for the diagnosis of atherosclerosis (Pan, 2017; Bitarafan et al., 2019). The study by Huang Y. et al. (2019) revealed that lncRNA H19 contributed to the occurrence of atherosclerosis by promoting ACP5 protein expression and increased the risk of ischemic stroke. LncRNA GAS5 was highly expressed in the plaques of atherosclerosis collected from patients and animal models. Inhibition of lncRNA GAS5 impaired the apoptosis of THP-1 cells after oxidized low-density lipoprotein (oxLDL) stimulation. Moreover, exosomes derived from lncRNA GAS5-overexpressing THP-1 cells enhanced the apoptosis of vascular endothelial cells, suggesting exosomal lncRNA GAS5 participated in the process of atherosclerosis (Chen L. et al., 2017). Compared with healthy controls, lncRNA TUG1 was upregulated in serum samples of patients with atherosclerosis. Gain- and loss-of-function approaches identified that lncRNA TUG1 was closely related to the progression of atherosclerosis (Li et al., 2018). Besides, a variety of lncRNAs including lncRNA LOC285194, lncRNA SNHG6, lncRNA OIP5-AS1, and lncRNA ZEB1-AS1 were proven to be important regulators of atherosclerosis (Cheng et al., 2020; Hua et al., 2020; Shan et al., 2020; Zhang C. et al., 2020). These findings will help to better understand the pathological process of atherosclerosis and aid in the development of novel therapeutic strategies for stroke.

LncRNAs and Neuroinflammation

At the beginning of an ischemic stroke, the decreased blood flow activates intravascular leukocytes and initiates proinflammatory mediators release, resulting in post-ischemic inflammation. Increasing evidence suggests that inflammatory response is a double-edged sword after stroke, as it not only aggravates secondary brain injury in the acute phase but also has protective effects on brain recovery (Ceulemans et al., 2010). Thus, neuroinflammation is closely related to the progression and prognosis of stroke. Microglia are the main resident immune cells in the central nervous system (CNS) and activated rapidly in response to cerebral ischemia. Stroke-induced brain injury activates microglia and polarizes microglia into pro-inflammatory M1 phenotype or anti-inflammatory M2 phenotype (Hu et al., 2012). Numerous studies showed that lncRNAs are related to neuroinflammation and the activation of microglia in ischemic stroke. It was reported that the expression of lncRNA ANRIL was negatively associated with hs-CRP, TNF-α, and IL-6 levels, but positively correlated with IL-10 levels in AIS patients, suggesting that lncRNA ANRIL play an anti-inflammatory role in AIS progression (Feng et al., 2019). A recent study found that knockdown of lncRNA MALAT1 attenuated the inflammatory injury after brain ischemia, whereas overexpression of MALAT1 exacerbated ischemic brain inflammation (Cao et al., 2020). Besides, silencing or knock-out of lncRNA MALAT1 significantly elevated the expression of proapoptotic factor Bim and proinflammatory cytokines MCP-1, IL-6, and E-selectin in cultured mouse BMECs after OGD as well as in isolated cerebral microvessels in mice after MCAO (Zhang X. et al., 2017). The study by Zhang X. et al. (2019) revealed that the upregulation of lncRNA 1810034E14Rik reduced the expression of inflammatory cytokines not only in ischemic stroke mice but also in OGD-induced microglial cells. Moreover, 1810034E14Rik overexpression could suppress the activation of microglial cells and inhibit the phosphorylation of p65, making it a potential target for stroke treatment (Zhang X. et al., 2019). In monocyte-derived macrophages (MoDMs), lncRNA Maclpil knockdown decreased pro-inflammatory gene expression while promoting anti-inflammatory gene expression, and *in vivo* studies demonstrated that adoptive transfer of macrophages with silenced lncRNA Maclpil robustly reduced infarction and improved behavioral performance of ischemic stroke mice (Wang et al., 2020b). LncRNA Nespas has been reported to play anti-inflammatory and anti-apoptotic

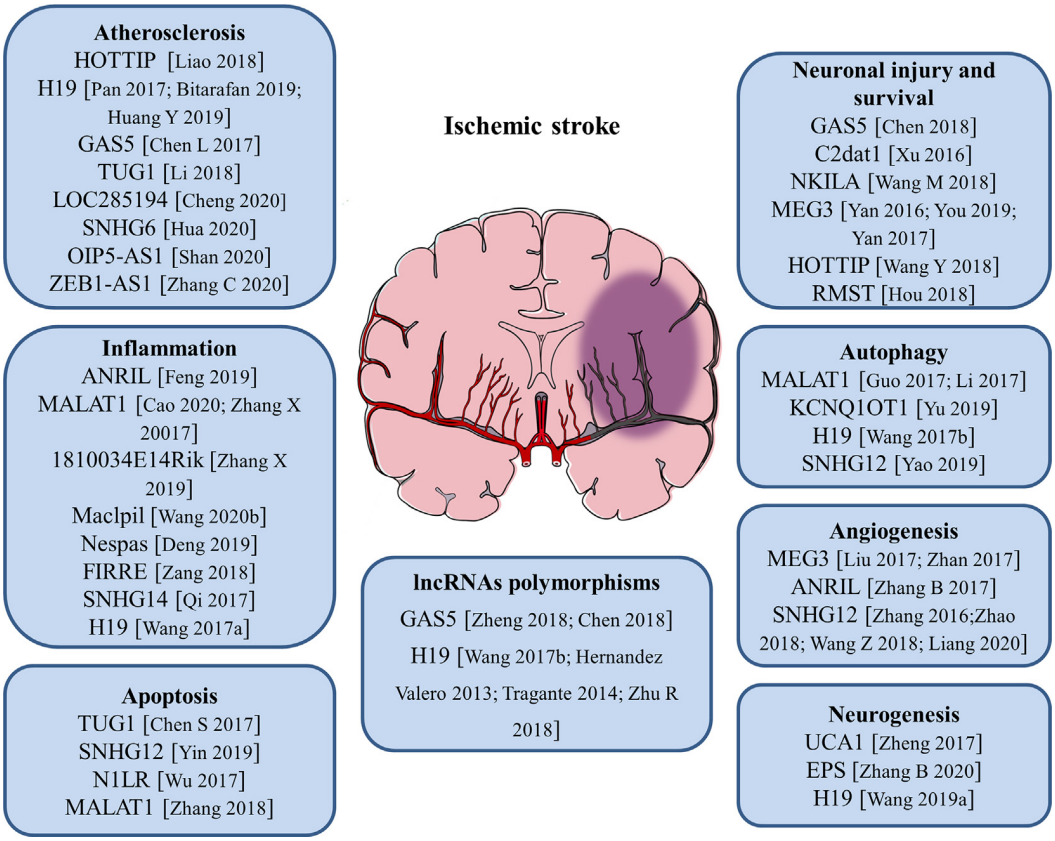

FIGURE 1 | Roles of long noncoding RNAs (lncRNAs) and LncRNA polymorphisms in the pathogenesis of ischemic stroke. The numbers in brackets refer to cited references.

roles in cultured microglial cells after OGD stimulation and mice after ischemic stroke by inhibiting TRIM8-related K63-linked polyubiquitination of TAK1 (Deng et al., 2019). Furthermore, lncRNA FIRRE was identified to be upregulated in microglial cells treated with OGD/R and functional experiments revealed that FIRRE upregulation contributed to the OGD/R-induced microglial cell injury through regulating NF-kB (p50)/NLRP3 inflammasome (Zang et al., 2018). The study by Qi et al. (2017) provided the first evidence that lncRNA SNHG14 was highly expressed in ischemic cerebral tissues and OGD-treated microglia. Also, lncRNA SNHG14 increased the expression of PLA2G4A by inhibition of miR-145-5p, which resulted in the activation of microglia in cerebral infarction (Qi et al., 2017). Our group has demonstrated for the first time that circulating lncRNA H19 levels were significantly higher in stroke patients compared with healthy controls. Moreover, this upregulation of plasma lncRNA H19 is positively related to neurological functional deficits and plasma TNF-α levels. Inhibition of lncRNA H19 reduced cerebral ischemic injury and promoted microglial M2 polarization through the downregulation of HDAC1. These findings support an immunomodulatory effect of lncRNA H19 and a novel H19-based diagnosis and therapy for ischemic stroke (Wang et al., 2017a).

Complex mechanisms are involved in the pathophysiology of ischemic stroke, and the inflammatory response plays an important role in its occurrence and development (Tuttolomondo et al., 2012; Anrather and Iadecola, 2016). Once the inflammatory cascade is activated, inflammatory cells secrete various cytotoxic factors such as cytokines, nitric oxide (NO), and matrix metalloproteinases (MMPs) and cause more cellular, blood-brain barrier (BBB), and extracellular matrix damage (Emsley and Tyrrell, 2002; Ouyang, 2013). Therefore, the findings mentioned above may have therapeutic implications and more endeavors are needed to investigate whether pharmacological manipulation of the lncRNAs affects neuroinflammation and stroke outcomes.

LncRNAs With Neuronal Injuries and Apoptosis

Apoptosis is a programmed, controlled process of cell death, which orderly and efficiently removes damaged cells from DNA damage or during development. Specific cellular signaling pathways and protein synthesis are involved in this self-destruction process (Pistritto et al., 2016). Apoptosis plays an important role in the homeostasis of normal tissues and participates in a variety of clinical diseases. Studies have disclosed that apoptosis may contribute to a significant

proportion of nerve cell death following acute brain ischemia, but the underlying mechanisms are still not fully understood. The expression of lncRNA TUG1 increased in the ischemic brain and cultured neurons under OGD insults. LncRNA TUG1 serves as a "sponge" to decrease miR-9 and positively regulates the pro-apoptosis gene Bcl2l11 expression at the post-transcriptional level under ischemia (Chen S. et al., 2017). LncRNA SNHG12 was found to be upregulated in mouse BMECs after cerebral ischemia. The knockdown of SNHG12 inhibited cell proliferation and induced apoptosis under OGD/R condition. Mechanistically, SNHG12 was proven to interact with miR-199a and activated SIRT1 expression, which ultimately led to the activation of the AMPK signaling pathway and attenuated cerebral ischemia/reperfusion injury (Yin et al., 2019). It has been shown that lncRNA-N1LR could enhance cell proliferation, inhibit apoptosis of N2a cells subjected to OGD/R, and reduce neuronal apoptosis and neural cell loss in ischemia/reperfusion (I/R)-induced mouse brains. A mechanistic study showed that lncRNA-N1LR promoted neuroprotection likely through p53 phosphorylation inhibition (Wu et al., 2017). Another study demonstrated that lncRNA MALAT1 regulated MDM2 expression, further restrained the proliferation, and increased the apoptosis of OGD/R induced human BMECs *via* the p53 signaling pathway (Zhang et al., 2018).

LncRNAs With Neuronal Injury and Survival

Cerebral ischemia/reperfusion post-ischemic stroke induces severe injury to neuronal cells. The role of lncRNAs in neuronal injury or survival has been illustrated. LncRNA GAS5 expression level was upregulated in MCAO-injured brain and OGD-injured primary brain neurons. The knockdown of GAS5 dramatically increased the cell viability and suppressed the activation of caspase-3 and cell apoptosis in neurons subjected to OGD insult. Mechanistically, GAS5 functioned as a ceRNA for miR-137 to decrease neuron survival through inactivating the Notch1 signaling pathway (Chen et al., 2018). Xu et al. (2016) reported a novel cerebral I/R-induced lncRNA, CAMK2D-associated transcript 1 (C2dat1), was augmented in a time-dependent manner in mouse cortical penumbra after focal ischemic brain injury. C2dat1 modulated the expression of CaMKIIδ to promote neuronal survival by activating the NF-κB signaling pathway following cerebral ischemia (Xu et al., 2016). The study by Wang M. et al. (2018) tested the expression and potential function of NKILA (NF-κB interacting lncRNA) in OGDR-treated neuronal cells. They showed that NKILA was upregulated in SH-SY5Y cells and primary murine hippocampal neurons after OGD/R. Silencing of NKILA largely reversed OGD/R-induced neuronal cell viability reduction, apoptosis, and necrosis *via* activating the NF-κB signaling pathway (Wang M. et al., 2018). LncRNA MEG3 was found to be a positive regulator of neuronal death in ischemia and physically and functionally interacted with p53 to mediate ischemic damage (Yan et al., 2016). Repression of lncRNA MEG3 inhibited the neuronal apoptosis, degeneration, and necrosis, enhanced nerve growth, and promoted neurological function restoration after cerebral ischemia-reperfusion injury through the activation of the Wnt/β-catenin signaling pathway (You and You, 2019). Another study reported that lncRNA MEG3 functioned as a ceRNA for miR-21 to regulate PDCD4 expression in ischemic neuronal death following reperfusion. Silencing of MEG3 protected against ischemic damage and improved overall neurological functions *in vivo* (Yan et al., 2017). The expression of lncRNA HOTTIP was decreased in both OGD-injured brain tissues of mice and primary neurons. Gain- and loss-of-function analysis revealed that HOTTIP attenuated OGD-induced neuronal injury and imbalanced glycolytic metabolism. HOTTIP could function as a ceRNA for miR-143 to modulate HK-2 expression and alleviate OGD-induced neuronal injury (Wang Y. et al., 2018). LncRNA RMST silencing is protected against MCAO-induced ischemic brain injury *in vivo* and OGD-induced primary hippocampal neuron injury *in vitro* (Hou and Cheng, 2018). Therefore, lncRNA-mediated epigenetic remodeling of brain/neuronal survival could determine the progression and outcomes of stroke.

LncRNAs and Autophagy

Autophagy is a highly conserved cellular self-protecting process to degrade misfolded proteins and impaired organelles into metabolic elements and recycle them for cellular homeostasis maintenance. It is widely accepted that autophagy is activated in numerous cell types in the brain such as neurons, glia cells, and microvascular cells upon ischemic stroke (Wang P. et al., 2018). Recent reports suggest that lncRNAs can affect cell survival in stroke by regulating autophagy. LncRNA MALAT1 is one of the most highly upregulated lncRNAs after I/R or OGD/R. It was reported that the knockdown of lncRNA MALAT1 suppressed ischemic injury and autophagy in cerebral cortex neurons after OGD as well as the mouse brain cortex after MCAO. Moreover, MALAT1 served as a molecular sponge for miR-30a and Beclin1 was a direct target of miR-30a (Guo et al., 2017). Another study demonstrated that lncRNA MALAT1 was a potent autophagy inducer, which protected BMECs against OGD/R-induced injury by sponging miR-26b and upregulating ULK2 expression (Li et al., 2017). Furthermore, lncRNA KCNQ1OT1 was highly expressed in the plasma of AIS patients. *In vivo* experiments revealed that inhibition of KCNQ1OT1 remarkably reduced the infarct volume and neurological impairments. Besides, the downregulation of KCNQ1OT1 enhanced cell viability and apoptosis by modulating autophagy in an OGD/R model. Mechanistically, KCNQ1OT1 might target miR-200a to regulate downstream FOXO3 expression, which is a transcriptional regulator of ATG7 (Yu et al., 2019). Additionally, lncRNA H19 induced cerebral ischemia-reperfusion injury *via* the activation of autophagy through the DUSP5-ERK1/2 axis, and OGD/R-induced autophagy activation could be prevented by knockdown of lncRNA H19 (Wang et al., 2017a). The study by Yao et al. (2019) demonstrated that overexpression of lncRNA SNHG12 alleviated OGD/R-induced SH-SY5Y cell injury and induced autophagy activation. On the contrary, inhibition of lncRNA SNHG12 exacerbated neuron cell injury and inhibited autophagy after OGD/R (Yao et al., 2019). These findings allow us to better understand the role of

lncRNAs and autophagy in the pathogenesis and development of ischemic stroke.

LncRNAs and Angiogenesis

Angiogenesis after ischemic brain injury has been discovered to facilitate the restoration of blood supply in the ischemic zone, and higher microvessel density is associated with less morbidity and better functional recovery (Ergul et al., 2012). Post-stroke angiogenesis is a complex biological process that is well-orchestrated by pro-angiogenic and anti-angiogenic factors such as VEGF, BDNF, and bFGF (Liu et al., 2014). Therefore, pro-angiogenesis may represent a potential therapeutic approach that requires more in-depth elaboration for patients with ischemic stroke. Recently, some studies have shown that lncRNAs act as key regulators involved in angiogenesis. Liu et al. (2017) found that lncRNA MEG3 was significantly decreased after ischemic stroke, and silencing of MEG3 increased endothelial cell migration, proliferation, sprouting, and tube formation, resulting in pro-angiogenesis and functional recovery from stroke. Furthermore, they showed that lncRNA MEG3 negatively regulated the notch pathway and inhibition of notch signaling in endothelial cells reversed the pro-angiogenic effect induced by MEG3 downregulation (Liu et al., 2017). Another study also proved that the downregulation of lncRNA MEG3 promoted angiogenesis in OGD/R-induced rat BMECs *via* the p53/NOX4 axis (Zhan et al., 2017). MEG3 may be a potential therapeutic target for promoting regeneration in cerebral infarction and ischemic vascular disease. LncRNA ANRIL could promote VEGF expression and enhance angiogenesis through activation of the NF-κB signaling pathway in rats with diabetes mellitus complicated with cerebral infarction (Zhang B. et al., 2017). LncRNA SNHG12 was significantly increased in OGD-induced primary BMECs and in microvessels isolated from mouse brains after MCAO (Zhang et al., 2016). Another study revealed that lncRNA SNHG12 could promote the angiogenesis in both OGD-injured BMECs and MCAO mouse models *via* regulating miR-150/VEGF signaling (Zhao et al., 2018). Wang Z. et al. (2018) identified that the upregulation of lncRNA SNHG1 promoted angiogenesis by inhibiting miR-199a and regulating HIF-1α and VEGF expression in an OGD/R-induced ischemic stroke model. Moreover, lncRNA SNHG1 functioned as a ceRNA of miR-140-3p to enhance cell proliferation, tube formation, and expression of VEGF, VE-cadherin, and MMP2 through HIF-1α/VEGF signaling (Liang et al., 2020). Undoubtedly, understanding the molecular mechanisms of angiogenesis after ischemic stroke will contribute to the development of pro-angiogenesis therapy for this deadly disease.

LncRNAs and Neurogenesis

Neural stem cells (NSCs) are a class of self-renewing and multipotent cells. Throughout the process of neural development, NSCs are gradually exhausted and reside in two major neurogenic niches—subventricular zone (SVZ) and subgranular zone (SGZ) in the adult brain. Recent studies revealed that after ischemic stroke, the endogenous quiescent NSCs become active and can differentiate into multiple cell lineages including neuron, astrocyte, and oligodendrocyte, as well as migrate to the ischemic region, which promotes the regeneration of the damaged cells induced by ischemia (Arvidsson et al., 2002; Huang and Zhang, 2019). It was discovered that lncRNAs are involved in the post-ischemic neurogenesis. For example, lncRNA UCA1 enhanced NSCs proliferation, increased nestin expression, and the neurosphere formation through regulating miR-1/Hes1 (Zheng et al., 2017). The study by Zhang B. et al. (2020) developed a novel targeting carrier for microglia with a lncRNA-EPS-loaded liposome. lncRNA-EPS promoted NSCs proliferation and anti-apoptotic ability *in vitro* and lncRNA-EPS-leukosomes improved neuron density in the ischemic core and boundary zone *in vivo* (Zhang B. et al., 2020). One of our studies demonstrated that circulating lncRNA H19 levels were negatively associated with the long-term neurological deficit recovery of patients with ischemic stroke. The knockdown of H19 reduced brain loss and promoted the recovery of neurological deficits through activating p53 to initiate the transcription of Notch1, and finally promoted the process of neurogenesis (Wang et al., 2019a). These studies further strengthen the clinical value of lncRNAs as therapeutic targets for ischemic stroke.

LncRNAs POLYMORPHISMS AND ISCHEMIC STROKE

Clinical epidemiology studies have reported several risk factors for ischemic strokes, such as hypertension, diabetes, obesity, dyslipidemia, and smoking (Yong et al., 2013). Besides, it is widely accepted that genetic factors are also involved in the pathogenesis of ischemic stroke (Dichgans, 2007; Cai et al., 2020). Currently, single nucleotide polymorphisms (SNPs) in some protein-coding genes, including BDNF, apolipoprotein A-V, apolipoprotein B, and ALOX5AP, have been demonstrated to be associated with susceptibility of ischemic stroke (Au et al., 2017; Chen Z. et al., 2017; Bao et al., 2018). Furthermore, lncRNA-related SNPs have been reported to be related to the risk of ischemic stroke (**Figure 1**). LncRNA GAS5 was observed to be upregulated in ischemic stroke. Zheng et al. (2018) demonstrated that the rs145204276 deletion allele was closely related to the increase of ischemic stroke susceptibility by promoting transcription activity of lncRNA GAS5 and subsequently increasing the expression of GAS5 (Chen et al., 2018; Zheng et al., 2018). LncRNA H19 polymorphisms were reported to participate in the regulation of lncRNA H19 expression. Wang et al. (2017b) found that lncRNA H19 rs217727 and rs4929984 variants were associated with the risk of ischemic stroke and the minor alleles of rs217727 (T) and rs4929984 (A) increased the risk. Moreover, lncRNA H19 rs4929984 was significantly associated with blood pressure. Rs217727 was correlated with coagulation function and homocysteine metabolism of patients with ischemic stroke in the southern Chinese Han population (Huang J. et al., 2019). Recent studies also found that polymorphisms of lncRNA H19 were associated with risk factors including obesity, birth weight,

and blood pressure for ischemic stroke patients (Hernández-Valero et al., 2013; Tragante et al., 2014). Additionally, Zhu R. et al. (2018) found that the TT genotype of lncRNA H19 rs217727 polymorphism was statistically associated with an increased risk of ischemic stroke in the northern Chinese Han population. Individuals with the TT genotype had a 1.941 times higher risk of small vessel ischemic stroke when compared with the subjects of CC + CT (Zhu R. et al., 2018; **Figure 1**).

LncRNAs IN INTRACEREBRAL HEMORRHAGE

The role of lncRNAs in intracerebral hemorrhage is an attractive field that scientists have tried to elucidate with limited success. Kim et al. (2019) performed microarray analyses and found that 83, 289, and 401 lncRNAs were significantly upregulated, whereas 52, 489, and 786 lncRNAs were significantly decreased of 1, 3, and 7 days after intracerebral hemorrhage, respectively. This study first revealed the temporal expression pattern of lncRNAs with an acute hemorrhagic stroke model induced by stereotactic collagenase injection. Gene ontology/pathway analysis revealed that inflammation is a key biological process after a hemorrhagic stroke and functional study disclosed that lncRNA H19 was the most upregulated lncRNA after intracerebral hemorrhage and closely related to the type I interferon signaling pathway (Kim et al., 2019). Therefore, lncRNA H19 plays an important role both in ischemic stroke and intracerebral hemorrhage. Another study analyzed the expression profiles of lncRNAs and mRNAs in subarachnoid hemorrhage (SAH) brain tissues of mice using high-throughput sequencing. The results showed that approximately 617 lncRNA transcripts and 441 mRNA transcripts were aberrantly expressed at 24 h after SAH. Fantom3_F730004F19, a differentially elevated lncRNA, was identified to be correlated with CD14/TLR4 and increased inflammation in BV-2 microglia cells in SAH (Peng et al., 2017). Also, lncRNA and mRNA microarray revealed a total of 625 lncRNAs, and 826 mRNAs were aberrantly expressed on day 21 after the experimental induction of intracerebral hemorrhage by collagenase. Mitochondrial matrix reduced G-protein coupled receptor activity, and impaired olfactory transduction was discovered to be involved in the late stage of intracerebral hemorrhage (Hanjin et al., 2018). LncRNA PTPRJ-AS1 was highly expressed in inflammatory tissues after intracerebral hemorrhage, activated the NF-κB pathway in microglia, and promoted the secretion of inflammatory cytokines, thereby aggravating inflammatory injury (Wen et al., 2018). Moreover, in type VII collagenase-induced intracerebral hemorrhage rats, silencing of lncRNA NKILA decreased neurological deficits, exacerbated hematoma and brain edema, and induced BBB breakdown, further leading to hippocampal neuron loss and inflammation cytokines production. The endoplasmic reticulum stress (ERS)/autophagy pathway and NF-κB signaling pathway were involved in this process (Jia et al., 2018). Dong et al. (2018) found that lncRNA FENDRR regulated the vascular endothelial growth factor A (VEGFA)/miR-126 axis and contributed to the apoptosis of BMECs in hypertensive intracerebral hemorrhage mice models. LncRNA SNHG3 suppressed the proliferation and migration abilities and increased cell apoptosis and monolayer permeability of BMECs. Pathway analysis revealed that lncRNA SNHG3 impaired cerebral microvascular cells function in intracerebral hemorrhage rats by activating the TWEAK/Fn14/STAT3 pathway (Zhang J. et al., 2019). The functional roles of lncRNAs in pathophysiological changes of intracerebral hemorrhage are summarized in **Figure 2**. Hence, these studies suggest lncRNAs function as novel targets for the attenuation or exacerbation of brain injuries after intracerebral hemorrhage.

LncRNAs AS PUTATIVE BIOMARKERS AND THERAPEUTIC TARGETS

There are various types of RNA in the circulation regarded as cell-free RNA. Circulating lncRNAs are emerging as promising biomarkers and participate in the screening, diagnosis, progression, treatment, and prognosis of multiple diseases. For example, lncRNA UCA1 in urine has been considered as a noninvasive biomarker of primary bladder cancer (BC; Srivastava et al., 2014). This finding is supported by the fact that UCA1 serves as a possible addition to cystoscopy and cytology treatments when primary BC is detected. UCA1 was identified as a non-coding RNA upregulated in BC compared to normal bladder tissues and is involved in embryogenesis and BC progression (Wang et al., 2006). UCA1 has been studied and confirmed as a biomarker for urothelial carcinoma and expression was increased in various urothelial neoplastic lesions. Increased expression of UCA1 can be associated with tumor proliferation, migration, and invasion. However, the exact mechanisms are still unclear (Srivastava et al., 2014). UCA1 plays an important role in BC pathogenesis and progression and has been shown to promote resistance to cisplatin-based chemotherapy in BC cells (Fan et al., 2014). Furthermore, UCA1 serves as a suitable biomarker in BC and provides significant contributions to other diagnostic procedures.

In regards to the use of lncRNAs as novel biomarkers for stroke, a recent study investigated the expression of lncRNA MIAT in the peripheral blood leukocytes of ischemic stroke patients. They found that lncRNA MIAT levels were significantly upregulated in peripheral blood leukocytes of ischemic stroke patients and were associated with stroke severity and infarct volume. Also, higher levels of MIAT were associated with poor prognosis. These findings suggest that lncRNA MIAT in the peripheral blood leukocytes could be used as a novel diagnostic and prognostic marker for ischemic stroke. However, the exact molecular mechanism of MIAT in ischemic stroke and validation with more cases are needed (Zhu M. et al., 2018). Additionally, another study elaborated that lncRNA ZFAS1 levels in the peripheral blood leukocytes were markedly lower in patients with large-artery atherosclerosis (LAA) strokes compared with non-LAA strokes and controls, indicating that lncRNA ZFAS1 has potential predictive value for the diagnosis of LAA stroke (Wang et al., 2019b; **Figure 3**).

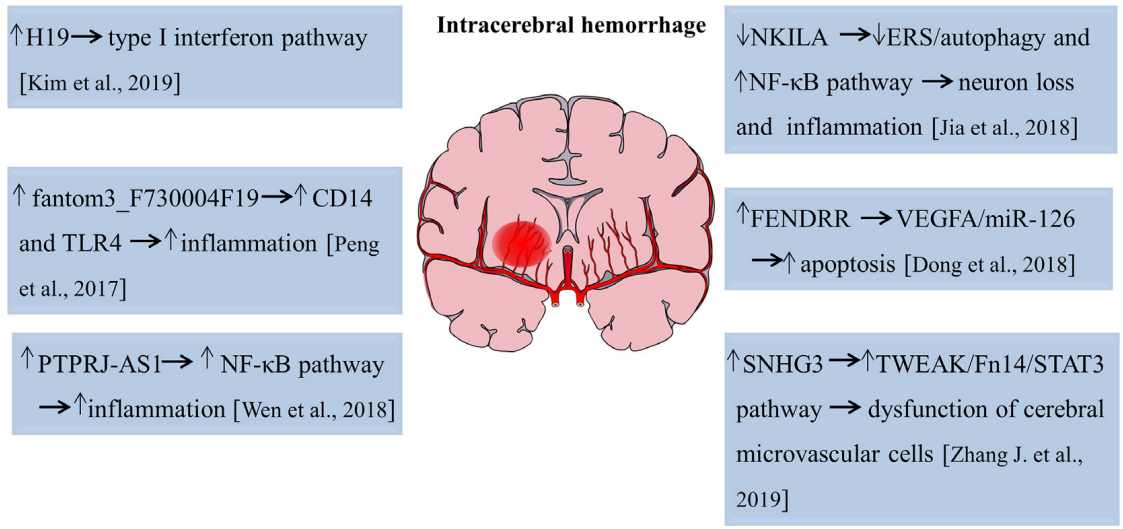

FIGURE 2 | Functions of lncRNAs in the pathophysiological process of intracerebral hemorrhage. The numbers in brackets refer to cited references.

lncRNA may serve as a novel therapeutic strategy for stroke. Elucidating lncRNA's mechanistic involvement in stroke pathology is key to establishing pharmaceutical treatment. Recent studies have explored specific lncRNAs and their role in stroke-induced neuroinflammation, apoptosis, and oxidative stress. lncRNAs may participate in neuroinflammation *via* macrophage modulation. As previously discussed, Maclpil suppression correlated with diminished expression of pro-inflammatory genes and bolstered expression of anti-inflammatory genes *in vitro*. Also, the delivery of Maclipil *in vivo* spurred a decrease in infarct volume and ameliorated neurological function. Moreover, stifling lncRNA-altered macrophages may bear therapeutic efficacy in alleviating stroke-induced neuroinflammation (Wang et al., 2020b). Also, human primary brain microvascular endothelial cells (HBMVECs) demonstrated truncated lncRNA FAL1 expression following OGD and reoxygenation (Gao et al., 2020). FAL1 overexpression decreased reactive oxygen species (ROS) levels and augmented glutathione (GSH), thereby attenuating oxidative stress. FAL1 overexpression diminished interleukin-6 (IL-6), monocyte chemotactic protein-1, and high mobility group box-1 (HMGB-1) levels, alleviating neuroinflammation. Depleted levels of PAK1 and AKT phosphorylation, along with proliferating cell nuclear (PCNA) numbers, were rehabilitated due to FAL1 overexpression (Gao et al., 2020).

Concerning stroke-induced apoptosis, there seems to be a multitude of various lncRNAs involved. N2a cells exposed to OGD displayed amplified advancement of the cell cycle and N2a proliferation, along with attenuated apoptosis, due to lncRNA-N1LR expression. *In vivo*, lncRNA-N1LR afforded neuroprotection, suppressing apoptosis, and enhancing cell viability, most likely through p53 phosphorylation obstruction (Wu et al., 2017). In parallel, depleting NR-120420 in SH-SY5Y cells exposed to OGD enhanced cell survival and reduced the number of apoptotic cells. *In vivo*, blocking NR_120420 repressed NF-κB phosphorylation, leading to suppressed apoptosis post brain infarction (Wu et al., 2017). Moreover, inhibition of NR_12040 *via* drug therapies may serve as an effective treatment for stroke (Tian et al., 2020). Notably, ischemic stroke samples displayed heightened expression of lncRNA MEG3 and Sema3A and reduced expression of miR-424-5p. When MEG3 was repressed, miR-424-5p was significantly enhanced and Sema3A was downregulated, contributing to bolstered cell survival, hindered apoptosis, and stimulation of the MAPK pathway. In MCAO rats models, the expression level of MEG3 increased gradually at 4, 8, and 24 h point in the process of ischemia-reperfusion, compared to the sham group. MEG3 down-regulated group has smaller ischemic area while it could be reversed by overexpression of Sema3A. Importantly, blocking MEG3 diminished infarct size and ameliorated neurological function, thereby elucidating a therapeutic strategy in stroke (Xiang et al., 2020).

lncRNA H19 has also been shown to make a significant contribution to stroke pathology. In NSCs isolated from the SVZ of rats afflicted with focal cerebral ischemia, H19 lncRNA expression was significantly increased (Fan et al., 2020). H19 knockdown hindered NSC proliferation and differentiation, along with spurring cell death. The elimination of H19 revealed its involvement in the regulation of transcription, apoptosis, cell proliferation, and reaction to ischemia post-stroke. While blocking of H19 enhanced the transcription of genes associated with the cell cycle like p27, H19 overexpression drastically downregulated the transcription of cell cycle-related genes. Also, H19 was shown to modulate miRNAs associated with neurogenesis. Notably, functional rehabilitation following stroke was retarded when H19 was blocked in NSCs (Fan et al., 2020). In another investigation, the sensorimotor cortex displayed upregulation of lncRNA H19 expression

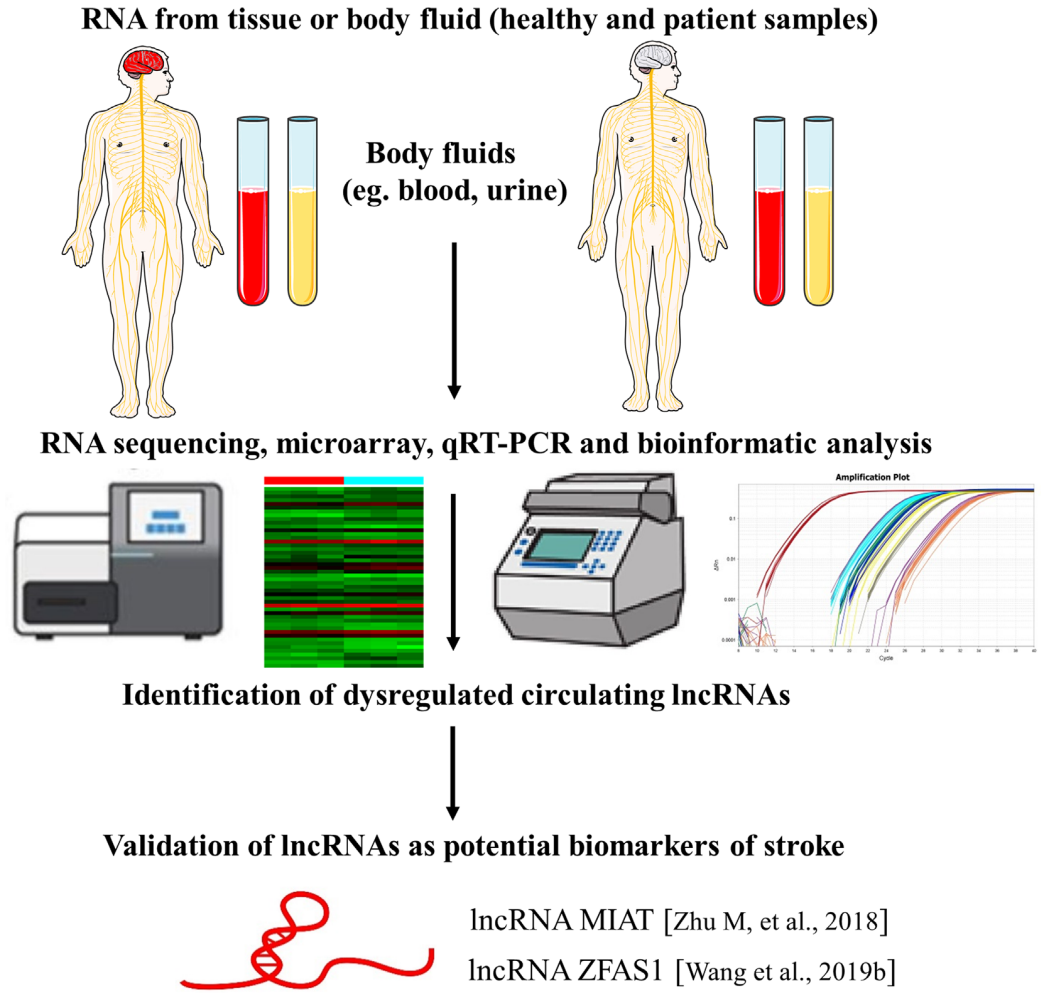

FIGURE 3 | LncRNAs as biomarkers of stroke. The identification of lncRNAs as novel biomarkers of stroke is a multistep process. The figure highlights examples of lncRNA molecules with reported biomarker potential for stroke. The numbers in brackets refer to cited references.

after MCAO. Corticospinal axons located in the spinal cord demonstrated bolstered midline-crossing sprouting due to H19 deletion, leading to ameliorated motor function (Hu et al., 2020). Altogether, these studies support the concept that pharmaceutical intervention regulating H19 expression may be therapeutically beneficial in stroke recovery.

In tandem with examining the function of lncRNA in stroke pathogenesis, potential modes of delivery for lncRNA drug therapy warrant further investigation to establish optimal stroke treatment. There is evidence suggesting the efficacy of exosomes in dispatching lncRNA-based therapeutics. Exosomes isolated from human UMSCs impeded cardiovascular malfunction spurred by aging, most likely *via* the secretion of lncRNA MALAT1, suppressing the NF-κB/TNF-α pathway (Zhu et al., 2019). Exosomes extracted from adipose-derived stem cells (hASCs) that carry lncRNA MALAT1 displayed substantial regenerative potential in traumatic brain injury (TBI) by attenuating inflammation. TBI-exposed rats intravenously treated with hASC-derived exosomes revealed that the exosomes were able to penetrate the brain and induced rehabilitation of motor function. Rats treated with exosomes that lacked MALAT1 displayed weaker regenerative capabilities, indicating MALAT1's pivotal role (Patel et al., 2018). Another study indicated that exosomes derived from adipose stem cells conditioned in hypoxia (HExos) were therapeutically beneficial in ameliorating SCI due to the heightened expression of lncGM37494. LncGM37494 delivery suppressed miR-130b-3p and enhanced expression of PPARγ, leading to greater microglial M1/M2 polarization, which likely contributed to HExos-induced SCI recovery (Shao et al., 2020). These studies support the use of exosomes as conveyers of lncRNA therapeutics, necessitating further investigations of exosome-lncRNA interactions in the context of stroke.

Along the lines of enhancing lncRNA delivery into the brain, liposomes and nanoparticles have also been demonstrated to exhibit as potent carriers of lncRNAs. Long intergenic noncoding RNA bearing (lincRNA-EPS) leukosomes enhanced proliferation of NSCs *in vitro* and hindered apoptosis by repressing

activated microglia-induced translocation and cytotoxicity. In transient middle cerebral arterial occlusion (tMCAO) models, penetration of inflammatory cells and cytotoxicity were reduced by lincRNA-EPS leukosomes, and neuronal volume was fortified in ischemic regions (Zhang B. et al., 2020). Regarding nano-based therapeutics, a nano-polymer Meg3 short hairpin RNA plasmid, designed to block Meg3, was conjugated with the OX26 antibody (MPO). *In vitro*, MPO heightened endothelial cell migration and tube generation. *In vivo*, MPO moved to the site of injury and diminished infarct volume, along with the increased expression of Vegfa and Vegfr2 genes, which are related to angiogenesis (Shen et al., 2018). In sum, finding safe and effective carriers of lncRNA that facilitate the proteins' bioavailability in the brain may potentiate lncRNA's therapeutic effects in stroke.

Genomics has illuminated particular genetic variants that are correlated with stroke pathology (Ferreira et al., 2019). Variants present in 35 genetic loci have been associated with a higher risk of stroke (Dichgans et al., 2019). However, ischemic stroke does display genetic heterogeneity, as various populations exhibit different genetic variants (Ferreira et al., 2019). Therefore, although evidence has pointed to lncRNA as a promising therapeutic strategy and diagnostic marker for stroke, disparities among individuals must be taken into account due to genotype heterogeneity. For instance, those who are genetically predisposed to have higher levels of circulating cytokines are more susceptible to stroke (Georgakis et al., 2019) and this must be considered when examining stroke outcomes following treatment with lncRNA therapeutics. Also, lncRNAs have numerous genetic variants, whose expression may vary among individuals and affect stroke susceptibility and pathogenesis. SNPs of MALAT1 may influence vulnerability to ischemic stroke. It was found that a variation of the MALAT1 promoter, rs1194338 C > A, could be linked to ischemic stroke susceptibility. Interestingly, those carrying the rs1194338 AC/AA genotypes may have greater resistance to ischemic stroke (Wang et al., 2020a). A study found that the genotype allocation of rs2383207, a variant of lncRNA ANRIL, differed among males with ischemic stroke and control groups (Yang J. et al., 2018). Interestingly, ischemic stroke patients with the GG genotype of rs1333049 demonstrated greater ANRIL expression than those with the CC or CG genotype. Gender also plays a role, as rs2383207 and rs1333049 expressions were linked to higher stroke susceptibility in males but not females (Yang J. et al., 2018). Moreover, these discrepancies among genotypes of individuals may engender inconsistencies in the lncRNA-based diagnosis and therapeutic outcome in stroke and should be further explored in preclinical and clinical investigations.

CLINICAL TRIALS SUPPORTING LncRNAs AS DIAGNOSTIC BIOMARKERS AND THERAPEUTICS IN STROKE

Recent clinical investigations have examined various lncRNAs in the context of stroke. Evaluation of blood serum from acute minor stroke (AMS) patients revealed substantial upregulation of lnc-CRKL-2 and lnc-NTRK3-4 expression and downregulation of RPS6KA2-AS1 and lnc-CALM1-7. Moreover, these lncRNAs may serve as early diagnostic markers in AMS (Xu et al., 2020). Also, a clinical study analyzed the correlation between H19 expression and risk for ischemic stroke in the Chinese Han population. Greater susceptibility to ischemic stroke could be linked to the expression of TT genotype rs217727 in H19. Moreover, H19 rs217727 bears significant potential as a biomarker for the risk of ischemic stroke (Zhu R. et al., 2018). Another clinical study demonstrated that lncRNA ZFAS1 serum levels in ischemic stroke patients were drastically downregulated compared to controls. Large artery atherosclerosis (LAA) stroke patients displayed much lower ZFAS1 expression than in non-LAA stroke patients (Wang et al., 2019b). In ischemic stroke patients, expression of lncRNA and mRNA changed drastically. Examination of blood serum suggests that ENST00000568297, ENST00000568243, and NR_046084 may serve as biomarkers for the diagnosis of ischemic stroke. Notably, analysis of serum revealed that lncRNAs may contribute to stroke pathology by inducing stroke-related mechanisms and mediating miRNA and mRNA expression (Guo et al., 2018). Further understanding of these processes may aid in establishing therapeutics utilizing ENST00000568297, ENST00000568243, and NR_046084 for stroke therapy.

Despite the positive clinical readouts of lncRNAs, equally compelling evidence indicates caution in the use of lncRNA ANRIL in stroke patients. A clinical trial investigated the relationship between antisense noncoding RNA in the INK4 locus (ANRIL) and high-sensitivity C-reactive protein (hs-CRP) and matrix metalloproteinase-9 (MMP-9) in blood serum of ischemic stroke patients. Patients with ischemic stroke exhibited drastic upregulation of ANRIL, hs-CRP, and MMP-9 in serum when compared to the control. A more severe neurological injury could be associated with higher concentrations of ANRIL, hs-CRP, and MMP expression (Zhang K. et al., 2019). On the other hand, another clinical study found that AIS patients demonstrated lower serum levels of lncRNA ANRIL than the control group. Reduced ANRIL expression could be linked to higher hs-CRP concentrations. ANRIL displayed an inverse relationship with inflammatory cytokines TNF-α and IL-6 and a positive association with IL-10 (Feng et al., 2019). These contradicting clinical findings suggest the necessity for careful application of lncRNA ANRIL in stroke. Whereas clinical trials have revealed lncRNA's capacity as both a diagnostic biomarker and a therapeutic strategy for stroke, additional preclinical studies are warranted to fully elucidate mechanisms and functions of lncRNA in the disease pathology which may aid in the optimal formulation of their clinical applications that are safe and effective in stroke patients.

CONCLUSION AND PERSPECTIVES

Taken together, the discovery of lncRNAs has completely transformed the way, we view the genetic code and the regulation network of gene expression. The emergence of lncRNAs as regulators of stroke provide novel insights and enhance our understanding of the complex regulatory network of pathological

cerebral stroke injury. With the development of new technologies such as RNA-seq, deep sequencing, microarray, and stem cell modality, a bulk of aberrantly expressed lncRNAs were identified during stroke onset and disease progression. Great progress has been made to elaborate on the potential roles of individual lncRNA in ischemic stroke and intracerebral hemorrhage. Elucidating the functions and mechanisms of these lncRNAs under normal and pathological conditions may contribute to identifying biomarkers and novel therapeutic targets of stroke.

However, there are still many challenges in this area. To date, only a very small quantity of lncRNAs have been studied in the pathological process of ischemic stroke and even fewer in intracerebral hemorrhage. Large-scale studies are needed to uncover lncRNA functions. Also, numerous lncRNAs have different isoforms due to splicing and the function of different isoforms may vary. Thus, more attention should be paid to the lncRNA isoforms. Moreover, the function of lncRNAs depends on their unique subcellular localization patterns. Many lncRNAs in the nucleus exhibit distinct nuclear localization patterns while others must be exported to the cytoplasm to carry out their regulatory roles. Stem cell technologies, such as the advent of induced pluripotent stem cells from stroke patients, may allow elucidation of lncRNA localization and function during homeostasis and pathological conditions. Linking lncRNA localization and function has the potential to better understand its specialized functions and cellular roles in depth (Chen, 2016). Given the poor-genetic conservation between species, much more work is needed to elucidate the specific role of lncRNAs in stroke. Furthermore, due to the large size of many lncRNAs, crossing through the BBB will be an important issue to be addressed. Exosomes, liposomes, nanoparticles, and lentivirus might be used for carrying lncRNA-based drugs into the cerebral infarction area (Zeng et al., 2016; Quan et al., 2017; Xiao et al., 2020; Zhang B. et al., 2020). The investigation of lncRNAs in stroke is still in its early stage, but its importance is being unraveled in many preclinical studies. Further investigations are still warranted to reveal lncRNA biological functions to accelerate the progress of lncRNA-based therapeutics for stroke.

AUTHOR CONTRIBUTIONS

JF, MS, NS, BG-P, YP, PS, CB, and YL conceptualized, drafted, edited, and finalized this manuscript. All authors contributed to the article and approved the submitted version.

FUNDING

YL is funded by the National Natural Science Foundation of China (NSFC), Grant/Award Numbers: 81771413, 81771412, 81971222 and 82001268; Natural Science Foundation of Beijing Municipality (Beijing Natural Science Foundation), Grant/Award Number: KZ201810025041. CB is funded by the National Institutes of Health (NIH) R01NS090962, NIH R01NS102395, and NIH R21NS109575.

ACKNOWLEDGMENTS

We acknowledge the excellent technical assistance of the staff from the laboratories of CB and YL.

REFERENCES

Ahad, M. A., Kumaran, K. R., Ning, T., Mansor, N. I., Effendy, M. A., Damodaran, T., et al. (2020). Insights into the neuropathology of cerebral ischemia and its mechanisms. *Rev. Neurosci.* 31, 521–538. doi: 10.1515/revneuro-2019-0099

Andersen, R. E., and Lim, D. A. (2018). Forging our understanding of lncRNAs in the brain. *Cell Tissue Res.* 371, 55–71. doi: 10.1007/s00441-017-2711-z

Anderson, D. M., Anderson, K. M., Chang, C. L., Makarewich, C. A., Nelson, B. R., McAnally, J. R., et al. (2015). A micropeptide encoded by a putative long noncoding RNA regulates muscle performance. *Cell* 160, 595–606. doi: 10.1016/j.cell.2015.01.009

Anrather, J., and Iadecola, C. (2016). Inflammation and stroke: an overview. *Neurotherapeutics* 13, 661–670. doi: 10.1007/s13311-016-0483-x

Arvidsson, A., Collin, T., Kirik, D., Kokaia, Z., and Lindvall, O. (2002). Neuronal replacement from endogenous precursors in the adult brain after stroke. *Nat. Med.* 8, 963–970. doi: 10.1038/nm747

Au, A., Griffiths, L. R., Irene, L., Kooi, C. W., and Wei, L. K. (2017). The impact of APOA5, APOB, APOC3, and ABCA1 gene polymorphisms on ischemic stroke: evidence from a meta-analysis. *Atherosclerosis* 265, 60–70. doi: 10.1016/j.atherosclerosis.2017.08.003

Bao, M. H., Zhu, S. Z., Gao, X. Z., Sun, H. S., and Feng, Z. P. (2018). Meta-analysis on the association between brain-derived neurotrophic factor polymorphism rs6265 and ischemic stroke, poststroke depression. *J. Stroke Cerebrovasc. Dis.* 27, 1599–1608. doi: 10.1016/j.jstrokecerebrovasdis.2018.01.010

Bär, C., Chatterjee, S., and Thum, T. (2016). Long noncoding RNAs in cardiovascular pathology, diagnosis, and therapy. *Circulation* 134, 1484–1499. doi: 10.1161/CIRCULATIONAHA.116.023686

Berkhemer, O. A., Fransen, P. S., Beumer, D., van den Berg, L. A., Lingsma, H. F., Yoo, A. J., et al. (2015). A randomized trial of intraarterial treatment for acute ischemic stroke. *N. Engl. J. Med.* 372, 11–20. doi: 10.1056/NEJMoa1411587

Bhan, A., Soleimani, M., and Mandal, S. S. (2017). Long noncoding RNA and cancer: a new paradigm. *Cancer Res.* 77, 3965–3981. doi: 10.1158/0008-5472.CAN-16-2634

Bhattarai, S., Pontarelli, F., Prendergast, E., and Dharap, A. (2017). Discovery of novel stroke-responsive lncRNAs in the mouse cortex using genome-wide RNA-seq. *Neurobiol. Dis.* 108, 204–212. doi: 10.1016/j.nbd.2017.08.016

Bitarafan, S., Yari, M., Broumand, M. A., SMH, G., Rahimi, M., Mirfakhraie, R., et al. (2019). Association of increased levels of lncRNA H19 in PBMCs with risk of coronary artery disease. *Cell J.* 20, 564–568. doi: 10.22074/cellj.2019.5544

Cai, H., Cai, B., Liu, Z., Wu, W., Chen, D., Fang, L., et al. (2020). Genetic correlations and causal inferences in ischemic stroke. *J. Neurol.* 267, 1980–1990. doi: 10.1007/s00415-020-09786-4

Cao, D. W., Liu, M. M., Duan, R., Tao, Y. F., Zhou, J. S., Fang, W. R., et al. (2020). The lncRNA Malat1 functions as a ceRNA to contribute to berberine-mediated inhibition of HMGB1 by sponging miR-181c-5p in poststroke inflammation. *Acta Pharmacol. Sin.* 41, 22–33. doi: 10.1038/s41401-019-0284-y

Ceulemans, A. G., Zgavc, T., Kooijman, R., Hachimi-Idrissi, S., Sarre, S., and Michotte, Y. (2010). The dual role of the neuroinflammatory response after ischemic stroke: modulatory effects of hypothermia. *J. Neuroinflammation* 7:74. doi: 10.1186/1742-2094-7-74

Chen, L. L. (2016). Linking long noncoding rna localization and function. *Trends Biochem. Sci.* 41, 761–772. doi: 10.1016/j.tibs.2016.07.003

Chen, L., Yang, W., Guo, Y., Chen, W., Zheng, P., Zeng, J., et al. (2017). Exosomal lncRNA GAS5 regulates the apoptosis of macrophages and vascular endothelial cells in atherosclerosis. *PLoS One* 12:e0185406. doi: 10.1371/journal.pone.0185406

Chen, S., Wang, M., Yang, H., Mao, L., He, Q., Jin, H., et al. (2017). LncRNA TUG1 sponges microRNA-9 to promote neurons apoptosis by up-regulated Bcl2l11 under ischemia. *Biochem. Biophys. Res. Commun.* 485, 167–173. doi: 10.1016/j.bbrc.2017.02.043

Chen, F., Zhang, L., Wang, E., Zhang, C., and Li, X. (2018). LncRNA GAS5 regulates ischemic stroke as a competing endogenous RNA for miR-137 to regulate the Notch1 signaling pathway. *Biochem. Biophys. Res. Commun.* 496, 184–190. doi: 10.1016/j.bbrc.2018.01.022

Chen, Z., Zheng, J., Liu, W., Yang, K., Li, K., Huang, B., et al. (2017). The SG13S114 polymorphism of the ALOX5AP gene is associated with ischemic stroke in Europeans: a meta-analysis of 8062 subjects. *Neurol. Sci.* 38, 579–587. doi: 10.1007/s10072-016-2804-6

Cheng, Q., Zhang, M., Zhang, M., Ning, L., and Chen, D. (2020). Long non-coding RNA LOC285194 regulates vascular smooth muscle cell apoptosis in atherosclerosis. *Bioengineered* 11, 53–60. doi: 10.1080/21655979.2019.1705054

Deng, Y., Chen, D., Wang, L., Gao, F., Jin, B., Lv, H., et al. (2019). Silencing of long noncoding RNA nespas aggravates microglial cell death and neuroinflammation in ischemic stroke. *Stroke* 50, 1850–1858. doi: 10.1161/STROKEAHA.118.023376

Deng, Q. W., Li, S., Wang, H., Sun, H. L., Zuo, L., Gu, Z. T., et al. (2018). Differential long noncoding RNA expressions in peripheral blood mononuclear cells for detection of acute ischemic stroke. *Clin. Sci.* 132, 1597–1614. doi: 10.1042/CS20180411

Dharap, A., Nakka, V. P., and Vemuganti, R. (2012). Effect of focal ischemia on long noncoding RNAs. *Stroke* 43, 2800–2802. doi: 10.1161/STROKEAHA.112.669465

Dharap, A., Pokrzywa, C., and Vemuganti, R. (2013). Increased binding of stroke-induced long non-coding RNAs to the transcriptional corepressors Sin3A and coREST. *ASN Neuro* 5, 283–289. doi: 10.1042/AN20130029

Dichgans, M. (2007). Genetics of ischaemic stroke. *Lancet Neurol.* 6, 149–161. doi: 10.1016/S1474-4422(07)70028-5

Dichgans, M., Pulit, S. L., and Rosand, J. (2019). Stroke genetics: discovery, biology and clinical applications. *Lancet Neurol.* 18, 587–599. doi: 10.1016/S1474-4422(19)30043-2

Djebali, S., Davis, C. A., Merkel, A., Dobin, A., Lassmann, T., Mortazavi, A., et al. (2012). Landscape of transcription in human cells. *Nature* 489, 101–108. doi: 10.1038/nature11233

Dong, B., Zhou, B., Sun, Z., Huang, S., Han, L., Nie, H., et al. (2018). LncRNA-FENDRR mediates VEGFA to promote the apoptosis of brain microvascular endothelial cells *via* regulating miR-126 in mice with hypertensive intracerebral hemorrhage. *Microcirculation* 25:e12499. doi: 10.1111/micc.12499

Dykstra-Aiello, C., Jickling, G. C., Ander, B. P., Shroff, N., Zhan, X., Liu, D., et al. (2016). Altered expression of long noncoding RNAs in blood after ischemic stroke and proximity to putative stroke risk loci. *Stroke* 47, 2896–2903. doi: 10.1161/STROKEAHA.116.013869

Emsley, H. C., and Tyrrell, P. J. (2002). Inflammation and infection in clinical stroke. *J. Cereb. Blood Flow Metab.* 22, 1399–1419. doi: 10.1097/01.WCB.0000037880.62590.28

Ergul, A., Alhusban, A., and Fagan, S. C. (2012). Angiogenesis: a harmonized target for recovery after stroke. *Stroke* 43, 2270–2274. doi: 10.1161/STROKEAHA.111.642710

Fan, B., Pan, W., Wang, X., Wei, M., He, A., Zhao, A., et al. (2020). Long noncoding RNA mediates stroke-induced neurogenesis. *Stem Cells* 38, 973–985. doi: 10.1002/stem.3189

Fan, Y., Shen, B., Tan, M., Mu, X., Qin, Y., Zhang, F., et al. (2014). Long non-coding RNA UCA1 increases chemoresistance of bladder cancer cells by regulating Wnt signaling. *FEBS J.* 281, 1750–1758. doi: 10.1111/febs.12737

Feng, L., Guo, J., and Ai, F. (2019). Circulating long noncoding RNA ANRIL downregulation correlates with increased risk, higher disease severity and elevated pro-inflammatory cytokines in patients with acute ischemic stroke. *J. Clin. Lab. Anal.* 33:e22629 33:e22629. doi: 10.1002/jcla.22629

Ferreira, L. E., Secolin, R., Lopes-Cendes, I., Cabral, N. L., and PHC, F. (2019). Association and interaction of genetic variants with occurrence of ischemic stroke among Brazilian patients. *Gene* 695, 84–91. doi: 10.1016/j.gene.2019.01.041

Fonarow, G. C., Smith, E. E., Saver, J. L., Reeves, M. J., Bhatt, D. L., Grau-Sepulveda, M. V., et al. (2011). Timeliness of tissue-type plasminogen activator therapy in acute ischemic stroke: patient characteristics, hospital factors and outcomes associated with door-to-needle times within 60 minutes. *Circulation* 123, 750–758. doi: 10.1161/CIRCULATIONAHA.110.974675

Gao, M., Fu, J., and Wang, Y. (2020). The lncRNA FAL1 protects against hypoxia-reoxygenation-induced brain endothelial damages through regulating PAK1. *J. Bioenerg. Biomembr.* 52, 17–25. doi: 10.1007/s10863-019-09819-2

Georgakis, M. K., Gill, D., Rannikmäe, K., Traylor, M., Anderson, C. D., Lee, J. M., et al. (2019). Genetically determined levels of circulating cytokines and risk of stroke. *Circulation* 139, 256–268. doi: 10.1161/CIRCULATIONAHA.118.035905

Gross, B. A., Jankowitz, B. T., and Friedlander, R. M. (2019). Cerebral intraparenchymal hemorrhage: a review. *JAMA* 321, 1295–1303. doi: 10.1001/jama.2019.2413

Guo, D., Ma, J., Yan, L., Li, T., Li, Z., Han, X., et al. (2017). Down-regulation of lncRNA MALAT1 attenuates neuronal cell death through suppressing beclin1-dependent autophagy by regulating miR-30a in cerebral ischemic stroke. *Cell. Physiol. Biochem.* 43, 182–194. doi: 10.1159/000480337

Guo, X., Yang, J., Liang, B., Shen, T., Yan, Y., Huang, S., et al. (2018). Identification of novel lncRNA biomarkers and construction of lncRNA-related networks in han chinese patients with ischemic stroke. *Cell. Physiol. Biochem.* 50, 2157–2175. doi: 10.1159/000495058

Hacke, W., Kaste, M., Fieschi, C., Toni, D., Lesaffre, E., Kummer, R., et al. (1995). Intravenous thrombolysis with recombinant tissue plasminogen activator for acute hemispheric stroke. The European Cooperative Acute Stroke Study (ECASS). *JAMA* 274, 1017–1025. doi: 10.1001/jama.1995.03530130023023

Hanjin, C., Tao, L., Pengfei, L., Ali, Y., Huajun, Z., Jiekun, L., et al. (2018). Altered long noncoding RNA and messenger RNA expression in experimental intracerebral hemorrhage-a preliminary study. *Cell. Physiol. Biochem.* 45, 1284–1301. doi: 10.1159/000487464

Hernández-Valero, M. A., Rother, J., Gorlov, I., Frazier, M., and Gorlova, O. (2013). Interplay between polymorphisms and methylation in the H19/IGF2 gene region may contribute to obesity in Mexican-American children. *J. Dev. Orig. Health Dis.* 4, 499–506. doi: 10.1017/S204017441300041X

Hou, X. X., and Cheng, H. (2018). Long non-coding RNA RMST silencing protects against middle cerebral artery occlusion (MCAO)-induced ischemic stroke. *Biochem. Biophys. Res. Commun.* 495, 2602–2608. doi: 10.1016/j.bbrc.2017.12.087

Hu, X., Li, P., Guo, Y., Wang, H., Leak, R. K., Chen, S., et al. (2012). Microglia/macrophage polarization dynamics reveal novel mechanism of injury expansion after focal cerebral ischemia. *Stroke* 43, 3063–3070. doi: 10.1161/STROKEAHA.112.659656

Hu, S., Zheng, J., Du, Z., and Wu, G. (2020). Knock down of lncRNA H19 promotes axon sprouting and functional recovery after cerebral ischemic stroke. *Brain Res.* 1732:146681. doi: 10.1016/j.brainres.2020.146681

Hua, Z., Ma, K., Liu, S., Yue, Y., Cao, H., and Li, Z. (2020). LncRNA ZEB1-AS1 facilitates ox-LDL-induced damage of HCtAEC cells and the oxidative stress and inflammatory events of THP-1 cells *via* miR-942/HMGB1 signaling. *Life Sci.* 247:117334. doi: 10.1016/j.lfs.2020.117334

Huang, J. Z., Chen, M., Chen, D., Gao, X. C., Zhu, S., Huang, H., et al. (2017). A peptide encoded by a putative lncRNA HOXB-AS3 suppresses colon cancer growth. *Mol. Cell* 68, 171.e6–184.e6.doi: 10.1016/j.molcel.2017.09.015

Huang, J., Yang, J., Li, J., Chen, Z., Guo, X., Huang, S., et al. (2019). Association of long noncoding RNA H19 polymorphisms with the susceptibility and clinical features of ischemic stroke in southern Chinese Han population. *Metab. Brain Dis.* 34, 1011–1021. doi: 10.1007/s11011-019-00417-0

Huang, Y., Wang, L., Mao, Y., and Nan, G. (2019). Long noncoding RNA-H19 contributes to atherosclerosis and induces ischemic stroke *via* the upregulation of acid phosphatase 5. *Front. Neurol.* 10:32. doi: 10.3389/fneur.2019.00032

Huang, L., and Zhang, L. (2019). Neural stem cell therapies and hypoxic-ischemic brain injury. *Prog. Neurobiol.* 173, 1–17. doi: 10.1016/j.pneurobio.2018.05.004

Jia, J., Zhang, M., Li, Q., Zhou, Q., and Jiang, Y. (2018). Long noncoding ribonucleic acid NKILA induces the endoplasmic reticulum stress/autophagy

pathway and inhibits the nuclear factor-k-gene binding pathway in rats after intracerebral hemorrhage. *J. Cell. Physiol.* 233, 8839–8849. doi: 10.1002/jcp.26798

Kim, J. M., Moon, J., Yu, J. S., Park, D. K., Lee, S. T., Jung, K. H., et al. (2019). Altered long noncoding RNA profile after intracerebral hemorrhage. *Ann. Clin. Transl. Neurol.* 6, 2014–2025. doi: 10.1002/acn3.50894

Kopp, F., and Mendell, J. T. (2018). Functional classification and experimental dissection of long noncoding RNAs. *Cell* 172, 393–407. doi: 10.1016/j.cell.2018.01.011

Kuo, C. C., Hänzelmann, S., Sentürk, C. N., Frank, S., Zajzon, B., Derks, J. P., et al. (2019). Detection of RNA-DNA binding sites in long noncoding RNAs. *Nucleic Acids Res.* 47:e32. doi: 10.1093/nar/gkz037

Kurian, L., Aguirre, A., Sancho-Martinez, I., Benner, C., Hishida, T., Nguyen, T. B., et al. (2015). Identification of novel long noncoding RNAs underlying vertebrate cardiovascular development. *Circulation* 131, 1278–1290. doi: 10.1161/CIRCULATIONAHA.114.013303

Li, F. P., Lin, D. Q., and Gao, L. Y. (2018). LncRNA TUG1 promotes proliferation of vascular smooth muscle cell and atherosclerosis through regulating miRNA-21/PTEN axis. *Eur. Rev. Med. Pharmacol. Sci.* 22, 7439–7447. doi: 10.26355/eurrev_201811_16284

Li, Z., Li, J., and Tang, N. (2017). Long noncoding RNA Malat1 is a potent autophagy inducer protecting brain microvascular endothelial cells against oxygen-glucose deprivation/reoxygenation-induced injury by sponging miR-26b and upregulating ULK2 expression. *Neuroscience* 354, 1–10. doi: 10.1016/j.neuroscience.2017.04.017

Liang, S., Ren, K., Li, B., Li, F., Liang, Z., Hu, J., et al. (2020). LncRNA SNHG1 alleviates hypoxia-reoxygenation-induced vascular endothelial cell injury as a competing endogenous RNA through the HIF-1α/VEGF signal pathway. *Mol. Cell. Biochem.* 465, 1–11. doi: 10.1007/s11010-019-03662-0

Liao, B., Chen, R., Lin, F., Mai, A., Chen, J., Li, H., et al. (2018). Long noncoding RNA HOTTIP promotes endothelial cell proliferation and migration *via* activation of the Wnt/β-catenin pathway. *J. Cell. Biochem.* 119, 2797–2805. doi: 10.1002/jcb.26448

Liu, J., Li, Q., Zhang, K. S., Hu, B., Niu, X., Zhou, S. M., et al. (2017). Downregulation of the long non-coding RNA Meg3 promotes angiogenesis after ischemic brain injury by activating notch signaling. *Mol. Neurobiol.* 54, 8179–8190. doi: 10.1007/s12035-016-0270-z

Liu, J., Wang, Y., Akamatsu, Y., Lee, C. C., Stetler, R. A., Lawton, M. T., et al. (2014). Vascular remodeling after ischemic stroke: mechanisms and therapeutic potentials. *Prog. Neurobiol.* 115, 138–156. doi: 10.1016/j.pneurobio.2013.11.004

Liu, C., Yang, J., Zhang, C., Liu, M., Geng, X., Ji, X., et al. (2018). Analysis of long non-coding RNA expression profiles following focal cerebral ischemia in mice. *Neurosci. Lett.* 665, 123–129. doi: 10.1016/j.neulet.2017.11.058

Matsumoto, A., Pasut, A., Matsumoto, M., Yamashita, R., Fung, J., Monteleone, E., et al. (2017). mTORC1 and muscle regeneration are regulated by the LINC00961-encoded SPAR polypeptide. *Nature* 541, 228–232. doi: 10.1038/nature21034

Mercer, T. R., Dinger, M. E., Sunkin, S. M., Mehler, M. F., and Mattick, J. S. (2008). Specific expression of long noncoding RNAs in the mouse brain. *Proc. Natl. Acad. Sci. U S A* 105, 716–721. doi: 10.1073/pnas.0706729105

Ouyang, Y. B. (2013). Inflammation and stroke. *Neurosci. Lett.* 548, 1–3. doi: 10.1016/j.neulet.2013.05.031

Pan, J. X. (2017). LncRNA H19 promotes atherosclerosis by regulating MAPK and NF-kB signaling pathway. *Eur. Rev. Med. Pharmacol. Sci.* 21, 322–328. doi: 10.1016/j.brainres.2020.146681

Patel, N. A., Moss, L. D., Lee, J. Y., Tajiri, N., Acosta, S., Hudson, C., et al. (2018). Long noncoding RNA MALAT1 in exosomes drives regenerative function and modulates inflammation-linked networks following traumatic brain injury. *J. Neuroinflammation* 15:204. doi: 10.1186/s12974-018-1240-3

Peng, J., Wu, Y., Tian, X., Pang, J., Kuai, L., Cao, F., et al. (2017). High-throughput sequencing and co-expression network analysis of lncRNAs and mRNAs in early brain injury following experimental subarachnoid haemorrhage. *Sci. Rep.* 7:46577. doi: 10.1038/srep46577

Pistritto, G., Trisciuoglio, D., Ceci, C., Garufi, A., and D'Orazi, G. (2016). Apoptosis as anticancer mechanism: function and dysfunction of its modulators and targeted therapeutic strategies. *Aging* 8, 603–619. doi: 10.18632/aging.100934

Ponting, C. P., Oliver, P. L., and Reik, W. (2009). Evolution and functions of long noncoding RNAs. *Cell* 136, 629–641. doi: 10.1016/j.cell.2009.02.006

Powers, W. J., Rabinstein, A. A., Ackerson, T., Adeoye, O. M., Bambakidis, N. C., Becker, K., et al. (2018). 2018 guidelines for the early management of patients with acute ischemic stroke: a guideline for healthcare professionals from the american heart association/american stroke association. *Stroke* 49, e46–46e110. doi: 10.1161/STR.0000000000000158

Qi, X., Shao, M., Sun, H., Shen, Y., Meng, D., and Huo, W. (2017). Long non-coding RNA SNHG14 promotes microglia activation by regulating miR-145–5p/PLA2G4A in cerebral infarction. *Neuroscience* 348, 98–106. doi: 10.1016/j.neuroscience.2017.02.002

Quan, Z., Zheng, D., and Qing, H. (2017). Regulatory roles of long non-coding RNAs in the central nervous system and associated neurodegenerative diseases. *Front. Cell. Neurosci.* 11:175. doi: 10.3389/fncel.2017.00175

Sahota, P., and Savitz, S. I. (2011). Investigational therapies for ischemic stroke: neuroprotection and neurorecovery. *Neurotherapeutics* 8, 434–451. doi: 10.1007/s13311-011-0040-6

Shan, H., Guo, D., Zhang, S., Qi, H., Liu, S., and Du, Y. (2020). SNHG6 modulates oxidized low-density lipoprotein-induced endothelial cells injury through miR-135a-5p/ROCK in atherosclerosis. *Cell Biosci.* 10:4. doi: 10.1186/s13578-019-0371-2

Shao, M., Jin, M., Xu, S., Zheng, C., Zhu, W., Ma, X., et al. (2020). Exosomes from long noncoding RNA-Gm37494-ADSCs repair spinal cord injury *via* shifting microglial M1/M2 polarization. *Inflammation* 43, 1536–1547. doi: 10.1007/s10753-020-01230-z

Shen, J., Zhao, Z., Shang, W., Liu, C., Zhang, B., Xu, Z., et al. (2018). Fabrication of a nano polymer wrapping Meg3 ShRNA plasmid for the treatment of cerebral infarction. *Artif. Cells Nanomed. Biotechnol.* 46, 894–903. doi: 10.1080/21691401.2018.1471483

Srivastava, A. K., Singh, P. K., Rath, S. K., Dalela, D., Goel, M. M., and Bhatt, M. L. (2014). Appraisal of diagnostic ability of UCA1 as a biomarker of carcinoma of the urinary bladder. *Tumour Biol.* 35, 11435–11442. doi: 10.1007/s13277-014-2474-z

St Laurent, G., Wahlestedt, C., and Kapranov, P. (2015). The landscape of long noncoding RNA classification. *Trends Genet.* 31, 239–251. doi: 10.1016/j.tig.2015.03.007

Taft, R. J., Pang, K. C., Mercer, T. R., Dinger, M., and Mattick, J. S. (2010). Non-coding RNAs: regulators of disease. *J. Pathol.* 220, 126–139. doi: 10.1002/path.2638

Tian, C., Li, Z., Zhang, L., Dai, D., Huang, Q., Liu, J., et al. (2020). lncRNA NR_120420 promotes SH-SY5Y cells apoptosis by regulating NF-κB after oxygen and glucose deprivation. *Gene* 728:144285. doi: 10.1016/j.gene.2019.144285

Tragante, V., Barnes, M. R., Ganesh, S. K., Lanktree, M. B., Guo, W., Franceschini, N., et al. (2014). Gene-centric meta-analysis in 87,736 individuals of European ancestry identifies multiple blood-pressure-related loci. *Am. J. Hum. Genet.* 94, 349–360. doi: 10.1016/j.ajhg.2013.12.016

Tuttolomondo, A., Di, R. D., Pecoraro, R., Arnao, V., Pinto, A., and Licata, G. (2012). Inflammation in ischemic stroke subtypes. *Curr. Pharm. Des.* 18, 4289–4310. doi: 10.2174/138161212802481200

Virani, S. S., Alonso, A., Benjamin, E. J., Bittencourt, M. S., Callaway, C. W., Carson, A. P., et al. (2020). Heart disease and stroke statistics-2020 update: a report from the american heart association. *Circulation* 141:e139.e596. doi: 10.1161/CIR.0000000000000757

Wan, P., Su, W., and Zhuo, Y. (2017). The role of long noncoding RNAs in neurodegenerative diseases. *Mol. Neurobiol.* 54, 2012–2021. doi: 10.1007/s12035-016-9793-6

Wang, J., Cao, B., Han, D., Sun, M., and Feng, J. (2017a). Long non-coding RNA H19 induces cerebral ischemia reperfusion injury *via* activation of autophagy. *Aging Dis.* 8, 71–84. doi: 10.14336/AD.2016.0530

Wang, J., Zhao, H., Fan, Z., Li, G., Ma, Q., Tao, Z., et al. (2017b). Long noncoding RNA H19 promotes neuroinflammation in ischemic stroke by driving histone deacetylase 1-dependent M1 microglial polarization. *Stroke* 48, 2211–2221. doi: 10.1161/STROKEAHA.117.017387

Wang, J., Cao, B., Zhao, H., Gao, Y., Luo, Y., Chen, Y., et al. (2019a). Long noncoding RNA H19 prevents neurogenesis in ischemic stroke through p53/Notch1 pathway. *Brain Res. Bull.* 150, 111–117. doi: 10.1016/j.brainresbull.2019.05.009

Wang, J., Ruan, J., Zhu, M., Yang, J., Du, S., Xu, P., et al. (2019b). Predictive value of long noncoding RNA ZFAS1 in patients with ischemic stroke. *Clin. Exp. Hypertens.* 41, 615–621. doi: 10.1080/10641963.2018.1529774

Wang, Y., Gu, X. X., Huang, H. T., Liu, C. H., and Wei, Y. S. (2020a). A genetic variant in the promoter of LncRNA MALAT1 is related to susceptibility of ischemic stroke. *Lipids Health Dis.* 19:57. doi: 10.1186/s12944-020-01236-4

Wang, Y., Luo, Y., Yao, Y., Ji, Y., Feng, L., and Du, F. (2020b). Silencing the lncRNA Maclpil in pro-inflammatory macrophages attenuates acute experimental ischemic stroke *via* LCP1 in mice. *J. Cereb. Blood Flow Metab.* 40, 747–759. doi: 10.1177/0271678X19836118

Wang, M., Jiang, Y. M., Xia, L. Y., Wang, Y., Li, W. Y., and Jin, T. (2018). LncRNA NKILA upregulation mediates oxygen glucose deprivation/re-oxygenation-induced neuronal cell death by inhibiting NF-κB signaling. *Biochem. Biophys. Res. Commun.* 503, 2524–2530. doi: 10.1016/j.bbrc.2018.07.010

Wang, Y., Li, G., Zhao, L., and Lv, J. (2018). Long noncoding RNA HOTTIP alleviates oxygen-glucose deprivation-induced neuronal injury *via* modulating miR-143/hexokinase 2 pathway. *J. Cell. Biochem.* 119, 10107–10117. doi: 10.1002/jcb.27348

Wang, P., Shao, B. Z., Deng, Z., Chen, S., Yue, Z., and Miao, C. Y. (2018). Autophagy in ischemic stroke. *Prog. Neurobiol.* 163–164, 98–117. doi: 10.1016/j.pneurobio.2018.01.001

Wang, Z., Wang, R., Wang, K., and Liu, X. (2018). Upregulated long noncoding RNA Snhg1 promotes the angiogenesis of brain microvascular endothelial cells after oxygen-glucose deprivation treatment by targeting miR-199a. *Can. J. Physiol. Pharmacol.* 96, 909–915. doi: 10.1139/cjpp-2018-0107

Wang, X. S., Zhang, Z., Wang, H. C., Cai, J. L., Xu, Q. W., Li, M. Q., et al. (2006). Rapid identification of UCA1 as a very sensitive and specific unique marker for human bladder carcinoma. *Clin. Cancer Res.* 12, 4851–4858. doi: 10.1158/1078-0432.CCR-06-0134

Wen, J., Yang, C. Y., Lu, J., and Wang, X. Y. (2018). Ptprj-as1 mediates inflammatory injury after intracerebral hemorrhage by activating NF-κB pathway. *Eur. Rev. Med. Pharmacol. Sci.* 22, 2817–2823. doi: 10.26355/eurrev_201805_14981

Wu, Z., Wu, P., Zuo, X., Yu, N., Qin, Y., Xu, Q., et al. (2017). LncRNA-N1LR enhances neuroprotection against ischemic stroke probably by inhibiting p53 phosphorylation. *Mol. Neurobiol.* 54, 7670–7685. doi: 10.1007/s12035-016-0246-z

Xiang, Y., Zhang, Y., Xia, Y., Zhao, H., Liu, A., and Chen, Y. (2020). LncRNA MEG3 targeting miR-424–5p *via* MAPK signaling pathway mediates neuronal apoptosis in ischemic stroke. *Aging* 12, 3156–3174. doi: 10.18632/aging.102790

Xiao, L., Wei, F., Zhou, Y., Anderson, G. J., Frazer, D. M., Lim, Y. C., et al. (2020). Dihydrolipoic acid-gold nanoclusters regulate microglial polarization and have the potential to alter neurogenesis. *Nano Lett.* 20, 478–495. doi: 10.1021/acs.nanolett.9b04216

Xu, Q., Deng, F., Xing, Z., Wu, Z., Cen, B., Xu, S., et al. (2016). Long non-coding RNA C2dat1 regulates CaMKIIδ expression to promote neuronal survival through the NF-κB signaling pathway following cerebral ischemia. *Cell Death Dis.* 7:e2173. doi: 10.1038/cddis.2016.57

Xu, X., Zhuang, C., and Chen, L. (2020). Exosomal long non-coding RNA expression from serum of patients with acute minor stroke. *Neuropsychiatr. Dis. Treat.* 16, 153–160. doi: 10.2147/NDT.S230332

Yan, H., Rao, J., Yuan, J., Gao, L., Huang, W., Zhao, L., et al. (2017). Long non-coding RNA MEG3 functions as a competing endogenous RNA to regulate ischemic neuronal death by targeting miR-21/PDCD4 signaling pathway. *Cell Death Dis.* 8:3211. doi: 10.1038/s41419-017-0047-y

Yan, H., Yuan, J., Gao, L., Rao, J., and Hu, J. (2016). Long noncoding RNA MEG3 activation of p53 mediates ischemic neuronal death in stroke. *Neuroscience* 337, 191–199. doi: 10.1016/j.neuroscience.2016.09.017

Yang, J., Gu, L., Guo, X., Huang, J., Chen, Z., Huang, G., et al. (2018). LncRNA ANRIL expression and ANRIL gene polymorphisms contribute to the risk of ischemic stroke in the chinese han population. *Cell. Mol. Neurobiol.* 38, 1253–1269. doi: 10.1007/s10571-018-0593-6

Yang, Q., Wan, Q., Zhang, L., Li, Y., Zhang, P., Li, D., et al. (2018). Analysis of lncRNA expression in cell differentiation. *RNA Biol.* 15, 413–422. doi: 10.1080/15476286.2018.1441665

Yao, X., Yao, R., Huang, F., and Yi, J. (2019). LncRNA SNHG12 as a potent autophagy inducer exerts neuroprotective effects against cerebral ischemia/reperfusion injury. *Biochem. Biophys. Res. Commun.* 514, 490–496. doi: 10.1016/j.bbrc.2019.04.158

Yin, W. L., Yin, W. G., Huang, B. S., and Wu, L. X. (2019). LncRNA SNHG12 inhibits miR-199a to upregulate SIRT1 to attenuate cerebral ischemia/reperfusion injury through activating AMPK signaling pathway. *Neurosci. Lett.* 690, 188–195. doi: 10.1016/j.neulet.2018.08.026

Yong, H., Foody, J., Linong, J., Dong, Z., Wang, Y., Ma, L., et al. (2013). A systematic literature review of risk factors for stroke in China. *Cardiol. Rev.* 21, 77–93. doi: 10.1097/CRD.0b013e3182748d37

You, D., and You, H. (2019). Repression of long non-coding RNA MEG3 restores nerve growth and alleviates neurological impairment after cerebral ischemia-reperfusion injury in a rat model. *Biomed. Pharmacother.* 111, 1447–1457. doi: 10.1016/j.biopha.2018.12.067

Yu, S., Yu, M., He, X., Wen, L., Bu, Z., and Feng, J. (2019). KCNQ1OT1 promotes autophagy by regulating miR-200a/FOXO3/ATG7 pathway in cerebral ischemic stroke. *Aging Cell* 18:e12940. doi: 10.1111/acel.12940

Zang, Y., Zhou, X., Wang, Q., Li, X., and Huang, H. (2018). LncRNA FIRRE/NF-kB feedback loop contributes to OGD/R injury of cerebral microglial cells. *Biochem. Biophys. Res. Commun.* 501, 131–138. doi: 10.1016/j.bbrc.2018.04.194

Zeng, L. L., He, X. S., Liu, J. R., Zheng, C. B., Wang, Y. T., and Yang, G. Y. (2016). Lentivirus-mediated overexpression of MicroRNA-210 improves long-term outcomes after focal cerebral ischemia in mice. *CNS Neurosci. Ther.* 22, 961–969. doi: 10.1111/cns.12589

Zhan, R., Xu, K., Pan, J., Xu, Q., Xu, S., and Shen, J. (2017). Long noncoding RNA MEG3 mediated angiogenesis after cerebral infarction through regulating p53/NOX4 axis. *Biochem. Biophys. Res. Commun.* 490, 700–706. doi: 10.1016/j.bbrc.2017.06.104

Zhang, J., Dong, B., Hao, J., Yi, S., Cai, W., and Luo, Z. (2019). LncRNA Snhg3 contributes to dysfunction of cerebral microvascular cells in intracerebral hemorrhage rats by activating the TWEAK/Fn14/STAT3 pathway. *Life Sci.* 237:116929. doi: 10.1016/j.lfs.2019.116929

Zhang, B., Li, Q., Jia, S., Li, F., Li, Q., and Li, J. (2020). LincRNA-EPS in biomimetic vesicles targeting cerebral infarction promotes inflammatory resolution and neurogenesis. *J. Transl. Med.* 18:110. doi: 10.1186/s12967-020-02278-z

Zhang, K., Qi, M., Yang, Y., Xu, P., Zhua, Y., and Zhang, J. (2019). Circulating lncRNA ANRIL in the serum of patients with ischemic stroke. *Clin. Lab.* 65:8. doi: 10.7754/Clin.Lab.2019.190143

Zhang, X., Tang, X., Liu, K., Hamblin, M. H., and Yin, K. J. (2017). Long noncoding RNA Malat1 regulates cerebrovascular pathologies in ischemic stroke. *J. Neurosci.* 37, 1797–1806. doi: 10.1523/JNEUROSCI.3389-16.2017

Zhang, B., Wang, D., Ji, T. F., Shi, L., and Yu, J. L. (2017). Overexpression of lncRNA ANRIL up-regulates VEGF expression and promotes angiogenesis of diabetes mellitus combined with cerebral infarction by activating NF-κB signaling pathway in a rat model. *Oncotarget* 8, 17347–17359. doi: 10.18632/oncotarget.14468

Zhang, T., Wang, H., Li, Q., Fu, J., Huang, J., and Zhao, Y. (2018). MALAT1 activates the P53 signaling pathway by regulating MDM2 to promote ischemic stroke. *Cell. Physiol. Biochem.* 50, 2216–2228. doi: 10.1159/000495083

Zhang, C., Yang, H., Li, Y., Huo, P., and Ma, P. (2020). LncRNA OIP5-AS1 regulates oxidative low-density lipoprotein-mediated endothelial cell injury *via* miR-320a/LOX1 axis. *Mol. Cell. Biochem.* 467, 15–25. doi: 10.1007/s11010-020-03688-9

Zhang, J., Yuan, L., Zhang, X., Hamblin, M. H., Zhu, T., Meng, F., et al. (2016). Altered long non-coding RNA transcriptomic profiles in brain microvascular endothelium after cerebral ischemia. *Exp. Neurol.* 277, 162–170. doi: 10.1016/j.expneurol.2015.12.014

Zhang, X., Zhu, X. L., Ji, B. Y., Cao, X., Yu, L. J., Zhang, Y., et al. (2019). LncRNA-1810034E14Rik reduces microglia activation in experimental ischemic stroke. *J. Neuroinflammation* 16:75. doi: 10.1186/s12974-019-1464-x

Zhao, F., Qu, Y., Liu, J., Liu, H., Zhang, L., Feng, Y., et al. (2015). Microarray profiling and co-expression network analysis of lncRNAs and mRNAs in neonatal rats following hypoxic-ischemic brain damage. *Sci. Rep.* 5:13850. doi: 10.1038/srep13850

Zhao, M., Wang, J., Xi, X., Tan, N., and Zhang, L. (2018). SNHG12 promotes angiogenesis following ischemic stroke *via* regulating miR-150/VEGF pathway. *Neuroscience* 390, 231–240. doi: 10.1016/j.neuroscience.2018.08.029

Zheng, Z., Liu, S., Wang, C., and Han, X. (2018). A functional polymorphism rs145204276 in the promoter of long noncoding RNA GAS5 is associated with an increased risk of ischemic stroke. *J. Stroke Cerebrovasc. Dis.* 27, 3535–3541. doi: 10.1016/j.jstrokecerebrovasdis.2018.08.016

Zheng, J., Yi, D., Liu, Y., Wang, M., Zhu, Y., and Shi, H. (2017). Long nonding RNA UCA1 regulates neural stem cell differentiation by controlling miR-1/Hes1 expression. *Am. J. Transl. Res.* 9, 3696–3704.

Zhu, M., Li, N., Luo, P., Jing, W., Wen, X., Liang, C., et al. (2018). Peripheral blood leukocyte expression of lncRNA MIAT and its diagnostic and prognostic value in ischemic stroke. *J. Stroke Cerebrovasc. Dis.* 27, 326–337. doi: 10.1016/j.jstrokecerebrovasdis.2017.09.009

Zhu, R., Liu, X., and He, Z. (2018). Long non-coding RNA H19 and MALAT1 gene variants in patients with ischemic stroke in a northern Chinese Han population. *Mol. Brain* 11:58. doi: 10.1186/s13041-018-0402-7

Zhu, B., Zhang, L., Liang, C., Liu, B., Pan, X., Wang, Y., et al. (2019). Stem cell-derived exosomes prevent aging-induced cardiac dysfunction through a novel exosome/lncRNA MALAT1/NF-κB/TNF-α signaling pathway. *Oxid. Med. Cell Longev.* 2019:9739258. doi: 10.1155/2019/9739258

Conflict of Interest: The authors declare that the research was conducted in the absence of any commercial or financial relationships that could be construed as a potential conflict of interest.

frontiers in Aging Neuroscience

SYSTEMATIC REVIEW
published: 11 December 2020
doi: 10.3389/fnagi.2020.539933

Effect of Bone Marrow Stromal Cells in Parkinson's Disease Rodent Model: A Meta-Analysis

*Jianyang Liu, Jialin He, Yan Huang and Zhiping Hu**

Department of Neurology, Second Xiangya Hospital, Central South University, Changsha, China

Background: Bone marrow stromal cells (BMSCs) has been reported to have beneficial effects in improving behavioral deficits, and rescuing dopaminergic neuron loss in rodent models of Parkinson's disease (PD). However, their pooled effects for dopaminergic neuron have yet to be described.

Objective: To review the neuroprotective effect of naïve BMSCs in rodent models of PD.

Methods: The PubMed, EMBASE, and Web of Science databases were searched up to September 30, 2020. Inclusion criteria according to PICOS criteria were as follows: (1) population: rodents; (2) intervention: unmodified BMSCs; (3) comparison: not specified; (4) primary outcome: tyrosine hydroxylase level in the substantia nigra pars compacta and rotational behavior; secondary outcome: rotarod test, and limb function; (5) study: experimental studies. Multiple prespecified subgroup and meta-regression analysis were conducted. Following quality assessment, random effects models were used for this meta-analysis.

Results: Twenty-seven animal studies were included. The median quality score was 4.7 (interquartile range, 2–8). Overall standardized mean difference between animals treated with naïve BMSCs and controls was 2.79 (95% confidence interval: 1.70, 3.87; $P < 0.001$) for densitometry of tyrosine hydroxylase-positive staining; −1.54 (95% confidence interval: −2.11, −0.98; $P < 0.001$) for rotational behavior. Significant heterogeneity among studies was observed.

Conclusions: Results of this meta-analysis suggest that naïve BMSCs therapy increased dopaminergic neurons and ameliorated behavioral deficits in rodent models of PD.

Keywords: bone marrow stromal cell, Parkinson's disease, meta-analysis, efficacy, animal experimentation

OPEN ACCESS

Edited by:
Thomas Wisniewski,
New York University, United States

Reviewed by:
Seong-Jin Yu,
National Health Research Institutes, Taiwan
Jea Young Lee,
University of South Florida, United States
Sachchida Nand Rai,
University of Allahabad, India
Jannette Rodriguez-Pallares,
University of Santiago de Compostela, Spain

****Correspondence:***
Zhiping Hu
zhipinghu@csu.edu.cn

Received: *03 March 2020*
Accepted: *23 November 2020*
Published: *11 December 2020*

Citation:
Liu J, He J, Huang Y and Hu Z (2020) Effect of Bone Marrow Stromal Cells in Parkinson's Disease Rodent Model: A Meta-Analysis. Front. Aging Neurosci. 12:539933. doi: 10.3389/fnagi.2020.539933

INTRODUCTION

Parkinson's disease (PD) is a neurodegenerative disorder characterized by clinical motor symptoms of bradykinesia, muscle rigidity, tremor, and postural instability (Jankovic, 2008), resulting from the selective degeneration of dopaminergic neurons in the substantia nigra pars compacta (SNpc) (Michely et al., 2015) and intraneuronal protein aggregates called Lewy bodies (Lashuel et al., 2013). As the fastest growing neurodegenerative disease in the world, PD prevalence is projected to exceed 12 million by 2040 (Dorsey et al., 2018). The main therapies of PD include

L-3,4-dihydroxyphenylalanine (L-DOPA) dopamine agonists, enzyme inhibitors and deep brain stimulation (Dong et al., 2016). However, the above therapies remain insufficient to recover the massive loss of dopaminergic neurons. Cellular therapy is another novel therapeutic tool that offers considerable hope and promise to promote neural recovery in PD (Lo Furno et al., 2018; Staff et al., 2019). Various source tissues have been tested for efficiency of mesenchymal stem cells therapy for PD, such as human bone marrow (Ye et al., 2007), adipose (Berg et al., 2015; Cucarian et al., 2019), olfactory mucosa (Simorgh et al., 2019), placenta (Kim et al., 2018), umbilical cord (Zhao et al., 2016), umbilical cord blood (Lee et al., 2019), and deciduous teeth (Zhang N. et al., 2018). Among the many kinds of mesenchymal stem cells in preclinical studies, bone marrow-derived mesenchymal stem cells are the most well-tested.

Bone marrow stromal cells (BMSCs, also known as bone marrow-derived mesenchymal stem and progenitor cells) have the potential to differentiate to mesenchymal lineage, such as osteoblasts, chondrocytes, adipocytes, and muscle (Prockop, 1997). BMSCs are easily accessible and isolated through aspiration of the bone marrow. They are free of ethical controversy, and are associated with fewer immunological reactions (Pittenger et al., 1999). They also have the ability to be easily expanded on a large scale, which is very convenient and suitable for clinical use (Dezawa, 2006). BMSCs have the potential to differentiate into functional dopaminergic neurons (Dezawa et al., 2004; Bae et al., 2011; Datta et al., 2011; Venkatesh and Sen, 2017) without forming tumors in preclinical studies (Rengasamy et al., 2016).

Numerous researches have evaluated the efficacy of BMSCs transplantation for PD, yet there are some disputes over results. Prior meta-analysis either took a broader approach to mesenchymal stem cells therapy (Riecke et al., 2015) or only included the induced pluripotent stem cells therapy (Zhang Y. et al., 2018). Neither have offered a meta-analysis of the relevant study to investigate both histopathological and functional efficiency of BMSCs transplantation for PD. Our aim was to perform a meta-analysis to review published animal studies employing the use of naïve BMSCs therapy following PD, and to provide information for the future clinical translation of BMSCs to the bedside.

MATERIALS AND METHODS

Preferred Reporting Items for Systematic Reviews and Meta-Analysis (PRISMA) was used to perform this meta-analysis (Moher et al., 2009).

Search Strategy

Studies of bone marrow-derived mesenchymal stem cell-based therapy for PD rodent models were identified from PubMed, EMBASE, and Web of Science through September 30, 2020 using the following search strategy: ("mesenchymal stem cells" OR "mesenchymal stromal cells" OR "mesenchymal stem cell" OR "mesenchymal stromal cell" OR "bone marrow stem cell" OR "bone marrow-derived stromal cell") AND ("Parkinson's disease" OR "Parkinson disease" OR "PD"). The publication language was limited to English. We also searched the reference lists of eligible studies.

Inclusion and Exclusion Criteria

The studies' eligibility criteria were set up according to the PICOS-scheme (population, intervention, control, outcome and study design) (Riva et al., 2012). The inclusion criteria were as follows: (i) Parkinson's animal model (rodent models); (ii) testing the effects of unmodified BMSCs in at least one experimental group; (iii) setting sham-controlled group or condition; (iv) providing adequate data on behavioral testing or densitometry of tyrosine hydroxylase-positive (TH^+) staining in the SNpc; (v) study: experimental studies presented in original research articles; and (vi) published in English. The exclusion criteria were as follows: (i) researches that only evaluated the efficacy of transfected or modified cell transplantation; (ii) studies that only tested stem cells other than bone marrow mesenchymal stem cells; (iii) BMSCs administered before PD model.

Study Selection

After removal of duplicates, all published articles were conducted by two investigators independently. When the two investigators agreed, irrelevant studies were excluded. All relevant articles were retrieved for a comprehensive review, and the two researchers independently evaluated these articles using criteria outlined above. Any differences or uncertainties were resolved through consensus and judged by a third investigator when necessary.

Data Abstraction

The following information were abstracted by two investigators independently and entered electronically: authors, year published, study country, source of BMSCs, species of animals, animal model, animal gender, anesthetic type, cell dose, delivery route, and timing of BMSCs, follow-up (the longest observation time of outcomes after BMSCs administration), the outcomes data.

When only graphs were available, values were obtained from images using GetData Graph Digitizer software. The average reading of the two researchers were used to analysis data. If the standard deviation was not reported, standard error was converted to standard deviation by multiplying the square root of the group size. If a research contained multiple experimental groups differentiated by cell dose or delivery route and timing that were contrasted with the control group, these experimental groups would be included separately as independent studies. If the outcomes were evaluated at different follow-up times, only the longest one was extracted.

Quality Assessment

To evaluate the quality of the eligible studies, we used the Collaborative Approach to Meta-Analysis and Review of Animal Data from Experimental Studies (CAMARADES) checklists (Macleod et al., 2004), which consist of the following items: (1) publication in a peer-reviewed journal, (2) statements describing temperature control, (3) randomized treatment allocation, (4) allocation concealment, (5) use of aged animal models, (6) blind assessment of outcome, (7) avoidance of

anesthetics with significant intrinsic neuroprotective activity, such as ketamine, (8) reporting of a sample size calculation, (9) statement of compliance with regulatory requirements, and (10) declarations of potential conflicts of interest. A sum of the quality scores was recorded for each study, with a total score of 10 points. Two researchers independently scored the studies. Any differences or uncertainty were resolved by consensus.

Statistical Analysis

Combined effect size was calculated as standardized mean difference (SMD) between BMSCs treated group and control group. The random-effects model and Hedges calculation (Durlak, 2009) were applied to get the pooled effect size, and all analysis was performed with Stata software (version 12.1). Overall, an effect size of 0.2 represents a small effect, 0.5 and 0.8 represent medium and large, respectively (Schulz et al., 1995). A P-value <0.05 was considered statistically significant. The I^2 statistic was used to analyze heterogeneity, and it was defined as low (25–50%), moderate (50–75%), or high (>75%) (Higgins et al., 2003).

Seven clinical characteristics were used to grouping the effect size of outcome: BMSCs species (Allogeneic or Xenogeneic); BMSCs dose (≤1E5, 1E5–1E6, ≥1E6); delivery time (<14, 14–21, ≥21 days); follow-up duration (≤4, 4–8, >8 weeks); delivery route (intrastriatal, intravenous, intracerebral, intranigral, intranasal); PD model [6-hydroxydopamine (6-OHDA), 1-methyl-4-phenyl-1,2,3,6-tetrahydropyridine (MPTP), Roteneone]; Gender (male, female). Pre-specified subgroup analysis and meta-regression analysis (Higgins and Thompson,

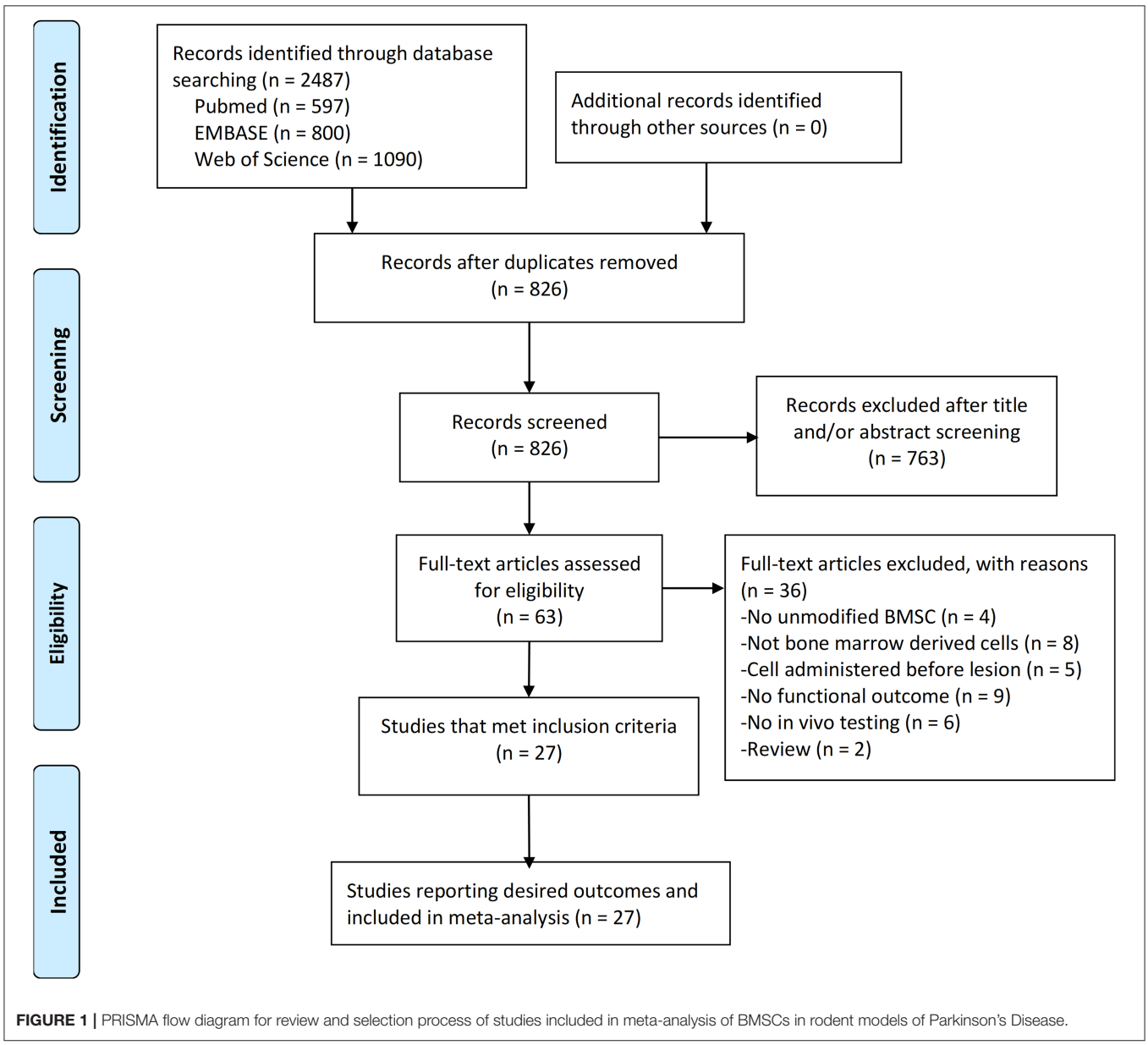

FIGURE 1 | PRISMA flow diagram for review and selection process of studies included in meta-analysis of BMSCs in rodent models of Parkinson's Disease.

2002) were performed to study the possible relations between the outcomes and the above clinical characteristics.

Publication bias was evaluated using funnel plots (Sterne et al., 2011), and the symmetry of funnel plots was performed with Egger regression (Egger et al., 1997). If necessary, any non-negligible bias would be corrected using the trim-and-fill approach (Sterne et al., 2001).

RESULTS

Study Inclusion

Electronic searching identified 597 articles in PubMed, 800 articles in EMBASE, and 1,090 articles in Web of Science. After removal of duplicates, 826 articles were screened by abstract and/or title, resulting in 763 articles excluded. By reading the full text of the remaining 63 articles, 36 were excluded due to review, not having unmodified BMSC experiments, not bone marrow derived cells, no *in vivo* experiment, BMSCs administered before lesion, or no primary outcomes. Therefore, 27 studies were included in the meta-analysis (**Figure 1**). All studies published in peer-reviewed journals.

TABLE 1 | Percentage of included studies satisfying each criterion of CAMARADES checklists.

Quality score criterion	Percentage of qualified studies (%)
Publication in a peer-reviewed journal	100
Control of temperature	44
Randomized treatment allocation	51.8
Allocation concealment	29.6
Use of aged animal models	0
Blind assessment of outcome	29.6
Avoidance neuroprotective anesthetics	55.5
Sample size calculation	0
Compliance with animal welfare regulations	100
Statement of conflict of interest	63

Study Characteristics

The characteristics of the 27 studies are summarized in **Supplementary Tables 1**, **2**. All studies were carried out in rodents (rats and mice). Intervention included MSCs obtained from mice, rat, or human bone marrow. The most common PD model was the 6-OHDA, although other methods were also used, such as the Rotenone and MPTP. Following induction of PD, BMSCs were administrated either immediately or over a period varying from 24 h to 5 weeks. The mean follow-up ranged from 8 days to 20 weeks. The most common delivery route used for BMSCs was intrastriatal route. Others used were the intravenous, intracarotid, intracerebral (into left/right ventricle), intrathecal (into subarachnoid space), and intranasal route. Histopathological outcome was assessed by densitometry of TH^+ staining in 18 studies. Behavioral outcomes were evaluated by rotational behavior in 20 researches, rotarod test in five researches, open field test in three researches, limb function (cylinder, adjusting step, staircase tests, treadmill locomotion test, and paw-reaching tests) in eight studies, and forced swimming test in one study. Considering that densitometry of TH^+ staining in SNpc and rotational behavior are the most common evaluations used in rodent studies of PD, we took them as co-primary outcomes in this review.

Quality Assessment

The quality assessment of included studies is summarized in **Table 1,** the details are presented in **Supplementary Table 3**. The quality scores varied from 2 to 8, with a mean value of 4.7.

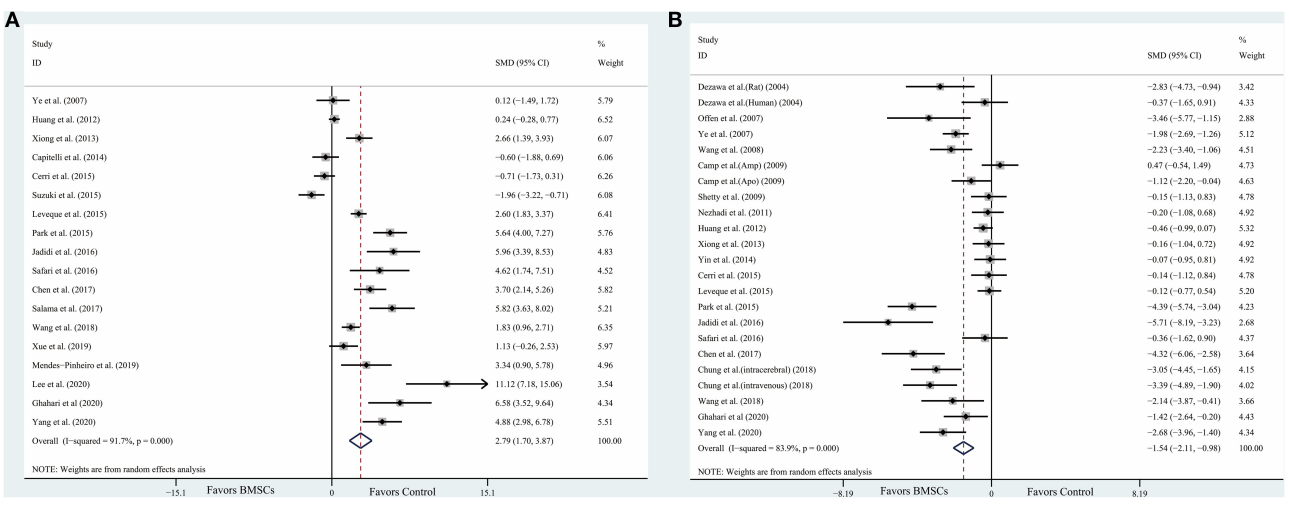

FIGURE 2 | Forest plot shows mean effect size and 95% CI for **(A)** densitometry of TH^+ staining in the substantia nigra pars compacta, **(B)** rotational behavior between BMSCs therapy group and control group in individual trials and all studies combined. Weights have been calculated using random effects model. Degree of heterogeneity in the pooled estimates is represented at I^2 statistic. SMD, standardized mean difference; BMSCs, Bone marrow stromal cells.

According to our statistical results, all the articles were published in a peer-reviewed journal and claimed compliance with animal welfare regulations. No study used aged animals.

Meta-Analysis

The data were extracted from the studies included (**Supplementary Table 2**). The composite weighted mean (95% confidence interval) effect size for densitometry of TH^+ staining was 2.79 (1.70, 3.87) ($P < 0.001$) (**Figure 2A**); for rotational behavior was −1.54 (−2.11, −0.98) ($P < 0.001$) (**Figure 2B**). We also conducted pooled analysis for rotarod tests ($n = 6$) and limb function ($n = 7$). The result was similar: The composite weighted mean (95% CI) effect size for rotarod tests was 1.77 (0.40, 3.15) ($P < 0.001$, $I^2 = 85.6\%$), and 0.28 (−0.52, 1.08) ($P = 0.001$, $I^2 = 73.4\%$) for limb function. The Higgins I^2 index indicated significant heterogeneity among four outcomes ($P < 0.001$).

Stratified Analysis and Meta-Regression Analysis

Table 2 summarizes the data of primary outcomes in diverse subgroup analysis. In general, significant efficacy of BMSCs transplantation were observed in most subgroups. Partial subgroups fail to reach the statistical significance ($P < 0.05$), which may be caused by insufficient sample size. Although significant difference was found between groups in partial subgroup analysis, we could not find the source of heterogeneity. In the most subgroups with two or more studies included, substantial heterogeneity was found ($I^2 > 75\%$). In order to further investigate the unexplained heterogeneity, multivariate meta-regression was used to test the influence of all clinical characteristics on the outcomes. However, for densitometry of TH^+ staining, no significant sources of heterogeneity were found. For rotational behavior, the administration time was the significant source of heterogeneity ($P = 0.009$).

Publication Bias

We assessed publication bias by funnel plots (**Figure 3A** for densitometry of TH^+ staining; **Figure 3B** for rotational behavior). No evident publication bias was observed by visual inspection. The Egger test presented significant publication bias for rotational behavior ($P = 0.001$) but not for densitometry of TH^+ staining ($P = 0.061$). After adopting trim-and-fill correction for rotational behavior outcomes, the estimated value remained unchanged.

DISCUSSION

The first open-labeled clinical study ascertaining the safety and efficacy of BMSCs in PD patients was performed in 2010, where seven patients who received unilateral injections of autologous BMSCs into the sublateral ventricular zone demonstrated the safety of transplantation (Venkataramana et al., 2010). The pilot clinical study in 2012 demonstrated a modest improvement during "on" and "off" period on the UPDRS scoring system in early-stage PD patients (Venkataramana et al., 2012). **Table 3** includes the related clinical trials that are registered with ClinicalTrails.gov. Although BMSCs have shown a promising role in PD in initial clinical pilot studies, there are a number of uncertain questions with respect to the delivery timing, route of administration, and BMSCs dose. As the evidence generated from animal model provide a framework for designing clinical trials, it is important to explore the pooled effects of preclinical studies. What stages (acute/chronic) of PD are indicated for stem cell therapy, what doses of BMSCs are optimal, how do we deliver BMSCs, how long to survive within the hostile ischemic microenvironment, and how do we improve neurological function? (**Figure 4**). Prior meta-analysis either took a broader approach to multiple different mesenchymal stem cell type (Riecke et al., 2015) or only included the induced pluripotent stem cell (Zhang Y. et al., 2018). These studies did not generate an effect size of histological outcomes of PD, only evaluate the behavioral outcomes. TH^+ staining has been frequently examined as histological identification of dopaminergic neurons (Barzilay et al., 2008). Thus, we took densitometry of TH^+ staining as the measure of histological outcomes in PD animal models.

Main Findings

This meta-analysis suggests the following: (1) Based on the defined quantification of the absolute value of the effect, we observed effect sizes of BMSCs on histological and behavioral outcomes were very large. All estimates other than limb function were statistically significant. In general, this meta-analysis suggested that deficits of both motor function and TH^+ levels in rodent models were alleviated by BMSCs therapy. (2) Administration time was correlated with effect size in densitometry of TH^+ staining and rotational behavior. BMSCs therapy initiated more than 3 weeks post-PD showed the greatest efficacy, followed by 2–3 weeks post-PD, and then therapy initiated within 2 weeks. (3) Intravenous seems to be more effective compared with intrastriatal to improve rotational behavior and increase densitometry of TH^+ staining. But the number of animals included for intravenous administration route in the pooled analysis were small, this comparison needs to be proved by more studies. (4) Xenogenic and allogenic cells showed similar beneficial effects for rotation behavior, although the latter increased the densitometry of TH^+ staining to a larger extent. But the number of studies included for xenogeneic group were small. (5) The included studies do not clearly provide a specific effective dose of BMSCs. With higher dose levels ($>1 \times 10^5$), a greater effect size of BMSCs therapy on densitometry of TH^+ staining was observed. Generally, the above various subgroup analysis can only generate hypothesis rather than confirming them.

Possible Mechanism of Neuroprotective Effects

MSCs-based therapy is a multimodal treatment for nervous system diseases (Badyra et al., 2020). The precise mechanism by which BMSCs may exert beneficial effects in PD is still being elucidated, but it appears that multiple mechanisms may contribute (Glavaski-Joksimovic and Bohn, 2013; Fan et al., 2020). First, anti-inflammatory properties of BMSCs. BMSCs administration in rats dramatically decreased dopaminergic

TABLE 2 | Subgroup analysis of rotational behavior and densitometry of TH^+ staining in animal models of Parkinson's disease associated with BMSC therapy.

Variable	Densitometry of TH^+ staining in the SNpc						Rotation behavior					
	No. of reports	Pooled estimates (95% CI)	Q statistic	*P*-value for heterogeneity	I^2 value (%)	Between group *P*-value	No. of reports	Pooled estimates (95% CI)	Q statistic	*P*-value for heterogeneity	I^2 value (%)	Between group *P*-value
BMSC species						<0.001						0.013
Allogeneic (mice/rats)	14	2.14 (1.03, 3.26)	146.17	<0.001	91.10%		16	−1.35 (−1.97, −0.73)	80.95	<0.001	81.50%	
Xenogeneic (human)	4	5.22 (2.54, 7.90)	20.89	<0.001	85.60%		7	−1.91 (−3.19, −0.63)	49.3	<0.001	87.80%	
BMSCs dose						<0.001						0.125
≤1E5	4	0.72 (−1.10, 2.53)	32.12	<0.001	90.70%		4	−1.84 (−3.54, −0.15)	22.07	<0.001	86.40%	
1E5–1E6	6	3.42 (1.58, 5.27)	28.94	<0.001	82.70%		9	−1.68 (−2.56, −0.79)	58.68	<0.001	83.00%	
≥1E6	8	3.59 (1.65, 5.52)	103.03	<0.001	93.20%		7	−1.20 (−2.23, 0.16)	35.33	<0.001	87.30%	
Administration time						0.101						<0.001
<2 weeks	5	3.31 (0.56, 6.06)	52.29	<0.001	90.00%		4	−0.58 (−1.45, 0.29)	7.06	0.07	57.50%	
2–3 weeks	5	1.82 (0.18, 3.47)	59.64	<0.001	93.30%		7	−0.94 (−1.82, −0.06)	37.69	<0.001	84.10%	
≥3 weeks	4	1.22 (−1.63, 4.07)	36.35	<0.001	91.70%		5	−3.03 (−3.96, −2.11)	8.68	0.07	53.90%	
Follow-up period						<0.001						0.026
≤4 weeks	10	3.18 (1.55, 4.81)	115.75	<0.001	92.20%		11	−1.78 (−2.78, −0.78)	77.37	<0.001	87.10%	
4–8 weeks	6	3.10 (1.23, 4.97)	50.37	<0.001	90.10%		8	−1.14 (−1.95, −0.34)	38.14	<0.001	81.60%	
>8 weeks	2	−0.99 (−3.02, 1.05)	4	0.045	75%		4	−1.87 (−3.23, −0.51)	13.59	0.004	77.90%	
Administration route						<0.001						<0.001
Intrastriatal	9	1.06 (0.01, 2.12)	59.32	<0.001	86.50%		14	−1.13 (−1.73, −0.53)	60.19	<0.001	78.40%	
Intravenous	4	4.65 (2.52, 6.77)	16.21	0.001	81.50%		5	−1.88 (−3.53, −0.24)	42.24	<0.001	90.50%	
Intracerebral	2	5.26 (3.73, 6.79)	0.44	0.507	0		3	−3.47 (−4.90, −2.04)	4.62	0.099	56.70%	
Intranasal	1	5.82 (3.63, 8.02)	NA	NA	NA		0	NA	NA	NA	NA	
Intracarotid	1	−0.71 (−1.73, 0.31)	NA	NA	NA		1	−0.14 (−1.12, 0.84)	NA	NA	NA	
Intrathecal	1	11.12 (7.18, 15.06)	NA	NA	NA		0	NA	NA	NA	NA	
PD model						0.001						0.006
6-OHDA	13	2.86 (1.54, 4.17)	162.80	<0.001	92.60%		21	−1.57 (−2.17, −0.97)	126.25	<0.001	84.20%	
Roteneone	2	4.11 (1.02, 7.20)	5.98	0.014	83.30%		1	−0.16 (−1.04, −0.72)	NA	NA	NA	
MPTP	3	1.73 (−1.14, 4.60)	21.88	<0.001	68.80%		1	−2.68 (−3.96, −1.40)	NA	NA	NA	
Gender						0.004						0.736
Male	15	3.15 (1.94, 4.36)	155.07	<0.001	91.60%		18	−1.74 (−2.43, −1.05)	113.31	<0.001	85.00%	
Female	3	0.27 (−2.56, 3.11)	25.78	<0.001	92.20%		4	−0.72 (−1.85, 0.41)	18.6	<0.001	83.90%	

BMSCs, bone marrow stromal cells; PD, Parkinson's disease; TH^+, tyrosine hydroxylase positive; NA, not available; SNpc, substantia nigra pars compacta.

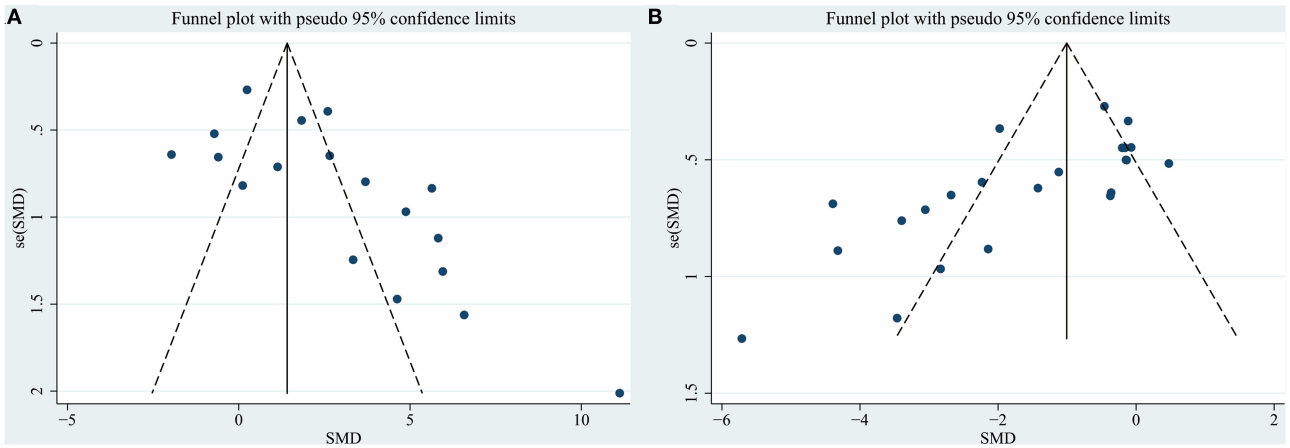

FIGURE 3 | Funnel plot for **(A)** densitometry of TH^+ staining in the substantia nigra pars compacta, **(B)** rotational behavior. Each dot in the figure represents a study, with the y-axis signifying study quality and the x-axis showing the study results. SMD, standardized mean difference.

TABLE 3 | Clinical trials using BMSCs in PD that are registered with ClincalTrials.gov (as of October 2020).

No. NCT	Years	Type of trial	Locations	Recruitment status	Phase	Ages (years)	Allo/Auto	Route of admistration	No. of BMSCs	Follow-up period
NCT00976430	2009	Open Label	India	Terminated	Not Applicable	35–70	Autologous	Stereotactically (striatum)	Not Applicable	18 months
NCT01446614	2011	Open Label	China	Unknown	Phase 1/2	30–65	Autologous	Intravenous	6×10^5 per kg, qw, for 4 weeks	12 months
NCT02611167	2015	Open Label	United States	Completed	Phase 1	45–70	Allogeneic	Intravenous	$1/3/6/10 \times 10^6$ per kg	52 weeks
NCT04506073	2020	Randomized controlled trial	United States	Not yet recruiting	Phase 2	50–79	Allogeneic	Intravenous	3 infusions of 10×10^6 per kg 3 months	78 weeks

BMSCs, bone marrow stromal cells.

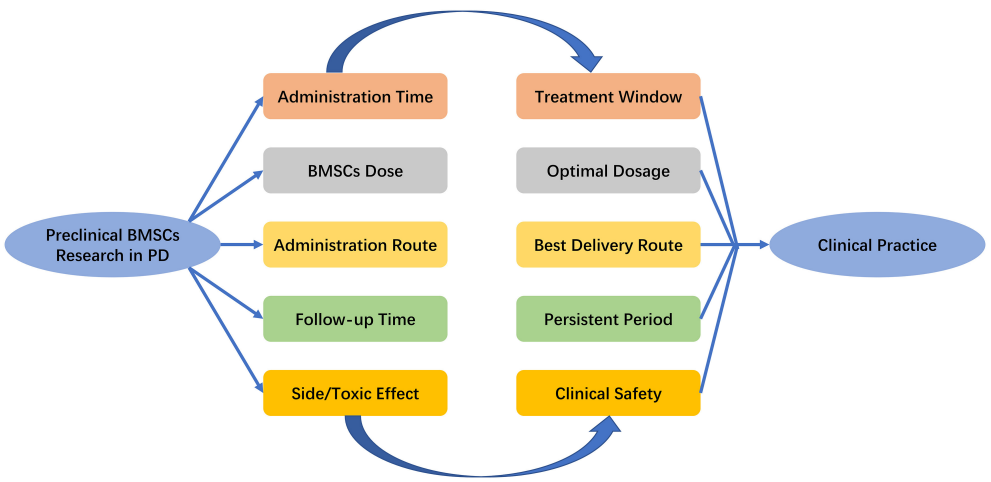

FIGURE 4 | Key issues that the settlement of which would facilitate the transition of BMSCs research in PD from bench to bedside. PD, Parkinson's Disease; BMSCs, Bone marrow stromal cells.

neuronal loss in the SNpc, which was obviously accompanied by reduced activation of microglia (Park et al., 2008; Suzuki et al., 2015), as well as the expression of inducible nitric oxide synthase and tumor necrosis factor-alpha (Kim et al., 2009). By inducing M2 microglia polarization, BMSCs can enhance α-synuclein clearance *in vitro* model (Park et al., 2016). Activated by

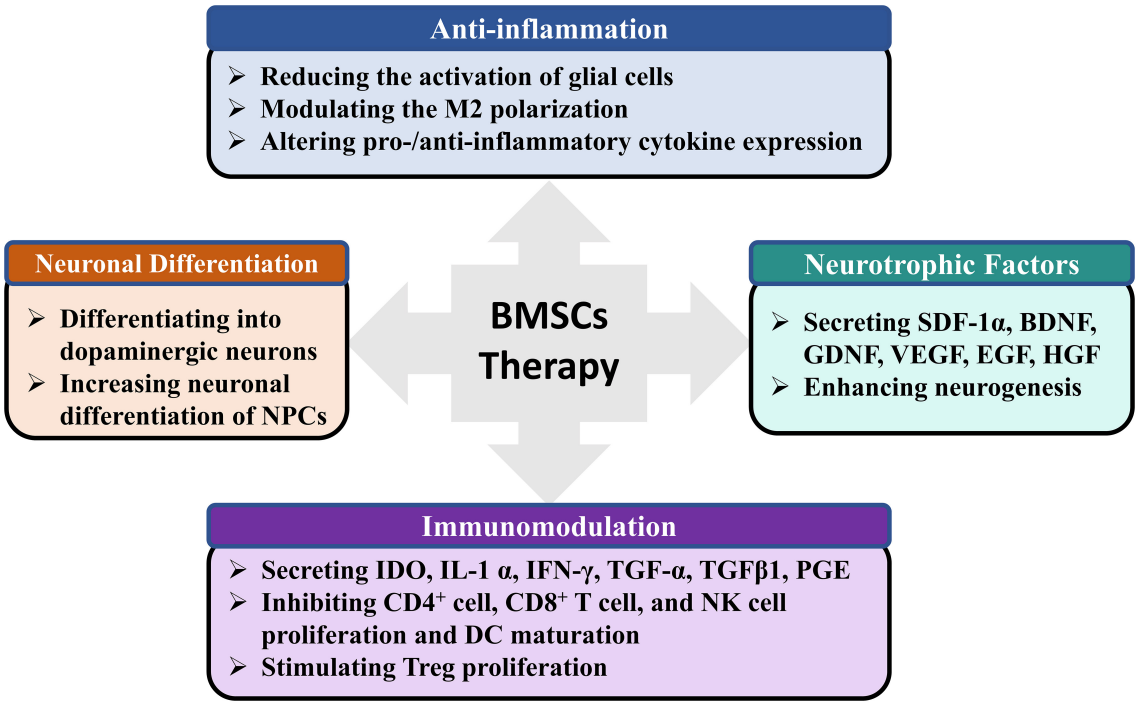

FIGURE 5 | The possible mechanisms of BMSCs therapy for PD. PD, Parkinson's Disease; BMSCs, Bone marrow stromal cells; GDNF, SDF-1α, Stromal cell-derived factor 1a; BDNF, Brain-derived neurotrophic factor; Glial cell-derived neurotrophic factor; VEGF, Vascular endothelial growth factor; EGF, Epidermal growth factor; HGF, Hepatocyte growth factor; NPCs, Neural progenitor cells; IDO, Indoleamine-2,3-dioxygenase; IFNγ, Interferon γ; TGF-α, Transforming growth factor alpha; TGFβ1, Transforming growth factor beta 1; PGE, Prostaglandin; DC, Dendritic cell.

inflammatory signals, MSCs also secrete the anti-inflammatory protein TNF-α-stimulated gene 6 protein (Choi et al., 2011), IL-6, and IL-10 (Jinfeng et al., 2016). But whether BMSCs can promote the switch of M1 microglia status into M2 phenotype and increase the anti-inflammatory protein in PD animal model needs further study. Second, paracrine activity of BMSCs. BMSCs can secrete factors including brain-derived neurotrophic factor, glial cell-derived neurotrophic factor, and vascular endothelial growth factor (Sadan et al., 2009), which can improve neuronal survival. Glial cell-derived neurotrophic factor released by BMSCs may protect catecholaminergic and serotonergic neuronal perikarya and transporter function (Whone et al., 2012), which may be effective for abrogating the non-motor symptoms of PD. As an important medium for paracrine effects, BMSCs-derived exosomes contain a variety of biomolecules, such as proteins, messenger RNA, and miRNA (e.g., miR-124, and miR-145), which contribute to neuroprotection and mediate immunomodulatory effects (Kojima et al., 2018; Mendes-Pinheiro et al., 2019). Finally, neuronal differentiation of BMSCs. Previous report has presented that BMSCs could be induced to form dopamine decarboxylase-positive cells along the line of restoring/replacing dopamine cell loss (Jiang et al., 2002). Alleviating motor symptoms of induced BMSCs transplantation has been tested in animal model of PD (Dezawa et al., 2004). Whether BMSCs can differentiate to a variety of neuronal phenotypes (such as noradrenergic, serotonergic, and cholinergic cell types), and improve the non-motor symptoms of PD requires further research. The above mechanisms have shown that transplantation of BMSCs can not only improve PD symptom directly by neuronal differentiation, but also trigger endogenous brain repair through the modulation of anti-inflammatory cytokines, proteomes, and neurotrophic factors (**Figure 5**).

Limitations

There are several limitations to our meta-analysis. First, our approach can only include the studies that have already been published in English. Unpublished data may change our results. In addition, none of the included studies investigated the safety of BMSCs injection on PD in animal models. we are incapable of evaluating the clinical safety of BMSCs application. Finally, a good study should have an adequate sample size with a formal calculation (Campbell et al., 1995). Nevertheless, no studies in the meta-analysis conducted sample calculation, which indicated the lack of statistical power to ensure proper estimation of the treatment effects (Schulz and Grimes, 2005).

Future Direction

There is significant work to be done for the future clinical translation. Firstly, most research subjects are rats, and their similarities to humans are limited. Therefore, since the outcomes for rodent model cannot be directly extended to humans, primates should be used to obtain more results. Secondly, PD is an age-related disease, and the majority of PD patients are elderly.

As previously stated, data shows a direct relation between age and the occurrence of PD (Tysnes and Storstein, 2017). Thus, the impact of age should be considered in preclinical studies given that the epidemiology of PD and response to therapy may vary widely in the developing, juvenile, adult, and elderly brains. However, the current research models are based almost exclusively on healthy adult animals. It is doubtful whether cell therapy can achieve the same treatment effect in elderly Parkinson's animal model.

CONCLUSION

Preclinical researches have showed the potential role of BMSCs to be an effective therapy for PD patients. But, determining the clinical parameters by our meta-analysis is inevitably confounded by high publication bias. Considering the limited internal and external validity, our conclusions should be confirmed in more strictly randomized control studies and carefully interpreted in relation to the design of future animal studies or clinical translation. Generally, the use of BMSCs as a novel therapeutic strategy for PD is promising.

DATA AVAILABILITY STATEMENT

All datasets generated for this study are included in the article/**Supplementary Material**.

AUTHOR CONTRIBUTIONS

JL analyzed the data. JH and YH supervised the project. JL and ZH wrote the paper. All authors contributed to the article and approved the submitted version.

FUNDING

This work was supported by grants from the National Natural Science Foundation of China (No. 81974213).

SUPPLEMENTARY MATERIAL

The Supplementary Material for this article can be found online at: https://www.frontiersin.org/articles/10.3389/fnagi.2020.539933/full#supplementary-material

REFERENCES

Badyra, B., Sulkowski, M., Milczarek, O., and Majka, M. (2020). Mesenchymal stem cells as a multimodal treatment for nervous system diseases. *Stem Cells Transl. Med.* 9, 1174–1189. doi: 10.1002/sctm.19-0430

Bae, K. S., Park, J. B., Kim, H. S., Kim, D. S., Park, D. J., and Kang, S. J. (2011). Neuron-like differentiation of bone marrow-derived mesenchymal stem cells. *Yonsei Med. J.* 52, 401–412. doi: 10.3349/ymj.2011.52.3.401

Barzilay, R., Kan, I., Ben-Zur, T., Bulvik, S., Melamed, E., and Offen, D. (2008). Induction of human mesenchymal stem cells into dopamine-producing cells with different differentiation protocols. *Stem Cells Dev.* 17, 547–554. doi: 10.1089/scd.2007.0172

Berg, J., Roch, M., Altschuler, J., Winter, C., Schwerk, A., Kurtz, A., et al. (2015). Human adipose-derived mesenchymal stem cells improve motor functions and are neuroprotective in the 6-hydroxydopamine-rat model for Parkinson's disease when cultured in monolayer cultures but suppress hippocampal neurogenesis and hippocampal memory function when cultured in spheroids. *Stem Cell Rev.* 11, 133–149. doi: 10.1007/s12015-014-9551-y

Campbell, M. J., Julious, S. A., and Altman, D. G. (1995). Estimating sample sizes for binary, ordered categorical, and continuous outcomes in two group comparisons. *BMJ* 311, 1145–1148. doi: 10.1136/bmj.311.7013.1145

Choi, H., Lee, R. H., Bazhanov, N., Oh, J. Y., and Prockop, D. J. (2011). Anti-inflammatory protein TSG-6 secreted by activated MSCs attenuates zymosan-induced mouse peritonitis by decreasing TLR2/NF-κB signaling in resident macrophages. *Blood* 118, 330–338. doi: 10.1182/blood-2010-12-327353

Cucarian, J. D., Berrio, J. P., Rodrigues, C., Zancan, M., Wink, M. R., and de Oliveira, A. (2019). Physical exercise and human adipose-derived mesenchymal stem cells ameliorate motor disturbances in a male rat model of Parkinson's disease. *J. Neurosci. Res.* 97, 1095–1109. doi: 10.1002/jnr.24442

Datta, I., Mishra, S., Mohanty, L., Pulikkot, S., and Joshi, P. G. (2011). Neuronal plasticity of human Wharton's jelly mesenchymal stromal cells to the dopaminergic cell type compared with human bone marrow mesenchymal stromal cells. *Cytotherapy* 13, 918–932. doi: 10.3109/14653249.2011.579957

Dezawa, M. (2006). Insights into autotransplantation: the unexpected discovery of specific induction systems in bone marrow stromal cells. *Cell. Mol. Life Sci.* 63, 2764–2772. doi: 10.1007/s00018-006-6191-7

Dezawa, M., Kanno, H., Hoshino, M., Cho, H., Matsumoto, N., Itokazu, Y., et al. (2004). Specific induction of neuronal cells from bone marrow stromal cells and application for autologous transplantation. *J. Clin. Invest.* 113, 1701–1710. doi: 10.1172/JCI200420935

Dong, J., Cui, Y., Li, S., and Le, W. (2016). Current pharmaceutical treatments and alternative therapies of Parkinson's disease. *Curr. Neuropharmacol.* 14, 339–355. doi: 10.2174/1570159X14666151120123025

Dorsey, E. R., Sherer, T., Okun, M. S., and Bloem, B. R. (2018). The emerging evidence of the Parkinson pandemic. *J. Parkinsons Dis.* 8, S3–S8. doi: 10.3233/JPD-181474

Durlak, J. A. (2009). How to select, calculate, and interpret effect sizes. *J. Pediatr. Psychol.* 34, 917–928. doi: 10.1093/jpepsy/jsp004

Egger, M., Davey Smith, G., Schneider, M., and Minder, C. (1997). Bias in meta-analysis detected by a simple, graphical test. *BMJ* 315, 629–634. doi: 10.1136/bmj.315.7109.629

Fan, X. L., Zhang, Y. L., Li, X., and Fu, Q. L. (2020). Mechanisms underlying the protective effects of mesenchymal stem cell-based therapy. *Cell. Mol. Life Sci.* 77, 2771–2794. doi: 10.1007/s00018-020-03454-6

Glavaski-Joksimovic, A., and Bohn, M. C. (2013). Mesenchymal stem cells and neuroregeneration in Parkinson's disease. *Exp. Neurol.* 247, 25–38. doi: 10.1016/j.expneurol.2013.03.016

Higgins, J. P., and Thompson, S. G. (2002). Quantifying heterogeneity in a meta-analysis. *Stat. Med.* 21, 1539–1558. doi: 10.1002/sim.1186

Higgins, J. P., Thompson, S. G., Deeks, J. J., and Altman, D. G. (2003). Measuring inconsistency in meta-analyses. *BMJ* 327, 557–560. doi: 10.1136/bmj.327.7414.557

Jankovic, J. (2008). Parkinson's disease: clinical features and diagnosis. *J. Neurol. Neurosurg. Psychiatry* 79, 368–376. doi: 10.1136/jnnp.2007.131045

Jiang, Y., Jahagirdar, B. N., Reinhardt, R. L., Schwartz, R. E., Keene, C. D., Ortiz-Gonzalez, X. R., et al. (2002). Pluripotency of mesenchymal stem cells derived from adult marrow. *Nature* 418, 41–49. doi: 10.1038/nature00870

Jinfeng, L., Yunliang, W., Xinshan, L., Yutong, W., Shanshan, W., Peng, X., et al. (2016). Therapeutic effects of CUR-activated human umbilical cord mesenchymal stem cells on 1-Methyl-4-phenylpyridine-induced Parkinson's disease cell model. *Biomed. Res. Int.* 2016:9140541. doi: 10.1155/2016/9140541

Kim, H. W., Lee, H. S., Kang, J. M., Bae, S. H., Kim, C., Lee, S. H., et al. (2018). Dual effects of human placenta-derived neural cells on neuroprotection and the inhibition of neuroinflammation in a rodent model of Parkinson's disease. *Cell Transplant.* 27, 814–830. doi: 10.1177/0963689718766324

Kim, Y. J., Park, H. J., Lee, G., Bang, O. Y., Ahn, Y. H., Joe, E., et al. (2009). Neuroprotective effects of human mesenchymal stem cells on

dopaminergic neurons through anti-inflammatory action. *Glia* 57, 13–23. doi: 10.1002/glia.20731

Kojima, R., Bojar, D., Rizzi, G., Hamri, G. C., El-Baba, M. D., Saxena, P., et al. (2018). Designer exosomes produced by implanted cells intracerebrally deliver therapeutic cargo for Parkinson's disease treatment. *Nat. Commun.* 9:1305. doi: 10.1038/s41467-018-03733-8

Lashuel, H. A., Overk, C. R., Oueslati, A., and Masliah, E. (2013). The many faces of alpha-synuclein: from structure and toxicity to therapeutic target. *Nat. Rev. Neurosci.* 14, 38–48. doi: 10.1038/nrn3406

Lee, J., Bayarsaikhan, D., Arivazhagan, R., Park, H., Lim, B., Gwak, P., et al. (2019). CRISPR/Cas9 edited sRAGE-MSCs protect neuronal death in Parkinsons disease model. *Int. J. Stem Cells* 12, 114–124. doi: 10.15283/ijsc18110

Lo Furno, D., Mannino, G., and Giuffrida, R. (2018). Functional role of mesenchymal stem cells in the treatment of chronic neurodegenerative diseases. *J. Cell. Physiol* 233, 3982–3999. doi: 10.1002/jcp.26192

Macleod, M. R., O'Collins, T., Howells, D. W., and Donnan, G. A. (2004). Pooling of animal experimental data reveals influence of study design and publication bias. *Stroke* 35, 1203–1208. doi: 10.1161/01.STR.0000125719.25853.20

Mendes-Pinheiro, B., Anjo, S. I., Manadas, B., Da Silva, J. D., Marote, A., Behie, L. A., et al. (2019). Bone marrow mesenchymal stem cells' secretome exerts neuroprotective effects in a Parkinson's disease rat model. *Front. Bioeng. Biotechnol.* 7:294. doi: 10.3389/fbioe.2019.00294

Michely, J., Volz, L. J., Barbe, M. T., Hoffstaedter, F., Viswanathan, S., Timmermann, L., et al. (2015). Dopaminergic modulation of motor network dynamics in Parkinson's disease. *Brain* 138, 664–678. doi: 10.1093/brain/awu381

Moher, D., Liberati, A., Tetzlaff, J., Altman, D. G., and Group, P. (2009). Preferred reporting items for systematic reviews and meta-analyses: the PRISMA statement. *J. Clin. Epidemiol.* 62, 1006–1012. doi: 10.1016/j.jclinepi.2009.06.005

Park, H. J., Lee, P. H., Bang, O. Y., Lee, G., and Ahn, Y. H. (2008). Mesenchymal stem cells therapy exerts neuroprotection in a progressive animal model of Parkinson's disease. *J. Neurochem.* 107, 141–151. doi: 10.1111/j.1471-4159.2008.05589.x

Park, H. J., Oh, S. H., Kim, H. N., Jung, Y. J., and Lee, P. H. (2016). Mesenchymal stem cells enhance α-synuclein clearance via M2 microglia polarization in experimental and human parkinsonian disorder. *Acta Neuropathol.* 132, 685–701. doi: 10.1007/s00401-016-1605-6

Pittenger, M. F., Mackay, A. M., Beck, S. C., Jaiswal, R. K., Douglas, R., Mosca, J. D., et al. (1999). Multilineage potential of adult human mesenchymal stem cells. *Science* 284, 143–147. doi: 10.1126/science.284.5411.143

Prockop, D. J. (1997). Marrow stromal cells as stem cells for nonhematopoietic tissues. *Science* 276, 71–74. doi: 10.1126/science.276.5309.71

Rengasamy, M., Gupta, P. K., Kolkundkar, U., Singh, G., Balasubramanian, S., SundarRaj, S., et al. (2016). Preclinical safety & toxicity evaluation of pooled, allogeneic human bone marrow-derived mesenchymal stromal cells. *Indian J. Med. Res.* 144, 852–864. doi: 10.4103/ijmr.IJMR_1842_15

Riecke, J., Johns, K. M., Cai, C., Vahidy, F. S., Parsha, K., Furr-Stimming, E., et al. (2015). A meta-analysis of mesenchymal stem cells in animal models of Parkinson's disease. *Stem Cells Dev.* 24, 2082–2090. doi: 10.1089/scd.2015.0127

Riva, J. J., Malik, K. M., Burnie, S. J., Endicott, A. R., and Busse, J. W. (2012). What is your research question? An introduction to the PICOT format for clinicians. *J. Can Chiropr. Assoc.* 56, 167–171.

Sadan, O., Bahat-Stromza, M., Barhum, Y., Levy, Y. S., Pisnevsky, A., Peretz, H., et al. (2009). Protective effects of neurotrophic factor-secreting cells in a 6-OHDA rat model of Parkinson disease. *Stem Cells Dev.* 18, 1179–1190. doi: 10.1089/scd.2008.0411

Schulz, K. F., Chalmers, I., Hayes, R. J., and Altman, D. G. (1995). Empirical evidence of bias. Dimensions of methodological quality associated with estimates of treatment effects in controlled trials. *JAMA* 273, 408–412. doi: 10.1001/jama.1995.03520290060030

Schulz, K. F., and Grimes, D. A. (2005). Sample size calculations in randomised trials: mandatory and mystical. *Lancet* 365, 1348–1353. doi: 10.1016/S0140-6736(05)61034-3

Simorgh, S., Alizadeh, R., Eftekharzadeh, M., Haramshahi, S. M. A., Milan, P. B., Doshmanziari, M., et al. (2019). Olfactory mucosa stem cells: an available candidate for the treatment of the Parkinson's disease. *J. Cell Physiol.* 234, 23763–23773. doi: 10.1002/jcp.28944

Staff, N. P., Jones, D. T., and Singer, W. (2019). Mesenchymal stromal cell therapies for neurodegenerative diseases. *Mayo Clin. Proc.* 94, 892–905. doi: 10.1016/j.mayocp.2019.01.001

Sterne, J. A., Egger, M., and Smith, G. D. (2001). Systematic reviews in health care: Investigating and dealing with publication and other biases in meta-analysis. *BMJ* 323, 101–105. doi: 10.1136/bmj.323.7304.101

Sterne, J. A., Sutton, A. J., Ioannidis, J. P., Terrin, N., Jones, D. R., Lau, J., et al. (2011). Recommendations for examining and interpreting funnel plot asymmetry in meta-analyses of randomised controlled trials. *BMJ* 343:d4002. doi: 10.1136/bmj.d4002

Suzuki, S., Kawamata, J., Iwahara, N., Matsumura, A., Hisahara, S., Matsushita, T., et al. (2015). Intravenous mesenchymal stem cell administration exhibits therapeutic effects against 6-hydroxydopamine-induced dopaminergic neurodegeneration and glial activation in rats. *Neurosci. Lett.* 584, 276–281. doi: 10.1016/j.neulet.2014.10.039

Tysnes, O. B., and Storstein, A. (2017). Epidemiology of Parkinson's disease. *J. Neural Transm.* 124, 901–905. doi: 10.1007/s00702-017-1686-y

Venkataramana, N. K., Kumar, S. K., Balaraju, S., Radhakrishnan, R. C., Bansal, A., Dixit, A., et al. (2010). Open-labeled study of unilateral autologous bone-marrow-derived mesenchymal stem cell transplantation in Parkinson's disease. *Transl. Res.* 155, 62–70. doi: 10.1016/j.trsl.2009.07.006

Venkataramana, N. K., Pal, R., Rao, S. A., Naik, A. L., Jan, M., Nair, R., et al. (2012). Bilateral transplantation of allogenic adult human bone marrow-derived mesenchymal stem cells into the subventricular zone of Parkinson's disease: a pilot clinical study. *Stem Cells Int.* 2012:931902. doi: 10.1155/2012/931902

Venkatesh, K., and Sen, D. (2017). Mesenchymal stem cells as a source of dopaminergic neurons: a potential cell based therapy for Parkinson's. *Curr. Stem Cell Res. Ther.* 12, 326–347. doi: 10.2174/1574888X12666161114122059

Whone, A. L., Kemp, K., Sun, M., Wilkins, A., and Scolding, N. J. (2012). Human bone marrow mesenchymal stem cells protect catecholaminergic and serotonergic neuronal perikarya and transporter function from oxidative stress by the secretion of glial-derived neurotrophic factor. *Brain Res.* 1431, 86–96. doi: 10.1016/j.brainres.2011.10.038

Ye, M., Wang, X. J., Zhang, Y. H., Lu, G. Q., Liang, L., Xu, J. Y., et al. (2007). Therapeutic effects of differentiated bone marrow stromal cell transplantation on rat models of Parkinson's disease. *Parkinsonism Relat. Disord.* 13, 44–49. doi: 10.1016/j.parkreldis.2006.07.013

Zhang, N., Lu, X., Wu, S., Li, X., Duan, J., Chen, C., et al. (2018). Intrastriatal transplantation of stem cells from human exfoliated deciduous teeth reduces motor defects in Parkinsonian rats. *Cytotherapy* 20, 670–686. doi: 10.1016/j.jcyt.2018.02.371

Zhang, Y., Ge, M., Hao, Q., and Dong, B. (2018). Induced pluripotent stem cells in rat models of Parkinson's disease: a systematic review and meta-analysis. *Biomed. Rep.* 8, 289–296. doi: 10.3892/br.2018.1049

Zhao, C., Li, H., Zhao, X. J., Liu, Z. X., Zhou, P., Liu, Y., et al. (2016). Heat shock protein 60 affects behavioral improvement in a rat model of Parkinson's disease grafted with human umbilical cord mesenchymal stem cell-derived dopaminergic-like neurons. *Neurochem. Res.* 41, 1238–1249. doi: 10.1007/s11064-015-1816-6

Conflict of Interest: The authors declare that the research was conducted in the absence of any commercial or financial relationships that could be construed as a potential conflict of interest.

frontiers in Aging Neuroscience

REVIEW
published: 14 December 2020
doi: 10.3389/fnagi.2020.575990

Revisiting Stem Cell-Based Clinical Trials for Ischemic Stroke

Joy Q. He[1], *Eric S. Sussman*[2] *and Gary K. Steinberg*[2,3,4]*

[1]*Institute for Stem Cell Biology and Regenerative Medicine, Stanford University School of Medicine, Stanford, CA, United States,* [2]*Department of Neurosurgery, Stanford University School of Medicine, Stanford, CA, United States,* [3]*Department of Neurology and Neurological Sciences, Stanford University School of Medicine, Stanford, CA, United States,* [4]*Stanford Stroke Center, Stanford Health Care, Stanford, CA, United States*

Stroke is the leading cause of serious long-term disability, significantly reducing mobility in almost half of the affected patients aged 65 years and older. There are currently no proven neurorestorative treatments for chronic stroke. To address the complex problem of restoring function in ischemic brain tissue, stem cell transplantation-based therapies have emerged as potential restorative therapies. Aligning with the major cell types found within the ischemic brain, stem-cell-based clinical trials for ischemic stroke have fallen under three broad cell lineages: hematopoietic, mesenchymal, and neural. In this review article, we will discuss the scientific rationale for transplanting cells from each of these lineages and provide an overview of published and ongoing trials using this framework.

Keywords: stem cells, clinical trials, ischemic stroke, transplantation, cell lineages

OPEN ACCESS

Edited by:
Ramesh Kandimalla, Texas Tech University Health Sciences Center, United States

Reviewed by:
Mikko T. Huuskonen, University of Southern California, United States
Vanessa Castelli, University of L'Aquila, Italy
Deepali Mathur, University of Valencia, Spain
Aurel Popa-Wagner, University Hospital Essen, Germany
Poornima Venkat, Henry Ford Health System, United States
Jukka Jolkkonen, University of Eastern Finland, Finland

***Correspondence:**
Gary K. Steinberg
gsteinberg@stanford.edu

Received: *24 June 2020*
Accepted: *23 November 2020*
Published: *14 December 2020*

Citation:
He JQ, Sussman ES and Steinberg GK (2020) Revisiting Stem Cell-Based Clinical Trials for Ischemic Stroke. Front. Aging Neurosci. 12:575990. doi: 10.3389/fnagi.2020.575990

INTRODUCTION

Stroke is the leading cause of serious long-term disability, significantly reducing mobility in almost half of affected patients aged 65 years and older (Benjamin et al., 2017). Each year, 795,000 strokes occur in the US alone, and the annual economic impact of stroke is estimated at $33.9 billion. The current standard of care for ischemic stroke is acutely time-sensitive: administration of intravenous tPA is recommended within 4.5 h of stroke onset, and endovascular therapy in select patients within 24 h of stroke onset (Hacke et al., 2008; Berkhemer et al., 2015; Campbell et al., 2015; Goyal et al., 2015; Jovin et al., 2015; Saver et al., 2015, 2016; Albers et al., 2018; Nogueira et al., 2018). Beyond the acute period, there are currently no proven neurorestorative treatments for stroke. Despite numerous clinical trials, drug-based therapies, including selective serotonin reuptake inhibitors, amphetamines, and ion channel modulators, have not yielded significant benefits, perhaps due to the complex cellular disruption that occurs within damaged ischemic tissue (Chollet et al., 2011; Mead et al., 2015; Simpson et al., 2015; Yeo et al., 2017).

Unlike other organs, the brain responds to ischemia by undergoing liquefactive necrosis, a process in which dead tissue liquefies and is cleared by brain resident phagocytes over months. This long-lasting inflammatory process results in substantial neurotoxicity, myelin degradation, and glial scarring, as well as releasing a host of neuroinflammatory mediators, including cytokines (TNF-a, IL-1b, IL-6, IL-20), chemokines (MCP-1, MIP1a), cellular adhesion molecules (immunoglobulins, cadherins, integrins), reactive oxygen species, and matrix metalloproteases (Lakhan et al., 2009; Ceulemans et al., 2010; Stonesifer et al., 2017; Chung et al., 2018; Zbesko et al., 2018). At the liquefactive core of the infarct, hematopoietic lineage (myeloid and lymphoid), mesenchymal lineage

(endothelial and other stromal), and neural lineage (neurons, astrocytes, and oligodendrocytes) cells undergo extreme stress, interacting and dying within this inflammatory, acidic, and hypoxic milieu (Chung et al., 2018).

To address the complex problem of restoring function in ischemic tissue, stem cell transplantation-based therapies have been investigated as potential restorative treatments for chronic stroke. Aligning with the major cell types found within the ischemic brain, stem-cell-based clinical trials for ischemic stroke have fallen under three broad cell lineages: hematopoietic, mesenchymal, and neural (**Table 1**). In this review, we will discuss the scientific rationale for transplanting cells from each of these lineages and provide an overview of published and ongoing trials using this framework.

HEMATOPOIETIC LINEAGE

Hematopoietic stem cells (HSCs) at rest reside within the bone marrow niche but can be mobilized to the general blood circulation in response to stimulant factors such as granulocyte colony-stimulating factor (G-CSF). A majority of trials conducted using HSC lineage cells have relied on autologous bone marrow transplantation, favoring the lack of immunogenicity and ethical challenges to obtaining a reliable source of hematopoietic cells. In these studies, bone marrow was obtained from the patient and purified, either by density gradient alone or combined with immunosorting to obtain the cell population for transplantation. The cell surface marker CD34 characterizes a population enriched for HSCs, and the proportion of CD34+ cells found in the peripheral blood immediately after stroke has been found to directly correlate with functional recovery (Dunac et al., 2007).

Bone Marrow Derived Cells

Bone Marrow Mononuclear Cell (BM-MNC) Transplantation

Early Phase I Trials (2009–2012)

The first Phase I trials of bone-marrow-derived cells demonstrated unequivocally that BM-MNCs could safely be transplanted in stroke patients at varying time points after stroke onset, and *via* various routes of administration. Suarez-Monteagudo et al. (2009) implanted 14–55 million autologous BM-MNCs by stereotactic intralesional injection in five chronic stroke patients at least 1 year and no more than 10 years post-stroke onset. This trial found that intracranially-injected autologous BM-MNCs were well-tolerated and safe,

TABLE 1 | Lineage origin of transplanted cells in published clinical trials for ischemic stroke.

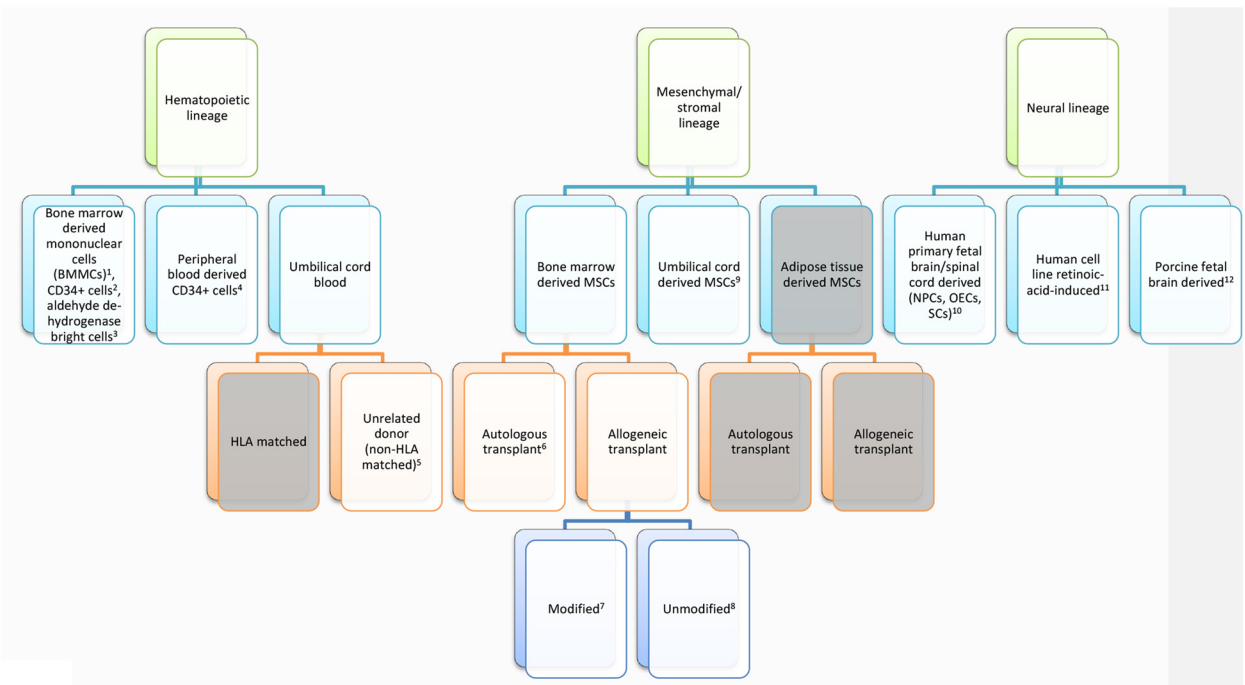

[1]*Suarez-Monteagudo et al. (2009), Barbosa da Fonseca et al. (2010), Savitz et al. (2011), Friedrich et al. (2012), Prasad et al. (2012), Prasad et al. (2014), Sharma et al. (2014) and Taguchi et al. (2015);* [2]*Moniche et al. (2012) and Banerjee et al. (2014);* [3]*Savitz et al. (2019);* [4]*Chen et al. (2014);* [5]*Laskowitz et al. (2018);* [6]*Bang et al. (2005), Lee et al. (2010), Bhasin et al. (2011), Honmou et al. (2011) and Fang et al. (2019);* [7]*Steinberg et al. (2016, 2018);* [8]*Hess et al. (2017) and Levy et al. (2019);* [9]*Chen et al. (2013) and Qiao et al. (2014);* [10]*Chen et al. (2013), Qiao et al. (2014), Kalladka et al. (2016) and Muir et al. (2020);* [11]*Kondziolka et al. (2000) and Kondziolka et al. (2005);* [12]*Savitz et al. (2005). Shading, in pending clinical trials only (no results published).*

with several patients reporting long-term neuropsychiatric improvements. Targeting the subacute phase of ischemic stroke, Barbosa da Fonseca et al. (2010) infused 125–500 million autologous BM-MNCs in six patients *via* intra-arterial injection 8–12 weeks after stroke onset and reported no cases of neurologic worsening. In the acute setting, Savitz et al. (2011) determined that intravenous infusion of 70–100 million cells per kilogram weight of autologous BM-MNCs in 10 patients with acute stroke (24–72 h after onset) was both safe and feasible. Additionally, Prasad et al.'s (2012) research group intravenously infused 11 patients with 80 million autologous BM-MNCs (mean 0.92×10^6 CD34+ cells) within 7–30 days of stroke onset and also confirmed the safety and feasibility of this treatment protocol. Friedrich et al. (2012) administered 50–600 million autologous BM-MNCs *via* intra-arterial (MCA) infusion to 20 patients within 3–10 days of stroke onset and found this method to be safe. Of note, while not known at the time, the brain biodistribution of intra-arterially and intravenously transplanted BM-MNCs was eventually determined to be comparable in a separate clinical trial completed a year later (Rosado-de-Castro et al., 2013). In both cases, brain biodistribution was low compared to that of lung or spleen, or liver. A summary of different routes of administration and their relative advantages and disadvantages concerning reaching ischemic brain tissue have been included in **Table 2**.

In the context of intracranial cell administration, transplantation into peri-ischemic vs. directly lesioned areas was extensively investigated in preclinical stroke models. The lesioned area was determined to be a poor injection target site due to unstable vascular supply and a highly inflammatory microenvironment. Moreover, the lesioned area was shown to eventually become a non-functional, fluid-filled cyst, suggesting that post-stroke recovery would be due to changes at the periphery of the lesion, not the cystic core (Veizovic et al., 2001; Modo et al., 2002; Smith et al., 2012). Of the clinical trials that utilized intracranial administration, only the porcine neural cell transplantation study conducted by Savitz et al. (2005) injected directly into the infarct. The study, discussed in a later section of this review, was terminated by the FDA after two of the five patients developed adverse events including cortical vein occlusion, complex partial seizures, and ring-enhancing lesions.

Phase I/II, Phase II Trials (2014–2015)

As Phase I/II trials progressed, the safety of these treatment protocols was consistently demonstrated, but BM-MNC administration was not found to significantly improve neurologic outcomes in transplant cohorts. In a follow-up to their initial Phase I trial, Prasad et al. (2014) performed a Phase II randomized study in which 120 patients received either 280 million autologous BM-MNCs or placebo intravenously within 7–30 days of stroke onset; this study yielded no clinical benefit for BM-MNC transplantation over placebo. Sharma et al.'s (2014) research group pursued a different route of administration, identifying 24 patients with chronic stroke (onset between 4 months to 10 years) to receive 1 million BM-MNCs per kilogram body weight intrathecally. Intrathecal administration proved safe, and functional improvement was noted in treated patients, however, there was no control group for comparison. In a phase I/IIa trial, Taguchi et al. (2015) intravenously administered either 250 million or 340 million cells of autologous BM-MNCs and found a trend toward improved neurologic outcomes and cerebral perfusion in the high dose group. Studies by Bhasin et al. (2016) additionally found that positive neurologic outcomes in patients given autologous BM-MNCs could be due to paracrine effects of secreted vascular endothelial growth factor (VEGF) and brain-derived neurotrophic factor (BDNF).

Sorted CD34+ From Bone Marrow

Hypothesizing that the hematopoietic stem cell-enriched CD34+ fraction of BM-MNCs contained the functional subset of cells responsible for repair during ischemic CNS injury, Moniche et al. (2012) conducted a Phase I/II study in which 160 million autologous CD34+ BM-MNCs were infused intra-arterially (MCA) into 10 patients within 5–9 days of stroke onset. The comparison group consisted of 10 subacute stroke patients who did not receive the intervention. In this trial, there was no clinical benefit at 180 days, but there was a statistically significant increase in b-NGF among the treated cohort ($p < 0.02$). Similarly, Banerjee et al.'s (2014) research group intra-arterially infused (*via* the MCA) 10 million autologous sorted CD34+ cells in five patients within 1–7 days of stroke onset, and found the intervention to be safe, and associated with a decrease in infarct size over time.

Sorted Aldehyde Dehydrogenase-Bright (ALDH-BR) From Bone Marrow

Aldehyde dehydrogenase (ALDH) was among the first markers used by immunologists to identify populations of human hematopoietic stem and progenitor cells in the 1990s. HSCs were found to express the highest levels of ALDH, while lymphocytes expressed the lowest (Kastan et al., 1990). Transplant of BM-derived ALDH-br cells was reported to improve functional recovery in limb ischemia and ischemic heart failure (Keller, 2009; Perin et al., 2011, 2012). Based on these findings, Savitz et al. (2019) transplanted up to eight million autologous ALDH-br BM-MNCs (dubbed autologous ALD-401 cells) *via* intracarotid infusion in 29 patients and compared this cohort to 19 control patients who received a sham procedure. Disappointingly, the study found no significant difference in primary or secondary efficacy measures between treatment and placebo groups.

Mobilized Peripheral Blood Stem Cells

Shyu's research group previously demonstrated peripheral blood-derived stem-cell (PBSC) transplant efficacy in treating chronic ischemia in rats (Shyu et al., 2006). To further evaluate the efficacy of this cell type in human subjects, Chen et al. (2014) conducted a Phase II trial in which autologous PBSCs were mobilized with G-CSF, and 3–8 million sorted CD34+ cells were stereotactically transplanted into 15 chronic stroke patients (stroke onset ranging from 6 months to 5 years prior).

TABLE 2 | Routes of administration of completed stem cell trials for ischemic stroke.

Intravenous (IV)	Intra-arterial (IA)	Intracranial (IC)	Intrathecal	Intranasal
Bang et al. (2005), Lee et al. (2010), Bhasin et al. (2011), Honmou et al. (2011), Savitz et al. (2011), Chen et al. (2013), Prasad et al. (2014), Qiao et al. (2014), Taguchi et al. (2015), Hess et al. (2017), Laskowitz et al. (2018), Fang et al. (2019) and Levy et al. (2019)	Barbosa da Fonseca et al. (2010), Friedrich et al. (2012), Moniche et al. (2012), Banerjee et al. (2014) and Savitz et al. (2019)	Kondziolka et al. (2000, 2005), Savitz et al. (2005), Suarez-Monteagudo et al. (2009), Chen et al. (2013, 2014), Kalladka et al. (2016), Steinberg et al. (2016, 2018) and Muir et al. (2020)	Chen et al. (2013) and Sharma et al. (2014)	
Systemic administration Advantage: • Simple procedure/ease of delivery Disadvantages: • Poor biodistribution to the brain: 0.9% after 24 h (Rosado-de-Castro et al., 2013) • Reperfusion of lesion after cell delivery not confirmed	**Systemic administration** Advantage: • When infused into the internal carotid or middle cerebral arteries, cell delivery to the brain occurs before other organs Disadvantages: • Reperfusion of lesion after cell delivery not confirmed • Lowest biodistribution to the brain overall: 0.6% after 24 h (Rosado-de-Castro et al., 2013) • Potential for complications and/or thrombosis	**Local administration** Advantage: • Greatest cell retention at lesion site compared to intra-arterial or intravenous: in mouse studies, 60% IC (compared to ∼1.5% IV) after 3 days (Barish et al., 2017) Disadvantages: • Uneven cell distribution throughout the lesion (Li et al., 2000; Giraldi-Guimardes et al., 2009) • An invasive procedure, requiring sedation and stereotactic localization	**Local administration** Advantages: • Direct access to CSF circulation throughout the brain and spinal cord • Less complex procedure than intracranial Disadvantage: • The mechanism of cellular migration from CSF space into brain parenchyma remains unknown	**Local administration** Advantages: • Enhanced blood-brain barrier permeability • Ease of delivery Disadvantage: • Unproven: clinical trials are ongoing and no data has been published to date

Shading = in pending clinical trials only (no results published).

The authors noted improvement in multiple neurologic and functional outcome scores in the treated cohort.

Umbilical Cord Blood Derived Cells

Allogeneic umbilical cord blood is an immunologically tolerant source of readily available cells. Unlike other sources of HSCs, HLA-matching is not required, and its safety and efficacy as a blood donor graft have been well established (Zhou et al., 2012). In this context, Laskowitz et al. (2018) conducted a Phase I study to establish the safety and feasibility of administering a single intravenous infusion of allogeneic (non-HLA matched) umbilical cord blood in stroke patients. The study included 10 patients treated between 3 and 9 days post-stroke onset, and noted an improvement in neurological and functional outcome, although there was no control group for comparison. A list of pending and ongoing clinical trials using cells of hematopoietic origin have been compiled in **Table 3**.

MESENCHYMAL LINEAGE

Mesenchymal stem cells (MSCs) are stromal cell precursors to cells of osteogenic, chondrogenic, and/or adipogenic lineages, and can be harvested and expanded from a variety of tissue types, including bone marrow (BM-MSCs, a cell population distinct from hematopoietic origin BM-MNCs), adipose tissue (adipose-derived MSCs, or AD-MSCs), and umbilical cord (UB-MSCs). This versatility, combined with low immunogenicity due to low expression of human leukocyte antigens, makes MSCs excellent candidates for allogeneic stem cell transplants (Le Blanc et al., 2003; Klyushnenkova et al., 2005). Unlike bone marrow-derived hematopoietic cells, MSCs from a single source can be expanded for transplant into many individuals, providing both standardization and scalability for large clinical studies.

BM-MSCs have been shown to cross the blood-brain barrier and improve functional recovery after acute ischemic stroke in animal models (Chen et al., 2001; Lee et al., 2016), likely due to a paracrine effect by secreting neurotrophic, mitogenic, and angiogenic factors, including VEGF, BDNF, nerve growth factor, basic fibroblast growth factor, and insulin-like growth factor 1 (Eckert et al., 2013; Shichinohe et al., 2015; Stonesifer et al., 2017). One hypothesized mode of delivery for these factors is *via* the secretion of membrane fragments (extracellular vesicles, EVs) from transplanted cells (Bang and Kim, 2019; Surugiu et al., 2019). Recent preclinical data in organoids suggest that EVs alone may be sufficient to significantly decrease injury in a hypoxia-starvation model of injury, opening the possibility for future early phase clinical trials of EV delivery for ischemic stroke (Zheng et al., 2020).

Additionally, AD-MSC transplants have also demonstrated success in experimental ischemic stroke models, in which animals treated with AD-MSCs demonstrated increased expression of BDNF and enhanced nerve regeneration, and simultaneously reduced expression of pro-apoptotic proteins such as BCL-2 and BAX within the ischemic lesion (Li et al., 2016). Multiple preclinical studies of UB-MSCs showed that transplanted cells quickly homed to the site of injury in rat ischemia models and resulted in improved long-term neurologic outcomes (Zhang et al., 2017; Wu et al., 2018). These results were

TABLE 3 | Ongoing and pending unpublished hematopoietic lineage trials.

ClinicalTrials.gov Identifier	Study type	Cell type	Planned enrollment	Timing of delivery	Delivery route	Status
NCT01518231 "AHSCTIS" China	Phase I Randomized Open-label	CD34+ from peripheral blood	40	<12 months	IA	Recruiting/unknown
NCT00473057 Brazil	Phase I Non-Randomized Open-label	Autologous BM-MNC	12	<90 days	IA or IV	Completed 2011, no publications to date
NCT01832428 "BMACS" India	Phase I/II Non-Randomized Open-label	BM-MNC	50	Chronic	IT	Not currently recruiting/unknown
NCT02290483 also identified by NCT02178657 Spain	Phase II Randomized Open-label	BM-MNC (2×10^6 or 5×10^6 cells/kg)	76	<7 days	IA	Recruiting/paper published on miRNAs from the trial but no study results to date
NCT02795052 "NEST" USA	Phase n/a Non-Randomized Open-label	Autologous BMSC (intranasal for hypothesized blood-brain barrier penetration)	300	>6 months	IV or intranasal	Recruiting

also most likely due to paracrine effects, as transplanted cells did not persist long term.

Bone Marrow Derived MSCs

Autologous Transplant

Bang et al. (2005) were the first to conduct autologous MSC transplants in stroke patients, to introduce cells with the potential to provide trophic support for neurogenesis and/or neuromodulatory effects—functions that are limited with hematopoietic cells. This group conducted a Phase I/II trial in which 100 million culture-expanded autologous BM-MSCs (grown in fetal bovine serum-containing media) were intravenously infused in five patients at 5–7 weeks post-stroke onset. Compared to a control cohort of 25 patients, treated patients demonstrated consistent neurologic improvement at 3, 6, and 12 months post-transplantation. Based on the success of this first study, the same group subsequently conducted a larger observer-blinded trial consisting of 52 patients (16 transplanted, 36 control; Lee et al., 2010). Due to the significant time required to expand MSCs in culture, the investigators opted to decrease the time-to-transplant by administering an initial dose of 50 million MSCs, and subsequently administering an additional 50 million MSCs 2 weeks later (rather than a one-time treatment with 100 million MSCs as in the Phase I/II trial). Notably, clinical improvement was found to be correlated with intactness of the subventricular zone—a known neurogenic site—as demonstrated on diffusion-weighted MR imaging. The MSC-transplanted cohort exhibited a higher rate of functional recovery and lower mortality compared to the control cohort. The authors reported that the use of bovine serum proteins to expand MSCs in culture did not appear to result in zoonoses or other adverse effects.

Due to ongoing concern regarding the use of bovine serum, particularly in the context of infectious diseases such as Creutzfield-Jakob, a Phase I study using MSCs expanded with autologous human serum was also conducted and published by a different group (Honmou et al., 2011). Honmou et al.'s (2011) research group demonstrated the safety and feasibility of BM-MSCs expanded in culture with human autologous serum, injected intravenously in 12 patients. Human serum resulted in more rapid MSC expansion *in vitro* compared to bovine serum, and at 1-week post-transplant, the mean infarct volume, as measured on MRI, was reduced by approximately 20% in patients treated according to this protocol. Circumventing the issue of serum altogether, Bhasin et al.'s (2011) research group conducted a Phase I/II trial in which autologous MSCs expanded in culture under serum-free conditions were intravenously administered to 20 chronic stroke patients between 3 months and 2 years following stroke onset. While both the control (n = 20) and transplanted groups experienced statistically significant improvement, there was no statistically significant difference between the groups in terms of functional outcome. Bhasin et al. (2013) presented a follow-up study in 2013 in which mesenchymal cells were compared with hematopoietic/mononuclear cells. Again, stem cell transplantation was found to be safe and feasible, with no conclusive evidence for efficacy but a trend toward functional improvement. Their 2016 study, again transplanting BM-MNCs, was discussed previously.

In a separate Phase I/IIa study, Fang et al. (2019) compared BM-MSCs to autologous endothelial progenitor cells (EPCs), as

well as to placebo in patients within 5 weeks of stroke onset. This study included 18 total patients: six transplanted with BM-MSC, six with EPCs, and six with saline (placebo). The BM-MSCs were expanded in fetal bovine serum culture, and EPCs were derived by seeding bone marrow mononuclear cells on fibronectin plates to select for adherent cells, and subsequently maintained in bovine serum culture with endothelial cell media. Two injections of 2.5 million cells per kilogram body weight were given approximately 1 week apart, and patients were followed for 4 years. While the trial was deemed safe, no functional or neurological difference was observed between the BM-MSC, EPC, and placebo groups.

Allogeneic Transplant

The fact that MSCs express low levels of human leukocyte antigen and are easily expanded in culture is a significant advantage over other cell-based therapies about stroke therapy (Le Blanc et al., 2003). These features allow for the development of large quantities of standardized single-source cells for allogeneic transplant and also mitigate many of the challenges of autologous cell therapy in terms of timing of treatment. This is of particular benefit in patients who are unable to provide autologous cells. Moreover, because MSCs may be cultured and expanded *in vitro* without sacrificing stemness potential (Reyes et al., 2001; Jiang et al., 2002), genetic modification of these cells prior to transplantation in order to enhance supportive properties has also opened new possibilities.

Unmodified Cell Transplants

In the largest MSC trial to date, Hess et al. (2017; MASTERS, Athersys) conducted a phase II randomized, double-blind, placebo-controlled dose-escalation trial of intravenous adult BM-MSCs for acute ischemic stroke at 33 centers across the US and UK. In this trial, patients were randomized to receive either 400 million or 1.2 billion allogeneic BM-MSCs ($n = 65$) or placebo ($n = 61$) within 24–48 h after stroke onset. The allogeneic BM-MSC product used in this study—MultiStem—was derived from two independent donors (Boozer et al., 2009). No dose-dependent toxicity was observed and the treatment was deemed safe, but the transplanted group and placebo groups exhibited no significant difference in terms of functional outcome at 90 days post-stroke. Of note, a *post hoc* analysis of those patients achieving an "Excellent Outcome" defined as mRS $\leq$1 and NIHSS $\leq$1 and Barthel $\geq$95, demonstrated a statistically significant benefit for all patients treated at 1 year (23.1% transplant vs. 8.2% placebo; $p = 0.02$) and for all patients treated within the originally planned time window of $\leq$36 h post-stroke the benefit at 1 year was even greater (29.0% transplant vs. 8.2% placebo; $p < 0.01$). This finding was encouraging enough for Athersys to initiate another Phase III prospective, randomized, placebo-controlled, double-blind trial treating patients between 18–36 h of stroke (MASTERS-2).

In a separate Phase I/II trial using allogeneic single-donor adult mesenchymal BM-MSCs (Levy et al., 2019; Stemedica) transplanted up to 1.5 million BM-MSCs per kg body weight intravenously in 38 patients with chronic stroke (>6 months post-stroke). The highest dose (1.5 million/kg) was found to be safe, and significant behavioral gains were observed. Excellent functional outcome (Barthel score >95) was reported in 35.5% of patients at 12 months post-transplant, compared to in 11.4% at baseline; however, there was no control group included in this study.

Modified MSC Transplants

SB623 is a BM-MSC line that has been transiently transfected with a plasmid containing the human Notch1 intracellular domain, which results in constitutive Notch1 expression. Importantly, the Notch1 plasmid is not replicated during mitosis and is therefore rapidly lost during cell division. In *in vitro* preclinical models, Notch1-modified MSCs promoted neural cell growth and rescued neural cell survival after ischemia by providing trophic support *via* the secreted extracellular matrix, promoting angiogenesis, and playing a protective, anti-inflammatory role (Aizman et al., 2009; Tate et al., 2010; Dao et al., 2011, 2013). Experimental stroke models transplanted with Notch-1-modified MSCs have demonstrated functional recovery and peri-infarct neuroprotection as measured by a reduction in cell loss. Despite these benefits, however, the SB623 cells themselves are short-lived *in vivo* (Yasuhara et al., 2009; Tajiri et al., 2013). This finding suggests that observed improvements are a result of supportive trophic activity rather than engraftment, and alleviates concerns over the challenges of achieving long-term allogeneic cell engraftment.

Based on this encouraging preclinical data, Steinberg et al. (2016) completed a Phase I/IIa trial in which 18 chronic stroke patients (6 months to 3 years post-stroke onset) received a stereotactic intracranial injection of either 2.5, 5, or 10 million allogeneic modified SB623 BM-MSCs (six patients per cohort). Each patient received five stereotactic image-guided injections of 20 μl each surrounding the infarct. Of note, the intracranial administration of SB623 was chosen because of the desire to prioritize trophic factor delivery by transplanted cells over cell engraftment (Bliss et al., 2010). In comparison to intra-arterial and intravenous delivery, the intracranial injection was shown to result in greater delivery of transplanted cells to the lesion, although cells are unequally distributed throughout (Rosado-de-Castro et al., 2013). Patients who received intracranial injections reported several treatment-emergent adverse events (TEAEs), including headache, nausea, and vomiting. It was determined that most, if not all, of the TEAEs, were due to the surgical procedure rather than the cell transplantation. No link between TEAE and cell dosage was identified, and all TEAEs recovered without sequelae. No antibody response to SB623 cells was observed, and a significant improvement in neurological function was noted after 3, 6 (the pre-determined efficacy endpoint), and 12 months. In a follow-up article detailing 2-year outcomes, the initial improvements were found to be stable at 2 years post-transplantation (Steinberg et al., 2018). Interestingly, the authors noted that the size of a transient T2-FLAIR signal (DWI negative) on MRI at an early time point (1–2 weeks post-transplant) was correlated with the degree of long-term functional improvements, and could be a possible indicator of functional transplant activity. A larger Phase IIb randomized,

double-blind, placebo-controlled study, ACTIsSIMA, has been completed but the results are as yet unpublished. Additional pending clinical trials using cells of mesenchymal origin have been detailed in **Table 4**.

NEURAL LINEAGE

Neural stem cells (NSCs) are multipotent cells that can differentiate into neurons, astrocytes, and oligodendrocytes. This native capacity to repopulate and support endogenous cell types within the brain has generated much interest in NSC transplantation for stroke. The subventricular zone of the lateral ventricle and the dentate gyrus of the hippocampus have been identified as neurogenic sites, and in murine models, NSC's have been shown to migrate from these niches to promote neurogenesis and vascular remodeling in response to ischemic stroke (Zhang et al., 2014; Hao et al., 2015).

One of the greatest barriers to developing an NSC transplantation model is the challenge of harvesting cells for transplantation. Clinical trials utilizing NSCs have attempted to overcome this barrier by: (1) modifying a human teratoma cell line [teratomas and cancer lines were the only non-embryonic source of pluripotent human cells before the development of induced pluripotent stem cells (iPSCs)] to induce neuronal differentiation by introducing the morphogen retinoic acid; (2) using NSCs harvested from human fetal tissue and/or clonal lines derived from these cells; or (3) using cells of non-human origin (i.e., porcine fetal NSCs).

Retinoic Acid-Induced Differentiated Tumor Cells

Kondziolka et al. (2000) were the first to conduct NSC transplants for chronic stroke. In a Phase I trial published in 2000, 12 patients received either two or six million human "LBS-Neurons" *via* intracranial injection between 6 months and 6 years post-stroke. These cells were derived by differentiating the NT2/D1 human cell line, originally derived from a lung metastasis of testicular embryonal carcinoma, into neurons using a 10 μM dose of retinoic acid. Before the discovery of iPSCs in 2007, NT2/D1 was among the lines widely used to represent human pluripotent cells and was shown to be capable of terminal differentiation into multiple cell types, including neurons and astrocytes (Bani-Yaghoub et al., 1999). Preclinical studies demonstrated that NT2/D1-derived neurons resulted in improved functional outcomes after ischemia when injected intracranially (Borlongan et al., 1998). In humans, treatment with NT2/D1-derived neurons was found to be safe and associated with significantly improved functional outcome at 6 months.

Subsequently, the same University of Pittsburg group, with the addition of Stanford University investigators, conducted a Phase II randomized observer-blinded trial in which 14 chronic stroke patients received an intracranial injection of either five or 10 million LBS-Neurons; four patients acted as nonsurgical controls. While the primary efficacy endpoint—improvement of European Stroke Scale score at 6 months — was not achieved, one of the prespecified secondary outcome measures (the Action Research Arm Test designed to measure gross hand-movement) improved significantly compared with controls and with baseline scores on the same test.

Porcine

Given the concerns surrounding implanting cells derived from malignant human tumors, compounded with the ethical implications and difficulty of obtaining fetal tissue, Savitz et al. (2005) attempted a Phase I trial to xenotransplant up to 50 million fetal porcine cells in five patients with chronic stroke, 18 months to 10 years post-stroke onset. Before intracranial transplantation, the cells were treated with anti-MHC to prevent rejection. While two patients reported clinical improvement, one patient developed seizures, and one experienced a temporary worsening of motor symptoms. As a result, this trial was halted due to safety concerns.

Human Primary Fetal Brain Derived

The human fetal brain represents a source of actively dividing NSCs that have demonstrated proven engraftment and functional capacity in both preclinical and clinical studies for disorders such as leukodystrophies (Uchida et al., 2000, 2012; Tamaki et al., 2002; Kelly et al., 2004; Gupta et al., 2012, 2019); however, fetal tissue is difficult to obtain in the US due to governmental policy. CTX0E03 is one such fetal tissue line, derived by a research group in the UK and is currently being studied in ischemic stroke in the PISCES clinical trials (ReNeuron). CTX0E03 cells are a clonally derived human fetal cortical cell line that was transfected with a single copy of c-mycERTAM, an immortalizing gene dependent on tamoxifen administration for function (Pollock et al., 2006). Despite c-myc's role as a known oncogene, preclinical stroke models indicated that CTX0E03 cells were safe to transplant, and promoted behavioral recovery *via* enhanced neurogenesis and angiogenesis in a dose-dependent fashion after ischemia (Stroemer et al., 2009). It is unclear if CTX0E03 cells exhibit long-term engraftment in the brain (Hicks et al., 2013; Baker et al., 2019). The PISCES 1 clinical trial for ischemic stroke transplanted 2.5, 5, 10, or 20 million CTX0E03 cells intracranially in 11 patients who had experienced a stroke 6–24 months prior (Kalladka et al., 2016). The treatment was found to be safe, and treated patients exhibited improved neurologic outcomes on several scales. However, the initial study was limited to cisgender male patients due to concerns about the potential for estrogen to activate c-myc. The PISCES 2 open-label Phase 2 trial transplanted 20 million CTX0E03 cells into the putamen of 23 patients, 13 males, and 10 females, 2–13 months after subcortical ischemic stroke (individuals actively taking tamoxifen were excluded). While the primary endpoint [two patients improving two points in the Action Research Arm Test (ARAT) subtest 2 at 3 months] was not met, there were substantial improvements in this metric as well as the mRS and Barthel Index (Muir et al., 2020). A Phase III prospective, randomized, controlled, double-blinded study (PISCES 3)

TABLE 4 | Ongoing and pending unpublished mesenchymal lineage trials.

ClinicalTrials.gov Identifier	Study type	Cell type	Planned enrollment	Timing of delivery	Delivery route	Status
NCT01678534 "AMASCIS-01" Spain	Phase I/II Randomized Double-blinded	Allogeneic cultured single donor Adipose-derived MSCs	40	<14 days	IV	Completed—no results to date
NCT01716481 "STARTING-2" South Korea	Phase III Randomized Open-label	Autologous BM-derived MSCs, expanded in serum	60	<90 days	IV	Recruiting/ unknown
NCT00875654 "ISIS" France	Phase II Randomized Open-label	Autologous BM-derived MSCs	31	<6 weeks	IV	Completed, no results to date
NCT02448641 "ACTIsSIMA" USA	Phase II Randomized Double-blinded	BMMNC SB623 (cultured single donor modified BM-derived MSCs)	156	6 months–7.5 years	IC	Completed, no results to date
NCT03570450 "RESSTORE-1" European Union	Phase I Randomized Open-label	Allogeneic adipose-derived mesenchymal stem cells	15	<1 week	IV	Recruiting
NCT02813512 Taiwan	Phase I Non-Randomized Open-label	Autologous ADSCs	6	>6 months	IC	Completed 2018
NCT03356821 "PASSIoN" Netherlands **Perinatal/neonatal stroke**	Phase I/II Non-Randomized Open-label	One dose of 50×10^6 Allogeneic BM-MSCs	10	<1 week	Nasal	Not yet recruiting
NCT03545607 "MASTERS-2" USA	Phase III Randomized Double-blinded	1.2×10^6 MultiStem (Allogeneic BM multipotent progenitors)	300	18–36 h	IV	Recruiting (see Hess et al., 2017 for MASTERS)
NCT02378974 S Korea	Phase I/II Randomized Double-blinded	Human Umbilical cord-derived Mesenchymal Stem Cells ("Cordstem-ST")	19	<7 days	IV	Completed, results not yet published
NCT04063215 USA **chronic brain injury**	Phase I/II Non-Randomized Open-label	Autologous adipose-derived Mesenchymal Stem Cells (HOPE biosciences)	24	>6 months	IV	Recruiting

TABLE 5 | Ongoing and pending unpublished neural lineage trials.

ClinicalTrials.gov Identifier	Study type	Cell type	Planned enrollment	Timing of delivery	Delivery route	Status
NCT01327768 China	Phase I Randomized Single blinded (participant)	OECs from nasal mucosa (autologous)	6	6–60 months	IC	Recruiting/unknown
NCT03629275 "PISCES-III" USA	Phase II Randomized	CTX0E03 modified NSCs, 20 million	130	6–24 months	IC	Recruiting

treating 130 patients 6–12 months post-stroke is currently ongoing in the US.

Cotransplant Studies of Primary Fetal NSC and UB-MSCs

Given the significant trophic support provided by mesenchymal cells and the regenerative capacity of NSCs, combined engraftment of fetal-derived neural and cord-blood-derived mesenchymal lineage cells together has been investigated as a potential therapeutic strategy to improve and support stem cell engraftment. Chen et al. (2013) sought to establish the safety and feasibility, as well as the optimal route of cell administration, of a multiple cell type co-transplantation in a group of 10 patients. The investigators isolated three distinct neural cell types from a single fetal donor: (1) olfactory ensheathing cells (OECs) from the fetal olfactory bulb; (2) neural progenitor cells (NPCs) from the subependymal zone; and (3) Schwann cells (SCs) from the sciatic nerve. Cord blood from a separate donor was used to derive UB-MSCs, and all transplanted UB-MSCs were derived from a single cord. Chronic stroke patients who were 6 months to 20 years post-stroke onset were included, and were divided amongst five distinct treatment protocols: (1) OECs alone (intracranial, $n = 2$); (2) OECs + NPCs (intracranial, $n = 2$); (3) OECs + NPCs (intracranial) with a second dose of NPCs at a later time point (intrathecal, $n = 4$); (4) OECs + NPCs (intracranial) + later doses of NPCs (intrathecal) and UB-MSCs

(intravenous, $n = 1$); and (5) OECs and NPCs (intracranial) + later doses of SC and NPCs (intrathecal) and UB-MSCs (intravenous, $n = 1$). Treatment was found to be safe and feasible in all cases, however, due to the variety of cell types and routes of administration evaluated, the authors concluded that the study was not sufficiently powered to conclude that co-transplantation is safe under all studied conditions. The authors also noted a trend towards functional benefits with intracranial injections, but not with intrathecal and intravenous cell administration.

Another Phase I study conducted by Qiao et al. (2014) involved co-transplantation of UB-MSCs with human fetal cells. Enrolled patients received either four intravenous doses of 0.5×10^6 UB-MSC cells per kg body weight or one intravenous dose of 0.5×10^6 UB-MSC cells per kg body weight followed by three intrathecal doses of 0.5×10^6 UB-MSC cells per kg body weight and 6×10^6 human fetal derived NPCs (Qiao et al., 2014). In total, the investigators treated six subacute to chronic stroke patients between 1 week and 2 years post-stroke onset. Two of these patients received UB-MSCs only. The trial demonstrated that co-transplantation was safe and feasible; no malignancies were observed from the use of multipotent fetal cells. Further, each treated patient experienced clinical improvement that was stable at 2 years post-transplant. A list of pending clinical trials using cells of neural origin has been compiled in **Table 5**.

CONCLUSIONS

The regenerative properties of stem cells have brought cell-based transplantation studies into the spotlight as appealing therapies for otherwise recalcitrant disorders such as subacute and chronic ischemic stroke. In this review article, we have detailed the clinical trials to date, which have featured transplantation of various cell types, administered *via* a variety of routes and in a variety of doses, to treat ischemic stroke of varying chronicity. We have discussed the history of and scientific rationale for the different cell types transplanted, their routes of administration, and associated trial outcomes, and have provided snapshots of current ongoing trials. Additional studies are necessary to strengthen our understanding of the relationship between neural cells and their surrounding stromal, endothelial, and immune landscape in both the healthy state and in pathologic conditions. As discussed in this review, specific attention should be given to the paracrine mechanisms by which transplanted cells exert their therapeutic effect, especially in light of data that suggests that these benefits persist even after the clearance of the originally transplanted cell type.

Furthermore, promising preclinical studies require adequate support and prudent design to overcome the "translational roadblock," a notable decrease in efficacy between preclinical studies and their clinical trial counterparts. The difference is thought to be due to a series of factors. First, a combination of publication bias and overstated efficacy in preclinical studies has led to overly optimistic preclinical data that fail to result in statistically meaningful clinical interventions (Dirnagl et al., 2009; Macleod et al., 2009). Poor translation to the clinic has also resulted from the differences in primary endpoints between animal models and trials, lengthening of time-to-treatment in the clinic compared to in animal models, nuances in translating dosage, and heterogeneity of patient characteristics such as age (Dirnagl et al., 2009; Hermann et al., 2019). Recent studies have shown patient age to be a significant prognostic factor, and have suggested that, for clinical improvement, the timing of interventions must be increased to account for increased age (Sandu et al., 2017). Additionally, the underpowered clinical trial design has also contributed significantly to the difficulty of translating otherwise promising preclinical interventions to the bedside (Dirnagl and Macleod, 2009; Schmidt-Pogoda et al., 2020). Judiciously guiding the development of future stem-cell-based clinical interventions, including those harnessing recent advances in cellular regeneration, trophic support, immunomodulation, and perhaps as-of-yet undiscovered mechanisms of repair, will be essential in achieving successful clinical trials of promising neurorestorative therapies.

AUTHOR CONTRIBUTIONS

ES and GS contributed to the conception of this review. JH and ES contributed to the design and organization of the material. JH and GS created and updated the tables. JH, ES, and GS wrote sections of the manuscript, contributed to manuscript revision, read, and approved the submitted version.

FUNDING

This article was supported in part by funding from Bernard and Ronni Lacroute, the William Randolph Hearst Foundation, Marc Paskin and Penny Bradley to GS, and from the National Cancer Institute (F30CA228215) and the Stanford Medical Scientist Training Program (T32GM007365) to JH.

ACKNOWLEDGMENTS

We thank Christine Plant for editorial support.

REFERENCES

Aizman, I., Tate, C. C., McGrogan, M., and Case, C. C. (2009). Extracellular matrix produced by bone marrow stromal cells and by their derivative, SB623 cells, supports neural cell growth. *J. Neurosci. Res.* 87, 3198–3206. doi: 10.1002/jnr.22146

Albers, G. W., Marks, M. P., Kemp, S., Christensen, S., Tsai, J. P., Ortega-Gutierrez, S., et al. (2018). Thrombectomy for stroke at 6 to 16 hours with selection by perfusion imaging. *N. Engl. J. Med.* 378, 708–718. doi: 10.1056/NEJMoa1713973

Baker, E. W., Kinder, H. A., and West, F. D. (2019). Neural stem cell therapy for stroke: a multimechanistic approach to restoring neurological function. *Brain Behav.* 9:e01214. doi: 10.1002/brb3.1214

Banerjee, S., Bentley, P., Hamady, M., Marley, S., Davis, J., Shlebak, A., et al. (2014). Intra-arterial immunoselected CD34+ stem cells for acute ischemic stroke. *Stem Cells Transl. Med.* 3, 1322–1330. doi: 10.5966/sctm.2013-0178

Bang, O. Y., and Kim, E. H. (2019). Mesenchymal stem cell-derived extracellular vesicle therapy for stroke: challenges and progress. *Front. Neurol.* 10:211. doi: 10.3389/fneur.2019.00211

Bang, O. Y., Lee, J. S., Lee, P. H., and Lee, G. (2005). Autologous mesenchymal stem cell transplantation in stroke patients. *Ann. Neurol.* 57, 874–882. doi: 10.1002/ana.20501

Bani-Yaghoub, M., Felker, J. M., and Naus, C. C. (1999). Human NT2/D1 cells differentiate into functional astrocytes. *Neuroreport* 10, 3843–3846. doi: 10.1097/00001756-199912160-00022

Barbosa da Fonseca, L. M., Gutfilen, B., Rosado de Castro, P. H., Battistella, V., Goldenberg, R. C., Kasai-Brunswick, T., et al. (2010). Migration and homing of bone-marrow mononuclear cells in chronic ischemic stroke after intra-arterial injection. *Exp. Neurol.* 221, 122–128. doi: 10.1016/j.expneurol.2009.10.010

Barish, M. E., Herrmann, K., Tang, Y., Argalian Herculian, S., Metz, M., Aramburo, S., et al. (2017). Human neural stem cell biodistribution and predicted tumor coverage by a diffusible therapeutic in a mouse glioma model. *Stem Cells Transl. Med.* 6, 1522–1532. doi: 10.1002/sctm.16-0397

Benjamin, E. J., Blaha, M. J., Chiuve, S. E., Cushman, M., Das, S. R., Deo, R., et al. (2017). Heart disease and stroke statistics-2017 update: a report from the american heart association. *Circulation* 135, e146–e603. doi: 10.1161/CIR.0000000000000485

Berkhemer, O. A., Fransen, P. S., Beumer, D., van den Berg, L. A., Lingsma, H. F., Yoo, A. J., et al. (2015). A randomized trial of intraarterial treatment for acute ischemic stroke. *N. Engl. J. Med.* 372, 11–20. doi: 10.1056/NEJMoa1411587

Bhasin, A., Srivastava, M. V., Kumaran, S. S., Mohanty, S., Bhatia, R., Bose, S., et al. (2011). Autologous mesenchymal stem cells in chronic stroke. *Cerebrovasc. Dis. Extra* 1, 93–104. doi: 10.1159/000333381

Bhasin, A., Srivastava, M. V., Mohanty, S., Bhatia, R., Kumaran, S. S., and Bose, S. (2013). Stem cell therapy: a clinical trial of stroke. *Clin. Neurol. Neurosurg.* 115, 1003–1008. doi: 10.1016/j.clineuro.2012.10.015

Bhasin, A., Srivastava, M. V. P., Mohanty, S., Vivekanandhan, S., Sharma, S., Kumaran, S., et al. (2016). Paracrine mechanisms of intravenous bone marrow-derived mononuclear stem cells in chronic ischemic stroke. *Cerebrovasc. Dis. Extra* 6, 107–119. doi: 10.1159/000446404

Bliss, T. M., Andres, R. H., and Steinberg, G. K. (2010). Optimizing the success of cell transplantation therapy for stroke. *Neurobiol. Dis.* 37, 275–283. doi: 10.1016/j.nbd.2009.10.003

Boozer, S., Lehman, N., Lakshmipathy, U., Love, B., Raber, A., Maitra, A., et al. (2009). Global characterization and genomic stability of human multistem, a multipotent adult progenitor cell. *J. Stem Cells* 4, 17–28. doi: jsc.2009.4.1.17

Borlongan, C. V., Tajima, Y., Trojanowski, J. Q., Lee, V. M., and Sanberg, P. R. (1998). Transplantation of cryopreserved human embryonal carcinoma-derived neurons (NT2N cells) promotes functional recovery in ischemic rats. *Exp. Neurol.* 149, 310–321. doi: 10.1006/exnr.1997.6730

Campbell, B. C., Mitchell, P. J., Kleinig, T. J., Dewey, H. M., Churilov, L., Yassi, N., et al. (2015). Endovascular therapy for ischemic stroke with perfusion-imaging selection. *N. Engl. J. Med.* 372, 1009–1018. doi: 10.1056/NEJMoa1414792

Ceulemans, A. G., Zgavc, T., Kooijman, R., Hachimi-Idrissi, S., Sarre, S., and Michotte, Y. (2010). The dual role of the neuroinflammatory response after ischemic stroke: modulatory effects of hypothermia. *J. Neuroinflammation* 7:74. doi: 10.1186/1742-2094-7-74

Chen, J., Li, Y., Wang, L., Zhang, Z., Lu, D., Lu, M., et al. (2001). Therapeutic benefit of intravenous administration of bone marrow stromal cells after cerebral ischemia in rats. *Stroke* 32, 1005–1011. doi: 10.1161/01.str.32.4.1005

Chen, D. C., Lin, S. Z., Fan, J. R., Lin, C. H., Lee, W., Lin, C. C., et al. (2014). Intracerebral implantation of autologous peripheral blood stem cells in stroke patients: a randomized phase II study. *Cell Transplant.* 23, 1599–1612. doi: 10.3727/096368914X678562

Chen, L., Xi, H., Huang, H., Zhang, F., Liu, Y., Chen, D., et al. (2013). Multiple cell transplantation based on an intraparenchymal approach for patients with chronic phase stroke. *Cell Transplant.* 22 Suppl. 1, S83–S91. doi: 10.3727/096368913X672154

Chollet, F., Tardy, J., Albucher, J. F., Thalamas, C., Berard, E., Lamy, C., et al. (2011). Fluoxetine for motor recovery after acute ischaemic stroke (FLAME): a randomised placebo-controlled trial. *Lancet Neurol.* 10, 123–130. doi: 10.1016/S1474-4422(10)70314-8

Chung, A. G., Frye, J. B., Zbesko, J. C., Constantopoulos, E., Hayes, M., Figueroa, A. G., et al. (2018). Liquefaction of the brain following stroke shares a similar molecular and morphological profile with atherosclerosis and mediates secondary neurodegeneration in an osteopontin-dependent mechanism. *eNeuro* 5:ENEURO.0076-18.2018. doi: 10.1523/ENEURO.0076-18.2018

Dao, M. A., Tate, C. C., Aizman, I., McGrogan, M., and Case, C. C. (2011). Comparing the immunosuppressive potency of naive marrow stromal cells and Notch-transfected marrow stromal cells. *J. Neuroinflammation* 8:133. doi: 10.1186/1742-2094-8-133

Dao, M., Tate, C. C., McGrogan, M., and Case, C. C. (2013). Comparing the angiogenic potency of naive marrow stromal cells and Notch-transfected marrow stromal cells. *J. Transl. Med.* 11:81. doi: 10.1186/1479-5876-11-81

Dirnagl, U., Becker, K., and Meisel, A. (2009). Preconditioning and tolerance against cerebral ischaemia: from experimental strategies to clinical use. *Lancet Neurol.* 8, 398–412. doi: 10.1016/S1474-4422(09)70054-7

Dirnagl, U., and Macleod, M. R. (2009). Stroke research at a road block: the streets from adversity should be paved with meta-analysis and good laboratory practice. *Br. J. Pharmacol.* 157, 1154–1156. doi: 10.1111/j.1476-5381.2009.00211.x

Dunac, A., Frelin, C., Popolo-Blondeau, M., Chatel, M., Mahagne, M. H., and Philip, P. J. (2007). Neurological and functional recovery in human stroke are associated with peripheral blood CD34+ cell mobilization. *J. Neurol.* 254, 327–332. doi: 10.1007/s00415-006-0362-1

Eckert, M. A., Vu, Q., Xie, K., Yu, J., Liao, W., Cramer, S. C., et al. (2013). Evidence for high translational potential of mesenchymal stromal cell therapy to improve recovery from ischemic stroke. *J. Cereb. Blood Flow Metab.* 33, 1322–1334. doi: 10.1038/jcbfm.2013.91

Fang, J., Guo, Y., Tan, S., Li, Z., Xie, H., Chen, P., et al. (2019). Autologous endothelial progenitor cells transplantation for acute ischemic stroke: a 4-year follow-up study. *Stem Cells Transl. Med.* 8, 14–21. doi: 10.1002/sctm.18-0012

Friedrich, M. A., Martins, M. P., Araujo, M. D., Klamt, C., Vedolin, L., Garicochea, B., et al. (2012). Intra-arterial infusion of autologous bone marrow mononuclear cells in patients with moderate to severe middle cerebral artery acute ischemic stroke. *Cell Transplant.* 21 Suppl. 1, S13–S21. doi: 10.3727/096368912X612512

Giraldi-Guimardes, A., Rezende-Lima, M., Bruno, F. P., and Mendez-Otero, R. (2009). Treatment with bone marrow mononuclear cells induces functional recovery and decreases neurodegeneration after sensorimotor cortical ischemia in rats. *Brain Res.* 1266, 108–120. doi: 10.1016/j.brainres.2009.01.062

Goyal, M., Demchuk, A. M., Menon, B. K., Eesa, M., Rempel, J. L., Thornton, J., et al. (2015). Randomized assessment of rapid endovascular treatment of ischemic stroke. *N. Engl. J. Med.* 372, 1019–1030. doi: 10.1056/NEJMoa1414905

Gupta, N., Henry, R. G., Kang, S. M., Strober, J., Lim, D. A., Ryan, T., et al. (2019). Long-term safety, immunologic response and imaging outcomes following neural stem cell transplantation for Pelizaeus-Merzbacher disease. *Stem Cell Reports* 13, 254–261. doi: 10.1016/j.stemcr.2019.07.002

Gupta, N., Henry, R. G., Strober, J., Kang, S. M., Lim, D. A., Bucci, M., et al. (2012). Neural stem cell engraftment and myelination in the human brain. *Sci. Transl. Med.* 4:155ra137. doi: 10.1126/scitranslmed.3004373

Hacke, W., Kaste, M., Bluhmki, E., Brozman, M., Davalos, A., Guidetti, D., et al. (2008). Thrombolysis with alteplase 3 to 4.5 hours after acute ischemic stroke. *N. Engl. J. Med.* 359, 1317–1329. doi: 10.1056/NEJMoa0804656

Hao, L., Zou, Z., Tian, H., Zhang, Y., Song, C., Zhou, H., et al. (2015). Novel roles of perivascular nerves on neovascularization. *Neurol. Sci.* 36, 353–360. doi: 10.1007/s10072-014-2016-x

Hermann, D. M., Popa-Wagner, A., Kleinschnitz, C., and Doeppner, T. R. (2019). Animal models of ischemic stroke and their impact on drug discovery. *Expert Opin. Drug Discov.* 14, 315–326. doi: 10.1080/17460441.2019.1573984

Hess, D. C., Wechsler, L. R., Clark, W. M., Savitz, S. I., Ford, G. A., Chiu, D., et al. (2017). Safety and efficacy of multipotent adult progenitor cells in acute ischaemic stroke (MASTERS): a randomised, double-blind, placebo-controlled, phase 2 trial. *Lancet Neurol.* 16, 360–368. doi: 10.1016/S1474-4422(17)30046-7

Hicks, C., Stevanato, L., Stroemer, R. P., Tang, E., Richardson, S., and Sinden, J. D. (2013). *In vivo* and *in vitro* characterization of the angiogenic effect of CTX0E03 human neural stem cells. *Cell Transplant.* 22, 1541–1552. doi: 10.3727/096368912X657936

Honmou, O., Houkin, K., Matsunaga, T., Niitsu, Y., Ishiai, S., Onodera, R., et al. (2011). Intravenous administration of auto serum-expanded autologous mesenchymal stem cells in stroke. *Brain* 134, 1790–1807. doi: 10.1093/brain/awr063

Jiang, Y., Jahagirdar, B. N., Reinhardt, R. L., Schwartz, R. E., Keene, C. D., Ortiz-Gonzalez, X. R., et al. (2002). Pluripotency of mesenchymal stem cells derived from adult marrow. *Nature* 418, 41–49. doi: 10.1038/nature00870

Jovin, T. G., Chamorro, A., Cobo, E., de Miquel, M. A., Molina, C. A., Rovira, A., et al. (2015). Thrombectomy within 8 hours after symptom onset in ischemic stroke. *N. Engl. J. Med.* 372, 2296–2306. doi: 10.1056/NEJMoa1503780

Kalladka, D., Sinden, J., Pollock, K., Haig, C., McLean, J., Smith, W., et al. (2016). Human neural stem cells in patients with chronic ischaemic stroke (PISCES): a phase 1, first-in-man study. *Lancet* 388, 787–796. doi: 10.1016/S0140-6736(16)30513-X

Kastan, M. B., Schlaffer, E., Russo, J. E., Colvin, O. M., Civin, C. I., and Hilton, J. (1990). Direct demonstration of elevated aldehyde dehydrogenase in human hematopoietic progenitor cells. *Blood* 75, 1947–1950.

Keller, L. H. (2009). Bone marrow-derived aldehyde dehydrogenase-bright stem and progenitor cells for ischemic repair. *Congest. Heart Fail.* 15, 202–206. doi: 10.1111/j.1751-7133.2009.00101.x

Kelly, S., Bliss, T. M., Shah, A. K., Sun, G. H., Ma, M., Foo, W. C., et al. (2004). Transplanted human fetal neural stem cells survive, migrate and differentiate in ischemic rat cerebral cortex. *Proc. Natl. Acad. Sci. U S A* 101, 11839–11844. doi: 10.1073/pnas.0404474101

Klyushnenkova, E., Mosca, J. D., Zernetkina, V., Majumdar, M. K., Beggs, K. J., Simonetti, D. W., et al. (2005). T cell responses to allogeneic human mesenchymal stem cells: immunogenicity, tolerance and suppression. *J. Biomed. Sci.* 12, 47–57. doi: 10.1007/s11373-004-8183-7

Kondziolka, D., Steinberg, G. K., Wechsler, L., Meltzer, C. C., Elder, E., Gebel, J., et al. (2005). Neurotransplantation for patients with subcortical motor stroke: a phase 2 randomized trial. *J. Neurosurg.* 103, 38–45. doi: 10.3171/jns.2005.103.1.0038

Kondziolka, D., Wechsler, L., Goldstein, S., Meltzer, C., Thulborn, K. R., Gebel, J., et al. (2000). Transplantation of cultured human neuronal cells for patients with stroke. *Neurology* 55, 565–569. doi: 10.1212/wnl.55.4.565

Lakhan, S. E., Kirchgessner, A., and Hofer, M. (2009). Inflammatory mechanisms in ischemic stroke: therapeutic approaches. *J. Transl. Med.* 7:97. doi: 10.1186/1479-5876-7-97

Laskowitz, D. T., Bennett, E. R., Durham, R. J., Volpi, J. J., Wiese, J. R., Frankel, M., et al. (2018). Allogeneic umbilical cord blood infusion for adults with ischemic stroke: clinical outcomes from a phase I safety study. *Stem Cells Transl. Med.* 7, 521–529. doi: 10.1002/sctm.18-0008

Le Blanc, K., Tammik, C., Rosendahl, K., Zetterberg, E., and Ringden, O. (2003). HLA expression and immunologic properties of differentiated and undifferentiated mesenchymal stem cells. *Exp. Hematol.* 31, 890–896. doi: 10.1016/s0301-472x(03)00110-3

Lee, J. S., Hong, J. M., Moon, G. J., Lee, P. H., Ahn, Y. H., Bang, O. Y., et al. (2010). A long-term follow-up study of intravenous autologous mesenchymal stem cell transplantation in patients with ischemic stroke. *Stem Cells* 28, 1099–1106. doi: 10.1002/stem.430

Lee, J. Y., Kim, E., Choi, S. M., Kim, D. W., Kim, K. P., Lee, I., et al. (2016). Microvesicles from brain-extract-treated mesenchymal stem cells improve neurological functions in a rat model of ischemic stroke. *Sci. Rep.* 6:33038. doi: 10.1038/srep33038

Levy, M. L., Crawford, J. R., Dib, N., Verkh, L., Tankovich, N., and Cramer, S. C. (2019). Phase I/II study of safety and preliminary efficacy of intravenous allogeneic mesenchymal stem cells in chronic stroke. *Stroke* 50, 2835–2841. doi: 10.1161/STROKEAHA.119.026318

Li, Y., Chopp, M., Chen, J., Wang, L., Gautam, S. C., Xu, Y. X., et al. (2000). Intrastriatal transplantation of bone marrow nonhematopoietic cells improves functional recovery after stroke in adult mice. *J. Cereb. Blood Flow Metab.* 20, 1311–1319. doi: 10.1097/00004647-200009000-00006

Li, X., Zheng, W., Bai, H., Wang, J., Wei, R., Wen, H., et al. (2016). Intravenous administration of adipose tissue-derived stem cells enhances nerve healing and promotes BDNF expression *via* the TrkB signaling in a rat stroke model. *Neuropsychiatr. Dis. Treat.* 12, 1287–1293. doi: 10.2147/NDT.S104917

Macleod, M. R., Fisher, M., O'Collins, V., Sena, E. S., Dirnagl, U., Bath, P. M., et al. (2009). Good laboratory practice: preventing introduction of bias at the bench. *Stroke* 40, e50–52. doi: 10.1161/STROKEAHA.108.525386

Mead, G., Hackett, M. L., Lundstrom, E., Murray, V., Hankey, G. J., and Dennis, M. (2015). The focus, affinity and effects trials studying the effect(s) of fluoxetine in patients with a recent stroke: a study protocol for three multicentre randomised controlled trials. *Trials* 16:369. doi: 10.1186/s13063-015-0864-1

Modo, M., Stroemer, R. P., Tang, E., Patel, S., and Hodges, H. (2002). Effects of implantation site of stem cell grafts on behavioral recovery from stroke damage. *Stroke* 33, 2270–2278. doi: 10.1161/01.str.0000027693.50675.c5

Moniche, F., Gonzalez, A., Gonzalez-Marcos, J. R., Carmona, M., Pinero, P., Espigado, I., et al. (2012). Intra-arterial bone marrow mononuclear cells in ischemic stroke: a pilot clinical trial. *Stroke* 43, 2242–2244. doi: 10.1161/STROKEAHA.112.659409

Muir, K. W., Bulters, D., Willmot, M., Sprigg, N., Dixit, A., Ward, N., et al. (2020). Intracerebral implantation of human neural stem cells and motor recovery after stroke: multicentre prospective single-arm study (PISCES-2). *J. Neurol. Neurosurg. Psychiatry* 91, 396–401. doi: 10.1136/jnnp-2019-322515

Nogueira, R. G., Jadhav, A. P., Haussen, D. C., Bonafe, A., Budzik, R. F., Bhuva, P., et al. (2018). Thrombectomy 6 to 24 hours after stroke with a mismatch between deficit and infarct. *N. Engl. J. Med.* 378, 11–21. doi: 10.1056/NEJMoa1706442

Perin, E. C., Silva, G., Gahremanpour, A., Canales, J., Zheng, Y., Cabreira-Hansen, M. G., et al. (2011). A randomized, controlled study of autologous therapy with bone marrow-derived aldehyde dehydrogenase bright cells in patients with critical limb ischemia. *Catheter. Cardiovasc. Interv.* 78, 1060–1067. doi: 10.1002/ccd.23066

Perin, E. C., Silva, G. V., Zheng, Y., Gahremanpour, A., Canales, J., Patel, D., et al. (2012). Randomized, double-blind pilot study of transendocardial injection of autologous aldehyde dehydrogenase-bright stem cells in patients with ischemic heart failure. *Am. Heart. J.* 163, 415–421, 421 e411. doi: 10.1016/j.ahj.2011.11.020

Pollock, K., Stroemer, P., Patel, S., Stevanato, L., Hope, A., Miljan, E., et al. (2006). A conditionally immortal clonal stem cell line from human cortical neuroepithelium for the treatment of ischemic stroke. *Exp. Neurol.* 199, 143–155. doi: 10.1016/j.expneurol.2005.12.011

Prasad, K., Mohanty, S., Bhatia, R., Srivastava, M. V., Garg, A., Srivastava, A., et al. (2012). Autologous intravenous bone marrow mononuclear cell therapy for patients with subacute ischaemic stroke: a pilot study. *Indian J. Med. Res.* 136, 221–228.

Prasad, K., Sharma, A., Garg, A., Mohanty, S., Bhatnagar, S., Johri, S., et al. (2014). Intravenous autologous bone marrow mononuclear stem cell therapy for ischemic stroke: a multicentric, randomized trial. *Stroke* 45, 3618–3624. doi: 10.1161/STROKEAHA.114.007028

Qiao, L. Y., Huang, F. J., Zhao, M., Xie, J. H., Shi, J., Wang, J., et al. (2014). A two-year follow-up study of cotransplantation with neural stem/progenitor cells and mesenchymal stromal cells in ischemic stroke patients. *Cell Transplant.* 23 Suppl. 1, S65–S72. doi: 10.3727/096368914X684961

Reyes, M., Lund, T., Lenvik, T., Aguiar, D., Koodie, L., and Verfaillie, C. M. (2001). Purification and ex vivo expansion of postnatal human marrow mesodermal progenitor cells. *Blood* 98, 2615–2625. doi: 10.1182/blood.v98.9.2615

Rosado-de-Castro, P. H., Schmidt Fda, R., Battistella, V., Lopes de Souza, S. A., Gutfilen, B., Goldenberg, R. C., et al. (2013). Biodistribution of bone marrow mononuclear cells after intra-arterial or intravenous transplantation in subacute stroke patients. *Regen. Med.* 8, 145–155. doi: 10.2217/rme.13.2

Sandu, R. E., Balseanu, A. T., Bogdan, C., Slevin, M., Petcu, E., and Popa-Wagner, A. (2017). Stem cell therapies in preclinical models of stroke. Is the aged brain microenvironment refractory to cell therapy? *Exp. Gerontol.* 94, 73–77. doi: 10.1016/j.exger.2017.01.008

Saver, J. L., Goyal, M., Bonafe, A., Diener, H. C., Levy, E. I., Pereira, V. M., et al. (2015). Stent-retriever thrombectomy after intravenous t-PA vs. t-PA alone in stroke. *N. Engl. J. Med.* 372, 2285–2295. doi: 10.1056/NEJMoa1415061

Saver, J. L., Goyal, M., van der Lugt, A., Menon, B. K., Majoie, C. B., Dippel, D. W., et al. (2016). Time to treatment with endovascular thrombectomy and outcomes from ischemic stroke: a meta-analysis. *JAMA* 316, 1279–1288. doi: 10.1001/jama.2016.13647

Savitz, S. I., Dinsmore, J., Wu, J., Henderson, G. V., Stieg, P., and Caplan, L. R. (2005). Neurotransplantation of fetal porcine cells in patients with basal ganglia infarcts: a preliminary safety and feasibility study. *Cerebrovasc. Dis.* 20, 101–107. doi: 10.1159/000086518

Savitz, S. I., Misra, V., Kasam, M., Juneja, H., Cox, C. S., Jr., Alderman, S., et al. (2011). Intravenous autologous bone marrow mononuclear cells for ischemic stroke. *Ann. Neurol.* 70, 59–69. doi: 10.1002/ana.22458

Savitz, S. I., Yavagal, D., Rappard, G., Likosky, W., Rutledge, N., Graffagnino, C., et al. (2019). A phase 2 randomized, sham-controlled trial of internal carotid artery infusion of autologous bone marrow-derived ALD-401 cells in patients with recent stable ischemic stroke (RECOVER-Stroke). *Circulation* 139, 192–205. doi: 10.1161/CIRCULATIONAHA.117.030659

Schmidt-Pogoda, A., Bonberg, N., Koecke, M. H. M., Strecker, J. K., Wellmann, J., Bruckmann, N. M., et al. (2020). Why most acute stroke studies are positive in animals but not in patients: a systematic comparison of preclinical, early phase and phase 3 clinical trials of neuroprotective agents. *Ann. Neurol.* 87, 40–51. doi: 10.1002/ana.25643

Sharma, A., Sane, H., Gokulchandran, N., Khopkar, D., Paranjape, A., Sundaram, J., et al. (2014). Autologous bone marrow mononuclear cells intrathecal transplantation in chronic stroke. *Stroke Res. Treat.* 2014:234095. doi: 10.1155/2014/234095

Shichinohe, H., Ishihara, T., Takahashi, K., Tanaka, Y., Miyamoto, M., Yamauchi, T., et al. (2015). Bone marrow stromal cells rescue ischemic brain by trophic effects and phenotypic change toward neural cells. *Neurorehabil. Neural Repair* 29, 80–89. doi: 10.1177/1545968314525856

Shyu, W. C., Lin, S. Z., Chiang, M. F., Su, C. Y., and Li, H. (2006). Intracerebral peripheral blood stem cell (CD34+) implantation induces neuroplasticity by enhancing beta1 integrin-mediated angiogenesis in chronic stroke rats. *J. Neurosci.* 26, 3444–3453. doi: 10.1523/JNEUROSCI.5165-05.2006

Simpson, D. M., Goldenberg, J., Kasner, S., Nash, M., Reding, M. J., Zweifler, R. M., et al. (2015). Dalfampridine in chronic sensorimotor deficits after ischemic stroke: a proof of concept study. *J. Rehabil. Med.* 47, 924–931. doi: 10.2340/16501977-2033

Smith, E. J., Stroemer, R. P., Gorenkova, N., Nakajima, M., Crum, W. R., Tang, E., et al. (2012). Implantation site and lesion topology determine efficacy of a human neural stem cell line in a rat model of chronic stroke. *Stem Cells* 30, 785–796. doi: 10.1002/stem.1024

Steinberg, G. K., Kondziolka, D., Wechsler, L. R., Lunsford, L. D., Coburn, M. L., Billigen, J. B., et al. (2016). Clinical outcomes of transplanted modified bone marrow-derived mesenchymal stem cells in stroke: a phase 1/2a study. *Stroke* 47, 1817–1824. doi: 10.1161/STROKEAHA.116.012995

Steinberg, G. K., Kondziolka, D., Wechsler, L. R., Lunsford, L. D., Kim, A. S., Johnson, J. N., et al. (2018). Two-year safety and clinical outcomes in chronic ischemic stroke patients after implantation of modified bone marrow-derived mesenchymal stem cells (SB623): a phase 1/2a study. *J. Neurosurg.* 131, 1–11. doi: 10.3171/2018.5.JNS173147

Stonesifer, C., Corey, S., Ghanekar, S., Diamandis, Z., Acosta, S. A., and Borlongan, C. V. (2017). Stem cell therapy for abrogating stroke-induced neuroinflammation and relevant secondary cell death mechanisms. *Prog. Neurobiol.* 158, 94–131. doi: 10.1016/j.pneurobio.2017.07.004

Stroemer, P., Patel, S., Hope, A., Oliveira, C., Pollock, K., and Sinden, J. (2009). The neural stem cell line CTX0E03 promotes behavioral recovery and endogenous neurogenesis after experimental stroke in a dose-dependent fashion. *Neurorehabil. Neural Repair* 23, 895–909. doi: 10.1177/1545968309335978

Suarez-Monteagudo, C., Hernandez-Ramirez, P., Alvarez-Gonzalez, L., Garcia-Maeso, I., de la Cuetara-Bernal, K., Castillo-Diaz, L., et al. (2009). Autologous bone marrow stem cell neurotransplantation in stroke patients. An open study. *Restor. Neurol. Neurosci.* 27, 151–161. doi: 10.3233/RNN-2009-0483

Surugiu, R., Olaru, A., Hermann, D. M., Glavan, D., Catalin, B., and Popa-Wagner, A. (2019). Recent advances in mono- and combined stem cell therapies of stroke in animal models and humans. *Int. J. Mol. Sci.* 20:6029. doi: 10.3390/ijms20236029

Taguchi, A., Sakai, C., Soma, T., Kasahara, Y., Stern, D. M., Kajimoto, K., et al. (2015). Intravenous autologous bone marrow mononuclear cell transplantation for stroke: phase1/2a clinical trial in a homogeneous group of stroke patients. *Stem Cells Dev.* 24, 2207–2218. doi: 10.1089/scd.2015.0160

Tajiri, N., Kaneko, Y., Shinozuka, K., Ishikawa, H., Yankee, E., McGrogan, M., et al. (2013). Stem cell recruitment of newly formed host cells *via* a successful seduction? Filling the gap between neurogenic niche and injured brain site. *PLoS One* 8:e74857. doi: 10.1371/journal.pone.0074857

Tamaki, S., Eckert, K., He, D., Sutton, R., Doshe, M., Jain, G., et al. (2002). Engraftment of sorted/expanded human central nervous system stem cells from fetal brain. *J. Neurosci. Res.* 69, 976–986. doi: 10.1002/jnr.10412

Tate, C. C., Fonck, C., McGrogan, M., and Case, C. C. (2010). Human mesenchymal stromal cells and their derivative, SB623 cells, rescue neural cells *via* trophic support following in vitro ischemia. *Cell Transplant.* 19, 973–984. doi: 10.3727/096368910X494885

Uchida, N., Buck, D. W., He, D., Reitsma, M. J., Masek, M., Phan, T. V., et al. (2000). Direct isolation of human central nervous system stem cells. *Proc. Natl. Acad. Sci. U S A* 97, 14720–14725. doi: 10.1073/pnas.97.26.14720

Uchida, N., Chen, K., Dohse, M., Hansen, K. D., Dean, J., Buser, J. R., et al. (2012). Human neural stem cells induce functional myelination in mice with severe dysmyelination. *Sci. Transl. Med.* 4:155ra136. doi: 10.1126/scitranslmed.3004371

Veizovic, T., Beech, J. S., Stroemer, R. P., Watson, W. P., and Hodges, H. (2001). Resolution of stroke deficits following contralateral grafts of conditionally immortal neuroepithelial stem cells. *Stroke* 32, 1012–1019. doi: 10.1161/01.str.32.4.1012

Wu, K. J., Yu, S. J., Chiang, C. W., Lee, Y. W., Yen, B. L., Tseng, P. C., et al. (2018). Neuroprotective action of human wharton's jelly-derived mesenchymal stromal cell transplants in a rodent model of stroke. *Cell Transplant.* 27, 1603–1612. doi: 10.1177/0963689718802754

Yasuhara, T., Matsukawa, N., Hara, K., Maki, M., Ali, M. M., Yu, S. J., et al. (2009). Notch-induced rat and human bone marrow stromal cell grafts reduce ischemic cell loss and ameliorate behavioral deficits in chronic stroke animals. *Stem Cells Dev.* 18, 1501–1514. doi: 10.1089/scd.2009.0011

Yeo, S. H., Lim, Z. I., Mao, J., and Yau, W. P. (2017). Effects of central nervous system drugs on recovery after stroke: a systematic review and meta-analysis of randomized controlled trials. *Clin. Drug Investig.* 37, 901–928. doi: 10.1007/s40261-017-0558-4

Zbesko, J. C., Nguyen, T. V., Yang, T., Frye, J. B., Hussain, O., Hayes, M., et al. (2018). Glial scars are permeable to the neurotoxic environment of chronic stroke infarcts. *Neurobiol. Dis.* 112, 63–78. doi: 10.1016/j.nbd.2018.01.007

Zhang, R. L., Chopp, M., Roberts, C., Liu, X., Wei, M., Nejad-Davarani, S. P., et al. (2014). Stroke increases neural stem cells and angiogenesis in the neurogenic niche of the adult mouse. *PLoS One* 9:e113972. doi: 10.1371/journal.pone.0113972

Zhang, L., Wang, L. M., Chen, W. W., Ma, Z., Han, X., Liu, C. M., et al. (2017). Neural differentiation of human Wharton's jelly-derived mesenchymal stem cells improves the recovery of neurological function after transplantation in ischemic stroke rats. *Neural Regen. Res.* 12, 1103–1110. doi: 10.4103/1673-5374.211189

Zheng, X., Zhang, L., Kuang, Y., Venkataramani, V., Jin, F., Hein, K., et al. (2020). Extracellular vesicles derived from neural progenitor cells–a preclinical evaluation for stroke treatment in mice. *Transl. Stroke Res.* doi: 10.1007/s12975-020-00814-z

Zhou, H., Chang, S., and Rao, M. (2012). Human cord blood applications in cell therapy: looking back and look ahead. *Expert Opin. Biol. Ther.* 12, 1059–1066. doi: 10.1517/14712598.2012.691161

Conflict of Interest: GS is a consultant for Qool Therapeutics, Peter Lazic US, NeuroSave, SanBio, Audaxion Therapeutics, Zeiss and Surgical Theater.

The remaining authors declare that the research was conducted in the absence of any commercial or financial relationships that could be construed as a potential conflict of interest.

frontiers in Aging Neuroscience

ORIGINAL RESEARCH
published: 17 December 2020
doi: 10.3389/fnagi.2020.602688

Age-Dependent Activation and Neuronal Differentiation of Lgr5+ Basal Cells in Injured Olfactory Epithelium *via* Notch Signaling Pathway

Xuewen Li[1†], Meimei Tong[5†], Li Wang[2†], Yumei Qin[3], Hongmeng Yu[2,4]* and Yiqun Yu[1,2]**

[1]School of Life Sciences, Shanghai University, Shanghai, China, [2]Department of Otolaryngology, Eye, Ear, Nose and Throat Hospital, Shanghai Key Clinical Disciplines of Otorhinolaryngology, Fudan University, Shanghai, China, [3]School of Food Science and Bioengineering, Zhejiang Gongshang University, Hangzhou, China, [4]Research Units of New Technologies of Endoscopic Surgery in Skull Base Tumor, Chinese Academy of Medical Sciences, Beijing, China, [5]Ear, Nose and Throat Department, Yuecheng People's Hospital, Shaoxing, China

OPEN ACCESS

Edited by:
Gary K. Steinberg,
Stanford University, United States

Reviewed by:
Kenji Kondo,
The University of Tokyo, Japan
Yongfu Wang,
Stowers Institute for Medical Research, United States

***Correspondence:**
Yiqun Yu
yu_yiqun@fudan.edu.cn
Hongmeng Yu
hongmengyush@fudan.edu.cn
Yumei Qin
yqin@zjgsu.edu.cn

[†]These authors have contributed equally to this work

Received: 04 September 2020
Accepted: 16 November 2020
Published: 17 December 2020

Citation:
Li X, Tong M, Wang L, Qin Y, Yu H and Yu Y (2020) Age-Dependent Activation and Neuronal Differentiation of Lgr5+ Basal Cells in Injured Olfactory Epithelium via Notch Signaling Pathway. Front. Aging Neurosci. 12:602688. doi: 10.3389/fnagi.2020.602688

Aging is an important factor affecting function of smell, leading to the degeneration of mature olfactory sensory neurons and inducing the occurrence of smell loss. The mammalian olfactory epithelium (OE) can regenerate when subjected to chemical assaults. However, this capacity is not limitless. Inactivation of globose basal cells and failure to generate sensory neurons are the main obstacles to prevent the OE regeneration. Here, we found the significant attenuation in mature sensory neuronal generation and apparent transcriptional alternation in the OE from aged mice compared with young ones. The recruitment of leucine-rich repeat-containing G-protein coupled receptor 5 (Lgr5)-positive cells in injured OE was weakened in aged mice, and more Lgr5+ cells remained quiescence in aged OE postinjury. Lineage-traced progenies from Lgr5+ cells were significantly fewer in the OE with aging. Moreover, Notch activation enhanced the neuronal regeneration in aged OE, making the regenerative capacity of aged OE comparable with that of young animals after injury. The growth and morphology of three-dimensional (3D)-cultured organoids from the OE of young and aged mice varied and was modulated by small molecules regulating the Notch signaling pathway. Thus, we concluded that activation of Lgr5+ cells in injured OE was age dependent and Notch activation could enhance the capacity of neuronal generation from Lgr5+ cells in aged OE after injury.

Keywords: olfactory epithelium, olfactory sensory neuron, aging, LGR5, Notch, organoid

INTRODUCTION

The mammalian olfactory epithelium (OE) is a neuroepithelial structure that has self-renewal capacity throughout life. Horizontal basal cells (HBCs) and globose basal cells (GBCs) are two types of stem/progenitor cell populations responsible for the regeneration of injured OE (Jang et al., 2003; Chen et al., 2004; Schnittke et al., 2015; Schwob et al., 2017).

When subjected to chemical assaults, dormant stem cells (mainly HBCs) are recruited to generate GBCs and then differentiate into olfactory sensory neurons, sustentacular cells, and other cellular subtypes constituting the OE (Leung et al., 2007). Acute injury drives proliferating cells to differentiate into immature neurons expressing Tuj1 and GAP43, and then grow into mature neurons expressing olfactory marker protein (OMP) and PGP9.5. However, the neuro-regenerative capacity of basal cells in the OE is not limitless and aging is a principal element causing the sensory neuronal death and inactivation of GBCs (Child et al., 2018). Studies on both human and laboratory animals such as mice have shown age-related morphology and functional changes in the olfactory nerve epithelium (Mobley et al., 2014). Age-associated decline in the neuro-regenerative capacity of the injured OE is related with the weakness in proliferative activity (Suzukawa et al., 2011). Spontaneous lesions occur in the neuroepithelium and Bowman's glands in mouse olfactory mucosa with progression of aging (Kondo et al., 2009). Several biomarkers have been identified as hallmarks of the aged olfactory mucosa, such as low expression of extracellular matrix genes (Ueha et al., 2018b) and ApoE deficiency (Zhang et al., 2018). With the increase of age, the recovery rate slows down and respiratory metaplasia may occur (Suzukawa et al., 2011; Child et al., 2018). Strategies against age-related neuronal degradation have been reported, including insulin-like growth factor 1 (IGF-1) administration (Ueha et al., 2018a), intranasal treatment with fibroblast growth factor-2 (FGF-2; Fukuda et al., 2018), activation of inositol trisphosphate receptor type 3 (IP3R3), and the neuroproliferative factor neuropeptide Y (NPY) signaling (Jia and Hegg, 2015).

The Notch signaling pathway plays important roles in the entire organism development process and in maintaining tissue self-renewal (Artavanis-Tsakonas and Muskavitch, 2010). Activation of Notch signaling transduction leads to proteolysis of the Notch receptor, allowing intracellular domain of Notch (NICD) to enter the nucleus, and subsequently binds to DNA-binding proteins and assembles transcription complexes that activate corresponding downstream target genes (Kopan and Ilagan, 2009). Notch expression is present in the neurogenesis of the peripheral olfactory system (Doi et al., 2004), and various Notch subtypes play different roles in determining neuronal and glial lineage during development of the OE (Carson et al., 2006). Notch signaling is necessary to direct the neuronal differentiation in the OE regeneration (Herrick et al., 2018), and Notch1 is required to maintain dormancy of reserve HBCs (Herrick et al., 2017). Our previous work indicated that Notch1 activation enhanced the proliferation in leucine-rich repeat-containing G-protein coupled receptor 5 (Lgr5)-positive progenitor cells and regulated the generation of mature sensory neurons in the OE (Dai et al., 2018). Thus, it is of interest to elucidate whether the effect of aging on the OE regeneration will be counteracted *via* Notch signaling activation.

In this study, we elucidated the transcriptional change in the OE from young and aged mice. Aging attenuated the recruitment of Lgr5+ cells in injured OE. Previous work reported that Lgr5 marked GBCs in the OE (Chen et al., 2014) and Lgr5+/Notch1+ cells participated in the OE regeneration postinjury (Dai et al., 2018). Based on these findings, here, we showed that aging altered the stemness of Lgr5+ cells in injured OE, keeping more Lgr5+ cells in dormancy. In aged OE, the capacity of neuronal generation from Lgr5+ cells were weakened, while Notch activation mimicking by NICD overexpression offset aging-induced intervention on neuronal regeneration in injured OE. *In vitro*-cultured OE organoids from aged mice showed more apparent cystic morphology compared with those from young mice, which was altered by chemical treatment regulating the Notch signaling. Thus, these data supported the conclusion that aging was a critical factor determining the participation of Lgr5+ cells in OE regeneration, and the adverse effect of aging on neuronal differentiation was counteracted by Notch activation. This study supplemented new evidence to elucidate the regulatory role of Notch signaling in aging and OE regeneration.

MATERIALS AND METHODS

Animals

Lgr5-EGFP-IRES-CreERT2 (#008875, harboring a "knock-in" allele that abolishes Lgr5 gene function and expresses EGFP and CreERT2 fusion protein from the Lgr5 promoter/enhancer elements), Rosa26-TdTomato (#007914, a Cre reporter strain with a loxP-flanked STOP cassette prevents transcription of the downstream red fluorescent protein), and RosaNICD (#008159, containing a sequence encoding an intracellular portion of the mouse Notch1 gene with a loxP-flanked STOP cassette, leading to elevating intracellular signal transduction and mimicking Notch signaling pathway activation by Cre reporter) mice were purchased from the Jackson Laboratory. Mice were housed with open access to food and water at the Experimental Animal Center of Eye, Ear, Nose, and Throat Hospital, Fudan University (Shanghai, China). The animals were housed in a temperature-controlled environment (23 ± 2°C) with a light/dark cycle of 12 h. All experiments were approved by the Shanghai Medical Experimental Animal Administrative Committee (Permit Number: 2009-0082). Both male and female mice were used in this study, and the data were grouped together because no sex difference was evident. All animals were maintained at C57BL/6J background.

Chemical Treatment

All the reagents were purchased from Sigma Aldrich unless specified. The final concentration of chemicals used in organoid culture was: 5 μM LY411575 (#SML0506) and 40 ng/ml Jagged 1 (aa 1-1067, #SRP8012). LY411575 was dissolved in sterile-filtered DMSO (#D2650) while Jagged 1 was dissolved in sterile phosphate-buffered saline (PBS) to make stock solution. Chemicals were diluted by 1,000 times into the cultures. Organoids were treated with chemicals on Day 3 after passaging and incubated with chemicals for 4 days.

Establishment of OE Injury Model

Methimazole leads to a dose-dependent olfactory toxicity (Genter et al., 1995). For OE lesion, animals were

intraperitoneally injected with methimazole (50 μg/g body weight, #46429; Leung et al., 2007). In the saline control, the animals were injected with the same amount of PBS. The Lgr5-EGFP-CreERT2 mice were killed at Days 3, 5, 10, 17, and 32 after methimazole administration. Lgr5-EGFP-CreERT2/Rosa26-TdTomato (LT) and Lgr5-EGFP-CreERT2/Rosa26-TdTomato/RosaNICD (LTN) mice were killed at Day 30 postinjury for further analysis.

Lineage Tracing and Notch Activation Mimicking

For lineage tracing and Notch activation mimicking in injured OE, 220 μg/g (body weight) tamoxifen (#T5648) was injected subcutaneously into LT and LTN mice for respective three consecutive days just prior to and after methimazole administration (the scheme is shown as **Figure 6A**). In the control group, mice were received with same doses of sunflower seed oil (#S5007), served as a solvent to tamoxifen. For lineage tracing in LT mice with different ages including 1-, 3-, 12-, and 24-month old, three doses of tamoxifen (1 dose/day) was injected prior to the methimazole treatment. The scheme for lineage tracing was shown as **Figure 5A**. For lineage tracing, administration of tamoxifen induced the generation of Cre, removed the STOP cassette, and induced the expression of TdTomato. Thus, all TdTomato+ cells were Lgr5+ cells or progenies derived from Lgr5+ cells. For Notch activation mimicking, Cre induced by tamoxifen administration led to the expression of NICD and then activated Notch signaling pathway.

Immunofluorescence Staining

Mice were deeply anesthetized with an intraperitoneal injection of sodium pentobarbital (40 mg/kg, #P3761) and perfused transcardially with 0.9% saline, followed by 4% paraformaldehyde (#16005). Brains were postfixed overnight in the 4% paraformaldehyde and then were decalcified in 0.5 M EDTA (#15575020, Invitrogen^{TM}) until the skull became transparent. After being washed in PBS, tissues were equilibrated sequentially in 10, 20, and 30% sucrose (#S0389) and embedded in Tissue-Tek O.C.T. Compound (#4583, Sakura). OE tissues were cryosectioned to 20 μm slices using a Leica CM3050S Cryostat.

Immunofluorescence staining was performed according to a standard protocol. After rinsing with PBST (PBS plus 0.3% Triton X-100), the sections were blocked in PBST with 5% bovine serum albumin (#0332, AMRESCO) for 60 min, and then incubated with the primary antibodies overnight at 4°C. Then, the sections were incubated in secondary antibodies at room temperature for 1 h. The nuclei were counterstained with DAPI (#D3571, Thermo Fisher Scientific). Tissues were mounted in Vectashield Mounting Medium (#H1200, Vector Laboratories). Images were captured under a confocal laser scanning microscope ZEISS with Zen Software. The primary antibodies used in the immunostaining and their marked cellular subtypes, dilutions, vendors, and category numbers were as follows: rabbit anti-OMP (#ab87338, Abcam, 1:200, mature olfactory sensory neurons), mouse anti-TUJ1 (#ab78078, Abcan, 1:200, immature olfactory sensory neurons), rabbit anti-PGP9.5 (#14730-1-AP, Proteintech, 1:400, olfactory sensory neurons), mouse anti-Krt14 (#10143-1-AP, Proteintech, 1:200, horizontal basal cells), mouse anti-Krt19 (TROMA-III-c, DSHB, 1:300, ciliated respiratory epithelial cells), rabbit anti-Sox2 (#ab92494, Abcam, 1:200, supporting and basal cells), chicken anti-GFP (#ab13970, Abcam, 1:1,000, Lgr5-EGFP+ cells), rabbit anti-GFP (#A11122, Thermo Fisher Scientific, 1:500, Lgr5-EGFP+ cells), goat anti-Sox2 (#sc-17320, Santa Cruz Biotechnology, 1:200, supporting and basal cells), mouse anti-Ki67 (#550609, BD Biosciences, 1:100, proliferative basal cells), goat anti-ICAM1(#AF796, R&D, 1:500, horizontal basal cells), and mouse anti-Mash1 (#556604, BD Biosciences, 1:100, globose basal cells). All the secondary antibodies used in this study were purchased from Thermo Fisher Scientific and diluted as 1:300, including Alexa Fluor 594 Donkey anti-Rabbit (#A21207), Alexa Fluor 488 Donkey anti-Rabbit (#A21206), Alexa Fluor 594 Donkey anti-Goat (#A11058), Alexa Fluor 568 Donkey anti-Mouse (#A10037), Alexa Fluor 488 Donkey anti-Goat (#A11055), Alexa Fluor 633 Donkey anti-Goat (#A21082), Alexa Fluor 488 Donkey anti-Mouse (#A21202), Alexa Fluor 647 Donkey anti-Mouse IgG (#A31571), and Alexa Fluor 647 Donkey anti-Rabbit (#A31573).

OE Organoid Culture

Single cells from OE were cultured according to previously reported protocol with some modifications (Dai et al., 2018). Briefly, intact nasal mucosa of C57BL/6J mice at 3- and 19-month old was dissected and minced into small pieces using scissors in Tyrode's solution (145 mM NaCl, 5 mM KCl, 10 mM HEPES, 5 mM NaHCO3, 10 mM pyruvate, 10 mM glucose). Tissues were digested in 0.25% Trypsin-EDTA (#25200056, Gibco^{TM}) and 10 mg/ml DNase I (#11284932001, Roche) for 20 min at 37°C. Then samples were centrifuged at 1,200 r.p.m. for 5 min, and supernatant was discarded; ∼1 ml organoid growth medium (see below, no addition of Matrigel) was added, and tissues were mechanically dissociated into single cells using a 1-ml fire-polished syringe needle. Single cell suspension was filtered with 40-μm nylon mesh cell strainers (#352235, BD Falcon). Cells were seeded in ultra-low-attached 24-well plates (#3473, Corning) at density of $\sim 1 \times 10^4$ cells per well. OE organoid growth medium was based on DMEM/F12 medium (#10565018, Thermo Fisher Scientific) supplemented with R-Spondin-1 (200 ng/ml, #4645-RS, R&D), Noggin (100 ng/ml, #250–38, PeproTech), Wnt3a (50 ng/ml, #5036-WN-010, R&D), Y27632 (10 μM, #Y0503, Sigma Aldrich), epidermal growth factor (EGF, 50 ng/ml, #PHG0311, Thermo Fisher Scientific), N2 (1%, #17502001, Thermo Fisher Scientific), B27 (2%, #17504044, Thermo Fisher Scientific), HEPES (1 mM, #15630080, Thermo Fisher Scientific), and Matrigel (3% (Vol/Vol), #356231, BD Biosciences). Medium was changed every 3 days. Visible organoids were observed at Day 3 after seeding. For passaging, organoids at Day 10 after *in vitro* culture were digested using 0.25% Trypsin-EDTA for 10 min at 37°C. Organoids were resuspended in culture medium without addition of Matrigel, and single cell suspension was prepared by drawing through a 1-ml microsyringe. Cells were reseeded in ultra-low-attached 24-well plates at density of ∼5,000 cells per well.

RNA Sequence

The protocol for RNA sequence was described previously (Ren et al., 2020). RNA was prepared from mouse olfactory mucosa using TRIZOL reagent. RNA-Seq analysis was performed by Majorbio Corp. (Shanghai, China). Briefly, sequencing reads were mapped to the mouse genome using HISAT2. Transcriptome from RNA-seq reads was reconstructed by StringTie, and expression differences were evaluated using DESeq2. Pearson's coefficient was calculated to determine the correlation among different groups. The clustering analysis of the global gene expression pattern in different samples was carried out using K-means clustering algorithm by RSEM software. Gene Ontology (GO) and Kyoto Encyclopedia of Genes and Genomes (KEGG) pathway analysis were performed at http://www.geneontology.org/ and http://www.genome.jp/kegg/. I-Sanger (www.i-sanger.com) was used to analyze all the sequence data.

Statistical Analysis

Each experiment was repeated in triplicate independently. Quantitative data were expressed as mean ± SEM. The evaluators involved in assessing organoid size and cell counting were blinded to the experimental design including age and genotypes of the animals from which the specimens were derived. Organoid counting for the ratio of cystic and filled appearance were based on the images captured under bright field. The number of positively stained cells (including OMP+, Tuj1+, Krt19+, Krt14+, Sox2+, Lgr5-EGFP+, Lgr5+/Sox2+, Lgr5+/Ki67+, Lgr5+/Mash1+, Lgr5+/ICAM1+, TdTomato+, PGP9.5+, TdTomato+ (TdT+)/PGP9.5+, and TdT+/Sox2+ cells), organoid size, and OE thickness were measured by Image J Software. All the cell counting data were derived from the number of cells on six OE sections per mice. We biologically triplicated each experiment, thus 18 sections from three animals were used for each cell counting analysis. Each slide had OE sections from anterior to posterior zones. On each OE section, six different regions (three in dorsal and three in ventral) were selected to measure the cell density. These selected regions were consistent among all groups. The density of positively stained cells was defined as the number of positively stained cells per 100 μm or 0.5 mm OE. The density of TdT+ cells in **Figure 5** was defined as the number of TdT+ cells per OE section. The OE thickness was averaged from five different places on each OE section. Two-way ANOVA with Sidak's multiple comparisons test and Tukey's multiple comparisons test was used to determine the statistical difference among multiple groups, while comparison between two groups was performed by unpaired *t*-test using GraphPad Prism 6.0 software. p values < 0.05 were considered statistically significant.

RESULTS

Aging Attenuates Sensory Neuronal Generation in the OE

To elucidate the effect of aging on the OE, we performed immunostaining against various biomarkers for cellular subtypes constituting the OE in wild-type C57BL/6J mice at 3- and 25-month old. The intensity of staining against mature sensory neuronal markers OMP was weaker in the OE of aged animals compared with the young mice (**Figures 1A,C,D**, differential OMP+ staining signals were noted by dash lines in **Figure 1A**). The density of OMP+ cells was decreased by 28.0 ± 4.4% in aged OE compared with the young one (**Figure 1M**, $p = 0.0072$, $n = 3$ mice). The intensity of staining against immature neuronal marker TUJ1 did not show apparent difference (**Figures 1A,C,D**), while the density of TUJ1+ cells in aged OE was still significantly lowered by 18.3 ± 4.9% than the OE of young mice (**Figure 1M**, $p = 0.0213$, $n = 3$ mice). Besides, the intensity of PGP9.5+ staining signals in the OE of young mice was more intensive than the old animals (**Figures 1B,E,F**, PGP9.5+ staining signals were labeled by asterisks in **Figure 1B**). By contrast, staining against Krt19, a biomarker for columnar ciliated respiratory epithelial cells, was more obvious in the OE of aged animals compared with the young mice (**Figure 1B**, noted by dash lines, **Figures 1G,H**, noted by arrows). The density of Krt19+ cells in the OE from aged mice was significantly increased by 2.3 ± 0.3-fold, compared with the young OE (**Figure 1M**, $p < 0.001$). However, we did not observe the apparent change in apical Sox2+ staining (marker for sustentacular cells, **Figures 1I,J**) or in Krt14+ staining (marker for HBCs, **Figures 1K,L**). The density of apical Sox2+ sustentacular cells or Krt14+ basal cells was not significantly changed in the OE between aged and young animals (**Figure 1M**, $p = 0.3769$ for Krt14+ cells and $p = 0.6724$ for apical Sox2+ cells, $n = 3$). The OE thickness of aged mice was not significantly different from the young animals (**Figure 1N**, $p = 0.3151$). Thus, we concluded that aging led to the attenuation in mature sensory neuronal generation in the OE.

Transcriptional Alteration in Aged OE

To elucidate the panoramic effect of aging on the OE, we performed transcriptional analysis between the OE from aged and young animals at 3- and 25-month old, respectively. Totally, 1,342 upregulated and 1,005 downregulated genes were found in aged OE. By KEGG enrichment analysis, we found five upregulated and 265 downregulated genes associated with olfactory transduction in the OE of aged mice (**Figure 2A**). The heatmap showed that the expression level of HBC markers Krt14, Krt5, ICAM1, and respiratory epithelial cell marker Krt19 was increased in aged OE, while level of GBC markers NeuroD1, NeuroG1, Ascl1, neuronal marker OMP, Tuj1, and GAP43, as well as sustentacular cell marker Cyp2g1 was decreased (**Figures 2B,C**). KEGG pathway analysis found that genes involved in inflammation pathway such as NF-kappa B, PI3K-Akt, TNFα, JAK/STAT, and MAPK signaling were upregulated in aged OE (**Figure 2D**). Genes participating in critical signal pathways such as Wnt, Notch, and Hippo were differentially expressed between the OE from young and aged mice (**Figure 2D**). Thus, we provided a transcriptional landscape showing the alteration in the OE with aging.

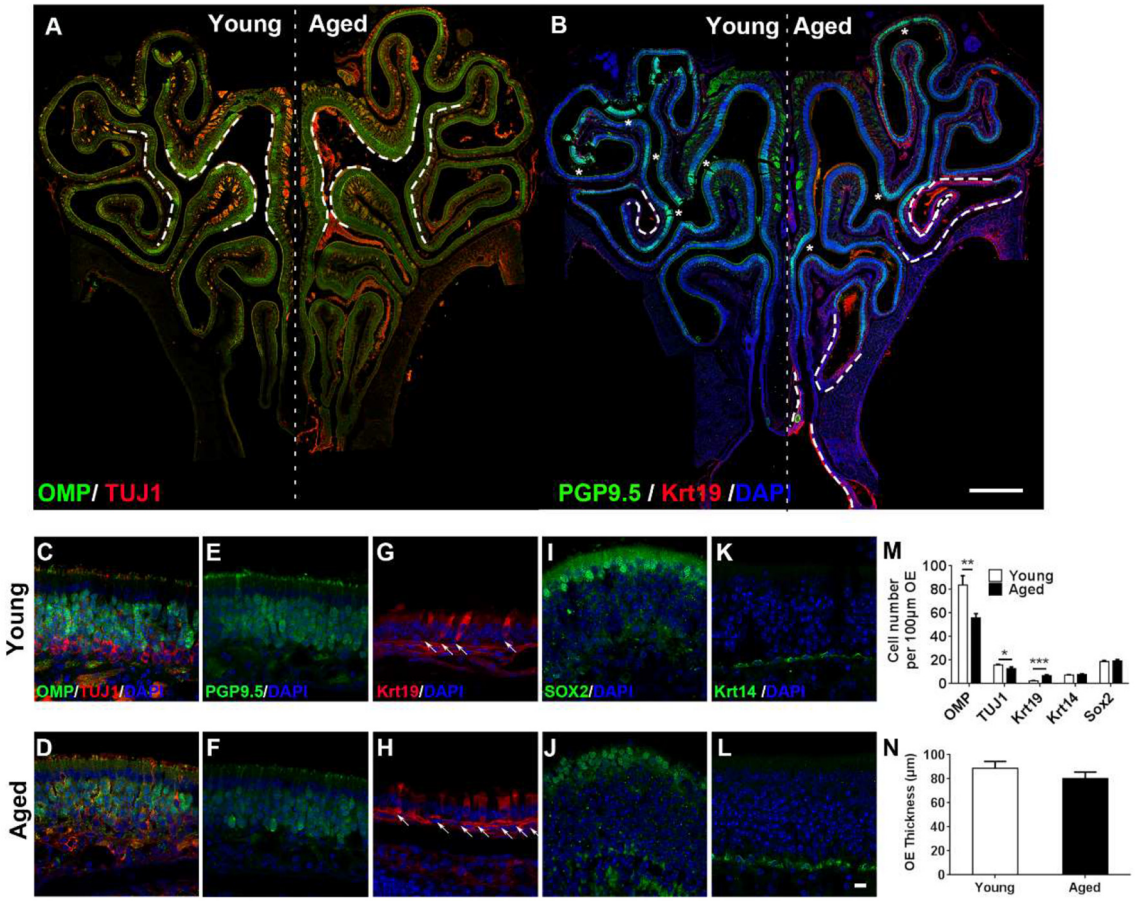

FIGURE 1 | Aging altered neuronal generation in the olfactory epithelium (OE). **(A)** Immunostaining against mature and immature sensory neuronal markers olfactory marker protein (OMP) and TUJ1 in the OE of young and aged mice at 3- and 25-month old. The positive signals against OMP were labeled by dash lines. **(B)** Immunostaining against sensory neuronal marker PGP9.5 (noted by asterisks) and columnar-ciliated respiratory epithelial cell marker Krt19 (noted by dash lines). **(C–L)** Confocal images of staining against OMP and TUJ1 **(C,D)**, PGP9.5 **(E,F)**, Krt19 (**G,H**, for respiratory epithelial cells, labeled by arrows), Sox2 (**I,J**, for apical supporting cells), and Krt14 (**K,L**, for HBCs) in the OE of young and aged mice. Nuclei were counterstained with DAPI, as shown in blue. **(M)** Statistical analysis of OMP+, TUJ1+, Krt19+, Krt14+, and apical Sox2+ cell density in the OE of young and aged mice. In young and aged OE, 1,406 and 723 OMP+, 262 and 179 TUJ1+, 162 and 133 Krt19+, 98 and 139 Krt14+, and 182 and 222 apical Sox2+ cells were counted. **(N)** Statistical analysis of OE thickness from young and aged mice. Each OE thickness was calculated from 18 sections of three mice. The statistical significance was determined by unpaired *t*-test with Mann–Whitney correction. $^{**}p = 0.0072$, $^{***}p < 0.001$ in **(M)**, $^{*}p = 0.3151$ in **(N)**. Scale bars: 0.5 mm in **(B)** and 10 μm in **(L)**.

Aging Leads to the Attenuation in Recruitment of Lgr5+ Cells in Injured OE

Lgr5 marks GBCs and Lgr5+ GBCs are recruited in injured OE (Chen et al., 2014; Dai et al., 2018). Since GBC markers such as Ascl1, NeuroD1, and NeuroG1 at transcriptional level were decreased in aged OE (**Figures 2B,C**), we determined whether aging weakened the recruitment of Lgr5+ GBCs in lesioned OE. Lgr5-EGFP-CreERT2 mice at 1- and 12-month old were injected with methimazole, and the density of Lgr5-EGFP+ cells was measured postlesion. The recruitment of Lgr5-EGFP+ cells in injured OE was not significantly different at Day 3 postinjury between 1- and 12-month-old mice (**Figures 3A,B**) but significantly retarded at Day 5 in aged OE (**Figures 3C,D**). Statistically, the density of Lgr5-EGFP+ cells was significantly increased in injured OE of both 1- and 12-month-old mice at Day 3 postlesion compared with the unlesioned controls (**Figure 3M**, $p < 0.001$ by unpaired *t*-test, $n = 3$). However, the density of Lgr5-EGFP+ cells was still drastically enhanced at Day 5 in young animals ($p < 0.001$ compared with Day 3, $n = 3$) while the density was reduced in the OE of 12-month-old mice at Day 5 compared with the density at Day 3 postinjury and not significantly changed in contrast to the saline control (**Figure 3M**). At Days 10, 17, and 32 postinjury, the density of Lgr5-EGFP+ cells at basal cell layer in the OE of both 1- and 12-month-old mice continued to decrease in contrast to the density at Day 5 and returned to the threshold level similar as the density of Lgr5-EGFP+ cells in the saline control (**Figures 3E–M**). Compared with the OE of young mice, the density of Lgr5-EGFP+ cells in aged OE at Days 5 and 32 postinjury was significantly decreased (**Figure 3M**, $p < 0.001$ at Day 5 and $p < 0.05$ at Day 32 using two-way ANOVA with Sidak's multiple comparisons test). Surprisingly, the Lgr5-EGFP+ cells appeared in the nonbasal cell layer during the

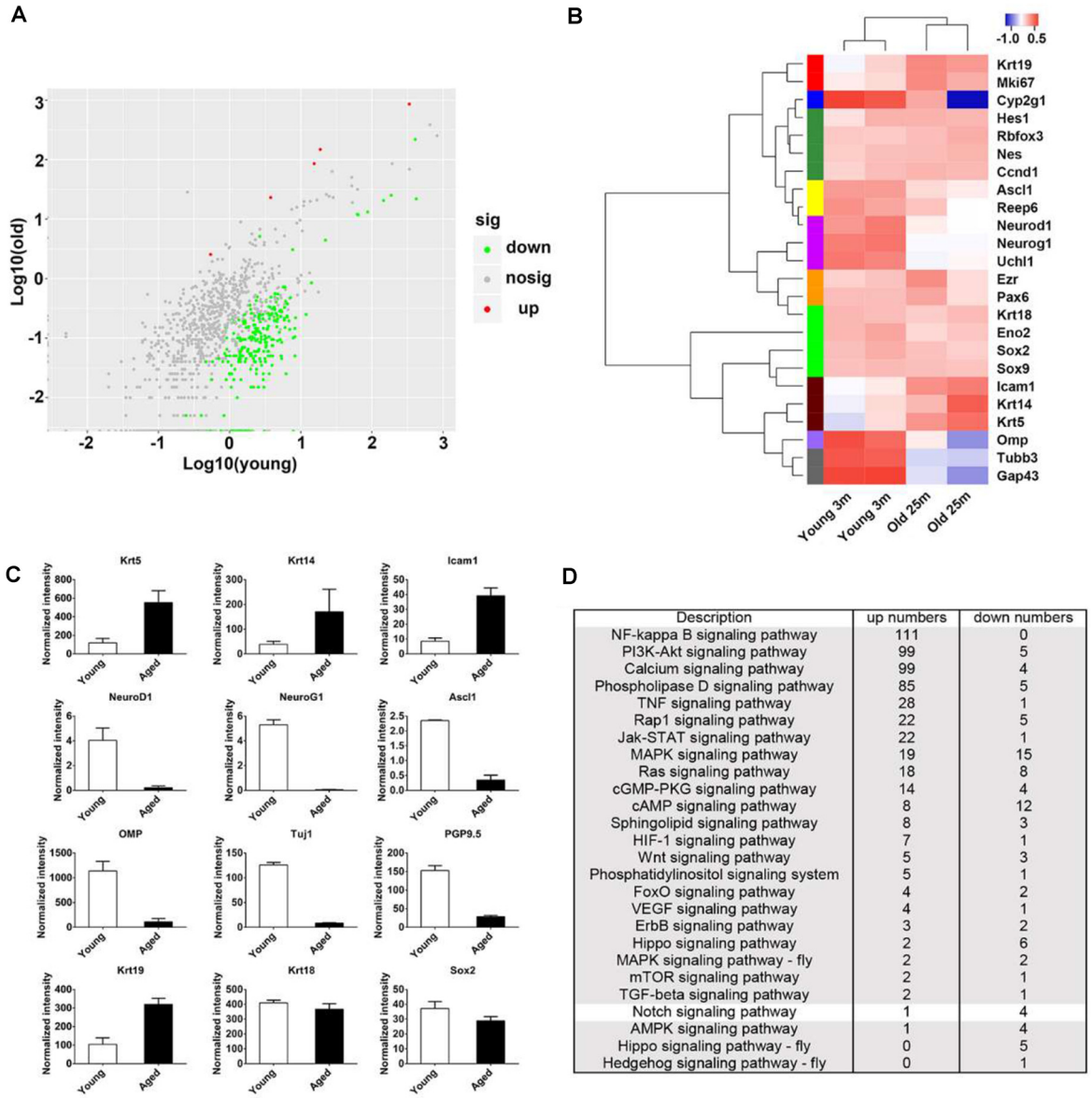

Description	up numbers	down numbers
NF-kappa B signaling pathway	111	0
PI3K-Akt signaling pathway	99	5
Calcium signaling pathway	99	4
Phospholipase D signaling pathway	85	5
TNF signaling pathway	28	1
Rap1 signaling pathway	22	5
Jak-STAT signaling pathway	22	1
MAPK signaling pathway	19	15
Ras signaling pathway	18	8
cGMP-PKG signaling pathway	14	4
cAMP signaling pathway	8	12
Sphingolipid signaling pathway	8	3
HIF-1 signaling pathway	7	1
Wnt signaling pathway	5	3
Phosphatidylinositol signaling system	5	1
FoxO signaling pathway	4	2
VEGF signaling pathway	4	1
ErbB signaling pathway	3	2
Hippo signaling pathway	2	6
MAPK signaling pathway - fly	2	2
mTOR signaling pathway	2	1
TGF-beta signaling pathway	2	1
Notch signaling pathway	1	4
AMPK signaling pathway	1	4
Hippo signaling pathway - fly	0	5
Hedgehog signaling pathway - fly	0	1

FIGURE 2 | Transcriptional analysis on the OE from young and aged mice at 3- and 25-month old. **(A)** Scatter plot showing the up- and downregulated as well as nondifferentially expressed genes in the OE from young and aged mice. **(B)** Heatmap showed the significantly differentially expressed biomarkers for cellular lineages in the OE from young and aged mice. **(C)** Statistical analysis of differential mRNA levels of OE biomarkers using RNA-seq data. **(D)** KEGG enrichment analysis indicated differentially expressed genes between the OE from young and aged mice participating in multiple signaling pathways including Notch.

recovery of OE from methimazole-induced lesion at Days 10, 17, and 31 (**Figures 3E–J**, labeled by arrowheads in **Figures 3E′–J′**). The density of nonbasal Lgr5-EGFP+ cells was significantly increased at Days 10, 17, and 31 postinjury in the OE of 12-month-old mice, compared with the density in unlesioned controls (**Figure 3N**, $p < 0.001$ by unpaired t-test, $n = 3$), while the density of Lgr5+ nonbasal cells was dramatically increased at Days 17 and 31 postinjury in the OE of young animals (**Figure 3N**, $p < 0.001$, $n = 3$). Compared with the young mice, the density of nonbasal Lgr5-EGFP+ cells in the aged OE was significantly increased at Days 10 and 17 postinjury (**Figure 3N**, $p < 0.01$ at Day 10 and $p < 0.001$ at Day 17 using two-way ANOVA with Sidak's multiple comparisons test). Collectively, these data demonstrated that aging weakened the recruitment of Lgr5+ basal cells in injured OE.

Aging Alters the Stemness of Lgr5+ Cells in Injured OE

Since aging attenuated the recruitment of Lgr5+ basal cells in injured OE, we determined whether the stemness of Lgr5+ cells was affected in aged mice compared with the young ones. At Days 3 and 5 postinjury, we observed the apparent recruitment

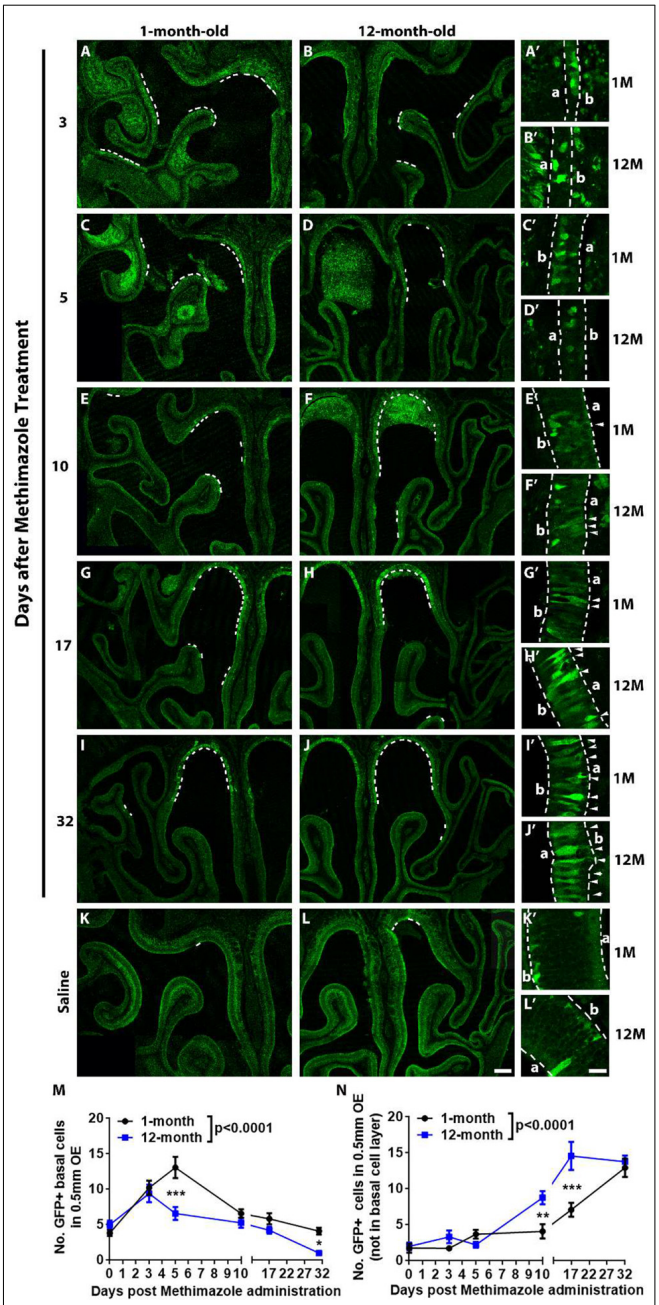

FIGURE 3 | Aging led to the attenuation in recruitment of Lgr5+ cells in injured OE. Confocal images of Lgr5-EGFP+ cells in the OE of 1- and 12-month-old Lgr5-EGFP-CreERT2 mice at Day 3 **(A,B)**, Day 5 **(C,D)**, Day 10 **(E,F)**, Day 17 **(G,H)**, and Day 32 **(I,J)** postinjury as well as in the OE of uninjured saline control **(K,L)**. Positive staining against GFP was labeled by dash lines in **(A–L)**. Panels **(A'–L')** were magnified regions in **(A–L)**. Lgr5-EGFP+ cells in the nonbasal layers were labeled by arrowheads. Dash lines in **(A'–L')** represented boundary of the OE. **(M,N)** Statistical analysis of Lgr5-EGFP+ cell density in basal and nonbasal cell layers of injured OE from young and aged mice. At Days 3, 5, 10, 17, and 32 postinjury, 207, 798, 549, 336, 333, and 222 Lgr5-EGFP+ basal cells were counted in saline controls and in 1-month-old mice. In 12-month-old mice, 150, 480, 237, 348, 279, and 51 Lgr5-EGFP+ basal cells were counted. In 1- and 12-month-old mice, 111, 141, 144, 258, 447, 738 Lgr5-EGFP+ nonbasal cells and 66, 180, 87, 474,

(Continued)

FIGURE 3 | Continued
831, and 744 Lgr5-EGFP+ nonbasal cells were counted. In **(A'–L')**, **a** and **b** denote apex and base. The statistical significance was determined by two-way ANOVA. $F_{(5,200)} = 24.75$, $p < 0.0001$ between 1- and 12-month-old mice in **(M)**; $F_{(5,207)} = 44.29$, $p < 0.0001$ in **(N)**. The significance at the same-day postinjury between 1- and 12-month-old mice (noted by asterisks) was determined by Sidak's multiple comparisons test. The significance at different time points postinjury compared with uninjured control was determined by unpaired *t*-test. Scale bars: 0.2 mm in **(L)** and 20 μm in **(L')**.

of Lgr5+/Sox2+ basal cells (**Figures 4A,B**), Lgr5+/Ki67+ proliferative cells (**Figures 4E,F**), and Lgr5+/Mash1+ GBCs (**Figures 4I,J**) in the OE of 1-month-old mice. By contrast, Lgr5+/Ki67+ and Lgr5+/Mash1+ cells were only recruited at Day 3 in injured OE of 12-month-old mice, but their densities was significantly decreased compared with the counterparts in young mice at Day 3 (**Figures 4E,G,I,K,Q**, $p < 0.001$ for Lgr5+/Ki67+ cell density, $p < 0.05$ for Lgr5+/Mash1+ cell density). However, there was barely Lgr5+/Ki67+ or Lgr5+/Mash1+ cells in injured OE of aged mice at Day 5 (**Figures 4H,L,Q**). However, Lgr5+/Sox2+ cells were apparently activated at Day 3 and still present at Day 5 postinjury in the OE of 12-month-old mice (**Figures 4C,D**). In 1-month-old mice, Lgr5+ cells were not co-immunostained with ICAM1, a biomarker for HBCs, at Days 3 and 5 postlesion (**Figures 4M,N**, squares were magnified as **Figures 4M′,N′**). By comparison, Lgr5+/ICAM1+ cells were found in the OE of 12-month-old mice at Days 3 and 5 postinjury (**Figures 4O,P**, labeled by arrowheads in magnified squares as **Figures 4O′,P′**). The density of Lgr5+/ICAM1+ cells was significantly increased in injured OE of 12-month-old mice at Days 3 and 5, compared with the density in the OE of 1-month-old mice (**Figure 4Q**, $p < 0.001$ by two-way ANOVA with Tukey's multiple comparisons test). This showed a portion of Lgr5+ cells remained in dormancy in injured OE of aged mice. Collectively, we concluded that aging led to the alteration in stemness of injury-recruited Lgr5+ cells in the OE, keeping some Lgr5+ cells in dormancy after OE injury.

Aging Weakens Progeny Generation From Lgr5+ Cells in Injured OE

Since Lgr5+ cells in the OE from young and aged animals were differentially recruited postinjury, we then determined whether the progeny generation from Lgr5+ cells in injured OE was affected by aging. Lineage tracing of Lgr5+ cells in LT mice through tamoxifen administration (**Figure 5A**) showed the TdT+ cell bundles (progenies from Lgr5+ cells) were obvious in the OE from mice at 1- and 3-month old (**Figures 5B,C**, noted by asterisks). In mice at 12-month old, single TdT+ cells were scattered throughout the OE while the cell bundles were seldom observed (**Figure 5D**). However, fewer TdT+ cells were present in injured OE of LT mice at 24-month old (**Figure 5E**). Statistical analysis indicated that the density of TdT+ cells (number of TdT+ cells per half OE section) was significantly lowered by 77.7 ± 14.4 and 75.3 ± 4.4% in injured OE of 12- and 24-month-old mice compared with that in the OE of 1-month-old animals (**Figure 5F**, $p = 0.0014$ and $p = 0.0002$ by unpaired *t*-test). Similarly, the density of TdT+ cells in the OE of 12-

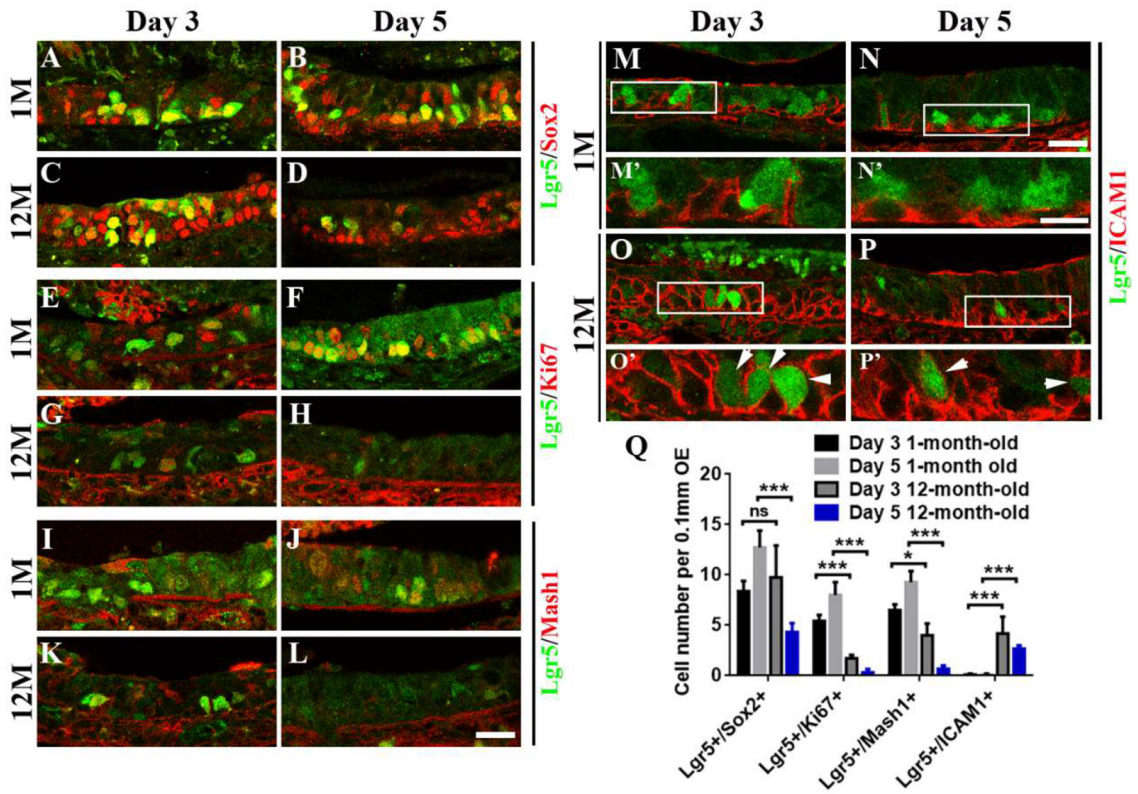

FIGURE 4 | Aging altered the stemness of Lgr5+ cells in injured OE. Immunostaining against GFP and basal cell marker Sox2 **(A–D)**, GFP and proliferative cell marker Ki67 **(E–H)**, GFP and GBC marker Mash1 **(I–L)**, GFP and HBC marker ICAM1 **(M–P)** in the OE of 1- and 12-month-old Lgr5-EGFP-CreERT2 mice at Days 3 and 5 postinjury. Panels **(M'–P')** were the magnification of squared regions in **(M–P)**. Lgr5-EGFP+/ICAM1+ cells were labeled by arrowheads in **(O',P')**. **(Q)** Statistical analysis on the density of Lgr5+/Sox2+, Lgr5+/Ki67+, Lgr5+/Mash1+, and Lgr5+/ICAM1+ cells in the OE of 1- and 12-month-old mice at Days 3 and 5 postinjury. At Days 3 and 5 postinjury, 603 and 420 Lgr5+/Sox2+ cells, 147 and 336 Lgr5+/Ki67+ cells, and 156 and 390 Lgr5+/Mash1+ cells were counted in 1-month-old mice. At Days 3 and 5, 375 and 195 Lgr5+/Sox2+ cells, 57 and 19 Lgr5+/Ki67+ cells, 108 and 18 Lgr5+/Mash1+ cells, and 153 and 72 Lgr5+/ICAM1+ cells were counted in 12-month-old mice. The statistical significance was determined by two-way ANOVA. $F_{(3,108)} = 84.92$, $p < 0.0001$. The asterisks were determined by Tukey's multiple comparisons test. Scale bars: 20 μm in **(L,N)** and 10 μm in **(N')**; ns, not significant.

and 24-month-old mice was decreased by 73.8 ± 16.9 and 70.9 ± 5.1% compared with the density in mice at 3-month old (**Figure 5F**, $p = 0.0055$ and $p = 0.0002$). Furthermore, we observed the apparent TdT+/PGP9.5+ cells in the OE of young mice at Day 30 postinjury (**Figure 5G**, noted by arrowheads), while significantly fewer TdT+/PGP9.5+ cells were found in the OE of 12-month-old mice at Day 30 postinjury (**Figure 5H**). Statistically, the density of TdT+/PGP9.5+ cells in LT mice at 12-month old was decreased by 51.6 ± 6.6% compared with 1-month-old mice (**Figure 5K**, $p = 0.0025$). Meanwhile, TdT+/Sox2+ cells were present in the OE of both 1- and 12-month old at Day 30 and did not show the apparent difference (**Figures 5I–K**, $p = 0.8356$, noted by arrowheads). Therefore, aging dampened neuronal differentiation of Lgr5+ cells in injured OE.

Notch Activation Strengthens Neuronal Regeneration in Aged OE

To determine whether the Notch signaling pathway could differentially regulate the neuronal regeneration in injured OE of young and aged mice, LTN mice at 1- and 12-month old were injected with tamoxifen to induce the overexpression of NICD (**Figure 6A**). With Notch activation mimicking, we found the significant increase in TdT+ cell density by 31.8 ± 6.5% in the OE of 12-month-old LTN mice compared with the density in 12-month-old LT mice (**Figures 6C,E,N**, $p = 0.0081$ by unpaired *t*-test). However, the TdT+ cell density was not significantly different between the OE of 1-month-old LT and LTN mice (**Figures 6B,D,N**, $p = 0.8864$). Furthermore, the TdT+ cell density in the OE of LTN mice at 12-month old was comparable with that in the OE of LT mice at 1-month old (**Figure 6N**, $p = 0.4518$), suggesting Notch activation enhanced the progeny generation from Lgr5+ cells in the OE of aged mice to the similar level as in the young animals. Staining against PGP9.5 was denser in the OE of LTN mice at both 1- and 12-month old, compared with the counterparts in LT mice (**Figures 6B–E**). The density of PGP9.5+ cells was higher in LTN mice at both 1- and 12-month old by 36.8 ± 7.4 and 26.7 ± 5.9%, compared with the counterparts in LT mice (**Figure 6O**, $p < 0.05$ by two-way ANOVA with Sidak's multiple comparisons test). By contrast,

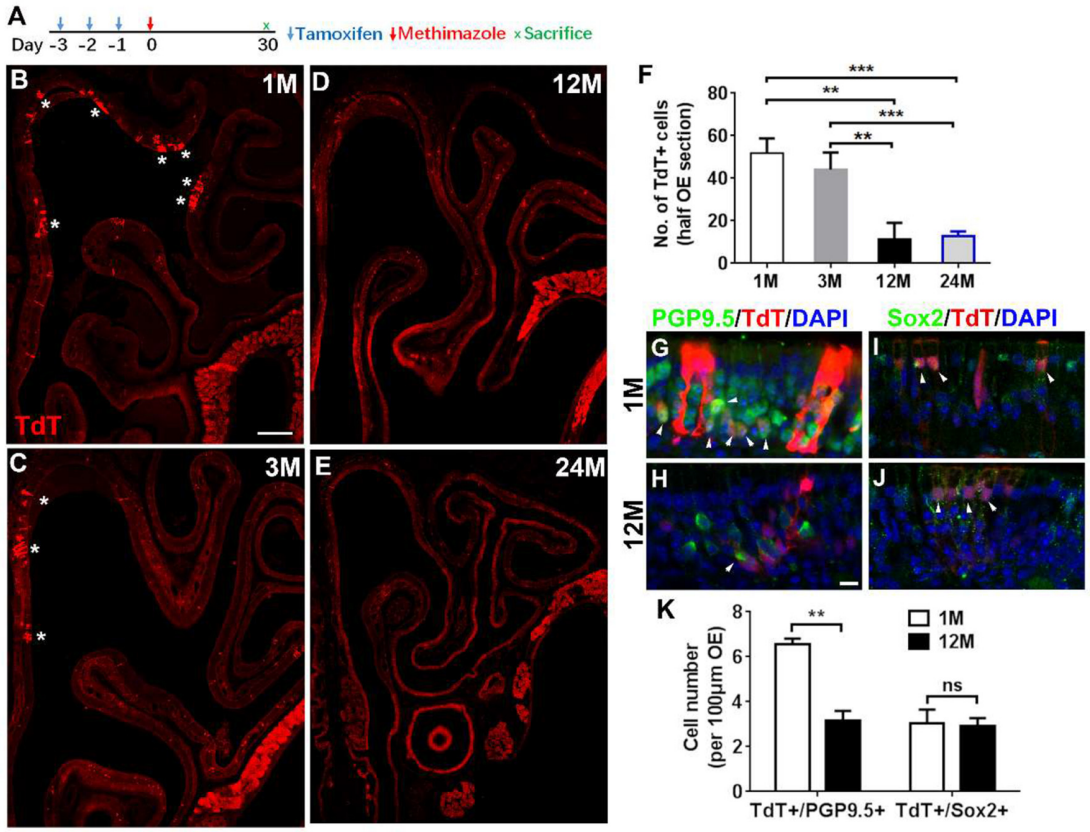

FIGURE 5 | Aging reduced the progenies of Lgr5+ cells in injured OE. **(A)** Scheme showing the lineage tracing of Lgr5+ cells in Lgr5-CreERT2/Rosa26-TdTomato (LT) mice. **(B–E)** Confocal images of lineage-traced TdT+ cells in the OE of LT mice at 1-, 3-, 12-, and 24-month old at Day 30 postinjury. *In **(B)** and **(C)** denoted TdT+ cell bundles. **(F)** Statistical analysis of TdT+ cell density in the OE at Day 30 postinjury. Totally, 2, 525, 921, 766, and 289 TdT+ cells were counted in mice at 1-, 3-, 12-, and 24-month old ($n = 3$). **(G,H)** Immunostaining against PGP9.5 in the OE of 1- and 12-month-old LT mice at Day 30. TdT+/PGP9.5+ cells were noted by arrowheads in **(G,H)**. **(I,J)** Confocal images of TdT+/Sox2+ cells (arrowheads labeled) in the OE of 1- and 12-month-old LT mice at Day 30. **(K)** Statistical analysis on the density of TdT+/PGP9.5+ and TdT+/Sox2+ cells in LT mice at 1- and 12-month old. Statistical significance was determined by unpaired *t*-test. ns, not significant. In **(F)** and **(K)**, $^{**}p < 0.01$, $^{***}p < 0.001$. Scale bars: 0.2 mm in **(B)** and 20 μm in **(H)**.

the density of apical Sox2+-supporting cells did not show a significant difference in the OE of LT and LTN mice at either 1- or 12-month old (**Figure 6O**, $p > 0.1$). The TdT+/PGP9.5+ cell density was significantly increased by 60.8 ± 14.5% ($p < 0.05$) and 125.3 ± 25.0% ($p < 0.01$) in the OE of young and aged LTN mice compared with the density in LT mice (**Figures 6F–I,P**, noted by arrowheads), while the density of TdT+/Sox2+ cells did not apparently change with Notch activation (**Figures 6J–M,P**, $p > 0.1$). Thus, Notch activation mimicking through NICD overexpression enhanced the neuronal regeneration capacity in aged OE postinjury, making it comparable with the young OE.

Notch Regulates Aging-Induced Morphological Alteration in OE Organoids

We then determined whether Notch signaling could regulate the aging-induced variation in OE organoid growth *in vitro*. The organoid size was not significantly different at Day 3 postculture but drastically increased in organoids from aged mice (19-month-old) at Day 7 (**Figures 7A–E**, $p < 0.001$ by two-way ANOVA with Sidak's multiple comparisons test). Compared with the organoids from young mice (3-month-old), percentage of organoids from aged mice with "filled" morphology was decreased by 23.7 ± 2.8%, while the ratio of cystic organoids was increased by 42.1 ± 2.8% (**Figures 7A–D,F**, $p < 0.001$). Then, we elucidated whether regulation of Notch signaling by small molecule chemicals *in vitro* could affect the organoid size and morphology. In the presence of Notch activator Jagged1, the size of organoids from aged mice was increased by 51.9 ± 5.1% compared with the organoids derived from young OE (**Figures 7H,K,M**, $p < 0.001$ by two-way ANOVA with Sidak's multiple comparisons test). By contrast, size of DMSO-treated control organoids from young animals was only increased by 16.2 ± 4.7% (**Figures 7G,J,M**, $p < 0.01$). The size change in organoids from young and aged mice was significantly different between DMSO- and Jagged1-treated groups ($p < 0.001$ by unpaired *t*-test). Notch inhibitor LY411575 led to an increase in organoid size only by 21.7 ± 4.0% (**Figures 7I,L,M**, $p < 0.05$), which was not significantly different from the size change between DMSO-treated organoids from young and aged OE ($p > 0.4$). Furthermore, regulation

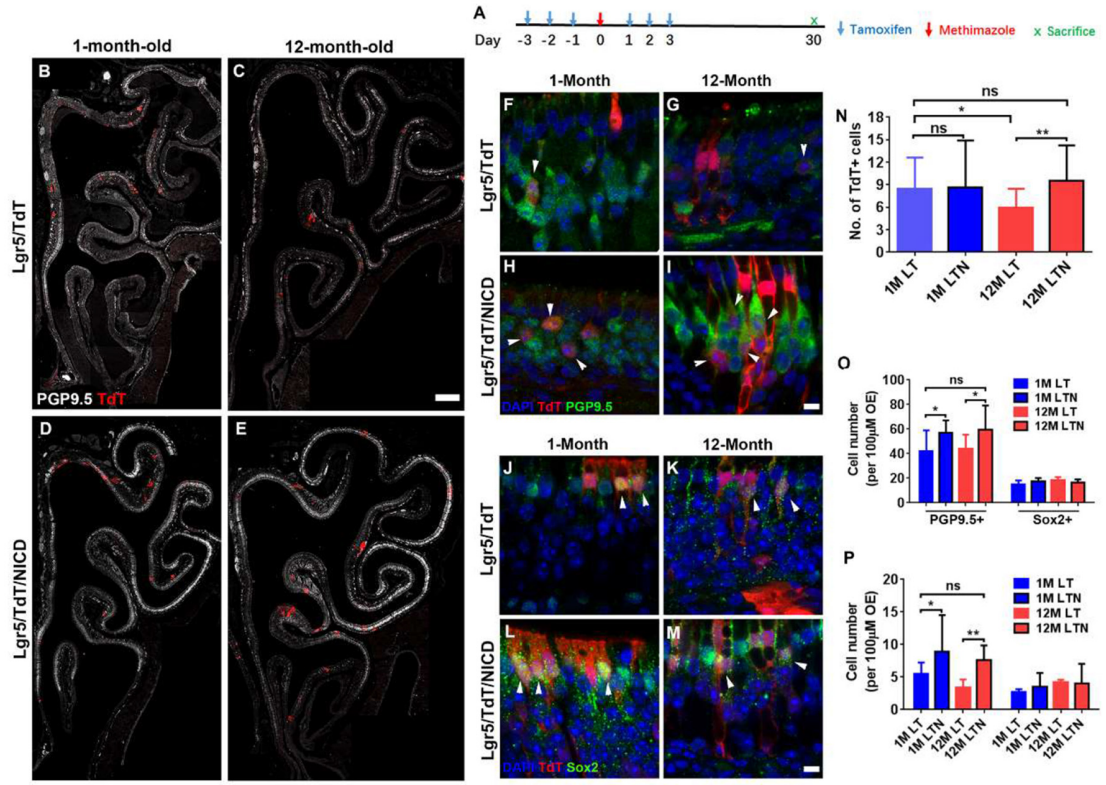

FIGURE 6 | Notch activation recovered neuronal regeneration of Lgr5+ cells in aged OE. **(A)** Scheme showing the tamoxifen and methimazole administration in Lgr5/TdT (LT) and Lgr5/TdT/NICD (LTN) mice. **(B–E)** Images showing PGP9.5+ and TdT+ cells in the OE from LT and LTN mice at Day 30 postinjury. **(F–I)** Immunostaining against PGP9.5 in injured OE from LT and LNT mice at 1- and 12-month old. The TdT+/PGP9.5+ cells were labeled by arrowheads. **(J–M)** Confocal images of TdT+/Sox2+ cells (noted by arrowheads) in the OE from LT and LNT mice at Day 30 postinjury. **(N)** Statistical analysis of TdT+ cell density (cell number per 100 μm OE) in LT and LTN mice at 1- and 12-month old. Totally, 461, 503, 421, and 588 TdT+ cells were counted in young LT, young LTN, aged LT, and aged LTN mice. **(O)** Statistical analysis of PGP9.5+ and Sox2+ cell density in the OE from young and aged LT and LNT mice at Day 30 postinjury. 1,256, 1,716, 1,419, and 1,429 PGP9.5+ cells and 224, 311, 329, and 247 Sox2+ cells were counted in young LT, young LTN, aged LT, and aged LTN mice. **(P)** Statistical analysis of TdT+/PGP9.5+ and TdT+/Sox2+ cell density in the OE. In young LT, young LTN, aged LT, and aged LTN mice, 103, 207, 125, and 172 TdT+/PGP9.5+ cells and 42, 62, 75, and 81 TdT+/Sox2+ cells were counted. The statistical significance was determined by unpaired *t*-test in **(N)** and by two-way ANOVA with Sidak's multiple comparisons test in **(O)** and **(P)**. ns, not significant. $^{*}p < 0.05$, $^{**}p < 0.01$.

of Notch signaling also changed the organoid morphology. LY411575 treatment led to significant increase in ratio of filled organoids from aged OE by 52.1 ± 6.5% compared with the DMSO-treated organoids (**Figures 7J,L,N**, $p < 0.001$). This was even higher than the ratio of filled organoids in untreated and LY411575-treated cultures from young mice by 16.0 ± 5.0 and 14.1 ± 4.9% (**Figures 7G,I,L,N**, $p < 0.001$). However, no apparent morphological change was observed in LY411575-treated organoids from young OE compared with the DMSO-treated control (**Figure 7N**). Collectively, these data demonstrated that regulation of Notch signaling by chemical stimulation affected aging-induced alteration in organoid size and morphology.

DISCUSSION

In this study, we reported the cellular and transcriptional alteration between young and aged OE. Aging weakened the recruitment of Lgr5+ cells, altered the stemness, and attenuated generation of neuronal progenies from Lgr5+ cells in the OE postinjury. Notch activation could recover the neuronal differentiation in aged OE, making it comparable with the OE of young animals. Therefore, this work provided the evidence to support the correlation between Notch signaling activation and alleviation in aging-induced incapacity of neuronal regeneration in injured OE, potentially providing a new concept in the therapy against aging-triggered anosmia.

Lgr5+ cells are active globose basal cells and are recruited in injured OE (Chen et al., 2014; Dai et al., 2018). However, it is still not clear whether dormant Lgr5+ cells are present in the OE, and this may lead to the discrepancy in the recruitment of Lgr5+ cells when OE is exposed to toxic reagent. Previous reports showed that Lgr5+ label-retaining cells were dormant stem cells in intestine (Li et al., 2016) and Lgr5+ intestinal stem cells were in G1 phase characterized by dormant periods (Carroll et al., 2018), showing the presence of Lgr5+ quiescent stem cells. In mammary gland, the deeply quiescent Lgr5+ mammary stem cells resided within the proximal region (Fu et al., 2017). These cells remained

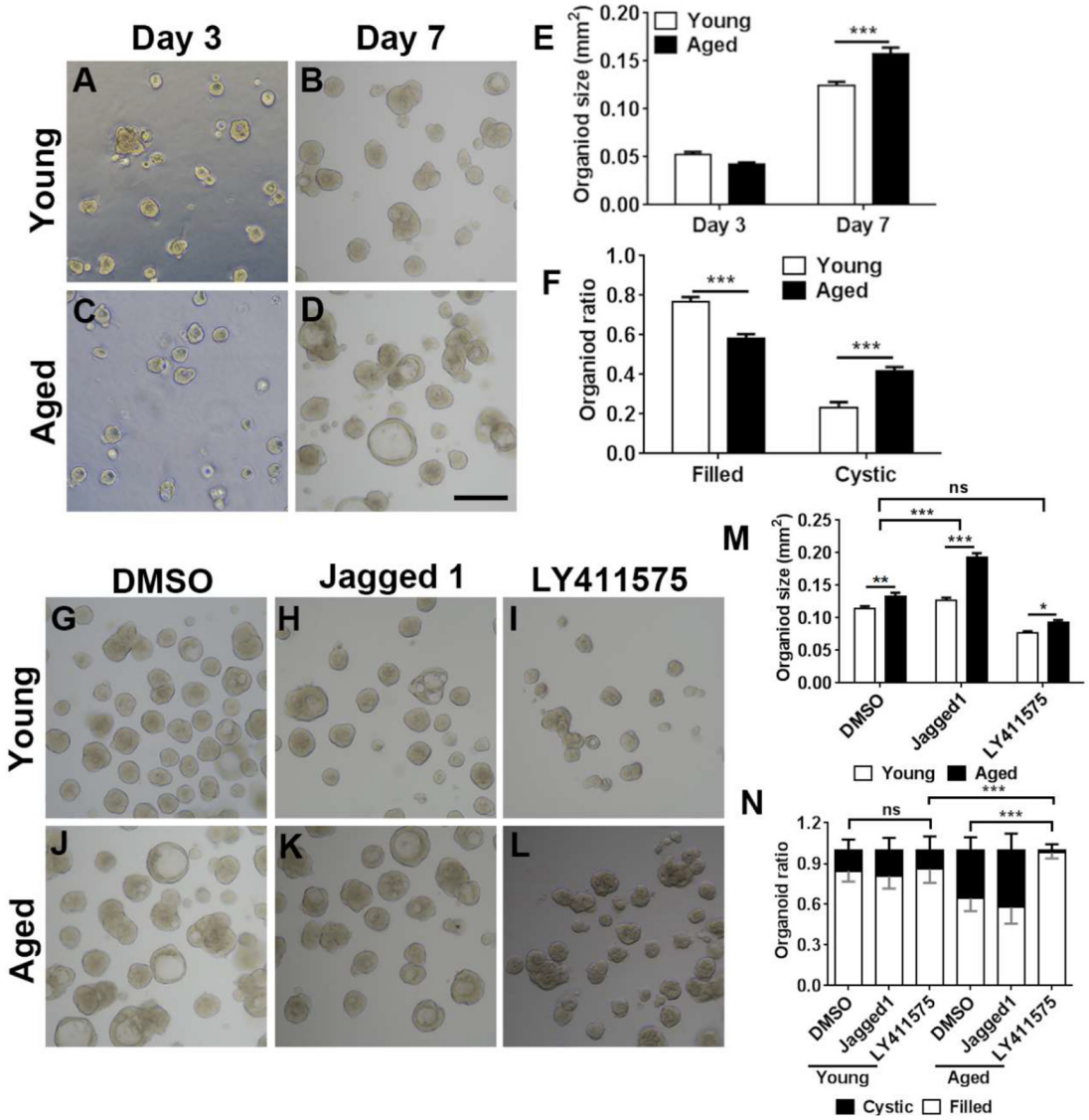

FIGURE 7 | Chemical cocktail regulated organoid growth and morphology *via* Notch signaling pathway. **(A–D)** Images showing the morphological difference in organoids derived from the OE of young (3-month-old) and aged (19-month-old) mice at Days 3 and 7 after *in vitro* culture. **(E)** Statistical analysis on size of organoids from young and aged mice at Days 3 and 7. At Days 3 and 7, 391 and 501, 1,113, and 604 organoids from aged and young OE were measured. **(F)** Statistical analysis on the ratio of filled and cystic organoids from young and aged mice; 825 and 934 organoids from young and aged OE were counted. **(G–L)** Images showing organoids from young and aged animals in the presence of DMSO **(G,J)**, Notch activator Jagged 1 **(H,K)**, and Notch inhibitor LY411575 **(I,L)**. **(M)** Statistical analysis on size of organoids treated with DMSO, Jagged 1, or LY411575; 518 and 415, 463 and 505, and 359 and 379 organoids from young and aged OE were measured when treated with DMSO, Jagged 1, or LY411575. **(N)** Statistical analysis on ratio of cystic and filled organoids from young and aged mice, treated with DMSO, Jagged 1, or LY411575; 973 and 1, 040, 518 and 717, and 683 and 300 organoids from young and aged OE were counted in the presence of DMSO, Jagged 1, and LY411575. The statistical significance was determined by two-way ANOVA with Sidak's multiple comparisons test. $F_{(1,814)} = 4.533$, $p = 0.0335$ in **(E)**; $F_{(1,56)} = 209.9$, $p < 0.0001$ in **(F)**; $F_{(2,1,493)} = 147.3$, $p < 0.0001$ in **(M)**. The statistical significance among different stimulation groups in **(M)** was determined by unpaired *t*-test. ns, not significant, $^{*}p < 0.05$, $^{**}p < 0.01$, $^{***}p < 0.001$. Scale bar: 250 μm.

active in embryonic mammary primordia before switching to a quiescent state after birth and can re-enter the cell cycling under ovarian hormone stimulation (Fu et al., 2017). This resembles the situation of Lgr5+ cells in the OE, which were active in early postnatal stage, remained in dormancy in adults, and were activated by chemical lesion (Chen et al., 2014; Dai et al., 2018). In aged OE, the recruitment of Lgr5+ cells was attenuated compared with that in young OE (**Figure 3**). This raises the possibility that more Lgr5+ cells in aged OE postinjury are still in quiescence. This was supported by the observation that Lgr5+/ICAM1+ cells were present in aged OE at Days 3 and 5 postlesion while it was seldom found in young OE (**Figure 4**). Thus, driving the quiescent stem cell to enter the cell cycle is applicable to alleviate aging-induced smell loss.

Multiple signaling pathways (ON or OFF state of Wnt, BMP, or IP3K signaling) regulated transition between quiescent and active state of intestinal stem cells (Richmond et al., 2016). Through RNA-Seq analysis, we found the transcriptional alteration in several signaling pathways between the OE from young and aged mice (**Figure 2**). A few pathways have been reported in previous studies to determine the stemness of active rapid cycling and dormant stem cells, such as Wnt (Li and Clevers, 2010) and PI3K-Akt (Richmond et al., 2015). Meanwhile, Notch signaling was involved in multiple diseases associated with advanced aging (Sun et al., 2013; Rizzo et al., 2018). Here, we found that Notch activation mimicking by NICD overexpression could restore the neuronal differentiation of Lgr5+ cells in aged OE (**Figure 6**), while aging weakened capacity to generate progenies from Lgr5+ cells compared with the young OE (**Figure 5**). Members of the Notch signaling pathway were significantly downregulated in HBCs following chemical lesion, demonstrating Notch pathway participated in activation of HBCs postinjury (Herrick et al., 2017). Our previous work showed that Notch activation enhanced the differentiation of Lgr5+ cells in the normal OE (Dai et al., 2018). Based on these data, we further elucidated that Notch activation offset the impairment in neuronal differentiation of Lgr5+ cells in aged OE postinjury and made it comparable with the young OE (**Figure 6**). This supplemented the role of Notch signaling in recovering the aging-induced attenuation of neuronal regeneration in injured OE, besides maintaining the cell turnover in normal OE.

OE organoid is an ideal tool to study the cellular proliferation and differentiation, mimicking the process in the OE tissue (Dai et al., 2018; Chen et al., 2020). Organoids showed the various morphologies, but the significance of it was still not very clear. Previous reports indicated that human intestinal organoids underwent maturation with morphological alteration (Jung et al., 2018). Morphological variation in Lgr5+ embryonic liver cell-formed organoids represented different cellular subtypes (Prior et al., 2019). Thus, different morphologies might represent various extents in cellular proliferation and differentiation. The OE from young and old mice as well as humans contained differential density of OMP+ and Tuj1+ neurons (**Figure 1**; Child et al., 2018). The increasing ratio of cystic organoids derived from old animals potentially showed their limited differentiation capacity. Furthermore, our data showed that addition of LY411575 in organoids from aged OE increased the ratio of filled organoids (**Figure 7N**), suggesting Notch signaling regulated organoid morphology and potentially affected the cellular differentiation in organoids. This will be strengthened by using OE organoids from RosaNICD mice to elucidate whether Notch activation could offset the aging-induced morphological alteration and cellular differentiation *in vitro*. This needs to be further investigated at cellular and transcriptional levels.

In conclusion, this work showed the attenuation in Lgr5+ cell recruitment in aged OE. Generation of neuronal progenies from Lgr5+ cells in aged OE postinjury was recovered through Notch activation, making it comparable with the young OE. Thus, we provided new evidence to support the role of Notch in regulating aged OE regeneration, potentially putting forward new therapeutic concept against smell loss in elder people.

DATA AVAILABILITY STATEMENT

The raw data supporting the conclusions of this article will be made available by the authors, without undue reservation.

ETHICS STATEMENT

The animal study was reviewed and approved by the Shanghai Medical Experimental Animal Administrative Committee (Permit Number: 2009-0082).

AUTHOR CONTRIBUTIONS

YY designed the research. YY, XL, MT, and LW performed the research. HY and YQ contributed unpublished reagents/analytic tools. YY and XL analyzed data and wrote the article. All authors edited the article. All authors agree to be accountable for the content of the work. All authors contributed to the article and approved the submitted version.

FUNDING

This work was supported by National Natural Science Foundation of China Grants (81700894 and 31771155 to YY, 81970856 to HY, 32072210 to YQ); Shanghai Municipal Education Commission, the Shanghai Eastern Scholar Program (TP2016029 to YY); Shanghai Municipal Human Resources and Social Security Bureau, Shanghai Talent Development Fund (2018112 to YY); the New Technologies of Endoscopic Surgery in Skull Base Tumor: CAMS Innovation Fund for Medical Sciences (CIFMS; 2019-I2M-5-003 to HY); Shanghai Municipal Commission of Heath and Family Planning (201740187 to HY); and Eye, Ear, Nose and Throat Hospital, Fudan University, Excellent Doctors-Excellent Clinical Researchers Program (SYB202002 to YY).

REFERENCES

Artavanis-Tsakonas, S., and Muskavitch, M. A. (2010). Notch: the past, the present and the future. *Curr. Top. Dev. Biol.* 92, 1–29. doi: 10.1016/S0070-2153(10)92001-2

Carroll, T. D., Newton, I. P., Chen, Y., Blow, J. J., and Nathke, I. (2018). Lgr5^{+} intestinal stem cells reside in an unlicensed G_1 phase. *J. Cell. Biol.* 217, 1667–1685. doi: 10.1083/jcb.201708023

Carson, C., Murdoch, B., and Roskams, A. J. (2006). Notch 2 and notch 1/3 segregate to neuronal and glial lineages of the developing olfactory epithelium. *Dev. Dyn.* 235, 1678–1688. doi: 10.1002/dvdy.20733

Chen, M., Tian, S., Yang, X., Lane, A. P., Reed, R. R., and Liu, H. (2014). Wnt-responsive Lgr5^{+} globose basal cells function as multipotent olfactory epithelium progenitor cells. *J. Neurosci.* 34, 8268–8276. doi: 10.1523/JNEUROSCI.0240-14.2014

Chen, X., Fang, H., and Schwob, J. E. (2004). Multipotency of purified, transplanted globose basal cells in olfactory epithelium. *J. Comp. Neurol.* 469, 457–474. doi: 10.1002/cne.11031

Chen, Z.-H., Luo, X.-C., Yu, C. R., and Huang, L. (2020). Matrix metalloprotease-mediated cleavage of neural glial-related cell adhesion molecules activates quiescent olfactory stem cells *via* EGFR. *Mol. Cell. Neurosci.* 108:103552. doi: 10.1016/j.mcn.2020.103552

Child, K. M., Herrick, D. B., Schwob, J. E., Holbrook, E. H., and Jang, W. (2018). The neuroregenerative capacity of olfactory stem cells is not limitless: implications for aging. *J. Neurosci.* 38, 6806–6824. doi: 10.1523/JNEUROSCI.3261-17.2018

Dai, Q., Duan, C., Ren, W., Li, F., Zheng, Q., Wang, L., et al. (2018). Notch signaling regulates $Lgr5^+$ olfactory epithelium progenitor/stem cell turnover and mediates recovery of lesioned olfactory epithelium in mouse model. *Stem Cells* 36, 1259–1272. doi: 10.1002/stem.2837

Doi, K., Ishida, H., and Nibu, K.-I. (2004). Notch expression in developing olfactory neuroepithelium. *Neuroreport* 15, 945–947. doi: 10.1097/00001756-200404290-00003

Fu, N. Y., Rios, A. C., Pal, B., Law, C. W., Jamieson, P., Liu, R., et al. (2017). Identification of quiescent and spatially restricted mammary stem cells that are hormone responsive. *Nat. Cell Biol.* 19, 164–176. doi: 10.1038/ncb3471

Fukuda, Y., Katsunuma, S., Uranagase, A., Nota, J., and Nibu, K.-I. (2018). Effect of intranasal administration of neurotrophic factors on regeneration of chemically degenerated olfactory epithelium in aging mice. *Neuroreport* 29, 1400–1404. doi: 10.1097/WNR.0000000000001125

Genter, M. B., Deamer, N. J., Blake, B. L., Wesley, D. S., and Levi, P. E. (1995). Olfactory toxicity of methimazole: dose-response and structure-activity studies and characterization of flavin-containing monooxygenase activity in the long-evans rat olfactory mucosa. *Toxicol. Pathol.* 23, 477–486. doi: 10.1177/019262339502300404

Herrick, D. B., Guo, Z., Jang, W., Schnittke, N., and Schwob, J. E. (2018). Canonical *notch* signaling directs the fate of differentiating neurocompetent progenitors in the mammalian olfactory epithelium. *J. Neurosci.* 38, 5022–5037. doi: 10.1523/JNEUROSCI.0484-17.2018

Herrick, D. B., Lin, B., Peterson, J., Schnittke, N., and Schwob, J. E. (2017). Notch1 maintains dormancy of olfactory horizontal basal cells, a reserve neural stem cell. *Proc. Natl. Acad. Sci. U S A* 114, E5589–E5598. doi: 10.1073/pnas.1701333114

Jang, W., Youngentob, S. L., and Schwob, J. E. (2003). Globose basal cells are required for reconstitution of olfactory epithelium after methyl bromide lesion. *J. Comp. Neurol.* 460, 123–140. doi: 10.1002/cne.10642

Jia, C., and Hegg, C. C. (2015). Effect of IP3R3 and NPY on age-related declines in olfactory stem cell proliferation. *Neurobiol. Aging* 36, 1045–1056. doi: 10.1016/j.neurobiolaging.2014.11.007

Jung, K. B., Lee, H., Son, Y. S., Lee, M.-O., Kim, Y.-D., Oh, S. J., et al. (2018). Interleukin-2 induces the *in vitro* maturation of human pluripotent stem cell-derived intestinal organoids. *Nat. Commun.* 9:3039. doi: 10.1038/s41467-018-05450-8

Kondo, K., Watanabe, K., Sakamoto, T., Suzukawa, K., Nibu, K.-I., Kaga, K., et al. (2009). Distribution and severity of spontaneous lesions in the neuroepithelium and Bowman's glands in mouse olfactory mucosa: age-related progression. *Cell Tissue Res.* 335, 489–503. doi: 10.1007/s00441-008-0739-9

Kopan, R., and Ilagan, M. X. (2009). The canonical notch signaling pathway: unfolding the activation mechanism. *Cell* 137, 216–233. doi: 10.1016/j.cell.2009.03.045

Leung, C. T., Coulombe, P. A., and Reed, R. R. (2007). Contribution of olfactory neural stem cells to tissue maintenance and regeneration. *Nat. Neurosci.* 10, 720–726. doi: 10.1038/nn1882

Li, L., and Clevers, H. (2010). Coexistence of quiescent and active adult stem cells in mammals. *Science* 327, 542–545. doi: 10.1126/science.1180794

Li, N., Nakauka-Ddamba, A., Tobias, J., Jensen, S. T., and Lengner, C. J. (2016). Mouse label-retaining cells are molecularly and functionally distinct from reserve intestinal stem cells. *Gastroenterology* 151, 298.e7–310.e7. doi: 10.1053/j.gastro.2016.04.049

Mobley, A. S., Rodriguez-Gil, D. J., Imamura, F., and Greer, C. A. (2014). Aging in the olfactory system. *Trends Neurosci.* 37, 77–84. doi: 10.1016/j.tins.2013.11.004

Prior, N., Hindley, C. J., Rost, F., Melendez, E., Lau, W. W. Y., Gottgens, B., et al. (2019). $Lgr5^+$ stem and progenitor cells reside at the apex of a heterogeneous embryonic hepatoblast pool. *Development* 146:dev174557. doi: 10.1242/dev.174557

Ren, W., Liu, Q., Zhang, X., and Yu, Y. (2020). Age-related taste cell generation in circumvallate papillae organoids *via* regulation of multiple signaling pathways. *Exp. Cell Res.* 394:112150. doi: 10.1016/j.yexcr.2020.112150

Richmond, C. A., Shah, M. S., Carlone, D. L., and Breault, D. T. (2016). An enduring role for quiescent stem cells. *Dev. Dyn.* 245, 718–726. doi: 10.1002/dvdy.24416

Richmond, C. A., Shah, M. S., Deary, L. T., Trotier, D. C., Thomas, H., Ambruzs, D. M., et al. (2015). Dormant intestinal stem cells are regulated by PTEN and nutritional status. *Cell Rep.* 13, 2403–2411. doi: 10.1016/j.celrep.2015.11.035

Rizzo, P., Bollini, S., Bertero, E., Ferrari, R., and Ameri, P. (2018). Beyond cardiomyocyte loss: role of notch in cardiac aging. *J. Cell. Physiol.* 233, 5670–5683. doi: 10.1002/jcp.26417

Schnittke, N., Herrick, D. B., Lin, B., Peterson, J., Coleman, J. H., Packard, A. I., et al. (2015). Transcription factor p63 controls the reserve status but not the stemness of horizontal basal cells in the olfactory epithelium. *Proc. Natl. Acad. Sci. U S A* 112, E5068–E5077. doi: 10.1073/pnas.1512272112

Schwob, J. E., Jang, W., Holbrook, E. H., Lin, B., Herrick, D. B., Peterson, J. N., et al. (2017). Stem and progenitor cells of the mammalian olfactory epithelium: taking poietic license. *J. Comp. Neurol.* 525, 1034–1054. doi: 10.1002/cne.24105

Sun, F., Mao, X., Xie, L., Ding, M., Shao, B., and Jin, K. (2013). Notch1 signaling modulates neuronal progenitor activity in the subventricular zone in response to aging and focal ischemia. *Aging Cell* 12, 978–987. doi: 10.1111/acel.12134

Suzukawa, K., Kondo, K., Kanaya, K., Sakamoto, T., Watanabe, K., Ushio, M., et al. (2011). Age-related changes of the regeneration mode in the mouse peripheral olfactory system following olfactotoxic drug methimazole-induced damage. *J. Comp. Neurol.* 519, 2154–2174. doi: 10.1002/cne.22611

Ueha, R., Kondo, K., Ueha, S., and Yamasoba, T. (2018a). Dose-dependent effects of insulin-like growth factor 1 in the aged olfactory epithelium. *Front. Aging Neurosci.* 10:385. doi: 10.3389/fnagi.2018.00385

Ueha, R., Shichino, S., Ueha, S., Kondo, K., Kikuta, S., Nishijima, H., et al. (2018b). Reduction of proliferating olfactory cells and low expression of extracellular matrix genes are hallmarks of the aged olfactory mucosa. *Front. Aging Neurosci.* 10:86. doi: 10.3389/fnagi.2018.00086

Zhang, J., Hao, C., Jiang, J., Feng, Y., Chen, X., Zheng, Y., et al. (2018). The mechanisms underlying olfactory deficits in apolipoprotein E-deficient mice: focus on olfactory epithelium and olfactory bulb. *Neurobiol. Aging* 62, 20–33. doi: 10.1016/j.neurobiolaging.2017.09.036

Conflict of Interest: The authors declare that the research was conducted in the absence of any commercial or financial relationships that could be construed as a potential conflict of interest.

frontiers in Aging Neuroscience

ORIGINAL RESEARCH
published: 26 March 2021
doi: 10.3389/fnagi.2021.612856

Conversion of Reactive Astrocytes to Induced Neurons Enhances Neuronal Repair and Functional Recovery After Ischemic Stroke

Michael Qize Jiang[1,2†], Shan Ping Yu[1,2†], Zheng Zachory Wei[1,2], Weiwei Zhong[1,2], Wenyuan Cao[1], Xiaohuan Gu[1,2], Anika Wu[1], Myles Randolph McCrary[1‡], Ken Berglund[2,3] and Ling Wei[1,4*]*

[1]Department of Anesthesiology, Emory University School of Medicine, Atlanta, GA, United States, [2]Center for Visual and Neurocognitive Rehabilitation, Atlanta Veterans Affair Medical Center, Decatur, GA, United States, [3]Department of Neurosurgery, Emory University School of Medicine, Atlanta, GA, United States, [4]Department of Neurology, Emory University School of Medicine, Atlanta, GA, United States

OPEN ACCESS

Edited by:
Cesar V. Borlongan,
University of South Florida,
United States

Reviewed by:
Jukka Jolkkonen,
University of Eastern Finland, Finland
Vanessa Castelli,
University of L'Aquila, Italy

***Correspondence:**
Ling Wei
lwei7@emory.edu
Shan Ping Yu
spyu@emory.edu

[†]These authors have contributed equally to this work

[‡]**Present address:**
Myles Randolph McCrary,
Emory University School of Medicine,
Atlanta, GA, United States

Received: 30 September 2020
Accepted: 08 March 2021
Published: 26 March 2021

Citation:
Jiang MQ, Yu SP, Wei ZZ, Zhong W, Cao W, Gu X, Wu A, McCrary MR, Berglund K and Wei L (2021) Conversion of Reactive Astrocytes to Induced Neurons Enhances Neuronal Repair and Functional Recovery After Ischemic Stroke. Front. Aging Neurosci. 13:612856. doi: 10.3389/fnagi.2021.612856

The master neuronal transcription factor NeuroD1 can directly reprogram astrocytes into induced neurons (iNeurons) after stroke. Using viral vectors to drive ectopic ND1 expression in gliotic astrocytes after brain injury presents an autologous form of cell therapy for neurodegenerative disease. Cultured astrocytes transfected with ND1 exhibited reduced proliferation and adopted neuronal morphology within 2–3 weeks later, expressed neuronal/synaptic markers, and extended processes. Whole-cell recordings detected the firing of evoked action potentials in converted iNeurons. Focal ischemic stroke was induced in adult GFAP-Cre-Rosa-YFP mice that then received ND1 lentivirus injections into the peri-infarct region 7 days after stroke. Reprogrammed cells did not express stemness genes, while 2–6 weeks later converted cells were co-labeled with YFP (constitutively activated in astrocytes), mCherry (ND1 infection marker), and NeuN (mature neuronal marker). Approximately 66% of infected cells became NeuN-positive neurons. The majority (~80%) of converted cells expressed the vascular glutamate transporter (vGLUT) of glutamatergic neurons. ND1 treatment reduced astrogliosis, and some iNeurons located/survived inside of the savaged ischemic core. Western blotting detected higher levels of BDNF, FGF, and PSD-95 in ND1-treated mice. MultiElectrode Array (MEA) recordings in brain slices revealed that the ND1-induced reprogramming restored interrupted cortical circuits and synaptic plasticity. Furthermore, ND1 treatment significantly improved locomotor, sensorimotor, and psychological functions. Thus, conversion of endogenous astrocytes to neurons represents a plausible, on-site regenerative therapy for stroke.

Keywords: ischemic stroke, direct reprogramming, induced neuron, glial scar, functional recovery, post-stroke depression

INTRODUCTION

Ischemic stroke is a devastating disease with limited therapies available (Liu et al., 2014; Ginsberg, 2016; Catanese et al., 2017). Stem cell transplantation has emerged as a promising regenerative therapy for stroke due to its potential for repairing damaged brain structures and improving functional recovery (Liu et al., 2014; Wei et al., 2017). However, cell transplantation therapies face multiple obstacles including the hosts' immune systems, poor transplanted cell survival, inappropriate migration/homing and differentiation, and the lack of specificity or integration into endogenous brain networks (Liu et al., 2014; Wei et al., 2017). Some clinical trials have also reported inconsistent results in the efficacy of cell transplantation therapies (Hatakeyama et al., 2020).

In the adult brain, neurogenesis mainly exists in two regenerative niches: the subventricular zone (SVZ) and the sub-granular zone (SGZ; Ohab and Carmichael, 2008). Unfortunately, endogenously generated cells are insufficient for enacting meaningful repair of damaged brain structures (Gogel et al., 2011). On the other hand, glial cells such as astrocytes exhibit great proliferative capacity (Khakh and Sofroniew, 2015). Astroglia are normally responsible for maintaining physiological homeostasis and supporting surrounding tissues by providing structural, trophic, and metabolic support to neurons while also playing a role in modulating synaptic activity (Chen and Swanson, 2003; Gibbs et al., 2008). Resident astrocytes in the brain remain mitotic throughout the lifespan and undergo rapid gliosis in response to injury. This characteristic response provides a rich source of cells adjacent to the site of injury (Liu and Chopp, 2016). After an ischemic insult, astrogliosis initially confers neuroprotective effects by forming a barrier to limit toxic substances (Pekny and Nilsson, 2005). As the gliotic tissue persists in subacute and chronic stages, the formation of a glial scar in the peri-infarcted region acts as physical and chemical barriers that release inhibitory paracrine factors which limit neuro-regeneration in and around the ischemic region (Sofroniew and Vinters, 2010; Pekny and Pekna, 2016). Thus, the accumulation of reactive astrocytes and astrogliosis during later phases after stroke is viewed as a major obstacle for regenerative therapy involving either endogenous or transplanted cells.

Several master transcription factors such as Neurogenic differentiation 1 (NeuroD1 or ND1), Neurogenin2 (Ngn2), Olig2, and Ascl1 have been identified for their role in controlling cell fate (Heinrich et al., 2010; Li and Chen, 2016). These discoveries provide a breakthrough opportunity to utilize endogenous and autologous cell substrates for regenerative therapy. More recently, the idea of direct reprogramming of non-neuronal cells allows for the trans-differentiation of glial cells (astrocytes, microglia, and oligodendrocytes) into induced neurons (iNeurons) without passing through a stem cell stage (Vignoles et al., 2019; Chen et al., 2020). Theoretically, this is a more efficient way to obtain desirable endogenous neurons from a large cellular pool for "on-site" repair in the brain (Torper et al., 2013; Vignoles et al., 2019). Being post-mitotic cells, iNeurons are not tumorigenic, which offers another advantage over naïve and differentiating stem cells.

Based on the efficiency and efficacy of glial cell reprogramming, we and others experimented with several combinations of transcription factors and settled on the use of the single neural transcription factor NeuroD1 (Guo et al., 2014; Gangal et al., 2017; Jiang et al., 2019b; Chen et al., 2020; Liu et al., 2020). Targeting astrocytes for neuronal reprogramming with different viral vectors has been tested in several animal models of neurodegenerative diseases including ischemic stroke with varying success (Guo et al., 2014; Rivetti di Val Cervo et al., 2017; Yamashita et al., 2019; Chen et al., 2020; Yavarpour-Bali et al., 2020). The exploration of this approach in animal disease models is at an early stage. The efficacy of neuronal conversion and its contribution to neuronal circuitry repair, the mechanisms involved in the regenerative process, and the functional benefits of this therapy have not been well defined. Concurrently, the specificity, reliability, and clinical potential of this novel regenerative gene therapy have sparked much debate. Investigations spanning various routes of administration and in animal models across the lifespan have yielded inconsistent results (Gresita et al., 2019). Our investigation examined the viability of reprogramming of astrocytes *in vitro* and *in vivo*. Reprogramming therapy was tested in a focal ischemic stroke model of rats, induced by occlusion of distal branches of the middle cerebral artery (MCA) accompanied with partial reperfusion (Wei et al., 1995; Jiang et al., 2017). This focal ischemic stroke represents common clinical cases of relatively small infarction followed by spontaneous or thrombolysis-induced partial recirculation (Hakim et al., 1987; Jorgensen et al., 1994; Neumann-Haefelin et al., 2004). The well-defined structure-function relationship of the damaged sensorimotor cortex is suitable for specific functional assessments during the acute, subacute, and chronic stages of stroke. After a stroke, we transduced ND1 using a lentivirus vector rather than other viral serotypes such as an adeno-associated virus (AAV) to preserve finer control over the scope of infection to study the mechanics of reprogramming on local circuitry and to limit the therapy to only the injured tissue. Neuronal network repair and functional recovery were confirmed using comprehensive assessments and behavioral tests up to 4 months after stroke.

MATERIALS AND METHODS

Animals

A total of 72 C57BL/6 adult mice (male, 26–28 g, n = 6–8 per experimental group) were used in this investigation. For *in vitro* direct reprogramming experiments, we dissected astrocytes from P1 C57 mouse pups. The near-pure astrocyte (>98%) cultures featured little contamination by other cell types (Choi et al., 1987). Astrocyte to neuron reprogramming using a GFAP promoter creates a closed-loop feedback system whereby initial translation of ectopic ND1 is high in hypertrophied reactive astrocytes but diminishes as the cell reprograms into neurons (Choudhury and Ding, 2016). For *in vivo* experiments, we crossed GFAP-Cre with Rosa-YFP mice to generate animals that exhibit constitutively active YFP expression in astrocytes regardless of cell phenotype changes; this property allowed

tracking the cell fate of reprogrammed cells from start to finish. In these mice, Cre recombinase expression is controlled by a GFAP promoter to inverts a loxP-flanked YFP in astrocytes. The resulting YFP reporter is both astrocyte-specific and remains activated independently of cell fate (McLellan et al., 2017). When astrocytes are reprogrammed into induced neurons, they no longer express GFAP but continue to express the YFP promoter while preexisting neurons do not express YFP. The specificity of Cre recombinase under a human GFAP promoter in mice has been thoroughly characterized. Specificity defined as the proportion of co-labeled S100β and reporter positive cells over the total number of reporter positive cells in the mouse has been reported as high as 96.02% (Park et al., 2018).

The animal protocol (DAR 2003027) was approved by the Institutional Animal Care and Use Committee (IACUC) of Emory University School of Medicine. Animal procedures followed institutional guidelines that meet NIH standards of principles of laboratory animal care (NIH publication No. 86-23). Animals were randomly assigned to different experimental groups and data were analyzed under blinded conditions.

NeuroD1 Lentiviral Production, Purification, and Titer Calculation

To express genes together with mCherry using a single plasmid, pEGIP was modified by replacing the GFP-IRES-Puro sequence with *BamHI-EcoRI*-IRES-mCherry-WPRE (EIMW). pEGIP was a gift from Linzhao Cheng (Addgene plasmid #26777; Zou et al., 2009). The mCherry tag was ligated to FUGW using two-step overlap PCR. A purified ND1 fragment was ligated into the FUGW plasmid. Verification of correct ligation and plasmid generation was confirmed using PCR and DNA sequence analysis. Plasmid production utilized Stbl3 bacteria and DNA was purified using Qiagen Miniprep and Maxiprep kits. Transduction efficacy was assayed compared to control GFP-FUGW in HEK 293FT cell cultures that were fixed and stained for both mCherry and ND1. To prevent interference from the mCherry reporter with ectopic ND1 translation, an internal ribosome entry site (IRES) preceding mCherry ensures that it is translated separately from ND1 (Martinez-Salas et al., 2001). The resulting ND1 and mCherry products are independent and able to be transported throughout the cell separately. While both proteins are translated in the cytoplasm, transcription factors such as ND1 contain nuclear localization signals while mCherry remains throughout the cytoplasm (Petersen et al., 2002).

Cloning experiments were performed in triplicates. A minimum of eight samples were required during cloning steps and three bacterial strains were sequenced to isolate a mutation-free strain. Of these, two contained point mutations, and one was mutation-free. All subsequent experiments used the mutation-free clone. In transduction experiments, three wells of HEK-293 cells were used to examine efficacy. DNA concentrations were assessed using Gen5 ultraviolet spectrophotometry by BioTek (Naldini et al., 1996). Plasmids were isolated using the following primers:

Ngn2-BamHI-F	5′-GGG GGATCC ATGTTCGTCA AATCTGAGA-3′
Ngn2-KpnI-myc-EcoRI-R	5′-CCCGAATTCT CACAGATCCT CTTCAGAGAT GAGTTTCTGC TCGGTACCGA TACAGTCCCT GGCGAGGG-3′
ND1-BamHI-F	5′-GGTGCCTTGCTATTCTAAGACGC-3′
ND1-EcoRI-R	5′-GCAAAGCGTCTGAACGAAGGAG-3′

Note: F, Forward primer; R, Reverse primer.

Generate ND1 Plasmid by Cloning ND1 Under GFAP Promoter With mCherry Tag Into the FUGW Plasmid

Lentivirus has been established as an effective method of transduction both *in vitro* and *in vivo* (Naldini et al., 1996; Blömer et al., 1997; Taoufik et al., 2007). Under a GFAP promoter, we packaged control GFP-FUGW and ND1-FUGW into a lentiviral vector. HEK 293FT cells were used as the substrate for lentiviral production (Tiscornia et al., 2006; Ansorge et al., 2009). We achieved a viral titer of at least 2.48×10^7 which was suitable for use *in vitro* and *in vivo*. The virus was harvested from culture media two times resulting in 144 ml total. To reach a high titer for *in vivo* use, the virus was concentrated using two rounds of ultracentrifugation to concentrate first from 144 to 1.2 ml and then from 1.2 to 30 μl. Phage titer was calculated by infecting triplicate HEK 293FT cell cultures with 1:10 and 1:100 dilutions of concentrated virus and then fixed and stained for mCherry.

Astrocyte Cultures and Lentivirus Infection

Astrocytes were dissected and cultured as described (Li et al., 2013). Briefly, cerebral cortex from postnatal day 1 (P1), and cells were cultured in a medium consisting of Dulbecco's Modification of Eagle's Medium (DMEM, Corning, Manassas, VA, USA), 15% FBS (Sigma), MEM non-essential amino acids (Life Technologies), 3.5 mM glucose (Sigma). One-week post-plating, cells were dissociated using trypsin-EDTA (Life Technologies) and passaged onto poly-D-lysine (Sigma) and laminin (Sigma) coated coverslips (80,000 cells per well for 24-well plates) in the same medium. A 4-day-long shaking procedure helped to remove microglia and neurons. By the end of this regimen, astrocyte activation and GFAP expression were induced uniformly across the culture by the addition of lipopolysaccharide (LPS). Neurons contained in initial cultures died within 10 days in culture. GFAP-ND1 expression is reliant on GFAP-positive astrocytes of the reactive state. We confirmed that 98.4% of the cells were positive for GFAP in our P10 astrocyte cultures.

Lentivirus was added into astrocyte cultures immediately after passage. One day post-transduction, the medium was completely replaced to minimize exposure to viral adjuvants into a medium consisting of DMEM/F-12 (Life Technologies), 3.5 mM glucose, penicillin/streptomycin (Life Technologies), B27 (Life Technologies), and 20 ng/ml brain-derived neurotrophic factor (BDNF, Sigma). After an initial media change, half-media changes occurred every 3–4 days subsequently.

Electrophysiological Examination of ND1 Converted Cells *In vitro*

Astrocyte cultures from 14 to 42 days *in vitro* after ND1 transduction were examined using whole-cell patch-clamp recordings on converted cells identified by the morphological phenotype of axonal outgrowth with neurite extension. Recordings were performed using an EPC9 amplifier (HEKA; Elektronik) were performed at 21–23°C. The external solution contained (in mM): 135 NaCl, 5 KCl, 1 $MgCl_2$, 2 $CaCl_2$, 10 HEPES, and 10 Glucose at a pH of 7.4. Recording electrodes pulled from borosilicate glass pipettes (Sutter Instrument) had a tip resistance between 5 and 8 MO when filled with the internal solution (in mM): 140 KCl, 2 $MgCl_2$, 1 $CaCl_2$, 2 Na_2ATP, 10 EGTA, and 10 HEPES at a pH of 7.2. Action potentials were recorded under the current-clamp mode using the Pulse software (HEKA, Elektronik).

MicroElectrode Array (MEA) Recording in Brain Slices

A high-resolution MEA2100-system (MultiChannel Systems, Reutlingen, Germany) was used to record field excitatory postsynaptic potentials (fEPSP) in brain slices. The MEA chamber (60pMEA200/30iR-Ti, MultiChannel Systems GmbH, Reutlingen, Germany) is composed of a 6-mm high glass ring and an 8 × 8 Titanium nitride electrode grid (59 electrodes and 1 internal reference electrode) with an electrode diameter of 30 μm and spacing of 200 μm. The brain slice was transferred to the MEA chamber that was perfused with oxygenated aCSF at a rate of 6–8 ml/min and stabilized at 34°C for at least 10 mins before recording. For evoked fEPSPs, electric stimuli (±1.5 V, 10 ms) were applied every 30 s and responses were simultaneously monitored in 58 locations. Pair-pulse facilitation was recorded by two electric stimuli (±1.0 V, 10 ms) with different intervals (20, 40, 60, 80, 100, 200 ms). The slopes of fEPSPs were analyzed with Multi-Channel Analyzer V 2.6.0 (Multichannel Systems) and GraphPad Prism 6 (GraphPad Software, San Diego, CA, USA).

Focal Ischemic Stroke in Mice

A focal cerebral ischemic stroke targeting the right sensorimotor cortex was induced as previously described (Choi et al., 2012; Li et al., 2013). Mice were anesthetized with 3% isoflurane and maintained using 1.5% isoflurane supplemented with regular air during surgery. Cortical ischemia was achieved by permanent occlusion of the distal branches of the right middle cerebral artery (MCA) supplying the sensorimotor cortex. The MCA occlusion was paired with 7-min ligation of both common carotid arteries (CCAs) to cause sufficient reduction of local cerebral blood flow (LCBF) in the sensorimotor region and followed by partial reperfusion. This relatively small stroke targets a well-defined brain structure, i.e., the sensorimotor cortex including the barrel cortex (Wei et al., 1995; Jiang et al., 2017). According to the epidemiological data from American Heart Association (AHA), small strokes are common and represent about 40% of all stroke cases (Roger et al., 2011). Importantly, partial reperfusion due to incomplete (spontaneous and post-thrombolytic) recanalization after an ischemic attack occurs in 30–70% of clinical cases at different times after the onset of ischemia (Hakim et al., 1987; Jorgensen et al., 1994; Barber et al., 1998; Neumann-Haefelin et al., 2004). Few animal models of ischemic stroke featuring partial reperfusion have been available. In this regard, the investigation on this stroke model possesses high face validity for translational research.

Body temperature was monitored during surgery and recovery period using a rectal probe and maintained at 37°C on a homoeothermic blanket in a ventilated incubator. Overall mortality resulting from ischemic stroke surgery was less than 2%. Before and after surgery the painkiller meloxicam was administered orally at a dosage of 5 mg/kg. Animals were housed with four to five mice per cage, with *ad libitum* access to food and water. At different time points after stroke, mice were sedated with overdose isoflurane and sacrificed by decapitation.

Stereotaxic Injection

Stereotaxic injection of control and ND1 lentivirus was performed using a 10 μL Hamilton GASTIGHT^{TM} syringe (Hamilton Company, NV). Injection locations included three areas around the infarcted region (Stereotaxic coordinates: AP −0.5, ML +3.2, DV +2.2) at a cortical depth of 0.5 mm and the sub-ventricular zone (SVZ; Stereotaxic coordinates: AP 0, ML +1.5, DV +2.5). Infected cells could be observed up to a distance of 3–4 mm from the injection site.

At time points of 24 and 48 h after the onset of MCAO, animals were sacrificed for assessment of brain infarct formation. 2,3,5-triphenyltetrazolium chloride (TTC; Sigma–Aldrich) staining was used to reveal damaged/dead brain tissue as previously described (Wang et al., 2014). Brains were removed and placed in a brain matrix then sliced into 1-mm coronal sections. Slices were incubated in 2% TTC solution at 37°C for 5 min, then stored in 10% buffered formalin for 24 h. Digital images of the caudal aspect of each slice were obtained by a flatbed scanner. Infarct, ipsilateral hemisphere, and contralateral hemisphere areas were measured using ImageJ software (NIH, Bethesda, MD, USA). The indirect method (subtraction of residual right hemisphere cortical volume from cortical volume of the intact left hemisphere) was used for infarct volume calculation. Infarct measurements were performed under double-blind conditions.

Western Blotting Analysis

Western blot analysis was used to detect the expression of trophic factors brain-derived neurotrophic factor (BDNF), FGF10, PSD-95, tyrosine hydroxylase (TH), NFKB, and GFAP (n = 3–6). Brain cortical tissue was lysed in a lysis buffer containing 0.02 M $Na_4P_2O_7$, 10 mM Tris-HCl (pH 7.4), 100 mM NaCl, 1 mM EDTA (pH 8.0), 1% Triton, 1 mM EGTA, 2 mM Na_3VO_4, and a protease inhibitor cocktail (Sigma–Aldrich). The supernatant was collected after centrifugation at 15,000 g for 10 min at 4°C. Protein concentration was determined with a bicinchoninic acid assay (Pierce Biotechnology, Rockford, IL, USA). Equivalent amounts of total protein, 15–20 μl were added per lane, were separated by molecular weight on an

SDS-polyacrylamide gradient gel, and then transferred to a polyvinyl difluoride (PVDF) membrane. The blot was incubated in 5% bovine serum albumin (BSA) for at least 1 h and then reacted with primary antibodies at 4°C for overnight. The primary antibodies used in this investigation included: anti-BDNF antibody (1:2,000; Cell Signaling, Danvers, MA, USA), anti-FGF-10 antibody (1:500, Abcam, Cambridge, MA, USA), anti-PSD-95 (1:750, Abcam), anti-TH antibody (1:1,000; Cell Signaling, Danvers, MA, USA), anti-FGF-10 antibody (1:500, Abcam), anti-GFAP antibody (1:500, Abcam), rabbit anti-actin antibody (1:500, Abcam), rabbit anti-beta tubulin antibody (1:500, Abcam) and rabbit anti-cleaved caspase-3 (1:500; Cell Signaling). After washing with Tris-buffered saline with Tween (TBST), membranes were incubated with AP-conjugated or HRP-conjugated secondary antibodies (GE Healthcare, Piscataway, NJ, USA) for 1–2 h at room temperature. After final washing with TBST, the signals were detected with bromochloroidolylphosphate/nitroblue tetrazolium (BCIP/NBP) solution (Sigma–Aldrich) or film. Signal intensity was measured by ImageJ and normalized to the actin signal intensity.

Immunocytochemistry and Immunohistochemical Staining

For immunocytochemistry (ICC), cell cultures were fixed using 10% formalin buffer, washed with −20°C precooled ethanol: acetic acid (2:1) solution for 10 min, and finally permeabilized with 0.2% Triton-X 100 solution for 5 min. All slides were washed three times with PBS (5 min each) after each step. Then, tissue sections were blocked with 1% fish gelatin (Sigma–Aldrich) in PBS for 1 h at room temperature, and subsequently incubated with the primary antibody: mouse anti-Tuj1 (1:500; Covance/Biolegend, CA, USA), rabbit synaptophysin (1:500; Ab32127, Abcam, Cambridge, MA, USA), rabbit anti-synapsin I (1:500; Millipore, Billerica, MA, USA), and rabbit anti-mCherry (1:400; Abcam) overnight at 4°C.

For immunohistochemistry (IHC), frozen brain tissues were sliced into 10 μm-thick coronal sections using a cryostat vibratome (Leica CM 1950; Leica Microsystems, Buffalo Grove, IL, USA). The sections were dehydrated on a slide warmer for 30 min, fixed with 10% formalin buffer, washed with −20°C precooled ethanol: acetic acid (2:1) solution for 10 min, and finally permeabilized with 0.2% Triton-X 100 solution for 5 min. All slides were washed three times with PBS (5 min each) after each step. Then, tissue sections were blocked with 1% fish gelatin (Sigma–Aldrich) in PBS for 1 h at room temperature, and subsequently incubated with the primary antibody: mouse anti-NeuN (1:400; Millipore, Billerica, MA, USA), rabbit anti-ND1 (1:400; Millipore, Billerica, MA, USA), chicken anti-GFAP (1:400; Abcam), mouse anti-iba-1 (1:400; Sigma–Aldrich), and rabbit anti-Beclin (1:5,000; Abcam, Cambridge, MA, USA), goat anti-collagen type IV (1:400; Millipore), rabbit anti-mCherry (1:400; Abcam), rabbit anti-vGluT1 (1:500; Abcam), rabbit anti-GAD67 (1:500; Abcam), rabbit anti-Iba1 (1:400; Abcam), rabbit anti-vGluT1 (1:500; Abcam), mouse anti-GFP (1:500; Sigma–Aldrich), Oct4 (1:250, Cell Signaling, Danvers, MA, USA) and Klf4 (1:500, Abcam) overnight at 4°C.

For both ICC and IHC, on the next day, the samples were washed three times with PBS for 5 min, then reacted with the secondary antibodies Alexa Fluor®488 goat anti-mouse or rabbit (1:300; Life Technologies, Grand Island, NY, USA) and Cy3-conjugated donkey anti-rabbit (1:300; Jackson ImmunoResearch Laboratories, West Grove, PA, USA) or Cy5-conjugated donkey anti-mouse or rabbit (1:400; Jackson ImmunoResearch Laboratories) for 80 min at room temperature. After three washes with PBS, nuclei were stained with Hoechst 33342 (1:20,000; Molecular Probes, Eugene, OR, USA) for 5 min as a counterstain; and then the brain sections were mounted, coverslipped, imaged, and photographed under a fluorescent microscope (BX51, Olympus, Japan) or a laser scanning confocal microscope (Carl Zeiss Microimaging, Inc., Thornwood, NY, USA).

For H&E, brains were sectioned with a vibratome and coronal sections (20 μm) of mouse brains were collected from the sensorimotor cortex (brains damaged during removal were not sectioned). Every 6th section and a total of 10 sections per brain were selected for H&E staining from the anterior start to the posterior end of the injury site.

Astroglia Scar Measurement

Glial scar measurements were taken using ImageJ against GFAP immunofluorescence contiguous to the ischemic core. The thickness of the glial scar was measured using the average distance across hypertrophied astrocytes lining the ischemic core based on a method previously described (Cai et al., 2017). GFAP area and intensity were determined using the ImageJ analysis of the area of GFAP-positive fluorescence in the glial scar region respectively. Median GFAP intensity was measured using a 100-pixel width rectangle across six different regions of the glial scar to measure median GFAP intensity across the area.

Cell Death Assessment

A terminal deoxynucleotidyl transferase dUTP nick end labeling (TUNEL) assay kit was used to examine cell death by detecting fragmented DNA in 10-μm-thick coronal fresh frozen sections as described previously (Lee et al., 2014). After fixation (10% buffered formalin for 10 min and then ethanol:acetic acid (2:1) solution for 5 min) and permeabilization (0.2% Triton X-100 solution), brain sections were incubated in equilibration buffer for 10 min. Recombinant terminal deoxynucleotidyl transferase (rTdT) and nucleotide mixture were then added on the slide at 37°C for 60 min in the dark. Reactions were terminated by 2× SSC solution for 15 min. Nuclei were counterstained with Hoechst 33342 (1:20,000; Molecular Probes) for 5 min. Cell counting was performed following the principles of design-based stereology (Lee et al., 2014). Systematic random sampling was used to ensure accurate and non-redundant cell counting. Eight brain sections per animal were collected at 90 μm distance between sections for non-overlapping multistage random sampling. For each animal, 6 "areas of interest" regions per slide were selected. Each field was scanned at 200× magnifications for cell counting. ImageJ (NIH) was used to analyze each picture. All experiments were performed in a blinded fashion, so the data collector

and data analysis were performed without knowledge of experimental groups.

Functional and Behavioral Tests

Rotarod Test

Rats were placed on an accelerating rotarod cylinder (Economex, Columbus In., Columbus, OH, USA) and the length of time the animals remained on the rotarod was measured. The speed was slowly increased from 4 to 40 rpm in 5 min. The animals were trained for 3 days before stroke surgery. The mean duration on the device was recorded with three measurements (Wittenberg et al., 2007; Spurlin and Nelson, 2017).

Corner Test

The corner test monitors unilateral whisker deficits. Mice were allowed to roam freely in a star-shaped arena with 30° angles. Upon entering a corner, the mouse would rear and turn toward the wall, which was sensed by intact whisker sensations. In our right sensorimotor cortex ischemic stroke model, mice lost sensation in their left whiskers. The percentage of right turns was measured before and after stroke (Calabresi et al., 2003; McCrary et al., 2019).

Forced Swimming Test

The forced swim test (FST) was carried out to measure depressive behaviors. Mice were dropped individually into a plexiglass cylinder (height: 30 cm, diameter: 22.5 cm) filled with water to a depth of 15 cm and maintained at 23–25°C. In this test, after the initial vigorous activity of 2 min, mice acquired an immobile posture which was characterized by motionless floating in the water and made only those movements necessary to keep the head above water. The duration of immobility was recorded in seconds during the last 4 min of the 6 min test. All mice received a 15-min training session under similar conditions 24 h before the formal test (Kronenberg et al., 2014; Frechou et al., 2019).

Sucrose Preference Test

The mice were given access to both water and a sucrose solution, and their preference for the sucrose solution was quantified. Briefly, mice were deprived of food and water for 20 h. One bottle of water and one containing 1% sucrose were simultaneously placed in the cages and were freely accessible to the mice for 3 h. The position of the two bottles (left or right side of the cage) was varied randomly from trial to trial. The volume of each liquid was measured before and after each trial, and sucrose preference was calculated according to the following equation: sucrose preference = (sucrose consumption)/(sucrose consumption + water consumption) × 100 (Heins et al., 2002; Grealish et al., 2016).

Tail Suspension Test (TST)

Mice were taped to a crossbar by their tails and their behavior was recorded for 10 min. In this test, after the initial vigorous activity of 2 min, mouse behavior was during an analysis period of 6 min. The duration of immobility was recorded in seconds during the time. In our laboratory, small movements that are confined to the front legs but without the involvement of the hind legs are not counted as mobility. Additionally, oscillations and pendulum-like swings that are due to the momentum gained during the earlier mobility bouts also are not counted as mobility. The same blinded observer was used to assess mobility in all experiments (Ge et al., 2012; Tsai et al., 2012).

Experimental Design and Statistical Analysis

Significant time and effort were initially spent to test several master transcription factors including NeuroD1 (ND1), Neurogenin2 (Ngn2; **Supplementary Figure 1**, Gangal et al., 2017; Jiang et al., 2019a,b), and Ascl1 to identify effective methods to efficiently carry out glia to neuron reprogramming. ND1 was eventually selected based on more than 2 years of *in vitro* and *in vivo* experiments and verification of combinations as well as individual applications of these factors. In cell culture experiments, at least three batches of cultures were tested per experiment, and the purity of astrocyte cultures was ensured by both GFAP staining and specific culture media/protocols. Multiple examinations were performed to independently replicate the virus infection efficacy and conversion efficiency, dose-response relationship, and cell phenotypes. In stroke animal experiments, the well-characterized focal ischemic stroke model with partial reperfusion represents common clinical cases (Wei et al., 2017; Zhong et al., 2020) and suitable for functional and behavioral tests. A specialized researcher with extensive rodent microsurgery training performed all ischemic surgery to ensure highly consistent ischemic insult in the sensorimotor cortex. Another experienced researcher performed all virus injection procedures to ensure consistent virus infections in the same brain region. The neuronal phenotype of reprogrammed cells was confirmed by at least two specific markers and the co-localization of cellular markers was examined by 3-D microscopy. We identified mature neurons not only rely on morphology and cell markers but also functional activity using electrophysiological recordings. In cell counting analysis, we followed stereology principles by separating analyzed by at least 100 μm to avoid double counting cells. In these experiments, sample sizes were six to eight per group and at least six sections were examined for each brain. In whole-cell recordings, over 20 cells per group were inspected; MEA recordings examined multiple brain slices from three to four brains per group. Functional and behavioral tests were performed using 6–14 animals per group, depending on the outcomes of Power analysis and our previous investigations. Data analysis was performed under blinded or double-blinded conditions.

All data were analyzed for normality using the D'Agostino and Pearson omnibus normality test (where $n > 7$) and Kolmogorov–Smirnov normality test (where $n < 7$). Unpaired Student's *t*-test or Fisher's test were used for pairwise comparisons. Comparisons of multiple groups were analyzed using one- or two-way ANOVA followed by *post hoc* Tukey's test or other tests as indicated in figure legends. In these statistical reports, the variance between populations was tested using Bartlett's test, F-factor, and *p*-values are provided. All results are expressed as Mean ± SEM Statistical comparisons were finished using Graph Pad Prism 6 (Graph Pad Software, Inc., San Diego, CA, USA). In general, $p < 0.05$ was considered significant for all comparisons; the exact *p*-value is reported for some important comparisons as a reference for readers.

RESULTS

Among single transcription factor-mediated direct reprogramming candidate genes, both ND1 and Ngn2 demonstrated an ability to reprogram reactive astrocytes but ND1 was selected based on both efficiency and efficacy (**Supplementary Figure 1**). A mCherry tagged ND1 lentivirus was generated under a mouse GFAP promoter and used for both *in vitro* and *in vivo* transduction. A viral titer of GFAP-ND1 was calculated to be approximately 4.8×10^7 units/μl by using a 10^7 dilution of virus that yielded ∼92% infection in HEK293FT cells. Astrocyte cultures were infected at 7 days *in vitro* (DIV 7) and followed for up to 8 weeks post-infection to examine cell fate and efficiency of transduction and conversion. After lentiviral transduction, successfully infected cells could be monitored over time by the expression a mCherry reporter carried by the ND1 virus (**Figures 1A–D**). Infected cells began to adopt neuronal features around 2 weeks following transduction, including the extension of one or more long processes that are uncharacteristic of astrocytes (**Figure 1C**). While neuronal axonal processes are often elongated beyond the length of the cell body (>100 μm), astrocytes are characterized by multiple shorter and spread-out processes. Staining using the neuronal lineage market Tuj1 verified this morphological difference between mCherry-positive astrocytes and immature neuron-like cells by morphological examination (**Figures 1D,H**). On the other hand, astrocytes infected with the empty vector did not exhibit any of these alterations (**Figure 1E**). The observed cell lineage switch from ectoderm to endoderm is a time-dependent process. By 4 weeks, 58.6% of astrocytes were positive for the immature neuronal marker Tuj1 (**Figure 1F**). Consistent with the expected reduction in cell proliferation and survival rate of converted cells under culture conditions, the cell numbers in cultures that received ND1 transduction were drastically less than that in control cultures infected by the empty vector where astrocytes continued to proliferate (**Figure 1G**).

In vitro Conversion of Astrocytes to Neuronal Cells

To confirm the maturity of astrocytes-converted iNeurons *in vitro*, we stained converted cells with the synaptic vesicle protein synaptophysin. As a marker for synapse formation, synaptophysin expression was detected in converted cells (**Figures 1H,I**). In the next experiment, we co-infected ND1 with a synapsin-GFP reporter to monitor cells. GFP expression emerged at 14 days post-transduction. In co-labeling experiments of Tuj1 and synapsin-1, around 20% of Tuj1-positive cells expressed the synaptic protein synapsin-1 (**Figures 1J,K**). During neuronal maturation, converted cells developed significantly longer processes (>20–100 μm) compared to cells infected by the control lentivirus, inspected at 6 weeks after transduction (**Figure 1L**).

Interestingly, reprogrammed cells also featured increased motility. In an *in vitro* scratch assay, reprogrammed cells moved into the scratched area much faster than vehicle control cells (**Figure 2A**). Three days later, the scratched area was significantly smaller compared to the control cultures (**Figures 2A,B**). Western blot analysis revealed that the phosphorylated focal adhesion kinase (p-FAK), a key mediator in cell adhesion and migration, was significantly increased (**Figure 2C**).

In electrophysiological examinations, the whole-cell recording was performed in mCherry-positive converted cells 28 days after ND1 transduction. In the current-clamp mode, gradually increased membrane depolarization triggered the firing of action potentials (**Figure 2D**). We patched a total of 10 mCherry positive cells with neuronal morphology; all cells exhibited sodium and potassium currents and action potentials upon membrane depolarization. Prolonged depolarization generated firing of repetitive action potentials, resembling functional activities of neuronal cells (**Figure 2E**).

Focal Ischemic Stroke in Mice and mCherry-ND1 Lentivirus Injection

Focal ischemic stroke of the right sensorimotor cortex was induced in adult GFAP-Cre × Rosa-YFP mice. Astrocytes in this mouse express the YFP reporter regardless of cell phenotype changes. This property is favorable for tracking astrocytes as they switch between inter-lineage phenotypes. After ischemic stroke, robust astrocyte accumulation took place in the peri-infarct region, and the ischemic core gradually forms a tissue cavity 2–3 weeks later (Kanekar et al., 2012; Pivonkova and Anderova, 2017). Proliferating astrocytes around the damaged tissue provided an abundant cell supply for reprogramming. Lentivirus containing mCherry-ND1 was injected into the peri-infarct region 7 days after ischemia, this time point was selected to avoid the acute phase when astrocytes are thought to be protective yet the virus transduction still catches hypertrophied astrocytes before the formation of a glial scar (**Figure 3A**).

Reprogramming of Reactive Astrocytes and Neuronal Conversion After Ischemic Stroke

At 28 days after ND1 lentivirus injection to the peri-infarct region, approximately 10% of total astrocytes were YFP/mCherry double-positive cells. We identified cells labeled by YFP (identifying their astrocyte origin), mCherry (infected by ND1 lentivirus), and NeuN (mature neuron marker; **Figure 3B**). The combination of these three markers in single cells indicated successful viral-mediated reprogramming of endogenous astrocytes to neurons. Co-labeling of NeuN and transduction marker YFP in a single converted cell was also confirmed using confocal microscopy, showing a pyramidal neuronal phenotype with a single axon and dendritic arbors (**Figure 3C**). In contrast, cells infected by the empty control vector showed separated cell populations of neurons and infected astrocytes, illustrating high specificity of the viral promoter and no conversion in the absence of ectopic ND1 (**Figure 3D**). In cell counts, around 66% of infected cells became mCherry/YFP/NeuN triple-positive iNeurons (**Figure 3E**). Immunohistochemical examination revealed that most reprogrammed cells (∼80%) expressed vesicular glutamate transporters (vGLUTs), which are the characteristics of glutamatergic neurons (**Figures 3F,G**). Western blotting of the peri-infarct tissue detected a significant increase in the expression of tyrosine hydroxylase (TH; **Figures 3H,I**),

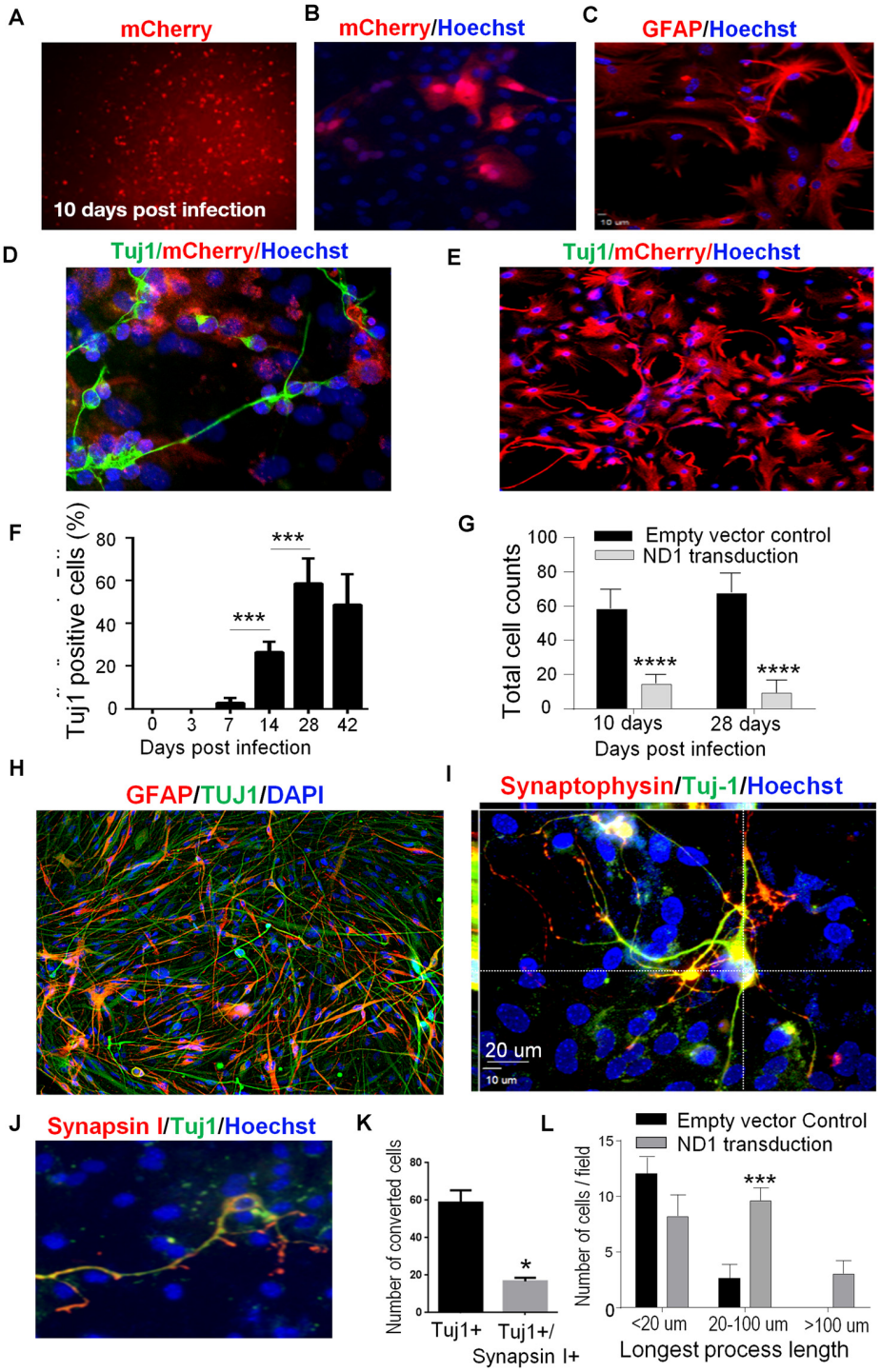

FIGURE 1 | *In vitro* direct reprogramming of astrocytes to induced neurons. Mouse astrocyte cultures were transduced with NeuroD1 (ND1) or empty vector control and stained for different cell markers. **(A)** Ten days after lentiviral transduction, successfully infected cells were monitored over time by the expression of the fluorescent mCherry reporter (red), implicating GFAP-ND1-IRES-Ubi-mCherry expression in these astrocytes. **(B–D)** Enlarged images of infected cells 14 days after transduction. Infected cells expressed the reporter gene mCherry **(B)**, GFAP stain revealing an astrocyte-like morphology of astrocytes before reprogramming **(C)**. In image **(D)**, some cells develop the neuronal lineage marker Tuj1 (green) and adopted either a unipolar or bipolar morphology that is uncharacteristic of astrocytes. **(E)** A representative image of control culture with the empty vehicle virus showing the lack of Tuj-1 expression in infected cells (mCherry, red). There were also no alterations to the morphology of astrocytes. **(F)** Time course and reprogramming rate of the expression of the immature neuron marker Tuj1 in infected astrocytes up to 42 days after transduction. One-way ANOVA ($F_{(5,36)}$ = 77.91) followed by Holm–Sidak's multiple comparisons test. *N* = 3 independent cell culture batches,

(*Continued*)

FIGURE 1 | Continued
$^{***}p < 0.001$. **(G)** Quantified cell counts of total cell numbers 10 and 28 days after transduction with ND1 or vector control. The reduced cell number implied attenuated cell proliferation after the ND1 transduction and neuronal conversion. Two-way ANOVA (interaction: $F_{(1,10)} = 2.377$, $p = 0.1542$; time: $F_{(1,10)} = 0.174$, $p = 0.6854$; *treatment*: $F_{(1,10)} = 358.9$, $^{****}p < 0.0001$). **(H)** An immunostaining image shows coexpression of Tuj1 and GFAP in cultured astrocytes 6 weeks after transduction. **(I)** Confocal microscopy of an enlarged image from 6 weeks post-transduction, showing complex processes that are positive for Tuj-1 and synaptophysin colocalized with mCherry. Those cells under the culture condition did not show positivity to NeuN; however, they expressed the synaptic protein synaptophysin. **(J)** At 6 weeks after transduction, astrocytes undergoing direct reprogramming extended processes and developed nerve terminals positive to the pre-synaptic protein synapsin I (red). **(K)** The bar graph shows quantified data that at 6 weeks post-transduction, 58.7% of reprogrammed cells (mCherry-positive) expressed Tuj-1 and 17.4% of these cells also expressed synapsin 1. $n = 3$, paired t-test, $^{*}p < 0.05$ vs. Tuj1 only cells. **(L)** Measurements of the length of extended processes from converted cells. There were drastically increased in the length of processes of cells received ND1 transduction. $N = 3$, two-way ANOVA (interaction: $F_{(3,9)} = 8.427$, $^{***}p < 0.001$).

which is consistent with the notion that activation of the Wnt/β-catenin pathway and ND1 upregulates TH expression (Jiang et al., 2020). We did not observe the GABAergic neuronal marker glutamic acid decarboxylase 67 (GAD67; data are not shown). Measured at 14 days into the reprogramming process, none of the stemness markers Oct4 and Klf4 were detected in transduced (mCherry-positive) cells (**Supplementary Figure 2**), supporting that ND1-mediated glia-to-neuron conversion did not pass through an intermediate stem cell stage.

Neurotrophic/growth factors such as BDNF and FGF10 play critical roles in important processes such as cell survival, proliferation, and maturation, angiogenesis, neurogenesis, and wound healing, each of which plays an essential part in the regenerative process (Matkar et al., 2017; Spurlin and Nelson, 2017; Ghosh, 2019). Western blot assay in the peri-infarct region detected significantly higher levels of BNDF and FGF10 in ND1 transfected mice compared to animals who received empty control vector (**Figures 4A,B**). Consistently, the ND1 treatment significantly attenuated the stroke-induced reduction of the synaptic protein PSD-95 expression in the post-stroke cortex (**Figure 4C**). Meanwhile, the inflammatory marker protein NFκB expression and the number of phagocytic Iba-1-positive microglia were significantly lower in the ND1 treated brains than in stroke mice that received a control vector (**Figures 4D**, **5A,B** and **Supplementary Figure 3**).

Reprogramming of Reactive Astrocytes and Reduced Glial Scar After Ischemic Stroke

In stroke mice that received lentiviral ND1 administration, the number of YFP-positive cells in the peri-infarct area decreased compared to that in the stroke control cortex (**Figures 5C,D**). The relative size, thickness and mean fluorescent intensity of the GRAP-positive glial scar were also reduced (**Figures 5D–H**). 6 weeks after stroke, Western blot data revealed decreased GFAP levels in the peri-infarct region of ND1-treated stroke mice (**Figure 5I**). The reduced astrogliosis appeared to facilitate regenerative activities in the peri-infarct region. Some newly converted iNeurons (mCherry/YFP/NeuN triple-positive cells) were even observed inside of the core region where no neuronal cells would normally be expected to survive at this delayed post-stroke time point (**Figure 5J**).

Astrocyte Reprogramming Improved Synaptic Transmission in the Peri-infarct Region

The MultiElectrode array (MEA) system was used to record evoked extracellular post-synaptic potentials (EPSPs) in brain slices of sham control, stroke control of empty vector, and stroke with ND1 transduced mice (**Figure 6A**). In peri-infarct locations 6 weeks (42 days) after stroke, the responsive area covered by 59 recording electrodes and the amplitude of EPSPs evoked by a stimulation electrode were noticeably absent or reduced (**Figure 6B**). In the similar areas of slices from stroke mice that received ND1 transduction, normal or enhanced EPSPs were detected in multiple locations (**Figure 6B**). To further understand changes at the synaptic level, we examined the synaptic plasticity by paired-pulse facilitation (PPF). In PPF recordings, the second evoked EPSPs were large than the first one in all three experimental groups (**Figure 6C**). In fact, in cortical layers II/III, layer IV, and layer V we observed even greater facilitation in stroke control slices, which was partly due to a smaller size of the first EPSP in stroke control slices (**Figures 6D–F**). ND1 transduction prevented the smaller initial EPSPs and the abnormally enhanced synaptic facilitation (**Figures 6D–I**). Similar increased synaptic facilitation has been reported in human stroke patients (Kronenberg et al., 2014). Increased synaptic modification such as ischemia-increased long-term potentiation (LTP), has been called "pathological plasticity" (Frechou et al., 2019), which was ameliorated in ND1-treated slices (**Figures 6G–I**).

Astrocyte Reprogramming Improves Functional Outcomes After Stroke

The focal ischemic stroke model results in well-defined motor and sensorimotor deficits detectable using the rotarod test and corner test (Grealish et al., 2016). Three weeks after stroke, the time that mice balanced on a rotating beam was significantly shorter compared to sham control mice (**Figure 7A**). Stroke mice that received the ND1 treatment, however, remained on the beam significantly longer than stroke mice received the empty control vector (**Figure 7A**). In the corner test, rodents normally make an equal left and right turn in their exploratory behavior. Stroke animals, however, show biased turns to one direction due to the unilateral injury to the right sensorimotor cortex (**Figure 7B**). Significant improvement in the turning behavior was seen with stroke mice received the ND1 treatment (**Figure 7B**). We and others have shown that stroke can induce chronically developed phenotypes of post-stroke depression-like behavior (Kronenberg et al., 2014; Frechou et al., 2019; Zhong et al., 2020). To further characterize long-term behavioral modifications, the sucrose solution preference test, forced swim test, and tail suspension test was performed 4 months after stroke. Stroke control mice exhibited obvious depressive-like behaviors in all these tests

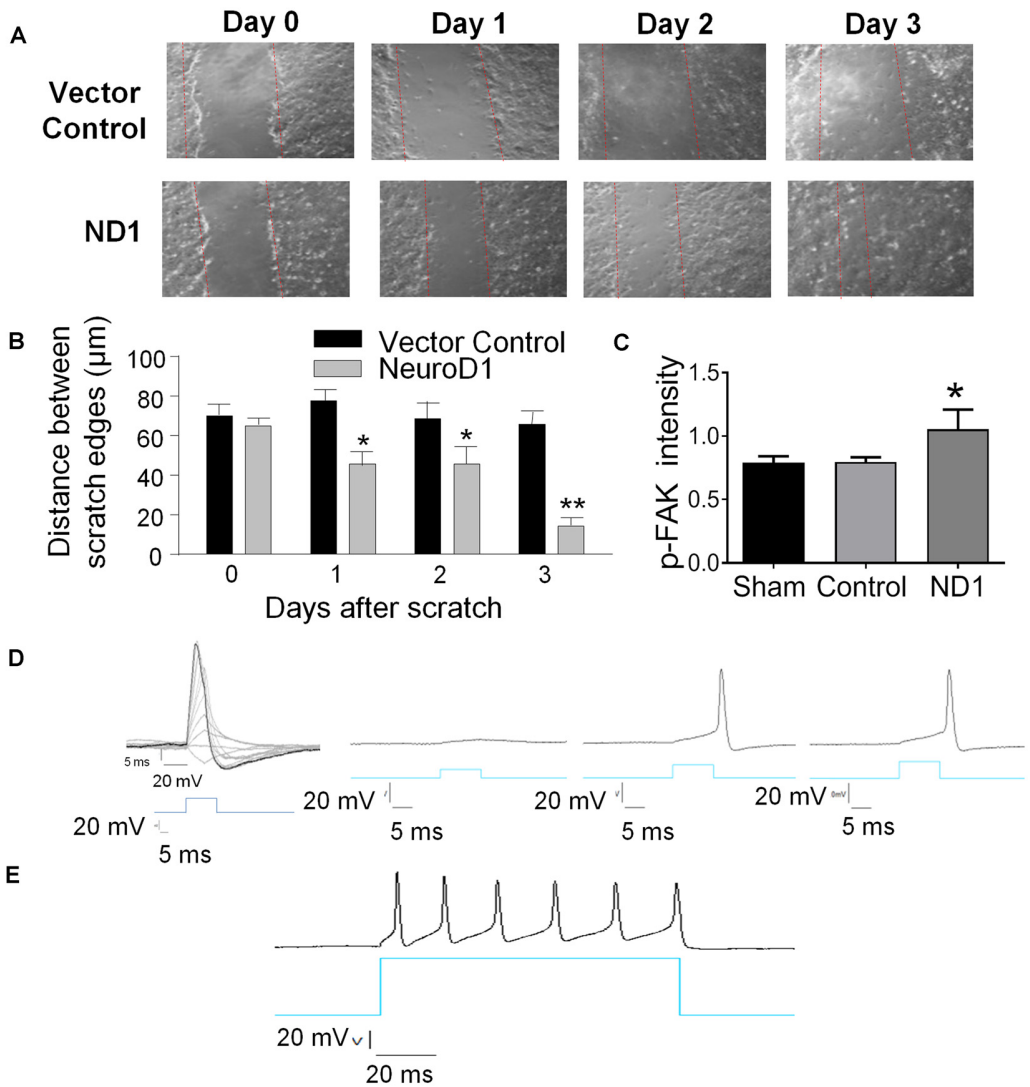

FIGURE 2 | Reprogramming induced cellular changes and functional activities *in vitro*. The ND1-mediated astrocytes reprogramming was monitored in cultures and functionally characterized. **(A,B)** Two weeks after ND1 virus or empty control vector transduction, astrocyte cultures were challenged by the scratch test to measure the motility of reprogrammed cells. From day 1 after the scratch insult, the damaged area recovered significantly faster by migrating cells in cultures infected by ND1 compared to the vector control culture. $N = 3$ cell cultures. Two-way ANOVA (Interaction: $F_{(3,24)} = 11.15$, $^{***}p < 0.0001$; Time: $F_{(3,24)} = 18.66$, $^{***}p < 0.0001$; ND1: $F_{(1,8)} = 53.87$, $^{***}p < 0.0001$) followed by Holm–Sidak's multiple comparisons test: $^{*}p < 0.05$ and $^{**}p < 0.01$ for ND1 vs. empty vector control. **(C)** Effect of the scratch test on the expression of migration factor focal adhesion kinase (FAK) in reprogrammed cells. In line with the increased motility 3 days after scratch, ND1-infected cells within 200 μm of the scratch expressed significantly higher immunofluorescence of phosphorylated FAK (p-FAK). $N = 3$ per group. One-way ANOVA, $F_{(2,6)} = 7.327$, $^{**}p = 0.0245$ followed by Holm–Sidak's multiple comparisons test: $^{*}p < 0.05$ vs. control. **(D)** mCherry-positive converted cells were subjected to whole-cell recordings 28 days after infection. In the current-clamp mode, membrane depolarization induced by current injections evoked depolarization generated action potentials. A hyperpolarization was observed upon the decay phase of the spikes, which is typical for neurons and suggestive of functional potassium channels in these cells. $n = 10$. **(E)** A longer membrane depolarization pulse evoked the firing of a chain of action potentials that are characteristics of functional neurons.

while no significant depressive-like changes were observed in mice that received ND1 treatment (**Figures 7C–E**).

DISCUSSION

The present investigation presents compelling evidence for the feasibility and effectiveness of utilizing reactive astrocytes as an endogenous cellular source for the generation of neuronal cells to repair damaged brain structures. Our *in vitro* experiments demonstrate the efficiency and the efficacy of the reprogramming process by ND1 as well as the neuronal activity of converted cells. Using an established sensorimotor ischemic stroke mouse model, we demonstrate that delivery of ND1 to reactive astrocytes in the peri-infarct region can be achieved in a temporally and spatially specific manner using a lentiviral vector. The ectopic expression of ND1 redirects reactive astrocytes into mature iNeurons, while reduced glial scar facilitates regenerative repair. MEA *ex vivo* recording revealed that ND1-induced reprogramming

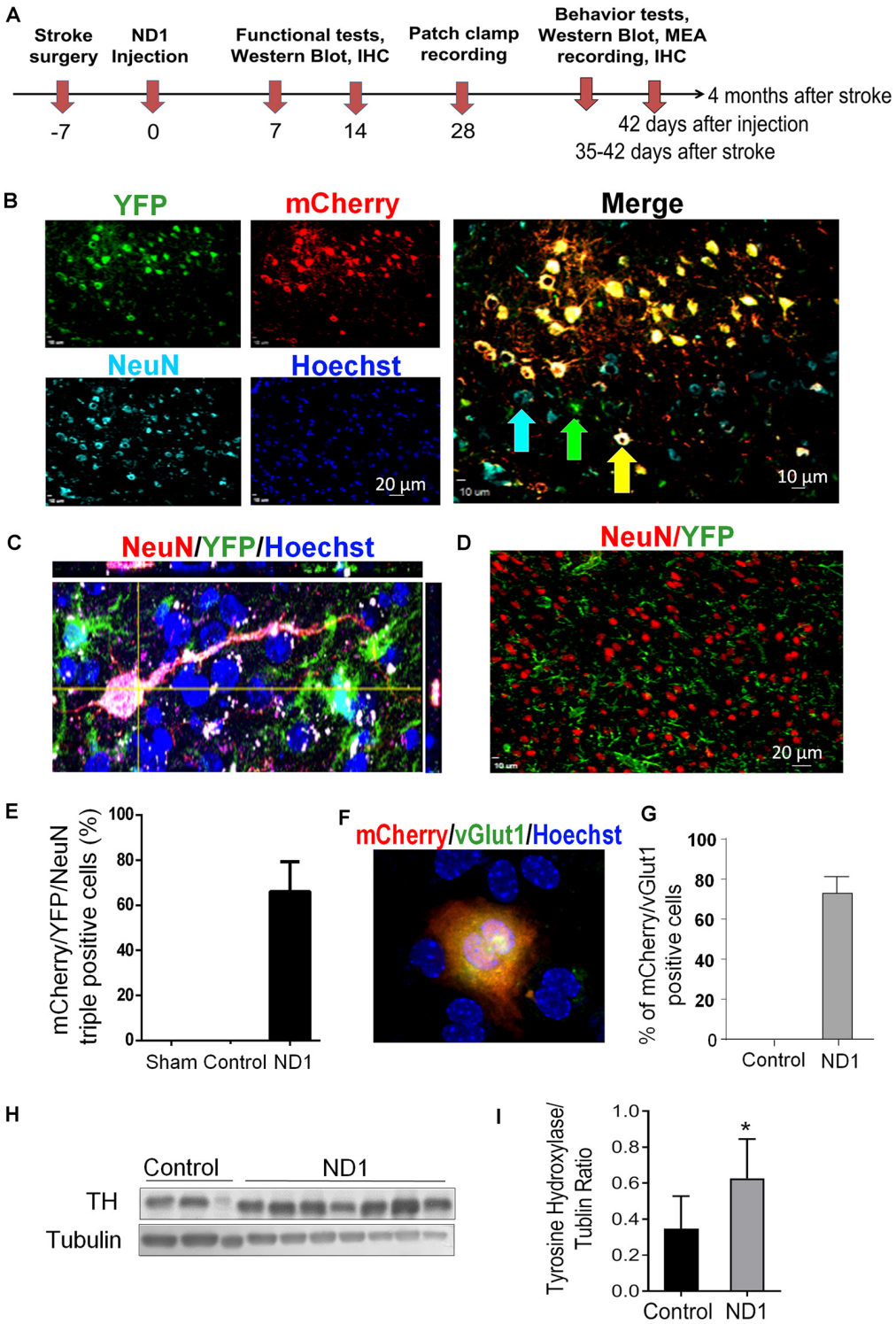

FIGURE 3 | Conversion of astrocytes to mature neurons *in vivo*. Adult GFAP-Cre x Rosa-YFP mice were subjected to a focal ischemic insult to the right sensorimotor cortex and subjected to control and ND1 treatments. **(A)** Timeline of *in vivo* reprogramming experiments. Animals received sham, stroke control, or ND1 lentivirus injection to the peri-infarct region 7 days after stroke. empty control vector or ND1 lentivirus. Functional and psychological assessments were performed different days after stroke. Six weeks later, brain coronel sections were subjected to immunohistochemical staining with cell phenotype markers. **(B)** Representative images show cells expressing YFP (green, astrocytes), mCherry (red, ND1 infected cells), NeuN (light blue, mature neurons), and Hoechst 33342 (dark blue, nuclei of all cells). The enlarged merged image illustrates overlapped markers (yellow/orange), indicating astrocyte-converted iNeurons. **(C)** A high

(*Continued*)

FIGURE 3 | Continued
magnificent confocal 3-D image showing a converted iNeuron with overlaid markers mCherry (red, transfection marker), YFP (green, astrocytes origin), and NeuN (blue, mature neuronal marker). The converted cell adopted neuronal morphology of an extended axon. **(D)** Control experiment where the brain region was infected with empty control virus. Due to the lack of cell reprogramming and lineage change, the neuronal and astrocytes populations (NeuN of red color and YFP of green color) were distinctively located without co-localization. **(E)** Quantified data of the image analysis of mCherry/YFP/NeuN triple-positive cells. No such cell could be seen in sham and empty control vector cells. There were over 66.06% of mCherry/YFP/NeuN triple-positive cells among ND1-infected cells. $N = 6$ for sham or control, $n = 8$ for ND1 group. **(F,G)** At 3–4 weeks after ND1 transduction, the glutamatergic neuronal marker vGLUT (green) was detected and colocalized with mCherry (red; overlay color: yellow/orange) in the converted cells. The bar graph in **(F)** shows that more than 72.9% of converted cells expressed vGLUT. There was no vGLUT expression in empty vector control cells. $N = 8$ animals per group. **(H,I)** The dopaminergic neuronal marker tyrosine hydroxylase was detected *via* western blot in peri-infarct tissue from control and ND1 treated brains. The bar graph in **(H)** indicates a significant increase of the tyrosine hydroxylase (TH) level in the ND1 treated tissue compared to injection of the empty vector control. $N = 3$ independent brain samples for control and $n = 7$ for ND1. Unpaired t-test, $^*p < 0.05$, $t = 1.937$, DF = 8; analysis of variance: $F_{(2,6)} = 1.433$, $p = 0.9279$.

can restore disrupted cortical neuronal networks and correct pathological synaptic activity in the peri-infarct region. Finally, we observed improved short- and long-term functional and behavioral recovery with ND1 treatment, suggesting the potential to improve multiple outcomes as a result of this innovative therapy.

Glia to neuron reprogramming has recently been tested in basic and translational research (Grealish et al., 2016; Li and Chen, 2016). Early *in vitro* work demonstrated successful reprogramming of postnatal astrocytes and NG2 cells into functional neurons through forced expression of Pax6, Ngn2, or Ascl1 (Heins et al., 2002; Berninger et al., 2007; Heinrich et al., 2010). In the last few years, reactive astrocytes have been explored as a reprogramming pool in the adult mouse brain (Torper et al., 2013; Liu et al., 2020). Astrocytes are normally quiescent, and proliferation is not activated without injury (Ge et al., 2012; Tsai et al., 2012). In response to brain injury or neurodegeneration, astrocytes become reactive and exhibit changes in morphology, gene expression, and engage in rapid proliferation (Sofroniew and Vinters, 2010; Robel et al., 2011). Reactivity of astrocytes to brain injury provides an advantageous step in the expression of transcription factors using the GFAP promoter to drive the expression of ectopic transcriptions factors and reprogramming of these cells.

Reactive astrocytes in the peri-infarct region encase the injury site and play a biphasic role during acute and chronic phases of stroke (Sofroniew and Vinters, 2010; Robel et al., 2011). At the early phase after ischemic stroke, accumulating astrocytes limit the expansion of tissue damage. At later phases after stroke, the formation of a physical and chemical barrier between the ischemic core and surrounding regions is inhibitory for regeneration. The glial scar comprised primarily of astrocytes secretes inflammatory and growth-inhibitory factors, i.e., TNF-α, Interleukins, and proteoglycan proteins that inhibit neurite outgrowth (Karimi-Abdolrezaee and Billakanti, 2012; Huang et al., 2014). This physical and chemical barrier during the later stage of stroke becomes a major hurdle for neuronal regeneration and tissue repair. In contrast to this theory, a recent study in a spinal cord injury model suggested that reactive astrocytes play an essential role in neuronal repair (Anderson et al., 2018). We presume that the role and process of astrogliosis may differ in the spinal cord and the brain. Nevertheless, the goal of conversion therapy is not to eliminate astrocytes in the local region. The strategy of converting only a portion of astrocytes aims to the remaining cellular homeostasis and supporting role of astrocytes while facilitating neuronal regeneration in the local microenvironment.

Recent evidence suggests that low-level neurogenesis can occur outside the two canonical niches in SVZ and SGZ. Neuroblasts have been observed in the striatum, cortex, and amygdala of rodents, rabbits, guinea pigs, and primates including humans (Ernst et al., 2014; Luzzati et al., 2014; Feliciano et al., 2015). Local generation of new neurons has also been reported in the cerebral cortex, where layer I progenitors traced by retrovirus-mediated labeling were shown to produce neurons (Ohira et al., 2010). These events imply that endogenous neurogenic activities do take place in different brain regions for tissue homeostasis and neuroplasticity. It is also likely that these same processes are enhanced after brain injuries such as stroke (Magnusson et al., 2014). This had led some to suggest that astrocytes already represent quiescent neuronal progenitors that can become activated after injury. Based on this view, the reprogramming strategy provides a method of enhancing this endogenous mechanism to further enforce the neurogenic competence of reactive astrocytes proximal to the site of injury.

Reactive astrocytes in the peri-infarct region may arise from remote areas including the SVZ (Niu et al., 2013). The present investigation was not intended to differentiate between local astrocytes and those that had migrated to the site. A major challenge and necessary task are to distinguish converted iNeurons from preexisting neurons and their relative contribution to tissue repair. Proteins that are specific to astrocytes are not typically expressed in mature neurons. Thus, an astrocyte-specific reporter cannot be used to trace converted cells. To this end, we employed a Cre-lox system to permanently switch on the expression of a fluorescent protein so that astrocytes could be traced throughout the reprogramming process regardless of cell phenotype transformation. Our Cre-lox-dependent YFP expression is "locked-in" before the injury and before the upregulation of GFAP expression in astrocytes, enabling us to determine the astrocyte origin of converted neurons by YFP expression.

Alterations in the epigenetically regulated enzymes, variations in DNA methylation, histone modifications, and chromatin accessibility have been shown to occur in glial cells upon spontaneous neurogenic activation or reprogramming (Endo et al., 2011; Holtzman and Gersbach, 2018). Current reprogramming strategies can generate both excitatory glutamatergic and inhibitory GABAergic neurons in the adult brain and spinal cord (Torper et al.,

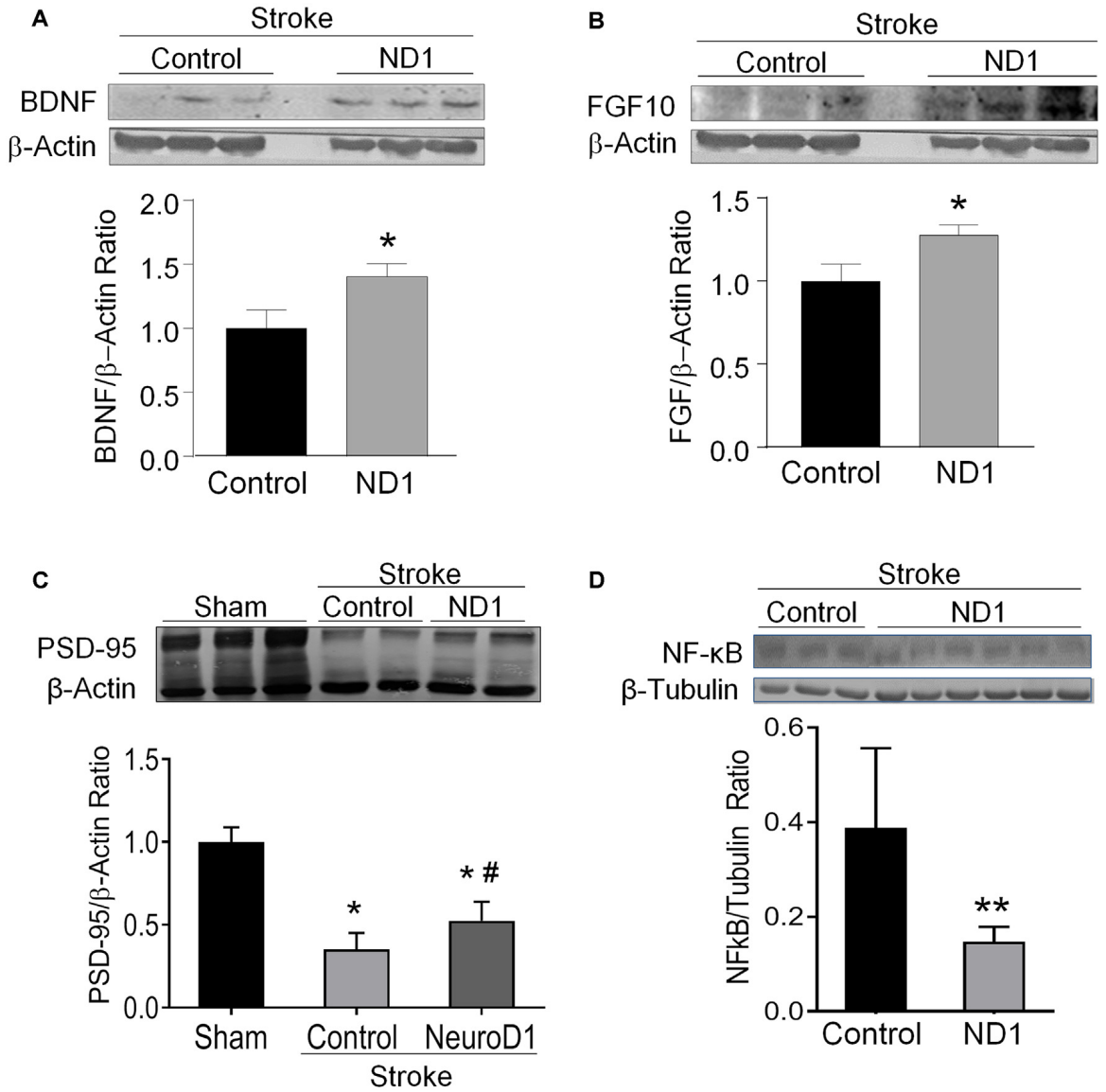

FIGURE 4 | Increased expression of regenerative genes and brain protection after ND1 treatment. Western blotting measured several key growth factors and synaptic proteins in the peri-infarcted region following stoke in control and ND1-treated animals 6 weeks after stroke. **(A,B)** The expression of BDNF (unpaired two-tailed Student's *t*-test: $n = 8$/group, $t = 2.305$, $^{*}p < 0.05$) and FGF (unpaired two-tailed Student's *t*-test: $n = 8$/group, $t = 2.407$, $^{*}p < 0.05$) were significantly increased in the brain subjected to ND1 vs. vehicle control of stroke mice. Panels **(A,B)** were performed in the same Western blot experiments with the same load control. **(C)** The expression of postsynaptic protein PSD-95 decreased after stroke and ND1 treatment partially recovered this synaptic protein loss. Two-way ANOVA (interaction: $F_{(2,4)} = 45.52$, $^{***}p = 0.0018$ followed by Holm–Sidak's Multiple Comparisons Test: $^{*}p < 0.05$ vs. sham; $^{\#}p < 0.05$ vs. empty vector control). **(D)** The ND1 treatment significantly reduced the NF-kB level in the post-stroke brain (unpaired two-tailed Student's *t*-test: $n = 3$ for vector control and $n = 6$ for ND1 group, $t = 3.613$, $^{**}p < 0.01$).

2013; Guo et al., 2014; Liu et al., 2015; Gascon et al., 2016). Consistent with these observations, we observed that ND1 primarily reprogrammed astrocytes into glutamatergic neurons, which are the most populous in the cerebral cortex. Since iNeurons are derived from a patient's own brain cells, they are compatible with the host and avoid possible rejection by the immune system or triggering inflammatory reactions. As shown in this investigation, ND1 mediated conversion did not trigger augmented inflammatory reactions; rather, it suppressed microglial activation and NFκB expression.

Aside from ND1 mediated direct reprogramming, alternative methods to increase neuronal production have been explored. For example, the removal of the p53-p21 pathway has also yielded significant promotion of direct reprogramming (Wang et al., 2016). Similarly, depletion of the RNA-binding protein PTBP1 also converted human astrocytes to functional neurons in a Parkinson disease model (Gao et al., 2017). Certain

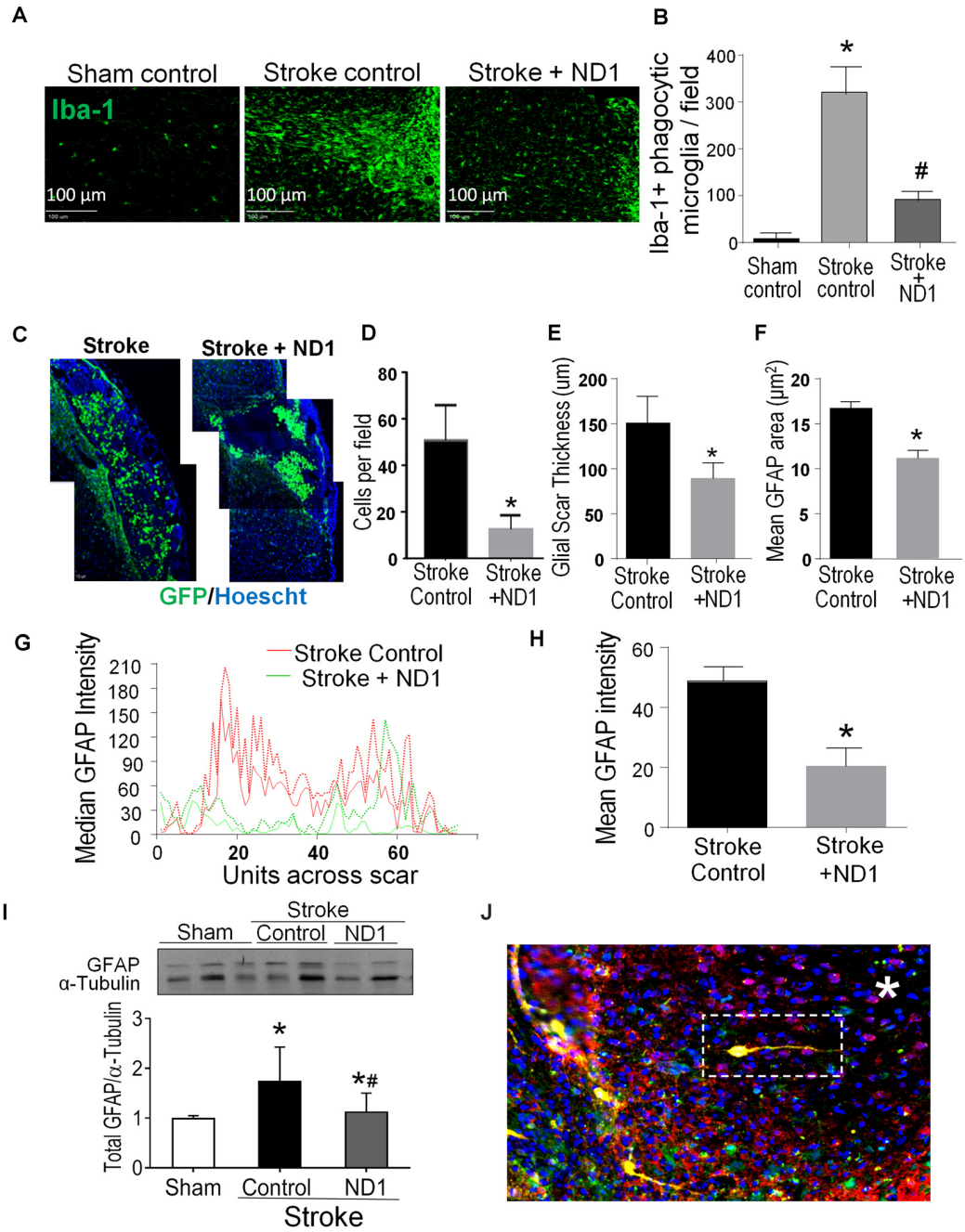

FIGURE 5 | Direct reprogramming of astrocytes attenuated microglial activation and astrogliosis in the post-stroke brain. Inflammatory activities including microglia activation and astrogliosis were examined in the peri-infarct region. **(A,B)** Iba-1 expression was examined 6 weeks post ND1 infection. Iba-1 positive microglia are present in significantly greater numbers in the ipsilateral cortex compared to sham control or contralateral cortex. The iba-1 fluorescence of phagocytic microglia was markedly less in the ND1-treated cortex. **(B)** The number of microglia in the ischemic cortex was significantly increased after stroke; ND1 injection showed a large reduction in the number of microglia cells in the region. N = 5/group; one-way ANOVA ($F_{(2,12)}$ = 118.4, $p < 0.0001$), $^{*}p < 0.05$ vs. sham control, $^{\#}p < 0.05$ vs. empty control vector. **(C–F)** Astrocyte accumulation or astrogliosis was evaluated in the peri-infarct region using immunohistochemical imaging 6 weeks after stroke after stroke. Images in C show accumulated astrocytes labeled by GFAP (green, arrows). The cell count **(D)**, the thickness of the gliosis **(E)**, and the mean GFAP area **(F)** were all significantly reduced. N = 6 per group paired t-test, $^{*}p < 0.05$ vs. stroke controls. **(G,H)** Gliosis profile analysis by mean gray value across scar transection. The graph plots show median values of stroke control (red lines) and stroke plus ND1 (green lines). The bar graph in **(H)** quantified the measurement, demonstrating a significant reduction in GFAP positive astrogliosis after ND1 treatment. N = 3 paired t-test, $^{*}p < 0.05$ vs. stroke controls. **(I)** Western blotting analysis of the GFAP level. The bar graph shows increased GFAP expression after stroke and the ND1 treatment attenuated this increase. N = 3, one-way ANOVA ($F_{(2,19)}$ = 4.525, p = 0.0247), Holm–Sidak's Multiple Comparisons Test; $^{*}p < 0.05$ vs. sham, $^{\#}p < 0.05$ vs. empty vector control. **(J)** An immunostaining image shows ND1-converted iNeurons (yellow) distributed inside the ischemic core (*). Cells were identified using mCherry (red), YFP (green), and NeuN (blue).

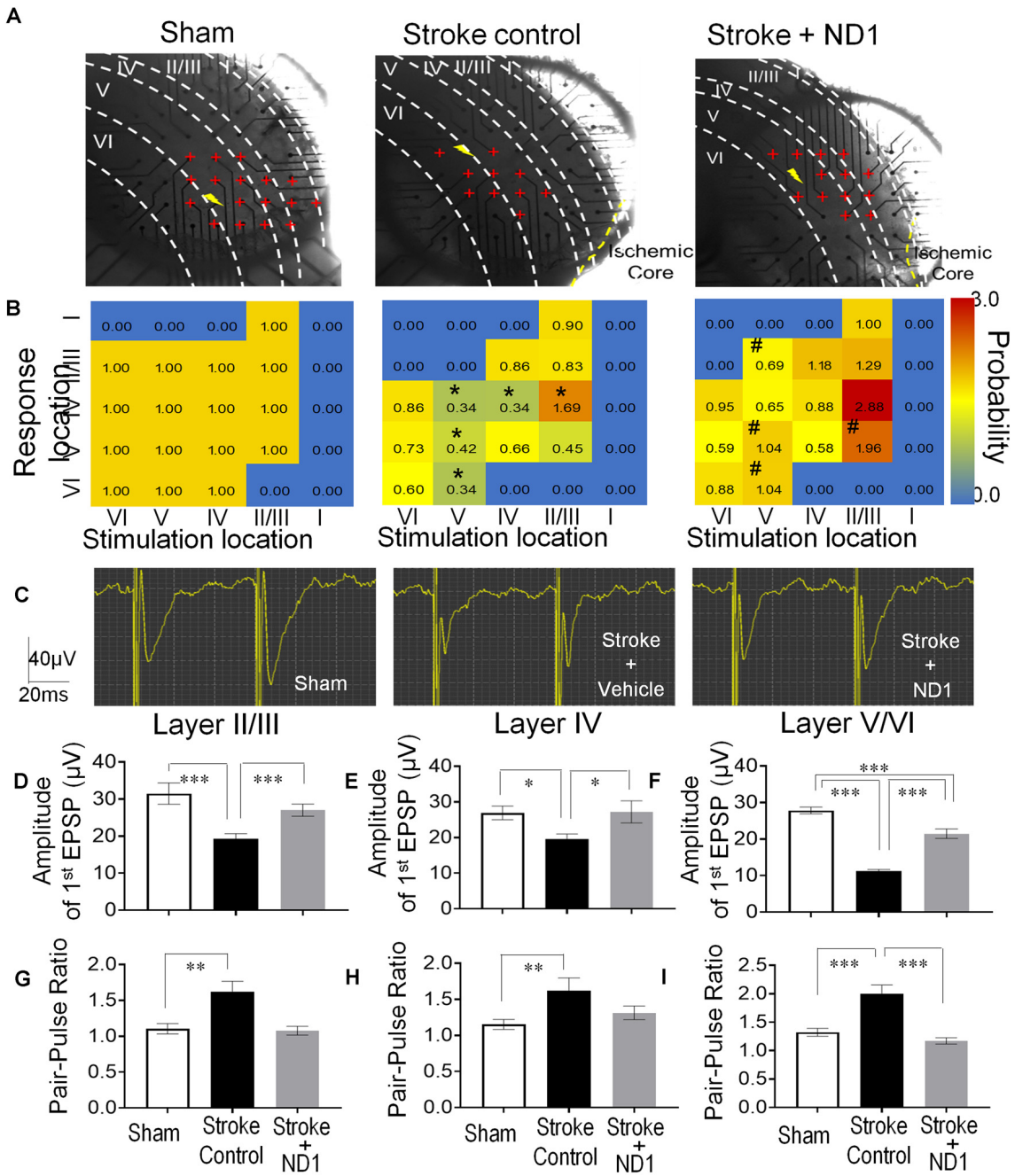

FIGURE 6 | Functional repair of neuronal networks in the ischemic cortex. The Multi-Electrode Array (MEA) recording was performed to detect neuronal connections and functional activities in the sensorimotor cortex of the brain sliced 42 days after stroke. **(A)** Photos of brain slices and locations of 59 recording electrodes (red cross) crossing the six cortical layers (I, II/III, IV, V, and VI) near the ischemic core or the similar area of the sham recording. The shock sign indicates the location of the stimulation electrode and red cross indicates the electrodes or area where evoked EPSPs can be recorded. **(B)** Heat maps of evoked EPSPs showing the location and intensity of the response. Non-response areas are shown in blue color, and responsive areas of evoked EPSPs are shown in a yellow to red spectrum according to the response probability normalized to sham controls. After a stroke, the EPSP response likelihood was significantly reduced or even disappeared in II/III, IV, V, and VI cortical layers (n = 4–5 animals in each group, $^{*}p < 0.05$, vehicle vs. sham controls, the Chi-square test). In recordings from slices subjected to ND1 transduction, there were more responsive areas (e.g., layer II/III) and the response probability of EPSPs was significantly greater than that in stroke controls (n = 4–5 animals in each group; $^{\#}p < 0.05$ vs. stroke controls, the Chi-square test). **(C)** Representative recordings of the pair-pulse facilitation. **(D–F)** Quantified data summarized from the pulse facilitation recording in different cortical layers. The amplitude of the first EPSPs was significantly smaller compared to sham control and it was restored in ND1-treated slices [**(D)** $F_{(2,561)} = 8.8$, **(E)** $F_{(2,352)} = 3.3$, **(F)** $F_{(2,1173)} = 89.7$, $^{*}p < 0.05$, $^{***}p < 0.001$, one-way ANOVA and Tukey's *post-hoc*]. **(G–I)** The ratio of the second to first EPSPs was significantly larger after stroke, while the ND1 treatment returned the ratio to the normal level. N = 4–5 per group, $^{**}p < 0.05$, $^{***}p < 0.001$ vs. sham or stroke controls [**(G)** $F_{(2,91)} = 10.2$, **(H)** $F_{(2,68)} = 5.2$, **(I)** $F_{(2,189)} = 16.8$, $^{*}p < 0.05$, $^{***}p < 0.001$, one-way ANOVA and Tukey's *post-hoc*].

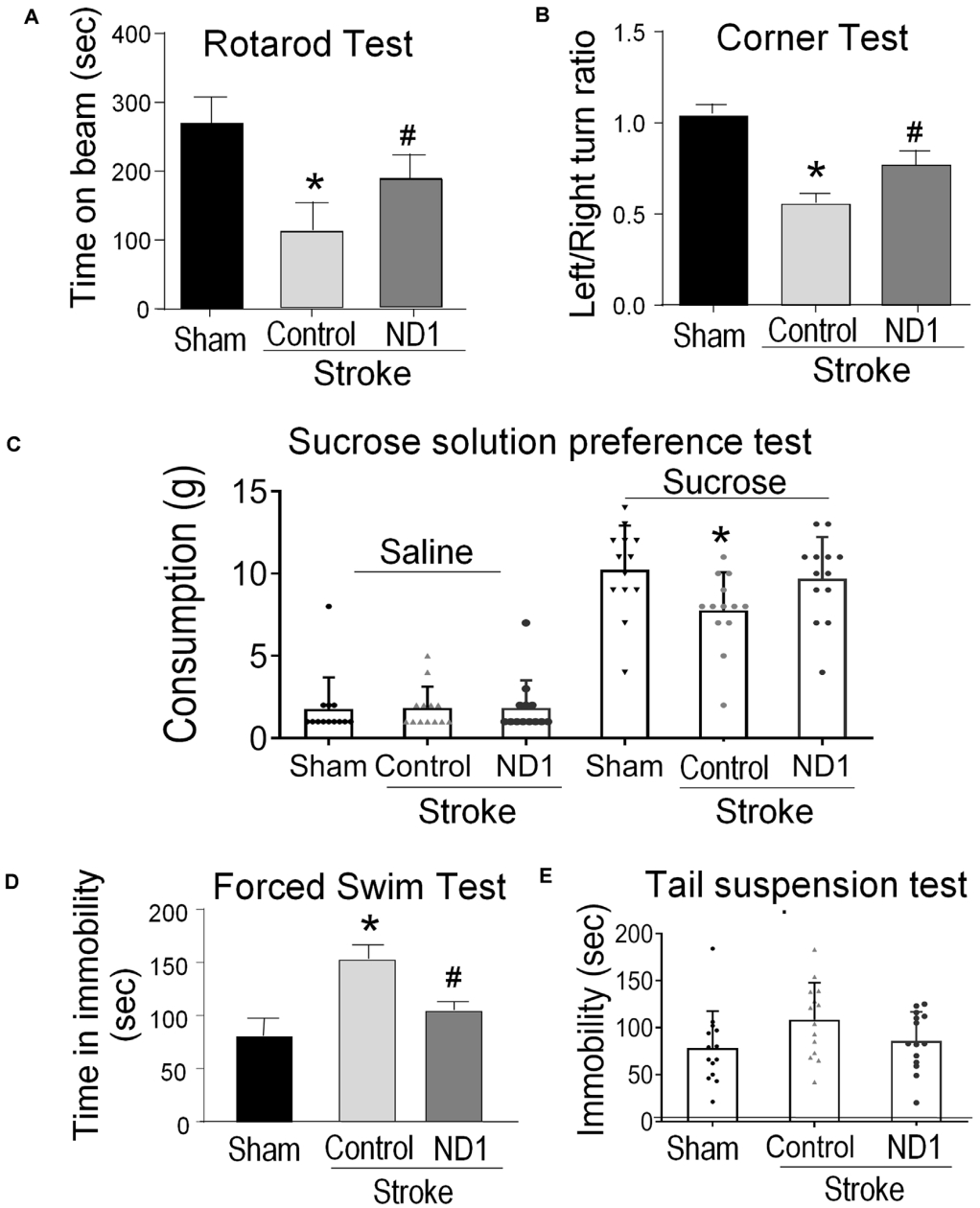

FIGURE 7 | Direct conversion of astrocytes to neurons improved functional recovery after stroke. Functional and behavioral tests were performed different days after stroke to evaluate the therapeutic benefits of the direct conversion therapy using ND1 transduction. **(A)** The rotarod test was performed 21 days after stroke to measure the motor function of stroke animals. Stroke animals disabled a disability in balancing on the rotarod beam, their time spent on the beam was significantly shorter than sham control mice. ND1 conversion treatment noticeably improved the motor function of maintaining on the beam with a longer time. N = 6/group, two-way ANOVA (interaction: $F_{(3,44)} = 29.9$, $^{***}p < 0.0001$ followed by Bartlett's test). Sidak's multiple comparisons test: $^{*}p < 0.05$ vs. Sham, $^{\#}p < 0.05$ vs. vector control. **(B)** In the corner test, normal mice make equal left and right turns so the ratio of turns is close to 1.0. After a stroke, animals revealed a sensorimotor deficit of biased turn behavior due to the side of ischemic damage in the sensorimotor cortex. ND1 treatment showed a significant correction in this sensorimotor functional deficit. N = 6/group, two-way ANOVA (interaction: $F_{(2,15)} = 19.91$, $^{***}p < 0.001$ followed by Bartlett's test). Sidak's multiple comparisons test: $^{*}p < 0.05$ vs. Sham, $^{\#}p < 0.05$ vs. vector control. **(C)** Long-term psychological behaviors were tested 4 months after stroke. In the sucrose preference test, sham animals showed a marked increase in consuming the sucrose solution compared to saline, while stroke resulted in a significantly reduced interest in the sucrose solution. Stroke mice that received ND1 treatment maintained a similar interest in drinking the sucrose solution as sham mice. N = 12–14/group, one-way ANOVA ($F_{(2,36)}$ 3.447, $p = 0.0427$), $^{*}p < 0.05$ vs. Sham. **(D)** In the forced swim test, stroke mice exhibited significantly longer idle time in the water, indicative of a chronically developed post-stroke depression-like phenotype. This depression-like behavior was significantly corrected in stroke mice treated with ND1. N = 6/group, One-way ANOVA ($F_{(4,82)} = 13.27$, $^{****}p < 0.0001$) followed by Holm–Sidak's multiple comparisons test: $^{*}p < 0.05$ vs. before stroke, $^{\#}p < 0.05$ vs. stroke control. **(E)** Tail suspension test of depression-like behavior in rodents. Stroke mice were observed to spend a longer time immobile compared to sham controls. ND1 treatment yielded a trend of reducing the immobility time. N = 14/group, one-way ANOVA (interaction: $F_{(2,39)} = 2.53$, $^{***}p = 0.0926$ followed by Bartlett's test).

neurotrophic factors have been shown to enhance the rate of direct conversion into neurons (Zhang et al., 2015). Supplemental treatments or co-expression of factors such as BDNF should also promote the maturation and survival of induced neurons (Zhang et al., 2015). Pathways involved in oxidative stress may act as key metabolic checkpoints during the glia-to-neuron conversion (Qian et al., 2020). Treatments with small molecules, such as VPA, calcitriol, or α-tocotrienol, may be tested since they also enhance neuronal survival and maturation, in addition to increased glia-to-neuron conversion (Su et al., 2014; Niu et al., 2015; Gascon et al., 2016). Cocktails of small molecules have been reported for the neuronal conversion of cultured human astrocytes (Zhang et al., 2015; Gao et al., 2017). Lastly, safety and efficiency are of paramount importance when these techniques are considered for clinical applications. Our study provides proof-of-principle data using a temporally and spatially specific lentivirus approach. Future research is required to explore more virus-mediated reprogramming therapies such as the non-integrating AAV vectors and non-virus approaches to prevent potential mutagenesis of genes critical for normal cell function or tumorigenesis. A balance must be maintained between the production of iNeurons with a supportive microenvironment to ensure safe and effective repairs at different time points after stroke. A better understanding of the molecular mechanisms underlying neuronal reprogramming may allow further flexibility in reprogrammed cell fate for specific brain disorders. Appropriate neuronal reprogramming schedules need to be explored for various applications in different injury models. Delayed reprogramming experiments are also needed to elucidate the therapeutic time window of this therapy.

CONCLUSIONS

The direct reprogramming of glial cells to neurons provides an unprecedented opportunity to repair damaged brain structures by a novel form of neurogenesis. This strategy utilizes an enriched endogenous cellular pool following injury, allowing on-site repair using autologous cells that are already integrated into the host tissue extracellular matrix. This approach also synergistically alters the pathology of stroke by ameliorating the inhibitory glial scar and associated inflammatory cascades. While this potential therapy is promising, it is also under debate due to previous inconclusive results. Data from this comprehensive investigation support that the glia-neuron conversion strategy is an effective and functionally beneficial therapy for ischemic stroke.

DATA AVAILABILITY STATEMENT

The original contributions presented in the study are included in the article/**Supplementary Material**, further inquiries can be directed to the corresponding author/s.

ETHICS STATEMENT

The animal study was reviewed and approved by Emory University IACUC.

AUTHOR CONTRIBUTIONS

SY and LW: conceptualization, resources, supervision, and funding acquisition. MJ, ZW, WZ, WC, XG, AW, MM, and KB: methodology and investigation. ZW and MJ: validation. MJ, ZW, and WZ: formal analysis. SY: data curation and project administration. SY and MJ: writing—original draft preparation. SY, MJ, MM, and KB: writing—review and editing. SY, MJ, AW, and LW: visualization. All authors have read and agreed to the published version of the manuscript. All authors contributed to the article and approved the submitted version.

FUNDING

This research was funded by NIH grants NS091585 (LW), NS099596 (LW/SY), NS114221 (LW/SY), S10 OD021773 (KB), Center for Integrated Healthcare, U.S. Department of Veterans Affairs; VA Merit grant RX001473 (SY), American Heart Association; AHA Career Development Award CDA34110317 (ZW); AHA Pre-doctoral Fellowship award AHA 0840110N (MJ). We acknowledge the Viral Vector Core of Emory Neuroscience NINDS Core Facilities supported by an NIH grant P30NS055077. The research was also supported by the O. Wayne Rollins Endowment fund, the Asa Griggs Candler Endowment fund (SY), and the John E. Steinhaus Endowment fund (LW).

SUPPLEMENTARY MATERIAL

The Supplementary Material for this article can be found online at: https://www.frontiersin.org/articles/10.3389/fnagi.2021.612856/full#supplementary-material.

REFERENCES

Anderson, M. A., O'Shea, T. M., Burda, J. E., Ao, Y., Barlatey, S. L., Bernstein, A. M., et al (2018). Required growth facilitators propel axon regeneration across complete spinal cord injury. *Nature* 561, 396–400. doi: 10.1038/s41586-018-0467-6

Ansorge, S., Lanthier, S., Transfiguracion, J., Durocher, Y., Henry, O., and Kamen, A. (2009). Development of a scalable process for high-yield lentiviral vector production by transient transfection of HEK293 suspension cultures. *J. Gene Med.* 11, 868–876. doi: 10.1002/jgm.1370

Barber, P. A., Davis, S. M., Infeld, B., Baird, A. E., Donnan, G. A., Jolley, D., et al (1998). Spontaneous reperfusion after ischemic stroke is associated with improved outcome. *Stroke* 29, 2522–2528. doi: 10.1161/01.str.29.12.2522

Berninger, B., Costa, M. R., Koch, U., Schroeder, T., Sutor, B., Grothe, B., et al (2007). Functional properties of neurons derived from *in vitro* reprogrammed postnatal astroglia. *J. Neurosci.* 27, 8654–8664. doi: 10.1523/JNEUROSCI.1615-07.2007

Blömer, U., Naldini, L., Kafri, T., Trono, D., Verma, I. M., and Gage, F. H. (1997). Highly efficient and sustained gene transfer in adult neurons with a lentivirus vector. *J. Virol.* 71, 6641–6649. doi: 10.1128/JVI.71.9.6641-6649.1997

Cai, H., Ma, Y., Jiang, L., Mu, Z., Jiang, Z., Chen, X., et al (2017). Hypoxia response element-regulated mmp-9 promotes neurological recovery *via* glial

scar degradation and angiogenesis in delayed stroke. *Mol. Ther.* 25, 1448–1459. doi: 10.1016/j.ymthe.2017.03.020

Calabresi, P., Centonze, D., Pisani, A., Cupini, L., and Bernardi, G. (2003). Synaptic plasticity in the ischaemic brain. *Lancet Neurol.* 2, 622–629. doi: 10.1016/s1474-4422(03)00532-5

Catanese, L., Tarsia, J., and Fisher, M. (2017). Acute ischemic stroke therapy overview. *Circ. Res.* 120, 541–558. doi: 10.1161/CIRCRESAHA.116.309278

Chen, Y. C., Ma, N. X., Pei, Z. F., Wu, Z., Do-Monte, F. H., Keefe, S., et al (2020). A neuroD1 AAV-based gene therapy for functional brain repair after ischemic injury through *in vivo* astrocyte-to-neuron conversion. *Mol. Ther.* 28, 217–234. doi: 10.1016/j.ymthe.2019.09.003

Chen, Y., and Swanson, R. A. (2003). Astrocytes and brain injury. *J. Cereb. Blood Flow. Metab.* 23, 137–149. doi: 10.1097/01.WCB.0000044631.80210.3C

Choi, D. W., Maulucci-Gedde, M., and Kriegstein, A. R. (1987). Glutamate neurotoxicity in cortical cell culture. *J. Neurosci.* 7, 357–368. doi: 10.1523/JNEUROSCI.07-02-00357.1987

Choi, K. E., Hall, C. L., Sun, J. M., Wei, L., Mohamad, O., Dix, T. A., et al (2012). A novel stroke therapy of pharmacologically induced hypothermia after focal cerebral ischemia in mice. *FASEB J.* 26, 2799–2810. doi: 10.1096/fj.11-201822

Choudhury, G. R., and Ding, S. (2016). Reactive astrocytes and therapeutic potential in focal ischemic stroke. *Neurobiol. Dis.* 85, 234–244. doi: 10.1016/j.nbd.2015.05.003

Endo, K., Karim, M. R., Taniguchi, H., Krejci, A., Kinameri, E., Siebert, M., et al (2011). Chromatin modification of Notch targets in olfactory receptor neuron diversification. *Nat. Neurosci.* 15, 224–233. doi: 10.1038/nn.2998

Ernst, A., Alkass, K., Bernard, S., Salehpour, M., Perl, S., Tisdale, J., et al (2014). Neurogenesis in the striatum of the adult human brain. *Cell* 156, 1072–1083. doi: 10.1016/j.cell.2014.01.044

Feliciano, D. M., Bordey, A., and Bonfanti, L. (2015). Noncanonical sites of adult neurogenesis in the mammalian brain. *Cold Spring Harb. Perspect Biol.* 7:a018846. doi: 10.1101/cshperspect.a018846

Frechou, M., Margaill, I., Marchand-Leroux, C., and Beray-Berthat, V. (2019). Behavioral tests that reveal long-term deficits after permanent focal cerebral ischemia in mouse. *Behav. Brain Res.* 360, 69–80. doi: 10.1016/j.bbr.2018.11.040

Gangal, A., Wei, Z. Z., Jiang, M. Q., Gu, H., Wei, L., and Yu, S. P. (2017). Overexpression of the neurogenic gene NGN2 in the peri-infarct region to reduce glial scar and support transplanted iPS cell-derived cells after neonatal stroke in rats. *Soc. Neurosci. Abstr.* 765:Y18.

Gao, L., Guan, W., Wang, M., Wang, H., Yu, J., Liu, Q., et al (2017). Direct generation of human neuronal cells from adult astrocytes by small molecules. *Stem Cell Rep.* 8, 538–547. doi: 10.1016/j.stemcr.2017.01.014

Gascon, S., Murenu, E., Masserdotti, G., Ortega, F., Russo, G. L., Petrik, D., et al (2016). Identification and successful negotiation of a metabolic checkpoint in direct neuronal reprogramming. *Cell Stem Cell* 18, 396–409. doi: 10.1016/j.stem.2015.12.003

Ge, W. P., Miyawaki, A., Gage, F. H., Jan, Y. N., and Jan, L. Y. (2012). Local generation of glia is a major astrocyte source in postnatal cortex. *Nature* 484, 376–380. doi: 10.1038/nature10959

Ghosh, H. S. (2019). Adult neurogenesis and the promise of adult neural stem cells. *J. Exp. Neurosci.* 13:1179069519856876. doi: 10.1177/1179069519856876

Gibbs, M. E., Hutchinson, D., and Hertz, L. (2008). Astrocytic involvement in learning and memory consolidation. *Neurosci. Biobehav. Rev.* 32, 927–944. doi: 10.1016/j.neubiorev.2008.02.001

Ginsberg, M. D. (2016). Expanding the concept of neuroprotection for acute ischemic stroke: the pivotal roles of reperfusion and the collateral circulation. *Prog. Neurobiol.* 145, 46–77. doi: 10.1016/j.pneurobio.2016.09.002

Gogel, S., Gubernator, M., and Minger, S. L. (2011). Progress and prospects: stem cells and neurological diseases. *Gene Ther.* 18, 1–6. doi: 10.1038/gt.2010.130

Grealish, S., Drouin-Ouellet, J., and Parmar, M. (2016). Brain repair and reprogramming: the route to clinical translation. *J. Intern. Med.* 280, 265–275. doi: 10.1111/joim.12475

Gresita, A., Glavan, D., Udristoiu, I., Catalin, B., Hermann, D. M., and Popa-Wagner, A. (2019). Very low efficiency of direct reprogramming of astrocytes into neurons in the brains of young and aged mice after cerebral ischemia. *Front. Aging Neurosci.* 11:334. doi: 10.3389/fnagi.2019.00334

Guo, Z., Zhang, L., Wu, Z., Chen, Y., Wang, F., and Chen, G. (2014). *In vivo* direct reprogramming of reactive glial cells into functional neurons after brain injury and in an Alzheimer's disease model. *Cell Stem Cell* 14, 188–202. doi: 10.1016/j.stem.2013.12.001

Hakim, A. M., Pokrupa, R. P., Villanueva, J., Diksic, M., Evans, A. C., Thompson, C. J., et al (1987). The effect of spontaneous reperfusion on metabolic function in early human cerebral infarcts. *Ann. Neurol.* 21, 279–289. doi: 10.1002/ana.410210310

Hatakeyama, M., Ninomiya, I., Otsu, Y., Omae, K., Kimura, Y., Onodera, O., et al (2020). Cell therapies under clinical trials and polarized cell therapies in pre-clinical studies to treat ischemic stroke and neurological diseases: A literature review. *Int. J. Mol. Sci.* 21:6194. doi: 10.3390/ijms21176194

Heinrich, C., Blum, R., Gascon, S., Masserdotti, G., Tripathi, P., Sanchez, R., et al (2010). Directing astroglia from the cerebral cortex into subtype specific functional neurons. *PLoS. Biol.* 8:e1000373. doi: 10.1371/journal.pbio.1000373

Heins, N., Malatesta, P., Cecconi, F., Nakafuku, M., Tucker, K. L., Hack, M. A., et al (2002). Glial cells generate neurons: the role of the transcription factor Pax6. *Nat. Neurosci.* 5, 308–315. doi: 10.1038/nn828

Holtzman, L., and Gersbach, C. A. (2018). Editing the epigenome: reshaping the genomic landscape. *Annu. Rev. Genomics Hum. Genet.* 19, 43–71. doi: 10.1146/annurev-genom-083117-021632

Huang, L., Wu, Z. -B., ZhuGe, Q., Zheng, W., Shao, B., Wang, B., et al (2014). Glial scar formation occurs in the human brain after ischemic stroke. *Int. J. Med. Sci.* 11, 344–348. doi: 10.7150/ijms.8140

Jiang, J., Piao, X., Hu, S., Gao, J., and Bao, M. (2020). LncRNA H19 diminishes dopaminergic neuron loss by mediating microRNA-301b-3p in Parkinson's disease *via* the HPRT1-mediated Wnt/beta-catenin signaling pathway. *Aging* 12, 8820–8836. doi: 10.18632/aging.102877

Jiang, M. Q., Yu, S. P., and Wei, L. (2019a). Direct reprogramming of reactive astrocytes to mature neurons reduces glia scar formation and enhances neuronal repair after ischemic stroke. *Soc. Neurosci. Abstr.* 16472:H14.

Jiang, M. Q., Yu, S. P., and Wei, L. (2019b). Direct conversion of astrocytes to neurons enhances neuronal repair and functional recovery after ischemic stroke. *Cell Transpl.* 28:472.

Jiang, M. Q., Zhao, Y. Y., Cao, W., Wei, Z. Z., Gu, X., Wei, L., et al (2017). Long-term survival and regeneration of neuronal and vasculature cells inside the core region after ischemic stroke in adult mice. *Brain Pathol.* 27, 480–498. doi: 10.1111/bpa.12425

Jorgensen, H. S., Sperling, B., Nakayama, H., Raaschou, H. O., and Olsen, T. S. (1994). Spontaneous reperfusion of cerebral infarcts in patients with acute stroke. incidence, time course and clinical outcome in the copenhagen stroke study. *Arch. Neurol.* 51, 865–873. doi: 10.1001/archneur.1994.00540210037011

Kanekar, S. G., Zacharia, T., and Roller, R. (2012). Imaging of stroke: part 2, pathophysiology at the molecular and cellular levels and corresponding imaging changes. *Am. J. Roentgenol.* 198, 63–74. doi: 10.2214/AJR.10.7312

Karimi-Abdolrezaee, S., and Billakanti, R. (2012). Reactive astrogliosis after spinal cord injury—beneficial and detrimental effects. *Mol. Neurobiol.* 46, 251–264. doi: 10.1007/s12035-012-8287-4

Khakh, B. S., and Sofroniew, M. V. (2015). Diversity of astrocyte functions and phenotypes in neural circuits. *Nat. Neurosci.* 18, 942–952. doi: 10.1038/nn.4043

Kronenberg, G., Gertz, K., Heinz, A., and Endres, M. (2014). Of mice and men: modelling post-stroke depression experimentally. *Br. J. Pharmacol.* 171, 4673–4689. doi: 10.1111/bph.12775

Lee, J. H., Wei, L., Gu, X., Wei, Z., Dix, T. A., and Yu, S. P. (2014). Therapeutic effects of pharmacologically induced hypothermia against traumatic brain injury in mice. *J. Neurotrauma* 31, 1417–1430. doi: 10.1089/neu.2013.3251

Li, H., and Chen, G. (2016). *In vivo* reprogramming for cns repair: regenerating neurons from endogenous glial cells. *Neuron* 91, 728–738. doi: 10.1016/j.neuron.2016.08.004

Li, W. L., Yu, S. P., Chen, D., Yu, S. S., Jiang, Y. J., Genetta, T., et al (2013). The regulatory role of NF-κB in autophagy-like cell death after focal cerebral ischemia in mice. *Neuroscience* 244, 16–30. doi: 10.1016/j.neuroscience.2013.03.045

Liu, M. H., Li, W., Zheng, J. J., Xu, Y. G., He, Q., and Chen, G. (2020). Differential neuronal reprogramming induced by NeuroD1 from astrocytes in grey matter versus white matter. *Neural Regen. Res.* 15, 342–351. doi: 10.4103/1673-5374.265185

Liu, X., Ye, R., Yan, T., Yu, S. P., Wei, L., Xu, G., et al (2014). Cell based therapies for ischemic stroke: from basic science to bedside. *Prog. Neurobiol.* 115, 92–115. doi: 10.1016/j.pneurobio.2013.11.007

Liu, Y., Miao, Q., Yuan, J., Han, S., Zhang, P., Li, S., et al (2015). Ascl1 converts dorsal midbrain astrocytes into functional neurons *in vivo*. *J. Neurosci.* 35, 9336–9355. doi: 10.1523/JNEUROSCI.3975-14.2015

Liu, Z., and Chopp, M. (2016). Astrocytes, therapeutic targets for neuroprotection and neurorestoration in ischemic stroke. *Prog. Neurobiol.* 144, 103–120. doi: 10.1016/j.pneurobio.2015.09.008

Luzzati, F., Nato, G., Oboti, L., Vigna, E., Rolando, C., Armentano, M., et al (2014). Quiescent neuronal progenitors are activated in the juvenile guinea pig lateral striatum and give rise to transient neurons. *Development* 141, 4065–4075. doi: 10.1242/dev.107987

Magnusson, J. P., Goritz, C., Tatarishvili, J., Dias, D. O., Smith, E. M., Lindvall, O., et al (2014). A latent neurogenic program in astrocytes regulated by Notch signaling in the mouse. *Science* 346, 237–241. doi: 10.1126/science.346.6206.237

Martinez-Salas, E., Ramos, R., Lafuente, E., and Lopez de Quinto, S. (2001) Functional interactions in internal translation initiation directed by viral and cellular IRES elements. *J. Gen. Virol.* 82, 973–984. doi: 10.1099/0022-1317-82-5-973

Matkar, P. N., Ariyagunarajah, R., Leong-Poi, H., and Singh, K. K. (2017). Friends turned foes: angiogenic growth factors beyond angiogenesis. *Biomolecules* 7:74. doi: 10.3390/biom7040074

McCrary, M. R., Jiang, M. Q., Giddens, M. M., Zhang, J. Y., Owino, S., Wei, Z. Z., et al (2019). Protective effects of GPR37 *via* regulation of inflammation and multiple cell death pathways after ischemic stroke in mice. *FASEB J.* 33, 10680–10691. doi: 10.1096/fj.201900070R

McLellan, M. A., Rosenthal, N. A., and Pinto, A. R. (2017). Cre-loxp-mediated recombination: general principles and experimental considerations. *Curr. Protoc. Mouse Biol.* 7, 1–12. doi: 10.1002/cpmo.22

Naldini, L., Blömer, U., Gage, F. H., Trono, D., and Verma, I. M. (1996). Efficient transfer, integration and sustained long-term expression of the transgene in adult rat brains injected with a lentiviral vector. *Proc. Natl. Acad. Sci. U S A.* 93, 11382–11388. doi: 10.1073/pnas.93.21.11382

Neumann-Haefelin, T., du Mesnil de Rochemont, R., Fiebach, J. B., Gass, A., Nolte, C., Kucinski, T., et al (2004). Effect of incomplete (spontaneous and postthrombolytic) recanalization after middle cerebral artery occlusion: a magnetic resonance imaging study. *Stroke* 35, 109–114. doi: 10.1161/01.STR.0000106482.31425.D1

Niu, W., Zang, T., Smith, D. K., Vue, T. Y., Zou, Y., Bachoo, R., et al (2015). SOX2 reprograms resident astrocytes into neural progenitors in the adult brain. *Stem Cell Rep.* 4, 780–794. doi: 10.1016/j.stemcr.2015.03.006

Niu, W., Zang, T., Zou, Y., Fang, S., Smith, D. K., Bachoo, R., et al (2013). *In vivo* reprogramming of astrocytes to neuroblasts in the adult brain. *Nat. Cell Biol.* 15, 1164–1175. doi: 10.1038/ncb2843

Ohab, J. J., and Carmichael, S. T. (2008). Poststroke neurogenesis: emerging principles of migration and localization of immature neurons. *Neuroscientist* 14, 369–380. doi: 10.1177/1073858407309545

Ohira, K., Furuta, T., Hioki, H., Nakamura, K. C., Kuramoto, E., Tanaka, Y., et al (2010). Ischemia-induced neurogenesis of neocortical layer 1 progenitor cells. *Nat. Neurosci.* 13, 173–179. doi: 10.1038/nn.2473

Park, Y. M., Chun, H., Shin, J. -I., and Lee, C. J. (2018). Astrocyte specificity and coverage of hGFAP-CreERT2 [Tg (GFAP-Cre/ERT2) 13Kdmc] mouse line in various brain regions. *Exp. Neurobiol.* 27, 508–525. doi: 10.5607/en.2018.27.6.508

Pekny, M., and Nilsson, M. (2005). Astrocyte activation and reactive gliosis. *Glia* 50, 427–434. doi: 10.1002/glia.20207

Pekny, M., and Pekna, M. (2016). Reactive gliosis in the pathogenesis of CNS diseases. *Biochim. Biophys. Acta* 1862, 483–491. doi: 10.1016/j.bbadis.2015.11.014

Petersen, H. V., Jensen, J. N., Stein, R., and Serup, P. (2002). Glucose induced MAPK signalling influences neuroD1-mediated activation and nuclear localization. *FEBS Lett.* 528, 241–245. doi: 10.1016/s0014-5793(02)03318-5

Pivonkova, H., and Anderova, M. (2017). Altered homeostatic functions in reactive astrocytes and their potential as a therapeutic target after brain ischemic injury. *Curr. Pharm. Des.* 23, 5056–5074. doi: 10.2174/1381612823666170710161858

Qian, H., Kang, X., Hu, J., Zhang, D., Liang, Z., Meng, F., et al (2020). Reversing a model of Parkinson's disease with in situ converted nigral neurons. *Nature* 582, 550–556. doi: 10.1038/s41586-020-2388-4

Rivetti di Val Cervo, P., Romanov, R. A., Spigolon, G., Masini, D., Martin-Montanez, E., Toledo, E. M., et al (2017). Induction of functional dopamine neurons from human astrocytes *in vitro* and mouse astrocytes in a Parkinson's disease model. *Nat. Biotechnol.* 35, 444–452. doi: 10.1038/nbt.3835

Robel, S., Berninger, B., and Gotz, M. (2011). The stem cell potential of glia: lessons from reactive gliosis. *Nat. Rev. Neurosci.* 12, 88–104. doi: 10.1038/nrn2978

Roger, V. L., Go, A. S., Lloyd-Jones, D. M., Adams, R. J., Berry, J. D., Brown, T. M., et al (2011). Heart disease and stroke statistics—2011 update: a report from the american heart association. *Circulation* 123, e18–e209. doi: 10.1161/CIR.0b013e3182009701

Sofroniew, M. V., and Vinters, H. V. (2010). Astrocytes: biology and pathology. *Acta Neuropathol.* 119, 7–35. doi: 10.1007/s00401-009-0619-8

Spurlin, J. W. III, and Nelson, C. M. (2017). Building branched tissue structures: from single cell guidance to coordinated construction. *Philos. Trans. R Soc. Lond B Biol. Sci.* 372:20150527. doi: 10.1098/rstb.2015.0527

Su, Z., Niu, W., Liu, M. L., Zou, Y., and Zhang, C. L. (2014). *In vivo* conversion of astrocytes to neurons in the injured adult spinal cord. *Nat. Commun.* 5:3338. doi: 10.1038/ncomms4338

Taoufik, E., Valable, S., Müller, G. J., Roberts, M. L., Divoux, D., Tinel, A., et al (2007). FLIPL protects neurons against *in vivo* ischemia and *in vitro* glucose deprivation-induced cell death. *J. Neurosci.* 27, 6633–6646. doi: 10.1523/JNEUROSCI.1091-07.2007

Tiscornia, G., Singer, O., and Verma, I. M. (2006). Production and purification of lentiviral vectors. *Nat. Protoc.* 1, 241–245. doi: 10.1038/nprot.2006.37

Torper, O., Pfisterer, U., Wolf, D. A., Pereira, M., Lau, S., Jakobsson, J., et al (2013). Generation of induced neurons *via* direct conversion *in vivo*. *Proc. Natl. Acad. Sci. U S A* 110, 7038–7043. doi: 10.1073/pnas.1303829110

Tsai, H. H., Li, H., Fuentealba, L. C., Molofsky, A. V., Taveira-Marques, R., Zhuang, H., et al (2012). Regional astrocyte allocation regulates CNS synaptogenesis and repair. *Science* 337, 358–362. doi: 10.1126/science.1222381

Vignoles, R., Lentini, C., d'Orange, M., and Heinrich, C. (2019). Direct lineage reprogramming for brain repair: breakthroughs and challenges. *Trends Mol. Med.* 25, 897–914. doi: 10.1016/j.molmed.2019.06.006

Wang, L. L., Chen, D., Lee, J., Gu, X., Alaaeddine, G., Li, J., et al (2014). Mobilization of endogenous bone marrow derived endothelial progenitor cells and therapeutic potential of parathyroid hormone after ischemic stroke in mice. *PLoS One* 9:e87284. doi: 10.1371/journal.pone.0087284

Wang, L. L., Su, Z., Tai, W., Zou, Y., Xu, X. M., and Zhang, C. L. (2016). The p53 pathway controls SOX2-mediated reprogramming in the adult mouse spinal cord. *Cell Rep.* 17, 891–903. doi: 10.1016/j.celrep.2016.09.038

Wei, L., Rovainen, C. M., and Woolsey, T. A. (1995). Ministrokes in rat barrel cortex. *Stroke* 26, 1459–1462. doi: 10.1161/01.str.26.8.1459

Wei, L., Wei, Z. Z., Jiang, M. Q., Mohamad, O., and Yu, S. P. (2017). Stem cell transplantation therapy for multifaceted therapeutic benefits after stroke. *Prog. Neurobiol.* 157, 49–78. doi: 10.1016/j.pneurobio.2017.03.003

Wittenberg, G. F., Bastings, E. P., Fowlkes, A. M., Morgan, T. M., Good, D. C., and Pons, T. P. (2007). Dynamic course of intracortical TMS paired-pulse responses during recovery of motor function after stroke. *Neurorehabil. Neural Repair* 21, 568–573. doi: 10.1177/1545968307302438

Yamashita, T., Shang, J., Nakano, Y., Morihara, R., Sato, K., Takemoto, M., et al (2019). *In vivo* direct reprogramming of glial linage to mature neurons after cerebral ischemia. *Sci. Rep.* 9:10956. doi: 10.1038/s41598-019-47482-0

Yavarpour-Bali, H., Ghasemi-Kasman, M., and Shojaei, A. (2020). Direct reprogramming of terminally differentiated cells into neurons: a novel and promising strategy for Alzheimer's disease treatment. *Prog. Neuropsychopharmacol. Biol. Psychiatry* 98:109820. doi: 10.1016/j.pnpbp.2019.109820

Zhang, L., Yin, J. C., Yeh, H., Ma, N. X., Lee, G., Chen, X. A., et al (2015). Small molecules efficiently reprogram human astroglial cells into functional neurons. *Cell Stem Cell* 17, 735–747. doi: 10.1016/j.stem.2015.09.012

Zhong, W., Yuan, Y., Gu, X., Kim, S. I., Chin, R., Loye, M., et al (2020). Neuropsychological deficits chronically developed after focal ischemic stroke and beneficial effects of pharmacological hypothermia in the mouse. *Aging Dis.* 11, 1–16. doi: 10.14336/AD.2019.0507

Zou, J., Maeder, M. L., Mali, P., Pruett-Miller, S. M., Thibodeau-Beganny, S., Chou, B. K., et al (2009). Gene targeting of a disease-related gene in human induced pluripotent stem and embryonic stem cells. *Cell Stem Cell* 5, 97–110. doi: 10.1016/j.stem.2009.05.023

Conflict of Interest: The authors declare that the research was conducted in the absence of any commercial or financial relationships that could be construed as a potential conflict of interest.

Advantages of publishing in Frontiers

OPEN ACCESS
Articles are free to read for greatest visibility and readership

FAST PUBLICATION
Around 90 days from submission to decision

HIGH QUALITY PEER-REVIEW
Rigorous, collaborative, and constructive peer-review

TRANSPARENT PEER-REVIEW
Editors and reviewers acknowledged by name on published articles

Frontiers
Avenue du Tribunal-Fédéral 34
1005 Lausanne | Switzerland

Visit us: www.frontiersin.org
Contact us: frontiersin.org/about/contact

REPRODUCIBILITY OF RESEARCH
Support open data and methods to enhance research reproducibility

DIGITAL PUBLISHING
Articles designed for optimal readership across devices

FOLLOW US
@frontiersin

IMPACT METRICS
Advanced article metrics track visibility across digital media

EXTENSIVE PROMOTION
Marketing and promotion of impactful research

LOOP RESEARCH NETWORK
Our network increases your article's readership